METEOR ASTRONOMY

LOVELL

523.5

523.
5
LOV

OXFORD

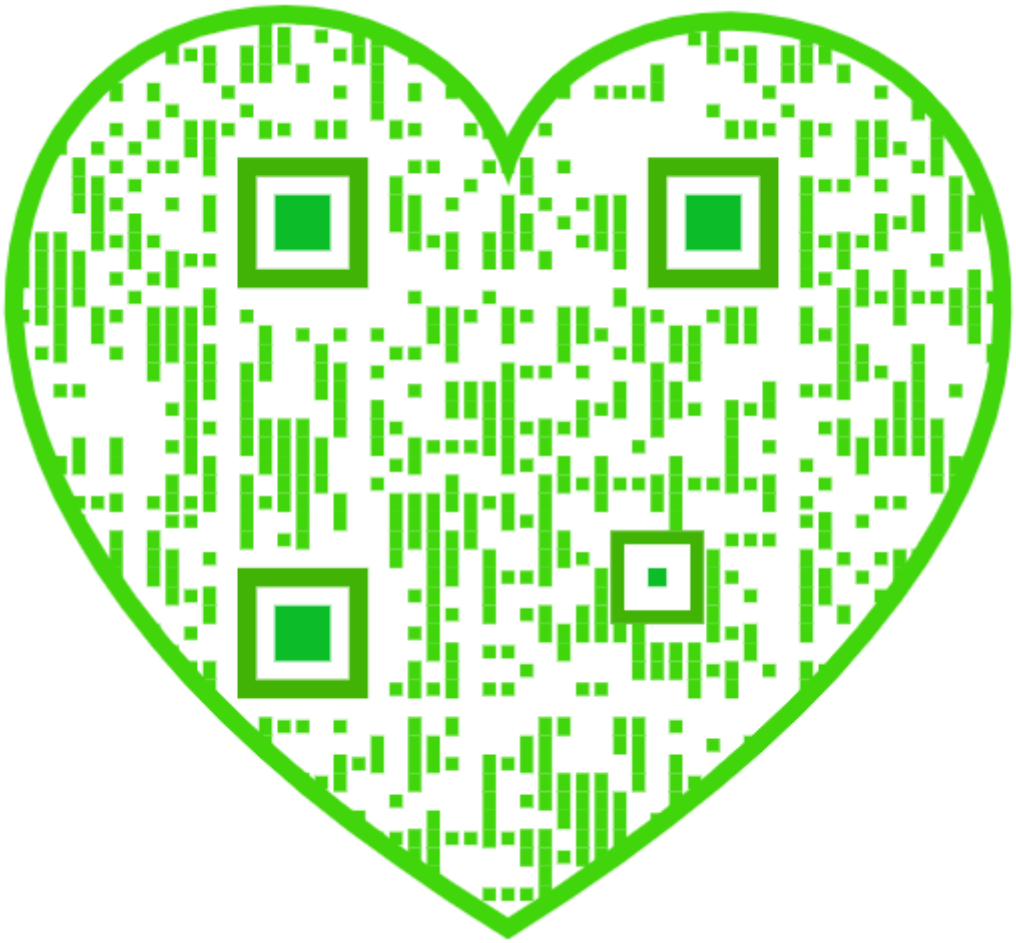

THE

INTERNATIONAL SERIES

OF

MONOGRAPHS ON PHYSICS

GENERAL EDITORS

N. F. MOTT E. C. BULLARD

THE INTERNATIONAL SERIES OF MONOGRAPHS ON PHYSICS

GENERAL EDITORS

N. F. MOTT
Cavendish Professor of Physics in the University of Cambridge

E. C. BULLARD
Director of the National Physical Laboratory Teddington

Already Published

THE THEORY OF ELECTRIC AND MAGNETIC SUSCEPTIBILITIES. By J. H. VAN VLECK. 1932.

THE THEORY OF ATOMIC COLLISIONS. By N. F. MOTT and H. S. W. MASSEY. *Second edition.* 1949.

RELATIVITY, THERMODYNAMICS, AND COSMOLOGY. By R. C. TOLMAN. 1934.

KINEMATIC RELATIVITY. A sequel to *Relativity, Gravitation, and World-Structure.* By E. A. MILNE. 1948.

THE PRINCIPLES OF STATISTICAL MECHANICS. By R. C. TOLMAN. 1938.

ELECTRONIC PROCESSES IN IONIC CRYSTALS. By N. F. MOTT and R. W. GURNEY. *Second edition.* 1948.

GEOMAGNETISM. By S. CHAPMAN and J. BARTELS. 1940. 2 vols.

THE SEPARATION OF GASES. By M. RUHEMANN. *Second edition.* 1949.

THE PRINCIPLES OF QUANTUM MECHANICS. By P. A. M. DIRAC. *Third edition.* 1947.

THEORY OF ATOMIC NUCLEUS AND NUCLEAR ENERGY SOURCES. By G. GAMOW and C. L. CRITCHFIELD. 1949. *Being the third edition of* STRUCTURE OF ATOMIC NUCLEUS AND NUCLEAR TRANSFORMATIONS.

THE PULSATION THEORY OF VARIABLE STARS. By S. ROSSELAND. 1949.

THEORY OF PROBABILITY. By HAROLD JEFFREYS. *Second edition.* 1948.

RADIATIVE TRANSFER. By S. CHANDRASEKHAR. 1950.

COSMICAL ELECTRODYNAMICS. By H. ALFVÉN. 1950.

COSMIC RAYS. By L. JÁNOSSY. *Second edition.* 1950.

THE FRICTION AND LUBRICATION OF SOLIDS. By F. P. BOWDEN and D. TABOR. 1950.

ELECTRONIC AND IONIC IMPACT PHENOMENA. By H. S. W. MASSEY and E. H. S. BURHOP. 1952.

THE THEORY OF RELATIVITY. By C. MØLLER. 1952.

MIXTURES. By E. A. GUGGENHEIM. 1952.

BASIC METHODS IN TRANSFER PROBLEMS. By V. KOURGANOFF with the collaboration of IDA W. BUSBRIDGE. 1952.

THE OUTER LAYERS OF A STAR. By R. V. d. R. WOOLLEY and D. W. H. STIBBS. 1953.

DISLOCATIONS AND PLASTIC FLOW IN CRYSTALS. By A. H. COTTRELL. 1953.

ELECTRICAL BREAKDOWN OF GASES. By J. M. MEEK and J. D. CRAGGS. 1953.

GEOCHEMISTRY. By the late V. M. GOLDSCHMIDT. Edited by ALEX MUIR. 1954.

THE QUANTUM THEORY OF RADIATION. By W. HEITLER. *Third edition.* 1954.

ON THE ORIGIN OF THE SOLAR SYSTEM. By H. ALFVÉN. 1954.

DYNAMICAL THEORY OF CRYSTAL LATTICES. By M. BORN and K. HUANG. 1954.

METEOR ASTRONOMY

BY

A. C. B. LOVELL

OXFORD
AT THE CLARENDON PRESS
1954

Oxford University Press, Amen House, London E.C.4
GLASGOW NEW YORK TORONTO MELBOURNE WELLINGTON
BOMBAY CALCUTTA MADRAS KARACHI CAPE TOWN IBADAN
Geoffrey Cumberlege, Publisher to the University

PRINTED IN GREAT BRITAIN

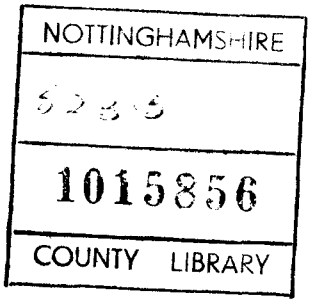

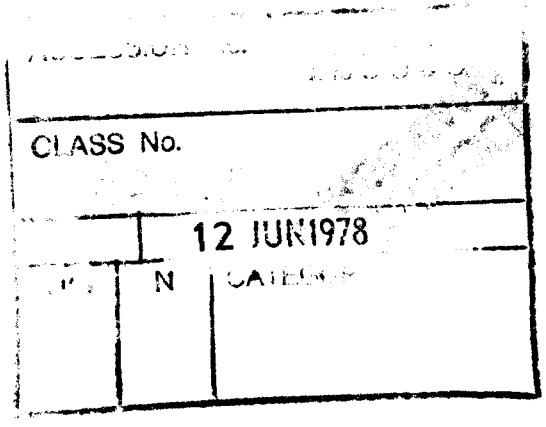

PREFACE

It is now twenty-seven years since the publication of the last comprehensive book on meteors. Recently the study of meteors has been transformed by the new photographic and radio-echo techniques and a modern treatment of the subject has become very desirable. When the present monograph was planned in 1949 it was intended to cover the entire field of meteors. However, it soon became evident that it would be impossible to compile such a work in any reasonable time, or in a single volume. With the publication of the present book, which deals only with the astronomy of meteors, the task is only half complete. A further volume, dealing with meteor physics, will be necessary to complete the original scheme and it is hoped that it may be possible to compile this at some future date.

In writing this book I have received much assistance from my colleagues working on meteors at Jodrell Bank. I am greatly indebted to Dr. J. G. Davies and Dr. G. S. Hawkins whose work, much of it still unpublished, forms the basis of certain sections of the book. I also wish to thank particularly, Prof. Z. Kopal, Mr. J. P. M. Prentice, Dr. Davies, Dr. Hawkins, and Miss M. Almond who have read and criticized the manuscript. The original for Plate I, and permission to reproduce, was kindly supplied by Dr. D. W. R. McKinley. The photograph for Plate II was taken by Mr. S. Evans of Jodrell Bank.

A. C. B. L.

UNIVERSITY OF MANCHESTER
JODRELL BANK EXPERIMENTAL STATION
LOWER WITHINGTON
CHESHIRE
December, 1952

CONTENTS

I. Introduction 1

II. Observational Methods 3
i. Visual and Photographic Techniques

III. Observational Methods 23
ii. The History and Fundamental Features of Radio-echo Observations

IV. Observational Methods 50
iii. Radio-echo Techniques for the Measurement of Meteor Radiants and Velocities

V. The Fundamental Equations of Meteoric Motion 86

VI. The Diurnal and Seasonal Distribution of Sporadic Meteors 96

VII. The Number and Mass Distribution of Sporadic Meteors 123

VIII. The Velocity of Sporadic Meteors 141
i. The von Niessl-Hoffmeister Fireball Catalogue

IX. The Velocity of Sporadic Meteors 155
ii. The Work of Öpik

X. The Velocity of Sporadic Meteors 190
iii. Porter's Analysis of the British Meteor Data

XI. The Velocity of Sporadic Meteors 198
iv. Photographic Results

XII. The Velocity of Sporadic Meteors 212
v. The Radio-echo Results and General Conclusion

XIII. The Major Meteor Showers 248
i. The Permanent Streams of January to June

XIV. The Major Meteor Showers 270
ii. The Permanent Streams of July and August

XV. The Major Meteor Showers 288
iii. The Permanent Streams of September to December

XVI. The Major Meteor Showers
iv. The Periodic Streams 326

XVII. The Major Meteor Showers
v. The Lost Streams 349

XVIII. The Major Meteor Showers
vi. The Day-time Streams 358

XIX. The Number and Mass Distribution of the Shower Meteors 384

XX. The Dispersive Effects in Meteor Streams 397

XXI. Cosmological Relationships of Meteors 413

Appendix I 435

Appendix II 438

Author Index 445

Subject Index 448

LIST OF TABLES

1. Correction to Zenithal Magnitude *page* 6
2. Relation between Observational Error ϵ and Magnitude m according to Öpik 7
3. Limiting Meteor Magnitude Visible at a given Angle from an Observer's Line of Vision 9
4. Numbers of Meteors of Different Magnitudes seen by a Visual Observer 10
5. Displacement of the Beginning and End Points for Common Meteors with Unequal Recorded Lengths in the Reticule Observations 11
6. Characteristics of the Harvard Cameras not Specifically Employed for Meteor Photography 15
7. Characteristics and Performance of the Meteor Cameras 20
8. Field Correction for the Harvard AI and FA Cameras 22
9. Data on a Single Meteor obtained in the 3-Station Radio Measurements of McKinley and Millman 54
10. Correction in Minutes of Time to be applied to Time of Transit for Various Heights of Meteor Showers 69
11. Correction Factors in Hoffmeister's Analysis 105
12. Probabilities of Telescopic Observations for Various Values of L/D 126
13. Effective Field of View for Different Meteor Magnitudes 127
14. Number of Meteors as a Function of Field of View and Magnitude 127
15. Path Length of Meteors as a Function of Magnitude 128
16. Correlation of Naked-eye and Telescopic Magnitude Scales 128
17. Path Length and Effective Area of Visibility for Meteors of Different Magnitudes 129
18. Number of Meteors of Different Magnitudes 130
19. Numbers of Meteors of Different Magnitudes entering the Earth's Atmosphere per Day 130
20. Frequency of Meteors as a Function of Magnitude in Williams's Analysis 134
21. Comparison of Observed and Computed Meteor Frequencies as a Function of Magnitude in Williams's Analysis 135
22. Relation of Meteor Magnitude and Mass 137
23. Daily Mass of Sporadic Meteors intercepted by the Earth as a Function of Meteor Magnitude 137
24. Mass and Energy brought into the Earth's Atmosphere by Sporadic Meteors 138
25. Space Distribution of Sporadic Meteor Material 139
26. Velocities in Fireball Catalogue for certain Radiant Clusters treated by Fisher 146
27. Comparison of Velocities of Meteors belonging to known Showers compared with the Values given in the Fireball Catalogue 150

28. Watson's Analysis of the Distribution in Latitude of Velocity Groups in the Fireball Catalogue 151

29. Results of Watson's Test of the Significance of Apparent Radiant Groups in the Fireball Catalogue 152

30. Comparison of Concentration of Meteors in the Arizona Results with those in the Fireball Catalogue 153

31. Öpik's Preliminary Grouping of 64 Stream Meteors 155

32. Corrections required to Angular Velocities w_1 in the Rocking-mirror Observations 156

33. Relative Weights to be assessed to Angular Velocities observed in Rocking Mirror 156

34. Relation between Height and Zenithal Angular Velocity 157

35. Example of Final Data produced by Öpik from the Rocking-mirror Observations 158

36. Distribution of Heliocentric Space Velocities $\overline{V}_h$ of 279 Naked-eye Observations 160

37. Distribution of Projected Heliocentric Velocities $\overline{V}_0$ of 279 Naked-eye Observations 161

38. Distribution of Heliocentric Space Velocities $\overline{V}_h$ for 580 Telescopic Observations 161

39. Distribution of Projected Heliocentric Velocities $\overline{V}_0$ for 580 Telescopic Observations 162

40. Percentage of Heliocentric Velocities exceeding 62 km./sec. according to the preliminary rocking-mirror results 163

41. Relation between w_z and h for 486 Observations in the complete Arizona Data 164

42. Provisional Distribution of Heliocentric Space Velocities for the 1,436 Arizona Velocities (all directions) 165

43. The Distribution of Geocentric Tangential Velocities v and the Correction for Error Dispersion 168

44. Stream Intensity n_η/C (for $\eta = 0°$ to $\eta = \eta$) for $k = 1$, $B = 1$ at $z = 45°$ N. 169

45. Stream Intensity n_η/C (for $\eta = 0°$ to $\eta = \eta$) for $k = 2$, $B = 1$ at $z = 45°$ N. 170

46. Calculated Stream Intensity 172

47. Relative Frequency of Projection Ratios ($\sin \eta$) 174

48. Distribution of Space Velocities 175

49. Distribution of Heliocentric Velocities 176

50. Distribution of Heliocentric Velocities for all Directions 178

51. Frequency of Solar and Hyperbolic Meteors in the Arizona Data 180

52. Relation between Uncorrected Geocentric Velocity v and Zenithal Magnitude m_z 180

53. Distribution of Heliocentric Velocities for High and Low Luminosity 181

54. Observed Frequency of Transverse Heliocentric Components of Velocity for Öpik's Arizona and Tartu Observations 183

55. Distribution of Space Velocities for 583 Sporadic Meteors observed by Öpik in Arizona and Tartu 186

56. Relation between the Heliocentric Tangential Velocity $\overline{V}_0$ and the Zenithal Magnitude m_z for Öpik's Combined Results 188

57. Mean Errors and Standard Deviations for the Multiple Accordances 191

58. Average and Median Errors for the Multiple Accordances 192

59. Comparison of r.m.s. Errors for Duplicate and Multiple Accordances 192

60. Relation between Height and Velocity for the Shower and Sporadic Meteors 194

61. Relation between Shower and Sporadic Meteors over the same range of ϵ and m 195

62. Distribution of v/v_p for Sporadic and Shower Meteors 196

63. Data on Seven Sporadic Meteors photographed by Millman and Hoffleit between 1932 and 1936 201

64. Example of Whipple's Trail Coordinates and Residuals for Meteor No. 642 204

65. Velocities and Deceleration of Meteor No. 642 204

66. Whipple's Double Station Data for Seven Sporadic Meteors 206

67. Additional List of Sixteen Sporadic Meteors extracted from Jacchia's First Analysis 208

68. Additional List of Ten Velocities extracted from Jacchia's Second Analysis 209

69. Anticipated Performance of Super Schmidt Camera compared with existing Cameras 211

70. Adopted Values of Errors in the Velocity Measurements 220

71. Collecting Areas of Aerial System 227

72. Distribution of Electron Densities observed in the Experiments on the Velocity Distribution 231

73. Comparison of Magnitudes obtained from Visual Rates and Electron Densities 233

74. Number of Meteors observed in Different Magnitude Groups during the Radio-echo Apex Experiments 233

75. Details of Seven Velocities in excess of 80 km./sec. 235

76. Mean Errors of Velocity Measurement at 70 km./sec. 236

77. Typical Transformations for McKinley's Velocity Distribution 243

78. The Major Meteor Streams 249

79. Maximum Rates of the Quadrantid Shower determined by the Radio-echo Apparatus 252

80. Radiant Coordinates for the Quadrantid Shower determined by the Radio-echo Technique 254

81. Parabolic Elements for the Quadrantids as computed by Wenz, Davidson, and Hoffmeister, compared with Comet 1860 I 256

82. Orbital Elements for the Quadrantids computed from the Radio-echo and Photographic Data 257
83. Maximum Hourly Rates of the Lyrid Meteor Shower 260
84. The Lyrid Shower of 1922 260
85. Lyrid Radiants 261
86. Radio-echo Determinations of the Velocity of Lyrid Meteors 263
87. Orbital Elements for Comet 1861 I and the Lyrid Meteor Shower 263
88. Epoch of Maximum of the η-Aquarid Shower 265
89. Ephemeris of the η-Aquarid Radiant 266
90. Orbital Elements of the η-Aquarid Shower compared with Halley's Comet 267
91. Radiant Coordinates of the δ-Aquarid Stream 272
92. Visual Velocity Measurements of possible δ-Aquarid Meteors 273
93. Orbital Elements for the δ-Aquarid Meteor Stream 275
94. Hourly Rate of the Perseid Stream since 1900 279
95. Radiant Positions of the Perseid Shower 280
96. Visual Velocity Measurements of Possible Perseid Meteors 283
97. Perseid Velocities Photographically determined by the Double-camera Method 284
98. Radio-echo Measurements of Perseid Velocities 285
99. The Orbital Elements of the Perseid Stream and of Comet 1862 III 287
100. Radio-echo Observations of the Orionid Activity 290
101. Orionid Radiants 1928 according to McIntosh 291
102. Prentice's Radiants for the Orionid Stream 291
103. Hoffmeister's Radiants for the Orionid Stream 293
104. Visual Velocity Measurements of possible Orionid Meteors 294
105. Comparison of the Orbits of the η-Aquarids, Orionids, and Halley's Comet 295
106. Denning's 1928 List of the Radiants in Taurus and Aries 298
107. Whipple's First List of seven Photographic Taurid Radiants 299
108. The Radiants in Taurus and Aries according to the Photographic Analysis of Miss Wright and Whipple 300
109. Predicted Mean Radiant with Date for the Taurid-Arietid Streams according to Miss Wright and Whipple 300
110. Velocities of the Taurids and Arietids according to Miss Wright and Whipple 302
111. Orbital Elements for nine Taurid-Arietid Meteors computed by Miss Wright and Whipple 304
112. Minimum Distances of Taurid Meteors from Planetary Orbits 307
113. Activity of the Geminid Meteor Shower as observed by the Radio-echo Technique 310
114. Ephemeris of the Geminid Radiant compiled by King in 1926 and by Maltzev in 1931 from Visual Observations 311

115. Whipple's Photographic Determinations of the Geminid Radiant from Five Doubly Photographed Trails 311
116. Whipple's Determination of the Daily Motion of the Geminid Radiant from Thirty-six Single and Five Doubly Photographed Trails 312
117. Radio-echo Observations of the Geminid Radiant Position 312
118. Daily Motion of the Geminid Radiant 312
119. Photographic Determinations of the Velocities of Geminid Meteors 315
120. Orbital Elements for the Geminid Meteors 317
121. Hourly Rates of the Bečvář Meteor Stream, 1945 December 22 320
122. Hourly Rate of the Ursid Stream subsequent to 1945 320
123. Radiant Positions of the Ursid Meteor Stream 322
124. Orbital Elements for the Ursid Meteor Stream and for Comet Tuttle 1939 k 324
125. Activity of the Giacobinid Shower 332
126. Visual Determinations of the Giacobinid Radiant during the 1933 Return 332
127. Photographic Determination of the Giacobinid Radiant during the 1946 Return 333
128. Computed Velocities of the Giacobinid Meteors 1946 335
129. Radio-echo Measurements of the Giacobinid Velocities 1946 335
130. Changes in the Orbit of Comet Giacobini–Zinner since 1900 336
131. Elements of the Giacobini–Zinner Comet 1946 and Predicted Elements for 1953 336
132. Activity of the Leonid Shower 339
133. Visual Observations of the Leonid Radiant according to King 341
134. Change of Mean Radiant Position of Leonids with Date according to King 342
135. King's predicted Ephemeris of the Leonid Radiant 342
136. The Visual Leonid Radiant 1934 according to Huruhata 342
137. Corrected Leonid Radiant at Maximum from the Harvard Photographic Data 343
138. Predicted Mean Radiant Position (1950·0) from the Harvard Photographic Data 344
139. The Velocities of Six Leonid Meteors determined by the Double-station Technique 346
140. The Orbits of the Leonids and of Temple's Comet 1866 I 347
141. The Activity of the Bielid Stream 350
142. Radiant Position of the Bielid Stream 352
143. The Changes in the Orbit of Biela's Comet 353
144. Orbital Elements of Biela's Comet and the Associated Meteor Streams 354
145. Radiant Positions of the Pons–Winnecke Shower 1916 355
146. Ephemeris of the Pons–Winnecke Radiant 356
147. Changes in the Orbital Elements of the Pons–Winnecke Comet 357

148. Activity of the Day-time Meteor Radiants 366
149. Mean Radiant Positions of the Day-time Meteor Streams 370
150. Daily Radiant Positions of the Day-time Streams 1950–2 371
151. Ephemerides of the Motion of the Radiants of the Day-time Arietids, ζ-Perseids, and β-Taurids 373
152. The Velocity Measurements of the Summer Day-time Streams 377
153. Observational Data and Orbital Elements for the o-Cetid Shower 379
154. Observational Data and Orbital Elements for the Arietid Stream 379
155. Observational Data and Orbital Elements for the ζ-Perseid Stream 381
156. Observational Data and Orbital Elements for the Day-time β-Taurid Stream and the Night-time Taurids 381
157. Distribution of Luminosities in the Perseid Shower according to Öpik 385
158. The Frequency Distribution Observed by de Roy and by Sandig and Richter during the 1933 Giacobinid Shower, as corrected by Watson 386
159. Distribution of Apparent Photographic Magnitudes for the 1946 Giacobinid Shower 387
160. Distribution of Integrated Absolute Photographic Magnitudes for the 1946 Giacobinid Shower 388
161. Scaling Factors for the Major Showers over the Sporadic Background derived from Fig. 184 392
162. Meteoric Mass entering the Earth's Atmosphere in Various Magnitude Groups due to the Major Showers 393
163. The Density and Total Mass in the Orbits of the Major Showers 395
164. Data for Calculation of Time of Fall of a Particle into the Sun as a Result of the Poynting–Robertson Effect 406
165. Times of Fall into the Sun of Meteoric Particles in the Major Shower Orbits 408
166. Times of Separation of Meteors of Magnitude -2 and $+5$ due to Poynting–Robertson Effect 409
167. Cometary–Meteor Stream Associations 413
168. Comets with Elliptical Orbits approaching the Earth to within 0·100 a.u. 415
169. Observed Perturbations for Encke's Comet 416
170. Elements of Comet Encke and three Taurid Meteors referred to Jupiter's Orbit (1920) and the Values of the Perturbation Constants 419
171. Major Meteor Showers without Cometary Association 422
172. Perturbations of the Geminid Orbit by Jupiter and the Earth in 100 years and changes in the least distance of the Orbit from the Earth 423
173. Relation of Comet Brightness and Meteor Characteristics 428
174. Comparison of the Orbits of Short-period Sporadic Meteors, Asteroids, and Comets 430
175. Times of Fall into the Sun for Meteors with an Asteroidal Type of Origin 431

LIST OF PLATES

Between pp. 72 and 73

I. Meteor echoes photographed on an intensity-modulated range-time display

II. The aerial system of the radiant survey apparatus at Jodrell Bank

III. Diffraction pattern from a meteor trail obtained with pulsed radio-echo equipment

The question of the velocity distribution of sporadic meteors is of such cardinal importance that considerable space has been devoted to the topic. The work of Öpik on this subject has been dealt with in particular detail. This seemed the only just course since the contemporary conclusions are in contradiction to his results; also his original papers are not readily available.

It must be emphasized that this book deals specifically with the astronomy of meteors. The subject of meteor physics will, it is hoped, be the topic of a complementary text at some future date. Thus the subject of meteor heights is introduced here only in so far as it is concerned with the determination of meteor velocities. An account of the extensive work in which the heights of appearance and disappearance of meteors are involved, in upper atmosphere measurements, and in the theories of meteor evaporation is reserved for this other work.

It must also be emphasized that the book does not deal with *meteorites*. Contemporary opinion is that these bodies, which are large enough to penetrate the atmosphere without complete evaporation, are likely to have a different origin from the meteors, or shooting stars, visible in the sky. In any case very little is known about the astronomy of meteorites, the subject at present being largely of geochemical interest.

At the other end of the scale the micro-meteorites which are small enough to be stopped before evaporation begins, and which are believed to fall to earth as fine dust, are of recent discovery. Insufficient is known about these micro-meteorites to justify the inclusion of the subject in this book, particularly as almost our entire knowledge of them is contained in two papers by Whipple.†

† Whipple, F. L., *Proc. Nat. Acad. Sci. Wash.* **36** (1950), 687; **37** (1951), 19.

LIST OF PLATES

Between pp. 72 and 73

I. Meteor echoes photographed on an intensity-modulated range-time display

II. The aerial system of the radiant survey apparatus at Jodrell Bank

III. Diffraction pattern from a meteor trail obtained with pulsed radio-echo equipment

I

INTRODUCTION

OLIVIER'S classical text on meteors appeared in 1925.† In the succeeding quarter of a century the subject of meteor astronomy was dominated by the great Arizona expedition for the study of meteors, and particularly by the work of Öpik.‡ Since the publication of Olivier's book, the literature of the subject has been composed largely of the results of the Arizona expedition and of two books by Hoffmeister§ dealing mainly with his own observations. In the years immediately preceding the Second World War, the observations of the amateur observing teams —particularly of those in America under Olivier, and in Great Britain under Prentice‖—together with the first results of Whipple's new photographic techniques at Harvard, cast serious doubt on the interpretation of the Arizona results and also of those of Hoffmeister. A controversy arose as to whether sporadic meteors were interstellar or solar in origin, and interest in the subject was further increased when the new techniques of radio astronomy were applied to the observation of meteors after the war. For some time the interest of the workers using this new technique was dominated by the ability to observe meteors systematically under all sky conditions, and particularly by the discovery of the great series of meteor streams active in the day-time sky. The evolution of the radio techniques for measuring meteor velocities and radiants soon enabled the radio astronomical work to be concentrated on the classical problem of the spatial orbits of the shower and sporadic meteors. Meanwhile the precision work at Harvard on meteor photography was extended and led to a deeper insight into the movement of meteors in the solar system.

Now a great many outstanding problems have been solved, and it seems unlikely that the next decade will witness such a revolution in meteor astronomy as has occurred during the past six years. Although the fundamental problem of the cosmical origin of meteors is not yet solved, much of the basic information on which the solution must be attempted already exists. The time would therefore seem to be appropriate for a new text describing the new methods and the integration of their results with the old problems.

† Olivier, C. P., *Meteors*, Williams and Wilkins, 1925. ‡ See Chap. IX.

§ Hoffmeister, C., *Die Meteore*, Leipzig, 1937; *Meteorströme*, Weimar, Leipzig, 1948.

‖ Valuable work in this period was also carried out by teams in Czechoslovakia under Guth, in Japan under Yumanoto, and in Russia under Astapovich and Sytinskaya.

The question of the velocity distribution of sporadic meteors is of such cardinal importance that considerable space has been devoted to the topic. The work of Öpik on this subject has been dealt with in particular detail. This seemed the only just course since the contemporary conclusions are in contradiction to his results; also his original papers are not readily available.

It must be emphasized that this book deals specifically with the astronomy of meteors. The subject of meteor physics will, it is hoped, be the topic of a complementary text at some future date. Thus the subject of meteor heights is introduced here only in so far as it is concerned with the determination of meteor velocities. An account of the extensive work in which the heights of appearance and disappearance of meteors are involved, in upper atmosphere measurements, and in the theories of meteor evaporation is reserved for this other work.

It must also be emphasized that the book does not deal with *meteorites*. Contemporary opinion is that these bodies, which are large enough to penetrate the atmosphere without complete evaporation, are likely to have a different origin from the meteors, or shooting stars, visible in the sky. In any case very little is known about the astronomy of meteorites, the subject at present being largely of geochemical interest.

At the other end of the scale the micro-meteorites which are small enough to be stopped before evaporation begins, and which are believed to fall to earth as fine dust, are of recent discovery. Insufficient is known about these micro-meteorites to justify the inclusion of the subject in this book, particularly as almost our entire knowledge of them is contained in two papers by Whipple.†

† Whipple, F. L., *Proc. Nat. Acad. Sci. Wash.* **36** (1950), 687; **37** (1951), 19.

II

OBSERVATIONAL METHODS—I

VISUAL AND PHOTOGRAPHIC TECHNIQUES

1. Direct visual techniques

(a) Introduction

From the historical records which are referred to in later chapters of this book it will be clear that meteors have been observed by the unaided eye for many hundreds of years. It was the end of the eighteenth century, however, before Brandes and Benzenberg in Germany noticed that, although separated by considerable distances, they saw the same meteor but that it appeared in different parts of the sky. From these and similar observations they deduced that the meteors were appearing at altitudes of 80 to 100 kilometres and that they must be due to bodies from space, entering the earth's atmosphere at speeds of many kilometres per second. In November 1833 the great shower of Leonid meteors occurred. On this occasion it became evident to Olmsted, Twining, and many others that the meteors were apparently radiating from a point. In the second half of the nineteenth century the work of Schiaparelli, Newton, and others drew attention to the importance of determining the spatial orbits in which the meteors were moving before they entered the atmosphere. It became evident that, apart from the counting of meteors, the accurate determination of their radiants and velocities was a prerequisite of any serious progress in meteor astronomy. From this era the techniques of naked-eye observation have been steadily improved and the contemporary work of experienced observers is a remarkable example of the excellence of the results which may be obtained in the recording of the transient and infrequent meteoric phenomena.

A single observer can only record the apparent path of a meteor projected against the star background. On the other hand, duplicate observations enable the parallactic displacement of the two apparent paths to be determined and, in principle, gives data on the radiant, height, path length, and velocity of the meteor. Originally, the method of recording appears to have been the plotting of the observed path of the meteor on a star map. As early as 1890, Denning† recommended the use of a

† Denning, W. F., *Telescopic work for Starlight Evenings*, London, 1891. *Mem. Brit. Astr. Ass.* **1** (1891), 20.

wand, or extended string, which the observer aligned along the meteor path and read the coordinates of the beginning and end of the path in terms of the star background. This gave more time for the establishment of the position of the trail, and also gave a more accurate 'flight direction' by enabling the meteor path to be extended to more suitable star fields. This method has been steadily improved, particularly under the influence of Prentice in Great Britain, such as by the use of cross bearings and the quotation of actual distances between known stars instead of estimates of angular distance. Thus the modern British observer rarely uses maps at the time of observation but presents his data in terms of the coordinates of stars for subsequent reduction to true paths. On the other hand the American observers, under Olivier, plot the path of the meteor on a prepared chart. An investigation of the accuracy of the data obtained by two of the best British observers between 1932 and 1935 has been carried out by Porter.† From an analysis of 102 meteor paths simultaneously observed by Prentice and Alcock, Porter plotted the frequency distribution of errors for the position of the beginning and end of the meteor path. The probable error for the beginning was $\pm 3{\cdot}26^\circ$ and for the end $\pm 2{\cdot}43^\circ$. These are comparable with the errors which Porter found in his subsequent analysis of the entire British meteor data,‡ referred to in Chapter X. In a later analysis of the accuracy of radiant determinations Porter§ concluded that the probable error was $\pm 2{\cdot}4^\circ$ and that the mean deviations in the height determinations were 3·6 km. at the beginning of the path and 2·8 km. at the end. As regards the accuracy of the radiant, Porter's conclusions were criticized by Prentice‖ on the grounds that Porter had assumed the Perseid radiant to be a point whereas, in fact, it is diffuse. Actually it seems that the probable error in the radiants determined by good observers is about $\pm 1^\circ$.

The accuracy of observations by inexperienced meteor observers has been discussed by Watson and Cook.†† As a result of tests made during the Leonid shower in 1933 they found probable errors in the direction given for the meteor path of between $\pm 10{\cdot}8^\circ$ and $\pm 18{\cdot}8^\circ$.

Unfortunately the timing errors are necessarily large in the visual techniques even with the best observers, mean errors of 20 to 30 per cent. being quoted by Porter. It will be evident from succeeding chapters

† Porter, J. G., *J. Brit. Astr. Ass.* **48** (1938), 337.
‡ Porter, J. G., *Mon. Not. Roy. Astr. Soc.* **103** (1943), 134.
§ Porter, J. G., *J. Brit. Astr. Ass.* **49** (1939), 113.
‖ Prentice, J. P. M., ibid. (1939), 146.
†† Watson, F., and Cook, E. M., *Pop. Astron.* **44** (1936), no. 5.

of this book that little confidence can be placed in many of the visual velocity determinations.

(*b*) *The Reduction of Visual Observations*

The difficulties in the reduction of the observed paths to true paths in the atmosphere will be clear from Fig. 1. Observers at O_1, O_2, record

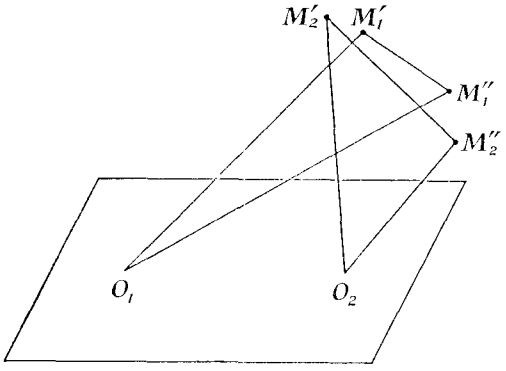

FIG. 1.

the beginning and end of the meteor path at M_1', M_2' and M_1'', M_2'', respectively. If the observations are simultaneous O_1M_1' and O_2M_2' will meet to define the beginning of the meteor path and O_1M_2'' and O_2M_2'' will meet to define the end. In this case the computation presents no difficulty. These ideal conditions are rarely fulfilled since one or other of the observers generally misses a portion of the flight. Various methods have been employed in the reduction† and arbitrary adjustments to the observations by the computors appear to have been common practice until about 1930. The method recommended by Porter‡ and the one now generally used in the reduction of the British observations is that devised by Davidson.§ The detailed procedure in the practical application of the method has been described by Porter.‖ In principle this method finds the point of intersection of the observations of O_1 with the plane of the observations of O_2, and no assumptions of simultaneity are made.

Using this method Porter†† has reduced the entire duplicate and multiple observations of meteors made in Great Britain between 1890

† For example, Schaeberle's method as described by Olivier, C. P., *Meteors*, ch. 14.
‡ Porter, J. G., *Mon. Not. Roy. Astr. Soc.* **103** (1943), 134.
§ Davidson, M., *J. Brit. Astr. Ass.* **46** (1936), 292.
‖ Porter, J. G., *Mem. Brit. Astr. Assoc.* **34** (1942), 37.
†† Porter, J. G., *Mon. Not. Roy. Astr. Soc.* **103** (1943), 134; **104** (1944), 257.

and 1940. The results and the analysis of the errors are discussed in Chapter X.

(c) *The Magnitude Correction*

The stellar magnitudes quoted by observers differ considerably on account of varying distance, atmospheric absorption, etc. It is customary to reduce the observed magnitude to zenithal magnitude, that is the magnitude the meteor would have if it were in the observer's zenith but at the same height. The reduction, which is simply made by applying the inverse square law, has been discussed by Öpik,† Porter,‡ and others. If the meteor is seen at a distance R and height h, the effect of bringing it to the observer's zenith would be to increase the luminosity in the ratio R^2/h^2. Then the stellar magnitude would be diminished by an amount Δm_1 where,

$$(2{\cdot}512)^{\Delta m_1} = R^2/h^2.$$

Thus

$$\Delta m_1 = 5 \log R/h = 5 \log \sec z$$

where z is the zenith distance of the observation.

The correction factors given by Porter,‡ which also include a small effect due to atmospheric absorption, are given in Table 1.

TABLE 1

Correction to Zenithal Magnitude

Height h km.	60	80	100	120	140	160	180	200
Distance R km.								
60	+1·1	..	..	..	..	..	..	..
80	+0·4	+0·5	..	..	..	..	..	..
100	−0·1	−0·1	0	..	..	..	..	..
120	−0·6	−0·5	−0·4	−0·4	..	..	..	..
140	−1·0	−0·9	−0·8	−0·7	−0·7	..	..	..
160	−1·4	−1·2	−1·1	−1·1	−1·0	−1·0	..	..
180	−1·7	−1·6	−1·5	−1·4	−1·4	−1·3	−1·3	..
200	−2·0	−1·8	−1·7	−1·6	−1·6	−1·6	−1·5	−1·5
220	−2·3	−2·1	−2·0	−1·9	−1·8	−1·8	−1·7	−1·7
240	−2·5	−2·3	−2·2	−2·1	−2·1	−2·0	−2·0	−1·9
260	−2·8	−2·6	−2·4	−2·3	−2·3	−2·2	−2·2	−2·1
280	−3·0	−2·8	−2·6	−2·5	−2·4	−2·4	−2·3	−2·3
300	−3·2	−3·0	−2·8	−2·7	−2·6	−2·6	−2·5	−2·5
320	−3·4	−3·2	−3·0	−2·9	−2·8	−2·7	−2·7	−2·6
340	−3·7	−3·4	−3·2	−3·1	−3·0	−2·9	−2·9	−2·8
360	..	−3·5	−3·4	−3·2	−3·1	−3·1	−3·0	−3·0
380	..	−3·7	−3·5	−3·4	−3·3	−3·2	−3·1	−3·1
400	..	−3·9	−3·6	−3·5	−3·4	−3·3	−3·3	−3·2

† Öpik, E. J., *Publ. Tartu Obs.* **25** (1922), no. 1; ibid. (1923), no. 4.

‡ Porter, J. G., *Mem. Brit. Astr. Ass.* **34** (1942), 62; *J. Brit. Astr. Ass.* **48** (1938), 337.

The variation in the magnitude estimates of a given meteor by different observers has been discussed by Öpik.† From an analysis of the discrepancies in the observation of 3,814 meteors observed during the Arizona meteor expedition Öpik deduces the relation in Table 2 between the observational error ϵ as a function of the magnitude m.

TABLE 2

Relation between Observational Error ϵ *and Magnitude* m *according to Öpik*

m	$\geqslant 4{\cdot}7$	4·2	3·7	3·2	2·7	2·2
ϵ	$\pm 0{\cdot}36$	$\pm 0{\cdot}37$	$\pm 0{\cdot}47$	$\pm 0{\cdot}56$	$\pm 0{\cdot}63$	$\pm 0{\cdot}65$
m	1·7	1·2	0·7	0·2	$-0{\cdot}3$	$\leqslant -0{\cdot}8$
ϵ	$\pm 0{\cdot}68$	$\pm 0{\cdot}77$	$\pm 0{\cdot}87$	$\pm 0{\cdot}96$	$\pm 1{\cdot}03$	$\pm 1{\cdot}05$

(*d*) *The Counting of Meteors*

The relation between the actual numbers of meteors and those seen by an observer has been investigated by several workers. Backhouse‡ appears to have been one of the first to investigate an observer's field of vision for meteors of different magnitude. He estimated the effective field for very bright meteors (magnitude $-4{\cdot}5$) to be 100°, decreasing to 25° for faint meteors of magnitude $+5$. His relationship is shown in Fig. 2.

The most thorough statistical investigation of the problem is by Öpik.§ If two observers watch the same area of sky the number of meteors seen in common will decrease as the brightness decreases. Öpik expresses this in terms of a Coefficient of Perception p. Then if n_1, n_2 are the numbers seen by two observers, and n_0 the number seen in common

$$n_0 = p_1 n_2 = p_2 n_1$$

and the true probable number N will be given by

$$N = \frac{n_1}{p_1} = \frac{n_2}{p_2} = \frac{n_1 n_2}{n_0}.$$

Öpik also shows that if there are k observers then the true number N will be given by

$$N = \frac{S}{1-(1-p_1)(1-p_2)\ldots(1-p_k)},$$

where S is the number of different meteors recorded by all the observers.

† Öpik, E. J., *Ann. Harv. Coll. Obs.* **105** (1936), 549.
‡ Backhouse, T. W., *Observatory*, **7** (1884), 299.
§ Öpik, E. J., *Publ. Tartu Obs.* **25** (1922), no. 1; (1923), no. 4.

After experience of this so-called 'double-count' method during the Perseid shower of 1920 Öpik concluded that the Coefficient of Perception could be represented as

$$p = \Psi\bar{\pi},$$

where the magnitude function Ψ depends only on the apparent magnitude and is the same for all observers, while the coefficient of attention $\bar{\pi}$ is an individual function depending on the observer and his position.

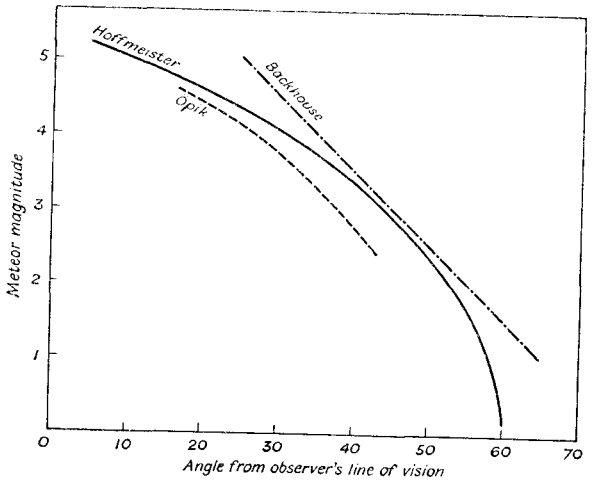

FIG. 2. Relation between limiting brightness of a meteor visible at a given angle from an observer's line of vision according to Hoffmeister (———), Öpik (– – – – –), and Backhouse (– · – · · · · –). In plotting Hoffmeister's data it has been assumed that a meteor of zero magnitude can just be seen at 60° from the line of vision.

The treatment of the observations of the Perseid showers in 1920 and in 1921 is very lengthy. It involves the evaluation of Ψ and $\bar{\pi}$ from a comparison of the observations of a number of observers on different nights with varying sky conditions. Here it is sufficient to summarize the conclusions about the effective field of vision as a function of magnitude. This result is given in Fig. 2 for comparison with the estimates of Backhouse.

The subject has also been treated in detail by Hoffmeister† in connexion with his extensive observations of the diurnal variation in meteor rates which are discussed in Chapter VI. He considered the

† Hoffmeister, C., *Meteorströme*, and private communication.

effects of fatigue,† increase in brightness with velocity of meteors, and decrease of apparent brightness with increasing angular velocity. In connexion with this work Hoffmeister carried out experiments with 'artificial meteors'. The various correction factors derived by him are given in Chapter VI, and the relation between the limiting brightness of a meteor visible at a given angle from the line of vision is plotted in Fig. 2 for comparison with the data of Backhouse and Öpik.

The subject has also been considered by Ceplecha,‡ whose results are in close agreement with those given in Fig. 2.

From a consideration of the results of Backhouse, Öpik, and Hoffmeister, Almond, Davies, and Lovell§ have estimated the actual collecting area of an observer for various meteor magnitudes. From the curves in Fig. 2 the limiting meteor magnitude visible at a given angle from an observer's line of vision was obtained as in Table 3.

TABLE 3

Limiting Meteor Magnitude Visible at a given Angle from an Observer's Line of Vision

Angle from line of vision .	60°	58°	53°	44°	30°	11°	0°
Limiting magnitude . .	0	1	2	3	4	5	5·5

If the observer's line of sight is directed upwards at 45°, the intersections of these cones of limiting visibility on a surface 95 km. above the earth can be plotted. The apparent magnitudes are then corrected to zenithal magnitudes according to § 1 (*c*) above, and the actual areas over which an observer sees meteors of a given magnitude can then be measured graphically. The results are given in column 2 of Table 4. Column 3 gives the relative number of meteors in the various magnitude groups falling on a square kilometre of the sky. This column is estimated on the basis of the data given in Chapter VII for the number and mass distribution of sporadic meteors. If it is assumed that one meteor of magnitude −1 falls per sq. km. per hour, the number of meteors seen in each magnitude group per hour can then be calculated as in column 4. The summation of this column then gives the total rate which would be seen by the observer on this assumption. If the actual observed hourly

† It is interesting to note that the effects of fatigue appear to be very small in meteor counts. See, for example, the tests made by Prentice, J. P. M., *J. Brit. Astr. Ass.* **52** (1942), 98.

‡ Ceplecha, Z., *Bull. Cent. Astr. Inst. Czech.* **2** (1950), no. 10, 145.

§ Almond, M., Davies, J. G., and Lovell, A. C. B., *Mon. Not. Roy. Astr. Soc.* **112** (1952), 21.

rate is known then the relative numbers in column 3 can be scaled down to give the actual numbers in the different magnitude groups falling on a sq. km. per hour. In column 5 this has been done for a case where the observed hourly rate by a single observer is one.

TABLE 4

Numbers of Meteors of Different Magnitudes seen by a Visual Observer

1 *Zenithal magnitude*	2 *Collecting area (sq. km.)*	3 *Relative number per sq. km.*	4 *Relative number seen*	5 *True number per sq. km. per hour for hourly rate of one*
				($\times 10^{-6}$)
$4\frac{1}{2}$	161	158	25,000	31·8
4	5,160	100	516,000	20·2
$3\frac{1}{2}$	9,845	63·1	620,000	12·7
3	16,125	39·8	641,000	8·02
$2\frac{1}{2}$	24,200	25·1	607,500	5·05
2	36,150	15·8	571,000	3·18
$1\frac{1}{2}$	50,000	10·0	500,000	2·02
1	66,000	6·31	420,000	1·27
$\frac{1}{2}$	87,500	3·98	348,000	0·80
0	115,700	2·51	291,000	0·50
$-\frac{1}{2}$	135,800	1·58	214,000	0·32
−1	200,000	1·00	200,000	0·20
			4,953,500	

2. The special visual techniques of the Arizona expedition

The famous Harvard expedition to Arizona† for the study of meteors took place between 1931 and 1933. For this expedition Öpik evolved special techniques of observation. It will be evident from later chapters of this book that many of the results of this work are in dispute. For this reason, and because the techniques have not been used since (except by Öpik in Tartu), they are treated separately here from the more conventional British and American methods.

(*a*) *Observation of Meteor Paths*

For the determination of meteor paths and heights, visual observers were placed at two stations over a 40 km. east–west base line. The meteors were registered in two areas of about 60° effective diameter centred on the meridian at 45° zenith distance north and south. Iron reticules projected on the sky were used as coordinates of reference for tracing the meteor trails. In this respect the technique differs markedly

† Shapley, H., Öpik, E. J., Boothroyd, S. L., *Proc. Nat. Acad. Sci. Wash.* **18** (1932), 16.

from the visual methods described in § 1. The reticules represented declination and hour angle at 10° intervals. The hour angle was transferred to right ascension from the recorded time of observation. These reticules were mounted on two opposite slopes of a wooden shelter which provided protection for the observers within. The observer looked through one eye-hole of 32 mm. diameter placed at a distance of 50 cm. from the centre of the reticule. In surveying the area it was only necessary for the observer to move his eye, the parallax introduced being only a fraction of a degree. It was considered that the reticules permitted direct reading of celestial coordinates to within half a degree, or with systematic corrections to within one tenth of a degree.

The widths of the wires forming the reticule were 0·5° to 0·8° and could be easily seen on the sky without artificial illumination. The obscuration was 10 per cent. Prepared maps gave exact reproductions of the reticules on a 1 : 4 scale, and the observer traced the trails on these maps. The time of appearance to the nearest second, magnitude and duration were also recorded. The total area of sky covered by each reticule was $80° \times 80°$, of which the observer could watch a field of about 60° diameter.

In the Arizona programme the observations were extended to infra visual meteors by using two 4-in. telescopes situated at an east–west spacing of about 3 km. The field of view was 4° using an eye-piece with a magnification of 17 times. Reticules in the focal plane were used as reference coordinates.

A comprehensive analysis of the errors involved in using these reticules has been given by Öpik.† An indication of the accuracy claimed is given in Table 5, which refers to the errors in the displacement of the beginning and end points for meteors observed in common by more than one observer.

TABLE 5

Displacement of the Beginning and End Points for Common Meteors with Unequal Recorded Lengths in the Reticule Observations

(The mean values are given in the sense: longer trail minus shorter trail without regard to observer.)

Difference in length limits . .	0·6°–2·2°	2·3°–4·8°	⩾ 4·9°
Difference in length, mean . .	1·18°	3·34°	7·56°
Mean displacement of beginning .	−0·39°	−1·96°	−4·42°
Mean displacement of end . .	+0·79°	+1·38°	+3·14°
Mean displacement of centre . .	+0·20°	−0·29°	−0·64°
Number of meteors . . .	720	564	394

† Öpik, E. J., *Ann. Harv. Coll. Obs.* **105** (1936), 549.

These are comparable with the errors quoted by Porter for the beginning and end points of the meteor paths in the British data referred to in § 1 (*a*). On the other hand Öpik† gives a probable error of 8° in the radiant determination by the reticule observations compared with the 1° claimed by the British observers.

The use of reticules for meteor observation has been criticized by Olivier‡ on the grounds that they force the employment of only one eye at a time by the observer. He justifies his criticism by reference to his own experience and also by referring to Öpik's coordinates† for the radiants of some of the major showers which differ considerably from the accepted radiant positions. Criticisms have also been made by Prentice,§ particularly that the base line, of less than 40 km., was too short.

(*b*) *Observation of Meteor Velocities*

For the measurement of angular velocities Öpik devised an ingenious technique which is now commonly known as the rocking-mirror method. The apparatus, which is described in detail by Shapley, Öpik, and Boothroyd,‖ consisted of a 6-in. square plate-glass mirror, resting freely on three supports forming an isosceles right triangle. The support at the right angle was motionless while the two others were tilted in the vertical direction to make harmonic oscillations with a difference of phase of 90°. Thus the normal to the mirror plane was given a conical motion of small amplitude. Assuming that the two oscillations are of equal amplitude, then a reflected stellar image will describe a circle if the object is in the zenith, and an ellipse if it is outside the zenith. A meteor will describe a more complicated curve, produced by the superposition of the elliptical oscillation upon its own motion. The shape of the apparent trajectory depends on a number of factors including the angular velocity of the meteor and its direction. The trajectories are pseudocycloidal of the type shown in Fig. 3, forming closed loops if the meteor is moving slowly and open loops for fast-moving meteors. Since the period of oscillation of the mirror is known, the angular speed can be derived from the trajectory shape, or from the length, of a complete oscillation. The calculation of the velocities is discussed in detail in Chapter IX.

In the Arizona apparatus the period of oscillation was 0·1 sec. and the

† Öpik, E. J., *Circ. Harvard Coll. Obs.* (1934), no. 388.
‡ Olivier, C. P., *Pop. Astron.* **46** (1938), 325.
§ Prentice, J. P. M., *Rep. Phys. Soc. Progr. Phys.* **11** (1948), 389.
‖ Shapley, H., Öpik, E. J., and Boothroyd, S. L., loc. cit.

oscillations were transmitted to the two supports from the same end of an eccentric shaft, the phase difference being attained by placing the two levers at right angles. The shaft was driven by a 60-r.p.s. synchronous motor through a gear reduction of 1:6, and the major axis of the mirror oscillation was 0·5°.

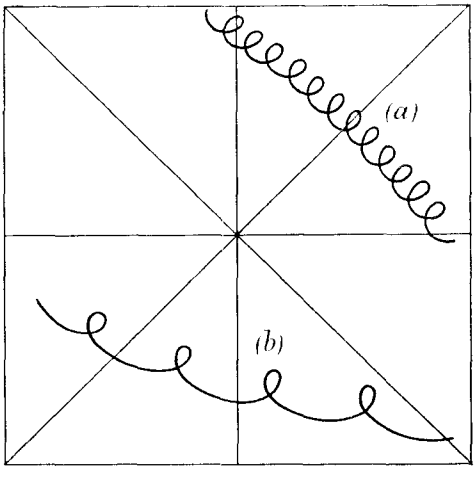

FIG. 3. The appearance of (*a*) a slow meteor, (*b*) a fast meteor in Öpik's rocking mirror apparatus.

The ellipses of oscillation for stars could be seen down to fourth magnitude out to an angle of 5° from the line of direct vision. The circumstances for meteor observation are stated to be more favourable because the linear dimensions of the oscillation are increased along the trail and the resolving power of the eye is therefore greater. Experience showed that about 80 per cent. of the meteors seen by a reticule observer could be observed in the rocking mirror with sufficient certainty to be traced on a map. Complete velocity data could be obtained for about half of these. It is claimed that fifth-magnitude meteors over an effective area of diameter 30° could be observed with the apparatus. Öpik's extensive treatment of the errors and results obtained with this rocking-mirror apparatus at Arizona and later in Tartu are described in Chapter IX.

In the Arizona expedition these visual observations were extended to infra visual meteors by adapting the rocking mirror so that it could be used in conjunction with a 4-in. telescope. In this modification a bar, rigidly connected at right angles to the mirror surface, was given a conical movement so that an elliptical oscillation of the image was

obtained. The observer then traced the apparent trajectory on a map which was a copy of the focal reticule in the telescope. The results obtained by Boothroyd using this device are also discussed in Chapter IX.

3. Photographic techniques

(*a*) *Introduction*

Although the main advances in photographic meteor studies have come from the application of special double-camera techniques as described later in this section, a great deal of valuable information has also accumulated from the chance occurrence of meteor trails on photographic plates exposed for other purposes. This is particularly the case with the Harvard collection. Later chapters (especially Chaps. XIII to XVII) contain many references to the analysis of these meteor trails in the Harvard collection back to 1896. In referring to these trails the Harvard notation is retained and the characteristics of the various cameras are listed in Table 6 for reference.

Watson† has given an account of meteors photographed with the 18-in. Schmidt camera on Mount Palomar, obtained by chance while the camera was in use on the supernova patrol. The field of this camera is about 9°. On 394 films, representing a total exposure time of 10,663 minutes, he found 81 meteor trails. From a comparison of this rate with the known visual rates Watson estimated that the camera recorded meteors down to second and third magnitudes.

(*b*) *Special Photographic Meteor Techniques*

Simultaneous photography of a meteor trail from two stations enables the trajectory of the meteor to be determined. If rotating shutters are used to cover the lenses at short intervals of time, a direct measure of the angular velocity of the meteor at various points along the trail is also obtained. Elkin‡ at Yale appears to have been the first to initiate successfully a programme of meteor photography with two cameras. His equipment, which was erected in 1894, consisted of a long polar axis driven by clockwork, carrying a number of cameras with apertures of 6 to 8 in. A simpler arrangement carrying four cameras was placed 2 miles north of the former. Some of the results obtained by Elkin with this equipment are discussed in Chapter XI. In 1900 Elkin§ described the modification whereby a rotating shutter was introduced. Elkin states that the idea of a rotating shutter was first suggested in 1860 by

† Watson, F., *Pop. Astron.* **50** (1942), no. 3.
‡ Elkin, W. L., *Astrophys. J.* **9** (1899), 20; **10** (1899), 25.
§ Ibid. **12** (1900), 4.

TABLE 6

Characteristics of the Harvard Cameras not Specifically Employed for Meteor Photography

Description	*Aperture (in.)*	*Focus (in.)*	*Remarks*	*Source of information*
E	..	..	The old series in use before 1900. A list of the various lenses used is given in the reference.	Fisher and Olmsted†
A	24	135	Bloemfontein, S.A., since 1926.8.	
AC	1·5	13	Oak Ridge since 1934.7.	
CA	1·5	13	Oak Ridge since 1934.7.	
AI	1·5	6	Oak Ridge since 1932.7, later equipped with rotating shutter for meteor work.	
AM	1·5	13	Bloemfontein, S.A., since 1925.2.	
AX	3	12	Bloemfontein, S.A., since 1927.8.	
AY	3	12	Cambridge, Mass., to 1928.	
B	8	44	Bloemfontein, S.A., since 1930.1.	Wright and Whipple‡
BI	1·5	Short focus attached to 8 in. (B)	Bloemfontein, S.A., since 1930.1.	
FA	1·5	6	Cambridge to 1948.7, later equipped with rotating shutter for meteor work.	
I	8	50	Cambridge.	
IR	8	50	Oak Ridge.	
J	24–33	84	Oak Ridge.	
MA	12	84	Oak Ridge since 1938.6.	
MC	16	83	Oak Ridge since 1932.5.	
MF	10	49	Bloemfontein since 1927.8.	
RB	3	21	Bloemfontein.	
RH	3	21	Oak Ridge since 1932.7.	
RL	4	28	Oak Ridge.	

J. H. Lane and that in 1885 Zenker in Berlin attempted to use the idea to photograph meteors but without success. The Yale apparatus consisted of a bicycle wheel rotating in front of the cameras. The wheel carried twelve opaque screens and the speed of rotation was 30 to 50 r.p.m. The first successful occulted trail was photographed on 1899 July 31, and the meteor was also recorded on the second camera, 2 miles distant. Some of Elkin's early measurements are referred to in Chapter XI. Elkin continued this work until 1909 but published very few results.

† Fisher, W. J., and Olmsted, M., *Bull. Harv. Coll. Obs.* (1929), no. 870.

‡ Wright, F. W., and Whipple, F. L., *Tech. Rep. Harv. Coll. Obs.* (1950), no. 6.

The analysis of the work was, however, made much later by Olivier.† Unfortunately the base line of approximately 3·5 km. between the two camera sites was inadequate for precision results.

The rotating-shutter technique was subsequently used by a number of workers, such as by Lindemann and Dobson,‡ Whitney,§ Fedynsky and Stanjukovitsch,‖ Waters,†† Ceplecha,‡‡ Thomson and Burland,§§ and others. Systematic results were not achieved by any of these workers (apart from the work of Jacchia, Kopal, and Millman‖‖ using Thomson and Burland's apparatus during the 1946 Giacobinid shower which is described in Chapter XVI). The main development of the technique has taken place at Harvard, where results of the highest quality and precision have been obtained.

(*c*) *The Harvard Techniques for Meteor Photography*

Meteor photography at Harvard using two cameras, one equipped with a rotating shutter, was commenced by Fisher in 1932. The cameras each used a Ross Xpres F/4 lens of 6 in. focal length covering a plate 8×10 in. One camera was equipped with a two-vane rotating shutter driven by a synchronous motor to give thirty occultations of the lens per second. With this equipment Fisher secured his first photograph in August 1932. The equipment was then assigned to Millman,††† who used it during the Leonid shower of 1932 and 1933, successfully photographing three Leonids and one sporadic meteor. Subsequently Millman dismantled the original rotating-shutter camera and in the summer of 1935 equipped the AI patrol camera with a shutter mechanism so that the lens was covered 20 times per second, the obscuration lasting for 0·0053 sec. and the exposure for 0·0447 sec. Approximately 90 hours of exposure time was required for one successful meteor photograph with this equipment. The method of analysis and the results obtained with this apparatus up to 1936 have been described by Millman and Hoffleit,‡‡‡ and are included in Chapter XI.

In 1936 the Harvard programme was continued by Whipple,§§§ using

† Olivier, C. P., *Astron. J.* **46** (1937), 41.
‡ Lindemann, F. A., and Dobson, G. M. B., *Mon. Not. Roy. Ast. Soc.* **83** (1923), 163.
§ Whitney, W. T., *Pop. Astron.* **45** (1937), 162.
‖ Fedynsky, V. V., and Stanjukovitsch, K. P., *Astr. J. U.S.S.R.* **12** (1935), 440.
†† Waters, H. H., *J. Brit. Astr. Ass.* **46** (1936), 153.
‡‡ Ceplecha, Z., *Bull. Cent. Astr. Inst. Czech.* **2** (1951), 114.
§§ Thomson, M. M., and Burland, M. S., *J. Roy. Astr. Soc. Can.* **34** (1940), 479.
‖‖ Jacchia, L. G., Kopal, Z., and Millman, P. M., *Astrophys. J.* **111** (1950), 104.
††† Millman, P. M., *Bull. Harv. Coll. Obs.* (1933), no. 891; *Publ. Amer. Astr. Soc.* **7** (1933), 181.
‡‡‡ Millman, P. M., and Hoffleit, D., *Ann. Harv. Coll. Obs.* **105** (1937), 601.
§§§ Whipple, F. L., *Proc. Amer. Phil. Soc.* **79** (1938), 499.

the AI patrol camera with the rotating shutter as described above, at Oak Ridge, together with a similar patrol camera (FA) situated at Cambridge, Mass., at a distance of 37·9 km. From 1936 February 15 the observing programmes of the two cameras were synchronized and seventeen pairs of meteor photographs were obtained in 27 months—representing 2,000 hours of exposure time. Each camera used Ross Xpres lenses of aperture 1·5 in. and focal lengths 5·95 in. (AI) and 5·99 in. (FA). The field of tolerable definition was about 60 degrees in each case. The two cameras were directed toward a point in space about 80 km. above the earth's surface, and were driven on polar axes. The exposures for each plate were 2 hours for AI and 1 hour for FA, the difference being necessary on account of the greater background fog on the FA camera, which was situated in the middle of a city. In 1939 the FA camera was also equipped with a rotating shutter, and according to Whipple† thirty doubly photographed meteor trails had been obtained by the end of 1942. Many of these results, and those obtained subsequently with these cameras, are referred to in Chapters XI and XIII–XVII. Chapter XI also gives an account of the method of measurement and reduction of the results.

This work of Whipple's yielded important results of high precision, but the programme suffered from the comparative insensitivity of the cameras. Only meteors brighter than magnitude zero or −1 could be satisfactorily recorded, giving an average yield of only 1 meteor per 100 hours exposure. In 1946 an investigation was commenced in an endeavour to overcome these difficulties. This resulted in the design by J. G. Baker of the Super Schmidt cameras which are now in operation in New Mexico and which are described separately below. In order to establish the routine, and to overcome the preliminary obstacles of observation at remote sites, the Harvard team set up the observing stations at Soledad and Dona Ana in 1948, using the Ross Xpres cameras described above, together with another pair constructed from aerial-camera lenses (K 24) of 3-in. aperture and 7½-in. focal length. Another pair used K 19 lenses of 5-in. aperture and 13-in. focal length. The shutter speed was increased to 1,800 r.p.m. for the K 19 cameras.‡ Whipple states that these aerial lenses were more effective for meteors than the old Ross Xpres ones, but that the gain was not proportional to the aperture. Some of the results from these New Mexico stations are

† Whipple, F. L., *Sky and Telescope*, **8** (1949), no. 4.

‡ The Harvard notation for the plates of the new camera lenses in New Mexico is KA, KB, KE.

included in Chapter XI. The relative performance of the various cameras is indicated on p. 20.

(d) The Harvard Super Schmidt Meteor Cameras

In order to improve the sensitivity of meteor cameras beyond the magnitude limit of zero to −1 and at the same time retain a wide field of view, Baker proposed the use of a new optical system known as the

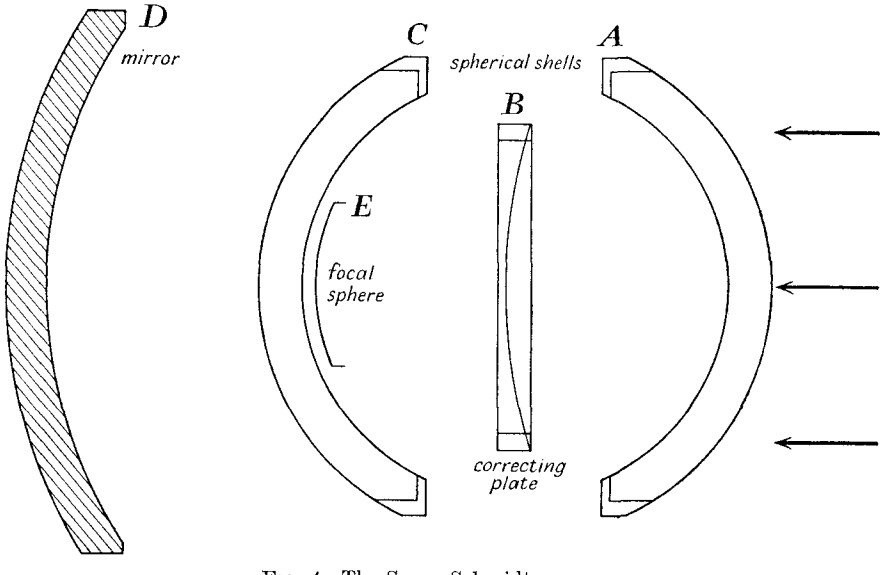

FIG. 4. The Super Schmidt camera.

Super Schmidt. Some preliminary accounts of the instrument have been published,† from which the following details are taken. The principle is illustrated in Fig. 4. Light from a distant point is refracted through the outer spherical shell A, the hyperchromatic correcting plate B, and the inner spherical shell C. It is then reflected at the mirror D, and passes again through C to the photographic plate on the focal sphere E. The concentric shells A and C greatly reduce the under-corrected spherical aberration of the mirror without destroying the spherical symmetry, and hence make possible the wide-angle properties of the system. The correcting plate B is weak compared with that in the ordinary Schmidt system. It is made of cemented elements of crown and flint glasses. The system gives almost complete correction over the range 3,800 to 7,000 A. In fact, the specification called for the on-axis image of a point source

† Whipple, F. L., *Sky and Telescope*, **8** (1949), no. 4; *Tech. Rep. Harv. Coll. Obs.* (1947), no. 1; *Sky and Telescope*, **10** (1951), 219.

at infinity in the range 3,500 to 8,000 A, to be concentrated 50 per cent. within a circle of diameter 0·015 mm. and 90 per cent. within 0·040 mm.

The spherical lenses are 18 in. diameter and the mirror 23 in. diameter. The effective aperture is 12·25 in. and focal length 8 in. The optical focal ratio is 0·65 and the effective field 55° without appreciable vignetting at the edges. However, the interposition of a $7\frac{3}{8}$-in. diameter photographic film reduces the effective clear aperture to 9·8 in. and the effective focal ratio to 0·81 in. Unusual problems are introduced by the position and shape of the film. The focal surface is spherical and the amount of flattening has to be compromised with additional complication in the optical system. The radius of curvature of the focal sphere in the Super Schmidt is 8 in., and to maintain the image quality it is necessary that the photographic emulsion should follow the focal sphere within 0·0005 in. The difficulties and technique of producing a large number of suitably shaped emulsions have been described by Carroll, McCrosky, Wells, and Whipple.† Standard flat acetate film coated with the appropriate emulsion is moulded to the required shape. A rubber diaphragm, heated by a radiant heater in a water-cooled tank, presses the flat film under the action of compressed air into a convex spherical polished mould of the required dimensions. Only 2 minutes is required for the complete cycle of diaphragm heating, compression, cooling, and cutting out the spherical surface from the 10×10 in. rectangular film. In the camera the film is supported by a vacuum on a spherical surface covered by a delicate spider-web of grooves emanating from the centre, to allow the transfer of air tangentially below the emulsion base.

The curved films are copied after exposure on to flat glass plates within a few weeks of processing by a special copying camera designed by Baker.† Since the optical system is a true concentric spherical projection, the star images appear on the spherical film in their relative configuration on the celestial sphere. The copying on to a flat plate renders the final projection accurately gnomic. Since a great circle on the sky becomes a straight line after gnomic projection, no new problems of measurement or reduction are introduced by the use of the Super Schmidt.

The large aperture of the system also makes a conventional type of rotating shutter external to the camera unsatisfactory. A shutter in the front of the camera would become a large and unwieldy 'windmill'. This difficulty has been solved by placing a small shutter immediately in front of the photographic plate. The shaft passes through both the

† See Carroll, P., McCrosky, R. E., Wells, R. C., and Whipple, F. L., *Tech. Rep. Harv. Coll. Obs.* (1951), no. 8.

mirror and the inner shell along the optical axis. The shutter revolves at 1,800 r.p.m. The limiting time of exposure is about 10 minutes, and in order to reduce the dead time during reloading, special automatic mechanisms are introduced which stop the rotating shutter after each exposure, turn the telescope for reloading, and then reset to a prearranged hour angle for the next exposure. Owing to the position of the film, reloading can only take place by separating the optical system. This is then reset automatically to within a few ten-thousandths of an inch.

According to reports† the first of the Super Schmidts to be completed by the Perkin–Elmer Corporation was installed at Soledad, New Mexico, during the summer of 1951. Estimates of the relative performance of these Super Schmidts compared with other meteor cameras have been made by Whipple‡ as in Table 7.

TABLE 7

Characteristics and Performance of the Meteor Cameras

Camera	*Aperture (in.)*	*Focal ratio*	*Number of elements*	*Number of air glass surfaces*	*Number of mirrors*	*Field diameter (deg.)*	*Light transmission taking Ross Xpres as unity*	*Performance meteors per 100 hours*
Ross Xpres .	1·5	4	5	6	0	60	1·0	1·0
Cooke-Taylor	1·5	8	3	6	0	33	1·1	0·3
3-in. Ross .	3·0	7	4	8	0	20	0·8	0·7
Aerial night lenses .	3·0	2·5	7	8	0	45	0·4	2·3
Classical Schmidt .	18·0	1·0	2	2	1	20	1·4	20
Super Schmidt .	12·0	0·67	5	10	1	50	1·3	260

The performance figures for the last three cameras listed in Table 7 are estimated. Allowing for the increased dead time due to the more frequent film-changes required—every 6 minutes instead of 1 or 2 hours for the Ross Xpres—Whipple§ estimates that the yield per annum for the Super Schmidt should be increased by about forty times over the older cameras. The limiting magnitude is expected to be $+3$ or $+4$ instead of -1 to 0 with the Ross Xpres.

(*e*) *Reduction of Data from the Photographic Plates*

The methods used in the Harvard work for obtaining the meteor path and velocity from the segmented trails on the photographic plates are described in Chapter XI. It is therefore only necessary in this section

† *Sky and Telescope*, **10** (1951), 219.

‡ Whipple, F. L., *Tech. Rep. Harv. Coll. Obs.* (1947), no. 1.

§ Whipple, F. L., *Sky and Telescope* (1949), loc. cit.

to refer to the problem of the photometry of the plates in order to obtain a measure of the magnitude of the meteor. Earlier discussions of the problem of photometry of meteor trails have been given by Sytinskaya† and by Millman and Hoffleit.‡ More recently Jacchia§ has dealt with the problem in connexion with the contemporary Harvard work. In this work the brightness of meteors was measured by comparison, emulsion against emulsion, with trailed-star images on unguided plates taken with the same instrument and the same focal ratio as the meteor plate. The trailed comparison plates, centred on equatorial regions rich in bright stars, were taken around culmination with an exposure time of 20 minutes. Two guided plates, each with an exposure time of 60 minutes and centred on the same region, were taken, one before and one after the trailed comparison plate. If no appreciable differences in the densities of the star images could be detected on the two guided plates, the series of two guided and one, or more, trailed plates taken in between was considered satisfactory for photometric purposes.

A number of stars over a range of three to five magnitudes were selected near the centre of the meteor plate, and their apparent brightness was compared with that of stars near the centre of the guided comparison plates. The magnitudes thus obtained for stars on the meteor plate generally differ by some constant amount Δm from the catalogued magnitude. Δm (which we assume to be catalogue magnitude *minus* observed magnitude) represents several factors arising from the differences in the conditions under which the meteor and comparison plates were obtained, such as differences in (i) exposure times, (ii) sky transparency, (iii) plate sensitivity, (iv) differential extinction. Difference (i) can be easily taken into account. If t_m and t_0 represent the exposure times of the meteor plate and comparison plate respectively, then

$$\Delta\overline{m} = \Delta m - k \log \frac{t_m}{t_0}$$

represents the correction that has to be applied to meteor magnitudes because of the combined effects of (ii), (iii), and (iv). k is a coefficient which allows for the reciprocity law failure ($k = 2{\cdot}2$ for the Cramer high-speed emulsions considered by Jacchia). The magnitude of the meteor at different points of the trail is obtained by comparison with the trailed-star images near the centre of the unguided comparison plate.

† Sytinskaya, H. N., *Astr. J. U.S.S.R.*, **12** (1935), 174.
‡ Millman, P. M., and Hoffleit, D., *Ann. Harv. Coll. Obs.*, loc. cit.
§ Jacchia, L. G., *Tech. Rep. Harv. Coll. Obs.* (1949), no. 3

Two further correction factors are necessary to the meteor magnitudes determined in this manner:

(α) A field correction to allow for the dimming of the trails at increasing distances from the plate centre. Jacchia† gives full details of this correction, made by comparison with the trailed plates. The corrections are considerable, as will be seen from Table 8, which gives representative values for the Harvard AI and FA cameras.

TABLE 8

Field Correction for the Harvard AI and FA Cameras

Distance from centre (r *cm.*)	*Correction in magnitudes*	
	AI camera	*FA camera*
0	0	0
2	−0·05	−0·04
4	−0·22	−0·21
6	−0·60	−0·52
8	−1·32	−1·22
10	−2·4	−1·52

(β) A velocity correction to allow for the different trailing velocities of the meteor and the comparison stars. If V_{met} and V_{star} are the trailing velocities (in mm./sec.) of the meteor and the comparison star respectively, this correction is given by

$$f(v) = -2{\cdot}5 \log \frac{V_{met}}{V_{star}}.$$

The average velocity of the meteors is about 1,000 times that of the comparison stars, hence the reciprocity law failure of the emulsion has to be considered. Jacchia shows that for the Cramer high-speed emulsion used with the AI and FA cameras a satisfactory expression which takes account of the reciprocity law failure is

$$f(v) = -2{\cdot}657 \log \frac{V_{met}}{V_{star}}.$$

In the case of meteor trails recorded with unguided cameras, the photometric measurements can be made by comparison with the trailed star images on the same plate. The only corrections necessary are the velocity corrections (β) above, and one to allow for the dimming effect of the shutter on the star trails. Finally the magnitude has to be reduced to the standard distance of 100 km. as described in § 1 (c). Jacchia also introduces a colour correction of $+1{\cdot}8^{m}$ for comparison with visual magnitudes, but until more is known about the colour index of meteors this latter correction is somewhat arbitrary.

† Jacchia, L. G., 1949, loc. cit.

III

OBSERVATIONAL METHODS—II

THE HISTORY AND FUNDAMENTAL FEATURES OF RADIO-ECHO OBSERVATIONS

1. Introduction: History of the radio-echo observation of meteors

THE radio-echo techniques for the study of meteors are derived directly from the basic techniques which were used in the pioneer work on the ionized layers by Appleton and Barnett† and by Breit and Tuve.‡ The former workers studied the reflection of radio waves from the ionized layers by using continuous wave-frequency modulation techniques and the latter by using the pulse technique. The main features of the ionized regions are now very well known, and here it is only necessary to mention that under normal conditions the electron density in the E region is subject to a marked solar control reaching a maximum at noon and a minimum during the night. For example, in Great Britain at noon on a summer day the density in the E region is about 10^5 electrons per c.c., decreasing to about 8×10^3 electrons per c.c. by midnight, the critical radio-wave frequencies being 3 mc./s. and 0·8 mc./s. respectively.

Abnormal effects,§ indicated by sudden increases in the electron density of the E region during the night, were reported by many of the early workers on the ionosphere, notably by Heising,‖ Eckersley,†† Appleton,‡‡ Appleton and Naismith,§§ and by Schafer and Goodall.‖‖ Heising described his results as indicating that 'great masses of electrons are tossed into the atmosphere rather quickly', while Appleton concluded that 'either the recombination of ions is prevented or there is some ionizing agent present which can influence the dark side of the earth'. Thus by 1930 it had become clear that although the sun was the main

† Appleton, E. V., and Barnett, M. A. F., *Nature*, **115** (1925), 333; *Proc. Roy. Soc.* A **109** (1925), 621.

‡ Breit, G., and Tuve, M. A., *Terr. Magn. Atmos. Elect.* **30** (1925), 15; *Nature*, **116** (1925), 357; *Phys. Rev.* **28** (1926), 554.

§ A survey of the work on ionospheric abnormalities, especially with regard to meteoric ionization, has been given by Lovell, A. C. B., *Rep. Phys. Soc. Prog. Phys.* **11** (1948), 415.

‖ Heising, R. A., *Proc. Inst. Radio Engrs.* **16** (1928), 75.

†† Eckersley, T. L., *J. Instn. Elect. Engrs.* **67** (1929), 992.

‡‡ Appleton, E. V., *Proc. Roy. Soc.* A **126** (1930), 542.

§§ Appleton, E. V., and Naismith, R., ibid. A **137** (1932), 36.

‖‖ Schafer, J. P., and Goodall, W. M., *Proc. Inst. Radio Engrs.* **19** (1931), 1434.

influence in controlling the ionization of the E region, some other ionizing agency must also be at work.

The suggestion that meteors might cause sufficient disturbance in the E region to affect the propagation of radio waves appears to have been made first by Nagaoka.† He considered that a meteor would sweep away the electrons in its path, and although it would ionize the air itself the number of electrons produced would be small compared with the number present before the passage of the meteor. Thus, in the track of the meteor there would be fewer electrons than in the surrounding air, and this would cause abrupt changes in the refractive index for an incident radio wave.

In 1931 Skellett‡ suggested that the actual ionization due to meteors might affect the conditions in the E region, and he pointed out that Heising's results might be explained in this manner. Skellett's theoretical estimates of the amount of ionization produced by meteors, which he developed further in 1932,§ were based on the theory of Maris‖ and are now known to be seriously in error.†† Nevertheless, the experimental work carried out by Schafer and Goodall‡‡ during the Leonid shower of 1931, and by Skellett§§ in conjunction with Schafer and Goodall, produced conclusive evidence that meteoric ionization was responsible for some of the night-time E region abnormalities. These workers used the pulse method and observed on frequencies between 1·6 and 6·4 mc./s. in rapid succession. During the 1931 Leonid shower very disturbed conditions were found in the E region, with sudden abnormal increases of ionization, reaching a peak on the night of November 16–17, which was known from visual observations to be the maximum of the shower. Unfortunately magnetic disturbances were also present on these nights and hence it was not possible to decide definitely that the effects were due to meteoric ionization. During the Leonid shower of 1932, however, successful visual correlations of meteors passing overhead with sudden transient increases in E region ionization were obtained.§§ Figures 5 and 6 show these sudden increases in ionization correlated with the passage of meteors for the nights of 1932 November 14–15

† Nagaoka, H., *Proc. Imp. Acad. Tokyo*, **5** (1929), 233; *Sci. Pap. Inst. Phys. Chem. Res., Tokyo*, **15** (1931), 169.

‡ Skellett, A. M., *Phys. Rev.* **37** (1931), 1668.

§ Skellett, A. M., *Proc. Inst. Radio Engrs.* **20** (1932), 1933.

‖ Maris, H. B., *Terr. Magn. Atmos. Elect.* **34** (1929), 309.

†† Herlofson, N., *Rep. Phys. Soc. Progr. Phys.* **11** (1948), 444.

‡‡ Schafer, J. P., and Goodall, W. M., *Proc. Inst. Radio Engrs.* **20** (1932), 1131; ibid., p. 1941.

§§ Skellett, A. M., *Proc. Inst. Radio Engrs.* **23** (1935), 132.

and 15–16. During nights when no meteor showers were active, these sudden increases in ionization were found to be rare—a similar plot given for the night of 1929 February 19–20 shows only one such increase.

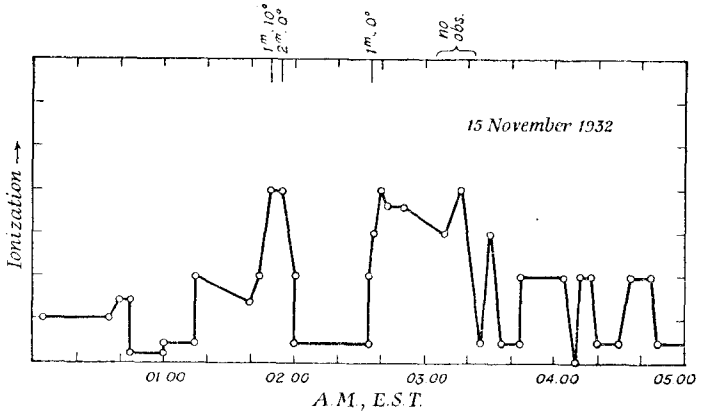

FIG. 5. Transient increases in ionization of the E region associated with meteors passing overhead obtained by Skellett, Schafer, and Goodall on 1932 Nov. 15.

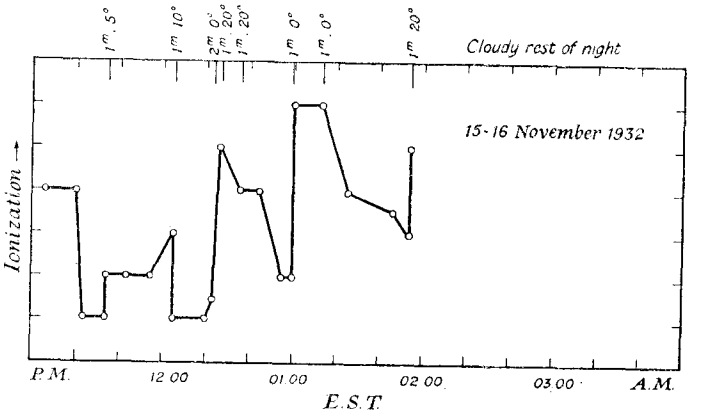

FIG. 6. Transient increases in ionization of the E region associated with meteors passing overhead obtained by Skellett, Schafer, and Goodall on 1932 Nov. 15-16.

From this work the following conclusions were made: (*a*) night-time increases in E region ionization were most marked during meteor showers, (*b*) for all major increases of ionization a meteor was observed to pass nearly overhead, (*c*) the intermittent reflections, lasting only for a period of seconds, were rare except during meteor showers, (*d*) observations of the critical frequency gave the ionization in the E region as 10^6

electrons per c.c. during the maximum of the Leonids, i.e. greater than its noon value on a summer day.

In Japan, Minohara and Ito† also investigated the effect of the 1932 Leonid shower. They found a large increase in the number of short-duration echoes during the shower, but do not appear to have associated specific echoes and meteors. Previous to this work Quäck‡ and Pickard§

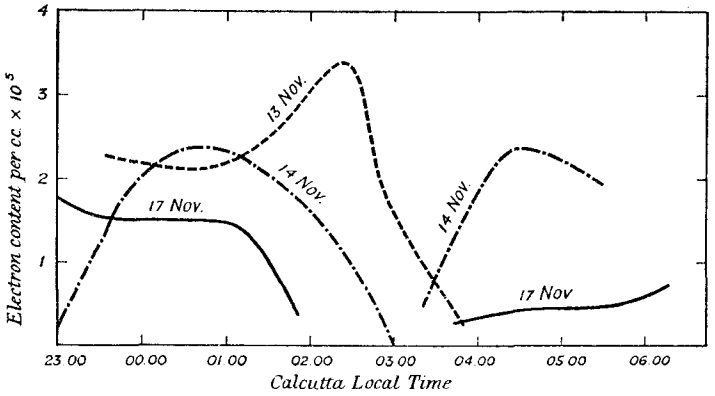

FIG. 7. Electron content of the E region during the 1933 Leonid shower as observed by Mitra, Syam, and Ghose.

investigated the disturbances on long-distance short-wave transmissions to see if any connexion with meteoric showers existed. Both investigators found correlations, but in view of the sensitivity of such transmissions to magnetic disturbances their analysis cannot be regarded as conclusive.

This work during the Leonid shower of 1932 was followed up in India during the 1933 Leonid shower by Mitra, Syam, and Ghose.‖ Their results for the electron density in the E region during the nights of 1932 November 13–14 and 16–17 are shown in Fig. 7. The electron densities reached values of $3{\cdot}3 \times 10^5$ and $2{\cdot}2 \times 10^5$ per c.c. respectively. The period was clear of magnetic and solar disturbances. Similar measurements were made by Bhar†† during the 1936 Leonid shower.

This early work was followed, during the next few years, by many studies of these transient increases in the ionization in the E region, and although several suggestions were made as regards their association with meteors, no specific relation seems to have been established. For

† Minohara, T., and Ito, Y., *Rep. Radio Res. Japan*, **3** (1933), 115.
‡ Quäck, E., *Elekt. Nachr.-Tech.* **8** (1931), 46.
§ Pickard, G. W., *Proc. Inst. Radio Engrs.* **19** (1931), 1166.
‖ Mitra, S. K., Syam, P., and Ghose, B. N., *Nature*, **133** (1934), 533.
†† Bhar, J. N., *Nature*, **139** (1937), 470; *Indian J. Phys.* **11** (1937), 109.

example, the transient echoes were widely observed during the 1932 Polar Year Expedition by Appleton, Naismith, and Ingram.† Eckersley‡ made extensive studies of the scattering of radio waves into the skip zone and measured the height, diurnal, and duration distributions of the echoes. He discussed these in terms of reflection of the radio waves from clouds of ions in the E region but did not discuss their origin. Skellett§ emphasized that these results strongly suggested a meteoric origin. Appleton and Piddington‖ also made detailed measurements on the transient echoes and concluded that the scattering centres consisted of clouds of 10^{16} electrons concentrated in a region of linear dimensions small compared with the wave-length (which in their case was about 30 m.). It was suggested that these results implied the entry into the atmosphere by day and night of an agency producing bursts of ionization. Similar measurements on the transient echoes were made by Watson-Watt, Wilkins, and Bowen†† in 1937 and by Harang‡‡ in 1942. In 1938 Pierce§§ made calculations which showed that the ionization due to meteors could maintain the E region ionization at its day-time value during the night. His calculations are now known to be in error by several orders of magnitude, however. In 1940‖‖ he repeated the observations of Skellett, Schafer, and Goodall by observing the echoes on a pulsed 3 mc./s. equipment during the 1940 Leonid shower.

The measurements on the transient signals described above were made either directly, using pulse technique, or by observations of scattering into the skip zone when the wave frequency was high enough to penetrate the normal E region but was reflected from the F region. A third type of phenomenon can also be caused by the occurrence of transient clouds of dense ionization in the E region—the scattering of radio signals to great distances in cases where the frequency is such that both E and F regions are penetrated and the signal is not normally received above the range of the ground ray. Taylor and Young††† reported abnormal scattering effects whereby high-frequency radio signals were received at a distant station after traversing a very long path. In 1931

† Appleton, E. V., Naismith, R., and Ingram, L. J., *Phil. Trans.* **236** (1937), 191.

‡ Eckersley, T. L., *J. Instn. Elect. Engrs.* **71** (1932), 405; **86** (1940), 548.

§ Skellett, A. M., *Nature*, **141** (1938), 472.

‖ Appleton, E. V., and Piddington, J. H., *Proc. Roy. Soc.* **164** (1938), 467.

†† Watson-Watt, R. A., Wilkins, A. F., and Bowen, E. G., ibid. **161** (1937), 181.

‡‡ Harang, L., *Geofys. Publ.* **13** (1942), no. 4.

§§ Pierce, J. A., *Proc. Inst. Radio Engrs.* **26** (1938), 892.

‖‖ Pierce, J. A., *Phys. Rev.* **59** (1941), 625.

††† Taylor, A. H., and Young, L. C., *Proc. Inst. Radio Engrs.* **16** (1928), 561; **17** (1929), 1491.

Beverage, Peterson, and Hansell† found occasional signals at very great distances on frequencies as high as 40 mc./s. In 1933 Jones‡ observed bursts of signals up to 200 miles from transmitters working on frequencies in the range 36 to 100 mc./s. with occasional maxima of great intensity. In 1938 Pierce§ discussed this type of phenomenon and pointed out that such bursts could be caused by meteor ionization. In 1942–4 workers of the Federal Communications Commission Engineering Department,‖ using transmitters in the frequency range 42 to 84 mc./s., and observing at distances of 100 to 340 miles, investigated these bursts in detail; visual correlation of the bursts with meteors was obtained on several occasions during 1944 August and November. The diurnal variation of numbers of bursts (Fig. 8) shows good agreement with the theoretical and experimental data on the diurnal variation in numbers of meteors. These workers observed that on 71·75 mc./s. the bursts were less frequent and of shorter duration than on 44 mc./s.

It will be seen that a large amount of evidence steadily accumulated, indicating that the entry of meteors into the atmosphere gave rise to transient increases of ionization which could be observed as short-lived echoes on suitably pulsed radio equipments. It was not until after the Second World War, however, that the radio techniques were deployed in the specific study of meteoric phenomena. The development of radio transmitters and receivers during the war, working on frequencies considerably in excess of the critical E and F region frequencies, gave a great impetus to the study of the transient meteoric echoes.

The work of Hey and Stewart††, ‡‡ in 1945 and 1946 and of Prentice, Lovell, and Banwell§§ in 1946 showed conclusively that with suitable equipment a close correspondence existed between the radio echoes and meteors. For example, Fig. 9 shows the mean hourly rate of occurrence

† Beverage, H. H., Peterson, H. O., and Hansell, C. W., *Proc. Inst. Radio Engrs.* **19** (1931), 1313.

‡ Jones, L. F., ibid. **21** (1933), 349.

§ Pierce, J. A., 1938, loc. cit.

‖ Federal Communications Commission; Engineering Dept. Docket (1944), no. 6651.

†† Hey, J. S., and Stewart, G. S., *Nature*, **158** (1946), 481; *Proc. Phys. Soc.* **59** (1947), 858.

‡‡ This work arose directly from observations made by Army G.L. Mark II radar equipments during the V2 rocket attacks on London in the latter part of 1944. These equipments were used to detect the approaching V2's in order that early warning could be given; but many echoes at the appropriate range were observed when no V2's had been launched. An analysis of these echoes was published as a secret memorandum (No. 462) by the Army Operational Research Group. The work immediately after the end of the war which confirmed their relationship with meteors was described in a further report (No. 348) by Hey and Stewart. Observations of the echoes made by the coastal radar chain in the British Isles were described by Eastwood, E., and Mercer, K. A. (*Proc. Phys. Soc.* **61** (1948), 122).

§§ Prentice, J. P. M., Lovell, A. C. B., and Banwell, C. J., *Mon. Not. Roy. Astr. Soc.* **107** (1947), 155.

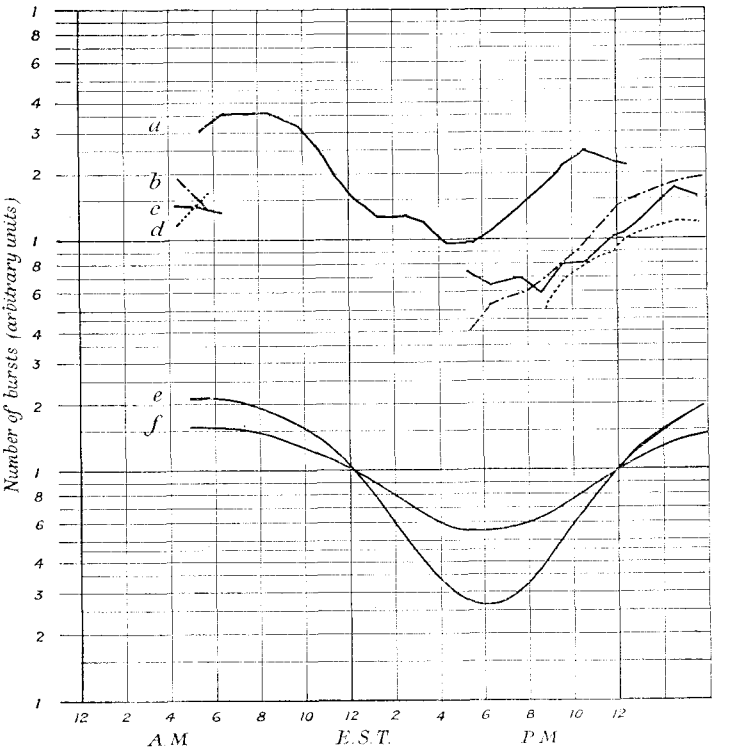

FIG. 8. Diurnal variation of the numbers of bursts of high-frequency radio signals compared with meteors by the Federal Communications Commission Engineering Department.

(*a*) Average of monthly median bursts/hr. 1943 Feb.–1944 Jan. (*b*) Observed number of meteors/hr. (Schmidt). (*c*) Observed number of meteors/hr. (Coulvier-Gravier). (*d*) Observed number of meteors/hr. (Hoffmeister). (*e*) Theoretical number of meteors/hr. (Hoffmeister) (parabolic). (*f*) Theoretical number of meteors/hr. (Hoffmeister) (hyperbolic).

of echoes observed by Hey and Stewart† in 1946 January to June with a pulsed apparatus on a wave-length of 5 m. The peak in the hourly rate in January corresponds to the Quadrantid meteor shower and that in April to the Lyrid shower, both agreeing in time with the visible occurrence of these showers. Similar curves of the activity during the summer of 1946 including the Perseid shower were obtained by Prentice, Lovell, and Banwell.‡ The very much more striking events observed during the great Giacobinid shower in October of that year are described in Chapter XVI. During this period several groups of workers in America, Canada,

† Hey, J. S., and Stewart, G. S., *Nature*, **158** (1946), 481; *Proc. Phys. Soc.* **59** (1947), 858.

‡ Prentice, J. P. M., Lovell, A. C. B., and Banwell, C. J., *Mon. Not. Roy. Astr. Soc.* **107** (1947), 155.

and Great Britain developed these radar and radio techniques for the study of specific problems in meteor astronomy and meteor physics. Some of the basic techniques are described in the remaining sections of this chapter, and the many results obtained in recent years are discussed in the appropriate later chapters of the book.

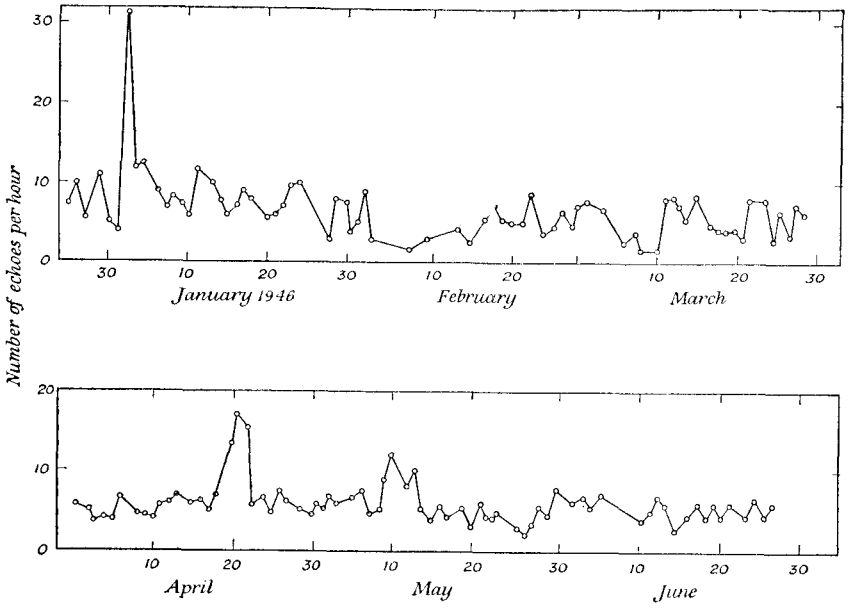

FIG. 9. Mean hourly rate of occurrence of radio echoes observed by Hey and Stewart in 1946.

2. Contemporary radio techniques for the study of meteors

(*a*) *Introduction*

The essential units in a radio apparatus for the study of meteors are the transmitter, receiver, aerial system, and display unit or recorder. The transmitter may generate either pulsed or continuous wave (c.w.) signals. In the former system the transmitted pulses are usually of the order of 10 microsec. in duration, and are radiated at a recurrence rate which generally lies between 50 and 1,000 pulses per second, depending on the particular problems under investigation. After scattering by the ionized meteor trail the returned pulses are received and can be most readily observed by displaying as an echo on a cathode-ray tube display with a linear time base, the commencement of which is synchronized with the transmitter pulse. On account of this synchronization the sequence of scattered pulses appear as an echo at a fixed point on the

time base for as long as the ionized trail exists. These basic facts are illustrated in Fig. 10. If the distance of the meteor trail from the station is R, then the time between the transmission and reception of a pulse will be $t = 2R/c$, where c is the velocity of radio waves. This time interval

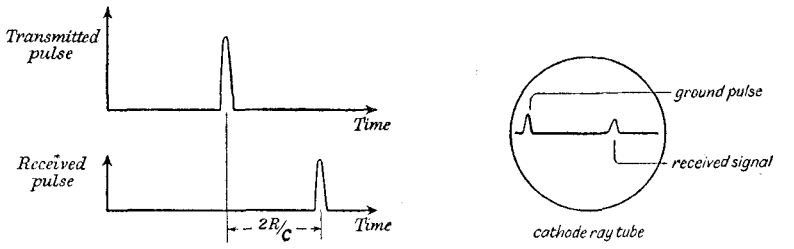

FIG. 10. The pulsed method of observing meteor trails.

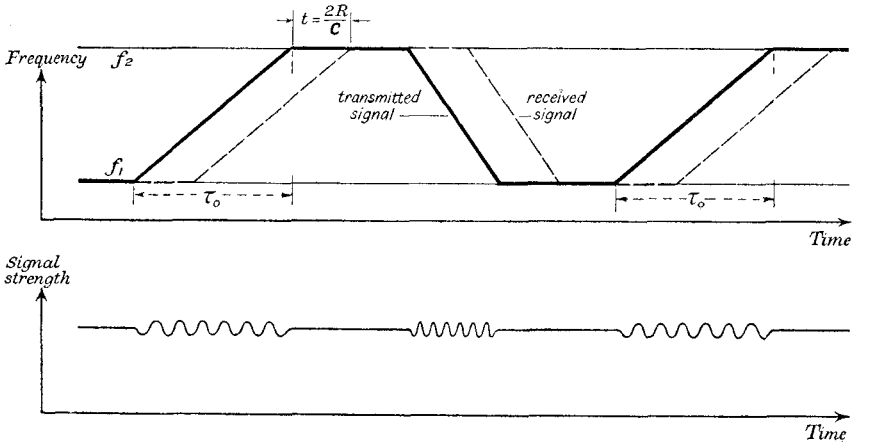

FIG. 11. The continuous-wave frequency modulation method.

can be measured accurately from the separation of the ground and echo pulses on the cathode-ray tube time base, and hence R can be determined readily.

If the transmitter radiates continuous waves, then it must be frequency modulated in order to determine ranges. This is illustrated in Fig. 11, where the transmitter frequency increases linearly from f_1 to f_2 in time τ_0. The wave returned from the meteor trail will be delayed by a time $t = 2R/c$: hence at a given instant the transmitted and received signals differ in frequency, and interference beats will be observed at the receiver output as indicated in the lower diagram of Fig. 11. The beat frequency

is clearly given by

$$\frac{t}{\tau_0}(f_2-f_1) = \frac{2R}{\tau_0 c}(f_2-f_1).$$

The total number of beats in one frequency sweep is therefore $\frac{2R}{c}(f_2-f_1)$ and hence the range is determined by counting the number of beats in each sweep.

It can be shown that for a given mean transmitter power, and other parameters constant, there is no difference in either pulse or frequency modulated systems as far as sensitivity and accuracy of range measurement are concerned. The pulse method has certain advantages in display, especially when the signals are scattered at the same time from more than one object. As far as meteor work is concerned the pulse method has been used almost exclusively in the applications requiring a range measurement. In fact it is difficult to find cases where the frequency modulation technique has been applied to meteor observation. On the other hand, as will be seen later, the continuous wave methods, without frequency modulation, have been extensively used for the determination of meteor velocities. In this case an auxiliary pulsed system is necessary to give the range of the meteor trail.

The basic circuits and techniques which are used in contemporary transmitters and receivers are largely identical with those applicable to radar. These are adequately described in the many texts devoted to radar† and it would be inappropriate to enter into details in this book. The factors governing choice of transmitter pulse width, receiver band width, aerial parameters, display systems, and wave-length are often different, however, when such equipment is used in the study of meteors. A brief discussion of some relevant points follows.

(*b*) *Pulse Width and Band Width*

The choice of transmitter pulse width and receiver band width for a meteor equipment depends on the various interdependent factors

† The following, amongst a large selection, may be recommended as filling in the background to this chapter.

All books in the Cambridge 'Modern Radio Technique' series, especially Taylor, D., and Westcott, C. H., *Principles of Radar*; Smith, R. A., *Aerials for Metre and Decimetre Wavelengths*; Moxon, L. A., *Radio Receivers for Metre and Decimetre Wavelengths*.

The chapter on 'Radar' by Smith, R. A., in *Electronics* (edited by Lovell, B.), Chapman & Hall.

Full accounts of radar techniques by many of the original workers are given in the special Radiolocation volume of the *J. Instn. Elect. Engrs.* (93 IIIA, 1946), and also by the Radar School Staff at the Massachusetts Institute of Technology in *Principles of Radar* (McGraw-Hill). A complete account is also given by Ridenour, L. N., *Radar System Engineering* (McGraw-Hill, 1947).

common in radar applications. In the latter the choice is mainly governed by consideration of range discrimination, range accuracy, and sensitivity. In the meteor case the question of discrimination is not usually significant. For example, with a pulse length of 10 microsec. two objects separated by 1 km. could be resolved. Apart from certain specialized techniques in the field of meteor physics such high discrimination is unnecessary, and the pulse length can therefore be determined by other considerations.

The pulse of transmitted radio frequency energy has a frequency spectrum spread around a mean value, which is the radio frequency of the transmitter. Ideally the receiver is required to pass this pulse without distorting it. Thus, in principle, the receiver should be able to pass the band of frequencies comprising the pulse spectrum. Since the pulse spectrum comprises an infinite range of frequencies this would entail a receiver with an infinitely wide pass band. In practice a compromise is made between finite band width and distortion of the pulse.

According to Fourier's theorem a periodic function $\Phi(t)$ repeating in time t_0 can be expanded in harmonic terms

$$\Phi(t) = k + \sum a \cos\left(\frac{2\pi nt}{t_0}\right) + \sum b \sin\left(\frac{2\pi nt}{t_0}\right).$$

The recurrent function is therefore an infinite series of harmonic oscillations of frequency n/t_0, where n is a positive integer. The full analysis of the spectrum of a train of pulses (as distinct from the spectrum of sinusoidal modulation), is somewhat complex and need not concern us here.† It is sufficient to note that the spectrum consists of a series of lines separated by the intervals between successive transmitted pulses (recurrence frequency $f_0 = 1/t_0$) as indicated in Fig. 12. The amplification of such a pulse sequence without distortion would require a receiver with an infinitely wide band width. It is evident from Fig. 12 that most of the spectrum is contained within a frequency band of the order $2/\tau$. It can be shown that τ corresponds to the width of the transmitted pulse, and in the practical design of receivers a band width of about $1/\tau$ is usually taken as the best compromise. It leads to a rounding of the pulse shape as shown in Fig. 13. The degree to which such rounding can be tolerated depends on the range accuracy required, since accurate ranging requires the transmission of a steep-fronted pulse and the maintenance of the steep front through the receiver. In the example

† A detailed discussion of the appropriate Fourier analysis for the case of pulsed transmission and reception is given by Lawson, J. L., and Uhlenbeck, G. E., in *Threshold Signals*, McGraw-Hill, 1950.

shown in Fig. 13 the limit of accuracy of the range measurement will be set by the time interval P'Q'. If it is required to measure the range of a meteor trail to $\pm 1{\cdot}0$ km. then this time interval must not be greater than $2\Delta R/c \simeq 6{\cdot}6$ microsec. If the receiver affects the pulse shape as shown in Fig. 13 (which approximates to the practical case of band width

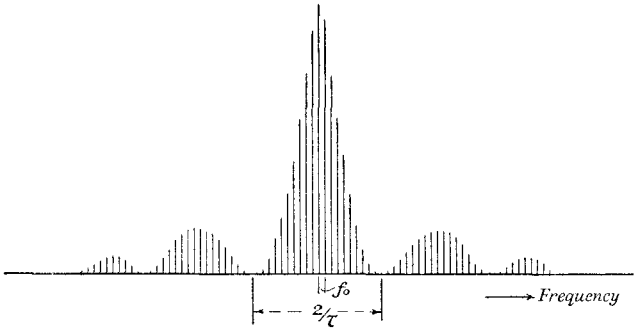

FIG. 12. Frequency spectrum of a sequence of pulses of recurrence frequency $f_0 (= 1/t_0)$.

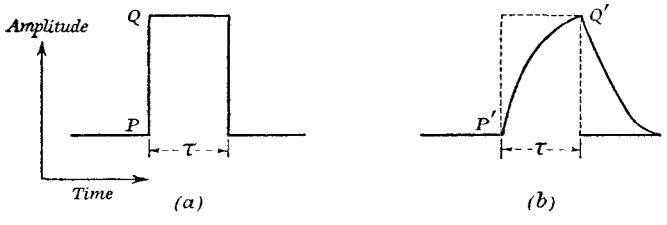

FIG. 13. Square-topped transmitted pulse (*a*) of length τ, and (*b*) the approximate shape of the pulse when passed through a receiver with band width $1/\tau$.

$\sim 1/\tau$), then the pulse width should also be about 6·6 microsec.; and hence the optimum receiver band width ($1/\tau$) about 150 kc./s. If greater range accuracy is required the receiver band width must be widened in order to increase the sharpness of the front of the pulse; but this will increase the noise level without increasing the pulse amplitude, and sensitivity will be lost. Conversely, if the receiver band width is decreased below the optimum value of $1/\tau$, the pulse shape will not only be more rounded but the amplitude of the pulse will be reduced. Hence although the noise level is decreased there will be no increase in sensitivity, and the accuracy of range determination will be worsened.

Of course, the same result could be obtained by, for example, using a pulse length of 66 microsec. and a band width of 15 kc./s. In normal radar applications this would be inadmissible because range discrimination would be no better than about 10 km., but in meteor work this would

not normally be a drawback. In fact, the over-all sensitivity of the system to meteor trails would be improved because of the reduction of receiver noise by virtue of the narrower band width. In practice, however, a limit is often set to such increases in pulse width because of transmitter power limitations. The benefit of increased sensitivity would only be obtained provided the peak power in the transmitter pulse remained constant, which for a given recurrence frequency would entail a tenfold increase in *mean* power. The mean power could be reduced by decreasing the recurrence frequency. It will be seen later, however, that the attainment of the utmost sensitivity is not an urgent problem in meteor astronomy, and that the requirements of velocity determination demand high recurrence frequencies, which in turn demand that the pulses should be short because of mean power limitations in the transmitter.

The result of these various criteria is that for the study of problems in meteor astronomy the pulsed radio equipments generally have transmitters radiating pulses of about 10 microsec., at a recurrence rate of a few hundred per second. Peak powers in the pulse generally range from about 5 to a few hundred kilowatts, but the mean powers are, of course, generally less than 1 kilowatt. Sufficient accuracy of range measurement is generally obtained when the receiver band width is adjusted in relation to pulse width as discussed above—in this case about 100 kc./s.

Although not of direct interest to meteor observations, it may be mentioned that in the case of the continuous wave techniques similar considerations apply. The range accuracy then depends on the beat frequency and the time of observation (Fig. 11). It is easy to show that the accuracy is of the order of the reciprocal of the receiver band width; and that for similar transmitter mean powers the over-all sensitivity of pulse and continuous wave equipments is identical. Actually, as mentioned earlier, the continuous wave techniques are not normally used in meteor work for range measurements. They are, however, widely used for meteor velocity measurements (see Chapter IV). The receiver band width requirements are then determined by the modulation frequency caused by the Fresnel zone oscillations during the formation of the meteor trail, which amounts to a few hundred cycles per second.

(*c*) *Aerial Systems*

A wide variety of aerial systems have been used for transmission and reception in meteor work. For some applications a wide coverage is

desirable; in others high directivity is required. The principles and practice in the design of these aerials have followed closely those used in the radar applications,† and here it is only necessary to refer to one or two general concepts. As a consequence of the reciprocity theorem the properties of an aerial may be regarded as identical whether it is in use for the transmission or reception of radio energy.

If the transmitter is connected to a system radiating a power P isotropically, then the power density at a distance R will be $P/4\pi R^2$. Any practicable aerial system will have a power gain G over an isotropic source, where G is defined such that the power density in a given direction is $GP/4\pi R^2$. The power gain G as normally used refers to the gain in the direction of maximum radiation. The power density in any other direction is obtained from the polar diagram of the aerial system $f(\theta, \phi)$, where θ and ϕ are the angles from the direction of maximum radiation in two planes at right angles. At a distance R in any direction (θ, ϕ) the power density will be $W_0 f^2(\theta, \phi)$, where W_0 is the power density in the direction of maximum radiation. The total flux of power from the aerial will be $\iint W_0 f^2(\theta, \phi)\, d\omega$, where $d\omega$ is the elementary solid angle and, by definition, this must be 1/G times the flux from an isotropic source radiating with a power density equal to that at the maximum. Hence we reach the general result that

$$G \iint f^2(\theta, \phi)\, d\omega = 4\pi. \tag{1}$$

The most elementary form of radiator is the Hertzian dipole, an electric doublet with dimensions small compared with the wave-length. All current elements in the dipole are in phase and the polar diagram is given by $f(\theta) = \cos\theta$ (Fig. 14). Thus, applying (1),

$$G \int_{-\frac{1}{2}\pi}^{\frac{1}{2}\pi} \int_{0}^{2\pi} \cos^3\theta \, d\theta d\phi = 4\pi,$$

or

$$G = 1{\cdot}5.$$

The simplest possible aerial system therefore has a power gain of 1·5 over the idealized isotropic radiator.

On the comparatively short wave-lengths which are mostly used in the radio investigation of meteors, the elementary form of radiator is more often the centre-fed half-wave dipole (Fig. 15). This dipole has a natural resonant frequency corresponding to a wave-length of twice its length, and if driven at this frequency it radiates strongly with a polar

† The books listed on p. 32 contain accounts of radar aerials.

diagram somewhat narrower than that of a Hertzian dipole shown in Fig. 15. It can be shown that for the half-wave dipole (1) becomes

$$G \int_{-\frac{1}{2}\pi}^{\frac{1}{2}\pi} \int_{0}^{2\pi} \frac{\cos^2(\frac{1}{2}\pi \sin\theta)}{\cos^2\theta} \cos\theta \, d\theta d\phi = 4\pi,$$

or

$$G = 1{\cdot}635.$$

The power gain of the half-wave dipole over that of the Hertzian dipole is therefore 1·09.

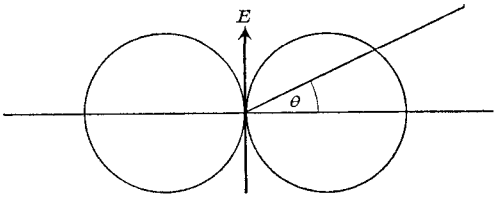

FIG. 14. Radiation from the Hertzian dipole in the plane of the electric vector. In the plane at right angles the radiation is constant with ϕ.

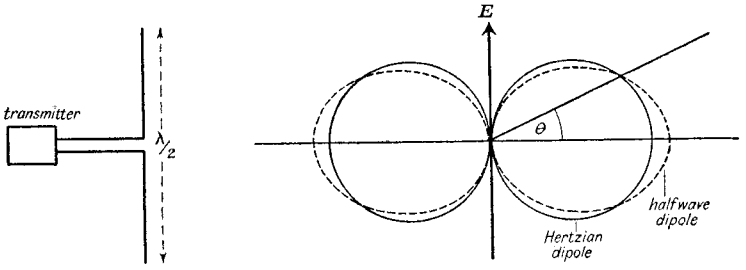

FIG. 15. Half-wave dipole and its radiation in the plane of the electric vector compared with the radiation from a Hertzian dipole. In the plane at right angles the radiation is constant with ϕ.

Unfortunately there is no universally accepted standard as to whether the power gain of an aerial system is expressed in terms of gain over an isotropic radiator, Hertzian dipole, or half-wave dipole. The expressions of power gain either in terms of an isotropic radiator or half-wave dipole are most commonly encountered, the latter being convenient in experimental work since the half-wave dipole is the fundamental driving element of most aerial arrays.

The simple half-wave dipole is a common aerial used for transmission and reception where wide coverage is required. In many applications much more highly directive aerial beams are required (for example, in the determination of meteor radiants described in Chapter IV). One

common method of achieving directivity is to feed the transmitter power into a number of elements, and by appropriate phasing to arrange for reduction of radiation in certain directions with consequent increase in others. For example, suppose the transmitter power is fed to n equally spaced elements in a row as in Fig. 16, each element of which has a polar

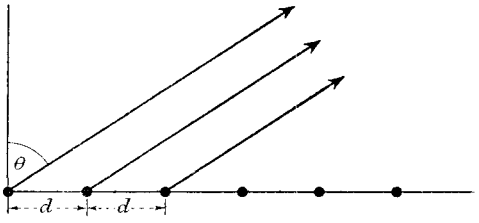

FIG. 16. Radiation from a linear array of n equally spaced elements.

diagram $f(\theta)$. If the rth element has current i_r and phase α_r then the field at (R_r, θ) from this element will be

$$E_r = kf(\theta)i_r e^{j\{(2\pi R_r/\lambda)+\alpha r\}},$$

where k is a constant and λ the wave-length. From the whole aerial

$$E = kf(\theta)\sum_{r=1}^{r=n} i_r e^{j\{(2\pi R_r/\lambda)+\alpha r\}}.$$

If d is the element spacing $R_r = R_1 + (r-1)d\sin\theta$, and for the same current in each element and for zero α's summation gives

$$|E| = kf(\theta)\frac{\sin\left(\frac{n\pi d\sin\theta}{\lambda}\right)}{\sin\left(\frac{\pi d\sin\theta}{\lambda}\right)}.$$

Maximum radiation occurs for $\theta = 0$ and zeros when $\sin\theta = N\lambda/nd$ ($N = 1, 2, 3, \ldots$). For spacing d of less than λ there is one principal maximum and a series of side lobes as shown in Fig. 17. The radiation of the main lobe falls to zero at $\sin\theta = \lambda/nd$: but if the total aperture of the aerial $(n-1)d \gg \lambda$, this reduces to $\theta = \lambda/a$, where a is the over-all dimension of the aerial.

The above is a simple example of a linear array producing directivity in one direction (θ). If directivity is also required in the plane at right angles (ϕ), then a series of such linear arrays must be placed side by side to form a broadside array. In 1928 a Japanese engineer Yagi devised an alternative form of directive aerial in which only the half-wave dipole

is fed, but which consists of a parasitic reflector and a number of parasitic directors as indicated in Fig. 18. This type of aerial has been widely used in meteor work, both singly and in arrays. It is easier to construct and more compact than a broadside array, but suffers from larger side

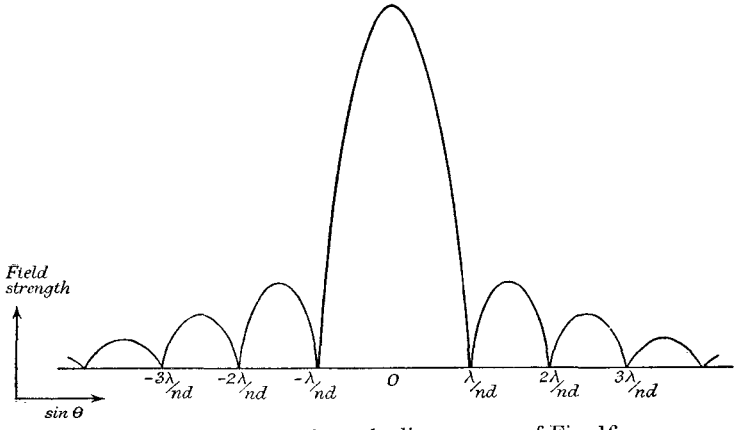

FIG. 17. Radiation from the linear array of Fig. 16.

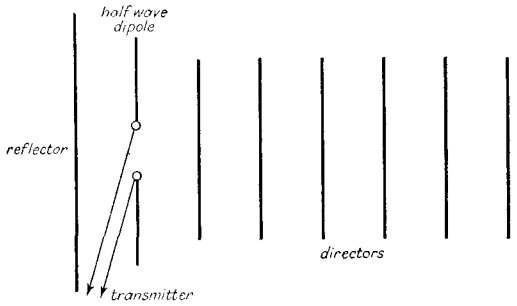

FIG. 18. Form of Yagi aerial for producing a directive beam.

lobes. The details of such broadside arrays and Yagis are given in many of the standard texts referred to previously.

The other main form of aerial used for obtaining directivity is the paraboloidal aerial, in which a half-wave dipole or small array is mounted at the focus of a parabolic surface in order to produce a uniform phase field across its aperture. One great advantage of this type of aerial is that the wave-length can be readily changed by adjusting the dipole feed system. If in Fig. 19 the curved surface is paraboloidal and the aperture rectangular with the focus in the aperture plane, the radiated field can be obtained as follows. Let E(x) be the field (in amplitude and phase) at a point in the aperture plane at a distance x from the edge of

the mirror. Then, by Huygens' principle, the field at a distant point can be obtained by summing the contributions from each element of the aperture with the appropriate phase relationship, giving

$$E(\theta) = k \int E(x) e^{\{(2\pi j x \sin\theta)/\lambda\}} \, dx, \tag{2}$$

the integral being taken over the aperture.

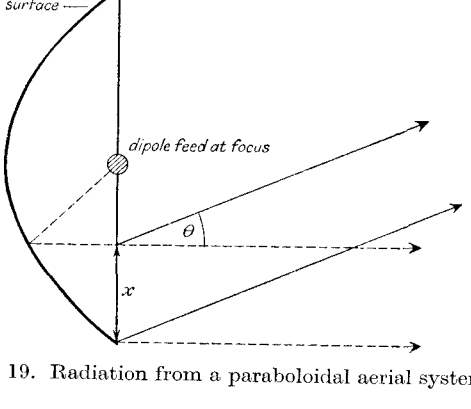

FIG. 19. Radiation from a paraboloidal aerial system.

For uniform phase and amplitude distribution across the aperture (2) gives the polar diagram as

$$E(\theta) = \text{const} \frac{\sin\left(\frac{\pi \, d' \sin\theta}{\lambda}\right)}{\frac{\pi \, d' \sin\theta}{\lambda}},$$

where d' is the length of the aperture.

If $d' \gg \lambda$, the first zero occurs at $\theta \simeq \lambda/d'$.

A similar expression will be appropriate in the ϕ plane. Thus for a rectangular aperture of sides d', d'', the first zeros in the principal planes will occur at λ/d', λ/d'' and the power will be effectively concentrated in a solid angle $\lambda^2/d'd''$. Then the power gain of the paraboloid will be

$$\frac{4\pi \, d'd''}{\lambda^2}.$$

In the case of a full paraboloid with circular aperture of radius a_0, uniformly illuminated, the beam will have circular symmetry. The polar diagram can be shown† to be given in terms of the first-order Bessel function

$$E(\theta) = \frac{2J_1(ka_0 \sin\theta)}{ka_0 \sin\theta}, \tag{3}$$

† See, for example, Slater, J. C., *Microwave Transmission*, McGraw-Hill, 1942.

and the power gain $$G = \frac{4\pi A}{\lambda^2},$$

where $A = \pi a_0^2$ is the area of the aperture. The first zero from (3) occurs at $\theta = 1{\cdot}22\lambda/a_0'$, where a_0' $(= 2a_0)$ is the diameter of the aperture. The beam from the uniformly illuminated circular aperture is therefore 1·22 times wider than that from the uniformly illuminated rectangular aperture with side the same as the diameter of the circular aperture. The field strength of the first side lobe is, however, reduced to 13 per cent. of the main lobe instead of 21 per cent. for the rectangular aperture.

In actual practice it is impossible to obtain uniform illumination of the aperture; neither is circular symmetry generally achieved because of the differing polar diagram of the primary feed source in the two planes. The general result is a broadening of the main beam, diminution of gain, and reduction of side-lobe intensity relative to the uniformly illuminated aperture.

The attainment of aerial systems of high directivity which are often required in meteor work is hindered by mechanical difficulties. The most useful wave-lengths for meteor work lie in the 3- to 10-metre wave band. Thus, to produce a beam of width $\pm 10°$ to the first zero on a wave-length of 5 metres would require an aerial aperture of about 36 metres. Such an arrangement can be fairly readily constructed to produce such a beam in a fixed direction, especially when the beaming is required only in one plane. On the other hand, if it is required to direct an aerial the mechanical difficulties become rather severe. One of the largest directional aerials so far used in meteor work consisted of an array of five Yagi systems mounted on a large army searchlight base, which gave a beam of about $\pm 16°$ to the first zero when used on a wave-length of 4 m.†

In the case of these large aerial structures it is almost always common practice to use an electronic switching arrangement whereby the same aerial may be employed both for transmission and reception simultaneously.

(d) Display and Recording Systems

Some form of cathode-ray tube display is used almost universally in all forms of apparatus for the observation of the radio echoes from meteor trails. For monitoring purposes the range amplitude display (Fig. 20) is generally used. The time base sweep C is synchronized with the transmitter pulse by electronic circuits of the type which are described

† Photographs of this and other aerials used in meteor work have been given in *Radio Astronomy* by Lovell, A. C. B., and Clegg, J. A., Chapman & Hall, 1952.

in the standard texts.† The recurrence period is rarely less than 50 per second, so the time base appears to the eye as a continuous line on which is superimposed the random noise output from the receiver. The transmitter pulse A appears at zero range, while the signal returned from

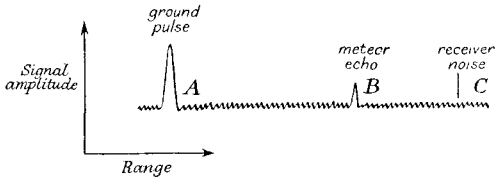

FIG. 20. Meteor echo on a range–amplitude cathode-ray tube display.

the meteor trail is applied to deflect the time base vertically as at B. The distance between A and B then gives the range of the trail directly. Thus, merely by visual inspection of such a display the numbers, range, time of occurrence, durations, and amplitudes of the echoes may be obtained. The duration of the echo from a given trail depends on a number of factors—principally the wave-length of the radio apparatus.‡ On a radio wave-length of 4 m. most of the echoes are shortlived—less than 0·1 second; but, especially during the major showers, echoes with durations of several seconds are commonly observed.

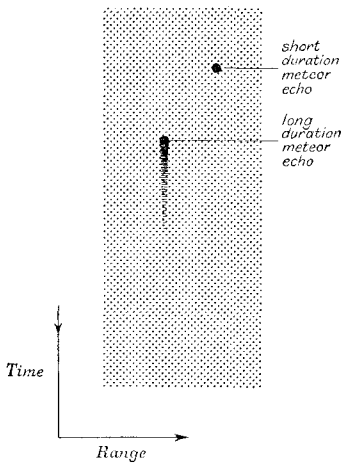

FIG. 21. Meteor echoes on an intensity modulated range-time display (see also photographic reproduction in Plate I).

Visual inspection of such a display is not conducive to high accuracy of measurement, and photographic methods are now almost always employed. For this purpose the type of display is changed so that the received signal is applied to increase the brightness of the time base. (Thus on visual inspection B would appear as a transient bright spot instead of a vertical deflexion of the time base.) A photographic film is then moved slowly past the cathode-ray tube face so that a continuous record of the

† See note on p. 32.

‡ This topic will not be discussed much in this book. It is hoped to deal with this and other similar features in *Meteor Physics*.

range, duration, and time of occurrence of the echoes is obtained as shown in Fig. 21. This is the type of display used in the apparatus for determining meteor radiants described in Chapter IV.

These may be regarded as the two basic types of display used in the radio-echo meteor work, but special adaptations have been made for specific purposes. Examples of those used in the work on the velocity measurements will be described in Chapter IV.

(*e*) *Radio Wave-length and Sensitivity of Equipment—the Fundamental Radio-echo Equation*

The choice of one of the most crucial parameters—the wave-length of the radio equipment—remains to be discussed. Originally, as mentioned in § 1, the transient echoes were observed on equipments designed for investigation of the ionosphere, and hence operated on wave-lengths of, say, 20 to 100 m. The pioneer post-war work of Hey and Stewart was carried out with army equipment which, for operational purposes, had been designed to work on wave-lengths in the 4- to 5-m. band. It was soon evident that on these shorter wave-lengths the transient echoes were much fewer, and were more clearly associated with the visual meteoric occurrences. However, only since the development of the theory of the scattering processes has there been any quantitative guide to the correct choice of wave-length for specific investigations. It is not intended to discuss these matters in any detail in the present book, but the deduction of the fundamental scattering equation will make clear the relations of the wave-length, receiver sensitivity, and other parameters discussed in this chapter. This treatment follows that of Lovell† and Lovell and Clegg.‡

Consider a cluster of N electrons at a distance R cm. from a radio transmitter and receiver working on a wave-length of λ cm. If the size of the cluster is small compared with λ and if the electrons reach their full velocity under the influence of the impressed e.m.f. and are not impeded by collisions, then the cross-section for scattering by the N electrons will be

$$\frac{8}{3}\pi\left(\frac{\mathbf{e}^2}{\mathbf{mc}^2}\right)^2 N^2 \text{ sq. cm.},$$

where **e** and **m** are the charge and mass of the electron and **c** the velocity of light.

If the peak power in the transmitter pulse is P watts, and if the aerial

† Lovell, A. C. B., *Nature*, **160** (1947), 670.
‡ Lovell, A. C. B., and Clegg, J. A., *Proc. Phys. Soc.* **60** (1948), 491.

system of the transmitter has a power gain G′ over an isotropic source, then the power density at R cm. will be

$$\frac{PG'}{4\pi R^2} \text{ watts/sq. cm.}$$

The power density of this scattered radiation when it returns to the receiving aerial will be

$$\frac{8\pi}{3}\left(\frac{e^2}{mc^2}\right)^2 N^2 \frac{PG'}{4\pi R^2} \frac{1{\cdot}5}{4\pi R^2} \text{ watts/sq. cm.}\dagger$$

If G_0' is the power gain of the receiving aerial over an isotropic source then its effective collecting area will be

$$G_0'\lambda^2/4\pi \text{ sq. cm.}$$

and the power delivered to a matched load when situated in a field of mean power density σ will be‡

$$\frac{G_0'\lambda^2}{4\pi}\sigma.$$

Thus the amount of energy $\bar{\omega}$ delivered to the receiver after scattering by the cluster of N electrons will be

$$\bar{\omega} = \frac{8}{3}\pi\left(\frac{e^2}{mc^2}\right)^2 N^2 \frac{1{\cdot}5PG'}{16\pi^2R^4} \frac{G_0'\lambda^2}{4\pi} \text{ watts.}$$

If we assume that the same aerial is used both for transmission and reception and express the power gain G in terms of a half-wave dipole, then $G' = G_0' = 1{\cdot}64G$ and the above expression reduces to

$$\bar{\omega} = \frac{8}{3}\pi\left(\frac{e^2}{mc^2}\right)^2 N^2 \frac{PG^2\lambda^2}{16\pi^3R^4} \text{ watts.} \tag{4}$$

If the voltage amplitude at the receiver input is V and the input resistance r then

$$V^2 = 2r\bar{\omega};$$

$$V = k_0 \frac{\lambda N}{R^2} \tag{5}$$

where

$$k_0^2 = \frac{8}{3}\pi\left(\frac{e^2}{mc^2}\right)^2 \frac{PG^2}{16\pi^3} 2r.$$

The meteor trail consists of a long narrow column of ionization whose diameter is small compared with λ, hence the appropriate number of electrons to be included in (4) can be calculated by using optical diffrac-

† The factor of 1·5 in this equation arises because the electrons scatter as Hertzian dipoles and not uniformly through 4π.

‡ This differs from the equation given by Lovell and Clegg (loc. cit.) which was incorrectly stated as $G_0'\lambda^2\sigma/8\pi$.

tion theory. The voltage amplitude returned to the receiver from a small element of track at an angle θ to the perpendicular from the receiver to the trail is given by (5) as

$$dV = \frac{k_0 \lambda \alpha_0 d\theta}{R},$$

where α_0 is the number of electrons per cm. path in the trail.

Then the voltage amplitude from the portion of the trail $\theta = 0$ to $\theta = \theta_1$ is given by Fresnel's integral in the form

$$V_{\theta_1} = \frac{k_0 \alpha_0}{2}\left(\frac{\lambda}{R}\right)^{\frac{3}{2}} \int_0^{\nabla} \cos\frac{\pi}{2}\nabla^2 \, d\nabla + \frac{ik_0 \alpha_0}{2}\left(\frac{\lambda}{R}\right)^{\frac{3}{2}} \int_0^{\nabla} \sin\frac{\pi}{2}\nabla^2 \, d\nabla,$$

where $\nabla = 2\theta\sqrt{(R/\lambda)}$.

The voltage amplitude at the receiver due to the whole track is then

$$V = \frac{1}{\sqrt{2}} k_0 \alpha_0 \left(\frac{\lambda}{R}\right)^{\frac{3}{2}},$$

and by comparison with (5) the appropriate number of electrons N is given by†

$$N = \alpha_0 \sqrt{\frac{\lambda R}{2}}.$$

Hence, from (4), the amount of energy at the receiver input due to scattering from a meteor trail with an electron density of α_0 electrons/cm. will be

$$\bar{\omega} = \frac{\alpha_0^2 P G^2 \lambda^3}{12\pi^2 R^3}\left(\frac{e^2}{mc^2}\right)^2 \text{ watts.} \qquad (6)$$

The above treatment applies only when the electron volume density in the meteor column is less than the critical value for the wave-length employed. Kaiser and Closs‡ have shown that the formula may be applied to the case of scattering from trails of electron line density less than about 10^{12} electrons/cm. when the electric vector is parallel to the trail. When the electric vector is transverse to the trail, plasma resonances may, under certain conditions, give a somewhat enhanced return of scattered power. For electron densities greater than 10^{12} electrons/cm. the trail behaves as a metallic cylinder and it has been shown by Kaiser and

† In this calculation the phase correction is applied twice because of the curvature of the incident and reflected wave surfaces. The wave-length is then effectively reduced to $\lambda/2$, giving $N = \alpha_0\sqrt{(\lambda R/2)}$ instead of the more familiar form $N = \alpha_0\sqrt{(\lambda R)}$ of optical theory.

‡ Kaiser, T., and Closs, R. L., *Phil. Mag.* **63** (1952), 1.

Closs† and by Greenhow† that (6) then becomes

$$\bar{\omega} = \frac{\alpha_0^{\frac{1}{2}} P G^2 \lambda^3}{20\pi^3 R^3} \left(\frac{e^2}{mc^2}\right)^{\frac{1}{2}}. \tag{7}$$

The ionized trail will immediately diffuse and when formula (6) applies the initial signal amplitude V_0 will decrease exponentially to a value V at time t given by‡

$$V = V_0 \exp\left(-\frac{16\pi^2 D t}{\lambda^2}\right), \tag{8}$$

where D is the diffusion coefficient. Thus the echo duration for trails with less than 10^{12} electrons/cm. varies as λ^2 and does not depend on the actual density in the trail.

On the other hand, for trails with more than 10^{12} electrons/cm. it can be shown† that the duration ΔT varies also with α_0 and is given by

$$\Delta T = \frac{\text{const.}\,\alpha_0 \lambda^2}{D}. \tag{9}$$

When (6) applies the signal amplitude $\sqrt{V}$ provides a direct measure of the line density α_0, but in (7) the signal amplitude increases only as the fourth root of the line density, and for these dense trails the actual duration as given by (9) provides a more satisfactory measure of the line density.

The validity of (6), (7), (8), and (9) has been well established experimentally. These results and their implications will not be discussed in the present work; it is sufficient to notice:

(*a*) that the received power $\bar{\omega}$ varies as P, G^2, and λ^3 for each scattering mechanism;

(*b*) that the combined visual and radio-echo observations§ show that a line density of about 10^{12} electrons/cm. is produced by a meteor of about 5th magnitude. Thus the majority of meteors in the range of visual magnitudes will fall into the high-density category, and formulae (7) and (9) are appropriate.

The over-all sensitivity of the equipment and the number of radio echoes obtained will therefore depend directly on the basic receiver noise level $\bar{\omega}_0$, and on P, G^2, and λ^3. The following are some of the main considerations governing the choice of these parameters in a practical meteor equipment.

(i) *The basic receiver noise level* $\bar{\omega}_0$. If an ideal noiseless receiver was matched to a resistance at its input, then according to Nyquist's theorem

† Kaiser, T., and Closs, R. L., *Phil. Mag.* **63** (1952), 1; Greenhow, J. S., *Proc. Phys. Soc.* **65** (1952), 169.

‡ Herlofson, N., *Rep. Phys. Soc. Progr. Phys.* **11** (1947), 444.

§ Greenhow, J. S., and Hawkins, G. S., *Nature*, **170** (1952), 355.

the thermal agitation in the resistor delivers a power $\mathbf{k}T\Delta f$ to the receiver, where $\mathbf{k}$ is Boltzmann's constant, T the absolute temperature of the resistance, and Δf the frequency acceptance band. The noise generated in the components of any practicable receiver will give rise to an additional noise power and the total noise of a receiver matched to a resistance is generally written as

$$\mathbf{N}\mathbf{k}T\Delta f,$$

where $\mathbf{N}$ is the noise factor of the receiver and is commonly used as a measure of the performance of the receiver. At room temperatures $\mathbf{k}T \sim 4\times 10^{-21}$ joules, and practicable noise factors with contemporary techniques vary from about three in the metre wave band to twelve or more in the centimetre wave band.

In addition to this receiver noise, a receiver connected to an aerial will also pick up solar and galactic radio emissions which appear with the same characteristics as the noise generated in the receiver itself. If this external noise is represented by P_e per unit band width, then the total noise in the receiver will be

$$\bar{\omega}_0 = (\mathbf{N}\mathbf{k}T + P_e)\Delta f. \tag{10}$$

Referring to equations (6) and (7), the signal scattered from the meteor trail will only be readily detectable if

$$\bar{\omega} > \bar{\omega}_0.$$

The common measure of the strength of the returned signal is the ratio of the amplitude of the signal to the amplitude of the noise, which will be proportional to $\sqrt{(\bar{\omega}/\bar{\omega}_0)}$.

Hence, with the other apparatus parameters in equations (6) and (7) fixed, the detection of the meteor echo will be determined by the value of $\bar{\omega}_0$. Whether the lower limit of $\bar{\omega}_0$ is determined by the receiver noise ($\mathbf{N}\mathbf{k}T$ in (10)), or the galactic noise (P_e in (10)) depends largely on the wave-length. As a general guide it may be stated that for wave-lengths longer than about 3 m. the galactic noise is generally greater than the receiver noise and this sets the limit to the sensitivity of the receiver. To a certain extent this can be avoided if special directional arrays are used to avoid the areas of maximum noise emission in the galaxy. On the other hand, for wave-lengths less than about 3 m., the receiver sensitivity is generally limited by the noise generated internally. It will be seen below that most meteor equipments operate on wave-lengths above 3 m. and hence the former case applies. $\bar{\omega}_0$ can, of course, be reduced by decreasing the receiver band width Δf, but the limitations here as regards accuracy of range measurement have already been discussed.

As regards the actual value of $\bar{\omega}_0$ if, as an example, we take $\Delta f = 1$ mc./s. then $\mathbf{k}T\Delta f \simeq 4\times10^{-15}$ watts. On a wave-length of 4 m., a noise factor N of about 3 is readily attainable, giving $\mathbf{N}\mathbf{k}T\Delta f \simeq 1{\cdot}2\times10^{-14}$ watts. If such a receiver was connected to a narrow beam aerial, the galactic noise on this wave-length would predominate when the beam was directed at the Milky Way. For a beam pointed in the neighbourhood of the galactic centre $\bar{\omega}_0$ would be limited to somewhere between 10^{-12} and 10^{-13} watts. For a direction away from the plane of the Milky Way it would, however, be possible to reach a value of $\bar{\omega}_0$ somewhere near the above limit of $1{\cdot}2\times10^{-14}$ watts.

(ii) *The peak transmitter power* P. According to equations (6) and (7) the power scattered from the meteor trail increases directly as the peak transmitter power P. As a guide to what is practicable it may be stated that peak powers of 100 kw. are fairly readily attainable on the wave-lengths under discussion. An increase of ten times over this figure requires a considerable technological enterprise, and so far in meteor work, peak powers of 200 to 300 kw. appear to be the maximum yet used. Whether such values can be attained with a given transmitter depends on a number of interlocking factors, especially on the pulse width τ and recurrence frequency f_0, since the mean power $\overline{W}$ is given by

$$\overline{W} = Pf_0\tau.$$

In a given transmitter $\overline{W}$ is generally limited by power supplies and valve dissipation, and within this limit it is possible to vary P, f_0, and τ considerably. The factors governing τ as regards range accuracy have already been discussed. For routine observations values of f_0 of 25 or 50 per second are satisfactory, but in certain specialized applications—such as the determination of velocities—it is necessary to use much higher recurrence frequencies of 600 or more. In one case where it was necessary to obtain the maximum over-all sensitivity of the equipment, Almond, Davies, and Lovell† employed a special device to retain a high peak power with such a high recurrence frequency. The high recurrence was required only for the duration of the Fresnel zone pattern. It was therefore arranged that the transmitter normally radiated with a pulse recurrence of 150, which was switched by an electronic device to 600 as soon as the first echo pulse was received.

(iii) *The aerial power gain* G. The factors governing the power gain G of aerial systems have been discussed in § 2 (*c*). According to equations (6) and (7) the scattered power received from a meteor trail increases

† Almond, M., Davies, J. G., and Lovell, A. C. B., *Mon. Not. Roy. Astr. Soc.* **111** (1951), 585.

as G^2 (assuming the same aerial is in use both for transmission and reception). It is important to notice, however, that the main effect of increasing G is to enable fainter meteors to be detected, and not necessarily to increase the number detected. It is implicit in (1) that increase in G means a decrease in beam width, and hence of collecting area. The actual change in numbers recorded with change of G depends both on the distribution of meteor radiants and on the mass distribution. In the case of a uniform distribution of meteor radiants and for the case where the number N of meteors of mass $\boldsymbol{m}$ is such that the total mass is constant for each magnitude range, then it can be shown that change of G will not change the numbers seen, but merely shift the magnitude range of those which are detected. This particular situation is found in the sporadic meteor distribution.

However, in many applications—particularly those concerned with the delineation of meteor radiants, or with the selection of meteors from a given direction—the width of the beam is the chief criterion. The actual numerical value of G is therefore not necessarily of chief significance in the design of aerials for meteor work.

(iv) *The wave-length* λ. The wave-length enters in equations (6) and (7) as λ^3 and is therefore the dominant factor as far as numbers of echoes are concerned. With the type of meteor apparatus readily available giving peak powers of say 100 kw. and with the best values of $\bar{\omega}_0$ it is found that very few meteor echoes can be seen on wave-lengths of 2 m. or less, even during active showers. The most commonly used wave-lengths are in the 4- to 10-m. range. The actual choice again depends on a number of other factors, particularly the requirements regarding beam width. Mechanical difficulties make directional systems difficult to achieve on wave-lengths of 8 m. or more, and hence the 4-m. range has been widely favoured for such applications as radiant determination. With conventional values of P and $\bar{\omega}_0$ the number of echoes on this wave-length is found to bear a fairly close relation to the number seen by a single visual observer under good sky conditions. The 8-m. range has been used in the experiments on the velocity distribution of sporadic meteors, both on account of the desire to study the faint meteors and also because on these longer wave-lengths the time of decay of echo amplitude (given by (8)) is sufficiently long for the Fresnel zone formation to be measured in the higher velocity groups. On wave-lengths much in excess of 10 m. the transient echoes associated with meteors become involved with various ionospheric effects and these longer wave-lengths have been little used for work in meteor astronomy.

IV

OBSERVATIONAL METHODS—III

RADIO-ECHO TECHNIQUES FOR THE MEASUREMENT OF METEOR RADIANTS AND VELOCITIES

In the years between 1945 and 1950 there was a rapid development in the application of the radio techniques discussed in Chapter III to specific problems in meteor astronomy. In this book we are chiefly concerned with the measurements of meteor radiants and velocities and the present chapter will describe the more important radio techniques which have been developed for these measurements. Various other radio techniques, such as those for the measurement of meteor heights and wind motions, lie outside the scope of this book.

1. The application of radio techniques to the measurement of meteor radiants

Pierce† first drew attention to the influence of the orientation of the meteor trail with respect to the observing station, and subsequent experimental work by Hey and Stewart‡ and by Lovell, Banwell, and Clegg§ has shown that meteor trails do, in fact, show a critical aspect effect. In most cases the radio echo is obtained only when the aerial beam is directed at right angles to the trail. This property of meteor trails has been used to determine the radiants of showers by observations of the radio echoes. At least three methods have been described in the literature, but the most widely used is that developed by Clegg (see (*c*)).

(*a*) *The Method of Hey and Stewart*

The first determination of meteor radiants by radio methods was made by Hey and Stewart‡ who used three separate stations operating on 73 mc./s. situated as shown in Fig. 22. The direction of the aerials was adjusted so that the beams intersected at a point about 100 km. in height, equidistant from each station. Since a meteor trail will give a radio echo only when it passes at right angles to the axis of the beam, it is to be expected that as a radiant moves across the sky it will not produce echoes simultaneously at the three stations, but in succession as the meteor trails become oriented at right angles to the respective

† Pierce, J. A., *Proc. Inst. Radio Engrs.* **26** (1938), 892.

‡ Hey, J. S., and Stewart, G. S., *Nature*, **158** (1946), 481; *Proc. Phys. Soc.* **59** (1947), 858.

§ Lovell, A. C. B., Banwell, C. J., and Clegg, J. A., *Mon. Not. Roy. Astr. Soc.* **107** (1947), 164.

aerial beams. The diurnal variations of the mean hourly rates obtained by Hey and Stewart on the stations B1, B2, B3 (Fig. 22) between 1945 July 26–August 1 are shown in Fig. 23.

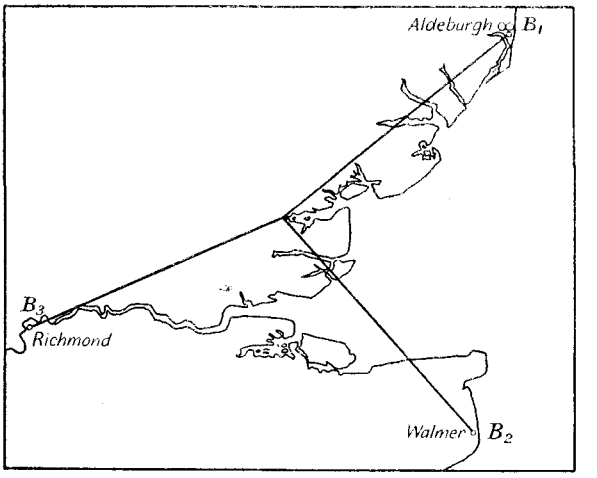

FIG. 22. Siting of the three equipments used by Hey and Stewart in 1945 June and July for the measurement of meteor radiants.

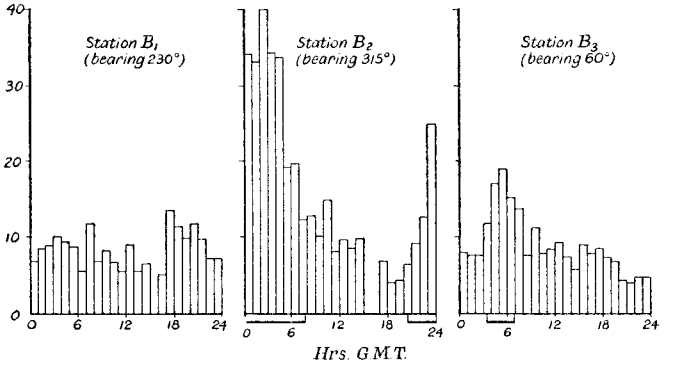

FIG. 23. Diurnal variations of mean hourly rate of echoes on the three equipments of Fig. 22 from 1945 July 26–Aug. 1. Times at which the radiant R (Fig. 24) is favourable are indicated by heavy-lines.

Ordinates = relative number. Abscissae = time G.M.T. O.A. = out of action.

The coverages of possible radiant points required to produce the peaks in echo rate for B2 at 02h. 30m. and B3 at 04h. 30m. are shown in Fig. 24. The centre of overlap R may be taken to be the radiant position and gives a radiant point at† $\alpha\,345°$, $\delta - 10°$. The station B1 shows no marked

† The notation adopted for giving radiant coordinates in this book is α 345°, δ −10°, indicating Right Ascension 345°, Declination −10°.

peak. This is to be expected since a radiant in this position never presents an aspect favourable to B1. This radiant corresponds well with the δ-Aquarid radiant, known to be prominent between these dates. The accuracy of such a determination depends on the width of the aerial beams. Hey and Stewart estimated that their errors in placing the radiant due to this reason may be 10°.

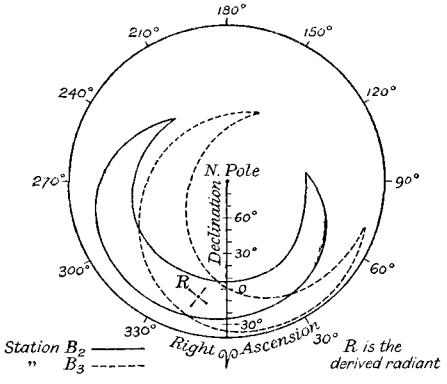

FIG. 24. Coverage of possible radiant positions for main peaks in hourly rate of stations B2 and B3.

The method requires triplicate radio echo apparatus worked over long base lines. Although important as the first radio determination of meteor radiants it does not compete in simplicity or accuracy with a method developed subsequently by Clegg (see below), and for these reasons it has not since been used for radiant work.

(*b*) *The Methods of McKinley and Millman*

(i) McKinley and Millman† have described a method by which the radiant of an isolated shower may be determined from a statistical analysis of the radio echoes obtained on an apparatus using a fixed, non-directional aerial system. The method is based on the possibility of deriving the elevation of the radiant from the observed range distribution of the echoes at given times. Assuming that all the meteors ionize in a thin layer at a height of 100 km. above the ground and that the meteors are entering the atmosphere at an angle ϕ (i.e. the elevation of the radiant) then the minimum slant range of the echoes observed will be $R = 100/\cos\phi$. The value of R is obtained for each hour when the radiant is above the horizon from the plot of the number/range distribution of the observed echoes. (Allowance for the sporadic meteor distribution is made from data obtained when there is no active radiant.) The

† McKinley, D. W. R., and Millman, P. M., *Proc. Inst. Radio Engrs.* **37** (1949), 364.

elevation of the radiant ϕ is then calculated from the above formula, for hourly intervals during the progress of the shower. The curve obtained in this manner for the Geminid radiant on 1947 December 12–13 is shown in Fig. 25. The maximum elevation was 76° determined at Ottawa at 02h. 08m. E.S.T. giving the radiant coordinates as α 112°, δ +31°. This is in good agreement with the best available data on the Geminid

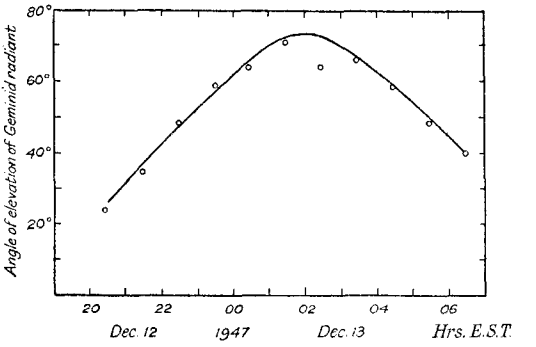

FIG. 25. Variation of elevation of Geminid radiant during the night of 1947 Dec. 12–13 as determined from the range distribution of the radio echoes by McKinley and Millman.

radiant.† The probable error of the radio-echo determination is stated to be between 2° and 3°.

This method can only be used if the echo rate is sufficient to yield a satisfactory value of R at not more than hourly intervals. It therefore requires the use of a comparatively long wave-length, high sensitivity equipment (the wave-length used by McKinley and Millman was 9·2 m.), and can only be used satisfactorily during an isolated active shower. In the example quoted, Fig. 25 was derived from the range measurements on 7,500 echoes. There are no published accounts of the use of this method to determine the radiant coordinates of showers other than the Geminid shower.

(ii) When fairly long radio wave-lengths of the order of 9 or 10 m. are used, the radio echo can often be observed from the ionization over a longer portion of the meteor path than in the neighbourhood of the right-angle reflecting point. McKinley and Millman‡ used this property to obtain simultaneous records of the meteor path from three triangularly situated stations, with spacings of 36 to 57 km. If the meteor is moving

† See Chap. XV.

‡ McKinley, D. W. R., and Millman, P. M., *Canad. J. Res.* **27** (1949), 53.

with constant velocity v, then the shape of the observed echo on a range-time display will be a hyperbola, defined by

$$R^2 = R_0^2 + v^2(t-t_0)^2, \qquad (1a)$$

where R is the range at time t, and R_0 is the minimum range at time t_0 (that is R_0 is the perpendicular reflecting point). Clearly, if the hyperbolae are sufficiently well defined on the three records then the R_0 points can be determined, and the path of the meteor in space can be delineated. As will be discussed in § 2 the velocity is obtained from the shape of the hyperbola. Thus, in principle, complete data are available from which the orbit of a single meteor can be determined. McKinley and Millman give one remarkable example of the three simultaneous records of a meteor observed on 1948 August 4 which is reproduced in Plate I, and from which it was possible to obtain the data given in Table 9.

TABLE 9

Data on a Single Meteor obtained in the 3-Station Radio Measurements of McKinley and Millman

	Ottawa Station (A)	*Arnprior Station (B)*	*Carleton Place Station (C)*
R_0 km.	117·8	108·6	122·1
t_0 sec.	47·22	48·71	48·36
v km./sec.	34·7 ± 0·6	35·3 ± 0·6	35·1 ± 0·6
Observed path length km.	270	175	160

Apparent geocentric velocity	35·0 ± 0·4 km./sec.
Apparent radiant: true bearing	074° ± 2°
elevation	+2° ± 2°
True height above sea-level:	
beginning of path	108 km.
end of path	104 km.

From these data it was possible to compute the orbit of the meteor. Unfortunately the type of echo which gave the above records is rarely observed. McKinley and Millman state that during 2,000 hours of observation, they obtained only fifty echoes displaying an ionized path well over 100 km. long, and of this number only a dozen while the three stations were operating. In order to yield the type of record illustrated in Plate I, the meteor must be travelling at a low angle to the horizontal plane and must be of a mass sufficient to ensure that it will not be completely vaporized during a period of several seconds. Although this three station technique can yield the complete orbital data for a single meteor it is unfortunately very restricted in its application. Apart from

the single case computed by McKinley and Millman there are no other published records of its use.

(c) *The Method of Clegg*

(i) *Theoretical considerations.* So far the most extensively used method for the determination of meteor radiants has been that devised by Clegg† whereby radiant positions can be determined with considerable accuracy from single station observations. The technique depends

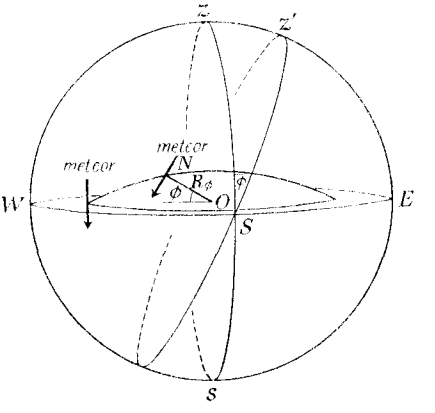

FIG. 26. The change in range R_ϕ of meteors detected at an elevation ϕ, as the radiant moves across the sky.

essentially on the specularly reflecting properties of meteor trails when observed on wave-lengths in the neighbourhood of 4 m. If, on such a wave-length, an infinitely narrow aerial beam is directed horizontally in an easterly direction then radio echoes will only be observed from meteors whose radiants lie in a great circle plane passing approximately overhead and cutting the horizon in the north and south. Thus the time of onset of echoes from an active radiant with such an idealized arrangement would give the right ascension of the radiant. By rotating the aerial through an angle, and observing the difference in time of the onset of the echoes in the two positions, the declination could also be found. Any practicable aerial beam has a finite width in azimuth and elevation, and thus echoes will be observed from a given radiant over a certain part of its movement across the sky. During this movement of the radiant, the range at which the echoes are observed will change as indicated in Fig. 26. If the meteors are assumed to originate at a constant height above the earth's surface, this layer will form a spherical cap above the

† Clegg, J. A., *Phil. Mag.* **39** (1948), 577; *J. Brit. Astr. Ass.* **58** (1948), 271.

observer at O due to earth curvature. Meteors detected due west at zero elevation will have radiants lying on the great circle plane NZS; those at elevation ϕ will have radiants on the great circle plane NZ'S. Hence, for an aerial directed towards the west, the ranges of the echoes observed from the meteors of a given radiant will increase as the radiant moves across the sky, but will decrease for an easterly directed aerial.

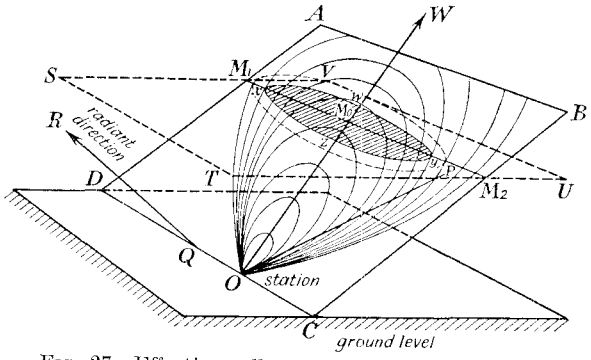

FIG. 27. Effective collecting area of aerial system.

The precise range-time relationships of the observed echoes depend on the shape of the aerial beam. This was treated in detail by Clegg as follows.

In an ideal meteor stream all meteors travel in parallel paths and due to the effect of perspective appear to emanate from a point radiant. Fig. 27 represents such a stream viewed from a station at O. The radiant lies in the direction QR from the station, and the plane ABCD, which contains O, is perpendicular to QR and cuts the celestial sphere in a great circle of which the radiant is the pole. The path of all the meteors will be parallel to QR and will cross ABCD normally, so that the reflecting points will lie in this plane.

The majority of trails occur within a limited range of heights and this further restricts the reflecting points to a strip of the plane of limited depth. The echoes detected by the station will be from the portion of this strip lying within the aerial beam. We thus define a collecting area lying in the plane ABCD whose depth is limited by the depth of the meteor zone, and whose lateral extent is determined by the width of the aerial beam. It will be shown that with a knowledge of the radiation pattern of the aerial it is possible to estimate the shape and size of this collecting area for any position of the radiant, and conversely by observation of the variations in range and echo rate to determine the radiant position.

The fundamental scattering formula (equation 6, Chap. III) may be written for the present purpose in the form

$$Z = \frac{kG(\theta, \phi)\alpha_0}{R^{\frac{3}{2}}}, \tag{1}$$

where

Z = amplitude of the echo measured as a signal to noise ratio,
G = effective power gain of the aerial system in the direction of the reflecting point,
θ = azimuth of the reflecting point from the station,
ϕ = elevation of the reflecting point from the station,
α_0 = line density of electrons in the trail at the reflecting point,
R = range of the reflecting point from the station,

and k is a constant depending on the parameters of the apparatus. It will be convenient to refer to α_0 as the effective electron density of the trail.

Equation (1) may be written

$$\frac{G(\theta, \phi)}{R^{\frac{3}{2}}} = \mathbf{q}, \tag{2}$$

where

$$\mathbf{q} = \frac{Z}{k\alpha_0}. \tag{3}$$

If $\mathbf{q}$ remains constant, equation (2) defines a closed surface in space on which the overall sensitivity of the apparatus is constant. There will be a family of such surfaces corresponding to different values of $\mathbf{q}$, those of lower value completely enveloping those of higher value. These surfaces will cut the great circle plane ABCD in a series of contours, as shown in Fig. 27. For a single meteor stream, where the velocities of the individual meteors are the same, it is assumed that all meteors of the same mass will produce identical trails. Let the horizontal surface STUV in Fig. 27 represent the height of maximum ionization for meteors of a certain mass group. For such meteors the effective electron density will be greatest when the trails cut the great circle plane in the line $M_1 M_2$ and will fall off with the increasing distance from this line. Thus the amplitude of an echo will depend not only on the $\mathbf{q}$ contour on which the reflecting point lies, but also on the distance of this point from $M_1 M_2$, and there will clearly be a closed curve such as xwyz in the plane ABCD on which all trails of this class give echoes of the same amplitude. A family of such curves can be drawn for different values of the signal to noise ratio Z. If xwyz corresponds to a value of Z equal to unity, it will represent the limit of visibility and the shaded area which it encloses

will be the effective collecting area for meteors of this mass. For smaller meteors the corresponding area will be less, and for the smallest detectable mass group it will reduce to a point inside xwyz lying on the axis of the beam OW. The collecting area for a larger mass group is shown as a dotted line in the figure, completely enveloping xwyz.

For a given mass group the horizontal width xy of the collecting area depends only on the conformation of the **q** contours on the great circle plane, and for the largest meteors tends to a limit defined by the width of the aerial beam. The depth wz increases indefinitely with the mass. The method of radiant determination assumes that there are relatively few meteors of great mass and that for the majority the depth of the collecting area is small in comparison with its mean height above the ground. In this case, if a surface such as STUV is drawn at the mean height of maximum ionization for the shower, all the echoes will originate at a point close to the line $M_1 M_2$, being most numerous close to the point M_0 and occurring less frequently near to the edge of the beam.

To find the rate and ranges of the echoes for any position of the radiant it is convenient to represent the aerial beam by a set of sensitivity contours on the surface STUV at the mean height of maximum ionization as indicated in the map in Fig. 28. Let this surface be at a height h above the ground. It can be shown that, allowing for earth curvature, the range R and the elevation ϕ at any point on it are related by the equation

$$R^2 + 2r_e R \sin\phi - 2r_e h + h^2 = 0, \qquad (4)$$

where r_e is the radius of the earth. The surfaces of constant sensitivity will cut this horizontal surface in a series of contours defined by equations (2) and (4). The map in Fig. 28 represents a polar projection of such a surface at a height of 95 km., which may be taken as the mean height of occurrence of a typical shower of medium velocity. The point O is vertically above the station and, in order to illustrate a specific case, the contours are drawn for one of the aerials at the Jodrell Bank Experimental Station.† This aerial has a half-amplitude beam-width of $\pm 8°$ horizontally and $\pm 12°$ vertically. For the present purpose the beam is maintained at a constant elevation of 12·5°, but can be directed at any azimuth. The **q** values of the contours are marked, the contour $\mathbf{q} = 1$ corresponding to the sensitivity at a point in this plane, situated vertically above an aerial of unit gain. The shaded portions represent side lobes in which the shape of the contours is not accurately known. Range circles

† Lovell, A. C. B., Banwell, C. J., and Clegg, J. A., *Mon. Not. Roy. Astr. Soc.* **107** (1947), 164.

are shown, giving distances from the station in kilometres. The dotted circle FHG indicates where the spherical 95-km. surface meets the horizon of the station. The radiant is in the azimuthal direction OR and the curved line $S_1 T_1 H$ shows where the great circle plane (ABCD, in Fig. 27) cuts the 95-km. surface when the elevation of the radiant is 30°. As the radiant elevation increases, the point T moves farther from

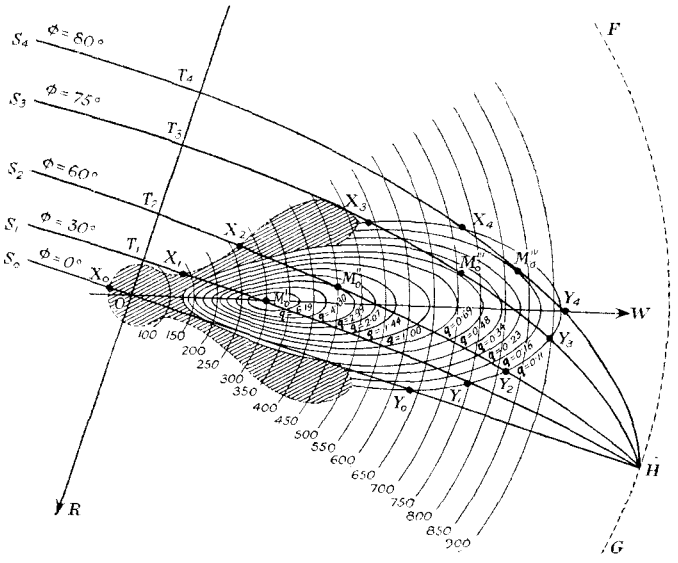

FIG. 28. Map of sensitivity contours on a surface at a height of 95 km. for a typical aerial in use at the Jodrell Bank Experimental Station. The radiant is in the azimuthal direction OR.

O and corresponding lines are shown for elevations of 60°, 75°, and 80°. When the radiant elevation is 90° the line STH lies on the horizon circle FHG, and for zero elevation it becomes the straight line $S_0 OH$, at right angles to OR.

Let the radiant be at the azimuth indicated in the figure and at an elevation 75°. The reflecting points of the trails will then lie close to $S_3 T_3 H$, but visible echoes will occur only within the limits of the aerial beam. Consider the meteors whose mass is such that they give echoes of noise amplitude when their point of maximum ionization lies on the outermost contour, for which $\mathbf{q} = 0{\cdot}11$. The horizontal limits of the collecting area for meteors of this class are defined by the points X_3 and Y_3 and, if the depth of the area (wz in Fig. 27) is not too great, these points will determine the maximum and minimum ranges at which such meteors can be detected. There will be a fairly well-defined upper mass limit above

which relatively few meteors are to be found. If $X_3 Y_3$ defines the extent of the collecting area for this limiting mass, it can be seen from the map that the majority of echoes will occur between ranges of 530 km. and 890 km. At these ranges only the largest meteors will be seen, but at points between X_3 and Y_3 meteors of smaller mass can be detected, and the most probable range of the echoes will be that of M_0''', where $S_3 T_3 H$

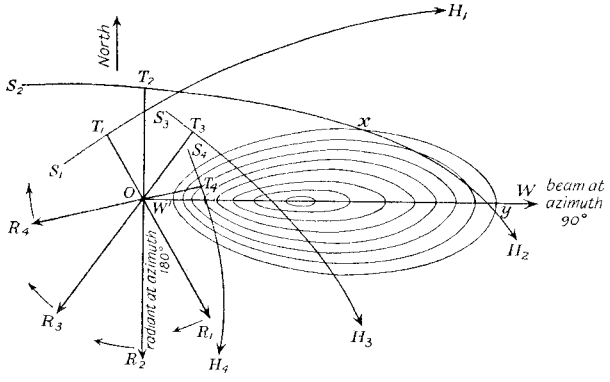

FIG. 29. Passage of radiant through central meridian with aerial beam directed due east.

touches the contour of highest value, and where the greatest number of meteors will give visible echoes.

It is evident from this figure that for a radiant at the same azimuth, but at elevation 60°, the ranges will be more scattered and the rate will tend to be higher, while for an elevation of 80° the range will be confined between narrower limits and the rate will be reduced.

As the celestial sphere rotates, the elevation and azimuth of the radiant, and consequently the position of the line STH in Fig. 28, will change. A typical case of a radiant sweeping through a low narrow beam is illustrated in Fig. 29. Let the aerial be directed at azimuth 90° and the radiant be about to cross the central meridian. Some time before transit it is in the azimuthal direction OR_1 and the line STH lies completely outside the beam so that no echoes will appear. As the azimuth approaches 180°, STH will cross the limiting contour and the rate will begin to rise, and at transit when the radiant is in the azimuthal direction OR_2 the collecting area for large meteors will be defined by xy. After transit the radiant passes through azimuths OR_3 and OR_4. This will cause a steady reduction in range and the echo rate will finally fall to zero as STH passes out of the beam at W′. The passage of the radiant through the beam is therefore characterized in this instance by a sudden

appearance of echoes at long ranges followed by a slow fall in the mean range and a final decay of the echo rate.

If the polar diagram of the aerial and the mean height of occurrence of the meteors are known, it is possible to estimate the most probable ranges of the echoes for any radiant position by means of a map such as that in Fig. 28, and, hence, to plot the range as a function of time for a radiant at any right ascension and declination. In Fig. 30 a set of theoretical range-time curves is plotted for the aerial described above at azimuth 90°, assuming that the mean height of occurrence of the echoes is 95 km. These curves are drawn for five different values of radiant declination δ (for an observer at the latitude of Jodrell Bank, 53° N.) and show the variation of maximum, minimum, and most probable range with time after transit, assuming that meteors can be detected out to the contour $\mathbf{q} = 0{\cdot}11$. In each case the point B corresponds to the time at which the line STH first crosses this contour, and, therefore, at which echoes can first appear.

The curves show that there is a sudden rise in echo rate at a time close to that of transit, and the rapid increase of the maximum and most probable ranges to their highest value, followed by a steady fall. For radiants at low declination whose elevation at transit is small, the initial rise in echo rate and range commences earlier and is less rapid than for high declinations. Thus for declination $-20°$, $\pm 0°$, and $+20°$ the rate has already become appreciable before transit and the maximum ranges occur at transit as indicated in Figs. 30 (*a*), (*b*), and (*c*). For high declinations the line STH does not pass through contours of sufficiently high value at the time of transit to ensure an appreciable rate, and the range curves are similar to those shown in Figs. 30 (*d*) and (*e*). For an aerial directed due west the variations occur in the opposite order and the time scale in Fig. 30 is reversed.

Curves such as these can be constructed for any azimuth of the aerial and it is always found that maximum ranges occur when the axis of the beam is perpendicular to the horizontal direction of the radiant, provided that the radiant elevation is not too great. If a different limiting contour is chosen, or if the map is drawn for a different mean height of ionization, the curves are of the same general form but the absolute values of the ranges are altered.

By observing the well-known visual night-time streams for which the radiant coordinates were known, Clegg† was able to show that the actual shape of the range-time plots of the echoes agreed well with the theoretical

† Clegg, J. A., loc. cit.

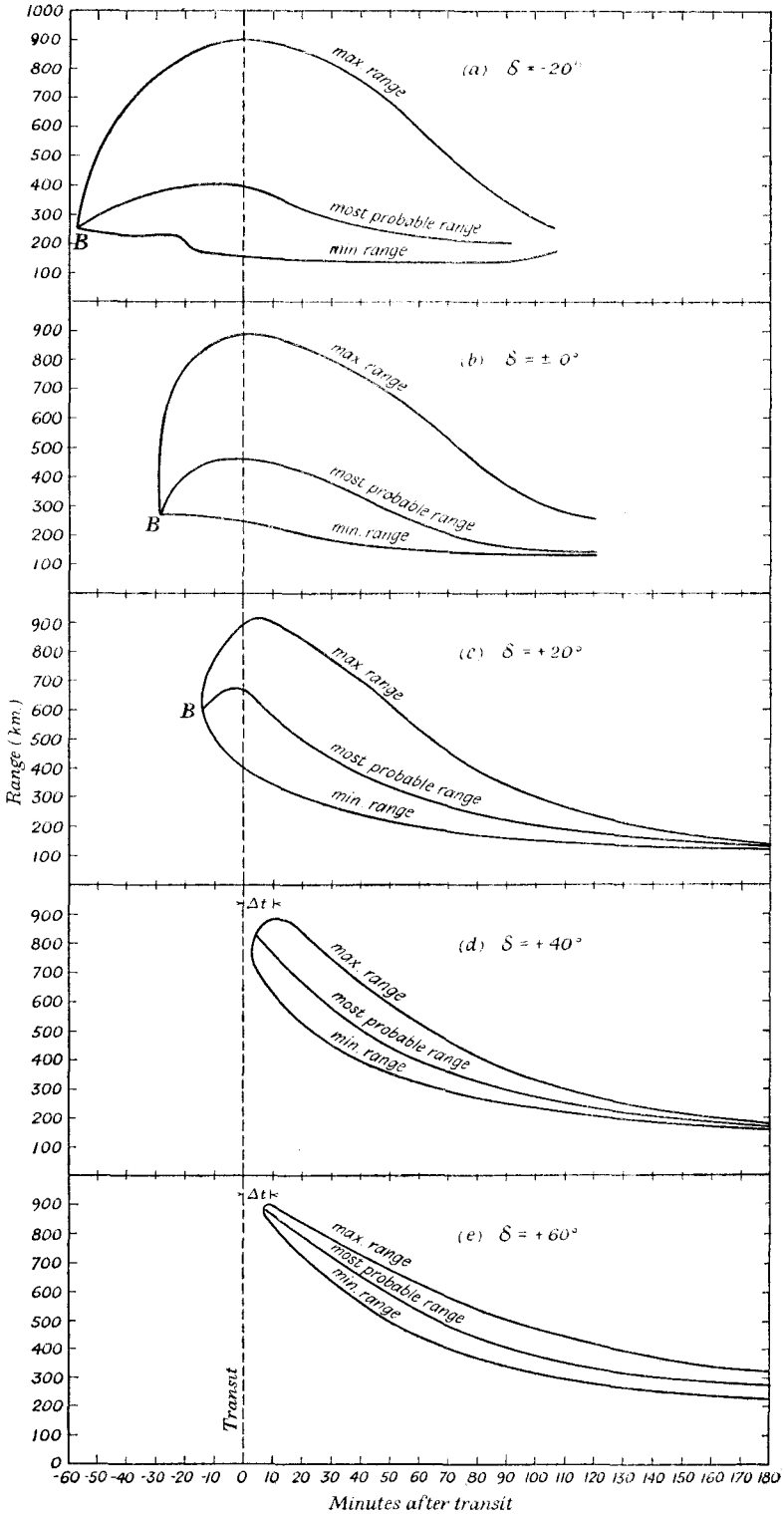

FIG. 30. Variation of maximum, minimum, and most probable range with time for observations taken on Jodrell Bank aerial directed at azimuth 90°. Curves are computed from contour map of aerial assuming a mean height of occurrence of 95 km. Maximum and minimum ranges apply to meteors which would be on the limit of visibility if their reflecting points lay on contours $\mathbf{q} = 0{\cdot}11$.

derivations discussed above. The method was then applied to the determination of unknown radiants in the following manner.

(ii) *Application to determine radiant coordinates of unknown showers.—Determination of right ascension.* Theoretical range-time curves such as those in Figs 30 (*a*), (*b*), and (*c*) show that for radiants at low elevation maximum ranges occur when the azimuth of the radiant differs from that of the aerial by 90°. The limiting elevation above which this no longer applies depends on the mean height of occurrence and the intensity of the ionization of the trails, but comparison of experimental results with the theoretical curves showed that for the original apparatus used† it was invariably greater than 60°. Thus for a radiant whose elevation never exceeds 60° (i.e. for which $\delta = +23°$) the right ascension can be found by directing the aerial at azimuth 90°. Maximum ranges will then occur at the time of transit. If the declination of the radiant is greater than +23°, maximum ranges will generally occur after transit at some time $(t_0+\Delta t_0)$, as indicated in Figs. 30 (*d*) and (*e*). The theoretical curves show that Δt_0 will never exceed 15m., so that the consequent error in right ascension will not be greater than 4°.

Determination of declination. It is possible to obtain some estimate of the declination from the range-time distribution of the echoes after transit, but for accurate determination it is necessary to make use of the relationship between the declination and the rate of change of azimuth of the radiant at the times close to transit. This relationship is indicated in Fig. 31, in which the azimuth and elevation of the radiant are plotted as functions of time. The curves are drawn for the approximate latitude of Jodrell Bank (53° N.) and for a number of declinations between δ −40° and δ +90°.

After observing the time t_0 of transit on azimuth 90°, the aerial is turned to some arbitrarily chosen azimuth $90°+\theta$. If the radiant is at sufficiently low elevation, maximum ranges will now occur when its azimuth is $180°+\theta$ at time t_θ. This gives the time $t_\theta - t_0$ required for the azimuth to change from 180° to $180°+\theta$ and immediately determines the appropriate azimuth-time curve in Fig. 31 (*a*) and, hence, the declination.

If the elevation of the radiant is greater than 60°, there will again be an error, maximum ranges occurring on this new azimuth at some time $(t_\theta+\Delta t_\theta)$. The apparent time required for the azimuth to change by θ will then be $(t_\theta - t_0 + \Delta t_\theta - \Delta t_0)$. If, however, θ does not exceed 20°, the elevation of the radiant will not change appreciably during this

† Lovell, A. C. B., Banwell, C. J., and Clegg, J. A., loc. cit.

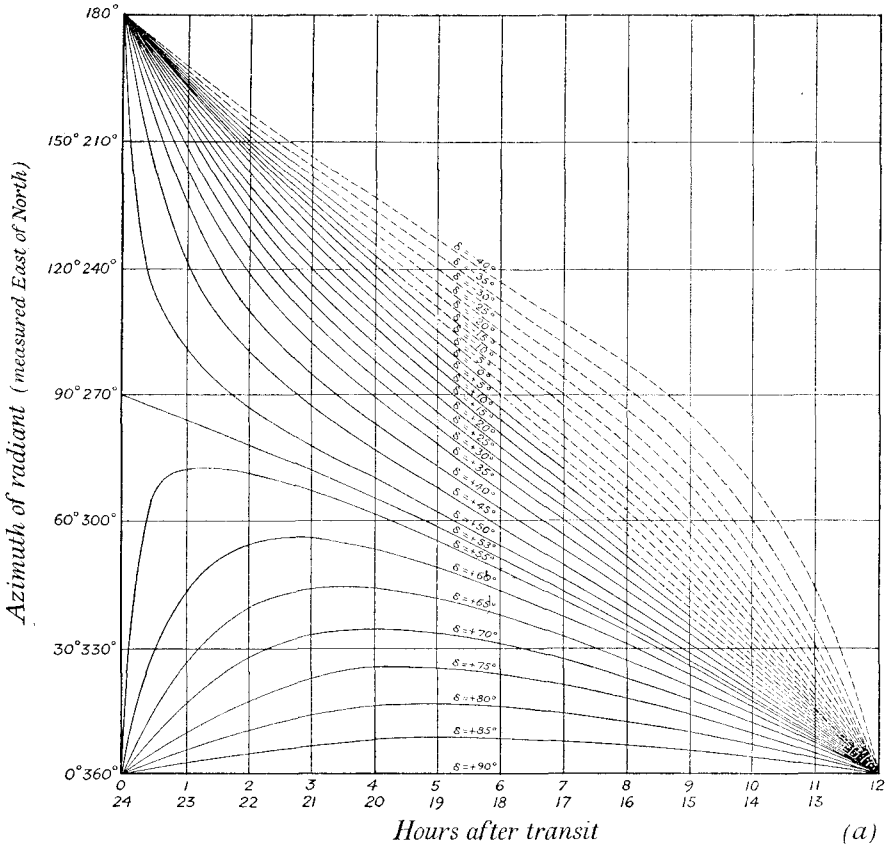

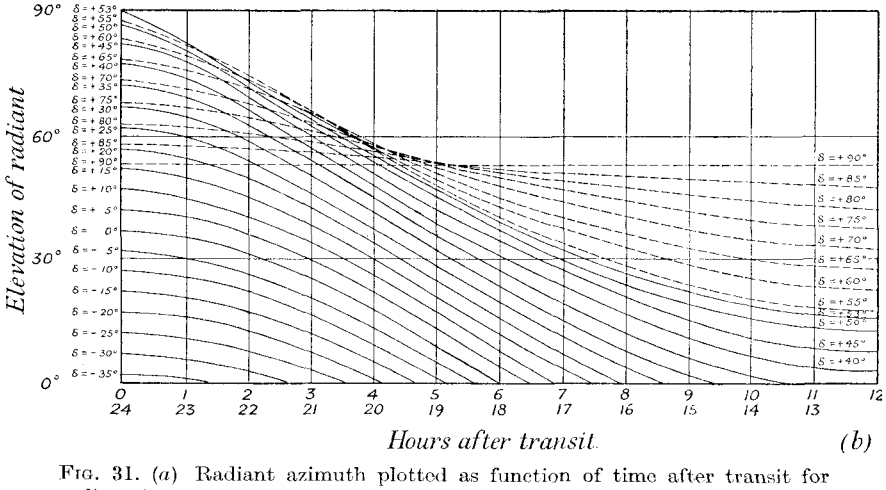

FIG. 31. (*a*) Radiant azimuth plotted as function of time after transit for radiant declinations at 5° intervals between $\delta -40°$ and $\delta +90°$ and for latitude 53° N.

(*b*) Radiant elevation plotted as function of time after transit for radiant declinations at 5° intervals between $\delta -35°$ and $\delta +90°$ and for latitude 53° N.

time and the errors Δt_0 and Δt_θ will be almost equal, so that the resultant error in the declination will be negligible.

Method for radiants at higher declinations. If the observations described above indicate that the declination is greater than $+23°$, the right ascension can be found more accurately by choosing two aerial positions $90°-\theta$ and $90°+\theta$ such that the elevation of the radiant when at right angles to the beam is less than 60°. If maximum ranges occur on these azimuths at time $t_{-\theta}$ and $t_{+\theta}$ respectively, the time of transit will be $\frac{1}{2}(t_{-\theta}+t_{+\theta})$ and the radiant will have moved from azimuth $180°-\theta$ to azimuth $180°+\theta$ in time $(t_{+\theta}-t_{-\theta})$.

This method of radiant determination using a single movable aerial was successfully employed to determine radiant coordinates during much of the early radio-echo meteor work, particularly for the first determinations of the radiants of the newly discovered summer day-time meteor streams in 1947.† The technique suffered, however, from the disadvantage that the aerial had to be moved in azimuth in order to determine the declination and it was often impossible to obtain both right ascension and declination measurements of a given radiant on the same day. The technique was therefore modified in order to use two fixed aerials at inclined directions with simultaneous photographic recording of the echoes occurring in each aerial beam. The technique, which has been described in detail by Aspinall, Clegg, and Hawkins‡ is outlined below.

(iii) *The radiant survey apparatus at Jodrell Bank.* In view of the success of the above method for the determination of meteor radiants, a special apparatus was constructed in order to determine both the right ascension and declination during a single transit of an active radiant. The apparatus also gives a continuous 24-hour record of meteoric activity and has been in continuous use since 1949.

A schematic diagram of the apparatus is shown in Fig. 32. It operates on a frequency of 72 mc./s., and comprises two independent beamed aerials A_1 and A_2, which are directed at low elevation, on azimuthal bearings of 242° and 292° respectively.§ These arrays are common to the transmitter and receiver, and the pulses from the transmitter are radiated simultaneously by both. The received signals are fed through the transmitter-receiver switches S_1, S_2, into the pre-amplifying stages

† Clegg, J. A., Hughes, V. A., and Lovell, A. C. B., *Mon. Not. Roy. Astr. Soc.* **107** (1947), 369. (See also Chap. XVIII.)

‡ Aspinall, A., Clegg, J. A., and Hawkins, G. S., *Phil. Mag.* **42** (1951), 504.

§ The azimuthal directions being measured in degrees east of north.

P_1, P_2, and after further amplification and detection are applied to the grids of the intensity modulated display tubes D_1 and D_2. The sequence of operations is initiated from a master control unit by the unit T_g, which provides pulses to trigger the transmitter, the multivibrator M, and the common time base TB of the two display tubes. The square waves from the multivibrator are used to suppress the preamplifying

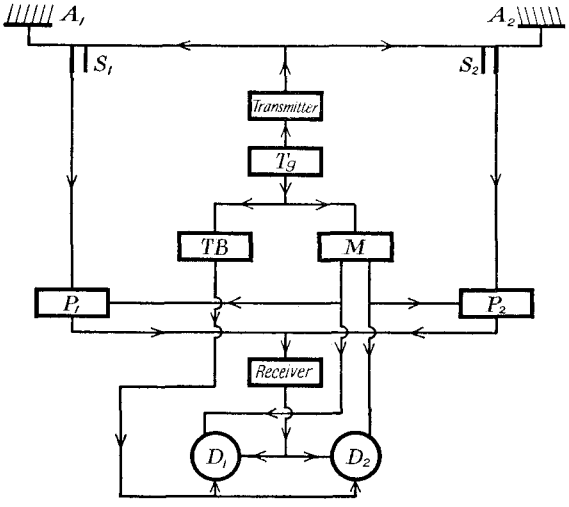

FIG. 32. Schematic diagram of the radiant survey apparatus.

stages P_1 and P_2 alternately, and are also applied to the grids of the cathode-ray tubes D_1 and D_2, so that the signals from each aerial are displayed separately side by side, and are photographed on a film which moves continuously in a direction perpendicular to that of the time bases.

The unit T_g is capable of providing pulses with a number of different recurrence frequencies, and the apparatus can be triggered in a variety of ways. For normal observations the transmitter is usually operated at a pulse recurrence frequency of 150 c./s. and the time base unit at a frequency of 75 c./s. Under these circumstances the transmitter pulses appear twice on each display, at the beginning of each time base and at a range of 1,000 km. This serves as a useful check on the range calibration, although subsidiary range markers can be supplied from the triggering system at intervals of 200 or 250 km. along the time base. One of the most serious difficulties encountered during the early experiments was that of differentiating between short duration echoes and the random noise impulses which present a similar appearance on the photographic record. This form of interference was considerably reduced

by inserting a discriminator unit, similar to that used by Davies and Ellyett† in the output of the receiver, but it has also been found advisable to trigger the transmitter with a pair of pulses separated by approximately 300 microsec., so that a true echo appears as a double. The photographic records are similar to the illustrations of Fig. 21 and Plate I.

Plate II shows the general arrangement of the two aerial systems, which are situated at longitude 2° 18′ W., latitude 53° 14′ N., and are placed symmetrically on either side of the building housing the transmitter and receiver. Each array consists of six Yagi aerials mounted at horizontal distances of $1{\cdot}2\,\lambda$ apart and at a height of $1{\cdot}57\,\lambda$ above the ground. They produce identical beams of elevation 8·5° and of half amplitude width ±5° and have a power gain of 165 over a half-wave dipole.

The minimum detectable signal at the receiver is 7×10^{-14} w., and in normal operation the peak power of the transmitter is 5 kw., with a pulse length of 8 microsec. Simultaneous visual and radio observations have shown that under these conditions the echo rate produced by an active shower, when the radiant is at 90° elongation to either of the aerial beams, corresponds closely to the rate of occurrence of visual meteors.

If the aerial characteristics are such that echoes can be detected down to the horizon, R_{max} is equal to the distance at which the meteor zone cuts the horizon circle of the station, and for a typical shower of medium velocity, for which the mean height of the zone can be taken as approximately 95 km., R_{max} = 1,100 km. Under these circumstances the time of maximum range, T, is the time at which the azimuth of the radiant differs from that of the beam by 90°. This would correspond to the transit of the radiant for aerials directed to the east or west. For aerials directed along azimuths $270°+\theta_1$ and $270°+\theta_2$, the echoes reach a maximum range at times $T+t_1$ and $T+t_2$. The time difference t_2-t_1 is a function of the declination, δ, of the radiant, θ_1, θ_2, and the latitude of the station. This function is plotted in Fig. 33 for the particular case of the radiant survey apparatus at Jodrell Bank ($\theta_1 = -28°$, $\theta_2 = +22°$ and lat. = 53° N.). From this curve the declination of the radiant may be found. t_1 and t_2 may be determined separately by using the curve labelled 1,100 km. in Fig. 34, and the time of transit then found from the observed values of $T+t_1$ and $T+t_2$.

It may be noted that t_1 is negative for radiants which transit south of

† Davies, J. G., and Ellyett, C. D. (see § 2).

the zenith and that echoes appear first in aerial 1 and then in aerial 2. For radiants which transit north of the zenith (decl. $> 53°$) this order is reversed, and $t_2 - t_1$ becomes negative. If the declination is greater than

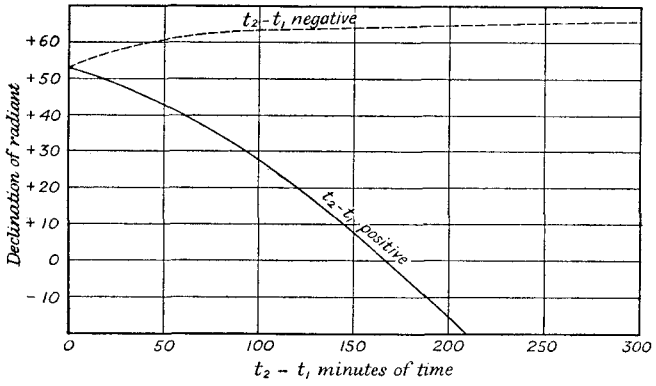

FIG. 33. Determination of declination from the times of maximum range occurrence in the radiant survey apparatus.

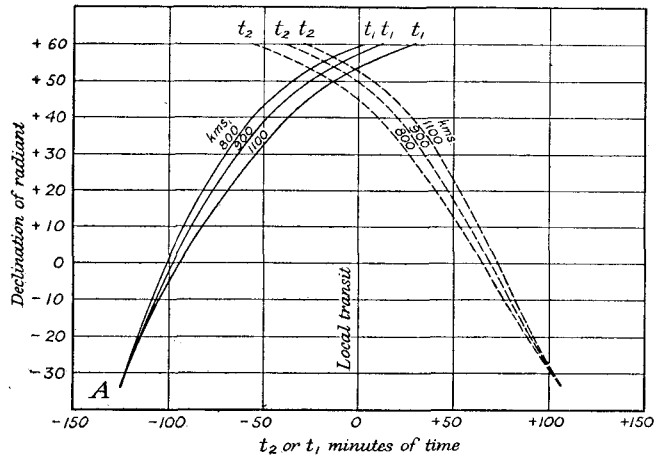

FIG. 34. Determination of right ascension from the times of maximum range occurrence in the radiant survey apparatus.

76° the echo zone never enters the coverage of aerial 2, but remains for many hours in the beam of aerial 1. A radiant position can still be determined, however, by fitting theoretical range curves to the range/time plots.

In practice, owing to the conditions governing the reflection of radio waves from the surface of the earth, the aerial sensitivity falls off rapidly in directions close to the horizontal, and echoes are never observed out

to ranges exceeding 1,000 km. Under these circumstances the time of occurrence of echoes of maximum range is advanced by an amount depending on the declination of the radiant and the observed value of R_{max}. This has been taken into account in the curves labelled 900 and 800 km. in Fig. 34, from which the time of transit is found, but since the displacement is to a close approximation the same for both aerials, the curve of Fig. 33 and the determination of declination are not affected. Finally, a small correction has to be applied if the mean height of the meteors in a stream is not 95 km. This correction, which affects only the time of transit, is given in Table 10.

The range-time plots for the Geminid showers of 1949 and 1950, which are shown in Fig. 35, provide a typical example of the results obtained with the apparatus. Times are shown as abscissae, and the ranges of individual echoes are indicated by the lengths of the vertical lines. The results obtained on each aerial between 00h. and 04h. U.T. on 1949 December 13 and 1950 December 13 are shown separately.

TABLE 10

Correction in Minutes of Time to be applied to Time of Transit for Various Heights of Meteor Showers

Height km.	*Declination δ*								
	−20°	−10°	0°	10°	20°	30°	40°	50°	60°
115	2	3	4	5	6	7	8	10	12
110	1	2	3	3	4	4	5	7	8
105	0	1	1	1	1	1	2	2	3
95	0	0	0	0	0	0	0	0	0
85	0	−1	−1	−1	−1	−1	−2	−2	−3
80	−1	−2	−3	−3	−4	−4	−5	−7	−8
75	−2	−3	−4	−5	−6	−7	−8	−10	−12

The plots in Fig. 35 show the variation in echo rate and range as the echo zone sweeps through each beam in turn. The occurrence of echoes at maximum range and the subsequent sharp fall in rate appear at about 01h. 10m. U.T. on the first aerial, and at about 02h. 40m. U.T. on the second aerial. The radiant positions obtained from these plots are as follows:

	Time of local transit	*Radiant coordinates*	
1949 Dec. 13	02 h. 14 m. U.T.	α 111·5°	δ 32·5°
1950 Dec. 13	02 h. 18 m. U.T.	α 112·2°	δ 32·5°

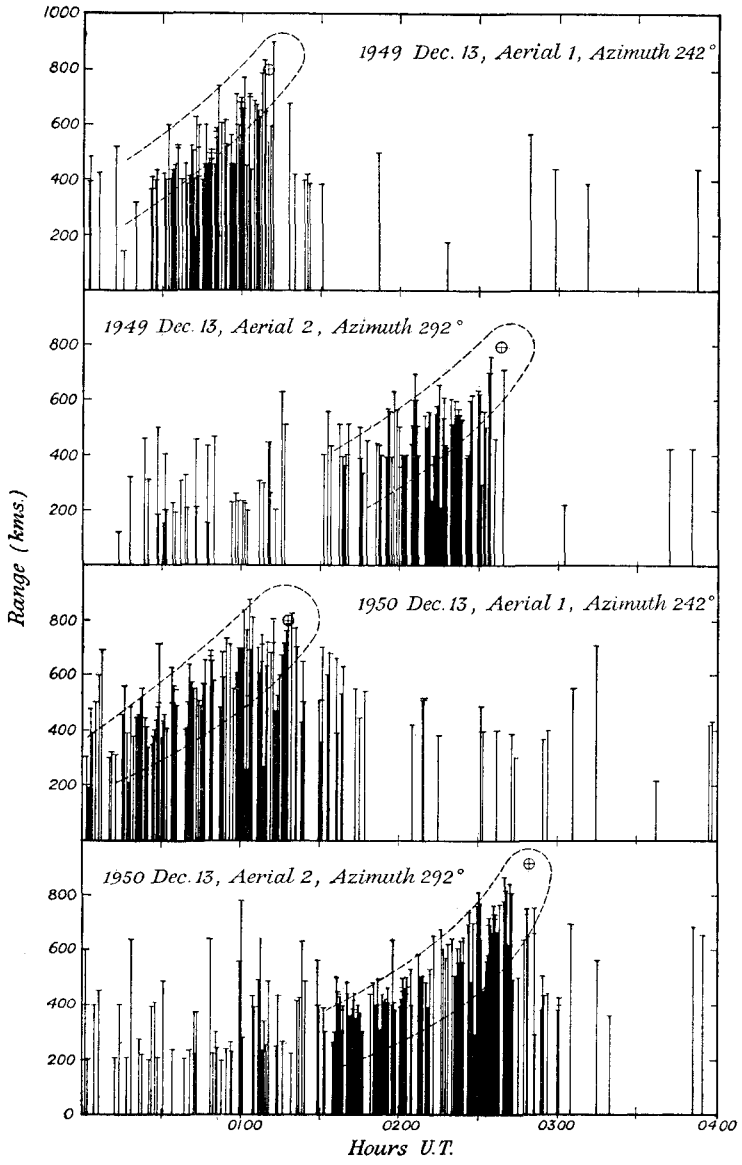

FIG. 35. Examples of range-time plots obtained with the radiant survey apparatus during the Geminid showers of 1949 and 1950 December.

The theoretical range-time plots for radiants in these positions are shown as broken lines in Fig. 35. They provide a useful indication of the diffuseness of the radiant, since, for a point radiant, all but sporadic meteors should fall inside the envelopes.

Examples of the range-time plots obtained during the summer day-time showers are given in Fig. 36.

The results with this apparatus during the major day-time and night-time showers have shown that if the echo rate exceeds 30 per hour, times t_1 and t_2 can be measured to within ± 5 minutes; which corresponds to an error of $\pm 1°$ in right ascension and $\pm 1{\cdot}5°$ in declination. In the

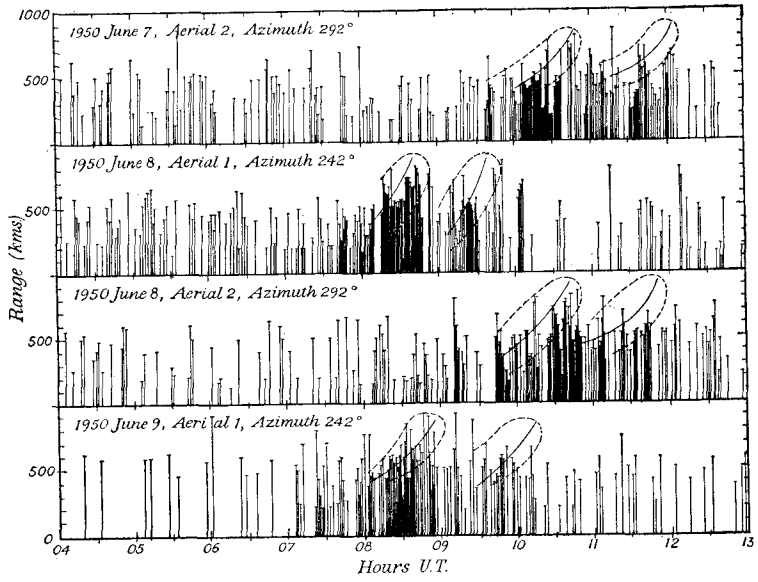

FIG. 36. Examples of range-time plots obtained with the radiant survey apparatus during the summer day-time streams. The examples include the Arietid and ζ-Perseid radiants (Chap. XVIII). The Arietid radiant culminates in aerial 1 at 08h. 30m.–09h. 00m. and in aerial 2 at 10h.–10h. 30m. In each case it is followed by the ζ-Perseid radiant.

exceptional case of a major stream with a radiant lying within 20° of the celestial pole the position must be determined by the curve-fitting method, and the accuracy is reduced. For weaker streams the accuracy falls off markedly with decreasing echo rate.

The apparatus can only resolve two radiants which are active simultaneously if their range-time plots on at least one of the aerials are separated by approximately 30 minutes. This time separation depends on the relative positions of the two radiants, and may be expressed in terms of their angular separation and relative position angle θ_0. Fig. 37 represents a small portion of the celestial sphere viewed internally, with two radiants at R_1, R_2. If ABC is the meridian bisecting the great circle arc $R_1 R_2$ at B, then θ_0 is defined as the angle ABR_2. Fig. 38 shows the angular

separation required for resolution on each of the two aerials, plotted as a function of θ_0 for different values of the declination of R_1. It is evident that any pair of radiants whose angular separation is greater than 20°

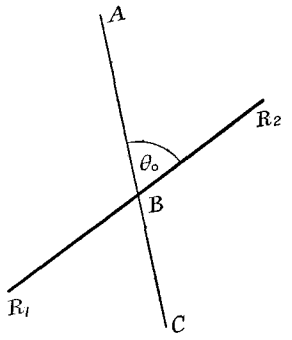

FIG. 37. Relative position angle θ_0 of radiants R_1 and R_2.

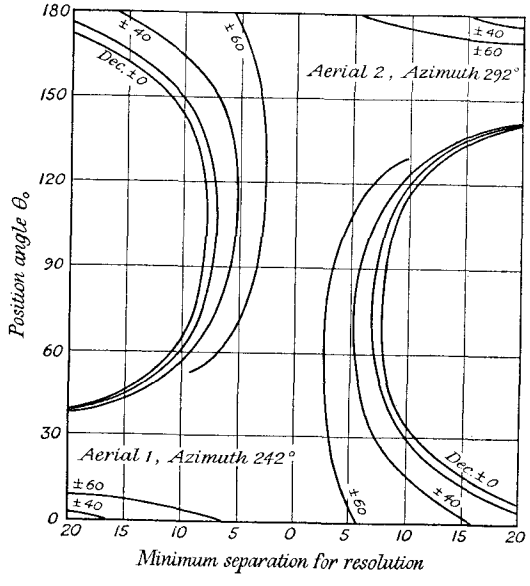

FIG. 38. Angular separation of two radiants required for resolution on each of the aerials of the radiant survey apparatus.

can be resolved by at least one of the two aerials, while for more favourable cases the degree of resolution is considerably higher than this.

All the radio-echo radiant determinations since 1949 quoted in Chapters XIII–XVIII have been made with this apparatus, which

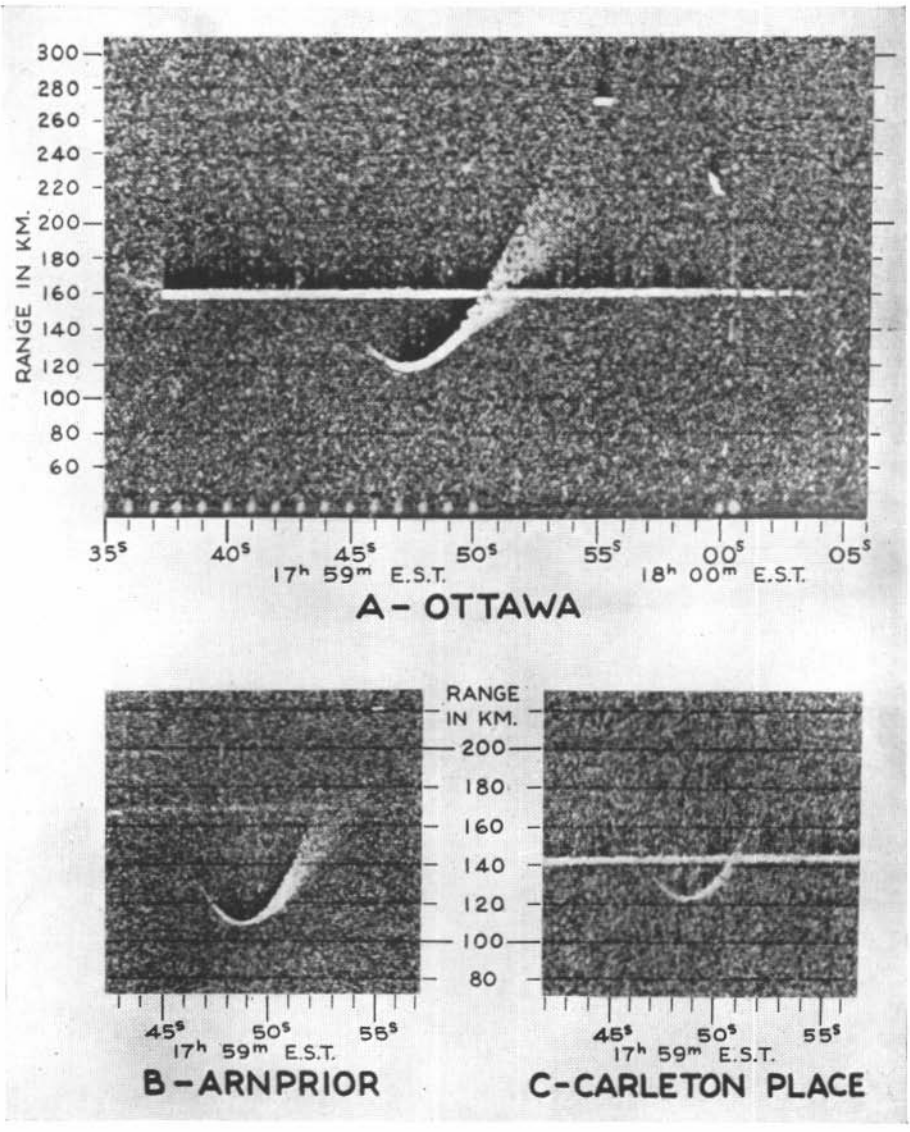

Meteor echoes photographed at three stations on 1948 August 4. (Reproduced by kind permission of Dr. D. W. R. McKinley and Dr. P. M. Millman.)

The photographs show:

(i) An echo of hyperbolic shape at 17h. 59m. 45–53s. from which the main data are obtained.

(ii) An echo at 17h. 59m. 37s., enduring for 27 sec. on the Ottawa record. This echo first appeared at a true height of 101 km. with bearing 197° and ground distance 120 km. from Ottawa. After 15 sec. the height of the echo was 94 km. and the apparent drift of the echo was about 20 km. in a south-east direction.

(iii) Visible on the Ottawa photograph only are an echo at 17h. 59m. 55s. range 270 km., duration one second, and an echo at 17h. 59m. 59s., range 228 to 216 km. As these echoes did not appear at the other stations it was not possible to triangulate heights and positions.

PLATE I

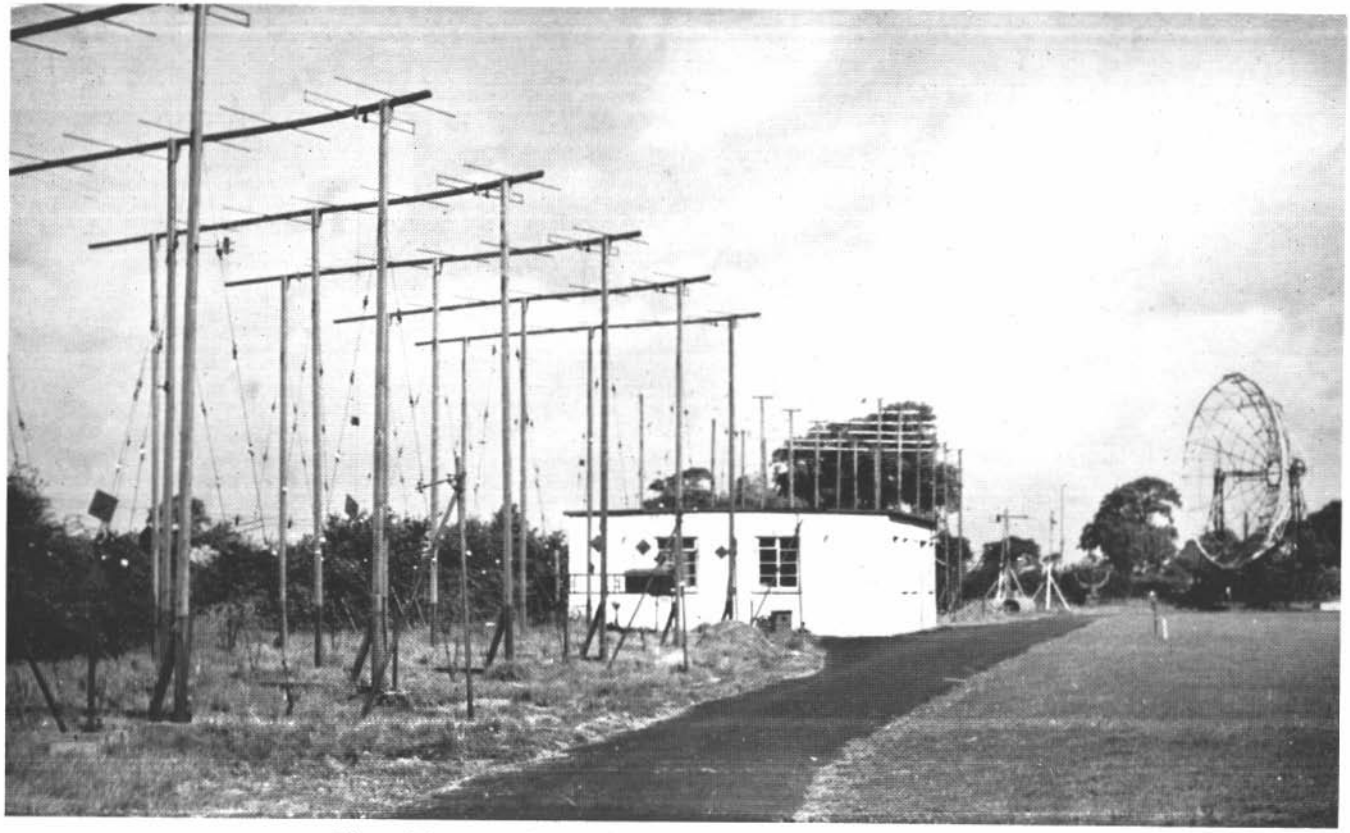

The aerial system of the radiant survey apparatus at Jodrell Bank.
In the right background can be seen a 30-ft. diameter steerable paraboloid.

PLATE II

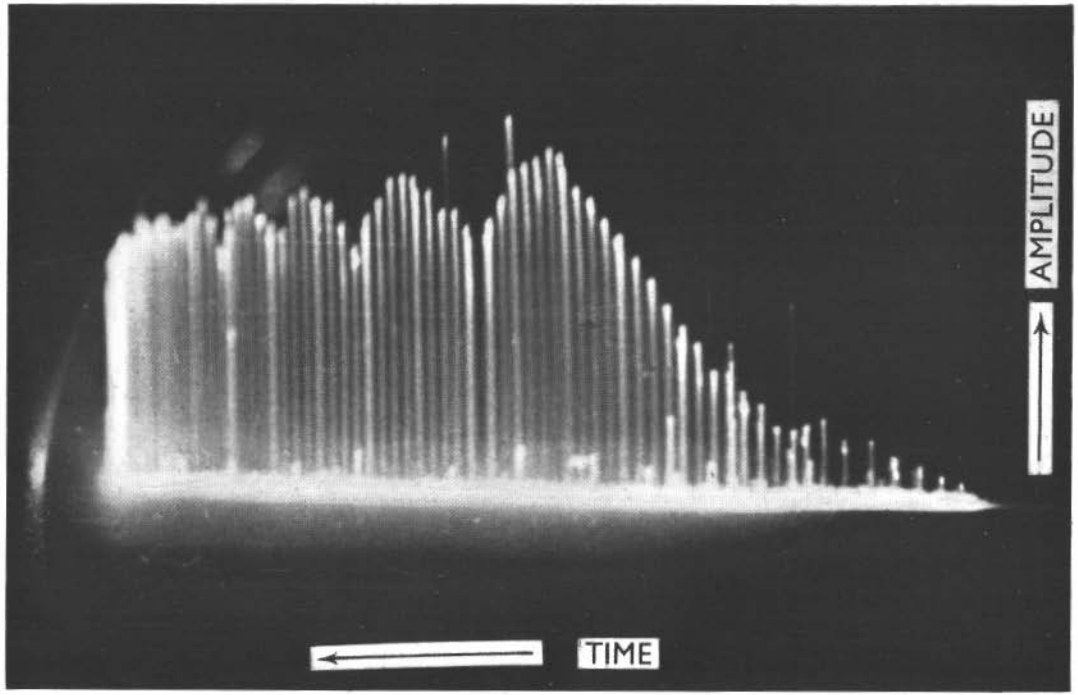

Diffraction pattern from a meteor trail obtained with pulsed radio-echo equipment. (Cf. theoretical shape in Fig. 39.)

The velocity of the meteor measured from the zone spacing was $51{\cdot}7 \pm 2{\cdot}3$ km./sec.

PLATE III

has also yielded the data on sporadic meteor radiants discussed in Chapter VI.

2. The application of radio techniques to the measurement of meteor velocities

Two distinct radio-echo methods of measuring meteor velocities have been developed. The first records the range of the meteor against time and can only be used satisfactorily with densely ionizing meteors under conditions when a radio echo is returned from the ionization near the head of the meteor. The second, more generally applicable method, records the amplitude variations with time as the meteor crosses the foot of the perpendicular from the observing station to the trail. This involves only a very short time interval near the instant when the meteor is at the perpendicular point and, in principle, can be employed for any meteor which gives a strong enough echo to be recorded. With conventional equipment of the type already discussed the number of meteors susceptible to velocity measurements by the two methods is about 1,000 to 1 in favour of the amplitude-time method. The range-time method is important, however, in the case of densely ionizing meteors which can be observed over a considerable length of their path since measurements of deceleration become possible, and triangulation enables the orbit of a single meteor to be determined as described in § 1 (*b*).

(*a*) *Range-time Methods*

In this method a pulsed transmitter is used and the received echo is displayed on an intensity-modulated range-time display. If the radio wave-length is long enough, and the ionization is sufficiently dense, then an echo may be recorded from parts of the ionized trail which are at a distance from the perpendicular reflecting point. In this case, as discussed in § 1 (*b*), the recorded echo will be in the shape of a hyperbola as given by equation (1 a). An extremely good example of this type of echo obtained by McKinley and Millman† is shown in Plate I. In this, both the approach and the regression of the meteor can be observed.

The production of a radio echo from the neighbourhood of the minimum range point (R_0) in terms of diffraction from a line source is now well understood (cf. Chap. III and later in this chapter). It is unlikely, however, that echoes of the type illustrated in Plate I can be explained in this way (that is apart from the minimum range point reflection). The intensity of the diffracted echo will vary inversely as the distance from R_0 and should therefore be very weak for remote

† McKinley, D. W. R., and Millman, P. M., *Canad. J. Res.* **27** (1949), 53.

points and increase steadily near R_0. The echoes do not show this behaviour, however, and have other features which make such an explanation of the reflection untenable. It seems certain that some mechanism exists in these densely ionizing meteors which is capable of giving a reflection from the ionization near the head of the meteor. No satisfactory explanation of the mechanism exists. It must differ from the conventional meteoric ionization processes discussed in Chapter III because if the idea of reflection from a line source is abandoned, then a considerable area of ionized matter above the critical density must exist in the region of the head. One hypothesis advanced by McKinley and Millman† is that ultra-violet light from the head of the meteor instantly ionizes the air at a considerable distance from the meteor. The echoing area of such a cloud would be relatively independent of the angle of incidence of the radio waves.

The geometrical analysis of the reflection of radio waves from such a 'moving-ball' type of target was considered by Manning,‡ who worked out the interference effects and the frequency of the Doppler whistle which would be observed when c.w. radio waves reflected from such a target interacted with the direct ground wave. Manning applied his analysis to all types of meteor echoes, the majority of which we now believe to arise from scattering near the R_0 point only and to be explained by the diffraction theory (§ 2 (*b*)). In actual fact Manning's analysis is now believed to apply only to the rare cases of the echoes discussed in this section. In fact, in the case of such densely ionizing meteors, McKinley§ has given evidence of the simultaneous observation of both the interference and diffraction effects near the R_0 point.

The first range-time velocity measurements were made by Hey, Parsons, and Stewart‖ during the great Giacobinid meteor shower of 1946 October. Although their apparatus worked on the comparatively short wave-length of 5 m. the shower contained meteors of sufficient magnitude to yield twenty-two faint fast-moving echoes prior to the R_0 echo from which they were able to measure the velocity†† by application of equation (1 a). The experiment is of great historic interest in representing the first successful measurements of meteor velocities by radio methods. The range-time methods were later developed further

† McKinley, D. W. R., and Millman, P. M., *Proc. Inst. Radio Engrs.* **37** (1949), 364; McKinley, D. W. R., *J. Appl. Phys.* **22** (1951), 202.

‡ Manning, L. A., *J. Appl. Phys.* **19** (1948), 689.

§ McKinley, D. W. R., loc. cit.

‖ Hey, J. S., Parsons, S. J., and Stewart, G. S., *Mon. Not. Roy. Astr. Soc.* **107** (1947), 176.

†† See Chap. XVI.

by McKinley and Millman† using longer radio wave-lengths in the region of 10 m., and have been applied by them to the measurement of velocities and of decelerations.‡ On these longer wave-lengths the echoes of hyperbolic shape appear more frequently and extend over a considerably greater path length than those observed by Hey, Parsons, and Stewart. Four methods of measuring the velocity from a range-time echo such as that illustrated in Plate I have been described by McKinley and Millman.§

(i) *Curve-fitting method.* Hyperbolic curves may be fitted directly to an enlargement of the echo and the best fit determined by trial and error. Owing to the various small distortions which are present in the record it is preferable to transfer the curve point by point to Cartesian co-ordinate paper, introducing any necessary corrections to each R and t point. A series of hyperbolic curves is then constructed with the observed values of R_0 and t_0 and various values of v, from which the probable upper and lower limits of v can be assigned.

(ii) *Range* $\times$ dR/dt *method.* Plate I is a good example of a range-time record which includes the (R_0, t_0) point, but in many cases only segments of the hyperbola are recorded, excluding this minimum range point. In this case the velocity can be derived from the curvature of the segment. Differentiating equation (1 a) (p. 54),

$$R\frac{dR}{dt} = v^2t - v^2t_0. \tag{5}$$

The slope of $R\dfrac{dR}{dt}\Big/t$ is therefore v^2. This curve can be constructed from the measured value of dR/dt along the segment.

(iii) *Three-point method.* In (1 a) v^2 may be evaluated by substituting three values of R and t from widely different parts of the observed curve. v is then given by

$$v^2 = \frac{R_1^2(t_3-t_2) - R_2^2(t_3-t_1) + R_3^2(t_2-t_1)}{(t_2-t_1)(t_3-t_2)(t_3-t_1)}. \tag{6}$$

(iv) *Parabolic regression method.* The velocity may also be computed by using the curvilinear regression method of least squares.‖ In (1 a) if R^2 is replaced by $\bar{\rho}$ then the observed values give a parabolic relation between $\bar{\rho}$ and t. The equations are then solved in the usual manner.

† Millman, P. M., and McKinley, D. W. R., *J. Roy. Astr. Soc. Can.* **42** (1948), 121; McKinley, D. W. R., and Millman, P. M., *Canad. J. Res.* **27** (1949), 53; McKinley, D. W. R., *J. Appl. Phys.* **22** (1951), 202.

‡ McKinley, D. W. R., loc. cit.

§ McKinley, D. W. R., and Millman, P. M., loc. cit.

‖ See, for example, Hoel, P. G., *Introduction to Mathematical Statistics*, Wiley, N.Y., 1947.

McKinley and Millman used all four methods in treating the example shown in Plate I, and found that the results agreed within the limits of error. The greatest source of error in the range-time measurements lies in the ambiguity as to the real outline of the echo hyperbola. In general it would appear to be difficult to reduce the final errors in the velocity below 1 or 2 per cent.

After the pioneer measurements of Hey, Parsons, and Stewart on the Giacobinid shower the range-time technique for velocity measurement has been almost exclusively developed by McKinley and Millman. Even on the long wave-lengths used by them the number of echoes suitable for analysis of this type is rather small and the greatest value of the technique is for special purposes such as measurement of decelerations, or the orbits of single meteors from three-station triangulation. The major part of the work on the measurement of meteor velocities has been carried out using one of the amplitude-time methods described below.

(b) Amplitude-time Methods

The diffraction theory of the scattering of radio waves from the neighbourhood of the R_0 point on a meteor trail was first given by Lovell and Clegg.† The idea that the change in intensity of the echo as the meteor passed the R_0 point might be used to measure the velocity was due to Herlofson‡ and the first successful application of the idea to measure velocities was made by Davies and Ellyett§ using the pulse method. Subsequently, continuous-wave techniques were applied to the problem by Manning, Villard, and Peterson,‖ and by McKinley.†† The shape of the diffraction pattern to be expected, and the strict analogy with the optical case of diffraction, was demonstrated by Davies and Ellyett.§ A later, more comprehensive, treatment by McKinley†† included various aspects of the continuous-wave case, and will be followed here.

Equation (1 a) will be written in the form

$$R^2 = R_0^2 + v^2(t-t_0)^2 = R_0^2 + s^2, \tag{7}$$

where s is the distance along the meteor path measured from the minimum range point (R_0, t_0). The wave scattered from an element of meteor

† Lovell, A. C. B., and Clegg, J. A., *Proc. Phys. Soc.* **60** (1948), 491. (See also Chap. II.)

‡ Herlofson, N., *Rep. Phys. Soc. Progr. Phys.* **11** (1948), 449.

§ Davies, J. G., and Ellyett, C. D., *Phil. Mag.* **40** (1949), 614; Ellyett, C. D., and Davies, J. G., *Nature*, **161** (1948), 596.

‖ Manning, L. A., Villard, O. G., and Peterson, A. M., *J. Appl. Phys.* **20** (1949), 475.

†† McKinley, D. W. R., *Astrophys. J.* **113** (1951), 225.

path ds will be

$$dA = g(R, \alpha_0)\sin\left(\omega t - \frac{4\pi R}{\lambda}\right) ds, \tag{8}$$

where ω and λ refer to the radio wave and $g(R, \alpha_0)$, involving the range and electron line density α_0, is a function which has been evaluated by Lovell and Clegg.† Since we are only concerned with a short section of the trail, $g(R, \alpha_0)$ will be treated as a constant. Then if the meteor is first detected at point s_1, the resultant instantaneous amplitude of the signal reflected from the section $s_1 s$ will be given by

$$A_r = g(R, \alpha_0) \int_{s_1}^{s} \sin\left(\omega t - \frac{4\pi R}{\lambda}\right) ds. \tag{9}$$

The integral can be evaluated by using the approximation near the t_0 point

$$R \simeq R_0 + (s^2/2R_0).$$

Writing

$$\Phi = \omega t - \frac{4\pi R_0}{\lambda}$$

and

$$\frac{\pi x^2}{2} = \frac{2\pi s^2}{R_0 \lambda},$$

$$A_r = E_r \int_{x_1}^{x} \sin\left(\Phi - \frac{\pi x^2}{2}\right) dx, \tag{10}$$

where E_r has the dimensions of field strength and is constant for a given meteor. Equation (10) may be expanded as

$$A_r = E_r(C \sin\Phi - S\cos\Phi), \tag{11}$$

where

$$C = \int_{x_1}^{x} \cos\frac{\pi x^2}{2}\, dx$$

and

$$S = \int_{x_1}^{x} \sin\frac{\pi x^2}{2}\, dx,$$

(C and S are the conventional Fresnel integrals of optical theory.) The frequency of the variations in C and S are small compared with ω. It can be shown that the contribution from the lower limit x_1 is generally negligible, and hence the lower limit can be taken as $-\infty$.

† Lovell, A. C. B., and Clegg, J. A., *Proc. Phys. Soc.* **60** (1948), 491. (See also Chap. II.)

The intensity of the reflected wave is given by (11) as

$$I_r = E_r^2(C^2+S^2), \tag{12}$$

an expression identical with that for the case of diffraction of light at a straight edge. It represents a steadily increasing intensity up to the t_0 point after which the intensity oscillates about a final mean value as shown in Fig. 39.

(i) *Pulse techniques for observation of the diffraction pattern.* The demonstration that the reflected wave followed the amplitude-time pattern of Fig. 39 was first made by Ellyett and Davies.† Special

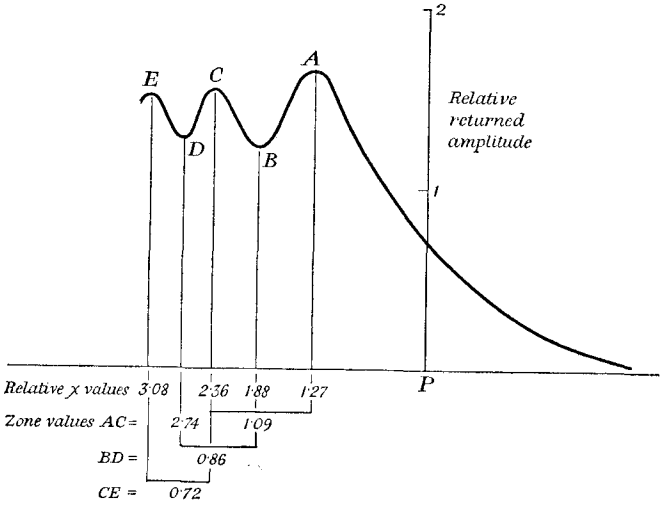

FIG. 39. The theoretical amplitude-time pattern to be expected as the meteor crosses the foot of the perpendicular P from the observing station to the trail.

technical developments were necessary in order to observe the diffraction pattern. On the wave-lengths used (say $\lambda = 4$ m.) the zone lengths are of the order of 0·5 km. for a meteor at a range of 100 km.; thus for meteor velocities of the order of 40 km./sec. the time intervals between successive maxima and minima are milliseconds only. In order to observe the amplitude variations of the scattered echo within this period the transmitter was pulsed at a recurrence frequency of about 600 per second giving a separation between pulses of about 1·7 millisec. The echo was photographed on a single-stroke time base of speed sufficient to resolve the individual pulses, giving an amplitude-time record of the type illustrated in Plate III in which the zone pattern is

† Ellyett, C. D., and Davies, J. G., loc. cit.

well in evidence. Since the measurements are required within the first few milliseconds of the life of an echo, the recording apparatus must be triggered by the echo itself with a minimum delay. This introduces the problem of making an apparatus which selects automatically a meteor echo in favour of the various noise impulses and other forms of interference which are always present. The technical solution of this problem and other details of the apparatus have been described by Davies and Ellyett.† The range of the echo was measured simultaneously by photographing a separate conventional range-time display.

The proof that the observed echo patterns similar to Plate III were actually the diffraction effects given by equation (12) was made by measuring the meteors in a shower of known homogeneous velocity, such as the Geminids. Then if v_0 is the apparent geocentric velocity of the meteors in the homogeneous group, p the number of pulses observed between specific zone maxima or minima, t the interval between specific zone maxima or minima, and f_0 the pulse recurrence frequency, it is evident that

$$v_0 = \frac{x}{2} f_0 \frac{\sqrt{(R\lambda)}}{p}. \tag{13}$$

Thus, for a series of meteors with identical velocities,

$$x \frac{\sqrt{R}}{p} = \text{const.}, \tag{14}$$

and, if such meteors are observed at various ranges, widely varying values should be obtained for $(x/p)_{mean}$ (which is a measure of the time required to traverse a Fresnel zone); but the values of $(x/p)_{mean} \sqrt{R}$ should remain constant. The validity of this result was first established by Davies and Ellyett during the Geminid meteor shower of 1947 December.

This pulse technique has since been extensively used at Jodrell Bank for the measurement of the velocities of shower and sporadic meteors, and many of the results are contained in later chapters.

(ii) *Continuous-wave techniques for the observation of the diffraction pattern.* If the transmitter radiates continuous waves instead of pulses then the fundamental diffraction theory given above will still apply but the recorded envelope will be continuous. If, in addition, the signal scattered from the meteor trail is allowed to beat with a direct ground wave from the transmitter then the diffraction pattern can be observed

† Davies, J. G., and Ellyett, C. D., loc. cit.

both before and after the minimum range point.† The extension of the diffraction theory given above to the case of continuous-wave signals with ground wave injection has been given by McKinley.‡

Suppose the receiver picks up a small fraction of the transmitted power directly of amplitude A_d given by

$$A_d = E_d \sin\left(\omega t - \frac{2\pi D}{\lambda}\right), \tag{15}$$

where D is the distance between transmitter and receiver. This will be added to the amplitude A_r from the meteor, given by equation (11), producing the combined intensity:

$$I_{r+d} = E_r^2(C^2+S^2)+E_d^2+2E_r E_d(C\cos\psi - S\sin\psi) \tag{16}$$

$$= (E_r C+E_d\cos\psi)^2+(E_r S - E_d\sin\psi)^2, \tag{17}$$

where $\psi = \dfrac{2\pi(2R_0-D)}{\lambda}$ is the phase difference between the direct and reflected paths at time t_0.

The signal actually obtained at the receiver output will depend on the type of detector. A square-law detector will reproduce the intensities given by (12), (16), and (17) directly. A linear detector will follow the square root of the intensity. The theoretical wave forms can be calculated for various ψ values and ratios of A_d to A_r. They are given in Fig. 40 for equal intensities of direct and reflected waves ($E_d^2 = 2E_r^2$) and in Fig. 41 for $2E_r^2 < E_d^2$.

If the region ($-1 > x > 1$) around the t_0 point is excluded, Cauchy's approximations for the Fresnel integrals give (assuming x_1 to be $-\infty$):

On the approach side of t_0, (−s)

$$C = \frac{1}{\pi x}\sin\frac{\pi x^2}{2}, \qquad S = -\frac{1}{\pi x}\cos\frac{\pi x^2}{2}.$$

On the receding side of t_0, (+s)

$$C = 1+\frac{1}{\pi x}\sin\frac{\pi x^2}{2}, \qquad S = 1-\frac{1}{\pi x}\cos\frac{\pi x^2}{2}.$$

† The term 'Doppler whistle' is often applied to the echoes obtained by the continuous-wave method because if the output of the receiver is connected to a loudspeaker, a whistle of varying pitch is heard (see, for example, Chap. II). The original idea that these whistles were a true Doppler effect arising from the wave reflected from the head of the meteor beating with the ground wave has been abandoned, since it can only occur in relatively infrequent cases of meteors of exceptional brightness. It is now recognized that the whistles arise from the amplitude and frequency changes in the diffraction patterns discussed in this chapter. Actually there is little difference in the calculated 'whistle' frequencies (except near the t_0 point) given by the interference and diffraction theories.

‡ McKinley, D. W. R., *Astrophys. J.*, loc. cit.

Thus

$$I_r(-s) = \frac{E_r^2}{\pi^2 x^2}, \tag{18}$$

$$I_r(+s) = 2E_r^2 + \frac{E_r^2}{\pi^2 x^2} + \frac{2\sqrt{2}}{\pi x} E_r^2 \sin\left(\frac{\pi x^2}{2} - \frac{\pi}{4}\right). \tag{19}$$

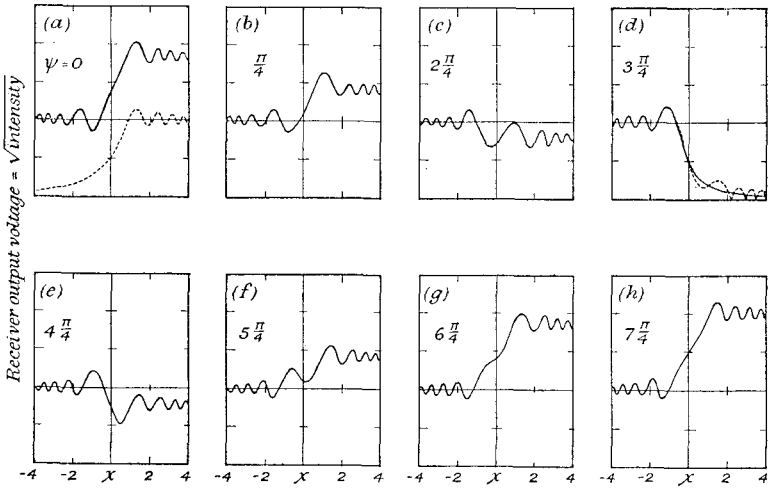

FIG. 40. Theoretical amplitude-time records. $2E_r^2 = E_d^2$.

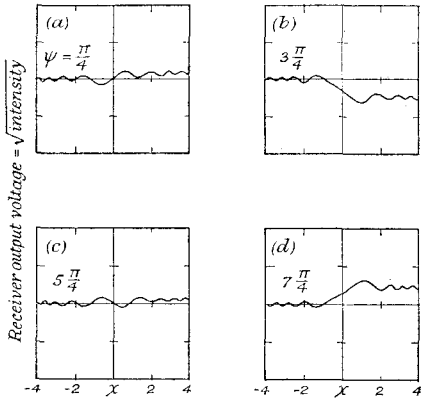

FIG. 41. Theoretical amplitude-time records. $2E_r^2 < E_d^2$.

Equations (18) and (19) are together equivalent to (12). Thus for the case of the reflected and ground wave

$$I_{r+d}(-s) = \frac{E_r^2}{\pi^2 x^2} + E_d^2 + \frac{2E_r E_d}{\pi x} \sin\left(\frac{\pi x^2}{2} + \psi\right), \tag{20}$$

which shows that the diffraction effect is also now observed on the

approach side, whereas without the ground wave it is only observed on the receding side.

After t_0

$$I_{r+d}(+s) = E_d^2 + 2E_r^2 + \frac{E_r^2}{\pi^2 x^2} - 2\sqrt{2}\, E_r E_d \sin\left(\psi - \frac{\pi}{4}\right) + \\ + \frac{2E_r}{\pi x}\left[E_d^2 + 2E_r^2 - 2\sqrt{2}\, E_r E_d \sin\left(\psi - \frac{\pi}{4}\right)\right]^{\frac{1}{2}} \times \\ \times \sin\left\{\frac{\pi x^2}{2} - \tan^{-1}\left(\frac{E_r - E_d \sin\psi}{E_r + E_d \cos\psi}\right)\right\}. \quad (21)$$

If **t** is the time relative to the t_0 point then the instantaneous frequency of the oscillatory terms in (19), (20), (21) can be shown to be

$$\mathbf{f} = \frac{2v^2}{R_0 \lambda}\mathbf{t}. \quad (22)$$

Thus the slope of **f** against **t** is proportional to the square of the meteor velocity which can be calculated if R_0 is also measured. As mentioned above, this measurement requires a separate pulsed equipment.

Equation (22) is the same relationship obtained by Manning† working on the basis of a 'moving-ball' type of target giving an interference effect. The agreement is fortuitous since the interference theory does not predict the other characteristics of the observed echoes, and, as discussed on p. 74, it is now believed to apply only to the infrequent cases of very large densely ionizing meteors.

The c.w. methods for velocity measurement have been used at Stanford by Manning, Villard, and Peterson‡ and most extensively by McKinley§ at Ottawa, whose technique will serve as an illustration of the experimental arrangements. The continuous-wave transmitter had a c.w. output of 1·5 kw. on 30·02 mc./sec. and fed into a half-wave dipole mounted a quarter wave-length above ground. A similar dipole was used as receiver, the axis of the two being collinear in order to reduce pick up of the direct ground wave. The receiving site was 7·5 km. from the transmitter. Two types of recording were used. In the so-called 'slow Doppler' method which was generally used, the receiver output was applied to a cathode-ray tube as vertical amplitude modulation of a horizontally moving trace which was photographed by a film moving vertically at 4 inches per minute. This speed was the same as that of the film recording the intensity-modulated range-time trace of the pulsed

† Manning, L. A., *J. Appl. Phys.* **19** (1948), 689.
‡ Manning, L. A., Villard, O. G., and Peterson, A. M., ibid. **20** (1949), 475.
§ McKinley, D. W. R., *Astrophys. J.* **113** (1951), 225.

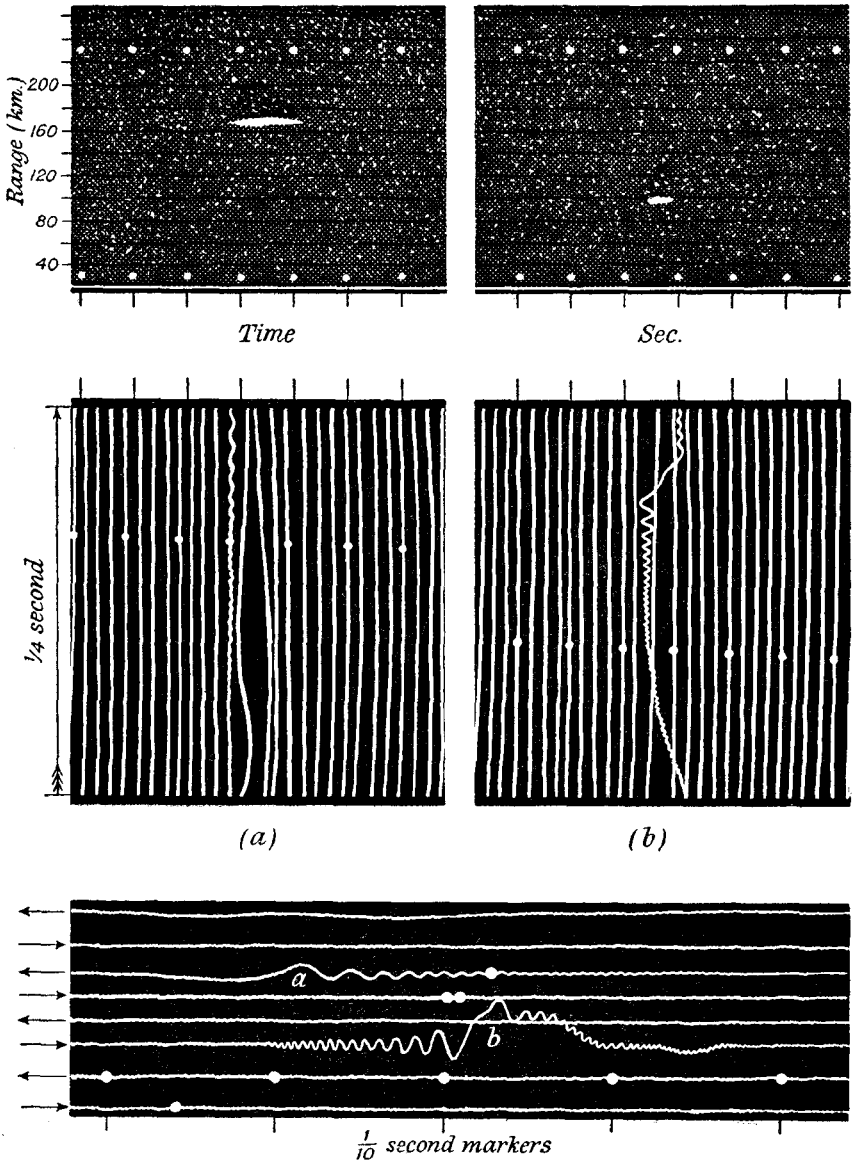

FIG. 42. Two meteor echoes. Velocities: (*a*) 28 km./sec.; (*b*) 47 km./sec. Top: range-time record (using pulsed equipment). Centre: c.w. amplitude-time record, 'slow Doppler' method. Bottom: c.w. amplitude-time record, 'fast Doppler' method.

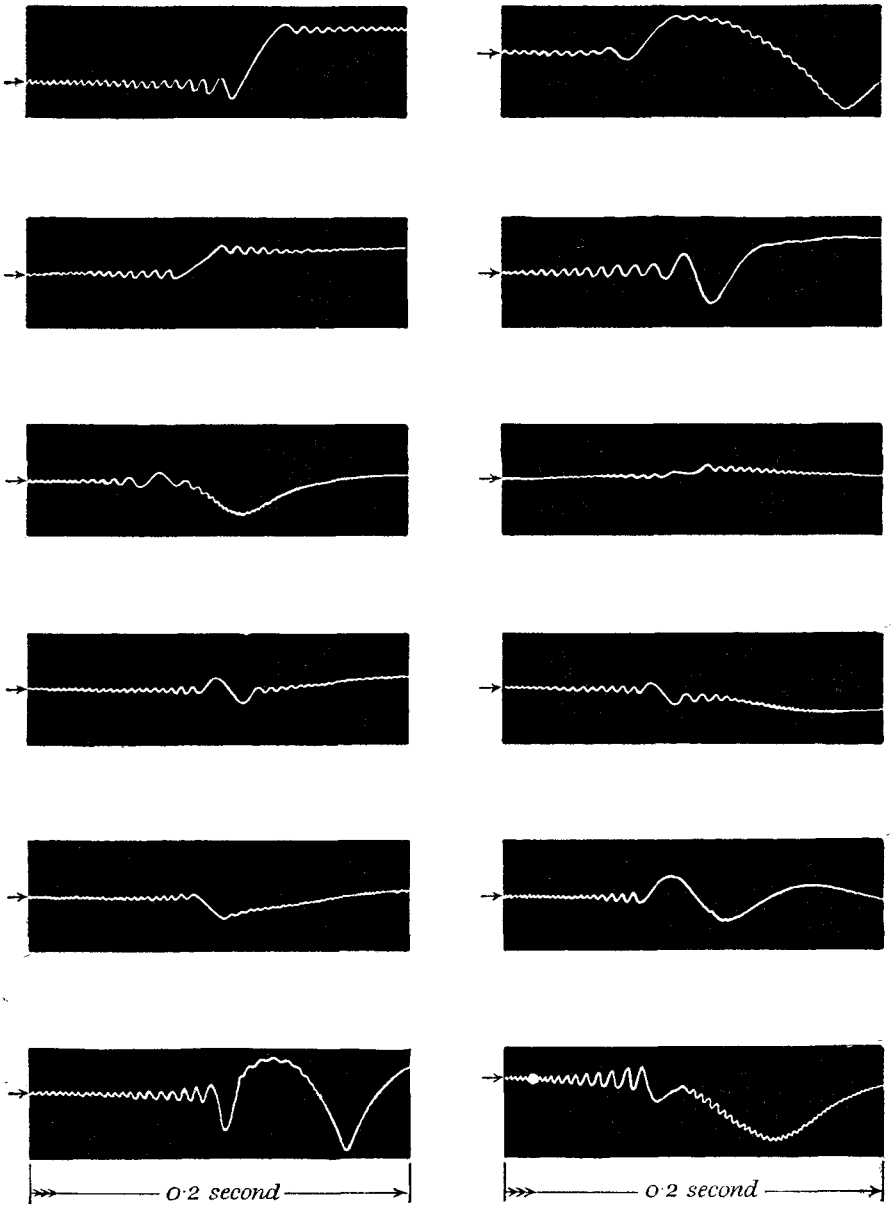

FIG. 43. Some examples of observed amplitude-time meteor echo records on a c.w. equipment recorded with the 'fast Doppler' system.

apparatus for range measurement. Records of this type are shown in Fig. 42 (*a*) and (*b*). The top records in each are the conventional range-time records of the pulsed system for range measurement. In the centre records the cathode-ray tube spot moves from the bottom to top in $\frac{1}{4}$ second, flashes back in a millisecond, and repeats while the record moves slowly to the right. In the other method—the 'fast Doppler'—the amplitude modulation is applied horizontally to a stationary cathode-ray tube spot and the film is drawn past at 4 inches per *second*. The equivalent 'fast Doppler' records of the meteors in Fig. 42 (*a*) and (*b*) are shown in the lower reproduction. Fig. 43 shows other examples of the 'fast Doppler' records, some of which show striking similarities to the theoretical patterns of Figs. 40 and 41.

In most of his velocity reductions McKinley† measured the time interval Δt between the m-th and n-th cycles and calculated the velocity from

$$v = \sqrt{(R_0 \lambda)}\left(\frac{\sqrt{n} - \sqrt{m}}{\Delta t}\right). \tag{23}$$

The probable error of the measurements, including contributions from all sources, was estimated as 5 per cent.

Many of the velocity measurements made by these c.w. techniques are referred to in later chapters on the sporadic and shower meteors. In comparing the c.w. and pulse techniques of amplitude-time velocity measurements, it is evident that the c.w. method has certain advantages in that the diffraction pattern can be observed both before and after the t_0 point, the zones are often more clearly defined and generally more are available for measurement than in the pulse case. There is, however, the great disadvantage that three separate aerial systems are needed—one at the transmitter, one at the receiver, which has to be separated by some kilometres for satisfactory ground-wave injection, and one for the separate pulse apparatus required for range measurement. Little difficulty arises as long as simple dipole systems are used, but when high-gain aerials are used for the investigation of faint meteors the c.w. system is scarcely a practicable alternative to the pulse arrangement which requires only a single aerial.

† McKinley, D. W. R., *Astrophys. J.*, loc. cit.

V

THE FUNDAMENTAL EQUATIONS OF METEORIC MOTION

It has already been mentioned in Chapter II that on the night of the great shower of Leonid meteors, 1833 November 12–13, many observers recognized that the meteors appeared to be diverging from a point in the sky. Very soon Olmsted and Twining suggested that the shower was caused by a cloud of particles through which the earth passed, and the idea of a periodic phenomenon arose. The quantitative developments of these ideas, which emphasized the importance of determining the spatial orbits of the meteoric particles, were made by Schiaparelli, H. A. Newton, and others in the second half of the nineteenth century.

Much of the observational effort described in this book has been devoted to the measurement of two quantities. Firstly the radiant, that is the point in space from which a meteor appears to originate, or in the case of a shower the point or area of space from which the meteors appear to diverge. Secondly the velocity with which the meteor—or, in the case of a shower, the meteors—travel in the earth's atmosphere. If these two quantities are known then it is possible to calculate the spatial orbit of the meteor. The computation is based on well-known principles of celestial mechanics and has been described by Olivier,† Porter,‡ and many others. The method will be summarized in this chapter in order to define the terms which occur later in the text.

1. The elements of the orbit

In Fig. 44 the sun S is at one focus of the ellipse PBA, with semi-major axis a and semi-minor axis b. If e is the eccentricity then the perihelion distance $q = a(1-e)$ and the aphelion distance $q' = SA = a(1+e)$. PA is the line of apsides. The semi-latus rectum $p = a(1-e^2)$. In the case of a hyperbola ($e > 1$), a will be negative. In the case of a parabola ($e = 1$) the shape of the orbit is defined completely by q, with $p = 2q$.

In Fig. 45, i is the inclination of the plane of the orbit to the plane of the ecliptic. If $i > 90°$ the motion of the meteor is retrograde (that is opposite to the direction of motion of the planets). The ascending node ☊ is the point at which the meteor passes from the south to north side

† Olivier, C. P., *Meteors*, 1925.
‡ Porter, J. G., *Comets and Meteor Streams*, Chapman & Hall, 1952.

of the ecliptic, and conversely for the descending node ☋. If ♈ is the vernal equinox in the plane of the ecliptic, then the longitude of the node is $\gamma\widehat{S}\Omega$, and Ω will be used for this angle. Clearly ☋ = $\Omega \pm 180°$. The angle $\Omega\widehat{S}P$ measured in the plane of the orbit is the argument of perihelion ω. The longitude of perihelion $\pi = \Omega + \omega$ is sometimes used.

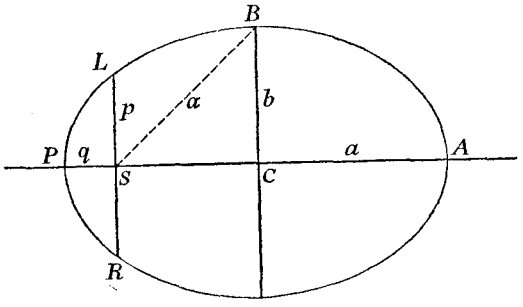

FIG. 44. Some elements of the meteor orbit.

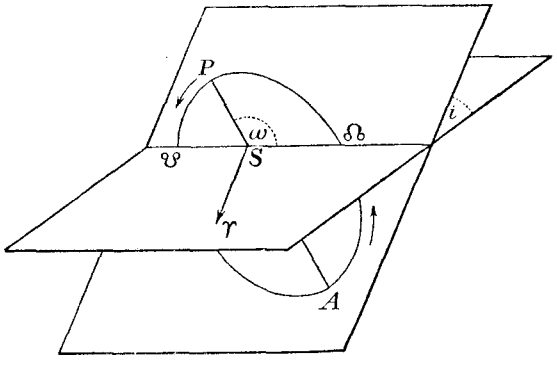

FIG. 45. The plane of the orbit.

Hence the size of the meteoric orbit is defined by a, its shape by e, the orientation of its plane in space by i and Ω, and the direction of the major axis in that plane by ω. The position in the orbit has to be defined by a sixth element—the time of perihelion passage T—given by angles known as 'anomalies'. In Fig. 46, if the meteor is at M, then the angle between the radius vector r and the line of apsides is the true anomaly ν. The eccentric anomaly is the angle E, the construction being evident from Fig. 46. The mean anomaly $M = n(t - T)$, where n is the mean daily motion in degrees and t the date.

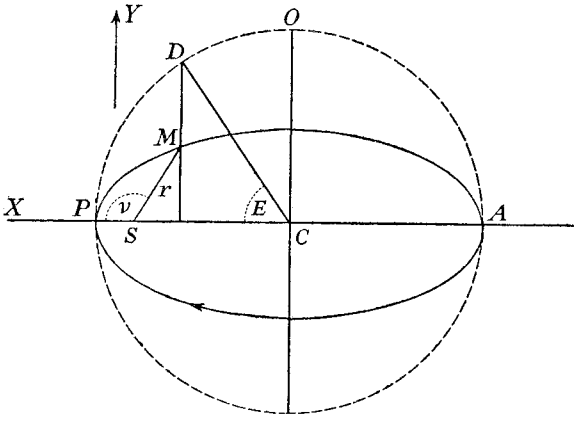

FIG. 46. True and eccentric anomalies.

2. The velocity of the meteor in its orbit

If, in Fig. 46, the sun S is taken as the origin of X and Y axes in the plane of the orbit then

$$\left.\begin{aligned} x &= r\cos\nu \\ y &= r\sin\nu \end{aligned}\right\}. \tag{1}$$

The velocity $\bar{V}$ of the meteor in the orbit is given by

$$\bar{V}^2 = \left(\frac{dx}{dt}\right)^2 + \left(\frac{dy}{dt}\right)^2 \tag{2}$$

$$= r^2\left(\frac{d\nu}{dt}\right)^2 + \left(\frac{dr}{dt}\right)^2. \tag{3}$$

This can be expressed in terms of r and a as follows:

The accelerations along X and Y are given by

$$\left.\begin{aligned} d^2x/dt^2 &= -A\cos\nu = -Ax/r \\ d^2y/dt^2 &= -A\sin\nu = -Ay/r \end{aligned}\right\}. \tag{4}$$

Thus

$$x\,d^2y/dt^2 - y\,d^2x/dt^2 = 0, \tag{5}$$

the integral of which is

$$x\,dy/dt - y\,dx/dt = h, \tag{6}$$

where h is the constant of integration.

Transferring to polar coordinates,

$$r^2\frac{d\nu}{dt} = h. \tag{7}$$

Further, from equations (4),

$$\frac{x}{r}\frac{d^2x}{dt^2}+\frac{y}{r}\frac{d^2y}{dt^2}=-A, \tag{8}$$

which becomes

$$\frac{d^2r}{dt^2}-r\left(\frac{d\nu}{dt}\right)^2=-A \tag{9}$$

in polar coordinates.

Since

$$r=\frac{p}{1+e\cos\nu}, \tag{10}$$

then, using (7),

$$\frac{dr}{dt}=\frac{eh\sin\nu}{p}. \tag{11}$$

Equations (7) and (11) can now be substituted in (3) giving

$$\bar{V}^2=\frac{h^2}{r^2}+\frac{e^2h^2\sin^2\nu}{p^2} \tag{12}$$

$$=\frac{h^2}{p^2}(1+e^2+2e\cos\nu) \tag{13}$$

$$=\frac{h^2}{p}\left(\frac{2}{r}-\frac{1}{a}\right). \tag{14}$$

Further, if M is the mass of the sun, the acceleration of a meteor of mass m relative to the sun will be $\frac{\gamma(M+m)}{r^2}$, or the acceleration at unit distance $\mu=\gamma(M+m)$. Writing $\gamma=k^2$, and expressing masses in terms of the sun's mass as unity,

$$\mu=\gamma(1+m)=k^2(1+m).$$

Also, since m is negligible, $\mu=\gamma=k^2$.

Manipulation of equations (7), (9), and (11) also gives

$$A=\frac{h^2}{pr^2}.$$

But the acceleration is also k^2/r^2: thus $k^2=h^2/p$, and (14) becomes

$$\bar{V}^2=k^2\left(\frac{2}{r}-\frac{1}{a}\right), \tag{15}$$

which is the fundamental expression for the velocity of a meteor in its orbit around the sun.

If the meteor is moving in a parabola, $a=\infty$ and (15) becomes

$$\bar{V}_p^2=\frac{2k^2}{r}. \tag{16}$$

If the meteor is moving in a hyperbola then a is negative and (15) becomes

$$\overline{V}_h^2 = k^2\left(\frac{2}{r}+\frac{1}{a}\right). \tag{17}$$

It will be seen later that the parabolic limiting velocity given by (16) is of great importance, and the question as to whether the velocity of sporadic meteors lies above or below this value has led to a deep controversy.

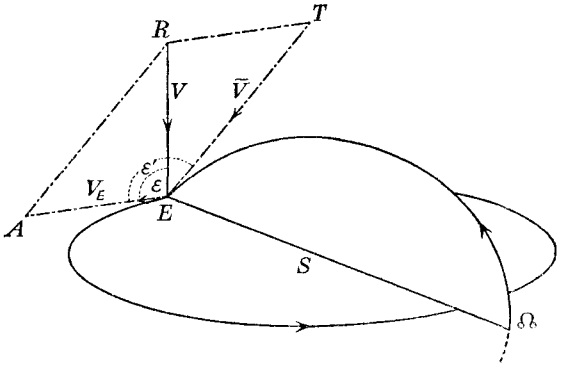

FIG. 47. The apparent radiant of a meteor.

3. The velocity of the meteor in the earth's atmosphere

The velocity $\overline{V}$ given by (15) is the heliocentric velocity of the meteor, or its velocity in the orbit before coming under the influence of the earth. In Fig. 47 it is represented in magnitude and direction by TE. The apparent velocity V of the meteor will be compounded of the heliocentric velocity $\overline{V}$ and the earth's velocity V_E.† In Fig. 47 it is represented by RE. The actual velocity measured by an observer on the earth will be greater than V because the attraction of the earth on the meteor forces it to move in a hyperbolic orbit about the earth's centre. This observed velocity v is known as the geocentric velocity of the meteor. If μ_c is the acceleration at unit distance from the earth, then by (17) the geocentric velocity will be given by

$$v^2 = \mu_e\left(\frac{2}{r_e}+\frac{1}{a_e}\right), \tag{18}$$

where r_e and a_e refer to the hyperbola about the earth's centre. The apparent velocity V outside the range of the earth's attraction must

† V_E is not, of course, constant. If its mean value is taken as unity then in (15) k^2 is unity and $V_E^2 = 2/R-1$, where R is the sun's radius vector, obtainable from standard tables for each day of the year.

also be given by (18) when $r = \infty$ so that

$$V^2 = \frac{\mu_e}{a_e}. \tag{19}$$

Hence
$$v^2 = V^2 + 2\frac{\mu_e}{r_e} \tag{20}$$

and
$$V^2(2a_e + r_e) = v^2 r_e. \tag{21}$$

$\mu_e = k^2 m_e$, where m_e is the mass of the earth. If this is taken as $3{\cdot}03 \times 10^{-6}$ of the sun's mass, and the distance as that from the centre of the earth to the meteor when it enters the atmosphere (say 6,450 km. $= 4{\cdot}31 \times 10^{-5}$ a.u.), then

$$\frac{2\mu_e}{r_e} = \frac{2k^2 m_e}{r_e} = 124{\cdot}9.$$

Hence
$$v^2 = V^2 + 124{\cdot}9. \tag{22}$$

4. Corrections to the observed radiant

(*a*) *Zenith Attraction*

The gravitational attraction of the earth on the meteor not only increases the velocity from V to v as given by (22), but also changes the direction in which the meteor is moving. In Fig. 48 the meteor M at a distance from the earth may be considered to be moving along the straight line MC, but on approaching the earth it will be forced into the hyperbola MPM′, with centre C and foci at S, the earth's centre, and at S′. Then $SC = CS' = a_e$ and $PS' = r_e + 2a_e$, where r_e is the radius of the earth. If TP is the tangent to the hyperbola at P then an observer at P measures the zenith distance of the radiant as $z = \widehat{TPR}$. In fact, the correct zenith distance is $\mathbf{z} = \widehat{TQR}$, where TQ is the asymptote to the hyperbola (meeting the major axis at C, so that $\sec\zeta = e$). Thus the measured radiant is always displaced towards the oberver's zenith, and the effect is known as zenith attraction. The value may be deduced as follows:

The projection of the sides of the triangle SPS′ on the asymptote gives

$$(r_e + 2a_e)\cos(2z - \mathbf{z}) - r_e \cos \mathbf{z} = 2a_e. \tag{23}$$

Adding r_e to each side and using (21),

$$V^2(1 - \cos \mathbf{z}) = v^2[1 - \cos(2z - \mathbf{z})]. \tag{24}$$

Writing $\Delta z = \mathbf{z} - z$

$$V \sin \tfrac{1}{2}(z+\Delta z) = v \sin \tfrac{1}{2}(z-\Delta z) \tag{25}$$

and

$$\tan \tfrac{1}{2}\Delta z = \frac{v-V}{v+V} \tan \tfrac{1}{2} z. \tag{26}$$

Thus, with v determined from (22), the correction Δz to be added to the observed zenith distance is obtained from (26). This correction is a

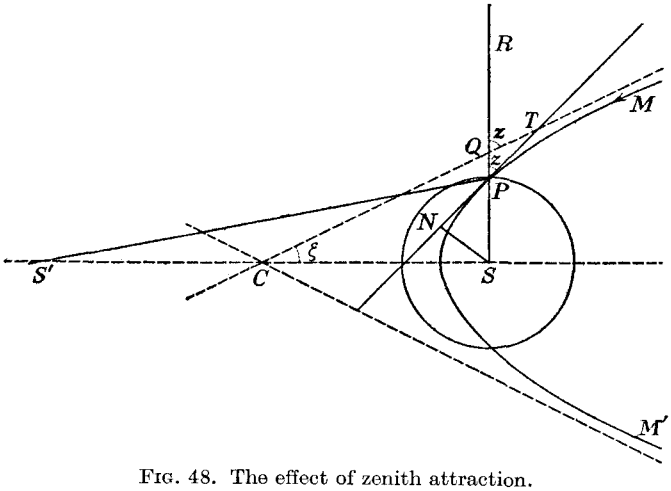

FIG. 48. The effect of zenith attraction.

maximum when the radiant lies on the horizon near the antapex when it may approach 17°. Tables and graphs for the rapid determination of the value of the zenith attraction in particular cases have been given by several authors, such as by Hardcastle,† Davidson,‡ and Nielsen.§

(*b*) *Diurnal Aberration*

A correction to the observed radiant must also be applied to allow for aberration due to the rotation of the earth. If V_E is the velocity of the observer due to the earth's rotation, and v the velocity of the meteor, then the aberrational displacement K will be given by

$$K = \frac{V_E}{v}.$$

At latitude ψ, $V_E = 0{\cdot}4639 \cos\psi$ km./sec. Thus

$$K = \frac{26{\cdot}58 \cos\psi}{v} \text{ deg.}$$

† Hardcastle, J. A., *J. Brit. Astr. Ass.* **21** (1910), 154.
‡ Davidson, M., ibid. **24** (1914), 307.
§ Nielsen, A. V., *Medd. Ole Rømer Obs.* (1938), no. 12.

The displacements in right ascension ($\Delta\alpha$) and declination ($\Delta\delta$) are then given by

$$\Delta\alpha = -\frac{26{\cdot}58}{v}\cos\psi\,.\cos H\,.\sec\delta, \tag{27}$$

$$\Delta\delta = -\frac{26{\cdot}58}{v}\cos\psi\,.\sin H\,.\sin\delta, \tag{28}$$

where δ is the declination and H the hour angle of the radiant.

The correction is small except for meteors of low velocity observed in the region of the poles.

(*c*) *The True Radiant*

After correction of the apparent radiant for zenith attraction and diurnal aberration as described above the true radiant can be readily calculated. In Fig. 47 if the elongation of the apparent radiant from the apex is ϵ (= $\widehat{\mathrm{REA}}$), and of the true radiant ϵ' (= $\widehat{\mathrm{TEA}}$), then

$$\frac{\overline{V}}{\sin\epsilon} = \frac{V}{\sin\epsilon'} = \frac{V_E}{\sin(\epsilon'-\epsilon)}. \tag{29}$$

In the normal observational case v and ϵ are measured. V is obtained from (22), and then from (29)

$$\cot\epsilon' = \cot\epsilon = -\frac{V_E}{V}\operatorname{cosec}\epsilon \tag{30}$$

and

$$\overline{V} = V\frac{\sin\epsilon}{\sin\epsilon'}. \tag{31}$$

(*d*) *The Elongation of the True Radiant*

The longitude (λ') and latitude (β') of the true radiant may be obtained as follows. The right ascension (α) and declination (δ) of the corrected radiant are converted into longitude (λ) and latitude (β) by means of the relations

$$\left.\begin{aligned}\cos\beta\,.\cos\lambda &= \cos\delta\,.\cos\alpha\\ \cos\beta\,.\sin\lambda &= \sin\delta\sin\boldsymbol{\epsilon} + \cos\delta\,.\sin\alpha\,.\cos\boldsymbol{\epsilon}\\ \sin\beta &= \sin\delta\cos\boldsymbol{\epsilon} - \cos\delta\,.\sin\alpha\,.\sin\boldsymbol{\epsilon}\end{aligned}\right\}, \tag{32}$$

where $\boldsymbol{\epsilon}$ is the obliquity of the ecliptic.

The positions of the apparent and true radiants (R and T of Fig. 47) on the celestial sphere in relation to the sun S and apex A are shown in Fig. 49. In the spherical triangle ARN

$$\left.\begin{aligned}\cos\beta\cos(\lambda-A) &= \cos\epsilon\\ \cos\beta\sin(\lambda-A) &= \sin\epsilon\cos\gamma\\ \sin\beta &= \sin\epsilon\sin\delta\end{aligned}\right\}, \tag{33}$$

from which ϵ and γ may be determined. ϵ' is then given by (29) and the spherical triangle ATN′ solved by equations similar to (33) for λ' and β' of the true radiant.

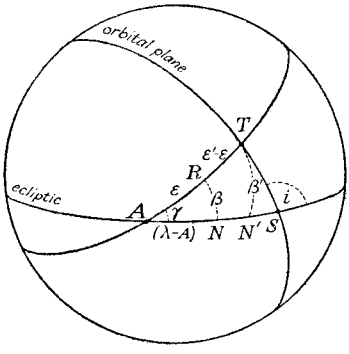

FIG. 49. The true radiant and orbital plane of the meteor.

5. Computation of the meteoric orbit

The computation of the elements of the meteoric orbit from the elongation of the radiant and velocity have been described by many authors. An account of the original methods of Schiaparelli and others is given by Olivier.† Subsequent methods have been devised by Bauschinger,‡ Davidson,§ and others. The contemporary method used in the British work is similar to that used by Laplace for cometary orbits and has been described by Porter.‖ It obviates the need for the solution of spherical triangles by the use of direction cosines and is a considerable simplification on the older methods.

In Fig. 49 the great circle TS is the projection on the celestial sphere of the plane of the orbit. Thus $\widehat{TSA} = (180° - i)$ and the elements of the orbit can be determined by the solution of the spherical triangle TSA. Alternatively, in the method used by Porter equation (15) is rewritten as

$$\overline{V}^2 = \frac{2}{r} - \frac{1}{a} = (x')^2 + (y')^2 + (z')^2, \tag{34}$$

where x', y', z' are the components of the meteor's velocity—the earth's mean velocity being taken as the unit.

Then
$$r^2 = x^2 + y^2 + z^2 \tag{35}$$

and
$$rr' = xx' + yy' + zz'. \tag{36}$$

† Olivier, C. P., *Meteors*, 1925.
‡ Bauschinger, J., *Die Bahnbestimmung der Himmelskörper*, Leipzig 1928.
§ Davidson, M., *J. Brit. Astr. Ass.* **44** (1934), 116, 146.
‖ Porter, J. G., *Comets and Meteor Streams*, Chapman & Hall, 1952.

Equations (10) and (11) may be written

$$\left.\begin{aligned} e\cos\nu &= \frac{p}{r} - 1 \\ e\sin\nu &= \frac{r'}{\sqrt{p}} \end{aligned}\right\}, \tag{37}$$

giving

$$p = \bar{V}^2 r^2 - (rr')^2. \tag{38}$$

The projection of twice the areal velocities on the planes of reference are given by the standard equations

$$\left.\begin{aligned} xy' - yx' &= C_1 \\ yz' - zy' &= C_2 \\ zx' - xz' &= C_3 \end{aligned}\right\}. \tag{39}$$

These equations (39) determine the position of the orbital plane and the other orbital elements are determined by equations (34)–(38). The evaluation of the true anomaly ν gives ω and the time of observation gives Ω. The details of the procedure using this method have been given by Porter,† and also that of the reverse problem of determining the radiant of a meteor moving in a given orbit.

† Porter, J.G., op. cit.

VI

THE DIURNAL AND SEASONAL DISTRIBUTION OF SPORADIC METEORS

THE number of meteors visible in a clear night sky to a single naked-eye observer may be from 2 to 20 per hour. There is a diurnal and seasonal variation, and the curve of variation is dominated by great increases in activity at irregular intervals due to the occurrence of major showers. These major showers are of paramount importance in meteor astronomy and will be discussed separately. Nevertheless, owing to the short time for which they are active, their contribution to the total number of meteors entering the earth's atmosphere during the year is considerably less than the contribution from the sporadic activity. This chapter will be concerned with these sporadic meteors. According to Prentice† the activity outside the major shower periods is maintained by a large number of minor streams (with rates not exceeding 1 per hour), as well as by meteors, which as a result of perturbations are pursuing isolated paths in space. It is unnecessary here to attempt such a distinction and we shall refer to all meteors occurring outside the major showers listed in Chapters XIII–XVIII as sporadic meteors.

1. The diurnal and seasonal variations of meteoric activity

The diurnal and seasonal variation of meteoric activity as found by visual and radio methods is shown in Figs. 50 and 51 respectively. The seasonal variations found by Wolf, Olivier, Denning, and Schmidt have been markedly influenced by the occurrence of the intense Perseid meteor shower in August. Even so, it is evident that all the results indicate two marked features: (*a*) the activity is higher after midnight than before, (*b*) the activity is higher during the second part of the year than the first.

The explanation of these variations was first attempted by Schiaparelli‡ in 1866. If the meteor radiants were of uniform intensity and were uniformly distributed over the celestial sphere, then, for an earth at rest, the number of meteors visible at any point would be constant. But the earth's orbital motion will lead to an apparent concentration of radiants around the apex of the earth's way. This point lies on the

† Prentice, J. P. M., *Rep. Phys. Soc. Progr. Phys.* **11** (1948), 389.

‡ Schiaparelli, G. V., *Note e Riflessioni sulla theoria astronomica delle stelle cadenti*, 1866, translated into German by G. von Bogusławski as *Entwurf einer astronomischen Theorie der Sternschnuppen*, 1871.

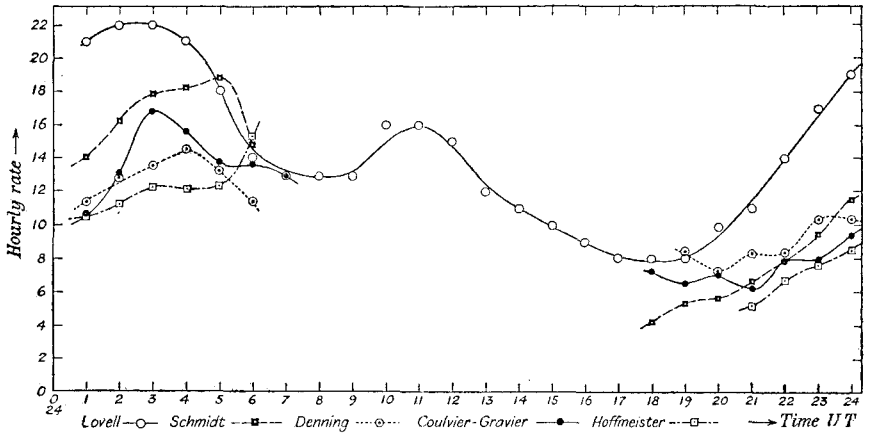

FIG. 50. Diurnal variation of meteoric activity. The radio observations are from a single run during 1947 Sept. 23–24, and the rates are scaled down for comparison with the visual observations. The visual observations are the mean observed hourly rates from a large number of observations. The sources of the data are as follows: Schmidt, Hoffmeister, Coulvier Gravier—plotted from information given by Olivier, *Meteors*, ch. 16 (Williams and Wilkins, 1925); Denning—plotted from information given by Davidson, M., *J. Brit. Astr. Ass.* **24** (1914), 352; Lovell A. C. B., *Rep. Phys. Soc. Progr. Phys.* **11** (1948), 429.

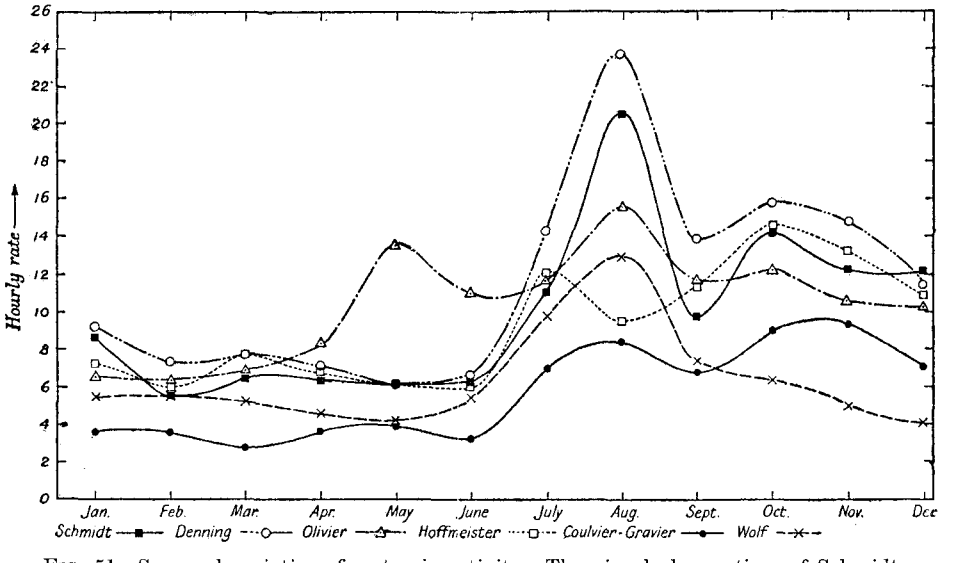

FIG. 51. Seasonal variation of meteoric activity. The visual observations of Schmidt, Denning, Olivier, Hoffmeister, Coulvier Gravier, and Wolf are plotted from information given by Olivier, *Meteors*, ch. 16 (Williams and Wilkins, 1925).

ecliptic approximately 90° from the sun, and hence during the course of the year its declination varies from −23·4° to +23·4°. The corresponding altitude of the apex when it is on the meridian in latitude +52° is 15° in spring and 61° in autumn. Similarly, the daily variation in the same latitude is from −38° in the evening to +38° in the morning. These changes in altitude of the apex account qualitatively for the observed diurnal and seasonal variation.

On the assumption of a uniform distribution of radiants of equal richness the form of the variation can be derived as follows.† In Fig. 47 the earth's direction and velocity is represented by V_E and the meteors' by $\bar{V}$. Equation (29), Chap. V, then gives

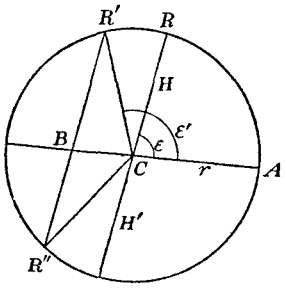

FIG. 52.

$$\frac{\sin(\epsilon'-\epsilon)}{\sin\epsilon} = \frac{V_E}{\bar{V}}, \qquad (1)$$

where ϵ' is the true elongation of the radiant from the apex and ϵ the apparent elongation. In Fig. 52 the earth's orbital motion is along CA (i.e. the direction of the apex), HH′ being the horizon. All meteor radiants above HH′ are visible and those below invisible. A radiant just visible on the horizon at R corresponds to a real radiant below the horizon at R′ with ϵ' given by (1) above. Let ϕ be the elevation of the apex above the horizon ($\sin\phi = \sin\epsilon$ in Fig. 52). Then

$$\sin(\epsilon'-\epsilon) = \frac{V_E}{\bar{V}}\sin\phi$$

and the meteors which are visible will come from the portion of the heavens R′AR″. The height of the spherical cap R′AR″ $= r + r\sin(\epsilon'-\epsilon)$ is therefore proportional to $\left(1+\frac{V_E}{\bar{V}}\sin\phi\right)$ and the area of the cap to

$$2\pi\left(1+\frac{V_E}{\bar{V}}\sin\phi\right).$$

Hence the ratio seen to the total number incident on the whole atmosphere will be

$$\frac{1}{2}\left(1+\frac{V_E}{\bar{V}}\sin\phi\right).$$

If we take the number in half the celestial sphere as unity, then the

† The final result is the same as that given by Schiaparelli (loc. cit.), but the derivation follows a method due to Davidson, M., *J. Brit. Astr. Ass.* **24** (1914), 352.

number of radiants F seen when the elevation of the apex is ϕ will be

$$F = 1 + \frac{V_E}{\bar{V}} \sin \phi. \qquad (2)$$

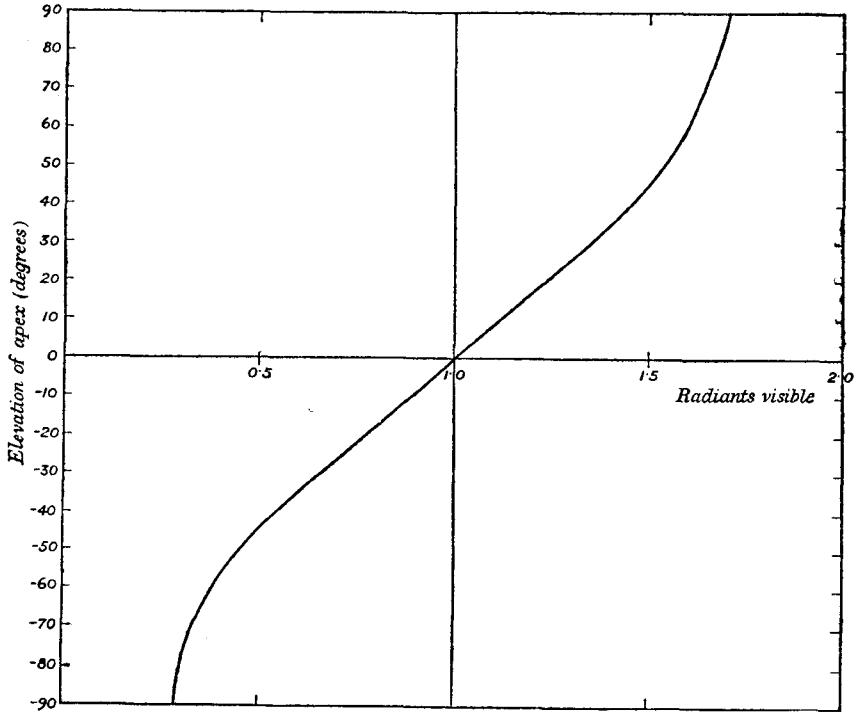

FIG. 53. The variation in the number of meteor radiants visible, with the elevation of the apex, according to Schiaparelli. The number is taken as unity for the apex on the horizon.

Schiaparelli further assumed a parabolic velocity for the meteors so that

$$\bar{V} = \sqrt{2}.V_E \quad \text{and} \quad F = 1 + \frac{1}{\sqrt{2}} \sin \phi.$$

The variation in the number of radiants with the elevation of the apex is shown in Fig. 53.

The above expressions give the variation in number of meteor *radiants* with ϕ. The number of meteors seen from a given radiant depends on the altitude of the radiant. Schiaparelli's derivation of the corrected expression for the number of *meteors* visible is as follows. The apex moves in the ecliptic with uniform motion at a distance of 90° behind the sun with a deviation of not more than $\pm 1°$. Choosing zero epoch at the summer solstice, the longitude λ_a of the apex will be nearly proportional to time

and we can express the increment in time by $d\lambda_a$. In Fig. 54 PZM is the observer's meridian, with sun S, pole P, zenith Z, apex A, and ecliptic ASM. Hour angle of the sun = H, with A 90° from S. It can be shown that the angle APS varies from 94° 56′ to 85° 04′ and is given to a close approximation by $\widehat{APS} = 90° + (4° 56')\sin 2\lambda_a$. Then $\widehat{APZ} = 90° + H + a \sin 2\lambda_a$ (where $a = 4° 56'$). In the triangle PZA, PZ is the

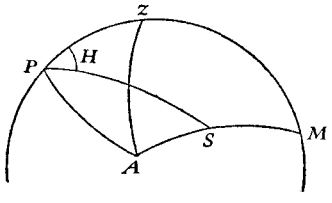

FIG. 54.

complement of the observer's latitude $(90° - \psi)$ and PA the polar distance of the apex, given by

$$\cos PA = \sin\lambda_a \sin\epsilon, \quad \text{where } \epsilon \text{ is the obliquity of the ecliptic.}$$

The zenith distance of the apex ZA = z is then given by

$$\cos z = \sin\psi \cos PA + \cos\psi \sin PA \cos(90° + H + a \sin 2\lambda_a). \tag{3}$$

The following approximations can be made:

$$\sin PA = \sqrt{(1 - \cos^2 PA)} = \sqrt{(1 - \sin^2\lambda_a \sin^2\epsilon)} = 1 - \tfrac{1}{2}\sin^2\lambda_a \sin^2\epsilon + \dots,$$

$$\cos(90° + H + a \sin 2\lambda_a) = -\sin(H + a \sin 2\lambda_a)$$

$$= -\sin H - a \sin 2\lambda_a \cos H.$$

Then (3) becomes

$$\cos z = \sin\psi \sin\lambda_a \sin\epsilon - \cos\psi(1 - \tfrac{1}{2}\sin^2\lambda_a \sin^2\epsilon)(\sin H + \sin^2\lambda_a \cos H). \tag{4}$$

In (2) let $\mu = V_E/\overline{V}$, then since $\phi = 90° - z$,

$$1 + \frac{V_E}{\overline{V}} \sin\phi = 1 + \mu \cos z.$$

The integral

$$\frac{1}{2\pi} \int_0^{2\pi} (1 + \mu \cos z)\, d\lambda_a \tag{5}$$

then gives the mean number of meteors for the hour angle H at latitude ψ.

Substituting cos z from (4) the integral reduces to

$$1 - \mu \cos\psi \sin H(1 - \tfrac{1}{4}\sin^2\epsilon). \tag{6}$$

Equation (6) gives the average mean frequency for all epochs and hours of the day. If K is the mean hourly number of meteors seen throughout

the year, then the average number of those meteors observed in an hour beginning ($H-30^m$) and ending ($H+30^m$) is given by

$$N = K\{1-\mu\cos\psi\sin H(1-\tfrac{1}{4}\sin^2\epsilon)\}. \quad (7)$$

Hence, according to this expression the number of meteors observed in any hour will remain constant at the poles and have its greatest variation on the equator.

For the latitude of Greenwich (7) gives

$$N = K(1-0{\cdot}598\mu\sin H). \quad (8)$$

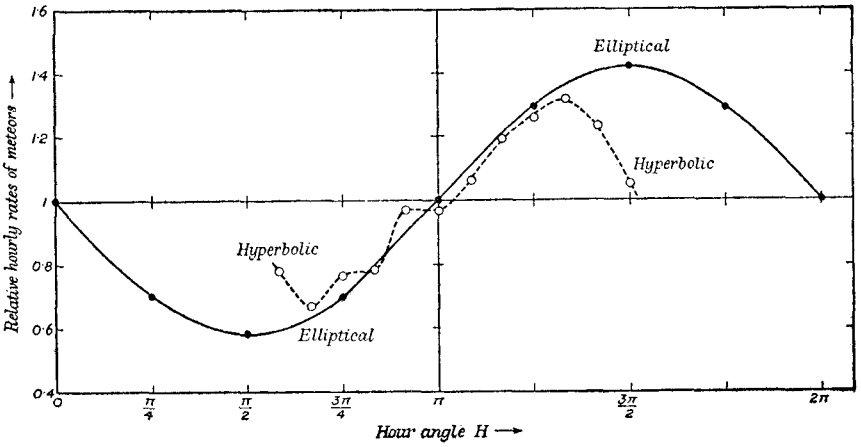

FIG. 55. The diurnal variation in meteor rates—as predicted by Schiaparelli's theory assuming a uniform distribution of meteor radiants and parabolic velocities. (Calculated for latitude 52°.) – – – – mean rates as observed by Denning in latitude 52°.

2. Comparison of the observed diurnal variation with Schiaparelli's theory

Schiaparelli assumed that the meteors were moving at the parabolic velocity limit so that $\overline{V} = \sqrt{2}.V_E$ and $\mu = 1/\sqrt{2}$. Hence for the latitude of Greenwich (8) becomes

$$N = K(1-0{\cdot}42\sin H). \quad (9)$$

The predicted diurnal variation plotted from (9) is shown in Fig. 55, taking a mean absolute rate of unity. Also plotted in Fig. 55 are Denning's† observations made in the same latitude, reduced to the same mean value. These observations are typical of the results on the diurnal variation found by various observers and shown in Fig. 50. The agreement between theory and observation is fairly good but far from complete. In

† See Fig. 50.

particular the maximum in the observations occurs considerably earlier than at 06h. as predicted by the theory. This discrepancy is evident in all the observations of diurnal variation plotted in Fig. 50, including the radio-echo observations which cannot have been influenced by dawn light. We shall return to this matter in § 4.

3. Comparison of the observed seasonal variation with Schiaparelli's theory

From (5) the theory predicts the relative number of meteors observed as the longitude of the apex varies from λ_{a_1} to λ_{a_2} to be

$$\int_{\lambda_{a_2}}^{\lambda_{a_1}} (1+\mu\cos z)\,d\lambda.$$

Introducing (4) this becomes

$$\int_{\lambda_{a_2}}^{\lambda_{a_1}} \{1+\mu[\sin\psi\sin\lambda_a\sin\epsilon-\cos\psi(1-\tfrac{1}{2}\sin^2\lambda_a\sin^2\epsilon)(\sin H+\sin^2\lambda_a\cos H)]\}\,d\lambda_a. \tag{10}$$

By integrating between values of λ_a appropriate to the longitude of the apex, eq. (10) gives the number of meteors to be expected at different periods of the year for hour angle H. For our present purpose it is sufficient to compare the average numbers predicted between the summer and winter solstice ($\lambda_a \to 0$ to π) and between the winter and summer solstice ($\lambda_a \to \pi$ to 2π). In comparing the seasonal rates we use the mean hourly rate averaged as H varies from 0 to 2π. Thus, since

$$\int_0^{2\pi} \sin H\,dH = 0,$$

the theory predicts the ratio

$$\frac{\text{mean hourly rate in second half of year}}{\text{mean hourly rate in first half of year}} = \frac{N_w}{N_s} = \frac{1+(2\mu/\pi)\sin\psi\sin\epsilon}{1-(2\mu/\pi)\sin\psi\sin\epsilon}.$$

For the latitude of Greenwich

$$\frac{N_w}{N_s} = \frac{1+0{\cdot}198\mu}{1-0{\cdot}198\mu},$$

and on the assumption of parabolic velocity ($\mu = 1/\sqrt{2}$)

$$\frac{N_w}{N_s} = 1{\cdot}325.$$

The observed seasonal ratio found in the extensive observations of Denning and his school averaged 2·1. The data have been treated by

Davidson† to remove the influence of the Perseid shower, whereby the ratio is reduced to 1·5. This is in fair agreement with the predicted value. The disagreement between theory and observation is discussed in § 9.

4. The discrepancy between theory and observation of the diurnal variation

In 1878 von Niessl‡ investigated in some detail the discrepancies which existed between the predictions of Schiaparelli's theory and the existing observations of the diurnal variation, particularly with regard to the disagreement in time of maximum. He developed an empirical expression involving assumptions about the density distribution of meteors with elongation from the apex but failed to obtain a satisfactory fit between the theoretical and observed variations. The assumption of a value for $\mu > 1/\sqrt{2}$, that is of hyperbolic velocities for the meteors, led to a better agreement. This suggestion, that the assumption of hyperbolic velocities enabled the theory to be brought into better accord with observations, formed the starting-point of a protracted discussion as to the reality of the hyperbolic meteor component. Essentially the dispute arises because the theory can be adapted to fit the observations either by abandoning the assumption of random distribution of meteor paths and retaining the parabolic velocity limit, or by retaining a measure of random distribution and exceeding the parabolic velocity limit. Unfortunately it has not been possible to settle the dispute by an appeal to actual velocity measurements, since as discussed in Chapters VIII–XII, these measurements have themselves been the subject of severe disagreement. In this chapter we shall proceed to discuss the measurements and interpretations of the diurnal variation as given by Hoffmeister and by Prentice, which illustrate the two opposing views on this subject. Finally the recent radio-echo investigations will be described.

5. Hoffmeister's investigation of the diurnal variation

During the past thirty years a very great number of observations have been collected by Hoffmeister, mainly under excellent conditions in South Africa. The results, and Hoffmeister's interpretation of them, have been presented in two books;§ here we shall only discuss Hoffmeister's later views on the interpretation of the diurnal variation.‖

As regards the original work of Schiaparelli, Hoffmeister draws

† Davidson, M., *J. Brit. Astr. Ass.* **24** (1914), 478.

‡ von Niessl, *Astr. Nachr.* **93** (1878), 209.

§ Hoffmeister, C., *Die Meteore*, Leipzig, 1937; *Meteorströme*, Weimar–Leipzig, 1948.

‖ The author is indebted to Professor Hoffmeister for much discussion in correspondence and for the opportunity of studying his unpublished papers.

attention to additional factors influencing the observed daily variation, particularly the effect of the acceleration due to the earth's gravitational attraction on the velocities, the effect of zenithal attraction upon the radiants, and the inability to observe meteors at less than 5° altitude even under good conditions. His fundamental expression for the number of meteors observed per unit time at any point on the earth, on the assumption of a uniform distribution of the original meteor directions, is then

$$N = \mathrm{f}(z, k, \bar{V}), \tag{11}$$

where z is the zenith distance of the earth's apex, k the average number for $z = 90°$, and $\bar{V}$ the effective heliocentric velocity.

In 1931† Hoffmeister discussed the computation of k and $\bar{V}$ in detail and pointed out that any shape of the diurnal curve might be possible if the assumption of the uniform distribution of original directions is abandoned. In other words any value of the velocity $\bar{V}$ derived from fitting the observed variation curves with the theoretical ones, calculated on the basis of uniform distribution, cannot be regarded as a real mean velocity, but rather as an apparent effective heliocentric velocity whose variations with time and locality might give information about the real distribution of meteor directions. Hoffmeister's initial extension of (11) took the form

$$N = k_1[\mathrm{f}(\bar{V}) + \mathrm{f}_2(\bar{V})\cos z + \mathrm{f}_3(\bar{V})\cos 2z], \tag{12}$$

where z is the zenith distance of the apex and $k_1 = k$ the average number of sporadic meteors for $z = 90°$.

The best fit with the observed material led Hoffmeister to conclude that nearly 70 per cent. of the meteors made up a strong interstellar component with a value for $\bar{V} = 2{\cdot}06 V_E$, instead of $\bar{V} = \sqrt{2}.V_E$ on the parabolic theory. However, his direct observations of a strong ecliptical component,‡ the work of Whipple, and the day-time radio-echo observations on the short-period orbits in the ecliptical plane§ led Hoffmeister to reinvestigate the distribution in order to test the effect of including a particular ecliptical component in the sporadic distribution.‖

His extension of (12) is then

$$N = k_1[\mathrm{f}(\bar{V}) + \mathrm{f}_2(\bar{V})\cos z + \mathrm{f}_3(\bar{V})\cos 2z] + k_2 \cos z_e, \tag{13}$$

where z_e is the zenith distance of the ecliptical radiant and k_2 the average of this component for $z_e = 90°$. The problem now is whether the inclusion of the ecliptical term enables the variation curves to be fitted with a value of $\bar{V} \not> \sqrt{2}.V_E$. For this latest analysis Hoffmeister's

† Hoffmeister, C., *Veröff. Berlin–Babelsberg*, **9** (1931), no. 1. ‡ *Meteorströme*.
§ See Chap. XVIII. ‖ Hoffmeister, C. Private communications (1951–2).

observations were obtained under excellent conditions in SW. Africa, long. 17° 5′ E., lat. 22° 35′ S., and include a total of 1,169 hourly numbers between 1937 April 30 and 1938 February 5. The effects of fatigue, increase in brightness with velocity, and decrease of apparent brightness with increasing angular velocity are considered as possible corrections. The last effect has been studied in great detail by making use of 'artificial meteors'.† The treatment of the two velocity effects is as follows. If N_m is the number of meteors between apparent magnitudes (m−0·5) and (m+0·5) then the real distribution function f(m) is given by

$$N_m = f(m).\Phi(m),$$

where $\Phi(m)$ is a probability function. In order to evaluate $\Phi(m)$ Hoffmeister assumed that within a certain area surrounding the resting point of the eye all meteors of a given magnitude will be seen, the area being greater for brighter meteors. By concentrating on a very small area the real distribution of different magnitudes will be seen, and by comparison with general observation not restricted to this small area, $\Phi(m)$ can be evaluated.

For $\Phi(m)$ Hoffmeister gives

m	0	1	2	3	4	5	6
$\Phi(m)$	1·00	0·95	0·78	0·51	0·25	0·05	0·001

The values refer to a unit area of sky defined so that meteors of apparent magnitude zero are seen without loss.

TABLE 11

Correction Factors in Hoffmeister's Analysis

Zenith distance of apex deg.	*Correction factor*	*Zenith distance of apex deg.*	*Correction factor*
0	1·456	90	1·000
10	1·396	100	0·959
20	1·339	110	0·920
30	1·285	120	0·882
40	1·232	130	0·846
50	1·182	140	0·812
60	1·133	150	0·778
70	1·087	160	0·747
80	1·043	170	0·716
90	1·000	180	0·687

In order to obtain a final correction curve it is necessary to make assumptions about the change of angular velocity during the night and the distribution of angular velocities. Hoffmeister uses his own values

† *Meteorströme.*

and those of Öpik derived from the rocking mirror observations† and gives the final correction factors of Table 11 to be applied to observed meteor frequencies.

Hoffmeister divided his observational material into nine groups as follows:

Group	*Dates*	*Sun's longitude deg.*
1	1937 April 30–May 22	40–62
2	May 27–June 20	66–89
3	June 25–July 20	94–118
4	July 25–Aug. 18	122–146
5	Aug. 24–Sept. 17	151–175
6	Sept. 22–Oct. 16	179–203
7	Oct. 22–Nov. 15	209–233
8	Nov. 20–Dec. 15	238–263
9	Dec. 19–1938 Feb. 5	267–317

The meteor counts in each group are divided into eight to eleven mean values for different zenith distances. Meteors identified as belonging to known showers are excluded. The nine curves of diurnal variation thus obtained are shown in Fig. 56 compared with the theoretical curves computed for uniform heliocentric velocity of $\overline{V} = 2{\cdot}5V_E$. Except for groups 7, 8, 9, the departures are considerable, but Hoffmeister points out that the discrepancies can be explained by a superposition of the classical variation curve with a secondary curve possessing a maximum after midnight. This indicates the effect of the ecliptical component, its decline in groups 7 to 9 being due to a real decrease of the average k_2 and to the change in the meridian zenith distances of the radiants. These curves, therefore, demonstrate that without the introduction of corrections due to the ecliptical component the new observations indicate a high heliocentric velocity in complete agreement with Hoffmeister's previous conclusions from earlier observations.

Now on the basis of (13) Hoffmeister gives a least square solution for k_1, k_2, and $\overline{V}$ with the following results:

Group	$\overline{V}/V_E$	k_1	k_2
1	$2{\cdot}11 \pm 0{\cdot}40$	$9{\cdot}80 \pm 1{\cdot}90$	$2{\cdot}78 \pm 2{\cdot}34$
2	$2{\cdot}23 \pm 0{\cdot}22$	$8{\cdot}75 \pm 1{\cdot}14$	$3{\cdot}88 \pm 1{\cdot}42$
3	$2{\cdot}08 \pm 0{\cdot}19$	$8{\cdot}99 \pm 0{\cdot}42$	$4{\cdot}0$
4	$2{\cdot}05 \pm 0{\cdot}15$	$10{\cdot}84 \pm 0{\cdot}36$	$6{\cdot}0$
5	$1{\cdot}98 \pm 0{\cdot}36$	$8{\cdot}16 \pm 1{\cdot}40$	$3{\cdot}34 \pm 1{\cdot}86$
6	$2{\cdot}04 \pm 0{\cdot}24$	$8{\cdot}41 \pm 0{\cdot}86$	$2{\cdot}12 \pm 1{\cdot}31$
7	$1{\cdot}55 \pm 0{\cdot}22$	$10{\cdot}70 \pm 1{\cdot}00$	$9{\cdot}46 \pm 1{\cdot}78$
8	$1{\cdot}60 \pm 0{\cdot}25$	$12{\cdot}75 \pm 1{\cdot}93$	$3{\cdot}93 \pm 3{\cdot}73$
9	$1{\cdot}48 \pm 0{\cdot}26$	$8{\cdot}12 \pm 0{\cdot}53$	$3{\cdot}0$

† See Chap. IX.

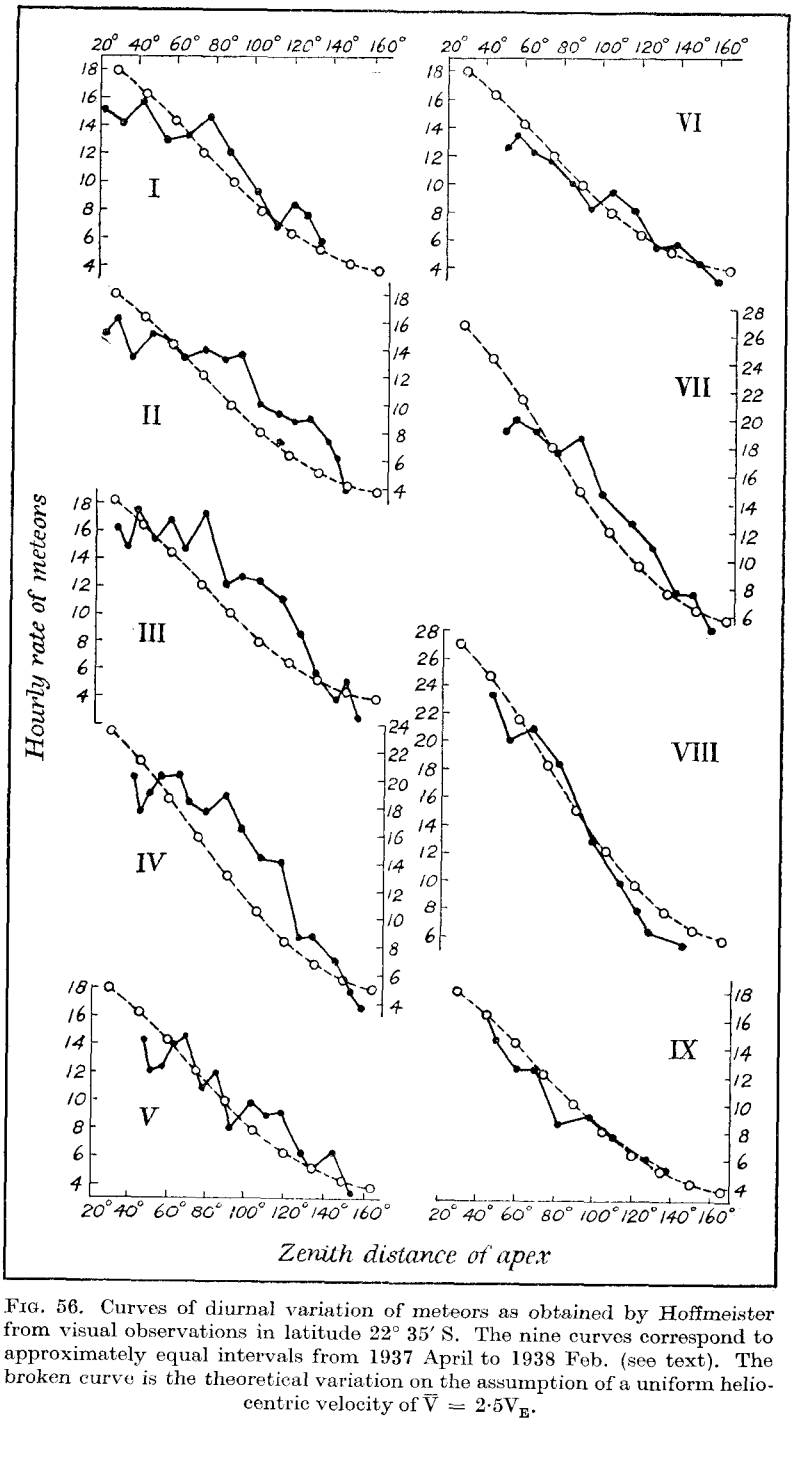

FIG. 56. Curves of diurnal variation of meteors as obtained by Hoffmeister from visual observations in latitude 22° 35′ S. The nine curves correspond to approximately equal intervals from 1937 April to 1938 Feb. (see text). The broken curve is the theoretical variation on the assumption of a uniform heliocentric velocity of $\overline{V} = 2{\cdot}5V_E$.

A comparison of the average number k_2 of ecliptical meteors (radiant in zenith) with former direct observations of this component† serves as a check on the computation. In the case of groups 3, 4, 9, it was necessary to use the previously observed value for k_2.

Hence, even when allowance is made for the strong ecliptical component, the value of $\overline{V}$ still emerges as distinctly hyperbolic though smaller than previously, its mean being $\overline{V} = 1{\cdot}90 \pm 0{\cdot}09 V_E$.

Hoffmeister then subtracts the ecliptical component by normalizing according to $N_{norm} = (N_{corr} - k_2 \cos z) k_1^{-1}$. The resultant mean corrected curves for groups 1 to 6 (May to October) and groups 7 to 9 (November to January) are compared with the theoretical variation curves in Figs. 57 and 58. In Fig. 58 the theoretical curve for $\overline{V} = \sqrt{2}.V_E$ agrees well with the corrected observational curve, and hence the results for the period November to January are in agreement with the parabolic theory. On the other hand the results for May to October (Fig. 57) indicate a markedly hyperbolic velocity ($\overline{V} \sim 2{\cdot}0 V_E$).

It will be seen later‡ that the most recent velocity measurements fail to demonstrate the markedly hyperbolic component required by the above analysis. The question therefore arises how Hoffmeister's observational data, to which great weight must be attached, can be aligned with these results. Hoffmeister offers the following possibilities:

(i) the data used on the velocity-luminosity relation, and the decrease of apparent brightness with increasing angular velocity, may be wrong. This would influence the correction factors listed on p. 105.

(ii) The deviation of the curve in Fig. 57 from the parabolic form might be compensated by an opposite deviation during the other part of the year. Hoffmeister's own southern hemisphere observations during March and April 1933 are irreconcilable with this possibility.

(iii) There may be another component with direct motion, thus requiring a further term in (13).

Hoffmeister gives reasons why it is unlikely that any such features could markedly influence the results; nevertheless the more recent results obtained both by the visual and radio analysis of the sporadic distribution indicate that either (i) or (iii) or a combination of both must have influenced Hoffmeister's analysis.

6. The distribution of sporadic meteors according to Prentice

The investigation of the sporadic distribution made by Hoffmeister discussed above is based on meteor counts, but the true path of the

† *Meteorströme.* ‡ Chap. XII.

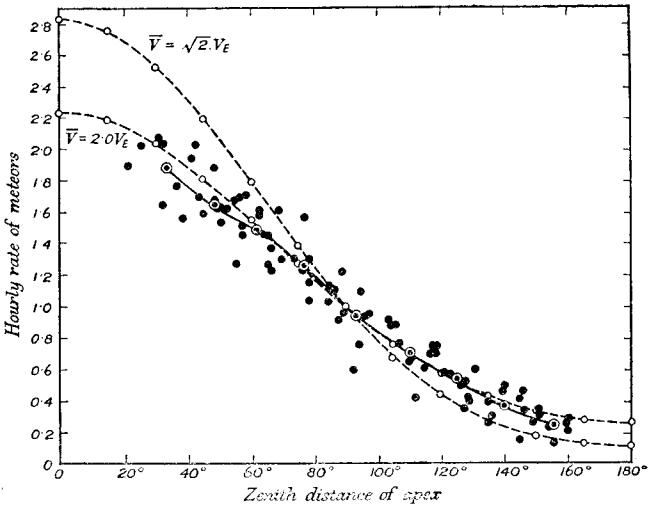

FIG. 57. The average values of groups 1 to 6 of Fig. 56 compared with the theoretical variation curve assuming $\overline{V} = \sqrt{2}.V_E$ and $\overline{V} = 2{\cdot}0V_E$.

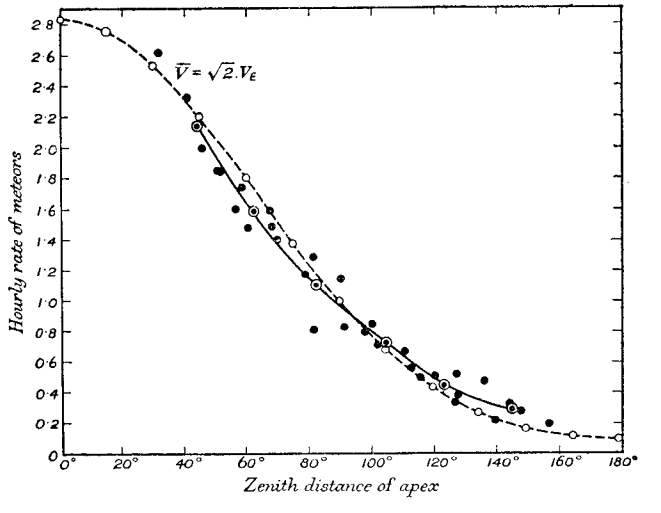

FIG. 58. The average values of groups 7 to 9 of Fig. 56 compared with the theoretical variation curve assuming a parabolic velocity $\overline{V} = \sqrt{2}.V_E$.

individual meteors remains unknown. Clearly a more direct attack on the problem of specific components in the sporadic distribution can be made if the true paths of the individual meteors are observed. This has been achieved by Prentice,† with members of the B.A.A. network of

meteor observers, using a visual technique in which the individual meteors are observed from two points on the earth's surface as described in Chapter II.

An observer O_1, Fig. 59, recorded the path of a meteor using the stellar background as a reference guide. In this way a plane was defined which contained the meteor path and the observer. The intersection of

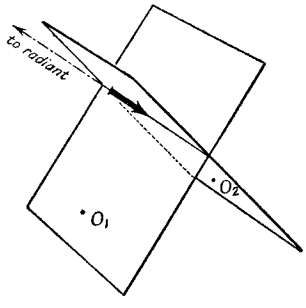

FIG. 59.

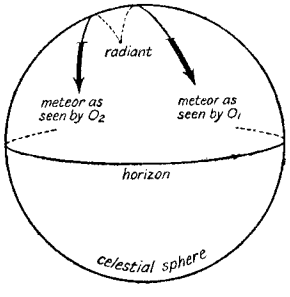

FIG. 60.

this plane with a similar plane recorded by another observer O_2 defined the path of the meteor in the atmosphere. These planes when projected on to the celestial sphere form great circles as shown in Fig. 60, the intersection of which defines the apparent radiant of the meteor.

The results of these observations are shown in Figs. 61 (*a*) and 61 (*b*). The distribution in ecliptic latitude (Fig. 61 (*b*)) shows that the sporadic meteors are largely concentrated in the plane of the ecliptic. The longitude distribution in Fig. 61 (*a*) shows a concentration from the anti-helion point at least as great as that from the apex of the earth's way. These directions may be visualized more clearly with the help of Fig. 62 which shows the earth's orbit EXYZ. The concentration in latitude is along QR with the maximum in the plane EXYZ. The concentrations in longitude, in the plane EXYZ, lie along the apex of the earth's way (EA) and towards the antihelion point EP. These results demonstrate in a striking manner the error in the original assumption of Schiaparelli that the meteor radiants are uniformly distributed. Before discussing the implications of these results we shall describe the radio-echo work on the sporadic meteors which confirms and extends these visual observations to the day-time sky.

† Prentice, J. P. M. (in preparation).

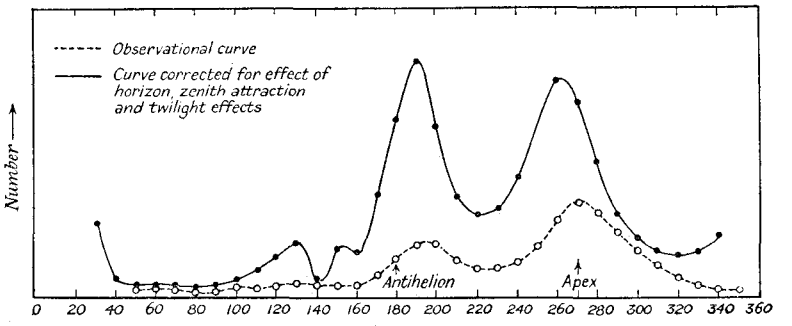
Observational curve
Curve corrected for effect of horizon, zenith attraction and twilight effects
Number
Antihelion
Apex
0 20 40 60 80 100 120 140 160 180 200 220 240 260 280 300 320 340 360
λ − ⊙

(a)

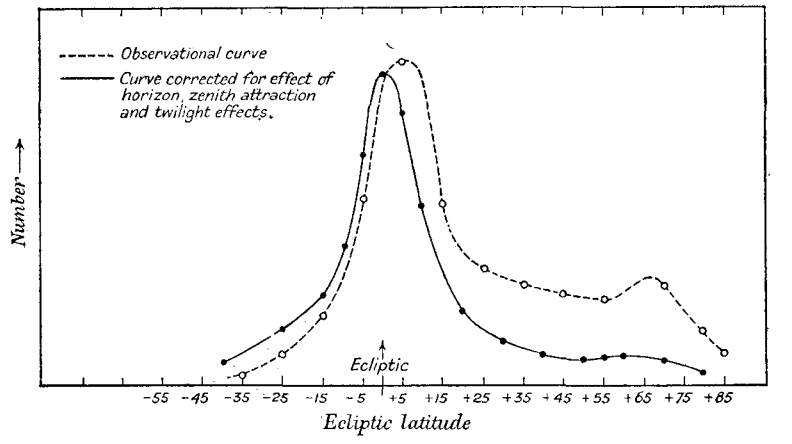
Observational curve
Curve corrected for effect of horizon, zenith attraction and twilight effects.
Number
Ecliptic
−55 −45 −35 −25 −15 −5 +5 +15 +25 +35 +45 +55 +65 +75 +85
Ecliptic latitude

(b)

FIG. 61. The distribution of sporadic meteors as derived from duplicate visual observations by Prentice.

(a) Distribution of visual radiants in local ecliptic longitude. (Abscissa: longitude λ − sun's longitude ⊙.)

(b) Distribution of visual radiants in ecliptic latitude.

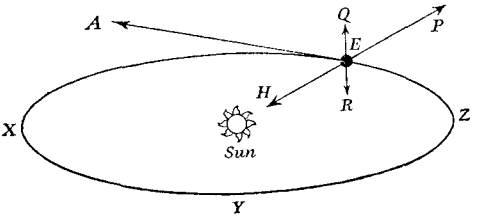

FIG. 62.

7. The radio-echo investigation of the sporadic distribution

The radio-echo apparatus designed for the continuous investigation of meteoric activity† has been used by Hawkins and Aspinall‡ to study the distribution of the sporadic meteors. As described elsewhere† this equipment uses two aerials beamed in azimuth and directed at 25° N. and S. of West respectively. On the radio frequency used (72 mc./s.) the radio reflection from the meteor trails is aspect sensitive, and hence

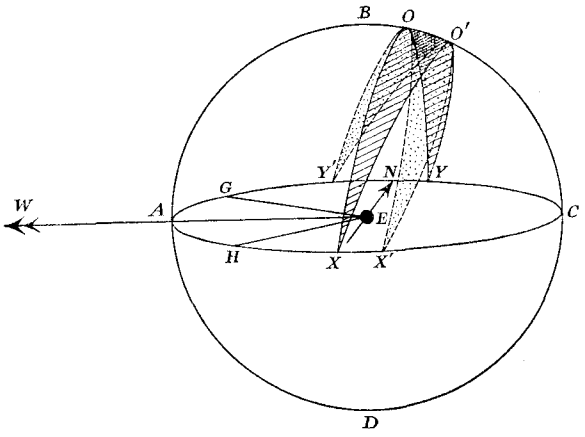

FIG. 63.

only those meteors whose paths lie in a restricted volume of space will be recorded at any given time. In Fig. 63 the observing station is at E. ABCD is the celestial sphere and ANCX the horizon circle. The beamed aerials are directed along EG and EH respectively. If the aerial EG produced an infinitely narrow beam, directed horizontally, then only those meteors would be recorded with paths in a vertical plane perpendicular to EG. The combination of finite beam widths, slight elevation of the maximum lobe, and a restriction on range measurement to 1,000 km., finally yield a collecting volume enclosed between two planes such as XOY and XO'Y, with a similar arrangement for EH as at X'OY', X'O'Y', the inclination between the two sectors being that of the aerials, that is 50°. The effect of the diurnal rotation of the earth can most easily be visualized as a rotation of the celestial sphere ABCD, with E and the sectors fixed. It will be seen that every day each of the aerials takes a complete sample of the meteor activity in the northern hemisphere. For example, meteors with paths lying in a plane through the apex will be recorded in the aerial EH when the apex is within the

† See Chap. IV.

‡ Hawkins, G. S., and Aspinall, A. (in preparation).

sector X′OO′Y′, and then later, when the celestial sphere has rotated 50°, in aerial EG when the apex is within the sector XOO′Y. If the

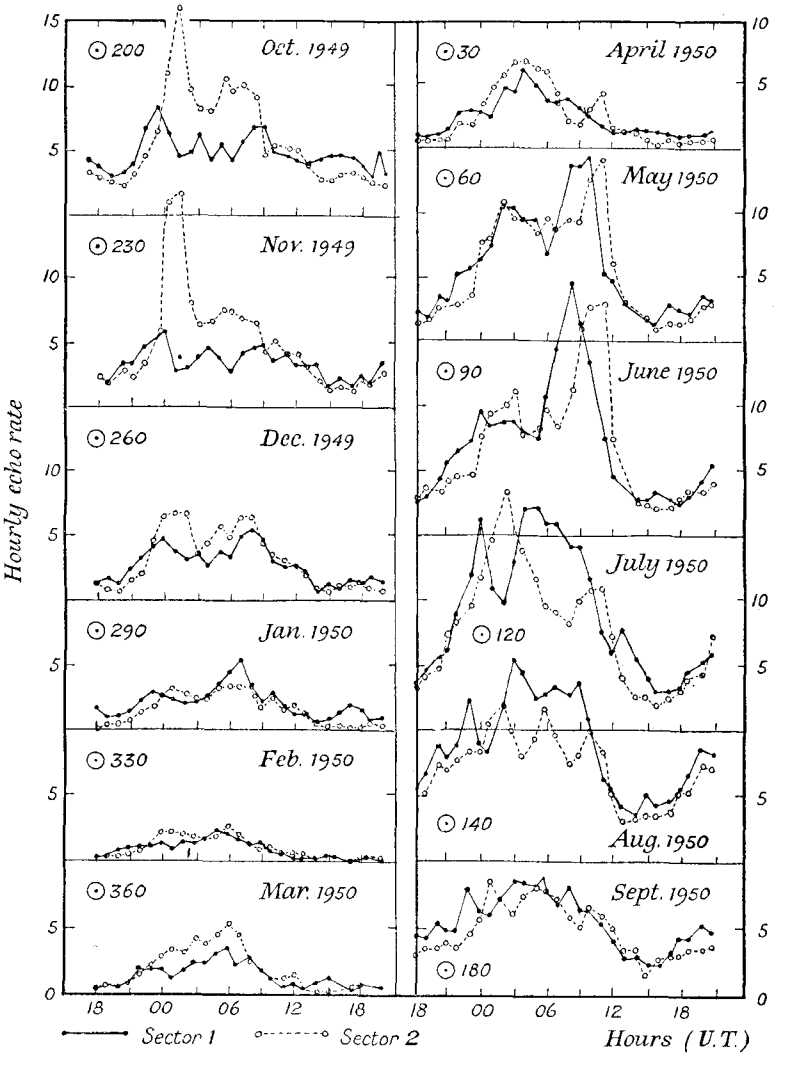

FIG. 64 (*a*). Monthly means of the diurnal variation of sporadic meteor radiants as measured by the radio-echo technique during the period 1949 Oct.–1950 Sept.

known meteor showers are eliminated from the records the distribution of the sporadic meteor directions can be obtained.

The mean monthly diurnal rate curves for both sectors are shown in Fig. 64 (*a*) for the year 1949–50, and in Fig. 64 (*b*) for the year 1950–1.

The average of all the monthly curves throughout the year is shown in Fig. 65 (*a*) (corresponding to Fig. 64 (*a*)) and in Fig. 65 (*b*) (corresponding

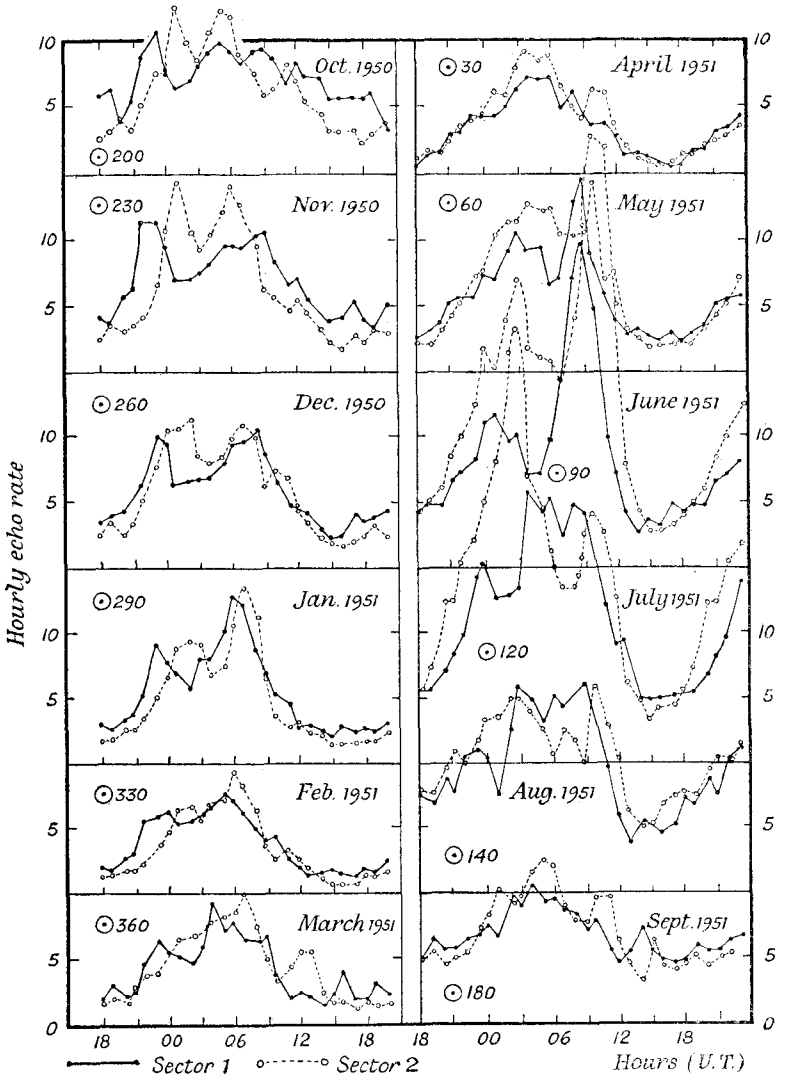

FIG. 64 (*b*). Monthly means of the diurnal variation of sporadic meteor radiants as measured by the radio-echo technique during the period 1950 Oct.–1951 Sept.

to Fig. 64 (*b*)). The displacement of the maximum in these curves is a result of the inclination of the two aerial beams. Figs. 66 (*a*) and 66 (*b*) (corresponding to 65 (*a*) and 65 (*b*) respectively) give the means of the separate curves for the two sectors corrected for this inclination. These

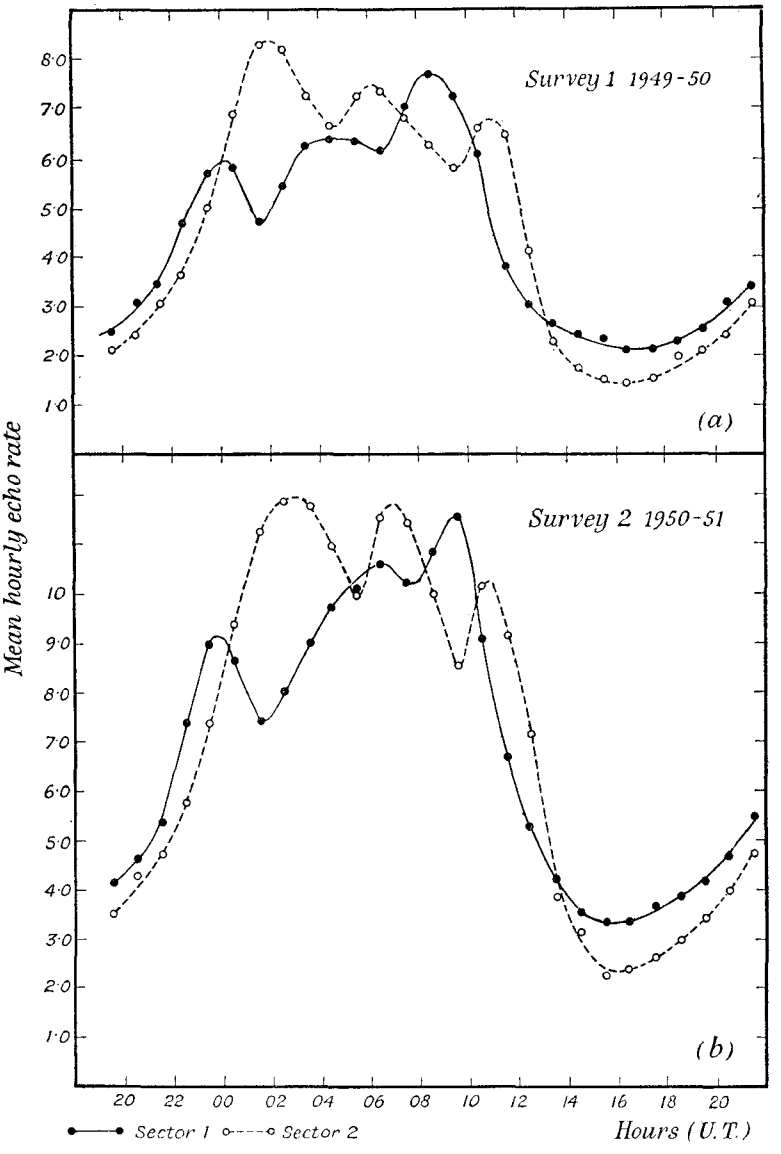

FIG. 65. The average diurnal variation of the sporadic meteor rates: (*a*) derived from Fig. 64 (*a*); (*b*) derived from Fig. 64 (*b*).

curves represent the distribution of the sporadic meteor activity in longitude and may be compared with the results of the visual observations shown in Fig. 61 (*a*). Both the radio-echo and visual observations show nearly equal concentrations towards the apex and antihelion points.

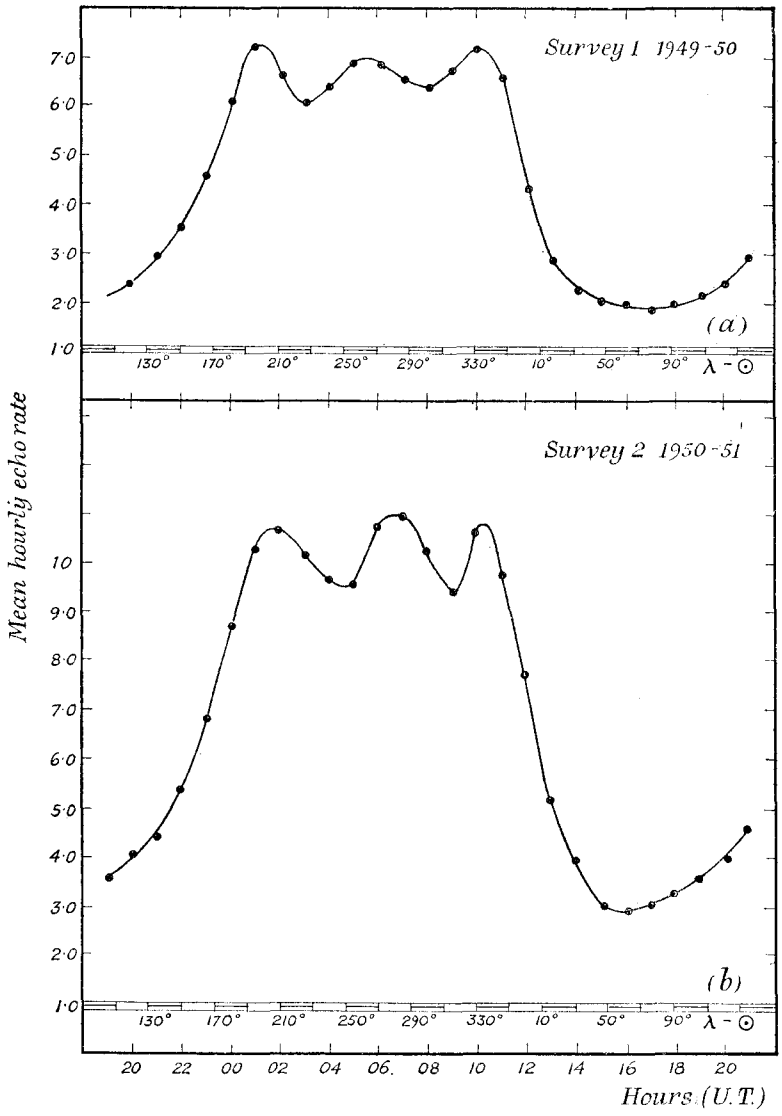

FIG. 66. The mean of the curves for the two sectors, combined by correcting for the inclination of the collecting areas: (*a*) corresponding to Fig. 64 (*a*); (*b*) corresponding to Fig. 64 (*b*).
Abscissae: (longitude λ − sun's longitude ⊙).

In addition, the radio-echo observations extend into the daylight sky and show a similar concentration towards the helion point (EH in Fig. 62). The radio-echo observations do not give a distribution in latitude to be compared with Fig. 61 (*b*), but the results can be satisfactorily

interpreted in terms of the concentration in the ecliptical plane shown in Fig. 61 (*b*). A mean value for the declination of 24° can be obtained from the displacement of the maximum in the two aerial beams as shown in Fig. 65, that is from the activity in the direction of the helion, antihelion, and apex points when they attain their maximum elevation.† Thus, if this activity was also concentrated in latitude in the plane of the ecliptic, the measured declination would be expected to be 23°. Comparison with the deduced value of 24° indicates general agreement with the visual results of Fig. 61 (*b*), that the concentration is near the ecliptical plane.

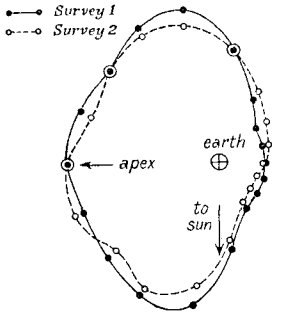

FIG. 67. Distribution of apparent radiants in local longitude.

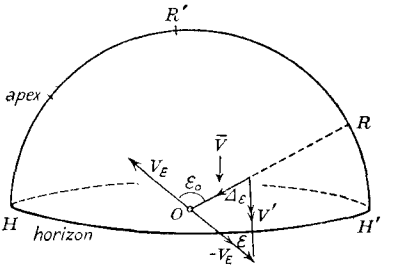

FIG. 68.

8. The true distribution of sporadic meteors

From the results described in §§ 6 and 7 it is possible to assess finally the true distribution of sporadic meteor orbits. In latitude most of the orbits lie in a narrow band enclosing the plane of the ecliptic. In longitude the rate curves plotted in polar coordinates around the earth are shown in Fig. 67. The distribution of sporadic orbits may be obtained from this by correcting for the earth's orbital motion in the following manner. In Fig. 68 the great circle HH′ represents the horizon of an observer O, moving with velocity V_E relative to the sun. If a meteor is moving with velocity $\overline{V}$ relative to the sun, then its apparent direction as seen by O may be obtained by reducing the earth to rest, and applying a velocity $-V_E$ to $\overline{V}$. Then the meteor will appear to radiate from R′ instead of R. If η_ϵ radiants are observed within a section $d\epsilon$ on the ecliptic, at an apparent elongation ϵ from the apex, then the true elongation ϵ_0 is given by

$$\epsilon_0 = \epsilon + \sin^{-1}\left(\frac{V_E}{\overline{V}}\sin\epsilon\right). \qquad (14)$$

† See Chap. IV, where the application of the apparatus to determine the declination of the shower radiants is described.

These radiants are located in a sector $d\epsilon'$, where

$$\frac{d\epsilon}{d\epsilon'} = \frac{V'}{\overline{V}} \sqrt{\left(1 - \frac{V_E^2}{\overline{V}^2} \sin^2 \epsilon\right)}. \tag{15}$$

An increase in the apparent velocity V′ increases the number of intercepted meteors, so that the true density in space is proportional to

$$\eta_\epsilon \frac{\overline{V}}{V'} = \frac{\eta_\epsilon \overline{V}}{\sqrt{(\overline{V}^2 + V_E^2 + 2\overline{V} V_E \cos \epsilon_0)}}. \tag{16}$$

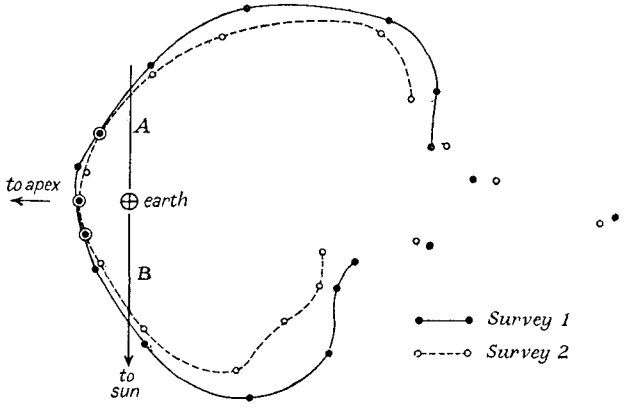

FIG. 69. Distribution of orbital directions of sporadic meteors.

By taking the parabolic limiting velocity for $\overline{V}$, the distribution of Fig. 67 can be corrected for the earth's motion by using the above equations. The corrected distribution is given in Fig. 69. It represents, for any point in the earth's orbit, the number of meteor orbits which cross in any specific direction. The distribution indicates a preponderance of directly moving meteors. Some indication of the actual orbits of these meteors can be obtained by using the velocity measurements of the sporadic distribution during the summer months.† These show that the meteors are moving in orbits of high eccentricity similar to the orbits of the intense summer day-time streams.‡

It is therefore evident that the original assumption of uniform distribution made by Schiaparelli has little relation to the true distribution. Finally, it is necessary to inquire if the true distribution as now derived is capable of yielding the form of the diurnal variation curve observed by Hoffmeister without the assistance of hyperbolic velocities. If the

† See Chap. XII.

‡ See Chap. XVIII.

radiants are assumed to lie on the ecliptic with a distribution in local longitude of $f(\lambda-\odot)$, as given in Fig. 66, then the rate at any instant may be found by summation, $N = \sum_1^n f(\lambda-\odot)\sin(\alpha+6°)$,† where n is the number of visible positions on the ecliptic taken at intervals of 20° in $(\lambda-\odot)$, and α is the elevation of the point on the ecliptic. Fig. 70 shows Hoffmeister's observed curve of diurnal variation for latitude

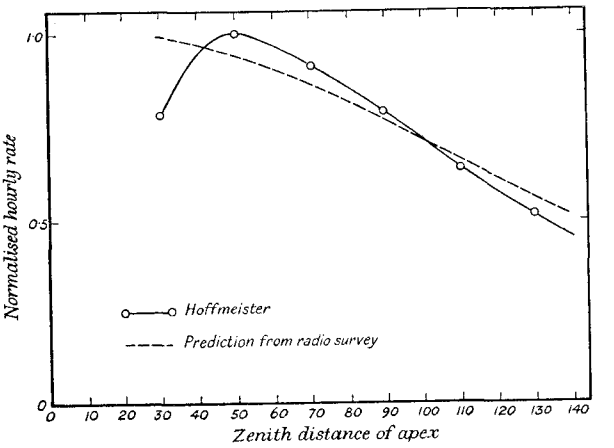

FIG. 70. Comparison of Hoffmeister's curve of diurnal variation observed in latitude 22° S., with the theoretical curve derived from the radio-echo observations made in latitude 53° N.

22° S. (§ 5) compared with the appropriate diurnal rate curve calculated as above from the intensity of the various components as measured in latitude 53° N. The sudden decrease in activity shown by the visual curve at low values of z is due to the decrease of visibility at dawn. The addition of this directly moving component of high eccentricity to Hoffmeister's analysis (§ 5) can also explain his observations without reference to the hyperbolic component.

The general agreement is so good that there no longer seem to be any grounds for the introduction of a hyperbolic component in the sporadic distribution. It will be seen in Chapter XII that the most recent measurements of the velocity distribution of sporadic meteors also fail to reveal any velocities in excess of the parabolic limit.

† The correction of the elevation α to $(\alpha+6°)$ has been determined empirically (see Prentice, J. P. M., *Rep. Phys. Soc. Progr. Phys.* **11** (1948), 389. It includes the allowance for the effective increase in elevation due to the zenith attraction, and the allowance for the thickness of the meteor layer on the effective collecting area of the observer.

9. The seasonal variation of sporadic meteor activity

In § 3 the observed seasonal variation was compared with Schiaparelli's theory with only fair agreement. In the light of the foregoing it will

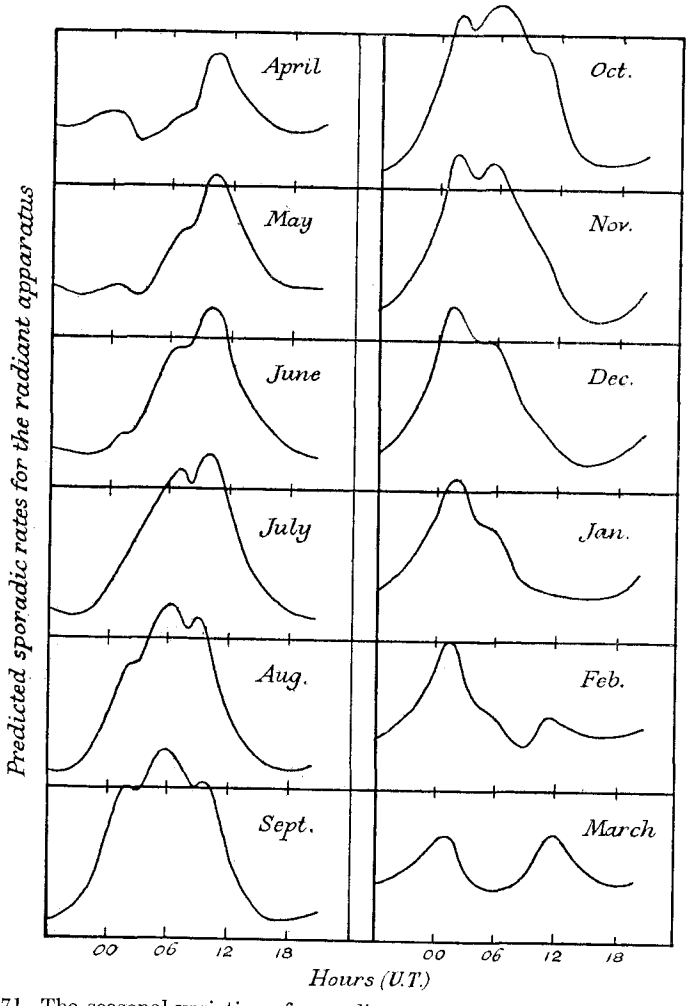

FIG. 71. The seasonal variation of sporadic meteor activity to be expected if the sporadic meteor orbits are uniformly distributed around the earth's orbit. Comparison with the observed seasonal variation (Fig. 64) indicates a marked asymmetry.

be apparent that no close agreement could be expected, since the true distribution of sporadic meteors is markedly different from the uniform distribution assumed in the original theory. The new results on the latitude and longitude distribution can be used to predict the seasonal variation

which should be observed with the radiant apparatus on the assumption that the density of meteor orbits along the length of the earth's orbit is

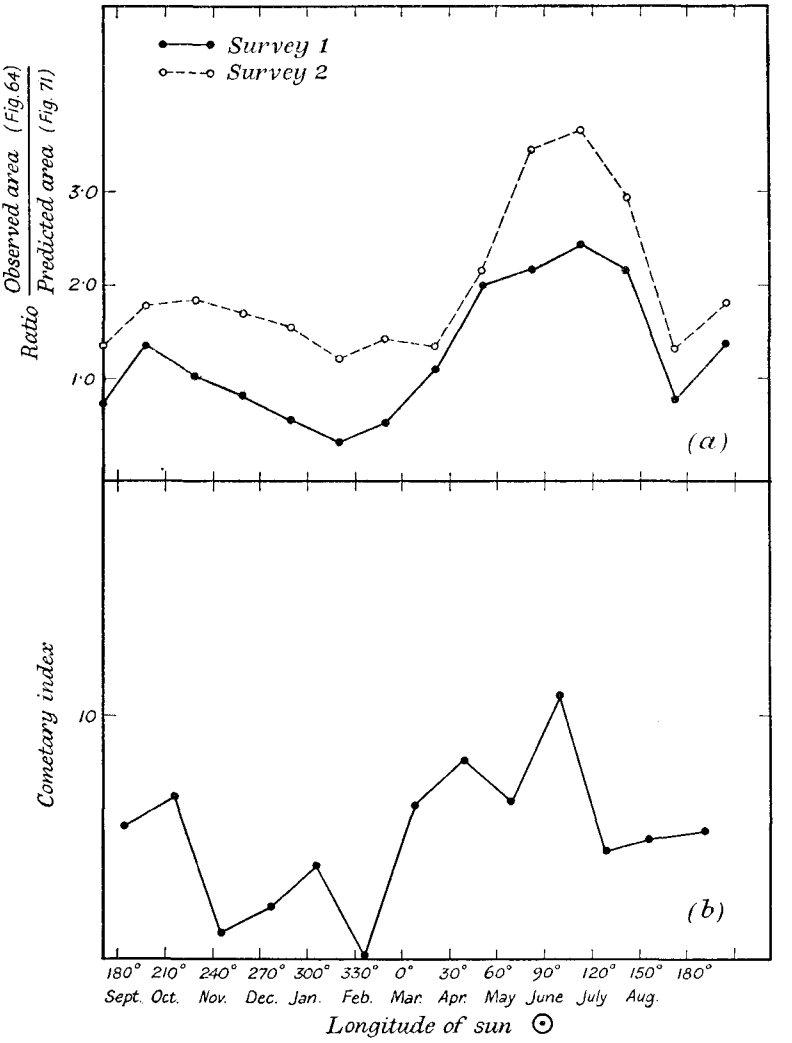

FIG. 72. (*a*) The actual modulation of sporadic orbits around the earth's orbit obtained from a comparison of the observed (Fig. 64) and theoretical (Fig. 71) seasonal variations.

(*b*) The variation of cometary index with sun's longitude ⊙.

uniform. From the mean distribution around the earth as shown in Fig. 69, the seasonal variation to be expected is obtained as in Fig. 71. The monthly averages are represented by the area under each curve, and

these can be compared with the actual observed monthly averages of Fig. 64. It is evident that the discrepancies are considerable and hence that the density of meteor orbits around the earth's orbit is far from uniform. A measure of the irregularity can be obtained from the ratio of the observed monthly averages (Fig. 64) to those to be expected on the assumption of uniform density (Fig. 71). This ratio is plotted throughout the year in Fig. 72 (*a*). The surprising feature of this distribution is that the activity is much higher in the summer (region of $\odot = 90°$) than in the autumn—a result in direct contradiction to the prediction of Schiaparelli's theory, and to the visual observations restricted to the night-time sky. The density of the sporadic meteor orbits in the region of the earth's orbit, around $\odot = 90°$, evidently more than compensates for the low altitude of the apex. Also plotted in Fig. 72 (*b*) is the index computed by Herschel and Hoffmeister,† proportional to the number of comets crossing the earth's orbit and their closeness of approach. The agreement of these curves, and the occurrence of the high-density sporadic meteoric orbits of direct motion and high eccentricity in the same region of the orbit as the intense summer day-time streams, is very suggestive and will be discussed in Chapter XXI.

† Hoffmeister, C., *Meteorströme*, 1948.

VII

THE NUMBER AND MASS DISTRIBUTION OF SPORADIC METEORS

Our present knowledge of the total numbers of meteors entering the earth's atmosphere is based largely on the work of Watson,† who has extended the results to tenth magnitude meteors by making telescopic observations. The fraction of the total number entering the atmosphere which can be observed at any given time depends on the length of the meteor path and hence upon magnitude. Further corrections are necessary to join the visual and telescopic magnitude scales and for the correction of the magnitude of meteors which are observed other than in the zenith.

1. The effective field of view for telescopic observations

The effective field of view for telescopic observations is greater than the normal visible field because of the finite length of the meteor paths. Thus, amongst the meteors counted will be those whose points of origin lie outside the visible field, but subsequently move into it. In Fig. 73 the circle of radius D/2 represents the normal field of view of the telescope. Meteors of path length L originating outside this field may move into it and the effective field can be calculated as follows. Consider an element AB of length $(D/2)\,\delta\gamma$ on the circle bounding the field of view of the telescope. Some of the meteors of path length L originating in the element PQRS (area $x\,\delta\zeta\,\delta x$) will pass through AB and enter the field of the telescope. The angle subtended by AB at PQRS is $\frac{AB\cos\zeta}{x}$ and the ratio of the number of meteors passing through AB to the total number from PQRS will be $\frac{AB\cos\zeta}{2\pi x}$. Hence the total number of meteors of path length L originating outside the field of view and subsequently entering it is given by

$$\int_{x=0}^{L}\int_{\gamma=0}^{2\pi}\int_{\zeta=-\frac{1}{2}\pi}^{+\frac{1}{2}\pi}\frac{D}{2}.d\gamma.\frac{\cos\zeta}{2\pi x}.x.dx.d\zeta=\frac{D}{4\pi}\int\int\int\cos\zeta.dx.d\gamma.d\zeta=DL.$$

† Watson, F., *Ann. Harv. Coll. Obs.* **105** (1937), 624; *Proc. Amer. Phil. Soc.* **81** (1939), 493.

The effective field of view for meteors with path length L is therefore given by

$$\frac{\pi D^2}{4} + DL.$$

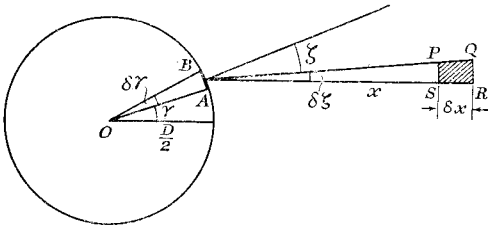

FIG. 73.

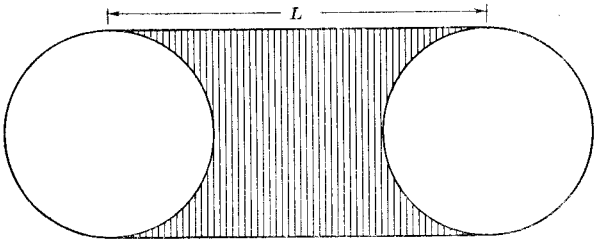

FIG. 74. Schematic representation of the total collecting area ($\pi D^2/4 + LD$) for telescopic observations of meteors when $L > D$. The area available for the beginning points of meteors which cross the field is vertically ruled.

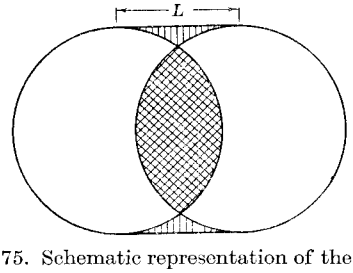

FIG. 75. Schematic representation of the total collecting area ($\pi D^2/4 + LD$) for telescopic observation of meteors when $L < D$. The area in which meteors both begin and end in the field is cross-hatched.

This expression was first deduced by Öpik.† Following Watson‡ this additional 'rectangular invisible' field DL can be represented diagrammatically as in Figs. 74 and 75.

† Öpik, E., *Publ. Tartu Obs.* **27** (1930), no. 2.
‡ Watson, F., *Proc. Amer. Phil. Soc.* **81** (1939), 493.

2. Probability of observation of different classes

We now consider the probabilities of observing four classes of meteors.

(*a*) Meteors which begin or end in the visible field. Since the visible field is a small fraction of the total field,

$$P_B = P_E = \frac{\pi D^2/4}{\pi D^2/4 + DL} = \frac{\pi D}{\pi D + 4L}.$$

(*b*) Meteors which cross the visible field. The probability is the fraction of the effective field available for the beginning points of meteors which cross the field:

$$P_C = 4\frac{\left\{\frac{LD}{4} - \int_0^{L/2}\left(\frac{D^2}{4} - x^2\right)^{\frac{1}{2}} dx\right\}}{(D/4)(\pi D + 4L)}$$

$$= 4\frac{\left\{L - \frac{L}{2}\left(1 - \frac{L^2}{D^2}\right)^{\frac{1}{2}} - \frac{D}{2}\sin^{-1}\left(\frac{L}{D}\right)\right\}}{\pi D + 4L}.$$

For $L \geqslant D$,
$$P_C = \frac{4L - \pi D}{\pi D + 4L}.$$

(*c*) Meteors which both begin and end in the visible field. The probability is proportional to the fraction cross-hatched in Fig. 75:

$$P_{BE} = \frac{\int_{L/2}^{D/2}\left(\frac{D^2}{4} - x^2\right)^{\frac{1}{2}} dx}{(D/4)(\pi D + 4L)}$$

$$= 2\frac{\left[\frac{\pi D}{2} - L\left(1 - \frac{L^2}{D^2}\right)^{\frac{1}{2}} - D\sin^{-1}\left(\frac{L}{D}\right)\right]}{\pi D + 4L}.$$

This vanishes when $L > D$.

Since meteors which both begin and end in the field will also be counted as either beginning or ending in the field:

$$P_B + P_E + P_C - P_{BE} = 1.$$

The probabilities that meteors with various values of L/D will be observed in these categories has been computed as above by Watson† and the results are given in Table 12 and Fig. 76.

† Watson, F., loc. cit.

TABLE 12

Probabilities of Telescopic Observations for Various Values of L/D

L/D	P_B *and* P_E	P_C	P_{BE}	*Area of effective field*	*Increase in area for doubled* D
0·0	1·0	0·0	1·0	1·0	4·0
0·1	..	..	0·775	..	..
0·2	0·803	0·003	0·609	1·25	3·32
0·3	..	..	0·451	..	..
0·4	0·663	0·005	0·333	1·51	3·00
0·5	..	..	0·237	..	..
0·6	0·569	0·016	0·154	1·76	2·78
0·7	..	..	0·097	..	..
0·8	0·497	0·062	0·056	2·02	2·66
0·9	..	..	0·024	..	..
1·0	0·440	0·120	0·000	2·27	2·56
1·25	0·386	0·228	..	2·59	..
1·5	0·344	0·312	..	2·90	2·42
1·75	0·310	0·380	..	3·22	..
2·0	0·282	0·436	..	3·54	2·32
2·5	0·239	0·522	..	4·18	..
3·0	0·207	0·586	..	4·81	2·22
3·5	0·183	0·634	..	5·45	..
4·0	0·164	0·672	..	6·10	2·18
5·0	0·135	0·730	..	7·35	2·15

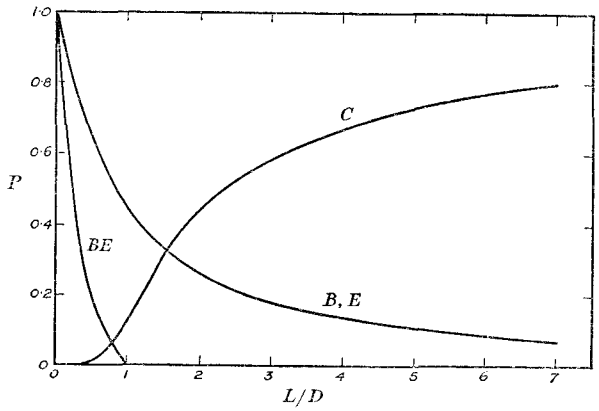

FIG. 76. Probability P of observing meteors of path length L with a telescopic field of diameter D. BE paths beginning and ending in the field. C paths which cross the field. B, E paths which begin or end in the field.

There data were used to determine the average path length for meteors of given brightness.

3. The observational data

(a) *Counts and Path Lengths*

The observations were made in 1934 at an elevation of 6,000 ft. in south California using a 4-in. telescope mounted horizontally with a 45° mirror in front of the lens for observing the meteors in the zenith. From star transits the field diameter was found to be 220 min. of arc. The magnification was 18 giving an observer's eye field of 66° diameter. The effective field of view for different magnitudes was determined by observing the distances of the beginning and ending points of trails from the centre of the field. The results were as shown in Table 13.

TABLE 13

Effective Field of View for Different Meteor Magnitudes

Apparent magnitude . .	< 3	3·5	4·5
Diam. of effective field . .	220′	140′	80′
Diam. of effective eye field .	66°	42°	24°

The numbers of meteors in the various categories outlined in § 2 were then counted for field diameters of 220′ (66°), 110′ (33°), 55′ (16·5°) and Fig. 76 used to determine the path lengths. The total numbers of all categories observed for various field diameters are given in Table 14.

TABLE 14

Number of Meteors as a Function of Field of View and Magnitude

Apparent magnitude	*Frequencies for fields of*			*Ratios*	
	220′ (N_a)	110′ (N_b)	55′ (N_c)	N_a/N_b	N_b/N_c
1·5	11	7	..	1·6±0·8	..
2·5	29	22	12	1·3±0·4	1·81±0·7
3·5	49	36	15	1·35±0·3	2·40±0·8
4·5	85	62	25	1·37±0·2	2·50±0·6

Some of the ratios N_a/N_b and N_b/N_c fall below 2, indicating that the effective field diameter was less than that used to obtain the ratio. These ratios can also be used to estimate the path lengths by using the last column of Table 12. The accuracies are rather low, the path length for different magnitudes varying as shown in Table 15 amongst the four different derivations.

TABLE 15

Path Length of Meteors as a Function of Magnitude

App. mag.	*Path length from Fig. 76*			*Path length from Table 12, column 6*
	220′ field	*110′ field*	*55′ field*	
1·5	530′	..	..	..
2·5	925′	..	..	..
3·5	240′	165′	160′	80′
4·5	66′	33′	44′	60′

(*b*) *Magnitudes*

In order to combine the results with the naked-eye observations it was necessary to associate the two scales of magnitude. During the telescopic observations simultaneous observations were made in the zenith by a naked-eye observer, and in a number of cases faint meteors seen by the naked-eye observer were observed in coincidence with the telescope. The results are given in Table 16; together with the results of similar observations made by Öpik.†

TABLE 16

Correlation of Naked-eye and Telescopic Magnitude Scales

Naked-eye magnitude	*Telescopic magnitude*								
	−2	−1	−0·5	0·0	0·5	1·0	1·5	2·0	2·5
1·0 . . .	1	1	..	..	..	..	..	..	..
1·5 . . .	..	..	..	..	..	..	?	..	..
2·0 . . .	..	..	..	..	..	..	..	1	..
2·5 . . .	..	..	..	..	..	..	..	..	..
3·0 . . .	..	1	..	..	..	1	..	..	..
3·5 . . .	..	..	..	..	1	1	..	..	..
4·0 . . .	..	..	..	..	..	3	1	1	?
Total coincidences	1	2	0	0	1	5	1	2	?
Telescopic but not naked eye .	..	..	..	..	..	2	4	7	17
Fractions obs. by naked eye .	1·0	1·0	..	..	1·0	0·71±0·6	0·25	0·22±0·14	?
Öpik's ratio .	1·0	1·0	..	..	0·62	0·50	..	0·21	..
Mean naked-eye magnitude .	1	2	..	..	3·5	3·7	4	4	..

The magnitude correction scale was extended to the eighth magnitude by observing the apparent magnitude of faint stars in the telescope; beyond, extrapolation was necessary to the limiting magnitude (tenth). The final correction curves used are shown in Fig. 77.

† Öpik, E., *Publ. Tartu Obs.* **25** (1923), no. 4.

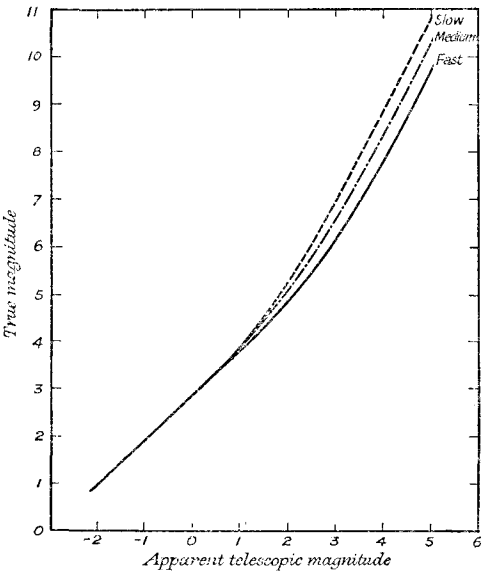

FIG. 77. Correction curves to true meteor magnitudes used by Watson for meteors of different speeds.

4. The frequency of different magnitudes

The final results of the work of Watson can be combined as in Tables 17 and 18. The mean path length is taken from Table 15 and the adjustment to kilometres made by assuming a height of 86 km. with no allowance for projection effects.

The total observing time was 1,529 minutes. Correcting for the difference between this and the length of a day (1,440 minutes), and using the data in Tables 17 and 18, gives the data shown in Table 19 for the numbers of meteors of different magnitudes entering the whole earth's atmosphere daily.

TABLE 17

Path Length and Effective Area of Visibility for Meteors of Different Magnitudes

Magnitude		*Path length*			*Effective area*	
Apparent	*True*	*Min. of arc*	*Km.*	*Effective field diam.*	*Sq. min.*	*Fraction of atmosphere*
1·5	4·5	500	12	220′	15×10^4	18×10^{-8}
2·5	5·8	500	12	220′	15	18
3·5	7·5	160	5·0	140′	3·8	4·6
4·5	9·5	50	1·3	80′	0·9	1·1

TABLE 18

Number of Meteors of Different Magnitudes

App. magnitude	−2	−1	0·0	0·5	1·0	1·5	2·0	2·5	3·0	3·5	4·0	4·5	5·0
No. of slow meteors .	0	0	0	1	0	0	3	1	1	0	0	4	2
No. of medium meteors .	1	2	1	1	2	4	5	15	17	20	28	21	2
No. of fast meteors .	0	0	0	0	4	1	1	3	6	9	19	11	3

TABLE 19

Numbers of Meteors of Different Magnitudes entering the Earth's Atmosphere per Day

True magnitude .	1	2	3	4	5	6	7	8	9	10
Number . .	2	2	6	28	53	143	292	790	2,240	$(1{,}660)\times 10^6$
Log N . .	6·3	6·3	6·76	7·47	7·72	8·16	8·47	8·90	9·36	(9·23)

The change in numbers dN with magnitude dm appears to be of the form

$$dN = \varkappa^m \, dm. \qquad (1)$$

The base $\varkappa$ is the increase in numbers per magnitude, and in the present case has a value of about 2·5 when averaged over the range of magnitudes given in Table 19. At the ninth magnitude some 2×10^9 meteors per day enter the atmosphere. The figures for the tenth magnitude cannot be regarded as complete since this is near the limiting magnitude for the observations.

5. Other observations of the frequency distribution

In an earlier analysis of the problem Watson† used data obtained by Öpik‡ and Boothroyd§ during the Arizona Meteor Expedition. He selected those meteors which were then recorded as having hyperbolic velocities in order to derive the mass distribution in interstellar space. It is now believed that these hyperbolic velocities were erroneous,‖ nevertheless this fact does not significantly influence Watson's analysis. Boothroyd§ listed 707 telescopic observations of which 488 were selected as having angular velocities 3 deg./sec. in excess of the parabolic limit. Öpik‡ listed 279 naked-eye observations of which 133 were selected as having heliocentric velocities greater than 50 km./sec.

† Watson, F., *Ann. Harv. Coll. Obs.* **105** (1937), 623.
‡ Öpik, E., *Circ. Harvard Coll. Obs.* (1934), no. 389.
§ Boothroyd, ibid., no. 390.
‖ See Chap. XII.

The observations described in §§ 1–4 were made in the zenithal direction. In the present observations corrections have to be applied to the observed magnitudes since the observations were not restricted to the zenith. Since meteors observed at low altitudes may be at considerable distances from the observer it is necessary to correct all observed magnitudes to the zenith where they become comparable.

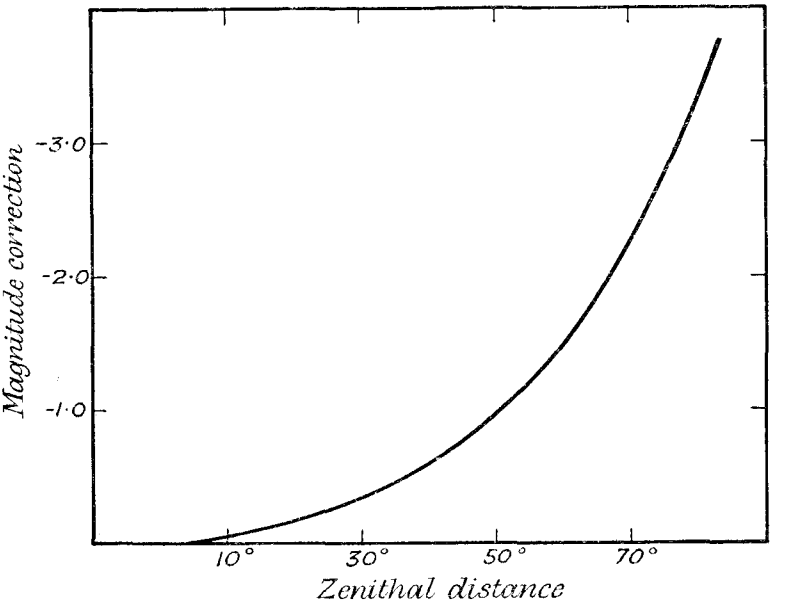

FIG. 78. Curve for correction of observed meteor magnitudes to zenithal magnitudes.

Boothroyd's telescopic observations were at 45° to the zenith and a constant zenithal correction of $-0{\cdot}76^{m}$ was applied. For the naked-eye observations the corrections derived by Öpik† and plotted in Fig. 78 were applied. The various other corrections for field of view of the telescope and the change of field diameter with brightness as described in §§ 1–4 were also applied. The results for the daily frequency over the entire atmosphere for the different magnitudes are plotted in Fig. 79. Also plotted are the later results of Watson (from Table 19), and other data by Öpik and Hoffmeister. Öpik's‡ results were obtained from an investigation of the luminosity function of Perseids and non-Perseids. Watson assumes that the non-Perseids were interstellar meteors, and

† Öpik, E., *Publ. Tartu Obs.* **25** (1923), no. 4, 70.
‡ Öpik, E., ibid. (1922), no. 1.

that the observers in all cases watched the same area of sky. The results of Hoffmeister† are from a list of 4,478 naked-eye observations made over a period of two years. Watson adjusts Hoffmeister's magnitude scale so that the fifth magnitude was the limiting magnitude, and not the sixth, as given by Hoffmeister.

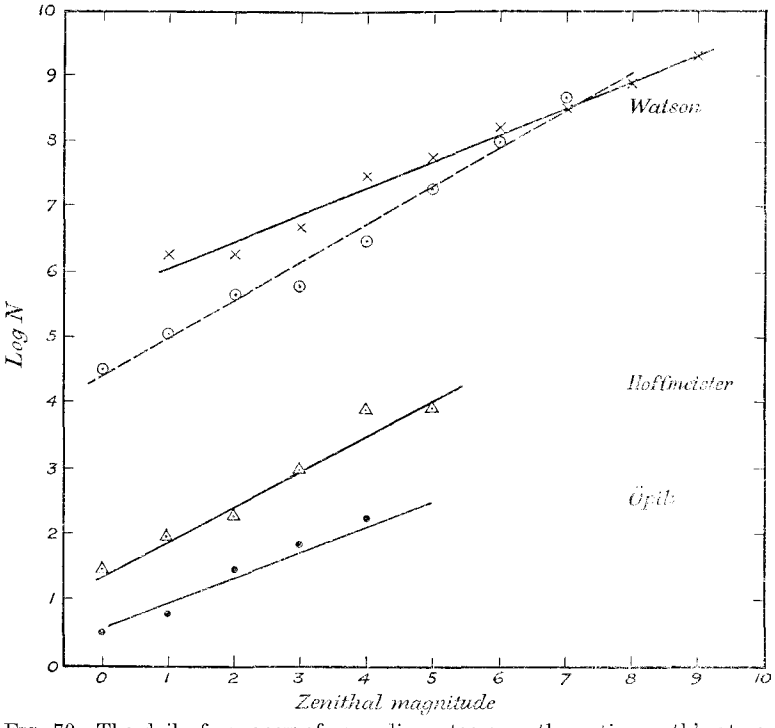

FIG. 79. The daily frequency of sporadic meteors on the entire earth's atmosphere, according to Öpik, Hoffmeister, and Watson.

⊙–⊙ Watson, derived from the telescopic observations of Boothroyd and Öpik.
– × – × Watson, from independent telescopic observation in the zenith (plotted from Table 19).

Probably not much weight can be attached to the difference in numerical magnitude between the results of Watson, Öpik, and Hoffmeister since the data from the two latter have not been taken from a specific investigation of daily frequency. The agreement between the slope of the various curves is satisfactory. According to McKinley,‡ Millman has determined the distribution from 1,938 visual observations made on clear moonless nights by a team of six observers. The slope of the curve from magnitude −3 to +3 is similar to those of Fig. 79 and

† Hoffmeister, C., *Veröff. Berlin-Babelsberg*, **9** (1931).
‡ McKinley, D. W. R., *Canad. J. Phys.* **29** (1951), 403.

gives a value of $\varkappa$ in equation (1) of 2·7, which is in satisfactory agreement with Watson's value of 2·5.

There is no good evidence as to whether the base $\varkappa$ remains constant over a wide range of magnitudes. In the data of Table 19 covering magnitudes from +1 to +10 there is no systematic trend, the value of $\varkappa$ varying in random fashion about the average of 2·5, showing a minimum of 1 between magnitudes +1 and +2, and a maximum of 4·66 between magnitudes +3 and +4. There is some evidence that, in the case of very bright meteors, the value of $\varkappa$ is greater. Thus Millman† investigated the theoretical frequency distribution of photographic meteors, and from a study‡ of Harvard meteor photographs in the magnitude range −2 to −7 found a value of $\varkappa = 3{\cdot}5$.

The distribution has also been investigated by Williams.§ Using naked-eye and binocular observations he first established that the value of $\varkappa$ had the same value at two points on the magnitude scale separated by 5 or 6 magnitudes. Two short magnitude intervals were chosen for comparison where the various selective processes could be expected to be the same. The value of $\varkappa$ obtained was $2{\cdot}29 \pm 0{\cdot}16$, but Williams considered that this could have only small weight owing to preferential selection. He therefore chose observations from the binocular series best suited to a determination of $\varkappa$ on the assumption that it was constant over the magnitude range. From the original observations, which were made by Knabe,‖ Williams selected meteors such that the initial points were not greater than 3° from the centre of the field of view, at which the observer's eyes were directed. The magnitude estimate corresponding to maximum light was adopted. Table 20 was thereby obtained, showing the frequency of initial points f for meteors of apparent magnitude m, at distances R from the centre of the field.

The unit of area is taken as that for $R = 0{\cdot}5°$, which is almost exactly the area observed by the *macula lutea* region in the retina of the human eye. The column F shows the frequency reduced to equal areas for meteors brighter than +8 mag. The decrease is almost linear as one recedes from the foveal region of the eye. Williams considers that the decrease is not due to lack of sensitivity outside the foveal region, but more probably to lack of attention as one recedes from this region. In view of the small size of the sample and of the roughness of the run in

† Millman, P. M., *Proc. Nat. Acad. Sci. Wash.* **19** (1933), 34.
‡ Millman, P. M., *J. Roy. Astr. Soc. Can.* **29** (1935), 210.
§ Williams, J. D., *Astron. J.* **48** (1939), 100; *Proc. Amer. Phil. Soc.* **81** (1939), 505; *Astrophys. J.* **92** (1940), 424.
‖ See Williams, J. D. (1939), ibid.

frequencies Williams obtained the most probable value of $\varkappa$ for each zone by an objective method of maximum likelihood due to Fisher.†

TABLE 20

Frequency of Meteors as a Function of Magnitude in Williams's Analysis

m / R	1	2	3	4	5	6	7	8	9	*Area*	*F*	$\varkappa$	$\sigma_\varkappa$
deg.													
0·5	0	0	1	4	3	2	8	8	4	1	1·00	1·75	±0·23
1·0	0	1	0	2	6	4	15	28	5	3	0·52	2·04	±0·28
1·5	0	3	0	1	4	6	25	38	7	5	0·43	2·22	±0·29
2·0	1	1	0	4	6	9	28	46	2	7	0·39	2·11	±0·23
2·5	0	0	0	3	6	11	22	36	5	9	0·26	2·31	±0·31
3·0	2	1	0	3	4	12	24	27	2	11	0·23	2·00	±0·21
f	3	6	1	17	29	44	122	183	25				

If the magnitude range is cut into $s+1$ intervals by the points

$$-\infty,\ \mathrm{m}_0,\ \mathrm{m}_0+\Delta\mathrm{m},\ \mathrm{m}_0+2\Delta\mathrm{m},\ldots,\ \mathrm{m}_0+s\Delta\mathrm{m}=\mathrm{m}'$$

then the probability $\mathbf{p}_i$ of finding a meteor in the sample whose magnitude lies in the $(i+1)$th interval is

$$\mathbf{p}_i = \mathrm{A}\int_{\mathrm{m}_0+(i-1)\Delta\mathrm{m}}^{\mathrm{m}_0+i\,\Delta\mathrm{m}} e^{\mathbf{a}\mathrm{m}}\,\mathrm{dm} \quad (i=1,2,\ldots s),$$

and

$$\mathbf{p}_0 = \mathrm{A}\int_{-\infty}^{\mathrm{m}_0} e^{\mathbf{a}\mathrm{m}}\,\mathrm{dm} \quad (e^{\mathbf{a}}=\varkappa),$$

where A is fixed by the normalization $1=\mathrm{A}\int_{-\infty}^{\mathrm{m}'} e^{\mathbf{a}\mathrm{m}}\,\mathrm{dm}$. $\mathbf{a}$ has to be determined in terms of the observed frequencies f_i $(i=0,1,\ldots,s)$. It can be established that the likelihood of the sample

$$P=\prod_0^s \mathbf{p}_i^{f_i}$$

is a maximum when

$$\coth\tfrac{1}{2}\mathbf{a}\Delta\mathrm{m}=1+\frac{2}{N-f_0}\left[N_s-\sum_1^s if_i\right],$$

where N is the total observed frequency, a result obtained when the logarithmic derivative of P with respect to $\mathbf{a}$ is equated to zero. This

† Fisher, R. A., *Proc. Camb. Phil. Soc.* **22** (1925), 700.

equation gives an optimum estimate of $\mathbf{a}$, and its standard deviation is estimated from

$$\sigma_a = \left[E\left(-\frac{d^2 \log P}{da^2}\right)\right]^{-\frac{1}{2}} = \frac{2 \sinh \frac{1}{2}a\Delta m}{\Delta m \sqrt{\{N(1-p_0)\}}},$$

where E indicates the operation of taking the mean value. Thus $\sigma_\kappa = \kappa\sigma_a$.

Using the above equations, Williams computed κ and σ_κ for each zone using only meteors brighter than magnitudes +7·75. These values are given in Table 20. The combination leads to a value of

$$\kappa = 2{\cdot}08 \pm 0{\cdot}10.$$

The computed frequencies compared with the observed are given in Table 21.

TABLE 21

Comparison of Observed and Computed Meteor Frequencies as a Function of Magnitude in Williams's Analysis

m	1·0	1·5	2·0	2·5	3·0	3·5	4·0	4·5	5·0
Observed	1	2	0	6	0	1	10	7	9
Computed	0·6	0·8	1·2	1·7	2·5	3·6	5·2	7·6	10·9

m	5·5	6·0	6·5	7·0	7·5	8·0	8·5	9·0	9·5
Observed	20	21	23	51	71	105	78	22	3
Computed	15·7	22·7	32·7	47·2	68·0	98·3	142	205	296

The result of these various observations is that the three most direct investigations of the frequency distribution give values of κ of 2·7 (Millman), 2·5 (Watson), and 2·08 (Williams) in the visual and near infra-visual magnitude range, while there is some evidence that for very much brighter meteors the value of κ is 3·5 (Millman). The position is not satisfactory, but there is good hope that in the near future the radio-echo techniques may be used to determine an independent value. A method depending on the measurement of the height distribution is described in Chapter XIX in connexion with the frequency distribution of the shower meteors. Preliminary application of this method to the sporadic distribution gives a value of $\kappa = 2{\cdot}5$.

6. The mass distribution

Since the magnitude of a meteor is proportional to the logarithm of the intensity, which, in turn, depends directly on the mass m, equation (1) for the frequency distribution of magnitudes becomes

$$dN = \frac{dm}{m^p}$$

for the mass-frequency distribution. The exponent p is related directly to the base $\varkappa$ of equation (1). For a likely value of $\varkappa = 2{\cdot}5$, the exponent $p = 2$, and the mass distribution follows an inverse square law.

In this section we shall be concerned with the actual meteoric mass entering the atmosphere in the various magnitude groups. Uncertainties in the mass estimates arise because of the incomplete state of the meteor evaporation theory. Whereas the relation between luminosity, mass, and velocity can be expressed as

$$I = \text{const.} \times m \times v^{s} = 10^{-0{\cdot}4 \times (\text{mag})}, \tag{2}$$

the possible values for the exponent s vary over a wide range. Thus Öpik† originally proposed a value for $s = 2{\cdot}5$, which has been adopted by Watson‡ in his work on the mass distribution. In his full theory, however, Öpik§ deduces $s = 3$, but more recently‖ concludes that $s \leqslant 1$. Similar uncertainty exists over the mass to be attributed to a meteor of given magnitude, but according to current ideas the original calculations of Öpik§ indicating a most probable mass of 12 milligrams for a Perseid meteor of second magnitude appears to be approximately correct.

By substitution in (2), taking $s = 2{\cdot}5$ and $v = 56$ km./sec., Watson‡ evaluated the constant as $5{\cdot}64 \times 10^{-7}$, giving the equation for mass determination in the form

$$\text{Mass (mg.)} = 1{\cdot}77 \times 10^{6} \times 10^{-0{\cdot}4(\text{mag})} \times v^{-2{\cdot}5}. \tag{3}$$

For the extreme limits of $s = 1$ to $s = 3$ the respective equations are

$$\text{Mass (mg.)} = 4{\cdot}25 \times 10^{3} \times 10^{-0{\cdot}4(\text{mag})} \times v^{-1}, \tag{4}$$

$$\text{Mass (mg.)} = 1{\cdot}33 \times 10^{7} \times 10^{-0{\cdot}4(\text{mag})} \times v^{-3}. \tag{5}$$

Thus taking Öpik's figure of 12 mg. as the most probable mass of a second magnitude Perseid meteor moving with a geocentric velocity of 56 km./sec., equations (4) and (5) give the mass limits in Table 22 for meteors of various magnitudes moving at the parabolic limiting velocity (72 km./sec.).

† Öpik, E. J., *Circ. Harvard Coll. Obs.* (1930), no. 355.
‡ Watson, F., loc. cit.
§ Öpik, E. J., *Publ. Tartu Obs.* (1933), no. 26. (Harvard Reprint, no. 100.)
‖ Öpik, E. J., *Observatory*, **68** (1948), 229.

TABLE 22

Relation of Meteor Magnitude and Mass

Magnitude	1	2	3	4	5	6	7	8	9	10
Mass (mg.) eq. (4)	23·5	9·35	3·7	1·48	0·59	0·23	0·093	0·037	0·014	0·0059
Mass (mg.) eq. (5)	11·3	5·66	2·25	0·89	0·35	0·14	0·056	0·022	0·0089	0·0036

Watson reduced his data to total masses by using equation (3) and accepting the geocentric velocities, which extended from 20 to 220 km./sec., as real. Velocities in excess of the parabolic limit are not now believed to exist† and hence it seems more satisfactory to reduce Watson's later data given in Table 19 assuming that all the meteors are moving with velocities near the parabolic limit and using the mass limits of Table 22. The results for the total daily mass intercepted by the earth's atmosphere for the magnitude range 1 to 9 are given in Table 23, for the two assumptions about the velocity term. Also included are Watson's results using the $v^{5/2}$ term, including his analysis for the presumed velocities up to 220 km./sec.‡

TABLE 23

Daily Mass of Sporadic Meteors intercepted by the Earth as a Function of Meteor Magnitude

Magnitude	1	2	3	4	5	6	7	8	9	Σ *Mass magnitudes* 1 *to* 9 *inclusive*
Σ Mass using eq. (4) ($\times 10^7$ mg.)	4·7	1·88	2·22	4·15	3·1	3·3	2·7	2·9	3·1	$2{\cdot}8\times10^8$
Σ Mass using eq. (5) ($\times 10^7$ mg.)	2·3	1·13	1·35	2·5	1·8	2·0	1·6	1·7	1·8	$1{\cdot}6\times10^8$
Σ Mass, Watson ($\times 10^7$ mg.)	0·13	0·19	0·20	0·72	0·53	1·4	2·0	1·2	(1·6)†	$0{\cdot}8\times10^8$

† Mean of 7 and 8.

In view of the uncertainties in the work the agreement is rather good. Even the difference between the extreme assumptions of the hyperbolic theory (last line) and the parabolic theory leads to no more than a factor 4 of uncertainty in the total daily mass for nine magnitudes. Greater importance must be attached to the first two estimates as based on more recent observations by Watson and calculated in line with the parabolic theory. A figure of 2×10^7 mg. per magnitude per day over

† See Chap. XII.

‡ Watson, F., loc. cit.

the entire atmosphere is probably correct to within a factor of 10 even allowing for uncertainties in the basic assumption of 12 mg. for the mass of a second magnitude Perseid meteor. It will be noticed that, although for each fainter magnitude there are about 2·7 times as many meteors (Table 19), the total mass in each magnitude remains constant.

Table 23 has been restricted to magnitudes 1–9 as representing the limits included in Watson's later observations. Watson's earlier analysis of the Arizona data† extended to magnitude −3 and indicates that the same mass distribution will be appropriate. There does not appear to be any published investigation of the magnitude ranges outside these limits of −3 to +10, although Watson‡ assumes that the relation will hold from −10 to +30. At the brighter limit the meteors will penetrate to the earth as meteorites, and the estimated mass falling per day is 550 kg.§ At the faintest limit the particles will be too small to enter the atmosphere, being dispersed by radiation pressure from the sun.‖ Table 24 summarizes these various estimates of mass and energy brought into the atmosphere assuming the meteors move at the parabolic velocity limit.

TABLE 24

Mass and Energy brought into the Earth's Atmosphere by Sporadic Meteors

Meteors	*Total daily mass over earth's atmosphere (kg.)*	*Total energy per day (ergs)*
(*a*) > −10 mag.—based on meteorite falls	550	$13{\cdot}0 \times 10^{18}$
(*b*) −4 to −9 mag.—extrapolation from (*c*)	120	3×10^{18}
(*c*) −3 to +9 mag.—observational data (Table 23)	260	$6{\cdot}5 \times 10^{18}$
(*d*) +10 to +30 mag.—extrapolation from (*c*)	400	$10{\cdot}0 \times 10^{18}$
Total	1,330	$3{\cdot}2 \times 10^{19}$

7. The space distribution

From the above data it is possible to calculate the density of meteoric matter in the solar system. The number of meteors swept up in time t by the earth will be those contained in the cylinder of volume

$$\pi r_e^2 \, \mathrm{t} \mathrm{v},$$

where r_e is the radius of the earth's atmosphere (6,400 km.) and v the

† Watson, F., *Ann. Harv. Coll. Obs.*, loc. cit.
‡ Watson, F., *Between the Planets* (Blakiston, 1948).
§ See Chap. XIX.
‖ See Chap. XX.

relative velocity of earth and meteors. Taking v = 72 km./sec. (the parabolic geocentric limit), the volume of this cylinder per day is $8{\cdot}0\times10^{14}$ km.^{3} From Table 23 we have deduced that the meteoric mass swept up per day per magnitude is 2×10^7 mg. Thus the spatial density is

$$2{\cdot}5\times10^{-11} \text{ gm./km.}^3\text{/magnitude}$$

$$= 2{\cdot}5\times10^{-26} \text{ gm./c.c./magnitude.}$$

The distribution of space density in the various mass groups derived from the information given in the previous tables is shown in Table 25.

TABLE 25

Space Distribution of Sporadic Meteor Material

Meteor magnitudes		*Mass range of individual particles*	*Number per day*	*Mass per day*	*Number per c.c.*	*Density gm./c.c.*
Extrapolation	−10 to −8	500 to 100 gm.	~ 300	$\sim 6.10^4$ gm.	4.10^{-28}	$7{\cdot}5.10^{-26}$
	−7 to −6	100 to 10 gm.	$\sim 2{,}500$	$\sim 4.10^4$	3.10^{-27}	$5{\cdot}0.10^{-26}$
	−5 to −4	10 to 1 gm.	$\sim 1{\cdot}8.10^4$	$\sim 4.10^4$	2.10^{-26}	$5{\cdot}0.10^{-26}$
	−3 to −1	1 gm. to 100 mg.	$\sim 4.10^5$	$\sim 6.10^4$	5.10^{-25}	$7{\cdot}5.10^{-26}$
Observational data	0 to +1	100 mg. to 10 mg.	10^6	4.10^4	$1{\cdot}5.10^{-24}$	$5{\cdot}0.10^{-26}$
	2 to 4	10 to 1	$3{\cdot}6.10^7$	6.10^4	$4{\cdot}5.10^{-23}$	$7{\cdot}5.10^{-26}$
	5 to 6	1 to 0·1	$1{\cdot}9.10^8$	4.10^4	$2{\cdot}4.10^{-22}$	$5{\cdot}0.10^{-26}$
	7 to 9	0·1 to 0·01	$3{\cdot}3.10^9$	6.10^4	$4{\cdot}1.10^{-21}$	$7{\cdot}5.10^{-26}$
	10 to 12	0·01 to 0·001	$6{\cdot}5.10^{10}$	6.10^4	$8{\cdot}1.10^{-20}$	$7{\cdot}5.10^{-26}$
Extrapolation	13 to 20	10^{-3} to 10^{-7}	$\sim 10^{19}$	16.10^4	$\sim 10^{-11}$	$\sim 20.10^{-26}$
	21 to 30	10^{-7} to 10^{-11}	$\sim 10^{29}$	18.10^4	$\sim 10^{-1}$	$\sim 20.10^{-26}$

In the range of masses from 1 gram to 10^{-3} mg. (−3 to +12 magnitude) the space density is about $8{\cdot}5.10^{-20}$ particles per c.c. and the mass density about 4×10^{-25} gm./c.c. These figures are probably reliable to within a factor of 10. The extrapolation to larger and smaller limits assumes that the same distribution applies as in the observed magnitude range and must be regarded as somewhat uncertain. If these are included the density increases to about 10^{-24} gm./c.c. These figures are of the same order as those obtained by Watson† using the Arizona data and allowing for the presumed hyperbolic velocities.

It is of interest to compare these figures with the density of matter in interstellar space, which is believed to be between 10^{-24} and 10^{-26} gm./c.c.‡ This is the same range of densities indicated above for the meteoric matter in the solar system. The absorption measurements indicate that these interstellar particles have radii of 10^{-5} or 10^{-6} cm. giving masses of less than 10^{-14} gm. Such particles, which lie well below the mass limit

† Watson, F., *Ann. Harv. Coll. Obs.*, loc. cit.
‡ *Centennial Symposium* (Harvard, 1948).

of 10^{-11} gm. considered here, would not be expected to appear as meteors in the earth's atmosphere.

The data considered in this chapter refer only to sporadic meteors. During the occurrence of the intense meteor showers these numbers and densities will be increased. This subject will be considered in Chapter XIX.

VIII

THE VELOCITY OF SPORADIC METEORS—I

INTRODUCTION AND THE VON NIESSL–HOFFMEISTER FIREBALL CATALOGUE

ACCORDING to equation (16) of Chapter V the limiting or parabolic velocity of a meteor of mass m at a distance r from the sun is given by

$$\overline{V}_p^2 = \gamma(M+m)\frac{2}{r}, \tag{1}$$

where γ is the constant of gravitation and M the mass of the sun. If for r we write the mean distance of the earth from the sun, then the limiting heliocentric velocity is

$$\overline{V}_p = 42{\cdot}1 \text{ km./sec.}$$

The question as to whether the velocities of sporadic meteors exceed this limit, and therefore have an interstellar origin, has provoked a major discussion in meteor astronomy. This problem arose in Chapter VI in connexion with the diurnal variation in sporadic meteor rates. In the next five chapters it will be discussed on the basis of the actual measurement of meteor velocities. There are at least three major difficulties which give rise to the uncertainty in providing a clear-cut answer to this problem:

(*a*) None of the existing methods of velocity measurement (Chapters II and IV), except the photographic, can provide a sufficiently precise measurement of an individual meteor velocity; and so far the photographic measurements have been restricted to comparatively small numbers of bright meteors.

(*b*) The velocity of a particle moving through space, at rest with respect to the sun, would be 20 km./sec. Further, it is known that the peculiar velocity of interstellar clouds relative to the sun is small, amounting to 10 km./sec. or less.† Hence it is reasonable to assume that the resultant velocity v of an interstellar particle in the solar system would be of the same order as that of the sun through space, that is 20 km./sec. The heliocentric velocity V of such a particle at the

† Adams, W. S., *Astr. J.* **97** (1943), 105; Whipple, F. L., *Centennial Symposium* (Harvard, 1946), p. 110; Greenstein, J., *Astrophysics* (McGraw Hill, 1952).

distance of the earth from the sun will be given by

$$v^2 = V^2 - \bar{V}_p^2 \qquad (2)$$

or $V = 46{\cdot}6$ km./sec. for $v = 20$ km./sec. Thus the most common interstellar particles would be expected to exceed the parabolic limiting velocity by only 10 per cent.

(*c*) The heliocentric velocity cannot be measured directly, but can only be inferred from a measurement of the geocentric velocity, v. For this to be done it is necessary to measure the spatial path of the meteor as well as its velocity, in order to allow for the earth's orbital motion and the gravitational attraction of the earth on the meteor. The velocity of a meteor in free fall (neglecting air resistance), which is initially at rest, reaches 11·1 km./sec. due to the earth's attraction. The correction for this alone varies from 1 to 5 km./sec. in the extreme cases of head-on and approach from behind, respectively.

1. The von Niessl–Hoffmeister fireball catalogue

If the length of the meteor path is divided by the time of flight and if the height is known, an estimate of the geocentric velocity of the meteor can be obtained. From such estimates Brandes and Benzenberg of Göttingen first decided that meteors were extra-terrestrial bodies. Since the estimates of duration (a fraction of a second) are very uncertain, the derived velocities are liable to gross errors. In the case of fireballs, or very bright meteors, the position is better because of the much greater length of the visible trail and the longer duration compared with ordinary meteors. The famous *Katalog der Bestimmungsgrößen für* 611 *Bahnen großer Meteore* by von Niessl and Hoffmeister† was compiled from such observations and has given rise to protracted discussion, because 79 per cent. of the fireballs are listed as possessing hyperbolic velocities. The catalogue is a critical selection from the available data on bright meteors. After von Niessl's death the catalogue was completed by Hoffmeister to No. 518. The list to No. 611 was added by Hoffmeister from unfinished discussions and new data. Of the entries in the catalogue 283 are from English observers,‡ 23 from America, and 71 from von Niessl's recomputation of other British data.§

† von Niessl, G., and Hoffmeister, C., *Denksch. d. Akad. d. Wiss. Wien, Math.-Naturw.* (1925), 100.

‡ Herschel or Denning 268, Tupman 10, Glaisher 1, Crumplen 1, Davidson 3.

§ From the Reports of the Committee on Luminous Meteors of the British Association for the Advancement of Science.

2. Fisher's first criticism

The conclusion in favour of such a high percentage of hyperbolic velocities was first criticized by Fisher,† who assembled fireball lists from four other sources in addition to the catalogue, in order to compare the seasonal trends. Fisher's sources were as follows the sequence corresponding to the respective plots in Figs. 80–84.‡

(i) Personal observations of 168 fireballs between 1841–53 by Coulvier-Gravier;§

(ii) personal observations of 987 fireballs between 1876–1925 by Torwald Køhl;‖

(iii) 1,500 cases compiled from the literature (excluding (i) and (ii)) in Prior's *Catalogue of Meteorites*, Eastman's *Progress of Meteoric Astronomy in America*, *L'Astronomie*, *Bulletin de la Société Astronomique de France*, *Ciel et Terre*, and the AI series of the Harvard photographs;

(iv) 285 cases from the Harvard meteor photographs (not entirely independent of (iii));

(v) the von Niessl–Hoffmeister catalogue (not entirely independent of (iii), although it contains only 23 examples from America).

The rate plots from these five sources are shown in Figs. 80–84, taken from Fisher's work, the year being divided into seventy-three groups of five days each. In the case of Fig. 84, for the von Niessl–Hoffmeister catalogue, the velocities (hyperbolic or non-hyperbolic) are also indicated. From a comparison of these rates Fisher formed the opinion that there was a definite periodicity in the arrival of fireballs and hence that their frequency depended on the position of the earth in its orbit. Also in Fig. 84 the frequency of the presumed hyperbolic velocities follows the same periodicity. Now, if there are 79 per cent. interstellar particles in the sample their distribution would be expected to be random. Fisher draws particular attention to the minimum around June 19–24 at sun's longitude 90°. He considers that the two possible influences on the randomness—the sun's motion and the possibility of interstellar streams—could not be responsible for the patchiness and that the clustering in the radiants of the fireballs, shown in Figs. 85, 86, and 87,‡ indicates that they are associated with well-known shower radiants with elliptic or nearly parabolic velocities. But the computed

† Fisher, W. J., *Circ. Harv. Coll. Obs.* (1928), no. 331.

‡ Figs. 80–87 are taken from Fisher, W. J., ibid.

§ Coulvier-Gravier, F. A.; F. Arago, *Astronomie Populaire*, **4** (1857), 275.

‖ Torwald Køhl, *Nordisk Astronomisk Tidsskrift*, **6** (1925), 97.

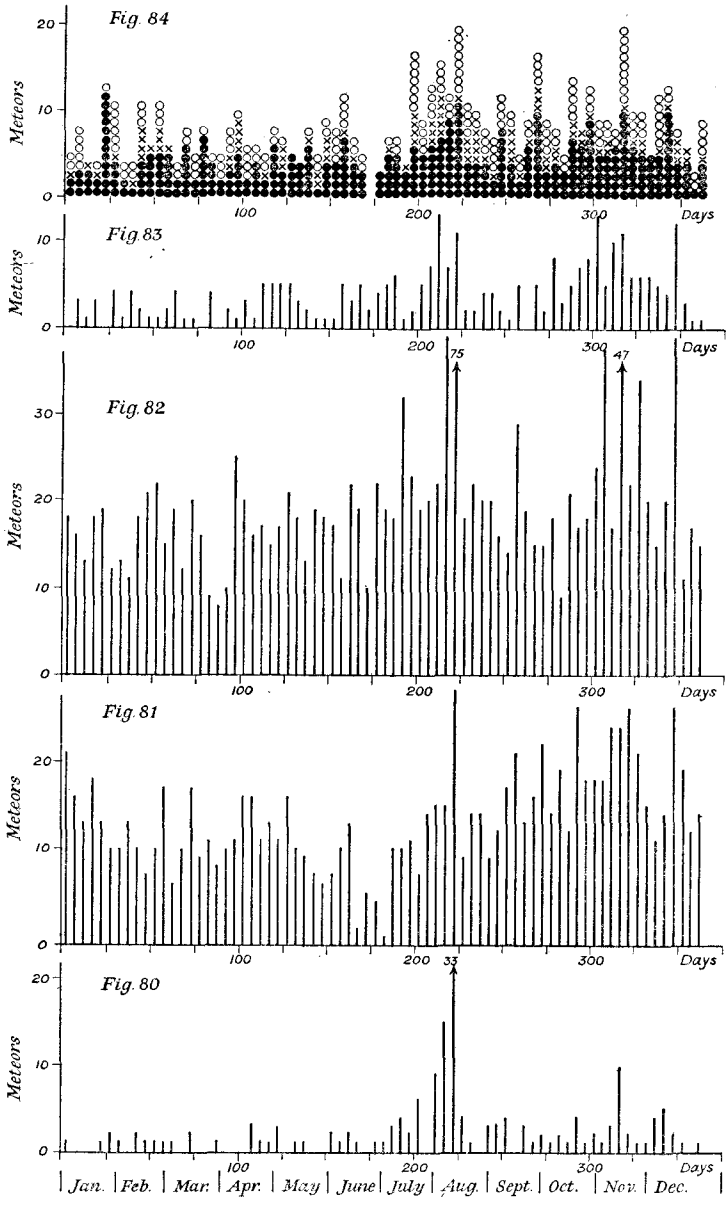

FIGS. 80–84. The fireball rates throughout the year as found by: (80) Coulvier-Gravier; (81) Torwald Køhl; (82) Miscellaneous catalogues (see text); (83) Harvard meteor photographs; (84) von Niessl-Hoffmeister fireball catalogue.
● hyperbolic velocities. × less than hyperbolic. ○ undetermined.

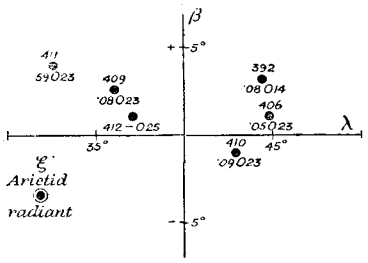

FIG. 85. Radiants of the fireballs in the von Niessl–Hoffmeister catalogue between Oct. 14–25 plotted in ecliptic coordinates. The ξ Arietid radiant (see Chap. XV) is that given in Denning's catalogue, no. xxvi.

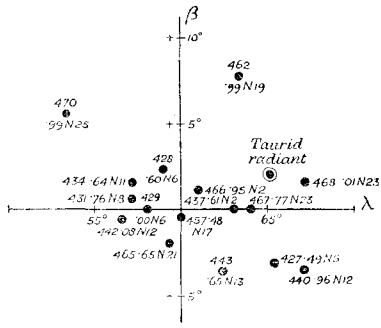

FIG. 86. Radiants of the fireballs in the von Niessl–Hoffmeister catalogue between Nov. 5–25 plotted in ecliptic coordinates. The ϵ Taurid radiant (see Chap. XV) is that given in Denning's catalogue, no. liii.

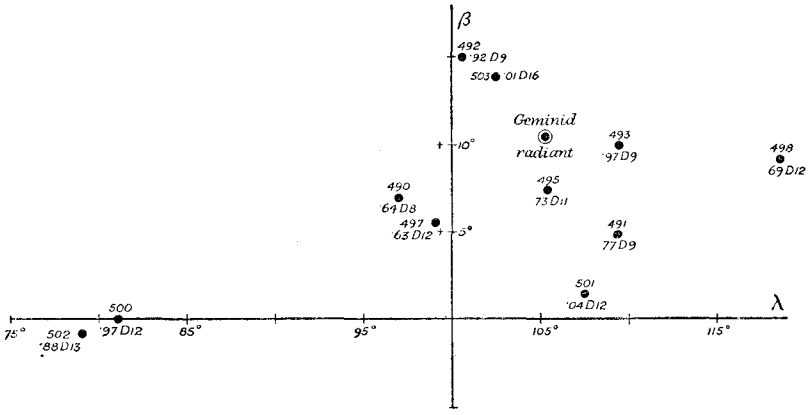

FIG. 87. Radiants of the fireballs in the von Niessl–Hoffmeister catalogue between Dec. 8–16 plotted in ecliptic coordinates compared with the Geminid radiant (see Chap. XV).

heliocentric velocities of von Niessl and Hoffmeister for these three groups are mostly hyperbolic as shown in Table 26.

Fisher also attempted to show that there must be a systematic error in the observations leading to an overestimate of geocentric velocities. However, Maltzev† pointed out that his basic equation contained an error in sign, which vitiates the argument and no purpose would be served in reproducing it.

† Maltzev, V. A., *Mon. Not. Roy. Astr. Soc.* **90** (1930), 568.

TABLE 26

Velocities in Fireball Catalogue for certain Radiant Clusters treated by Fisher

Fig. 85. *Oct.* 14–25.		*Fig.* 86. *Nov.* 5–25.		*Fig.* 87. *Dec.* 8–16.	
No. in catalogue	*Heliocentric velocity (km./sec.)*	*No. in catalogue*	*Heliocentric velocity (km./sec.)*	*No. in catalogue*	*Heliocentric velocity (km./sec.)*
392	38	427	82	490	77
406	49	428	58	491	49
409	..	429	39	492	45
410	50	431	67	493	..
411	62	434	80	495	97
412	60	437	57	497	82
		440	..	501	94
		442	49	503	36
		443	99	498	38
		457	..	500	56
		462	47	502	54
		465	37		
		466	45		
		467	41		
		468	..		
		470	51		

3. Maltzev's analysis

Maltzev further objected to Fisher's assumption that, because of the association with known radiants, the velocities must be less than parabolic, citing the beliefs of Kleiber† and von Niessl‡ that these were actually interstellar streams. We shall see in Chapter XV that the subsequent accurate velocity measurements showed that the presumed hyperbolic stream in Taurus is actually a stream in a short-period elliptical orbit. Maltzev then analysed the heights of appearance and disappearance of the fireballs in the von Niessl–Hoffmeister catalogue. His results are shown in Fig. 88, from which he concluded that the heights of appearance and disappearance increase with the geocentric velocity and that the appearance of ordinary shooting stars is 20–30 km. lower and the disappearance 20–25 km. higher than that of the hyperbolic fireballs. From a further analysis Maltzev concluded that for equal geocentric velocities the heights of appearance and disappearance depended on the heliocentric velocity of the fireballs. These data were all considered to be in favour of the hyperbolic fireball theory.

† Kleiber, J. A., *The Astronomical Theory of Shooting Stars* (St. Petersburg, 1884).
‡ von Niessl, G., *Encyklop. d. math. Wissensch.* vi (2), **10** (1910), 454.

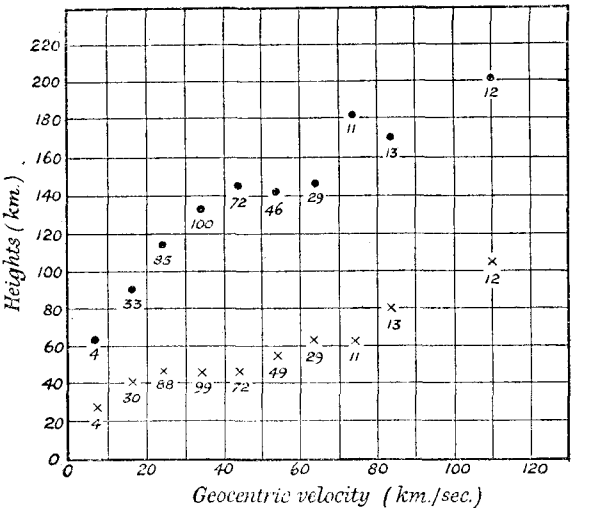

FIG. 88. Maltzev's analysis of the mean heights of appearance (●) and disappearance (×) of the fireballs in the von Niessl–Hoffmeister catalogue. The number of cases used is indicated beside each plot.

4. Fisher's second criticism

Shortly after the publication of Maltzev's work Fisher† produced further evidence that the velocities in the von Niessl–Hoffmeister catalogue must be overestimated. He effectively carried out a test, first suggested by Galle in 1874, in which the velocities of meteors belonging to well-known elliptical orbits, such as the Perseids and Leonids, are measured by the same visual technique and compared with the fireball catalogue. Fisher therefore collected observations (mostly from British sources to agree with the preponderance of data used in the fireball catalogue) on the Quadrantids, Lyrids, Perseids, Orionids, Leonids, and Geminids: all being meteor showers with generally acknowledged closed orbits. The data collected by Fisher from these sources is plotted in Figs. 89 and 90 for each of the showers and for the fireball catalogue, as a function of velocity against path length. The slant lines through the origin are the loci of points for which velocity and path length correspond to durations of $\frac{1}{2}$ sec., 1 sec., etc., as marked. The points with serial numbers also appeared in the fireball catalogue and those marked H were quoted as having a hyperbolic velocity. From these figures Fisher draws three conclusions. (i) The plots tend to group along lines of equal duration (notably 1 second)—a result due to observational

† Fisher, W. J., *Circ. Harv. Coll. Obs.* (1932), no. 375.

convenience since generally estimates, as distinct from measurements, of the time of flight were used. (ii) The spread of path lengths and velocities for equal observed durations is very great, and does not improve for long flights. The same is true of the spread with regard to the periodic velocity. (iii) Nearly all the points above the line of periodic velocity

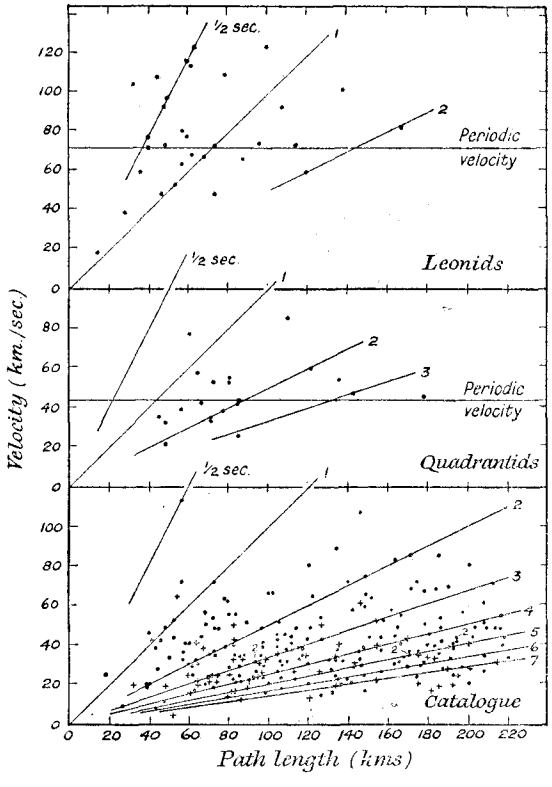

FIG. 89. (For explanation see under Fig. 90.)

would mean hyperbolic heliocentric velocities, were the meteors not otherwise identified as belonging to circumsolar streams. Thus 61 per cent. of the Leonids would have been judged to be hyperbolic meteors on this criterion, and certain Perseids, Orionids, and Geminids actually appear as hyperbolic meteors in the fireball catalogue. A further analysis of the data is given in Table 27.

Again it is evident that the means found from the observational path length/time of flight data tend to exceed considerably the geocentric velocity of the shower meteors. Thus Fisher concludes that, since the visually observed periodic meteor velocities are unreliable and high,

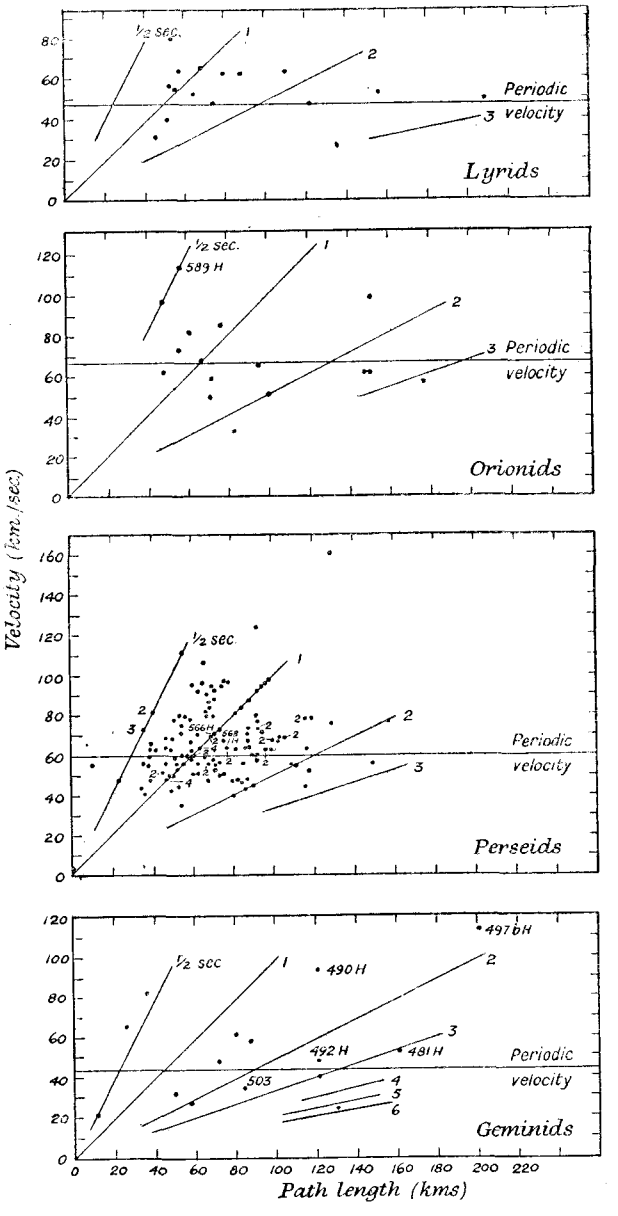

FIG. 90.

FIGS. 89 and 90. Fisher's data on the visually observed meteors from the Lyrid, Orionid, Perseid, Geminid, Leonid, and Quadrantid streams as a function of velocity against path length. Where there is ambiguity the single numbering indicates the duration groups (e.g. 2). The multiple numbering indicates that the meteor was actually used in the von Niessl–Hoffmeister catalogue (e.g. 503 = no. 503 in the catalogue, 490 H = no. 490 (hyperbolic velocity).

the von Niessl–Hoffmeister catalogue velocities with the same range of durations must be equally unreliable and high, with the probability that the same defects must influence others of longer durations.

TABLE 27

Comparison of Velocities of Meteors belonging to known Showers compared with the Values given in the Fireball Catalogue

Streams	*No. plotted in Figs. 89 and 90*	*No. tabulated*	*Spread km./sec.*	*Arithmetical mean*	*Harmonic mean*	*Median*	*Geocentric velocity estimated from stream period*†
Quadrantids	21	22	21–85	45·1	40·8	41·8	42·55‡
Lyrids	15	15	31–80	55·9	53·1	54·6	47·1§
Perseids	145	147	40–161	68·1	63·6	64·4	61·25‖
Orionids	15	16	48–113	69·6	65·2	62·7	65·2††
Leonids	31	38	19–215	83·1	70·5	75·6	71·4‡‡
Geminids	16	18	24–113	52·0	43·1	48·3	43·6††

† The velocities quoted here are those used by Fisher, and are not necessarily the values now accepted. For example, the Geminid velocity is now known to be 35 km./sec. (see Chap. XV) and this still further strengthens Fisher's argument.

‡ Kirkwood, D., *Proc. Amer. Phil. Soc.* **13** (1873), 501.

§ Maltzev, V. A., *Mirovedine Astr. Bull.* (1929), no. 24, 1.

‖ Velocity assumed parabolic.

†† Kirkwood, D., *Proc. Amer. Phil. Soc.* **11** (1871), 229.

‡‡ Newton, H. A., and Adams, J. C., *Amer. J. Sci.* **37** (1864), 377; **38** (1864), 53; *Mon. Not. Roy. Astr. Soc.* **27** (1866–7), 247.

5. Later discussions of the fireball catalogue and Watson's analysis

Following Fisher's second criticism Maltzev† made a further analysis of the harmonic mean velocities and concluded that they were principally hyperbolic. Knopf‡ plotted the distribution of apparent radiants and believed that he had evidence for the activity of streams in Taurus and Scorpius throughout the year, thus indicating that they were truly interstellar. On the other hand Wylie§ concluded from the study of several well-observed fireballs that the paths given in the fireball catalogue were too long, which would mean that the derived velocities were too high. If Wylie's belief is correct then the high altitudes given by Maltzev‖ for the appearance of the fireballs can be explained.

† Maltzev, V. A., *Tashkent Obs. Bull.* (1934), no. 3, 57.

‡ Knopf, *Astr. Nachr.* **242** (1931), 161.

§ Wylie, C. C., *Pop. Astron.* **43** (1935), 241, 312, 379, 602, 657; **44** (1936), 42, 152; **45** (1937), 101, 209.

‖ Maltzev, V. A., *Mon. Not. Roy. Astr. Soc.* **90** (1930), 568.

In the face of these contradictions Watson† attempted a more detailed analysis of the apparent radiants than that made by Knopf. Watson first reduced the apparent radiants given in the catalogue to space radiants. In Fig. 91 if A is the apex of the earth's way; AB the true radiant of the fireball moving with heliocentric velocity $\overline{V}$, and BC the

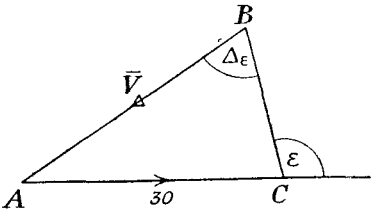

FIG. 91.

apparent radiant at elongation ϵ to the apex, then the shift $\Delta\epsilon$ necessary to correct the apparent radiant is given by

$$\sin(\Delta\epsilon) = \frac{30}{\overline{V}} \sin\epsilon,$$

the displacement being along the great circle passing through the apparent radiant and the apex. Using this correction and the velocities for 411 fireballs given in the catalogue, Watson obtained the distribution shown in Fig. 92. The concentration towards the ecliptic is further shown in Table 28, which gives the frequencies in 10-degree zones north of the ecliptic for three groups with $\overline{V} < 43$ km./sec., $43 < \overline{V} < 50$, $50 < \overline{V}$.

TABLE 28

Watson's Analysis of the Distribution in Latitude of Velocity Groups in the Fireball Catalogue

Mid-latitude of zone	5°	15°	25°	35°	45°	55°	65°	75°	85°
$\overline{V} < 43$	33%	20	15	11	10	7	2	2	0
$43 < \overline{V} < 50$	40%	12	20	14	5	5	1	2	1
$50 < \overline{V}$	45%	18	9	9	9	2	5	2	1

In Fig. 92 there are several groupings which might indicate streams of fireballs—particularly those at α 160°, δ +5°; α 175°, δ +3°; α 210°, δ +2°. The latter is the 'Scorpius stream' with a mean heliocentric velocity of 51 km./sec., agreeing with the concentration as selected by

† Watson, F., *Proc. Amer. Phil. Soc.* **81** (1939), 473.

von Niessl† in Scorpius. Watson tested the significance of these groupings by applying Poisson's equation

$$P(N) = \frac{N_0^N}{N!} e^{-N_0},$$

where N_0 is the average number of radiants per unit area and N is the anticipated number. Between latitudes 0° and +10° there are 141

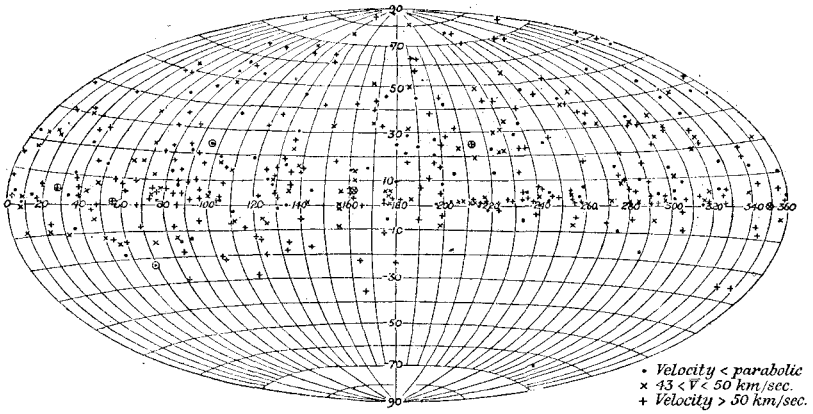

FIG. 92. Distribution of space radiants from the von Niessl–Hoffmeister catalogue as plotted by Watson.

radiants which, when considered over 36 intervals, 10 degrees wide, gives $N_0 = 3{\cdot}91$. The number of the 36 intervals $\overline{N}$ in which we expect to find N radiants is compared with the observed number in Table 29.

TABLE 29

Results of Watson's Test of the Significance of Apparent Radiant Groups in the Fireball Catalogue

N	$P(N)$	$\overline{N}$ *expected*	$\overline{N}$ *obs.*	N	$P(N)$	$\overline{N}$ *expected*	$\overline{N}$ *obs.*
0	0·024	0·9	2±1·4	5	0·15	5·6	4±2·0
1	0·090	3·3	2±1·4	6	0·094	3·5	5±2·2
2	0·17	6·4	4±2·0	7	0·050	1·9	3±1·7
3	0·21	7·9	8±2·8	8	0·018	0·6	1±1·0
4	0·20	7·5	7±2·6				

Table 29 gives no indication that the groupings are anything but accidental. Finally Watson made a similar reduction for the radiants found in the Arizona Meteor Expedition,‡ assuming parabolic velocity,

† von Niessl, G., *Sitz. d. k. Akad. d. Wiss. Wien*, **121** (1912), 1925.
‡ *Circ. Harv. Coll. Obs.* (1934), no. 388.

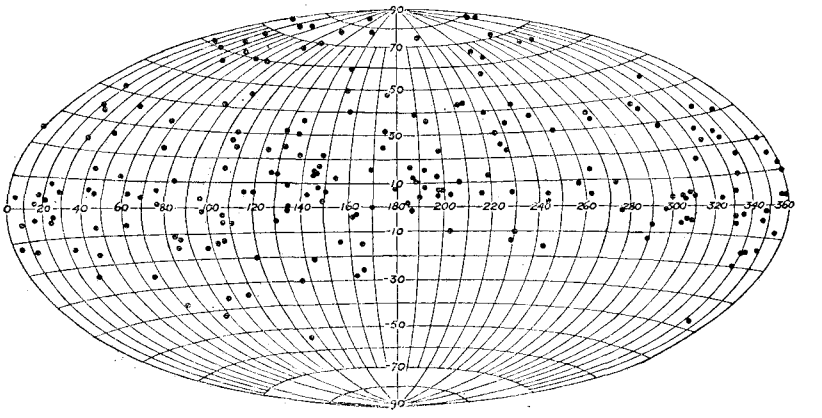

FIG. 93. Watson's analysis of the distribution of space radiants of meteors observed during the Arizona expedition.

with the result shown in Fig. 93. The concentration towards the ecliptic compared with the concentrations in the fireball catalogue are listed in Table 30.

TABLE 30

Comparison of Concentration of Meteors in the Arizona Results with those in the Fireball Catalogue

Mid-latitude . .	5°	15°	25°	35°	45°	55°	65°	75°	85°
Concentration in fireball catalogue .	41%	17	12	11	8	4	3	2	1
Concentration in Arizona results .	33%	14	16	13	6	4	7	6	1

On the whole the fireball radiants are even more concentrated towards the ecliptic than the Arizona radiants, which almost certainly had periodic orbits. Hence there are only two possible conclusions: either (*a*) the fireballs are from interstellar space and just by chance have motions principally in the ecliptic like the periodic streams, or (*b*) the velocities in the fireball catalogue are not significant and the fireballs are actually members of the solar system like the periodic streams.

6. Summary of discussions on the von Niessl–Hoffmeister fireball catalogue

In the above sections some examples have been given of the discussions which have centred around the velocity data in the von Niessl–Hoffmeister catalogue. Evidently an appeal to further measurements is necessary before any decision on the validity of these measurements

can be taken. Even Öpik, who from his measurements (described in Chapter IX) firmly believed in the hyperbolic theory, nevertheless doubted whether the velocity data in the catalogue were well founded.† In a critical analysis of British meteor data Porter‡ showed that little reliance could be placed on the paths of the meteors observed by Denning or Herschel. Hence, since 44 per cent. of the paths in the fireball catalogue are from this source, Porter§ considers that the velocity data in the catalogue are essentially unreliable. On the other hand there are one or two cases of observations of meteorites or fireballs by reliable observers which indicate a marked hyperbolic velocity. Perhaps the most famous of these is the case of the Pultusk meteorite which fell on 30 January 1868, where the two principal observers were an astronomer and a trained army officer. In his analysis of the data, Galle‖ found the velocity to be hyperbolic. The conditions were unusually favourable since the meteorite was overtaking the earth. The average observed velocity was 28 km./sec., corresponding to an average duration of 6·7 sec. derived from 26 estimates. From this material Galle derived a marked hyperbolic heliocentric velocity of 57 km./sec. For a parabolic velocity the duration would have to be doubled. More recently the case of the Pultusk meteorite has been thoroughly discussed by Nielsen,†† who again arrived at the conclusion that the velocity was hyperbolic; the revised heliocentric value being 56 km./sec. giving an interstellar velocity of 37 km./sec.

† Öpik, E., *Irish Astr. J.* **1** (1950), 84.
‡ Porter, J. G., *Mon. Not. Roy. Astr. Soc.* **103** (1943), 134.
§ Porter, J. G., ibid. **104** (1944), 257.
‖ Galle, J. G., *Abh. Schles. Gesellschaft. Nat. u. Med.* (Breslau, 1868).
†† Nielsen, A. V., *Meddel. Ole Rommer Obs.* (1943), no. 17.

IX

THE VELOCITY OF SPORADIC METEORS—II

THE WORK OF ÖPIK

THE rocking-mirror apparatus designed by Öpik has been described in Chapter II. It was used by Öpik and his colleagues to measure meteor velocities during the Arizona Meteor Expedition† (1931–3), and after 1934 at Tartu in Esthonia. A meteor seen in the mirror describes a cycloid. This curve was redrawn as it appeared visually and the angular velocity was calculated by two methods: (i) from the shape of the trajectory (w_1), (ii) from the observed length and duration as given by the number of the loops (w_n). The heights and paths of the meteors were obtained from simultaneous observations by two observers separated by about 40 km.‡ In the final reduction of the data to linear velocities, however, mean heights were used, because the spread in meteor heights was found to be smaller than the observational error in the observed heights.

1. Treatment of data

The systematic and accidental errors were estimated from meteors belonging to specific radiants where a parabolic velocity could be assumed (in the later reductions a correction for the probable ellipticity of these meteors was introduced.) For example, in his reduction of some of the preliminary data§ Öpik took sixty-four stream meteors and divided them into two groups according to geocentric velocity, as shown in Table 31.

TABLE 31

Öpik's Preliminary Grouping of 64 Stream Meteors

Mean geocentric velocity v, km./sec. . . .	36	71
Number of heights	22	16
Harmonic mean‖ height of trail centre h, km. .	79·0	85·8
Probable error in mean height, km. . . .	±2·0	±3·7

Because of the small change in height with velocity, and because the real spread is of the same order as the observational errors, Öpik

† Shapley, H., Öpik, E. J., and Boothroyd, S. L., *Proc. Nat. Acad. Sci. Wash.* **18** (1932), 16.

‡ See Chap. II.

§ Öpik, E. J., *Circ. Harv. Coll. Obs.* (1934), no. 389.

‖ Harmonic mean heights are computed in this work instead of arithmetical means because the observational errors are in parallax, and because a mean angular velocity corresponds to a mean harmonic height.

considered that the use of mean heights, instead of individual heights, was justified. In this way many meteors observed in the rocking mirror, but without measured heights, could be included in the analysis of linear velocities.

The theoretical values of the angular velocity **w** of these meteors were computed from

$$\mathbf{w} = 57{\cdot}3\mathrm{v}\frac{\sin\eta\cos\mathrm{z}}{\mathrm{h}}\ \text{deg./sec.}, \qquad (1)$$

where η is the angular distance of the centre of the trail from its radiant and z the zenith distance of the trail. This value was compared with the measured rocking-mirror value w_n. The errors in angular velocity were of a logarithmic character with the average $\log(w_n/\mathbf{w}) = 1{\cdot}067 \pm 0{\cdot}035$. No systematic dependence of this ratio on duration, length of trail, or angular velocity could be found. Öpik concluded that w_n did not involve any large systematic error and that the constant systematic error probably consisted of an overestimate of the angular velocity by about 7 per cent. The errors in the individual observations he considered to be due to errors in the length of the trail as traced on a star map. The durations were thought to be very accurate, the error amounting to no more than $\frac{1}{100}$ sec. for short durations ($< 0{\cdot}4$ sec.).

Öpik applied this systematic correction in the ratio 1 : 1·067 for w_n to investigate the corrections of w_1 relative to w_n. The resultant corrections necessary to w_1 are given in Table 32.

TABLE 32

Corrections required to Angular Velocities w_1 in the Rocking-mirror Observations

w_1 observed (deg./sec.)	0·0	4·0	8·0	12·0	16·0	20·0	24·0	30·0	36·0	44·0	60·0	72·0
w_1 corrected (deg./sec.)	0·0	7·1	11·6	15·9	20·4	25·3	29·8	36·3	42·2	49·0	65·0	75·2

Assuming uniform accuracy for w_n the relative weights of Table 33 were derived from the internal agreement of w_n and w_1.

TABLE 33

Relative Weights to be assessed to Angular Velocities observed in Rocking Mirror

Method and angular velocity .	w_n	$w_1 \leqslant 17{\cdot}9$	$w_1 = 18{\cdot}0 - 23{\cdot}9$	$w_1 \geqslant 24{\cdot}0$
Relative weight . . .	1·0	0·5	0·8	1·0

By applying Tables 32 and 33 to the observed angular velocities the final weighted mean angular velocity $\bar{w}$ was obtained.

In the subsequent computation of linear velocities, average heights of the trail centre were assumed to be a function of the zenithal angular velocity

$$w_z = \bar{w} \sec z. \tag{2}$$

The relation between h and w_z was obtained from the data in Table 34.

TABLE 34

Relation between Height and Zenithal Angular Velocity

w_z deg./sec.	0–19·9	20·0–39·9	40·0–79·9	⩾ 80·0	All
No. of heights	34	53	35	12	134
Harmonic mean h, km.†	78·6	81·8	86·8	83·7	82·4
Probable error, km.	±1·5	±1·3	±1·8	±2·8	±0·8

Smoothed relation finally adopted

w_z	0	10	20	30	40	50	60	70	80
h	77·5	77·9	79·6	82·0	83·8	84·9	85·8	86·2	86·3

The linear velocity was then computed from

$$v = \frac{\bar{w} h \sec z}{57{\cdot}3}. \tag{3}$$

In both (1) and (2) the curvature of the earth is neglected. Öpik's justification is that errors thereby introduced tend to cancel in the mean, and in any case the average error produced by neglecting the curvature is only 2·3 per cent. with a spread of ±1·7 per cent. for the actual region of observation.

The spread in $\log\left(\frac{w_{obs}}{w_{comp}}\right)$ for the 64 radiant meteors was ±0·165 (standard deviation). Correcting for an assumed 7 stray meteors gave ±0·157. This gives for the empirical value of the observational probable error in $\log \bar{w}$ a figure of ±0·106, or ±25 per cent., which is larger than would have been expected from the internal agreement of w_n and w_1. The velocities were finally corrected for the earth's orbital motion graphically to give the heliocentric velocity $\bar{V}_0$. An example of the final data produced in this manner is shown in Table 35, these being the data given by Öpik‡ for 1931 November 14.

† The arithmetical mean of all the heights was 85·0 km. These are relative to Flagstaff, Arizona; reduction to sea-level requires a correction of +2·1 km.

‡ Öpik, E. J., *Circ. Harv. Coll. Obs.*, loc. cit.

TABLE 35

Example of Final Data produced by Öpik from the Rocking-mirror Observations

Sidereal time (deg.)	*Estimated magnitude*	*R.A. (beginning of trail) (deg.)*	*Decln. (deg.)*	*Direction of motion†*	*Duration (sec.)*	*Angular velocity $\bar{w}$ (centre of trail) (deg./sec.)*	*Apparent direction‡*	*Heliocentric velocity $\bar{V}_0$ (km./sec.)§*	*Height of trail centre (km.)*	*No. of observers‖*
335·6	3·0	299	56	126	0·25	20	291	52	74	3
338·6	1·5	46	83	180	0·52	7	345	45	69	3
343·8	0·0	16	58	93	1·50	16	257	34	80	3
351·4	3·8	350	66	78	0·24	16	234	25	..	1
6·1	4·0	164	83	189	1·00	6	327	46	55	3
13·8	4·0	78	68	160	0·25	16	295	53	..	2
19·8	3·0	144	82	155	0·33	12	279	42	100	3
81·8	4·0	99	68	218	0·41	19	284	48	82	3
87·1	4·0	35	74	243	0·27	19	303	61	62	3
88·6	2·8	17	53	162	0·21	21	225	37	66	3
94·6	3·8	329	84	99	0·07	36	149	82	..	1
114·4	4·0	107	68	178	0·16	22	213	22	..	1
117·1	4·0	355	80	157	0·15	20	186	34	94	2
123·4	3·5	148	68	145	0·14	39	167	40	143	3

† This is the direction of motion measured on the chart relative to the vertical line passing through the centre of the map (the North Pole), from south through west. Thus 0° means vertically up; 90° means E. to W.

‡ The apparent direction relative to the orbital apex of the earth; 0° means direction from the antapex; 270° towards the sun.

§ This is the projected component of the heliocentric velocity of the meteors, without correction for the earth's attraction.

‖ Heights could only be determined when two observers, one at each end of the base line, recorded the meteor.

2. The Arizona results of Öpik and Boothroyd

Although a very large number of velocities were measured during the Arizona expedition, those measured by Öpik† (naked eye) and by Boothroyd‡ (telescopic) represent data obtained by experienced observers. They were therefore considered by Öpik§ to be worthy of separate treatment. The adaptation of Öpik's technique to the telescopic observations has been described in Chapter II. The data treated by Öpik§ consisted of 279 naked-eye observations made by himself and of 580 telescopic observations‖ made by Boothroyd.‡

The lists of observations (for example Table 35) give the observed distribution of projected heliocentric velocities. From these Öpik attempted to deduce the true distribution of heliocentric velocities in space in two steps. (i) The observed distribution was freed from the effects of accidental errors of observation to obtain the true distribution of projected heliocentric velocities. (ii) By making plausible assumptions about the distribution of angles between the velocity vectors and the line of sight, the probable distribution of heliocentric space velocities was obtained.

(i) As discussed in § 1 above, the observational error in the angular velocities had a logarithmic character. For a constant relative accuracy in the observed angular velocity, the relative error in the heliocentric velocity $\overline{V}_0$ depends upon the direction (for directions from the apex the relative error will be larger than average; for directions from the antapex, smaller than average). By comparison with meteors from known radiants the probable error in the linear velocity was found to be $\pm 0{\cdot}106$ in log v. Assuming this constant relative error in the observed velocity, the probable error in the transverse heliocentric velocity $\overline{V}_0$ (that is at right angles to the line of sight) was calculated graphically for each case. Further detailed treatment gave the frequency of errors for different limits of $\overline{V}_0$, and enabled a table to be constructed showing the complicated law of observational errors in $\overline{V}_0$. With the aid of these data the true distribution of the projected heliocentric velocities was calculated by a method of successive approximations.

(ii) In order to find the distribution of space velocities from these data it is necessary to know the frequency of the ratio

$$x = \frac{\overline{V}_0}{\overline{V}_h},$$

† Öpik, E. J., *Circ. Harv. Coll. Obs.*, loc. cit.

‡ Boothroyd, S. L., ibid. (1934), no. 390. § Öpik, E. J., ibid. (1934), no. 391.

‖ These are about five-sixths of the data given by Boothroyd (loc. cit.). Öpik rejects Boothroyd's observations of durations $< 0{\cdot}027$ sec., owing to the uncertainty of the data.

where $\overline{V}_0$ is the projected velocity, and $\overline{V}_h$ the heliocentric space velocity. Since x was continuous, Öpik calculated the frequency of x for two cases, (i) for a random distribution of directions, (ii) for a spherical surface density of radiants proportional to $\cos^2 z$ (z being the zenith distance of the radiant). The distribution of x is rather similar in both cases. Actually Öpik gave reasons for taking the $\cos^2 z$ distribution for $\overline{V}_h > 42$ km./sec. and the random distribution for $\overline{V}_h < 42$ km./sec.

Öpik's solutions for his 279 naked-eye observations are given in Tables 36 and 37.

TABLE 36

Distribution of Heliocentric Space Velocities $\overline{V}_h$ *of 279 Naked-eye Observations*

$\overline{V}_h$ *km./sec.*			
Uncorrected	*Corrected*†	*Number*	*Percentage*
36	32	7	2·5
42	39	76	27·3
50	47	52	18·7
60	57	47	16·8
72	69	26	9·3
85	83	16	5·7
101	98	12	4·3
120	116	15	5·4
143	139	16	5·7
170	165	10	3·6
202	197	2	0·7
	All	279	100·0

† The uncorrected values of $\overline{V}_h$ are here corrected for (i) the earth's gravitational attraction, (ii) an estimated average constant correction of −2·5 per cent. to allow for the possible ellipticity of the stream meteor orbits which were used in standardizing the data. The gravitational correction was calculated by averaging three cases: (*a*) direction from apex, weight one, (*b*) direction from antapex, weight one, (*c*) radial heliocentric direction, weight four, giving the following values:

$\overline{V}_h$ *km./sec.*	*Correction km./sec.*
28	−3·6
30	−3·3
34	−2·9
38	−2·5
42	−2·1
50	−1·6
60	−1·1
100	−0·7
140	−0·5
200	−0·3

TABLE 37

Distribution of Projected Heliocentric Velocities $\overline{V}_0$ of 279 Naked-eye Observations

$\overline{V}_0$ *km./sec. uncorrected*	*Number*					
	Observed unsmoothed			*Observed smoothed, all magnitudes*	*True, corrected for accidental errors*	*Computed from distribution of $\overline{V}_h$ (Table 36)*
	m ⩽ 3·7	m > 3·7	*All magnitudes*			
⩽ 14·9	10	3	13	13·0	10·7	11·7
15·0–17·8	3	1	4	3·6	1·1	4·9
17·9–21·1	8	0	8	5·4	3·5	7·4
21·2–25·1	5	2	7	8·4	6·5	10·7
25·2–29·9	12	1	13	15·7	4·7	16·3
30·0–35·7	28	8	36	34·9	33·8	28·5
35·8–42·3	36	12	48	48·0	71·5	59·4
42·4–50·3	27	15	42	39·0	49·6	42·4
50·4–59·9	16	9	25	28·5	29·9	30·0
60·0–71·5	12	11	23	21·3	18·6	18·4
71·6–84·7	10	7	17	16·2	12·7	12·8
84·8–100	4	7	11	13·0	10·6	10·8
101–119	8	3	11	11·0	11·0	10·9
120–143	6	5	11	8·5	9·0	9·1
144–169	2	1	3	5·5	4·7	4·8
170–201	2	1	3	3·0	1·1	0·9
> 201	2	2	4	4·0	0·0	0·0
All	191	88	279	279·0	279·0	279·0

TABLE 38

Distribution of Heliocentric Space Velocities $\overline{V}_h$ for 580 Telescopic Observations

$\overline{V}_h$ *km/sec.*		*Average magnitude = 6·5*		*Average magnitude = 8·5*	
Uncorrected	*Corrected†*	*Number*	*Percentage*	*Number*	*Percentage*
30	27	0	0	14	4·1
36	33	77	32·1	11	3·2
42	40	32	13·3	0	0
50	48	0	0	0	0
60	59	0	0	19	5·6
72	71	16	6·7	23	6·8
85	84	36	15·0	28	8·2
101	100	38	15·8	10	2·9
120	120	30	12·5	0	0
143	143	10	4·2	192	56·6
170	170	0	0	43	12·6
202	202	0	0	0	0
239	239	1	0·4	0	0
	All	240	100·0	340	100·0

† Correction only for earth's gravitational attraction.

TABLE 39

Distribution of Projected Heliocentric Velocities $\bar{V}_0$ for 580 Telescopic Observations

	Average magnitude = 6·5 (*subjective mag.* ⩽ 3·7)				*Average magnitude* = 8·5 (*subjective mag.* > 3·7)			
$\bar{V}_0$ *km./sec. uncorrected*	*Observed unsmoothed*	*Observed smoothed*	*True, corrected for accidental errors*	*Computed from distribution of* $\bar{V}_h$ *in Table* 38	*Observed unsmoothed*	*Observed smoothed*	*True, corrected for accidental errors*	*Computed from distribution of* $\bar{V}_h$ *in Table* 38
⩽ 14·9	13	11·0	10·7	16·8	8	6·0	6·4	9·8
15·0– 17·8	11	8·6	8·8			2·0	0·0	
17·9– 21·1	8	10·4	6·7	7·3	4	5·0	0·7	5·0
21·2– 25·1	11	15·0	8·9	11·8	11	10·0	14·0	7·2
25·2– 29·9	22	22·6	24·8	20·2	12	12·2	15·2	14·3
30·0– 35·7	32	28·4	46·1	50·8	13	12·8	13·0	13·2
35·8– 42·3	20	21·3	21·9	21·7	12	13·8	8·5	10·0
42·4– 50·3	15	15·0	1·8	8·1	20	18·1	17·3	15·5
50·4– 59·9	17	16·2	10·1	12·1	26	22·8	24·5	24·7
60·0– 71·5	22	21·7	27·7	20·7	29	26·8	28·5	28·2
71·6– 84·7	23	22·2	27·1	27·0	26	31·2	31·3	31·3
84·8–100	19	20·2	24·1	23·4	36	36·8	30·3	29·9
101 –119	17	14·4	15·5	15·1	40	42·8	25·3	39·3
120 –143	6	7·7	4·7	4·5	52	47·0	106·0	92·5
144 –169	1	3·0	0·0	0·1	35	36·7	19·0	19·0
170 –201	2	1·3	0·2	0·2	15	15·0	0	0
> 201	1	1·0	0·8	0·4	1	1·0	0	0

Öpik treated the 580 telescopic observations of Boothroyd in a similar manner. In this case no standardization with shower meteors was possible because of lack of knowledge of radiants and individual heights. An average height for all meteors was therefore assumed. The probable error in Boothroyd's log $\bar{w}_0$ was found to be $\pm 0{\cdot}065$ corresponding to a relative probable error of ± 11 per cent. The solution for the heliocentric space velocities was made in a similar manner as for the naked-eye observations. The results, corresponding to Tables 36 and 37 for the naked-eye data, are given in Tables 38 and 39.

Although these results are inadequate for a discussion of small differences in heliocentric velocity, such as would be necessary to distinguish between parabolic and highly eccentric elliptical orbits, the data show the existence of an appreciable number of high hyperbolic velocities and the fact that the percentage increases with decreasing brightness. Öpik gives the data in Table 40 for the percentage of heliocentric velocities exceeding 62 km./sec. for different magnitudes.

TABLE 40

Percentage of Heliocentric Velocities exceeding 62 km./sec. according to the preliminary rocking-mirror results

Magnitude	2·5	4·5	6·5	8·5
Percentage of high-velocity meteors .	20	45	56	87

Furthermore in the period October to November 1931, covered by the naked-eye observations, Öpik concluded that all the sporadic meteors possessed hyperbolic velocities and were therefore of extra-solar origin.

3. Preliminary treatment of the complete Arizona velocity measurements

The naked-eye data on 279 meteors discussed above were obtained from the personal observations of Öpik in Arizona during October and November 1931. After Öpik's departure the observations were continued by R. Wilson and D. Hargrave until the end of the expedition. From the combined observations a total of 1,436 meteor velocities was obtained (611 by R. W., 546 by D. H., 279 by E. Ö.). A lengthy and comprehensive analysis of these data has been made by Öpik.† The method of reduction was essentially the same as that described above. Meteors belonging

† Öpik, E. J., *Publ. Tartu Obs.* **30** (1940), no. 5. A short account is given in Öpik, E. J., *Mon. Not. Roy. Astr. Soc.* **100** (1940), 315.

to showers where a parabolic velocity could be assumed were used to determine the systematic errors of the observers. The standard deviation in log $\bar{w}$ for the shower meteors was found to be $\pm 0{\cdot}165$ (D. H.); $\pm 0{\cdot}176$ (R. W.); $\pm 0{\cdot}165$ (E. Ö). Including the error dispersion in the assumed mean height the observational probable error in log $\bar{w}$ was taken as $\pm 0{\cdot}106$, the same as previously. The number of shower meteors used in this standardization was small—69 for E. Ö., 41 for R. W., 32 for D. H., from which 5, 6, and 11 were rejected respectively. Öpik justifies this rejection on the grounds that these represent a peculiar selection of stray meteors.

The correlation between height and angular velocity was obtained from 486 cases observed by R. W. and D. H., in which both height and velocity were measured. The relation adopted is given in Table 41, which is to be compared with Table 34 for the earlier analysis, from which it differs somewhat.

TABLE 41

Relation between w_z and h *for* 486 *Observations in the complete Arizona Data*

w_z deg./sec. .	0	4	8	12	16	20	24	28	32	$\geqslant 36$
h km. . .	81·0	83·0	84·7	86·3	88·0	89·7	91·2	92·4	92·8	93·0

The linear velocity at right angles to the line of sight was then calculated as described above.

The Arizona records showed that the results of R. W. yielded 20 per cent. velocities, D. H. 19·6 per cent., and E. Ö. 66·7 per cent. In view of these differences Öpik gives attention to the question of selection of the data, with respect to angular velocity, magnitude, position in the field of observation, length of trail, and direction of motion. Although, from an analysis of the data, Öpik found marked selection effects relative to these variables, there were also various equalizing factors which led him to conclude that the uncorrected velocity list must represent fairly well the distribution of intermediate w, with a deficiency in very large and very small w. He decided to use the statistical data, uncorrected for selection, because a satisfactory determination of all the selection factors was not possible on the basis of the existing data.

Following the same law of observational error dispersion in $\overline{V}_0$, and of the relative frequency of projection ratios $\overline{V}_0/\overline{V}_h$ (p. 159), Öpik gives the provisional distribution of heliocentric space velocities as shown in

Table 42 for the three observers. This is to be compared directly† with the distribution given in Table 36 for the 279 measurements of Öpik which are also included in Table 42.

TABLE 42

Provisional Distribution of Heliocentric Space Velocities for the 1,436 *Arizona Velocities* (*all directions*)

$\bar{V}_h$ *km./sec.*	*E. Ö.* (*number*)	*R. W.* (*number*)	*D. H.* (*number*)	*All observers* (*number*)
$\leqslant$ 15	0	0	23	23
18	0	0	0	0
21	0	0	2	2
25	0	0	3	3
30	0	0	3	3
36	7	84	34	125
42	76	173	64	313
50	52	125	113	290
60	47	102	164	313
72	26	101	77	204
85	16	25	61	102
101	12	0	0	12
120	15	0	0	15
143	16	0	0	16
170	10	0	0	10
202	2	1	0	3
240	0	0	2	2
All	279	611	546	1,436

4. Detailed treatment of the complete Arizona velocity measurements

Although the individual differences in the results of the three Arizona observers were considerable Table 42 indicates that the statistical data are not radically different. Öpik therefore joined together the data of all three observers, which then provided sufficient material for a detailed analysis of the different directions of motion. Following Öpik† we shall first outline his method of correction for observational error dispersion, the results of which have already been presumed in deriving Tables 36 and 42 (§ 2 (i), p. 159, and § 3, p. 164). Secondly, his more precise method for finding the distribution of space velocities will be described. This supersedes the elementary treatment described in § 2 (ii) used in the computation of Tables 36 and 42.

† The values of $\bar{V}_h$ in Table 42 are not corrected for the earth's gravitational attraction or for the effect of the ellipticity of the shower meteors on the standardization of the velocity scales.

‡ Öpik, E. J., *Publ. Tartu Obs.* **30** (1940), no. 5, p. 27.

(a) Öpik's Corrections for Observational Error Dispersion

The correction made by Öpik for observational errors is of primary importance in his analysis. In this section an outline of the treatment will be given, with an example of its influence on the observational results.

Let x = true quantity,

$F(x)\,dx$ = frequency of x,

y = observational error,

$\chi(y, x)\,dy$ = frequency of y,

$\xi = x+y$ = observed quantity,

$\Phi(\xi)\,d\xi$ = observed frequency between ξ and $\xi+d\xi$.

Then the integral equation of diffusion is

$$\Phi(\xi) = \int_{-\infty}^{+\infty} F(\xi-y)\chi(y, \xi-y)\,dy. \tag{4}$$

When Φ and χ are known, the true distribution is determined by (4). An analytical solution for the case of a Gaussian $\chi = \chi(y)$ has been given by Eddington† but even in this case the method cannot be used for a large error dispersion. Öpik used a method of successive approximation. With $\Phi_1 = \int \Phi\chi\,dy$ the first approximation to F is

$$F_1 = \Phi+(\Phi-\Phi_1) = 2\Phi-\Phi_1.$$

With $\Phi_2 = \int F_1\chi\,dy$ the second approximation is

$$F_2 = \Phi+(F_1-\Phi_2),$$

and so on. The numerical procedure is actually a direct calculation of $(F_1-\Phi_2)$ instead of Φ_2. Generally one to three approximations lead to a good solution, which is checked by substitution in (4).

The dispersions Δ (mean square deviations from the arithmetical mean) satisfy

$$\Delta_x^2 = \Delta_\xi^2-\Delta_y^2. \tag{5}$$

This is true when ξ is a directly measured quantity, and χ is the error function representing the distribution of $y = (\xi-x)$ for a given value of x. But if the observed quantity η is a statistical average value of x, corresponding to a certain observed criterion ξ' (Öpik cites as example

† Eddington, A. S., *Mon. Not. Roy. Astr. Soc.* **73** (1913), 359.

spectroscopic absolute magnitudes), $\boldsymbol{\eta} = \bar{x}(\xi')$, then

$$F(x) = \int_{-\infty}^{\infty} \psi(x-y)\chi_1(y, x-y)\, dy, \tag{6}$$

$$\boldsymbol{\Delta}_x^2 = \boldsymbol{\Delta}_{\boldsymbol{\eta}}^2 + \boldsymbol{\Delta}_y^2, \tag{7}$$

where

$x = \boldsymbol{\eta} + y$,

$\psi(\boldsymbol{\eta})\, d\boldsymbol{\eta}$ = observed frequency of $\boldsymbol{\eta}$,

$\chi_1(y, \boldsymbol{\eta})\, dy$ = apparent error function determining the distribution of $x - \boldsymbol{\eta} = x - \bar{x}(\xi')$.

Thus the first case involves a subtraction of the error dispersion (eq. 5) and the second case an addition (eq. 7).

In the present observations $x = \log v$ and χ is assumed to be Gaussian depending on the error alone $\chi = \chi(y)$. Also we have seen that the probable error in $\log v = \pm 0{\cdot}106$. The solution was then made according to (4). Table 43 gives the distribution of the geocentric tangential velocity v for all three observers together, for different values of $\boldsymbol{P}$, the direction of motion with respect to the apex ($\boldsymbol{P} = 180°$ is from the apex; $\boldsymbol{P} = 270°$ is towards the sun and downwards). For each $\boldsymbol{P}$, the first column gives the smoothed observed value of v, and the second column the value of v corrected for the error dispersion as above. The roman figures at the head of this column give the order of the final approximation in F adopted.

(b) Öpik's Calculation of the Distribution of Space Velocities

The approximations described in § 2 (ii) were used by Öpik in the preliminary treatment to derive the distribution of space velocities given in Tables 36 and 42. His exact treatment for the complete Arizona data is described in this section.

(i) *The frequency of the projection ratios.* In order to find the distribution of space velocities from the data in Table 43 it is necessary to know the frequency of the projection ratios $\sin \eta$ for each '$\boldsymbol{P}$-sector', η being the angle between the line of sight and the trajectory of the meteor (or the angular distance of the centre of the trail from its radiant).

Certain assumptions are still made in order to simplify the analysis: (1) the whole area of observation is replaced by a point at its centre 45° N. of the zenith ($\delta = +90°$); (2) in each $\boldsymbol{P}$ sector a homogeneous distribution of $\boldsymbol{P}$ is assumed, $dn/d\boldsymbol{P}$ = constant, of a density corresponding to the median value of $\boldsymbol{P}$.

TABLE 43

The Distribution of Geocentric Tangential Velocities v *and the Correction for Error Dispersion*

v km./sec.	$P = 15°$ Obs.	Corr. III	45° Obs.	Corr. II	75° Obs.	Corr. II	105° Obs.	Corr. III	135° Obs.	Corr. III	165° Obs.	Corr. III	195° Obs.	Corr. IV	225° Obs.	Corr. II	255° Obs.	Corr. III	285° Obs.	Corr. III	315° Obs.	Corr. III	345° Obs.	Corr. II
0·0–7·4	0·1	0·0	0·5	0·5	0·6	0·0	0·3	0·2	0·0	0·0	0·0	0·0	0·0	0·0	0·0	0·0	0·0	0·0	1·5	0·2	0·9	0·0	0·0	0·0
7·5–8·8	0·3	0·0	0·5	0·5	0·7	1·0	0·3	0·3	0·0	0·0	0·0	0·0	0·0	0·0	0·0	0·0	1·0	0·0	2·5	0·4	1·2	0·4	0·2	0·0
8·9–10·5	0·9	0·0	0·5	0·5	0·8	1·2	0·4	0·2	0·4	0·0	0·0	0·0	0·3	0·0	0·4	0·0	3·0	0·0	4·0	2·0	1·9	0·9	0·6	0·0
10·6–12·5	1·9	1·5	0·5	0·6	0·8	1·1	0·5	0·0	1·0	0·0	0·0	0·0	1·0	0·0	0·8	0·0	6·0	0·0	6·7	3·4	3·1	2·0	1·8	0·0
12·6–14·9	2·6	3·0	0·5	0·4	0·6	0·5	0·9	0·1	1·6	0·8	0·5	0·0	2·3	0·0	1·6	0·0	11·0	2·8	10·6	8·3	4·7	4·4	4·1	3·8
15·0–17·8	3·0	3·8	0·5	0·4	0·5	0·0	1·6	1·0	2·6	2·2	1·5	0·3	4·1	2·7	4·4	0·0	18·5	14·3	15·0	13·6	6·4	7·0	5·2	7·5
17·9–21·1	3·2	3·7	0·5	0·2	0·4	0·0	2·5	2·6	3·7	3·3	3·1	0·2	6·3	7·0	8·5	6·9	27·3	27·0	20·4	22·9	7·8	9·7	5·3	7·4
21·2–25·1	3·2	3·6	0·7	0·4	0·8	0·4	3·3	4·2	5·0	4·6	5·4	1·6	8·7	7·9	12·3	12·1	36·0	42·5	24·5	29·6	8·6	11·3	4·5	5·0
25·2–29·9	3·1	3·7	1·1	1·1	1·3	1·5	3·8	5·2	6·4	6·8	8·5	3·0	11·5	10·4	16·2	16·5	42·6	56·9	26·5	32·5	8·1	9·3	3·6	3·1
30·0–35·7	2·6	2·7	1·3	1·1	1·7	2·3	3·7	4·5	7·8	9·7	14·0	11·7	14·8	12·9	20·0	21·3	43·6	58·5	26·1	30·1	7·2	7·6	3·0	2·5
35·8–42·3	2·2	1·9	1·7	1·4	1·7	2·1	3·3	3·4	8·2	9·9	21·0	28·2	18·0	13·8	22·8	24·3	38·6	45·8	24·0	25·8	6·1	5·8	2·6	2·2
42·4–50·3	1·8	1·5	2·1	2·3	1·6	1·8	2·9	3·0	8·0	9·3	24·5	34·8	22·0	20·4	25·5	28·3	30·4	27·9	21·2	21·2	5·1	5·1	2·3	2·3
50·4–59·9	1·5	1·4	2·7	3·7	1·5	2·0	2·4	2·7	7·2	7·4	23·5	31·2	27·0	36·8	27·3	33·7	23·5	20·1	18·3	18·8	4·0	3·9	2·0	2·1
60·0–71·5	1·3	1·5	3·1	5·3	1·2	1·1	1·8	1·7	6·3	6·4	19·8	22·0	28·4	44·5	26·5	36·3	17·5	15·9	15·2	16·9	3·0	3·0	1·6	1·7
71·6–84·7	1·0	1·2	2·0	0·6	0·8	0·0	1·3	0·9	5·4	5·8	15·8	16·0	23·8	33·3	20·2	24·3	12·0	10·5	11·2	11·8	1·9	1·5	1·2	1·1
84·8–100	0·7	0·5	0·8	0·0	0	0	0·8	0·0	4·2	4·3	11·4	10·0	15·8	9·1	11·5	5·0	7·3	0·8	7·3	2·5	1·0	0·0	0·9	0·9
101–119	0·4	0·0	0·0	0·0	0	0	0·2	0·0	3·2	3·5	7·0	3·5	10·7	3·1	5·4	0·0	3·7	0·0	4·0	0·0	0·5	0·0	0·6	0·4
120–143	0·2	0·0	0·0	0·0	0	0	0·0	0·0	1·9	0·0	3·7	0·0	7·5	1·8	3·0	0·0	1·0	0·0	1·0	0·0	0·3	0·1	0·4	0·0
144–169	0	0	0	0	0	0	0	0	0·9	0·0	1·7	0·0	5·8	4·7	1·6	0·0	0·0	0·0	0	0	0·2	0·0	0·1	0·0
170–201	0	0	0	0	0	0	0	0	0·2	0·0	0·8	0·0	4·6	5·9	1·2	0·3	0·0	0·0	0	0	0	0	0	0
202–239	0	0	0	0	0	0	0	0	0·0	0·0	0·5	0·3	3·6	4·7	1·0	1·5	0·0	0·0	0	0	0	0	0	0
⩾ 240	0	0	0	0	0	0	0	0	0·0	0·0	0·3	0·2	2·8	0·0	0·8	0·5	0·0	0·0	0	0	0	0	0	0
All velocities	30	30	19	19	15	15	30	30	74	74	163	163	219	219	211	211	323	323	240	240	72	72	40	40

If **B** is the density of radiants per unit solid angle at vertical incidence and ϵ the angular distance from the apex, then Öpik has shown† that the surface density of radiants $f(\epsilon, \eta)$ can be written as

$$f(\epsilon, \eta) = \mathbf{B}(\cos z)^{k},$$

where z is the zenith distance of the radiant. ($k = 1$ would correspond to a case in which all meteors were sufficiently massive to be observed, or in which the apparent brightness did not depend upon the angle of incidence; $k = 2$ corresponds to brightness varying as cos z and with the numbers of meteors increasing by a factor of 2·5 per magnitude.)

TABLE 44

Stream Intensity $n_\eta/\mathbf{C}$ (*for* $\eta = 0°$ *to* $\eta = \eta$) *for* $k = 1$, $\mathbf{B} = 1$ *at* $z = 45°$ N.

	A						
η	0° (*up*)	30° 330°	60° 300°	90° 270°	120° 240°	150° 210°	180° (*down*)
deg.							
0	0·000	0·000	0·000	0·000	0·000	0·000	0·000
10	0·027	0·027	0·028	0·030	0·032	0·033	0·033
20	0·090	0·094	0·104	0·117	0·130	0·140	0·144
30	0·159	0·171	0·204	0·250	0·296	0·329	0·341
40	0·207	0·235	0·310	0·413	0·516	0·591	0·619
45	0·215	..	..	..	..	..	..
49·1	..	0·258	..	..	..	..	..
50	..	..	0·396	0·587	0·778	0·917	0·968
60	..	..	0·443	0·750	1·057	1·282	1·364
63·4	..	..	0·466	..	..	..	..
70	..	..	..	0·883	1·334	1·663	1·784
80	..	..	..	0·970	1·582	2·031	2·195
90	..	..	..	1·000	1·786	2·360	2·571
100	..	..	..	..	1·928	2·629	2·886
110	..	..	..	..	2·005	2·826	3·126
116·6	..	..	..	..	2·016	..	..
120	..	..	..	..	..	2·940	3·278
130	..	..	..	..	..	2·978	3·348
130·9	..	..	..	..	..	2·980	..
135	..	..	..	..	..	..	3·356

In the present analysis we use A as the direction of the meteor with respect to horizontal coordinates‡ ($A = 0°$ denotes motion vertically

† Öpik, E. J., *Ann. Harv. Coll. Obs.* **105** (1937), 568.
‡ $A = P - 90° + t$, where t is the mean local time.

up in the northern hemisphere), then putting $A = \epsilon$ and $\mathbf{B} = 1$

$$\frac{n_\eta}{C} = \sin^2\eta - (\eta - \sin\eta\cos\eta)\cos A \quad (\text{for } k = 1), \tag{8}$$

$$\frac{n_\eta}{C} = \frac{\sqrt{2}}{3}\sin^2 A(1-\cos^3\eta) + \sqrt{2}\cos^2 A(1-\cos\eta) - \frac{2\sqrt{2}}{3}\cos A\sin^3\eta$$

$$(\text{for } k = 2), \tag{9}$$

where $\mathbf{C} = (\sqrt{2}/4)\,dA$. These expressions give the integral number of radiants n_η from $\eta = 0$ to η, within the directions A to $(A+dA)$.

From (8) and (9) Tables 44 and 45 respectively can be calculated, giving the relation between n_η/C and A for $k = 1$ and $k = 2$.

TABLE 45

Stream Intensity n_η/C (*for* $\eta = 0°$ *to* $\eta = \eta$) *for* $k = 2$, $\mathbf{B} = 1$ *at* $z = 45°$ N.

	A						
η	0° (*up*)	30° 330°	60° 300°	90° 270°	120° 240°	150° 210°	180° (*down*)
deg.							
0	0·000	0·000	0·000	0·000	0·000	0·000	0·000
10	0·016	0·017	0·019	0·021	0·023	0·025	0·026
20	0·047	0·051	0·062	0·080	0·100	0·117	0·123
30	0·071	0·081	0·112	0·165	0·230	0·285	0·307
40	0·080	0·096	0·152	0·260	0·402	0·530	0·582
45	0·080	..	..	..	..	..	..
49·1	..	0·099	..	..	..	..	..
50	..	..	0·175	0·346	0·597	0·830	0·928
60	..	..	0·182	0·412	0·792	1·161	1·319
63·4	..	..	0·182	..	..	..	..
70	..	..	..	0·452	0·963	1·487	1·712
80	..	..	..	0·469	1·094	1·772	2·068
90	..	..	..	0·471	1·179	1·993	2·357
100	..	..	..	..	1·222	2·142	2·560
110	..	..	..	..	1·235	2·223	2·697
116·6	..	..	..	..	1·235	..	..
120	..	..	..	..	..	2·251	2·733
130	..	..	..	..	..	2·256	2·746
130·9	..	..	..	..	..	2·257	..
135	..	..	..	..	..	..	2·748

As regards the actual value of k to be taken in the reduction Öpik represents the law between $k = 1$ and $k = 2$ by linear interpolation:

$$(\cos z)^k = \beta\cos z + (1-\beta)\cos^2 z \tag{10}$$

(where for $k = 1$, $\beta = 1$; for $k = 2$, $\beta = 0$).

During the entire Arizona expedition the observed meteor streaming near the meridian was as follows:

	Meteors moving up			*Meteors moving down*			*Ratio down/up*
	A	*Number*	$\bar{\delta}$	A	*Number*	$\bar{\delta}$	
N. of zenith	0°–29°	143	+76°	150–179	3,266	+14°	20·0/1
	330–359	141		180–209	2,419		
S. of zenith	150–179	138	−34°	0–29	1,935	+56°	13·4/1
	180–209	108		330–359	1,369		

$\bar{\delta}$ is the mean declination for the given sector estimated on the basis of Tables 44 and 45 with $\beta = 0{\cdot}5$. Öpik considers the inequality in the N/S ratios to be an effect of declination which he represents by an additional factor $\mathbf{b}^{\cos^2\delta}$ in (10). For the limits of A the theoretical ratio down/up is $\frac{3{\cdot}16}{0{\cdot}236} = 13{\cdot}4$ for $k = 1$ (Table 44), and $\frac{2{\cdot}50}{0{\cdot}090} = 27{\cdot}8$ for $k = 2$ (Table 45). With these and the observed ratios (10) gives

$$\beta = 0{\cdot}54 \pm 0{\cdot}045; \qquad \mathbf{b} = 1{\cdot}374.$$

In the subsequent analysis Öpik takes $\beta = 0{\cdot}5$ (actually the sum of Tables 44 and 45 was used, which corresponds to $2n_\eta/C$).

As regards the increase in the apparent density of radiants towards the apex Öpik shows that the distribution can be represented satisfactorily by the expression

$$\mathbf{B}(\epsilon_1) = \mathbf{a}^{\cos\epsilon_1} \times \text{const.}, \tag{11}$$

where ϵ_1 is the distance of the apparent radiant from the apex. From the relative frequency of velocities in the region $P = 165° + 195°$, compared with $P = 15° + 345°$ (Table 43) and with the value of $\mathbf{b}$ found above, Öpik evolves the working formula

$$\mathbf{B}' = \mathbf{a}^{\cos\epsilon_1}\,\mathbf{b}^{\cos^2\delta_1} \tag{12}$$

with $\mathbf{a} = 2{\cdot}77$, $\mathbf{b} = 1{\cdot}374$, for the apparent density of radiants (vertical incidence).

Tables 44 and 45 are arranged according to the angle A, whereas the statistics (Table 43) refer to the apex direction P. For the centre of the observational area these angles are connected by $A = (P - 90° + t)$, where t is the mean local time. Hence, for a given P sector, different A sectors contribute during the night. The theoretical distribution for a given P sector is computed by weighting the data of Tables 44 and 45 according to the observational times. For the calculation of $\mathbf{B}'$ in (12)

it is assumed that $\delta_{apex} = 0$ and for a point (δ_1, P) that

$$\cos \epsilon_1 = -\cos \delta_1 \cos P. \tag{13}$$

The original coordinates are η, P. The declination varies slightly with A. The average declination for given (η, P) is found, weighting the data according to the observational times as above. $\mathbf{B}'$ is then calculated using (12) and (13). A selection of the final theoretical distributions is given in Table 46. (The original contains the distribution for P in 30° intervals from $P = 15°$ to 345°.) The three columns of this table give the following data for the limits η_1 and η_2, and for $\Delta P = 1$ (one radian), corresponding to a solid angle $\mathbf{S} = \cos \eta_1 - \cos \eta_2$:

(i) N_z, the intensity of streaming for $\mathbf{B}' = 1$ (uniform distribution of directions),

$$N_z = 4\sqrt{2} \int_{\eta_1}^{\eta_2} (\cos z + \cos^2 z) \sin \eta \, d\eta,$$

found by summation of Tables 44 and 45 and by taking the corresponding differences between η_1 and η_2;

(ii) the provisional radiant density $\mathbf{B}'$, computed by using (12);

(iii) the final intensity of radiation corresponding to $\mathbf{B}'$,

$$N_\eta = \mathbf{B}' N_z.$$

TABLE 46

Calculated Stream Intensity

(Northern Region, Arizona)

	$P = 45°$			$P = 135°$			$P = 225°$			$P = 315°$		
η	N_z	$\mathbf{B}'$	N_η	N_z	$\mathbf{B}'$	N_η	N_z	$\mathbf{B}'$	N_η	N_z	$\mathbf{B}'$	N_η
0°	0·046	1·000	0·046	0·046	1·000	0·046	0·054	1·140	0·062	0·055	0·893	0·049
10	0·120	0·893	0·107	0·118	1·140	0·134	0·179	1·325	0·237	0·180	0·813	0·146
20	0·152	0·813	0·123	0·144	1·324	0·191	0·301	1·545	0·465	0·310	0·757	0·235
30	0·152	0·757	0·115	0·144	1·545	0·223	0·409	1·799	0·734	0·420	0·719	0·301
40	0·124	0·720	0·089	0·113	1·799	0·203	0·483	2·089	1·006	0·500	0·698	0·349
50	0·098	0·698	0·068	0·084	2·09	0·175	0·513	2·38	1·220	0·533	0·678	0·361
60	0·072	0·678	0·049	0·062	2·38	0·147	0·503	2·59	1·300	0·527	0·676	0·355
70	0·051	0·676	0·034	0·041	2·59	0·106	0·442	2·73	1·204	0·468	0·673	0·314
80	0·029	0·673	0·020	0·024	2·73	0·065	0·360	2·82	1·015	0·383	0·668	0·255
90	0·013	0·668	0·009	0·010	2·82	0·028	0·262	2·73	0·716	0·278	0·673	0·187
100	0·006	0·673	0·004	0·004	2·73	0·011	0·172	2·59	0·445	0·183	0·676	0·123
110	0·002	0·675	0·001	0·001	2·59	0·003	0·076	2·38	0·181	0·087	0·678	0·059
120	0·000	..	0·000	0·000	..	0·000	0·034	2·09	0·071	0·029	0·698	0·020
130	0·000	..	0·000	0·000	..	0·000	0·003	1·94	0·006	0·003	0·708	0·002
135												
Sum	0·865	..	0·665	0·791	..	1·332	3·791	..	8·662	3·956	..	2·756
	$\eta_{eff} = 34°·9$; $\delta_1 = +60°$; $\bar{\epsilon}_1 = 111°; \bar{z} = 72°·9$			$\eta_{eff} = 43°·5$; $\delta_1 = +53°$; $\epsilon_1 = 65°; \bar{z} = 80°·3$			$\eta_{eff} = 64°·7$; $\delta_1 = +20°$ $\bar{\epsilon}_1 = 48°; \bar{z} = 48°·3$			$\eta_{eff} = 58°·3$; $\delta_1 = +27°$; $\bar{\epsilon}_1 = 129°; \bar{z} = 38°·7$		

If $\overline{\mathbf{B}}$ is the true mean density of apparent radiants, the observable probable number of meteors originating from the sector $\boldsymbol{P}$ to $\overline{\boldsymbol{P}+\Delta\boldsymbol{P}}$ and from a distance η_1 to η_2 is

$$\mathrm{n}_\eta = \frac{\Delta \boldsymbol{P}}{4\sqrt{2}}\overline{\mathbf{B}}\boldsymbol{N}_z,$$

with $\Delta\boldsymbol{P}$ in radians.

For the 30° sector width considered here this becomes

$$\mathrm{n}_\eta = \frac{\overline{\mathbf{B}}\boldsymbol{N}_z}{10{\cdot}80}.$$

By using this formula the relative figures in Table 46 can be converted into absolute ones for the specific value $\Delta\boldsymbol{P} = 30°$. At the foot of Table 46 the coordinates of the effective point of radiation are given. η_{eff} is the value of η which halves $\sum \boldsymbol{N}_\eta$; $\bar{\delta}_1, \bar{\epsilon}_1$, and $\bar{z}$ refer to the point $(\boldsymbol{P}, \eta_{\mathrm{eff}})$.

Öpik compares the observed distribution of velocities according to $\boldsymbol{P}$ with the theoretical distribution determined by the sum of $\boldsymbol{N}_\eta$ and shows that the degree of approximation in Table 46 is reasonable. There are systematic trends for different $\boldsymbol{P}$ in the ratio observed/calculated within the limits 0·68 to 1·54. Öpik considers this to be reasonable since the error in the distribution of $\sin\eta$ inside a given $\boldsymbol{P}$ sector, which is required, must be smaller by an order of magnitude than the errors in the absolute frequencies for different $\boldsymbol{P}$ sectors. Finally the distribution of the projection ratios, $\sin\eta$, is given in Table 47 for cases of $\mathbf{B}$ = const., and $\mathbf{B}'$ defined by (12). (Table 47 is a selection of the original corresponding to the $\boldsymbol{P}$ values in Table 46.) The similarity of the two solutions leads Öpik to conclude that no further approximation is required and the results in Table 47 for $\mathbf{B}'$ defined by (12) are used in the subsequent analysis.

(ii) *The distribution of space velocities.* From the above data Öpik determines the distribution of space velocities by employing equation (4), used in calculating the error dispersion. In this case χ is the frequency function of projection ratios given by Table 47, Φ the frequency of tangential velocities corrected for error dispersion (Table 43), and F the frequency function of space velocities which is required. Successive approximations are not required and the numerical solution proceeds as follows:

The discrete values of the space velocity $\mathbf{v}$ are spaced in the ratio $\sqrt[4]{2}/1$ as for v in Table 43 and $\sin\eta$ in Table 47. Let v_1 be the highest value of v and let the number between v_1 and $\mathrm{v}_2 = \mathrm{v}_1/\sqrt[4]{2}$ be n_1 (Table 43 corrected). Let the frequency of projection ratios from 1·000 to

TABLE 47

Relative Frequency of Projection Ratios ($\sin\eta$)

Case (*a*): **B** = const.; case (*b*): **B′** defined by formula (12). Case (*b*) is adopted in the solution for space velocities.

	$P = 45°$		$P = 135°$		$P = 225°$		$P = 315°$	
$\sin\eta$	(*a*)	(*b*)	(*a*)	(*b*)	(*a*)	(*b*)	(*a*)	(*b*)
1·000								
0·842	0·228	0·202	0·206	0·303	0·516	0·598	0·523	0·503
0·707	0·157	0·144	0·151	0·175	0·173	0·170	0·170	0·168
0·594	0·131	0·123	0·133	0·131	0·100	0·087	0·099	0·100
0·500	0·116	0·116	0·121	0·112	0·072	0·056	0·071	0·073
0·421	0·090	0·102	0·094	0·079	0·044	0·030	0·043	0·047
0·354	0·073	0·072	0·076	0·056	0·030	0·021	0·030	0·033
0·297	0·060	0·063	0·057	0·041	0·020	0·012	0·019	0·022
0·250	0·042	0·048	0·043	0·031	0·014	0·008	0·014	0·016
0·210	0·031	0·033	0·033	0·021	0·010	0·006	0·010	0·011
0·177	0·021	0·026	0·026	0·015	0·007	0·004	0·007	0·008
0·148	0·015	0·021	0·018	0·011	0·004	0·003	0·004	0·005
0·125	0·010	0·015	0·012	0·008	0·003	0·002	0·003	0·004
0·105	0·007	0·011	0·009	0·005	0·002	0·001	0·002	0·003
0·000	0·019	0·024	0·021	0·012	0·005	0·002	0·005	0·007
Sum	1·000	1·000	1·000	1·000	1·000	1·000	1·000	1·000
Mean $\sin\eta$	0·596	0·570	0·583	0·655	0·775	0·819	0·777	0·764

0·842 be χ_0 (Table 47); the frequency of space velocities $\mathbf{v}_1 = \mathrm{v}_1$ is $\mathrm{N}_1 = \mathrm{n}_1/\chi_0$: this number is then multiplied consecutively by the fractions χ from Table 47 and the products subtracted from the corresponding v frequencies. A new distribution of v is obtained with v_2 the highest value, and with n_2 between v_2 and v_3. The frequency of space velocities $\mathbf{v}_2 = \mathrm{v}_2$ is then $\mathrm{N}_2 = \mathrm{n}_2/\chi_0$ and so on. A selection of the distribution of space velocities for the same $\boldsymbol{P}$ values as in Tables 46 and 47 determined by this method is given in Table 48. The various columns in Table 48 are as follows:

1. $\mathbf{v}$ = the discrete values of the space velocities corrected for the ellipticity of the standard shower meteors.
2. $\mathrm{v} = \sqrt{(\mathrm{v}^2 - 125)}$ the geocentric velocity corrected for the attraction of the earth.
3. $\bar{\epsilon}_1, \bar{\delta}_1$ = the apparent distance from the apex, and the declination of the centre of radiation of the $\boldsymbol{P}$ sector.
4. $\overline{V}$ = mean heliocentric velocity corresponding to the centre of radiation.
5. ϵ, δ = the true or heliocentric distance from the apex and the declination of the centre of radiation.

In standardizing the velocity scales Öpik assumed that the shower meteors were moving at the parabolic velocity limit. In deriving Table 48 he introduces a tentative correction of 0·986 based on the velocities then believed to apply for the Lyrids, η-Aquarids, Perseids, and Leonids.

(iii) *The distribution of heliocentric velocities.* Öpik derived correction factors for the above data to allow for the gravitational attraction and orbital velocity of the earth, and after transforming from geocentric to heliocentric coordinates presented the final data given in Table 49. The table is arranged according to the observed direction of motion $\boldsymbol{P}$, and for different limits of the heliocentric velocity $\overline{V}$ it gives: $\bar{\epsilon}$ the distance from the apex and $\bar{\delta}$ the declination of the true (heliocentric) centres of radiation; n the number of observed meteors; $\bar{\mathrm{v}}$ the mean velocity of impact on the atmosphere upon which the luminosity of a given mass depends.

TABLE 48

Distribution of Space Velocities

v *km./sec.*	v *km./sec.*	n	$\bar{\epsilon}_1$	δ_1	$\overline{V}$ *km./sec.*	ϵ	$\bar{\delta}$	n	$\bar{\epsilon}_1$	δ_1	$\overline{V}$ *km./sec.*	ϵ	$\bar{\delta}$
		$\boldsymbol{P}$ = 45°						$\boldsymbol{P}$ = 135°					
			deg.	*deg.* +		*deg.*	*deg.* +		*deg.*	*deg.* +		*deg.*	*deg.* +
281	281	0	111	60	293	116	56	0	65	53	270	71	56
235	235	0	111	60	247	117	55	0	65	53	224	72	57
198	198	0	111	60	210	119	54	0	65	53	187	73	58
166	166	0	111	60	179	120	54	0	65	53	156	75	59
141	141	0	111	60	154	121	53	0	65	53	131	77	60
117	117	0	111	60	131	123	51	11·4	65	53	108	80	61
99	98·5	0	111	60	113	125	49	7·5	65	53	89·9	82	62
83·5	82·7	3·0	111	60	97·3	128	47	9·6	65	53	75·0	86	62
70·5	69·6	16·0	111	59	84·9	130	45	7·6	65	52	63·0	90	61
59·0	58·0	0	111	59	74·0	133	42	9·2	65	52	52·7	96	60
49·6	48·3	0	111	59	65·1	136	39	13·0	65	52	44·7	102	58
41·7	40·2	0	112	58	58·4	140	36	9·8	64	51	38·1	108	55
35·2	33·4	0	112	58	52·4	144	33	5·9	64	50	33·7	117	49
29·5	27·3	0	112	57	47·4	148	29	0	64	50	30·3	126	44
24·7	22·0	0	113	56	43·4	152	25	0	63	48	27·9	135	36
20·8	17·5	0	114	54	40·2	157	20	0	62	46	26·5	144	28
17·5	13·5	0	116	51	37·7	161	16	0	61	43	26·1	153	21
14·7	9·5	0	119	44	35·4	167	11	0	57	35	25·9	161	12
12·3	5·1	0	125	33	33·1	173	5	0	52	22	26·8	172	4
Sum		19						74					

TABLE 48 (*cont.*)

v *km./sec.*	v *km./sec.*	n	$\bar{\epsilon}_1$	δ_1	$\bar{V}$ *km./sec.*	ϵ	δ	n	$\bar{\epsilon}_1$	δ_1	$\bar{V}$ *km./sec.*	ϵ	δ
		$P = 225°$						$P = 315°$					
			deg.	*deg.* +		*deg.*	*deg.* +		*deg.*	*deg.* +		*deg.*	*deg.* +
281	281	0·8	48	20	262	53	22	0	129	27	301	133	25
235	235	1·5	48	20	216	54	22	0	129	27	255	134	25
198	198	0·0	48	20	180	55	22	0	129	27	218	135	24
166	166	0·0	48	20	148	57	23	0	129	27	186	136	24
141	141	0·0	48	20	123	58	23	0·1	129	27	161	137	23
117	117	0·0	48	20	99·8	61	24	0·0	129	27	138	139	23
99	98·5	8·4	48	20	81·9	64	24	0·0	129	27	120	140	22
83·5	82·7	37·8	48	20	66·9	67	25	3·0	129	27	104	142	21
70·5	69·6	47·8	48	20	54·6	72	26	5·0	129	27	91·3	144	20
59·0	58·0	35·3	48	20	44·2	78	27	5·6	129	27	80·2	146	19
49·6	48·3	25·1	47	19	35·5	85	26	6·8	130	26	71·2	149	17
41·7	40·2	20·1	47	19	29·5	95	26	6·9	130	26	63·6	151	16
35·2	33·4	16·7	47	19	25·5	106	25	9·7	130	26	57·3	154	15
29·5	27·3	10·5	46	19	22·5	119	23	11·2	131	26	52·0	157	13
24·7	22·0	5·9	46	18	21·5	132	18	13·0	131	26	47·2	160	12
20·8	17·5	1·1	45	17	21·3	145	14	7·7	131	25	43·3	162	10
17·5	13·5	0·0	43	15	22·0	156	9	2·7	133	24	40·2	166	8
14·7	9·5	0·0	39	12	23·2	165	5	0·3	136	22	37·2	170	6
12·3	5·1	0·0	33	6	25·4	174	1	0·0	143	18	34·2	175	3
Sum		211						72					

TABLE 49

Distribution of Heliocentric Velocities†

$\bar{V}$ *km./sec. limits*		P 135°	P 165°	P 195°	P 225°	$\bar{V}$ *km./sec. limits*		P 135°	P 165°	P 195°	P 225°
	$\bar{\epsilon}$	163°	..	..	..		$\bar{\epsilon}$	..	..	123°	..
	δ	+11°	..	..	..		δ	..	..	+48°	..
29·8..	n	0·0	—	—	—	14·9..	n	—	—	6·6	—
..25·1	$\bar{v}$	14	..	..	..	..12·5	$\bar{v}$	..	..	26	..
	$\bar{\epsilon}$	..	169°	174°	152°		$\bar{\epsilon}$	..	..	107°	..
	δ	..	+8°	+6°	+11°		δ	..	..	+56°	..
25·1..	n	—	0·0	0·0	0·8	12·5..	n	—	—	8·7	—
..21·1	$\bar{v}$	..	14	13	16	..14·9	$\bar{v}$	..	..	32	..
	$\bar{\epsilon}$	..	151°	167°	..		$\bar{\epsilon}$	..	121°	85°	..
	δ	..	+24°	+12°	..		δ	..	+50°	+60°	..
21·1..	n	—	0·0	0·0	—	14·9..	n	—	0·0	6·4	—
..17·7	$\bar{v}$	..	20	16	..	..17·7	$\bar{v}$	..	28	37	..
	$\bar{\epsilon}$	..	135°	155°	..		$\bar{\epsilon}$	..	106°	72°	..
	δ	..	+40°	+21°	..		δ	..	+58°	+56°	..
17·7..	n	—	0·0	2·2	—	17·7..	n	—	0·0	3·2	—
..14·9	$\bar{v}$	..	24	20	..	..21·1	$\bar{v}$	..	34	42	..

† The data for $\bar{V} < 29·8$ occur twice, representing different heliocentric directions. A dash indicates that the corresponding limits of $\bar{V}$ cannot occur at given P.

TABLE 49 (*cont.*)

$\bar{V}$ km./sec. limits		P											
		15°	45°	75°	105°	135°	165°	195°	225°	255°	285°	315°	345°
	$\bar{\epsilon}$	..	..	..	..	..	86°	65°	122°	..	..	..	..
	$\bar{\delta}$	..	..	..	..	..	+63°	+51°	+21°	..	..	..	..
21·1..	n	—	—	—	—	—	8·6	4·6	21·9	—	—	—	—
..25·1	$\bar{v}$	..	..	..	..	..	40	46	27	..	..	..	..
	$\bar{\epsilon}$	..	..	..	166°	138°	78°	59°	101°	158°	..	..	..
	$\bar{\delta}$	..	..	..	+10°	+33°	+62°	+48°	+25°	+7°	..	..	..
25·1..	n	—	—	—	0·0	0·0	17·6	5·6	20·8	0·5	—	—	—
..29·8	$\bar{v}$	..	..	..	13	22	46	52	38	16	..	..	..
	$\bar{\epsilon}$	175°	168°	159°	148°	121°	72°	50°	90°	139°	163°	175°	177°
	$\bar{\delta}$	+4°	+9°	+18°	+28°	+47°	+59°	+42°	+26°	+13°	+5°	+3°	+3°
29·8..	n	0·0	0·0	0·0	0·0	5·1	24·6	19·6	20·8	67·2	1·3	0·0	0·0
..35·4	$\bar{v}$	12	13	16	20	33	52	57	46	24	14	12	12
	$\bar{\epsilon}$	166°	163°	146°	133°	108°	65°	49°	83°	125°	152°	167°	172°
	$\bar{\delta}$	+11°	+18°	+31°	+42°	+55°	+55°	+41°	+26°	+16°	+10°	+8°	+8°
35·4..	n	2·3	0·0	0·0	3·1	11·8	27·4	26·5	23·6	103·6	36·1	3·7	2·7
..42·1	$\bar{v}$	16	19	24	30	42	59	64	54	34	22	17	16
	$\bar{\epsilon}$	161°	149°	136°	124°	101°	61°	46°	78°	115°	143°	160°	166°
	$\bar{\delta}$	+18°	+28°	+40°	+49°	+58°	+52°	+38°	+27°	+17°	+13°	+12°	+13°
42·1..	n	6·3	0·0	0·0	5·0	13·2	22·8	38·6	29·8	66·5	60·3	21·1	14·5
..50·1	$\bar{v}$	23	28	34	40	51	68	71	62	44	31	24	22
	$\bar{\epsilon}$	155°	142°	128°	117°	95°	57°	43°	72°	108°	136°	155°	161°
	$\bar{\delta}$	+24°	+34°	+47°	+55°	+60°	+50°	+36°	+26°	+18°	+15°	+14°	+18°
50·1..	n	8·1	0·0	0·0	0·9	9·0	20·5	37·1	39·8	34·2	49·0	18·5	6·6
..59·6	$\bar{v}$	32	35	44	50	62	76	80	70	55	42	32	30
	$\bar{\epsilon}$	151°	136°	122°	111°	89°	54°	41°	68°	103°	130°	151°	158°
	$\bar{\delta}$	+28°	+39°	+52°	+60°	+61°	+49°	+34°	+25°	+19°	+16°	+16°	+20°
59·6..	n	3·8	0·0	0·0	7·0	7·8	18·4	27·1	33·0	24·6	31·9	11·1	3·8
..70·9	$\bar{v}$	43	50	56	62	73	87	90	82	66	53	44	40
	$\bar{\epsilon}$	147°	132°	118°	106°	85°	51°	39°	65°	98°	126°	147°	156°
	$\bar{\delta}$	+31°	+43°	+55°	+62°	+62°	+46°	+33°	+25°	+19°	+18°	+18°	+22°
70·9..	n	2·3	6·7	15·0	6·4	9·1	14·1	9·5	14·8	19·9	29·2	8·7	4·3
..84·3	$\bar{v}$	56	63	69	76	86	100	102	94	80	66	56	53
	$\bar{\epsilon}$	144°	129°	114°	103°	82°	48°	37°	62°	95°	123°	144°	153°
	$\bar{\delta}$	+34°	+46°	+58°	+64°	+62°	+44°	+31°	+24°	+20°	+18°	+20°	+25°
84·3..	n	3·1	11·2	0·0	7·6	7·3	6·2	2·5	3·4	6·1	24·9	6·3	3·9
..100·2	$\bar{v}$	71	78	84	91	101	114	117	109	96	81	72	68
	$\bar{\epsilon}$	142°	126°	111°	100°	80°	47°	35°	60°	92°	119°	141°	151°
	$\bar{\delta}$	+37°	+49°	+60°	+66°	+61°	+43°	+30°	+24°	+20°	+19°	+21°	+27°
100·2..	n	3·2	1·1	0·0	0·0	10·5	2·2	0·6	0·0	0·4	7·3	2·5	2·1
..119·2	$\bar{v}$	88	96	103	108	119	132	134	127	114	98	88	86
	$\bar{\epsilon}$	140°	123°	108°	97°	77°	45°	34°	58°	89°	117°	139°	149°
	$\bar{\delta}$	+39°	+51°	+63°	+67°	+60°	+41°	+29°	+23°	+20°	+19°	+22°	+28°
119·2..	n	0·9	0·0	0·0	0·0	0·2	0·0	2·1	0·0	0·0	0·0	0·0	1·6
..141·7	$\bar{v}$	110	116	124	130	140	152	156	148	135	120	110	106

TABLE 49 (*cont.*)

$\bar{V}$ *km./sec. limits*	P											
	15°	45°	75°	105°	135°	165°	195°	225°	255°	285°	315°	345°
$\bar{\epsilon}$	138°	121°	106°	95°	75°	44°	34°	57°	87°	115°	137°	148°
$\bar{\delta}$	+40°	+53°	+64°	+68°	+59°	+40°	+29°	+23°	+20°	+20°	+23°	+30°
141·7.. n	0·0	0·0	0·0	0·0	0·0	0·0	5·0	0·0	0·0	0·0	0·1	0·5
..168·5 $\bar{v}$	134	142	150	155	166	176	180	173	160	145	134	131
$\bar{\epsilon}$	136°	119°	103°	92°	72°	41°	33°	54°	84°	112°	135°	146°
$\bar{\delta}$	+42°	+54°	+66°	+68°	+57°	+38°	+28°	+22°	+20°	+20°	+24°	+32°
>168·5 n	0·0	0·0	0·0	0·0	0·0	0·6	13·1	2·3	0·0	0·0	0·0	0·0
$\bar{v}$	200	210	220	220	230	284	226	252	224	230	200	200

The final data in Table 49 can be conveniently summarized to give the distribution of heliocentric velocities for all directions as shown in Table 50.

TABLE 50

Distribution of Heliocentric Velocities for all Directions

$\bar{V}$ *km./sec.*	*Semi-major axis* a	n	%
12·5	0·55	15·3	1·1
14·9	0·57	8·6	0·6
17·7	0·61	3·2	0·2
21·1	0·67	35·9	2·5
25·1	0·77	44·5	3·1
29·8	1·00	138·6	9·6
35·4	1·71	240·8	16·8
42·1	∞	278·1	19·4
50·1	..	223·4	15·6
59·6	..	168·5	11·7
70·9	..	140·0	9·8
84·3	..	82·5	5·7
100·2	..	29·9	2·1
119·2	..	4·8	0·3
141·7	..	5·6	0·4
168·5	..	7·0	0·5
200·5	..	7·6	0·5
238·3	..	1·4	0·1
283·3	..		
All		1,436	100·0

For the elliptical meteors the corresponding values a of the semi-major axis are given. It is of interest to compare Table 50 with the preliminary distribution given in Table 42, derived before the application of the detailed analysis of the projection ratios, and with the distribution of Table 36 for Öpik's personal 279 observations. These comparisons are

made in Fig. 94. There is considerable difference in detail between the provisional and final distribution and between Öpik's own observations and the total number of 1,436 velocities. Nevertheless they all show the same main feature of a large component exceeding the parabolic limiting velocity.

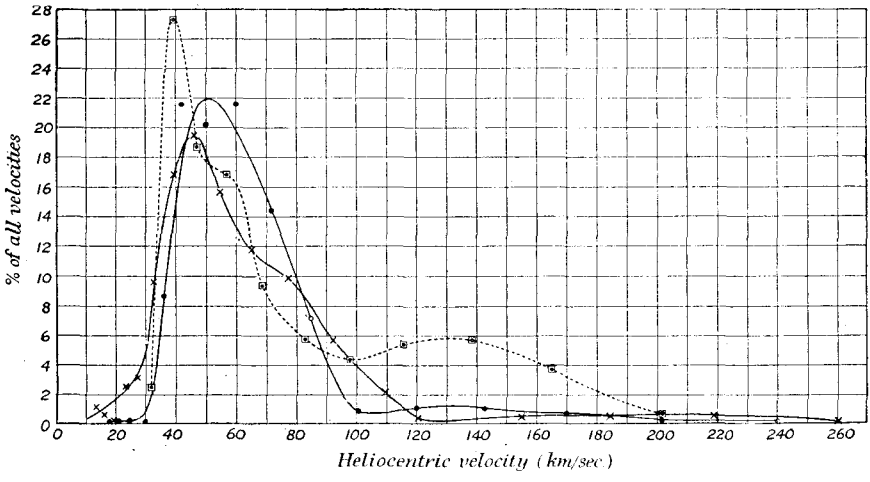

FIG. 94. The distribution of heliocentric velocities (all directions) from Öpik's rocking-mirror apparatus during the Arizona expedition.

Öpik's 279 observations with approximate solution for the distribution of space velocities.

The complete 1,436 velocities with approximate solution for the distribution of space velocities.

The complete 1,436 velocities with final solution for the distribution of space velocities.

The broad outline of the distribution of heliocentric velocities in different directions is given in Table 51. The data show only few solar meteors from the antapex ($\boldsymbol{P} = 315°$–$15°$) and few moving upwards ($\boldsymbol{P} = 45°$–$105°$); but numerous solar meteors for the apex ($\boldsymbol{P} = 165°$–$195°$) and downward ($\boldsymbol{P} = 225°$–$285°$) directions. The percentage of solar meteors in Table 51 is 38·8 per cent., of moderate hyperbolic meteors 46·6 per cent., and of 'high' hyperbolic meteors 19·6 per cent.

(iv) *The relation between velocity and luminosity.* As regards the relation between velocity and luminosity in the Arizona records, Öpik gives the data of Table 52, which refer to the uncorrected observed tangential geocentric velocity v and zenithal magnitude m_z.

TABLE 51

Frequency of Solar and Hyperbolic Meteors in the Arizona Data

P	15°		45°		75°		105°		135°		165°		195°		225°		255°		285°		315°		345°	
	n	%	n	%	n	%	n	%	n	%	n	%	n	%	n	%	n	%	n	%	n	%	n	%
Solar ($\bar{V} < 42{\cdot}1$)	2·3	7·7	0	0	0	0	3·1	10·3	16·9	22·8	78·2	48·0	83·4	38·1	87·9	41·7	171·3	53·0	37·4	15·6	3·7	5·1	2·7	6·8
Moderate hyperbolic ($\bar{V} = 42{\cdot}1$ to 70·9)	18·2	60·7	0	0	0	0	12·9	43·0	30·0	40·5	61·7	37·8	102·8	46·9	102·6	48·6	125·3	38·8	141·2	58·8	50·7	70·4	24·9	62·2
High hyperbolic ($\bar{V} > 70{\cdot}9$)	9·5	31·7	19·0	100	15·0	100	14·0	46·7	27·1	36·6	23·1	14·2	32·8	15·0	20·5	9·7	26·4	8·2	61·4	25·6	17·6	24·4	12·4	31·0
Sum	30	100	19·0	100	15·0	100	30	100	74	100	163	100	219	100	211	100	323	100	240	100	72	100	40	100

TABLE 52

Relation between Uncorrected Geocentric Velocity v *and Zenithal Magnitude* m_z

	$\bar{m}_z$	⩾3·5	3·2	2·7	2·2	1·45	0·45	−0·55	−1·55	⩽ −2·0
High hyperbolic	n	23	25	34	42	77	51	15	3	2
	%	21	21	20	18	20	20	15	13	7
Moderate hyperbolic	n	59	54	72	130	160	93	51	13	15
	%	54	44	42	55	42	37	50	52	56
Solar	n	28	43	66	64	148	111	36	9	10
	%	25	35	38	27	38	43	35	36	37

An analysis for heliocentric velocities by using the provisional approximation method gives the data in Table 53.

TABLE 53

Distribution of Heliocentric Velocities for High and Low Luminosity

$\bar{V}$ km./sec.		$\leqslant 36$	42	50	60	72	85	101	120	143	170	$\geqslant 202$	All
$m_z < 0$	n	4	35	62	44	3	0	0	0	0	0	6	154
($\bar{m}_z = 0{\cdot}6$ true)	%	2·6	22·7	40·3	28·6	1·9	0	0	0	0	0	3·9	100
$m_z > 0$	n	152	278	228	269	201	102	12	15	16	9	0	1,282
($\bar{m}_z = 2{\cdot}5$ true)	%	11·8	21·7	17·8	21·0	15·7	8·0	0·9	1·2	1·2	0·7	0	100

These figures indicate that bright meteors have a distribution in velocity different from the faint meteors. There are no bright meteors in the range $\bar{V} = 72$ to 170 km./sec., but only bright meteors for $\bar{V} \geqslant 202$ km./sec.

5. The complete observations of Öpik—Arizona and Tartu

Eighty per cent. of the Arizona measurements were made by two comparatively inexperienced observers. In order to obtain a more homogeneous series of results Öpik observed with the rocking-mirror apparatus in Tartu from the autumn of 1934 to the spring of 1938. He obtained an additional 506 observations (202 of which were shower meteors), which, with his previous 279 Arizona observations, made a total of 785 velocities determined by Öpik. This total material Öpik discusses separately in a publication† which contains a detailed list of the actual individual observations.

In an effort to improve the accuracy of the Tartu observations Öpik observed through a fixed reticule or grid for recording the meteor trails, instead of the star maps used in Arizona. Also during the observations attention was concentrated on the number of apparent waves produced in the meteor trail by the oscillating mirror. Thus only the duration of flight was observed and not other details, such as the shape of the oscillations, as in the Arizona work.

† Öpik, E. J., *Publ. Tartu Obs.* **30** (1941), no. 6. Summaries of the work have also been given by Öpik in *The Observatory*, **68** (1948), 228, and *Irish Astr. J.* **1** (1950), 85. In the latter publication Öpik states that the observations were continued at Tartu until the summer of 1941, when the observing station fell into the front line of the fighting forces, where it was damaged by an artillery shell and essential parts of the apparatus were stolen. No results subsequent to those considered here (up to 1938) have been published, however.

(*a*) *Reduction of Observations*

In the Tartu observations the rectangular coordinates of the beginning and end of the meteor trail were measured. Observations of the coordinates of a number of stars were also made, these being used to determine the constants in the formulae for the transition from rectangular to celestial coordinates. If L is the length of the trail computed in this manner, then the angular velocity of the meteor is determined from the observed number of waves n by

$$w_n = \frac{f\mathrm{L}}{(0{\cdot}1n)},$$

where f is a personal correction factor. (The frequency of the rocking mirror was 10 per second.) f was found from observations of 53 shower meteors to be 0·832 for the Tartu observations, compared with 0·938 for the Arizona observations.

In cases where the duration τ was observed the angular velocity is given by

$$w_\tau = \frac{f'\mathrm{L}}{\tau},$$

where f' is a correction factor varying with τ from 0·62 (τ = 0·05 sec.) to 1·00 (τ = 1·0 sec.) For Arizona f' was taken as a constant = 0·848. f' again was determined from observations of shower meteors (35 Tartu, 45 Arizona).

This observed angular velocity was reduced to the zenithal angular velocity w_z by using

$$w_z = \frac{w_{n \text{ or } \tau}}{\overline{\cos z}},$$

where $\overline{\cos z}$ is the mean for the beginning and end of the trail. As before (p. 157) the linear tangential velocity v km./sec. is then given by

$$\mathrm{v} = \frac{\mathrm{h}w_z}{57{\cdot}3} \tag{14}$$

with the height h in kilometres. For a shower meteor of geocentric velocity **v** observed at a distance η from the radiant, the tangential velocity is

$$\mathrm{v} = \mathbf{v} \sin \eta.$$

Hence the above equations give the predicted angular velocity of a shower meteor as

$$w_c = \mathbf{v} \sin \eta \, \overline{\cos z} \, \frac{57{\cdot}3}{\mathrm{h}}. \tag{15}$$

The equivalent predicted duration τ_c adapted to the observed trail length L is

$$\tau_c = \frac{L}{w_c}.$$

The average heights of the shower meteors in (15) and the mean heights as a function of w_z in (14) were assumed on the basis of the Arizona height observations as described previously. For the Tartu work the heights were increased by a constant amount of 1·9 km. to allow for the different level of the Arizona and Tartu stations.

The velocity scale was standardized by using the data on 202 shower meteors (compared with 73 in the Arizona work). By means of eight diagrams Öpik shows the correlation between the observed (w_f) and computed (w_c) angular velocity for the shower meteors as observed by the different workers for the case of oscillations and durations. The best correlation is that of Öpik's own Tartu observations for oscillations (Fig. 95). The worst correlations are those in which the durations were estimated—an example (R.W., Arizona) is shown in Fig. 96. Figs. 95 and 96 illustrate well the dispersion in the fundamental material of the rocking-mirror observations.

(*b*) *Analysis of the Complete Results*

Öpik discusses in some detail the influence of the observational errors and selection of data, comparing the various Arizona observers with his own Tartu observations. By various analyses which will not be reproduced here he draws the general conclusion that the effects of selection and systematic influences of the particular method, as well as the personality of the observer have little influence upon the statistics of the meteor velocities. He concludes that the observational material referring to meteor velocities appears to be well established. Öpik's total observational data are summarized in Table 54, uncorrected for error dispersion.

TABLE 54

Observed Frequency of Transverse Heliocentric Components of Velocity for Öpik's Arizona and Tartu Observations

Velocity km./sec.	*0–14*	*15–21*	*22–29*	*30–42*	*43–59*	*60–84*	*85–119*	*Over 120*
Sporadic meteors								
Number .	26	27	57	162	161	82	44	24
Percentage .	4·6	4·6	9·8	27·8	27·6	14·1	7·5	4·1
Shower meteors								
Number .	20	14	24	65	44	24	4	7
Percentage .	9·9	6·9	11·9	32·2	21·8	11·9	2·0	3·5

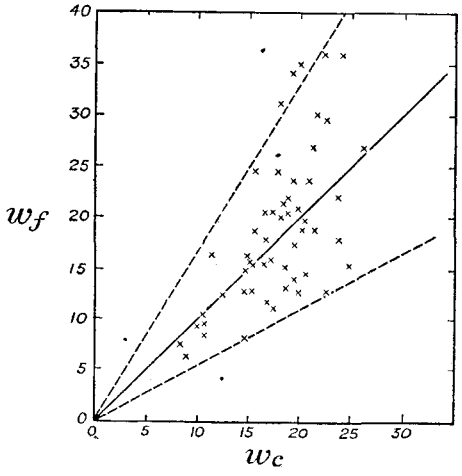

FIG. 95. The correlation of the observed (w_f) and computed (w_c) angular velocity for the shower meteors observed by Öpik at Tartu using oscillations of rocking mirror. The full line represents the true correlations and the broken lines the approximate limits of possible observational error.

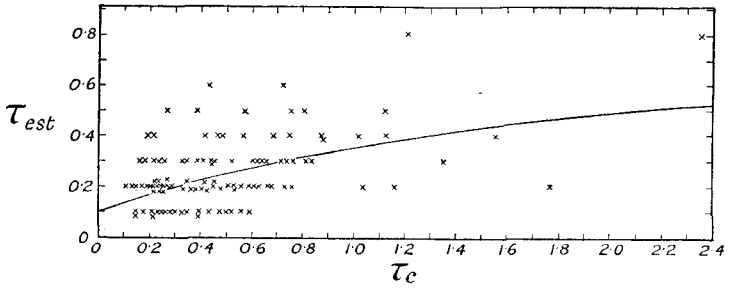

FIG. 96. The correlation of the observed (τ_{est}) and computed (τ_c) durations for the shower meteors observed by R.W. in Arizona. From estimates of duration with the rocking-mirror apparatus.

Öpik considers that any uncertainty in the final conclusions must be attributed to the method of interpretation of these results, in particular to the hypothesis upon which the distribution of space velocities is derived.

Here there are two contrasting influences. Firstly if a large observational error dispersion is assumed, the spread in meteor velocities and the relative number of high velocities will be small and vice versa. Secondly if a large spread in projection ratios is assumed, the mean velocity and the relative number of high velocities will be large and vice versa. Öpik

proceeds to take certain limiting cases for these two functions in order to set extreme limits to the true velocity distribution.

A maximum-error dispersion is obtained by assuming that all the deviations of the observed angular velocity from the computed values of the shower meteors are errors of observation; that is, none of the 'shower' meteors are rejected. Some 20 per cent. of the meteors included as 'shower' meteors may be stray meteors and hence this will certainly be an overestimate of the error dispersion. The lower limit—the most probable observational-error dispersion—is obtained from an analysis which rejects the probable number of stray meteors from the 'shower' meteors. The dispersion is then obtained from the deviation of the observed and computed angular velocity of the remaining, presumably true, shower meteors.

As regards the limits in the spread of the projection ratios, Öpik takes the maximum concentration to be that derived for the shower meteors, which are strongly concentrated towards the ecliptic. The minimum concentration is taken as that derived from the formula

$$\mathbf{f}_1 = \mathbf{f}_0 + \frac{n_2}{n_1}(\mathbf{f}_0 - \mathbf{f}_2)$$

for values of sin η from 0 to 1, where $\mathbf{f}_1$ is the frequency of sporadic meteors, $\mathbf{f}_2$ for shower meteors, $\mathbf{f}_0$ for all meteors, n_1 the number of sporadic, and n_2 of all meteors. With $n_1 = 621$, $n_2 = 164$ (the probable number of 38 stray meteors being subtracted from the shower total), $\mathbf{f}_2$ the concentration derived for the shower meteors and $\mathbf{f}_0$ the concentration for all the Arizona meteors, Öpik calculates the frequency of sin η for his own observations. He considers that this must be smaller than the true concentration of the sporadic meteors because the 1,436 Arizona results, used to obtain $\mathbf{f}_0$, contain a smaller relative fraction of shower meteors than Öpik's meteors. Also the values used for $\mathbf{f}_2$ were for the geocentric velocities which are more concentrated than the distribution of the heliocentric velocities. Thus it is possible that the value of $\mathbf{f}_1$ given by the formula is doubly overestimated, and hence that the true distribution lies between these values and the values obtained for the shower meteors alone.

Since the direct observational data of the various Arizona observers are statistically similar to the Tartu data, Öpik considers that with the same method of reduction both the observational series should yield the same results. He does not, therefore, apply the full complicated method of analysis, described earlier, to the Tartu data, but by variations in the

basic assumptions he estimates the possible range of uncertainty in the final results. Öpik's final summarized results for his 583 observations of sporadic meteors (Arizona 279, Tartu 304) are given in Table 55 and Fig. 97 for the various possibilities of maximum errors in observational error and projection ratios.

TABLE 55

Distribution of Space Velocities for 583 Sporadic Meteors observed by Öpik in Arizona and Tartu

aD = maximum observational error and maximum concentration of projection ratios.
aE = maximum observational error and minimum concentration of projection ratios.
bD = probable observational error and maximum concentration of projection ratios.
bE = probable observational error and minimum concentration of projection ratios.

$\bar{V}$ km./sec.					
uncorrected	*corrected*†	aD	aE	bD	bE
$\leqslant$ 15·0	$\leqslant$ (12)	11	0	16	0
17·9	(15)	0	0	0	0
21·2	(18)	25	0	24	0
25·2	(21)	2	0	5	0
30·0	26	4	0	14	0
35·8	32	64	9	65	17
42·4	39	115	77	100	69
50·4	47	153	188	128	171
60·0	57	86	121	78	104
71·6	69	58	83	59	84
84·8	83	39	62	39	56
101	98	17	28	26	39
120	116	6	10	11	15
144	140	2	4	6	5
$\geqslant$ 171	$\geqslant$ 166	1	1	12	23
All		583	583	583	583
Short period solar .	n ($\bar{V} \leqslant 32$)	106	9	124	17
	%	18·2	1·6	21·3	2·9
Long period solar .	n ($\bar{V} = 39$)	115	77	100	69
	%	19·7	13·2	17·1	11·8
Hyperbolic . .	n ($\bar{V} \geqslant 47$)	362	497	359	497
	%	62·1	85·2	61·6	85·2

† Corrected for zenithal attraction and ellipticity of shower orbits used for standardization.

The summary of the distribution for the wider velocity classes given at the bottom of Table 55 shows that the relative frequency of the short-period meteors is very uncertain and depends largely upon the assumed law of projection ratios; the same applies to the high hyperbolic velocities ($\bar{V} \geqslant 116$ km./sec.), but Öpik concludes that the relative

frequency of the intermediate velocities ($\overline{V} = 39$ to $\overline{V} = 98$ km./sec.) does not show variations of fundamental importance, and that the distribution may be considered as being satisfactorily established, independently of the assumptions regarding the law of errors and of projection ratios.

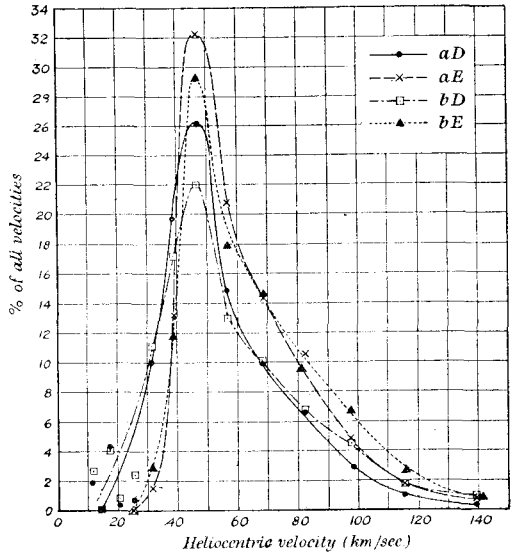

FIG. 97. The distribution of heliocentric space velocities for 583 sporadic meteors observed by Öpik in Arizona and Tartu.

aD = maximum observational error and maximum concentration of projection ratios;

aE = maximum observational error and minimum concentration of projection ratios;

bD = probable observational error and maximum concentration of projection ratios;

bE = probable observational error and minimum concentration of projection ratios.

(c) *The Relation between Velocity and Luminosity*

The relation between the heliocentric tangential velocity $\overline{V}_0$ and the zenithal magnitude for the combined observations of Öpik is given in Table 56. There is no systematic change in the distribution of luminosity with velocity—a result which is in disagreement with the combined Arizona data described in § 4 (*b*) (iv) above.

6. Criticisms of Öpik's velocity measurements

Although there are various discrepancies in the results of the rocking-mirror observations described in this chapter, the final conclusion

TABLE 56

Relation between the Heliocentric Tangential Velocity $\bar{V}_0$ *and the Zenithal Magnitude* m_z *for Öpik's Combined Results*

$\bar{V}_0$ *km./sec.*		⩽ 35	35–42	43–50	51–59	60–71	⩾ 72	All
$\bar{m}_z$								
−1·0	n	17	15	5	7	8	10	62
	%	28	24	8	11	13	16	100
+1·5	n	53	30	33	26	20	38	200
	%	26	15	17	13	10	19	100
+2·5	n	64	37	34	26	9	32	202
	%	32	18	17	13	4	16	100
+3·6	n	32	30	17	13	11	22	125
	%	26	24	14	10	9	17	100
All	n	166	112	89	72	48	102	589
	%	28	19	15	12	8	18	100

reached by Öpik is that at least 60 per cent. of the sporadic meteors are moving with velocities in excess of the parabolic limit. This work of Öpik has been subjected to severe criticism by the groups of observers whose results lead to a contrary conclusion—namely that the sporadic meteors are similar to the shower meteors and do not have velocities in excess of the parabolic limit. The main criticisms of the work have been made by Olivier† in America and by Porter‡ and Prentice§ in Great Britain. Olivier† complains of the absence of a determination of the velocity of a well-known shower group as a fundamental check on the reliability of the method, and refers to the peculiar positions of some of the centres of radiation. He criticizes the method because reticules were used in making the observations and these force the employment of only one eye at a time by the observer. Olivier's wide experience of meteor observation had convinced him that the reticule method was inferior to that of direct plotting upon prepared star maps. He then gives attention to the 279 preliminary results analysed by Öpik,‖ in particular to the number of meteors belonging to the well-known major showers. Since these showers are well spread throughout the year, Olivier considers that a comparison of Öpik's conclusions during these epochs should represent

† Olivier, C. P., *Pop. Astron.* **46** (1938), 325.

‡ Porter, J. G., *Mon. Not. Roy. Astr. Soc.* **103** (1943), 134; **104** (1944), 257; *J. Brit. Astr. Ass.* **60** (1949), 1.

§ Prentice, J. P. M., *Rep. Phys. Soc. Progr. Phys.* **11** (1948), 389.

‖ Öpik, E. J., *Circ. Harv. Coll. Obs.* (1934), no. 388.

a fair criterion for his results on the sporadic distribution. Olivier shows that many of the positions found by Öpik differ considerably from the accepted radiant positions of the showers, and that on many of the major shower nights no radiants whatever for them were obtained. This failure is especially marked in the case of the Orionids and Geminids. In view of the failure to observe the major showers adequately Olivier considers that the whole of the 279 radiants in the preliminary list must be regarded with suspicion. As to the cause of these errors Olivier writes as follows:† 'Such a result must have causes. These may be sought, first in an inferior method of observing, but I do not think this can possibly explain such abnormal results. I can only assign them, therefore, to a purely mathematical way of treating data when a graphical one, with proper safeguards, has been generally conceded by the best observers to be the proper procedure.'

Prentice‡ considers that the base line was too short and that the technique was not accurate enough for the determination of individual radiants, hence assumptions had to be made about the probable mean centres of radiation. Porter§ concludes that Öpik's paths were so erroneous that his results had to be based on mere assumptions as to the radiants and mean heights.

The detailed analysis of the visual observations which lead to this contrary view have been made by Porter§ and will be described in the following chapter.

† Olivier, C. P., loc. cit.
‡ Prentice, J. P. M., loc. cit.
§ Porter, J. G., *Mon. Not. Roy. Astr. Soc.* **104** (1944), 257.

X

THE VELOCITY OF SPORADIC METEORS—III

PORTER'S ANALYSIS OF THE BRITISH METEOR DATA

1. The British meteor data

THE main analysis of the British meteor data has been made by Porter† from a total of 2,669 observations, 90 per cent. of which were made by thirteen first-line observers.‡ From these observations a list of 1,253 accordances was compiled, that is observations made by different observers at the same time, and bearing other evidence of being different views of the same meteor. The source of these accordances was as follows:

The A. S. Herschel letters to Denning	1877–1900	36	accordances
B.A.A. Journals and Memoirs . .	1890–1914	68	,,
Denning's Notebook§ . . .	1895–1900	133	,,
A. King's Notebook . . .	1898–1920	17	,,
B.A.A. Observations . . .	1921–1931	274	,,
B.A.A. Modern Observations . .	1932–1940	725	,,
	Total	1253	

Only about two-thirds of these accordances show any real agreement in path, and thus the material finally treated by Porter consists of a total of about 800 paths.

(a) Observational Details and Method of Reduction

During the period of the observations treated by Porter there was a distinct change in the method of observation. In the early years the observed meteor paths were plotted on a map, and the observers undoubtedly concentrated on the brighter meteors with the longer paths. Although the extended wand, or string, was recommended in 1890‖ there is no certainty that its advantage was fully realized until 1929, by which time the British observers were quoting coordinates for the beginning and end of the meteor path, together with points on the path to define the actual position of the luminous path. In the subsequent years the method was further improved in the hands of Prentice, particularly by

† Porter, J. G., *Mon. Not. Roy. Astr. Soc.* **103** (1943), 134; **104** (1944), 257.

‡ T. H. Astbury, G. E. D. Alcock, D. Booth, T. W. Backhouse, J. H. Bridger, W. E. Besley, H. Corder, Miss A. Grace Cook, W. F. Denning, A. S. Herschel, A. King, J. P. M. Prentice, Mrs. F. Wilson.

§ Denning actually computed the paths of some 1,400 meteors but unfortunately the only notebook recovered after his death contained only the 133 accordances referred to by Porter.

‖ *Mem. Brit. Astr. Ass.* **1** (1891), 20.

using cross bearings, and distances between stars rather than estimates of angular distance. The method derived by Davidson† for the reduction of the meteor data has been used by Porter.‡ In this method the point of intersection of one of the observations with the plane of the observations of the other observer is found, so that no assumptions of simultaneity are made.

(*b*) *Reduction of Multiple Accordances*

In the sample treated by Porter there were 100 multiple accordances (the remainder being duplicate). Sixty-one of these gave satisfactory results on reduction, and Porter§ has used these to estimate the various errors. The mean errors and standard deviations of these results are given in Table 57 divided into 'old' and 'new' to indicate the change in observational method from map plotting to the extended wand referred to above.

TABLE 57

Mean Errors and Standard Deviations for the Multiple Accordances

Error	*120 old observations*		*68 new observations*		*All observations*	
	Mean	*Standard deviation*	*Mean*	*Standard deviation*	*Mean*	*Standard deviation*
	deg.	deg.	deg.	deg.	deg.	deg.
$\Delta \boldsymbol{R}$ Radiant . .	−0·06	1·62	−0·07	1·13	−0·06	1·47
$\boldsymbol{\tau}$ Twist . . .	−0·26	3·07	−0·19	2·27	−0·22	2·81
$\boldsymbol{\Delta}_1$ Offset (beg.) . .	+0·06	1·10	0·00	0·65	+0·03	0·96
$\boldsymbol{\Delta}_2$ Offset (end) . .	+0·10	1·28	+0·05	0·81	+0·09	1·13
ΔE_1 Sliding error (beginning) . .	−0·28	3·30	+0·09	2·97	−0·15	3·19
ΔE_2 Sliding error (end)	+0·04	3·45	−0·06	2·60	0·00	3·16
$\Delta\boldsymbol{\pi}$ Angular path .	0·00	3·80	−0·16	3·29	−0·06	3·61
ΔL Path length km. .	+3·7	21·1	+0·6	12·3	+2·5	18·2
Δh_1 Height (beg.) km..	4·6	3·5	4·2	3·3	4·4	3·5
Δh_2 Height (end) km. .	4·6	3·8	2·9	2·2	4·0	3·4
Δv Speed % . .	−4·8	38·2	0·0	30·6	−2·1	34·3
Δm Magnitude . .	0·0	1·30	−0·5	1·06	0·0	1·25

The radiant errors are the residuals in the observational equations, the positive sign indicating that the observed path passed north of the correct radiant. The actual angular errors made by the observers are divided into sliding errors ΔE along the path (positive in direction of motion) and offset errors $\boldsymbol{\Delta}$ perpendicular to the path (positive if north of the true path). The twist $\boldsymbol{\tau}$ is a guide to the accuracy of direction, computed from the angle between the observed and computed planes of

† Davidson, M., *J. Brit. Astr. Ass.* **46** (1936), 292.
‡ *Mem. Brit. Astr. Ass.* **34** (1942), pt. 4.
§ Porter, J. G. (1943), loc. cit.

observation. The offset errors were found to be an excellent guide to the value of an accordance. Any observations with an offset r.m.s. error exceeding 0·060 radians were rejected. The average and median errors for the quantities of Table 57 are given in Table 58.

TABLE 58

Average and Median Errors for the Multiple Accordances

	Averages			*Medians*		
Error	*Old* (*deg.*)	*New* (*deg.*)	*Total* (*deg.*)	*Old* (*deg.*)	*New* (*deg.*)	*Total* (*deg.*)
ΔR Radiant . .	1·23	0·78	1·07	1·0	0·45	0·7
τ Twist . . .	2·47	1·60	2·15	2·1	1·1	1·7
Δ_1 Offset (beginning) .	0·86	0·49	0·73	0·7	0·35	0·6
Δ_2 Offset (end) .	0·95	0·57	0·81	0·7	0·35	0·6
ΔE_1 Sliding error (beginning) . .	2·46	2·32	2·41	1·8	1·7	1·7
ΔE_2 sliding error (end) . . .	2·71	2·04	2·46	2·2	1·5	1·7
Δv Speed % . .	29·9	24·9	27·1	29	21·5	23
Δm magnitude .	0·98	0·91	0·95	0·75	0·75	0·75

(*c*) *Reduction of Duplicate Accordances*

The majority of the meteors in the sample were duplicate accordances. Comparison between the r.m.s. errors for these duplicate observations† and those for the multiples is given in Table 59.

TABLE 59

Comparison of r.m.s. Errors for Duplicate and Multiple Accordances

	Δh_1 (*km.*)	Δh_2 (*km.*)	Δm	ΔL (*km.*)	Δv† (*km./sec.*)	ΔE_1 (*deg.*)	ΔE_2 (*deg.*)
Multiples . .	5·7	4·5	1·05	14·8	11·3	2·81	2·72
Duplicates .	6·6	4·9	0·78	12·2	10·1	2·72	2·65
All meteors .	6·5	4·9	0·80	12·4	10·2	2·73	2·65

† In the later analysis Porter uses Δv—the mean difference in speeds—instead of the percentage Δv (Tables 57 and 58).

Porter investigates the error correlations in these data and finds a clear positive correlation between the sliding errors ΔE and the apparent angular length of the path. A possible explanation is that a meteor with a short path lies in a star field which can be embraced in one glance,

† Porter, J. G., 1944, loc. cit.

whereas a long path taxes the observer's memory. In any case it is clear that the values of the computed quantities are more reliable for the shorter paths. Definite positive correlations are also found between magnitude error and luminosity—probably because no reference standards are readily available for the very bright meteors—and between timing errors and duration.

The final data available for analysis from the multiple and duplicate observations amounted to 298 shower meteors† and 480 sporadic meteors.

2. The relation between height, velocity, and elongation

Porter investigates the correlation between the various physical quantities of the meteor, but here we shall be concerned only with height and velocity as involved in a comparison of the shower and sporadic meteors. The dominant factor amongst those affecting the heights is the elongation of the radiant—smaller elongation giving greater heights. The chief effect here must be a velocity one, small elongation being associated with high velocities as seen amongst the various shower meteors. Porter's data on this relation are summarized in Table 60.

Table 60 indicates that the average shower meteor appears and disappears at greater heights than the average sporadic meteor—a fact previously well known from Öpik's‡ analysis of the Arizona results. Porter points out, however, that the two groups are drawn from very different ranges of elongation and that a comparison can be made only for groups covering a similar range of elongation and magnitude. Such a comparison is made in Table 61, where the shower meteors are compared with the sporadic meteors over the same range of ϵ and m for two groups —(A) over the same dates, (B) over all other dates.

† Comprising the following showers:

Perseids, July 22–Aug. 6	152
Orionids, Oct. 16–29	35
Taurids, Nov. 2–9	28
Leonids, Nov. 15–17	27
δ-Aquarids, July 27–Aug. 18	15
α-Capricornids, July 23–Aug. 10	14
Camelids, Aug. 6–11	8
Quadrantids, Jan. 1–7	8
Lyrids, April 13–24	6
β-Piscids, Aug. 27–Sept. 18	5
Total	298

‡ Öpik, E. J., *Ann. Harv. Coll. Obs.* **105** (1937), 549.

TABLE 60

Relation between Height and Velocity for the Shower and Sporadic Meteors

	Number in sample	*Elongation from apex* ϵ	*Height of beginning of path* h_1 *km.*	*Height of end of path* h_2 *km.*	*Path length* L *km.*	v *km./sec.*	m	τ *(sec.)*	v/v_p†
		deg							
Leonids . .	27	10·5	125·6±2·34	94·1±2·00	56·2±5·70	57·8	−1·78±0·45	1·23±0·20	0·76
Orionids . .	35	24·1	119·7±2·14	100·9±1·79	27·0±2·23	51·6	+1·20±0·30	0·65±0·06	0·69
Perseids . .	152	39·2	114·9±1·32	94·7±0·98	31·7±1·61	43·4	+0·51±0·19	0·66±0·02	0·68
δ-Aquarids . .	15	69·4	101·1±4·43	89·0±4·39	49·9±8·22	29·3	+0·63±0·48	1·91±0·37	0·61
Taurids . .	28	81·4	101·6±2·24	77·7±1·97	33·5±3·49	25·7	−0·26±0·64	1·52±0·18	0·65
α-Capricornids .	14	93·0	95·5±4·25	85·3±3·42	22·5±3·64	24·2	+0·75±0·30	1·31±0·05	0·67
All showers . .	298	44·9	112·3±1·03	91·8±0·75	34·5±1·32	41·7	+0·39±0·14	0·93±0·04	0·67
Sporadic . .	480	68·1	103·1±0·93	85·8±0·84	33·6±1·61	34·9	+1·00±0·10	1·25±0·08	0·67

† v_p is the theoretical parabolic velocity of the meteor computed from the elongation.

TABLE 61

Relation between Shower and Sporadic Meteors over the same range of ϵ *and* m

		Shower	*Sporadic*	
			Group (A) (same dates)	*Group (B) (all other dates)*
Leonids	h_1	125·6±2·34	..	121·2±4·52
$\epsilon = 10{\cdot}5°$	h_2	94·1±2·00	..	101·3±3·17
	n	27	..	21
Orionids	h_1	119·7±2·14	117·0±4·06	114·4±1·90
$\epsilon = 24{\cdot}1°$	h_2	100·9±1·79	99·5±2·77	101·1±1·65
	n	35	14	53
Perseids	h_1	114·9±1·32	108·8±2·15	112·0±2·56
$\epsilon = 39{\cdot}2°$	h_2	94·7±0·98	93·2±2·73	94·4±2·20
	n	152	26	29
δ-Aquarids	h_1	101·1±4·43	101·9±2·99	100·3±2·23
$\epsilon = 69{\cdot}4°$	h_2	89·0±4·39	84·9±1·96	83·8±2·49
	n	15	16	36
Taurids	h_1	101·6±2·24	90·9±4·43	98·8±2·94
$\epsilon = 81{\cdot}6°$	h_2	77·7±1·97	78·8±3·49	77·9±1·94
	n	28	14	62
α-Capricornids	h_1	95·5±4·25	100·9±3·24	93·3±2·09
$\epsilon = 93{\cdot}0°$	h_2	85·3±3·42	82·7±2·24	80·5±2·48
	n	14	13	37

It is evident from this comparison that the mean heights of the shower and sporadic meteors are now significantly the same, that the height of appearance and disappearance is determined mainly by ϵ and m, and that in this respect both shower and sporadic meteors behave in an identical manner.

The relation between velocity and elongation is shown in Fig. 98, where the full curve is the theoretical geocentric parabolic velocity; and the results for six showers and nine groups of sporadic meteors are plotted. The close similarity between the groups indicates that the velocities of the sporadic and shower meteors are of the same order. The actual distribution of v/v_p amongst the shower and sporadic meteors is shown in Table 62.

Sixteen per cent. of the sporadic meteors have a v/v_p ratio greater than unity (that is hyperbolic velocity), but this also applies to 14 per cent. of the shower meteors so that the figures merely represent the tail of the distribution curve.

3. Comparison of Öpik's and Porter's analysis

It is evident that Öpik's analysis of the Arizona results, and Porter's analysis of the British results lead to opposite conclusions about the

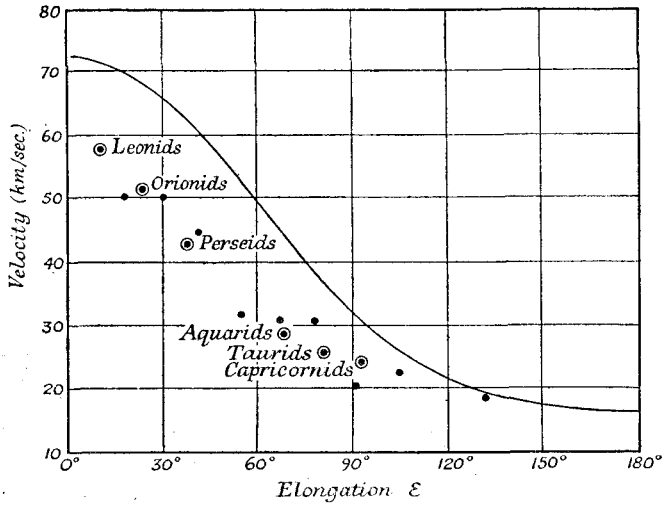

FIG. 98. Relation between elongation and velocity from Porter's analysis of the British meteor data. ⊙ shower meteors. ● nine groups of sporadic meteors separated in elongation. —— parabolic velocity limit.

TABLE 62

Distribution of v/v_p *for Sporadic and Shower Meteors*

v/v_p	*Number of sporadic meteors*	*Number of shower meteors*
0·0–	2	..
0·2–	62	25
0·4–	145	77
0·6–	95	85
0·8–	52	36
1·0–	23	20
1·2–	18	6
1·4–	12	4
1·6–	7	4
1·8–	2	1
2·0–	7	2
3·0–	1	..

existence of a meteor component with hyperbolic velocities. Öpik concludes that some 62 per cent. of sporadic meteors have hyperbolic velocities, whereas Porter concludes that there is nothing in his analysis of the British data to justify the belief in more than an occasional meteor with hyperbolic velocity. Porter's criticism of Öpik's data has been referred to on p. 189, while Öpik† likewise discusses Porter's conclusions on the grounds of the heterogeneity of the basic data. One serious difficulty to the acceptance of the hyperbolic theory lies in the problem of

† Öpik, E. J., *Irish Astr. J.* **1** (1950), 80.

the height range of the sporadic meteors. Since there appears to be a correlation between height and velocity it would be expected that the hyperbolic meteors would appear and disappear at very much greater heights than the shower meteors. This, however, is not found to be the case, a difficulty which Öpik† overcomes by the somewhat arbitrary assumption that the chemical composition of the sporadic meteors is different from that of the shower meteors.

Evidently an appeal to less subjective methods of velocity measurement is necessary to overcome this impasse, and in the next two chapters we shall review the contributions of the photographic and radio-echo work to this problem.

† Öpik, E. J., *Ann. Harv. Coll. Obs.* **105** (1937), 549.

XI

THE VELOCITY OF SPORADIC METEORS—IV

PHOTOGRAPHIC RESULTS

THE first successful attempts to measure the velocity of meteors by using a rotating shutter in front of the camera lens appear to have been made by Elkin of Yale between 1893 and 1909.† An analysis of Elkin's work has been presented by Olivier.‡ Elkin appears to have recorded 131 meteor trails, but only scanty data could be found for some of the records. In any case the base lines used by Elkin (3·3 and 5·0 km.) were too short for accurate velocity measurements and no useful purpose would be served in giving further details of the work. Subsequently the photographic work was carried out elsewhere, such as by Lindemann and Dobson§ in England and by Fedynski and Stanjukowitsch‖ in Russia, but the main results have been obtained by successive workers at Harvard. In this chapter we shall be concerned mainly with the Harvard results on the velocity of sporadic meteors.

1. The results of Millman and Hoffleit

Meteor photography at Harvard with rotating shutters was initiated by Fisher, who used two cameras fitted with Ross Xpress F/4 lenses of 6 in. focal length. Fisher obtained preliminary photographs with this equipment and assigned the programme to Millman in 1932. The first published analysis by Millman and Hoffleit†† concerns fourteen meteors photographed between 1932 August and 1936 July—one successful photograph being obtained for approximately 90 hours of exposure time.

(a) Reduction of Data from the Photographic Plates

The photographic meteor trails obtained by Millman and Hoffleit were segmented by the operation of the rotating shutter which occulted the lens 20 times per second. The determination of the velocity of the meteor was made in the following manner. In Fig. 99, L is the camera lens, which, in the present analysis, is assumed to be distortionless. AB is the meteor in the atmosphere and PQ the image on the photographic plate. Let A and P be fixed points on the trail and plate respectively and

† Elkin, W. J., *Astrophys. J.* **9** (1899), 20; **10** (1899), 25; **12** (1900), 4.
‡ Olivier, C. P., *Astr. J.* **46** (1937–8), 41.
§ Lindemann, F. A., and Dobson, G. M. B., *Mon. Not. Roy. Astr. Soc.* **83** (1923), 163.
‖ Fedynski, V., and Stanjukowitsch, K., *Astr. J. U.S.S.R.* **12** (1935), 440.
†† Millman, P. M., and Hoffleit, D., *Ann. Harv. Coll. Obs.* **105** (1937), 601.

B and Q variable points moving in the direction of the arrows. Then with the geometrical construction as shown:

$$\frac{x+z}{s} = \frac{r+d}{r},$$

$$\frac{z}{y+r+d} = \frac{s}{y+r}.$$

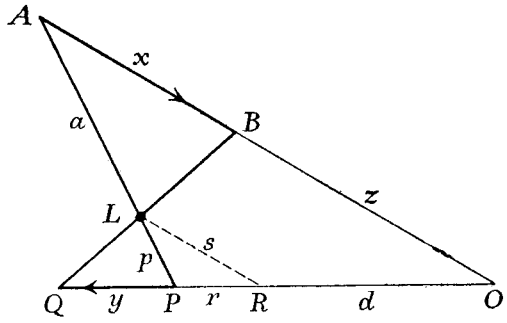

FIG. 99.

Hence $x = \mathrm{K}\frac{y}{y+r}$, where $\mathrm{K} = \frac{ds}{r} = \frac{as}{p}$ is a constant for a given meteor.

If the meteor has constant velocity v, then $x = \mathrm{vt}$ and

$$\mathrm{t} = \frac{\mathrm{K}}{\mathrm{v}}\frac{y}{y+r};$$

also $$\frac{\mathrm{d}y}{\mathrm{d}t} = \frac{(y+r)^2}{\mathrm{C}r} \quad \text{where } \frac{\mathrm{K}}{\mathrm{v}} = \mathrm{C} \text{ (constant)}.$$

Differentiating, $\frac{\mathrm{d}^2y}{\mathrm{d}y\mathrm{d}t} = \frac{2(y+r)}{\mathrm{C}r}$, giving a straight line relation between $\frac{\mathrm{d}^2y}{\mathrm{d}y\mathrm{d}t}$ and y. In principle these quantities can be found from the plate measurements, and the constants r and C evaluated giving the radiant point and geocentric velocity of the meteor. If instead of constant velocity, a constant deceleration $\dot{\mathrm{v}}$ is assumed, then $\left(\mathrm{vt} - \frac{\dot{\mathrm{v}}\mathrm{t}^2}{2}\right)$ is substituted for x, and the relation between $\frac{\mathrm{d}^2y}{\mathrm{d}y\mathrm{d}t}$ and y becomes more complicated and deviates from a straight line.

Unfortunately a very small error in measurement leads to a large percentage error in the second derivative $\frac{\mathrm{d}^2y}{\mathrm{d}y\mathrm{d}t}$; and the measurements

made by Millman and Hoffleit were not sufficiently accurate to justify its use.

A simplification ensues because the trail is generally short compared with its distance from the radiant, that is, y small compared with r. In such cases higher powers of y with respect to r can be neglected and we obtain

$$\frac{dy}{dt} = \frac{2}{C}y + \frac{r}{C},$$

which is a straight line relation between dy/dt and y with slope

$$S = \frac{2}{C} \quad \text{and intercept on the } y\text{-axis } Y = \frac{-r}{2}.$$

Y and S are obtained graphically or by least squares. r and C are thus determined. p and the angle at P are obtained from plate measurements, then s can be computed. If the distance of the meteor from the camera, a, is known, the velocity v is then given by

$$v = \frac{K}{C} = \frac{Sas}{2p}.$$

For the case of constant deceleration

$$\frac{dy}{dt} = \left(\frac{2}{C} - \frac{\dot{v}}{v}\right)y + \frac{r}{C} \quad \text{(neglecting higher powers of } y\text{)},$$

which is also a straight line relation between dy/dt and y, with slope

$$S' = \frac{2}{C} - \frac{\dot{v}}{v}$$

and intercept

$$Y' = \frac{-rv}{2v - \dot{v}C}.$$

Hence

$$r = -\left(2 - \frac{\dot{v}C}{v}\right)Y'$$

and

$$v = \frac{S'as}{2p} + \frac{\dot{v}}{v}\frac{as}{2p}.$$

Millman and Hoffleit did not have sufficient data available to evaulate any possible deceleration and based their computations on the assumption that the meteor was moving with constant velocity when the curve between dy/dt and y was a straight line. The procedure was to measure the distances between successive breaks and to determine the velocity from the plot of dy/dt against y, as indicated above.

(b) Results

Seven of the meteors analysed by Millman and Hoffleit were either Perseids, Leonids, or Orionids. The remaining seven sporadic meteors are listed in Table 63.

Although such photographic measurements are capable of great accuracy, the present analysis suffered because for all the meteors listed in Table 63 only one camera was operating and hence no height measurements were obtained. The heights quoted are assumed heights based on early data given by Öpik† for the relation between height, magnitude, and velocity.

TABLE 63

Data on Seven Sporadic Meteors photographed by Millman and Hoffleit between 1932 *and* 1936

Meteor No.†	*Date and Time (E.S.T.)*	*Magnitude (zenithal at 100 km.)*	*Radiant (1900)*		*Elongation from apex*	*Height km.*	*Velocity*‡ *km./sec.*		
			α *(deg.)*	δ *(deg.)*	ϵ *(deg.)*		v	v_g	$\bar{V}$
5	1933 Nov. 16d. 0h. 38m.	−2	75	+45	67	68	26	24	30§
7	1935 Sept. 7d. 1h. 36m.	−4	339·5	−1·6	93	65	20	16	35
8	1935 Sept. 30d. 20h. 28m.	−4	350·6	+43·2	85	62	13	6	30
9	1935 Oct. 20d. 1h. 04m.	−5	20·6	+11·1	92	60	14	8	31
12	1935 Dec. 29d. 4h. 36m.	−9	183·0	+18·6	21	70	72	71	44
13	1936 Feb. 29d. 4h. 08m.	−4	238	−7	17	70	55	54	27
14	1936 July 6d. 23h. 55m.	−6	247·8	+34·7	115	60	15	10	35

† Catalogue number corresponding to the nomenclature of Millman and Hoffleit.

‡ v = observed velocity relative to the earth.
v_g = observed velocity v corrected for zenith attraction.
$\bar{V}$ = heliocentric velocity obtained by correcting v_g for the earth's motion.

§ The speed of rotation of the shutter was uncertain during this photograph, and the velocity may be double the value given.

The times given are the mid-points of the exposure times of the plate, which varied from 71 min. to 120 min. The magnitude was estimated for the brightest part of the trail by photometry.

The heliocentric velocities $\bar{V}$ computed for these seven sporadic meteors are well below the parabolic limit with the exception of No. 12 for which the parabolic limit is just exceeded. Similar analysis of the seven shower meteors indicated that there may have been a loss in velocity of some 10 km./sec. due to deceleration. Even if allowance is made for this, only two more of the velocities are raised slightly above the parabolic limit, and there is little indication of the very marked hyperbolic velocities to be expected on the basis of Öpik's work.

† Öpik, E. J., *Proc. Nat. Acad. Sci. Wash.* **22** (1936), 526.

2. The results of Whipple

In 1936 Whipple instituted a new two-camera programme at Harvard for meteor photography. His results represent the first real precision measurements in meteor astronomy. The definitive orbits which he was soon able to give for the Taurid and Geminid showers are amongst the highest achievements in the subject. This work on the shower meteors will be considered in Chapter XV; here we are concerned only with Whipple's data on the sporadic meteors.

The two cameras were situated at the ends of a 38-km. base line; the AI patrol camera at Oak Ridge, and the FA patrol camera at Cambridge. Both cameras were equipped with Ross Xpress lenses of 5·9 in. focal length and aperture 1·5 in. The occulting shutters gave 20 interruptions per second. The routine observing programmes were synchronized so that the two cameras were directed towards a point in space about 80 km. above the earth's surface.

(*a*) *Reduction of Data*

In the first† of the publications dealing with this work, Whipple describes in detail the method of measurement of the segmented trails on the photographic plate and the treatment of the data. The apparent radiant was determined by measurement of the trail position relative to several faint stars symmetrical about the trail. The plate centre was determined from the position of three stars by a method due to Olmsted‡ and from this centre standard coordinates were determined for all the stars according to Turner's method.§ These coordinates were related to the measured coordinates by means of a number of comparison stars of known coordinates distributed along the trail, at small distances from it. Hence, theoretical coordinates for each star measured on the plate could be calculated. The differences between these and the measured coordinates give the corrections necessary for lens distortion, and also for measurement errors, and the effects of differential refraction. Whipple considered that the radiant coordinates determined from the photographic plates were correct to an accuracy of 2 minutes of arc.

For a doubly photographed meteor the height of any point of the trail can be determined from the direction of the trails on the two plates, provided the time of appearance of the meteor is known. This latter presents some difficulty with long exposures except when the meteor is also seen visually. Otherwise it is necessary to determine the times of

† Whipple, F. L., *Proc. Amer. Phil. Soc.* **79** (1938), 499.
‡ Olmsted, M., *Ann. Harv. Coll. Obs.* **87** (1931), 221.
§ Turner, H. H., *Mon. Not. Roy. Astr. Soc.* **60** (1900), 201.

appearance by identification of natural irregularities in the trails as seen from the two stations. This determination is the least satisfactory part of the early measurements. For example, in the first six results described by Whipple,† one meteor was also seen visually and hence an exact time could be given, but accurate times could be found only for two others. In one case of a faint trail (No. 660), the possible time of apparition extended for the duration of the exposure (60 min.). The detailed method of height computation depends on the position of the intersection of the two planes passing through the stations and not on the identification of points on the two trails. The method of computation which is due to Schaeberle has been described by Olivier.‡

The coordinates of the shutter breaks on the trails were transferred to a distance s along the actual trail in space by the method of Millman and Hoffleit described in § 1. An example to illustrate the accuracy obtainable is given in Table 64 for a single meteor (No. 642). The first column gives the time in mean seconds from the first break, the second column the square root of the weight assigned to the measurement, based on the appearance of the breaks at the time of measurement. Three types of equations were then fitted to the measured distances, s, by means of least squares:

$$s = A + Bt + Ct^2, \tag{1}$$

$$s = A + Bt + Ct^3, \tag{2}$$

$$s = A + Bt + Ce^{ct}, \tag{3}$$

where A, B, and C are unknown constants, and c is a constant arbitrarily chosen for each meteor. The last three columns of Table 64 give the residuals from the solutions according to (1), (2), and (3). It is to be expected that equation (3) would represent most accurately the motion of a meteor in an atmosphere in equilibrium with gravity, since the exponential increase of density with decreasing height should produce an exponentially increasing deceleration. c was estimated for each meteor on the assumption that the air resistance was proportional to the density. The velocities and deceleration of this meteor calculated according to the three equations are given in Table 65.

It is evident from the data in Tables 64 and 65 that the three equations fit the observations equally well, and the same is true for the other meteors discussed by Whipple. Whipple concludes that the observed

† Whipple, F. L. (1938), loc. cit.

‡ Olivier, C. P., *Meteors*, ch. xiv, Williams & Wilkins (1925).

TABLE 64

Example of Whipple's Trail Coordinates and Residuals for Meteor No. 642

Time from first break t (sec.)	*√(Weight)*	*Distance along trail in space* s *(km.)*	*Residuals for equations* (1)–(3)		
			O−C eq. (1) *(km.)*	*O−C eq.* (2) *(km.)*	*O−C eq.* (3) *(km.)*
0·00	0·3	0·0000	−0·0594	−0·0795	−0·0832
0·05	0·8	1·6339	+0·0098	+0·0037	+0·0014
0·10	0·8	3·1884	+0·0065	+0·0087	+0·0082
0·15	0·8	4·7376	+0·0046	+0·0105	+0·0119
0·20	1·0	6·2696	−0·0077	−0·0015	+0·0010
0·30	1·0	9·3358	−0·0097	−0·0090	−0·0071
0·35	0·8	10·8697	+0·0004	−0·0025	−0·0024
0·40	0·8	12·3916	+0·0052	−0·0003	+0·0024
0·45	0·8	13·9083	+0·0116	+0·0056	+0·0018
0·50	0·8	15·4094	+0·0091	+0·0059	+0·0026
0·55	1·0	16·8928	−0·0042	−0·0004	+0·0012
0·60	0·3	18·3470	−0·0399	−0·0238	−0·0094
Probable errors of observation (weight unity)			±0·0067	±0·0067	±0·0065

TABLE 65

Velocities and Deceleration of Meteor No. 642

Equation	A *(km.)*	B *(km.)*	C *(km.)*	*c*	*Mid-time* t_0 *(sec.)*	*Velocity* v_0 *(km./sec.)*	*Acceleration* $\dot{v}_0$ *(km./sec.²)*	$\dot{v}_0/v_0$
(1)	+0·0594	+31·3612±0·0626	−1·3590 ±0·0992	..	0·300	30·546	−2·718	−0·089
(2)	+0·0795	+31·0172±0·0382	−1·4770 ±0·1068	..	0·300	30·618	−2·659	−0·087
(3)	+0·1035	+31·1015±0·0425	−0·02031±0·00142	5	0·300	30·646	−2·276	−0·074

decelerations are consistent with an assumption that the density decreases exponentially with height, and utilizes the observed decelerations to determine the absolute values of the density. In any case it is seen from Table 65 that the calculated velocities v_0 at the mid-point are almost independent of the law of deceleration assumed, and that the decelerations are only slightly dependent on the law.

Finally the velocity v_0 has to be reduced to the corresponding velocity V for the case of no atmosphere. Whipple applies the equation

$$\log V = \log v_0 + \frac{9{\cdot}0\times10^{11}}{v_0^2}\left[\log\left(1-9{\cdot}73\times10^{-7}\frac{\dot{v}_0}{\cos z}\right)\right],$$

where z is the true zenith distance of the radiant and c.g.s. units are used.

(b) Whipple's Analysis for Seven Sporadic Meteors

Whipple's analysis of the results with the double camera photography have so far been given in six publications (*a*)-(*f*).† Of these, three publications (*c*), (*d*), and (*f*) contain only double station results applicable to shower meteors and will be discussed in Chapters XIII–XV. The remaining three publications contain data for seven sporadic meteors, the details of which are given in Table 66. Of these No. 642, although originally given as sporadic in (*a*), was later classed as a Taurid meteor in (*e*), a classification also continued in Jacchia's analysis (see § 3). The data given in (*b*) for Nos. 505 and 756 were obtained from the sinuosity of the trails in two double cameras, caused by vibration of the camera supports. The reduction of the data is the same as for the occulted lens systems. Table 66 contains the essential published information on these seven meteors. The most complete data are given in the 1938 publication for meteors 642, 660, 663, 670, 694. The data for numbers 505 and 756 are given in the 1940 publication and the incomplete data for number 694 in the 1943 publication.

For three of the meteors (660, 663, 505) the times of apparition are uncertain, and solutions for the extreme ranges of possible time are given in each case. The following notes, numbered to correspond with the entries in Table 66, explain the data which are not self-evident:

(vi) The magnitudes were determined from a comparison of faint star images in the vicinity of the trail. The effective exposure times varied from 4×10^{-4} sec. for a fast meteor to 8×10^{3} sec. for the star images. Whipple‡ discusses the possible failure of the reciprocity law and other matters relating to the magnitude estimates in some detail.

(vii) Q is the angle between the poles of the great circle motion as seen from the two stations. $\sin Q$ represents the relative accuracy with which the apparent radiant is determined for equal precision in the determination of the great circle motion. The trail length multiplied by $\sin Q$ is an approximation to the relative accuracy of the apparent radiant. The data in Table 66 indicate that all the radiant determinations have an accuracy of about two minutes of arc.

† Whipple, F. L., (*a*) *Proc. Amer. Phil. Soc.* **79** (1938), 499; (*b*) **82** (1940), 275; (*c*) **83** (1940), 711; (*d*) **91** (1947), 189; (*e*) *Rev. Mod. Phys.* **15** (1943), 246; (*f*) Wright, F. W., and Whipple, F. L., *Tech. Rep. Harv. Coll. Obs.*, no. 6 (Harvard Reprint Series II–35), 1950.

‡ Whipple, F. L. (1938), loc. cit.

TABLE 66

Whipple's Double Station Data for Seven Sporadic Meteors

Meteor number	642	660		663		670	694	505		756
(i) Sidereal time	4h. 22m. 0s.	9h. 50m. 0s.	9h. 0m. 0s.	10h. 20m. 0s.	10h. 0m. 0s.	15h. 8m. 1s.	..	23h. 0m.	0h. 30m.	17h. 43m. 5s.
(ii) U.T.	1936 Oct. 21·2972	1937 Feb. 4·2364	1937 Feb. 4·2017	1937 Feb. 12·2353	..	1937 Mar. 12·3583	1937 Oct. 12·35	1932 Nov 4·0363	1932 Nov. 4·0987	1938 July 30·1663
(iii) Length of trail (degrees)	6	20	..	43	..	8	..	13·4	..	1·4
(iv) Number of breaks	12	48	..	18	..	11	5	41†	..	14†
(v) Time observed (sec.)	0·60	2·25	..	0·95	..	0·55	..	2·00	..	0·81
(vi) Average visual magnitude	−2·3	−2·2	..	−4·0	..	−3·1	−3·0	−3·91‡	−3·16‡	+0·40‡
(vii) sin Q	+0·9998	+0·2286	..	+0·1109	..	+0·1594	..	..	..	..
(viii) cos **z**	+0·8151	+0·5620	+0·6820	+0·1226	+0·0739	+0·4647	+0·681	+0·885	+0·860	+1·000
(ix) Height at first break (km.)	89·69	66·54	73·81	119·53	101·90	76·27	..	86·5	71·9	98·4
(x) Height at last break (km.)	74·74	49·88	50·22	110·26	97·11	70·14	..	42·5	41·6	74·0
(xi) Height at middle (km.)	82·08	57·97	61·68	114·90	99·50	73·15	..	..	..	..
(xii) Height at max. light (km.)	77	53	55	114	99	70	100·3	61·2	54·5	86·2
(xiii) Apparent radiant										
α (1900·0)	42° 59′·7	90° 9′·1	..	208° 4′·0	..	169° 41′·6	..	351°·1	351°·1	267°·1
δ (1900·0)	+12° 31′·9	+14° 44′·2	..	−23° 59′·7	..	+5° 33′·8	..	+15·1	+15·1	+42·5
(xiv) Corrected radiant										
α (1900·0)	41° 48′	78° 31′	83° 33′	208° 14′	208° 23′	166° 44′	..	..	..	..
δ (1900·0)	+11° 24′	+4° 28′	+8° 45′	−24° 28′	−24° 38′	+2° 53′	..	..	..	..
(xv) Elongation (ε)	75° 19′	141° 51′	138° 20′	20° 47′	20° 47′	93° 17′	..	131°·4	131°·4	95°·0
(xvi) v_0 apparent velocity (km./sec.)	30·646	13·256	15·472	79·690	68·429	23·876	69·6	18·43	13·00	27·92
(xvii) V no-atmosphere velocity (km./sec.)	31·360	13·823	15·937	79·963	68·861	25·273	..	..	..	..
(xviii) v_g geocentric velocity (km./sec.)	29·466	8·672	11·744	78·941	67·694	23·020	..	14·7	6·9	25·6
(xix) $\bar{V}$ heliocentric velocity (km./sec.)	36·285	37·397	39·740	51·859	40·884	38·814	..	41·5	35·7	40·8
(xx) a (a.u.)	1·910	2·222	4·062	−0·990	7·189	3·206	..	14·5	1·72	11·0
(xxi) q (a.u.)	0·2962	0·9684	0·9517	0·8342	0·7484	0·6178	..	0·927	0·963	0·951
(xxii) e	0·8449	0·5641	0·7657	1·8423	0·8959	0·8073	..	0·936	0·442	0·914
(xxiii) Period in orbit **P** (years)	2·639	3·311	8·186	hyperbolic	19·275	5·740	..	55	2·3	37
(xxiv) Mean anomaly	−15° 35′	−4° 13′	−2° 0′	..	−1° 48′	−7° 16′	..	359°·6	351°·4	353°·5
(xxv) ω (1900·0)	122° 14′	18° 4′	22° 53′	40° 28′	60° 44′	81° 10′	..	210°·3	204°·4	210°·2
(xxvi) Ω (1900·0)	27° 14′	134° 32′	134° 33′	142° 36′	142° 33′	170° 53′	..	220°·9	220°·9	97°·2
(xxvii) i (1900·0)	6° 0′	4° 15′	4° 19′	159° 13′	156° 39′	1° 53′	..	5°·3	2°·2	36°·3

† Number of vibrations (sinusoidal trail). ‡ At maximum light.

(viii) **z** is the zenith distance from Oak Ridge.

(ix) to (xii) Heights refer to the horizon plane through Oak Ridge. Height at maximum refers to the brightest part of the trail, including flares.

(xiv) Corrected radiant obtained by correcting the apparent radiant successively for the aberration effect of the earth's rotation and for zenith attraction.

(xv) ϵ is the elongation of the corrected radiant from the apex of the earth's way.

(xx) to (xxvii) Notation according to Chapter V.

(*c*) *Discussion of Whipple's Measurements on the Seven Sporadic Meteors*

The fundamental accuracy of Whipple's data given in Table 66 can be checked against the data which he derives for the shower meteors with the same photographic system and analysis.† The agreement in the velocities shows that the velocities determined by the rotating shutter method are not subject to large errors produced by deceleration in the atmosphere as suggested by Millman and Hoffleit.‡ The comparisons also show that the correction for atmospheric deceleration discussed in (*a*) above is of the right order.

The velocity results show that the sporadic meteors 642, 660, 670, 694, 505, 756 are moving in short-period elliptical orbits around the sun. In the case of 663, however, there is an uncertainty of 20 minutes in the time of appearance of the meteor. Whipple§ states that the natural irregularities in the trails were difficult to measure and no certain identification could be made. From repeated trials with two different matching techniques it seemed that the sidereal time of 10h. 20m. was correct. This implies a marked hyperbolic velocity (78·9 km./sec. geocentric, 51·8 km./sec. heliocentric). On the other hand Whipple considers that the various physical data of the meteor compared with the others indicates a solar system origin and his final decision is against the hyperbolic value. The other extreme of the solution for this meteor yields a velocity less than the parabolic value (67·7 km./sec. geocentric, 40·8 heliocentric). Öpik's views on these results will be referred to later (§ 4).

† Whipple, F. L., 1938, 1940, 1949, *loc. cit.* See also Chapter XIII et. seq.
‡ See this chapter, § 1.
§ Whipple, F. L., 1938, loc. cit.

TABLE 67

Additional List of Sixteen Sporadic Meteors extracted from Jacchia's† First Analysis

Meteor number	*Date*	*Number of breaks in trail*	*Velocity km./sec.*	*Acceleration km./sec.²*	*Height km.*
663‡	1937 Feb. 12·22	18	71·03	−0·05	98·6
815	1939 Jan. 24·11	13	19·71	−3·31	61·6
828	1939 Mar. 20·16	24	32·58	−1·62	80·4
982	1940 Aug. 29·20	11	39·97	−2·72	91·6
1005	1940 Oct. 27·07	11	26·74	−1·98	86·2
1068§	1941 Mar. 23·08	9	22·59	−2·84	67·2
		11	21·55	−5·00	62·8
		9	19·77	−10·07	58·8
1071	1941 Mar. 31·34	16	57·33	−3·23	84·2
1103	1941 Nov. 25·38	8	75·49	+1·06	94·7
1170§	1942 Aug. 2·20	5	67·93	−7·07	90·6
		6	67·35	−25·63	90·0
1180§	1942 Oct. 4·15	22	20·39	−0·743	79·4
		10	19·98	−3·85	73·3
1205§	1943 Mar. 25·23	22	33·10	−0·437	74·5
		18	31·85	−6·25	61·3
1241	1944 Dec. 10·07	24	29·14	−1·37	79·1
1242§	1945 Feb. 6·22	31	11·98	−0·178	62·6
		34	11·62	−0·572	54·6
		38	10·52	−1·315	46·1
		17	9·35	−1·941	41·8
1243§	1945 Feb. 6·30	19	28·05	−1·19	78·1
		20	27·03	−2·98	66·1
		25	27·20	−3·74	66·1
		16	24·65	−9·83	57·1
1514	1947 Oct. 12·30	32	13·52	−1·613	56·4
1544§	1947 Dec. 10·01	20	25·04	−0·198	85·5
		21	24·86	−0·508	79·6
		21	24·44	−1·162	73·2
		19	23·43	−2·860	67·0
		15	21·50	−7·101	62·4
1556§	1947 Dec. 17·35	22	35·07	−0·70	92·4
		19	34·75	−1·31	88·0

† Jacchia, L. G. (1948), loc. cit.
‡ Included also in Table 66—see note in text.
§ The reason for the alternative solutions is not given. They are presumably either due to timing uncertainties or split components of the trail.

3. Jacchia's analysis of the double-camera data

In two reports† on ballistics and upper atmospheric air densities Jacchia gives the most complete list of velocities, determined by the double-camera system, which has yet been published. The 1948 report† gives a list of 50 velocities, 14 of which have been previously published by

† Jacchia, L. G., *Tech. Rep. Harv. Coll. Obs.* (1948), no. 2 (Harvard Reprint Series, II–26); (1949), no. 4 (Harvard Reprint Series, II–32).

Whipple (§ 2 above). The remaining 36 contain 16 sporadic meteors which are listed in Table 67. Most of these were photographed using the two-camera system employed by Whipple at Oak Ridge (AI) and Cambridge (FA) with shutters rotating at 600 r.p.m. After August 1947 some results were obtained with new, unguided cameras—KA at Cambridge, KB at Oak Ridge. These each used Kodak-Ektar lenses of 7-in. focal length and aperture F/2·5, with shutter speeds of 1,800 r.p.m. (KA) and 1,200 r.p.m. (KB). In the summer of 1948 these cameras were removed to sites in New Mexico at Doña Ana and Soledad Canyon.

The data given by Jacchia for these meteors are rather incomplete compared with the data given by Whipple in Table 66. The velocities correspond to the apparent measured velocities v_0 of Table 66, and the heights to the point for which v_0 is given (corresponding approximately to 'Height at middle' of Table 66). Unfortunately no data are given for the computation of heliocentric velocities or orbital elements. One meteor (1103) has a velocity of 75·49 km./sec., which is in excess of the geocentric parabolic velocity. The much disputed meteor, number 663, is also included in Table 67 since Jacchia gives a value for v_0 almost exactly at the parabolic limit, intermediate between the extremes quoted by Whipple in Table 66.

Jacchia's 1949 report† gives a list of fifty-two meteors photographed in the double-camera programme. Forty-two of these are repeats of previously published data. The relevant velocity information on the remaining ten is given in Table 68, but there is no indication as to whether the meteors are shower or sporadic.

TABLE 68

Additional List of Ten Velocities extracted from Jacchia's Second Analysis†

Meteor number	*Velocity km./sec.*	*Height km.*
808	36·31	93·8
1065	49·09	113·2
1158	29·85	90·5
1270	60·25	106·3
1360	71·78	107·3
1447	72·28	105·3
1472	58·88	103·9
1542	23·71	77·5
1550	36·64	95·8
1587	68·39	105·1

4. Discussion of the photographic velocities

The double-camera photographic technique is capable of such high accuracy that it can, in principle, settle the hyperbolic velocity problem

† Jacchia, L. G. (1949), loc. cit.

without ambiguity. Unfortunately, with the types of camera so far used, the collection of data is a long task since only very bright meteors can be photographed satisfactorily. Even in the cases of the meteors already photographed the unfortunate ambiguity in the time of appearance of number 663 has perpetuated the dichotomy of views as to the reality of the hyperbolic component. Further, in the most complete published lists (those of Jacchia, Tables 67 and 68) there is no information which enables the heliocentric velocity to be computed, but, even so, one meteor (1103) has a velocity exceeding the geocentric parabolic limit, and two others (1360 and 1447) are at the limit.

Whereas the adherents of the solar system origin for meteors point to the lack of any very high velocities such as found by Öpik (Chap. IX), Öpik† accepts the photographic data as proof of the hyperbolic theory. Whereas Whipple‡ considers from physical evidence that the low elliptical velocity for meteor 663 is correct, Öpik† investigates the relation between luminosity and velocity in Whipple's data and concludes that meteor 663 fits this relationship well when it is given the hyperbolic velocity; but that it lies six magnitudes away from the curve connecting magnitude and velocity when the lower elliptical velocity is assigned. Öpik also criticizes the photographic results on two other grounds:

(i) that the preponderance of shower meteors in the photographic results, compared with his visual Arizona results, indicates that the solar component amongst the bright meteors is strongly enhanced;

(ii) that the photographic selection favours meteors with low angular motion across the photographic plate.

5. The future of the photographic programme

The failure of the double-camera technique to provide an unambiguous answer to the velocity problem has been due basically to the fact that the techniques used were restricted to very bright meteors. Firstly, this implies that the collection of sufficient data is a prolonged task since with the AI and FA cameras it required an average of some 100 hours exposure to obtain a satisfactory duplicate photograph. Secondly, the results are open to a criticism that they refer to very bright meteors, which may possibly represent a different selection of the meteoric material than the visual observations referred to in Chapters IX and X.

The development and construction of Super Schmidt cameras to

† Öpik, E. J., *Irish Astr. J.* **1** (1950), 80.
‡ Whipple, F. L. (1938), loc. cit.

overcome these basic difficulties has been described by Whipple† and have been discussed in Chapter II. The magnitude limit is expected to be reduced to about +4 compared with zero to −1 on the existing instruments. Table 69 gives the anticipated details of characteristics and performance compared with the various cameras used for the work described earlier in this chapter.

TABLE 69

Anticipated Performance of Super Schmidt Camera compared with existing Cameras

Camera	*Aperture (in.)*	*Focal ratio*	*Field diameter (degrees)*	*Light transmission*†	*Performance meteors/100 hours*
Ross Xpress .	1·5	4	60	1·0	1·0
Cooke Taylor .	1·5	8	33	1·1	0·3
3-in. Ross .	3·0	7	20	0·8	0·7
Aero-Ektar .	3·0	2·5	45	0·4	2·3
Super-Schmidt .	12·0	0·85	52	1·3	260

† Ross Xpress taken as unity for comparison.

Allowing for the increasing 'dead time' due to the more frequent film changes required—even on a perfectly dark night the limiting exposure is expected to be about 15 minutes—Whipple‡ estimates that the yield per annum should be increased by some 40 times on the existing instruments, and anticipates satisfactory double station information from about 100 meteors per annum.§ According to a recent announcement‖ the construction of two of these Super Schmidt instruments was completed by the Perkin Elmer Corporation during 1951. The first was installed at Soledad, New Mexico, during the summer of 1951. The results from these instruments, which should give a precise answer to the problem of the hyperbolic velocity component, will be awaited with interest.††

† Whipple, F. L., *Sky and Telescope*, **8** (1949), 90; *Tech. Rep. Harv. Coll. Obs.* (1947), no. 1.

‡ Whipple, F. L. (1949), loc. cit.

§ Whipple, F. L. (1947), loc. cit.

‖ *Sky and Telescope*, **10** (1951), 219.

†† In a private communication received at the end of October 1952, Dr. Whipple stated that the Super Schmidt cameras were working excellently, and that in September 1952 nearly 200 doubly photographed meteors were obtained. It is therefore evident that the photographic meteor studies have entered a new epoch and that the information given in this chapter will become of historic interest only during the course of the next few years.

XII

THE VELOCITY OF SPORADIC METEORS—V

THE RADIO-ECHO RESULTS AND GENERAL CONCLUSION

In the previous four chapters we have seen that the conventional visual and photographic techniques have led to an impasse over the question of the velocities of sporadic meteors. The new radio-echo techniques for the measurement of velocities, developed in the years following 1945 (Chaps. III and IV), have since been applied to this problem independently in Great Britain and Canada. The workers in Great Britain used the pulsed techniques with narrow-beam aerials in order to select particular groups of sporadic meteors; whilst the Canadian workers used the continuous-wave techniques with wide-beam aerials. The details of the two programmes and the results will be discussed separately in this chapter.

1. The work of Almond, Davies, and Lovell

(*a*) *Equipment*

The measurements in Great Britain have been made at the Jodrell Bank Experimental Station by Miss Almond, Davies, and Lovell.† The radio apparatus was essentially similar to that described in Chapter IV. The transmitter radiated 600 pulses per second each of 10 microsec. duration. Since the separation between pulses corresponds to only 250 km. in range it was necessary to double every fourth pulse so that ranges could be measured to 1,000 km. without ambiguity. Two radio wavelengths were used in a series of four equipments designed successively to record meteors of fainter magnitudes.

	Equipment I	*Equipment II*	*Equipment III*	*Equipment IV*
Wavelength λ . . .	4·16 m.	8·13 m.	8·13 m.	8·20 m.
Peak transmitter power P .	20 kw.	30 kw.	240 kw.	240 kw.
Aerial beam width to half power { azimuth	$\pm 6{\cdot}5°$	$\pm 12°$	$\pm 12°$	$\pm 12°$
Aerial beam width to half power { elevation	$\pm 14{\cdot}0°$	$\pm 7°$	$\pm 5°$	$\pm 12°$
Aerial power gain over isotropic source G . .	50	25	36·6	28
Receiver noise level $\bar{\omega}_0$.	$5{\cdot}7\times10^{-14}$ watts	$1{\cdot}3\times10^{-13}$ watts	$1{\cdot}3\times10^{-13}$ watts	$1{\cdot}3\times10^{-13}$ watts

The 4-m. aerial system was steerable and was used at various azimuths with the elevation fixed at 10°. The 8-m. aerial system was fixed to

† Almond, M., Davies, J. G., and Lovell, A. C. B., *Observatory*, **70** (1950), 112; *Mon. Not. Roy. Astr. Soc.* **111** (1951), 585; **112** (1952), 21; **113** (1953), 411.

produce a beam with its main axis in an easterly direction (azimuth 90°). In equipments II and III the aerial was horizontal and the elevation of the main beam about 10 deg. In equipment IV the aerial of III was rebuilt at an angle of 45° to the horizontal. Although the maximum power gain of the aerial was thereby decreased somewhat owing to the loss of ground reflections, the mean range of the observed meteors was reduced. The net result was an improvement in sensitivity over equipment III to the extent of about 1·5 magnitudes in the limiting magnitude of meteors detected (see § 1 (*f*)). The recording instrument and the method of determining velocities has been described in Chapter IV.

(*b*) *Organization of Experiments*

The basic purpose of the experimental arrangements was to measure the velocity distribution of sporadic meteors whose paths lay in the great circle plane through the apex of the earth's way. The specular reflection properties of meteor trails (see Chapter III) enable this selection to be achieved partially with narrow-beam aerials oriented at right angles to the plane through the apex. Actually, owing to the finite width of the aerial beams, the meteors recorded are those lying between two small circle planes enclosing the great circle; the thickness of the 'slice' depending on the width of the beam. In order that the hourly rates could be sufficiently large the apex experiments were carried out in the autumn mornings in the neighbourhood of 06h. when the apex of the earth's way lies near its highest altitude, on a great circle plane passing approximately overhead and cutting the horizon in the north and south. Similarly, 'antapex experiments' were carried out during the spring evenings in the neighbourhood of 18h. when the antapex of the earth's way occupies this position. Thus for all the experiments the aerial beams were either fixed in an easterly direction or movable for a small angle around it. Since for a given heliocentric velocity the geocentric velocity depends on the elongation of the meteor radiant from the apex of the earth's way, it was possible with these arrangements to obtain distributions for velocities in the neighbourhood of maximum velocity (apex) and minimum velocity (antapex). These distributions were then compared with the theoretical distribution to be expected if all the meteors were moving at the parabolic velocity limit so that an appreciable hyperbolic component would be immediately apparent.

The following specific experiments were made:

(i) Equipment I was used in the early morning hours between 1948 September 18 and December 18, with a certain amount of aerial

movement in order to keep the apex on the circle of echo. The 230·5 hours of observation yielded 67 velocities which are plotted in Fig. 100.

(ii) Equipment II was used in the early morning hours between 1949 October 10 and December 20 with the aerial fixed at azimuth 90°. In 43·5 hours of observation 187 velocities were measured as shown in Fig. 101.

(iii) Equipment II was used between 17h. and 19h. from 1950 February 18 to April 29 with the aerial fixed at azimuth 90°. The 213 hours of observation yielded 87 velocities which are plotted in Fig. 102.

(iv) Equipment III was used in the early morning hours between 1950 November 8 and December 14 with the aerial fixed at azimuth 90°. In 10·7 hours of observation 335 velocities were measured as shown in Fig. 103.

(v) Equipment III was used between 17h. and 19h. from 1951 March 29 to May 18 with the aerial fixed at azimuth 90°. The 56·5 hours of observation yielded 57 velocities which are plotted in Fig. 104.

(vi) Equipment IV was used in the early morning hours between 1951 November 18 and December 6 with the aerial fixed at azimuth 90°. The 21 hours of observation yielded 362 velocities which are plotted in Fig. 105.

(c) *Experimental Errors*

In order to provide a standard of comparison and a basis for the estimation of errors, equipment II was also employed to measure the velocities of the Geminid meteors in 1949 December. The measured velocity distribution is shown in Fig. 106. In 05h. 48m. 122 velocities were measured, giving a mean of 35·9 km./sec. and a standard deviation of 4·6 km./sec. The errors of the individual velocity measurements can be estimated from the diffraction photographs. The effect of errors in range measurement is small, and it is found that the error depends principally on the number of echo pulses between the maxima and minima, and on the number of Fresnel zones observable. In deriving the individual errors in these Geminid velocities it was assumed that the position of each maximum or minimum could be estimated to ± 1 pulse. The r.m.s. value of the error for the 122 individual velocities calculated on this basis was 2·4 km./sec. This value is considerably less than the standard deviation of the histogram in Fig. 106. This discrepancy could arise either because the basis of error estimation is wrong or because of

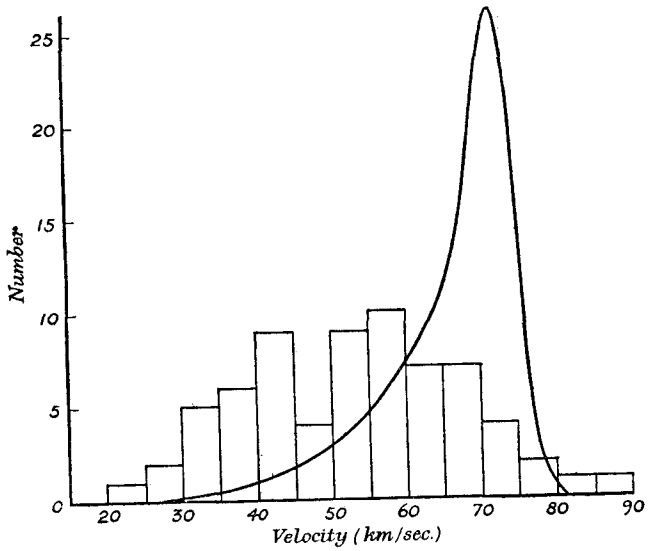

FIG. 100. The measured velocity distribution (histogram) for the first apex experiment (equipment I, autumn 1948). The theoretical distribution calculated as described in the text is shown as a smooth curve, and is normalized to the equivalent number of observations.

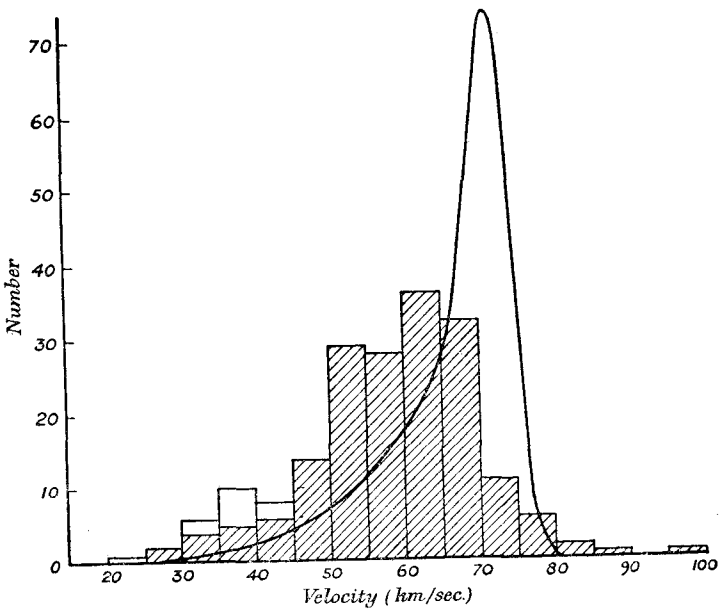

FIG. 101. The measured velocity distribution (histogram) for the second apex experiment (equipment II, autumn 1949). The unshaded parts are referred to in § 1 (*g*) (iii). The theoretical distribution calculated as described in the text is shown as a smooth curve, and is normalized to the equivalent number of observations.

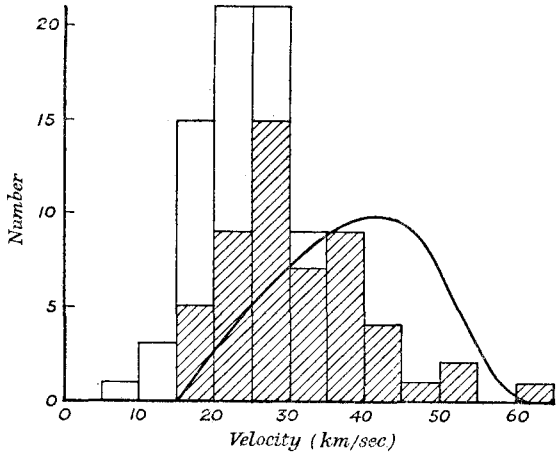

FIG. 102. The measured velocity distribution (histogram) for the first antapex experiment (equipment II, spring 1950). The unshaded parts are referred to in § 1 (*g*) (iii). The theoretical distribution calculated as described in the text is shown as a smooth curve, and is normalized to the equivalent number of observations.

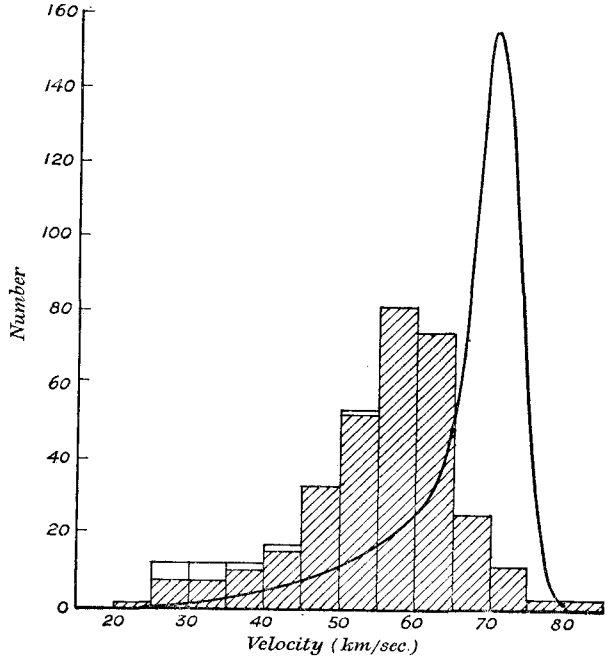

FIG. 103. The measured velocity distribution (histogram) for the third apex experiment (equipment III, autumn 1950). The unshaded parts are referred to in § 1 (*g*) (iii). The theoretical distribution calculated as described in the text is shown as a smooth curve, and is normalized to the equivalent number of observations.

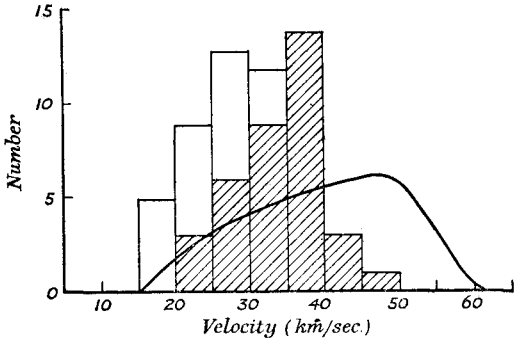

FIG. 104. The measured velocity distribution (histogram) for the second antapex experiment (equipment III, spring 1951). The unshaded parts are referred to in § 1 (*g*) (iii). The theoretical distribution calculated as described in the text is shown as a smooth curve, and is normalized to the equivalent number of observations.

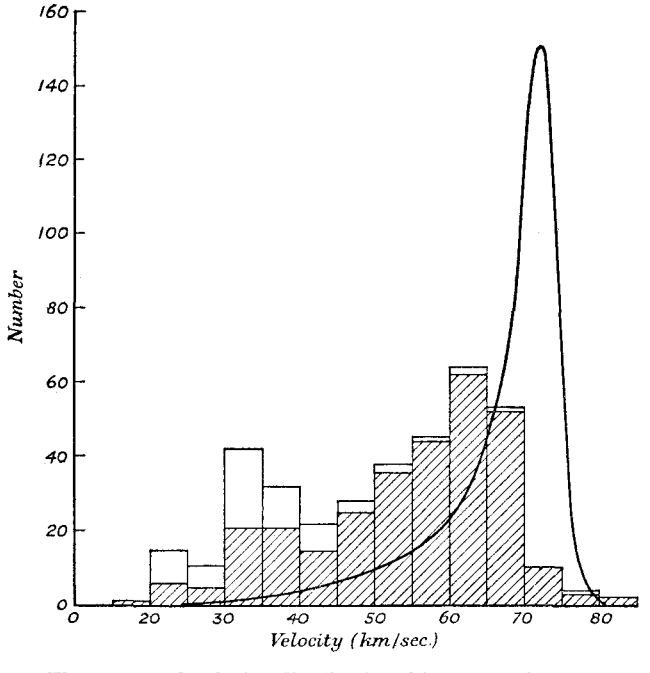

FIG. 105. The measured velocity distribution (histogram) for the fourth apex experiment (equipment IV, autumn 1951). The unshaded parts are referred to in § 1 (*g*) (iii). The theoretical distribution calculated as described in the text is shown as a smooth curve, and is normalized to the equivalent number of observations.

the existence of an actual spread in the Geminid velocities. The matter was investigated as follows.

In the largest group of homogeneous velocities between 34 and 38 km./sec. (Fig. 106), N meteors were selected on which the average number of independent measurements of velocity per meteor was greater

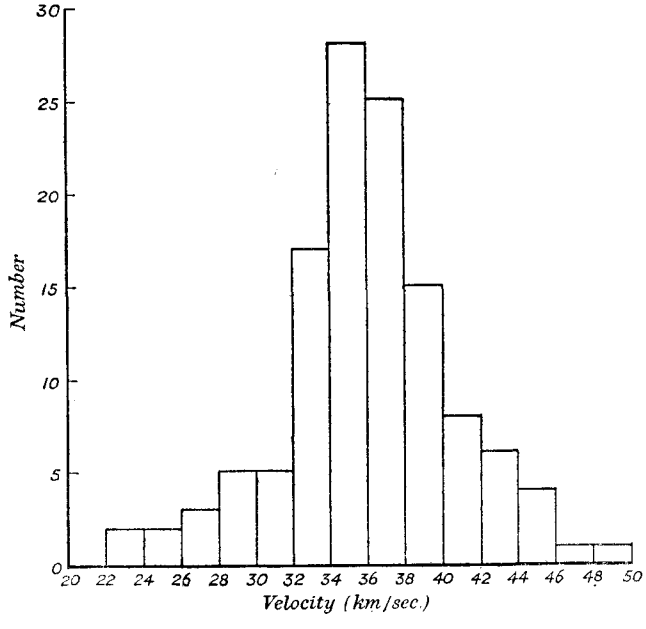

FIG. 106. The velocity distribution for the Geminid meteor shower measured during the period 9–15 Dec. 1949, with equipment II for the purpose of assessment of errors in the velocity measurements.

than three. Let the mean velocity of the nth meteor be v_n, and the separate measurements of its velocity be v_{na}, v_{nb}, etc. Let the average number of measurements of velocity per meteor be Γ. Then, if we write $\Delta_{na} = v_n - v_{na}$, the quantity

$$\sqrt{\frac{\sum \Delta^2}{N\Gamma}} \tag{1}$$

is a measure of the accuracy of a single measurement, the sum being taken over the $N\Gamma$ measurements made. The mean standard deviation of each meteor velocity is then

$$\sqrt{\frac{\sum \Delta^2}{N\Gamma(\Gamma-1)}}.$$

A sample of sixteen Geminid meteors was selected which yielded

fifty-seven individual velocity measurements, giving $\Gamma = 3{\cdot}56$. The value of (1) is then 1·75 km./sec., and the mean error in the velocity of a meteor for the group 1·1 km./sec.

An alternative method of estimating the individual errors from the group result has been described by Davies.† Let v represent the true velocity of the meteor, and v_1, v_2 two independent measures of its velocity. If the mean velocity of the group, v′, is known accurately then errors of measurement ξ_1 and ξ_2 can be defined by

$$\xi_1 = v - v_1,$$
$$\xi_2 = v - v_2.$$

The true deviation $x = v' - v$

and the observed deviations

$$x_1 = v' - v_1, \qquad x_2 = v' - v_2.$$

Since $x_1 = v' - v + \xi_1 = x + \xi_1$

$$\sum (x_1 x_2) = \sum (x+\xi_1)(x+\xi_2)$$
$$= \sum x^2 \text{ (since } \xi_1 \text{ and } \xi_2 \text{ are uncorrelated).}$$

If the standard deviation of the observed velocities is σ' and of the true velocities σ_x then

$$\sigma'^2 = \sigma_x^2 + \frac{\sum \xi^2}{N} \tag{2}$$

or

$$\frac{\sum x'^2}{N} = \frac{\sum x^2}{N} + \frac{\sum \xi^2}{N},$$

where x′ is the mean of the measured deviations x_1, x_2.

Thus

$$\frac{\sum \xi^2}{N} = \frac{\sum x'^2}{N} - \frac{\sum (x_1 x_2)}{N}.$$

In a group of fifty-six meteors, with two measures of velocity for each, $\frac{\sum x'^2}{N}$ was 20·1 and $\frac{\sum (x_1 x_2)}{N}$ was 17·5. This represents a measured deviation $\sigma' = 4{\cdot}5$ km./sec. and a true deviation $\sigma_x = 4{\cdot}2$ km./sec. The errors of measurement are then given by (2) as 1·6 km./sec.

In view of the different number of velocity measures in the two methods the discrepancy between the first figure of 1·1 km./sec. and the second figure of 1·6 km./sec. is reasonable, and a final value of 1·4 km./sec. was adopted as the standard deviation in a velocity of 35 km./sec. The value of 2·4 km./sec. estimated from the errors in the zone spacing is therefore too great, and it appears that the zone maxima and minima can be estimated to better than ± 1 pulse.

† Davies, J. G., unpublished (Ph.D. thesis, Manchester, 1952).

For the work on the sporadic distribution it is necessary to find this error for other velocities. If the fractional error in estimating a zone length is constant, the error should be proportional to the velocity. At higher velocities more zones are measured and the error therefore increases less rapidly. Consequently the adopted values of the errors given in Table 70 have been based on the empirical formula $\Delta v \propto \sqrt{v}$, the proportionality being fitted to the point at 35 km./sec.

TABLE 70

Adopted Values of Errors in the Velocity Measurements

v km./sec.	20	30	40	50	60	70
Δv km./sec.	1·06	1·29	1·50	1·67	1·83	1·98

A check on these values at $v = 60$ km./sec. has been applied by using the first method described above on a sample of forty-three sporadic meteors with velocities between 58 and 61 km./sec. measured in 1950 November and December. These yielded 172 independent velocity measurements and gave the standard deviation as 1·3 km./sec. Scaling as above to achieve the mean of the first and second methods gives a value to be adopted of 1·7 km./sec., in agreement with Table 70.

The mean range of the Geminid measurements was 400 km. and the wave-length 8 m. In cases where R and λ differ, the errors have to be adjusted in proportion to $\sqrt{(R\lambda)}$.

These error values were applied to the theoretical distributions calculated as described in the next section, in order to produce the distributions with which the experimental results could be directly compared.

(*d*) *The Theoretical Velocity Distribution*

The theoretical velocity distributions appropriate to the above experimental conditions have been calculated by Clegg.† As a basis for the comparison it was assumed that all sporadic meteors moved in parabolic orbits, and approached the earth from random heliocentric directions. The radiant concentration and velocity are then expressed as functions of the elongation from the apex of the earth's way. The actual velocity distribution observed from such a distribution depends on the directional characteristics of the aerial system. The main features of the calculation will be described in this section.

(i) *Calculation of the radiants and geocentric velocities.* In Fig. 107 a meteor is approaching the earth O from heliocentric direction X at

† Clegg, J. A., *Mon. Not. Roy. Astr. Soc.* **112** (1952), 399.

elongation ϵ_0 from the apex. Its geocentric direction will be Y, and the elongation ϵ will be given by

$$\sin\epsilon = (\Lambda_0 \sin\epsilon_0)(1+\Lambda_0^2+2\Lambda_0\cos\epsilon_0)^{-\frac{1}{2}}, \tag{3}$$

where $\Lambda_0 = \bar{V}/V_E$, $\bar{V}$ being the heliocentric velocity of the meteor and V_E the orbital velocity of the earth. The geocentric velocity of the meteor v can be written as ΛV_E, where

$$\Lambda = (\Lambda_0^2 - 1 + \cos^2\epsilon)^{\frac{1}{2}} + \cos\epsilon. \tag{4}$$

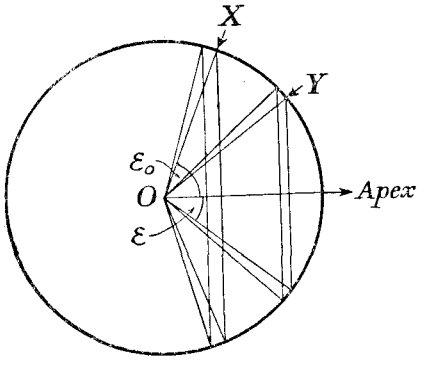

FIG. 107.

If the density of meteors near the earth is $4\pi N$ per km.^{3} then the number approaching per second from heliocentric directions between ϵ_0 and $\epsilon_0 + d\epsilon_0$ will be

$$2\pi N \Lambda V_E \sin\epsilon_0 \, d\epsilon_0$$

and the corresponding geocentric flight directions lie between ϵ and $\epsilon + d\epsilon$, concentrated within a solid angle $2\pi \sin\epsilon \, d\epsilon$.

The number whose radiants lie within a small solid angle $d\Omega$ at elongation ϵ is therefore

$$N_\epsilon \, d\Omega = N\Lambda V_E \, d\Omega \left(\frac{\sin\epsilon_0}{\sin\epsilon}\right) \frac{d\epsilon_0}{d\epsilon},$$

which, using (3) and (4), becomes

$$\frac{N_\epsilon}{N} = \frac{2\Lambda^4 V_E}{\Lambda_0(\Lambda_0^2+\Lambda^2-1)}. \tag{5}$$

These formulae neglect the effect of the earth's gravitational attraction. For the present purpose the modification to (5) can be neglected but the true geocentric velocity v_g from (4) becomes

$$v_g^2 = \Lambda^2 V_E^2 + 2 r_e g, \tag{6}$$

where r_e is the radius of the earth and g the acceleration due to gravity.

In the present case the calculations have been made for meteors moving in parabolic orbits ($\Lambda_0 = \sqrt{2}$). Fig. 108 shows the values of v_g and N_ϵ/N for this case, plotted as functions of ϵ for $V_E = 29{\cdot}8$ km./sec.

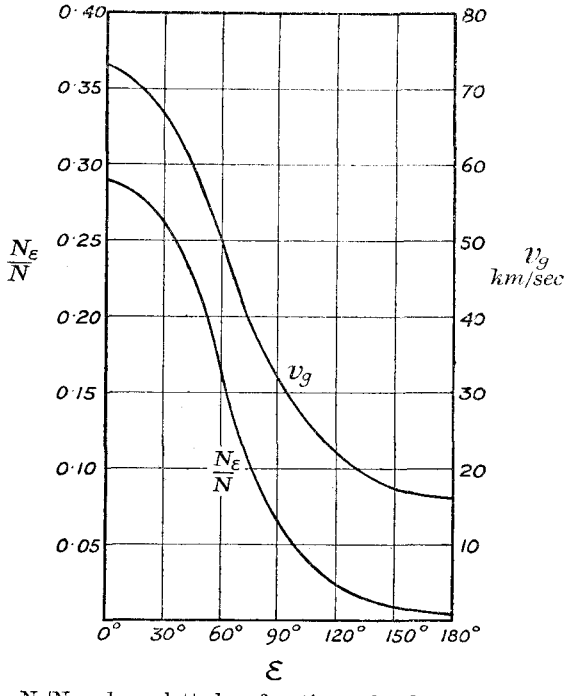

FIG. 108. N_ϵ/N and v_g plotted as functions of ϵ, for meteors approaching the earth from random heliocentric directions, with parabolic velocities.

(ii) *The directional characteristics of the aerial.* The beamed aerial used in the experiments described above is represented in Fig. 109, which shows the celestial sphere drawn for the observing station at O. The cone aOb represents the limits of the main lobe of the aerial beam. Since the reflection from the meteor trails is specular, the apparatus recorded only those meteors whose radiants lay in the strip of sky enclosed by the small circle arcs xzy, x′z′y′, lying symmetrically about the great semi-circle Sz_0N which has X as its pole, where OX is the axis of the aerial beam. The measurements were restricted to the times when either the apex, or antapex, A, was crossing this strip.

To find the relative numbers of meteors of different velocities which enter the aerial coverage, the strip can be divided into a number of elementary segments, in the way indicated by the dotted lines. If these are sufficiently small, the meteors emanating from any one will have the

XVI

THE MAJOR METEOR SHOWERS—IV

THE PERIODIC STREAMS

THE previous three chapters have described the major night-time meteor showers which recur annually with appreciable intensity, and from which the debris must be fairly uniformly distributed around the orbit. At least three remarkable cases are known, however, in which great showers occur periodically and in which the debris must still be localized in a small section of the orbit. Two of these, which are still active—the Giacobinids and Leonids—are described in this chapter. The third—the Bielids—was last observed in 1899, and has since disappeared. It is therefore classed under the lost streams of Chapter XVII. It is also possible that periodic streams may exist amongst the sequence of day-time meteor showers described in Chapter XVIII, but sufficient time has not yet elapsed for the existence of such periodicities to be manifest.

1. The Giacobinid shower

(a) History

By far the most spectacular meteor displays of the present century have been given by the Giacobinid, or Draconid, meteor shower. The last intense shower seen visually was in 1946 October, but in 1952 October an appreciable shower was recorded by radio-echo apparatus during the day-time. The possibility that the debris of the Comet 1900 (III) discovered by Giacobini in December 1900† might give rise to a meteor shower seems to have been first suggested by Davidson‡ in 1915. Davidson investigated the list of comets observed since 1892 and selected those with elliptical orbits. Of these he found only two which passed close to the earth's orbit, one of which, Comet 1900 (III), had a periodic time of 6·5 years. Davidson concluded that, if the debris was spread across the orbit for some 2,000,000 miles, a shower might be expected at the descending node around October 10 with a radiant at α 267°, δ +50°, and that the relative velocity of the meteors should be about 22 km./sec. He referred to a feeble shower observed by Denning between October 4 and 17 at α 270°, δ +46°. Denning§ also mentioned the topic in 1918,

† The comet was found again by Zinner in 1913 November, and is now generally referred to as the Giacobini–Zinner Comet.

‡ Davidson, M., *J. Brit. Astr. Assoc.* **25** (1915), 292.

§ Denning, W. F., *J. Brit. Astr. Assoc.* **28** (1918), 229.

The similarity between these various orbits is emphasized in Fig. 160, where the mean orbit of the Ursids as given in Table 124 is shown with the orbit of the comet. In their presentation of these results in 1950, Hawkins and Miss Almond† had available only the original data from Czechoslovakia, which, as mentioned above, were subsequently shown to be in error by Ceplecha. They were therefore forced to conclude that the orbit of the intense stream observed in 1945 differed from that of the later returns, and that considerable difficulties existed in postulating a common relationship for the two streams and the comet. The corrected data given above remove this difficulty and it now seems certain that the intense 1945 stream was due to a condensation in the orbit of the Ursids, although on the opposite side of the orbit to the comet.

† Hawkins, G. S., and Almond, M. (1950), loc. cit.

observations, and by Hawkins and Miss Almond† for the British visual and radio-echo observations. The elements are compared with those for Periodic Comet Tuttle 1939 k in Table 124.

TABLE 124

Orbital Elements for the Ursid Meteor Stream and for Comet Tuttle 1939 k

Date	1945	1947	1948	1949	
Source	Ceplecha	Hawkins and Miss Almond			*Periodic Comet Tuttle* 1939 k
		Mean of radio-echo and visual	*Radio-echo*	*Radio-echo*	
Radiant α	217·1°	199·3±8	206·8±10	207·1±8	..
Radiant δ	+75·81°	+76·5±5	+82·8±8	77·6±3	..
☊	270·66°±05	270·5	269·4	270·2	269·8
Δ☊ Shower limits	..	..	−1·0	−0·5	..
	..	..	+1·2	+1·1	..
ω	205·85°±·03	213±4	212±5	210±3	207
i	53·57°±·08	57±6	50±9	56±3	55
q (a.u.)	0·93887±0·00011	0·91±·02	0·91±·02	0·92±·01	1·02

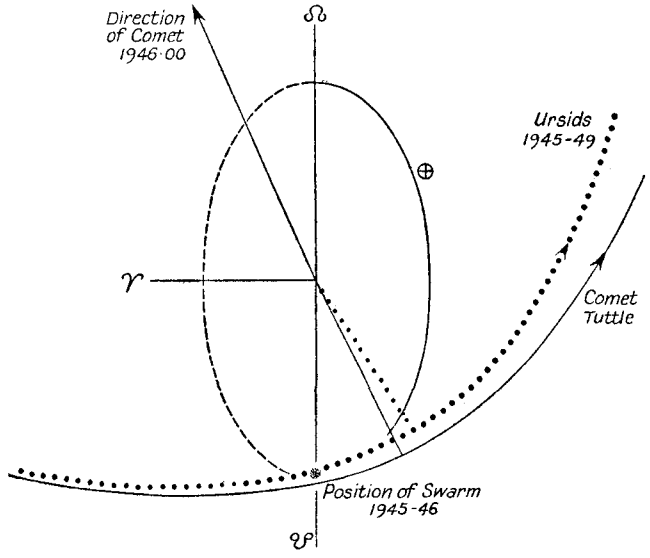

FIG. 160. The mean orbit of the December Ursids as plotted from the data of 1945–9, compared with the orbit of Comet Tuttle 1939 k. The orbit of the comet has been drawn in the plane of the paper, and the orbits of the earth and the meteor streams have been projected on to it.

All radiant positions have been corrected for zenithal attraction and diurnal aberration, and reduced to the common equinox of 1950.

† Hawkins, G. S., and Almond, M. (1950), loc. cit.

(*d*) *Velocities*

There are no published records of visual or photographic determinations of the velocities of meteors in the Ursid stream. Attempts to measure the velocities by the radio-echo technique have been made in each year, but owing to the low hourly rate only partial success has been

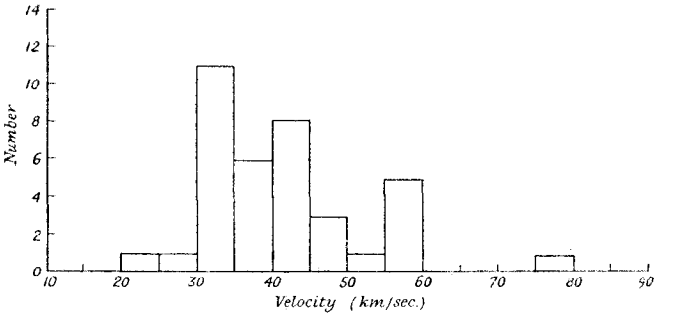

FIG. 159. Distribution of velocities measured during the epoch of the 1951 Ursids.

achieved. The velocities of three possible Ursid meteors were measured in 1948 as follows:†

1948 Dec. 21d. 19h. 20m. 52s. $39{\cdot}5 \pm 4{\cdot}8$ km./sec.;
1948 Dec. 22d. 06h. 01m. 31s. $34{\cdot}6 \pm 2{\cdot}0$ km./sec.;
1948 Dec. 22d. 08h. 50m. 15s. $38{\cdot}7 \pm 1{\cdot}6$ km./sec.;

giving a weighted mean of $37{\cdot}4 \pm 1{\cdot}3$ km./sec. No further success was achieved in 1949 or 1950, but in 1951 a larger scale effort was made using two equipments simultaneously. Over the period of the Ursid stream thirty-six velocities were measured with a distribution shown in the histogram of Fig. 159. The wide spread in this distribution indicates well the difficulties of measurement where the hourly rate is only a little in excess of the sporadic background rate. It was unfortunate that on this occasion the maximum hourly rate of the Ursid stream was only thirteen, which is considerably lower than in the previous years.

(*e*) *Orbit*

So far the velocity measurements are not precise enough to justify any orbital calculations other than on the assumption that the meteors are moving with the parabolic velocity. The appropriate orbital elements for this case have been calculated by Ceplecha,‡ for the Skalnaté Pleso

† Clegg, J. A., Lovell, A. C. B., and Prentice, J. P. M. (1949), loc. cit.
‡ Ceplecha, Z. (1951), loc. cit.

in the visual and photographic positions. The correct position of the 1945 radiant is therefore the one given by Ceplecha and not the original position quoted by Bečvář. Radiant positions from visual observations have also been obtained by Bochníček† and by Vanýsek‡ in 1946, and by Prentice§ in 1947. These are listed in Table 123 together with the radio-echo determinations of the radiant coordinates. The low hourly rate and high declination make determination of the radiant coordinates difficult by the radio-echo technique, and the limits of error quoted in Table 123 are therefore large.

TABLE 123

Radiant Positions of the Ursid Meteor Stream

Source	*Technique*	*Date*	*Radiant* α	*Radiant* δ	*Whether corrected for diurnal aberration and zenithal attraction*
Ceplecha‖	Photographic	1945 Dec. 22·773	217° 05′±4′	+75° 51′±3′	Yes
Bochníček†, ††	Visual	1946 Dec. 22·9	213°±4°	+75°±1°	Yes
Vanýsek‡	Visual	1946 Dec. 22·9	217·8°±0·8°	+76·7°±1°	Yes
Prentice§	Visual	1947 Dec. 23·15	207°	+74°	No
Clegg, Hughes, and Lovell‡‡	Radio-echo	1947 Dec. 22·23	195°±8°	+78°±5°	No
Clegg, Lovell, and Prentice§§	Radio-echo	1948 Dec. 20·23	210°±10°	+82°±8°	No
Hawkins and Miss Almond‖‖	Radio-echo	1949 Dec. 22	207·1°±8°	+77·6°±3°	Yes
Hawkins and Miss Almond†††	Radio-echo	1950 Dec. 22	199°±8°	+77°±3°	No
Jodrell Bank (unpublished)	Radio-echo	1951 Dec. 23	≏ 200°	≏ +77°	No
	Radio-echo	1952 Dec. 22	Rate too low for accurate determination		
	Radio-echo	1953 Dec. 23			

Considering the limits of error of the radio-echo determinations, the agreement amongst these observations is satisfactory. The most serious discrepancy occurs in the declination measurement for 1948, but Hawkins and Miss Almond‖‖ have pointed out that this need not be considered significant since there was a gap in the observations at the critical period of the shower which probably gave rise to a false value for $\odot_{max}$ and may have interfered with the coordinate measurements.

† Bochníček, Z., *Bull. Cent. Astr. Inst. Czech.* **1** (1948), 26.
‡ Vanýsek, V., ibid. **1** (1947), 10.
§ Prentice, J. P. M. (1948), loc. cit.
‖ Ceplecha, Z. (1951), loc. cit.
†† Unfortunately, in the original announcement of the 1946 results Bečvář (*I.A.U. Circ.* 1078) quoted the right ascension as 203° instead of 213°.
‡‡ Clegg, J. A., Hughes, V. A., and Lovell, A. C. B. (1948), loc. cit.
§§ Clegg, J. A., Lovell, A. C. B., and Prentice, J. P. M. (1949), loc. cit.
‖‖ Hawkins, G. S., and Almond, M. (1950), loc. cit.
††† Hawkins, G. S., and Almond, M. (1952), loc. cit.

activity for the radio-echo observations of 1949 December.† In this case the stream was active for 34 hours between ⊙ 269·5° and 271·3° with a maximum at ⊙ = 270·2°. The results for the year 1947, 1948, 1950, 1951, and 1952 are very similar.

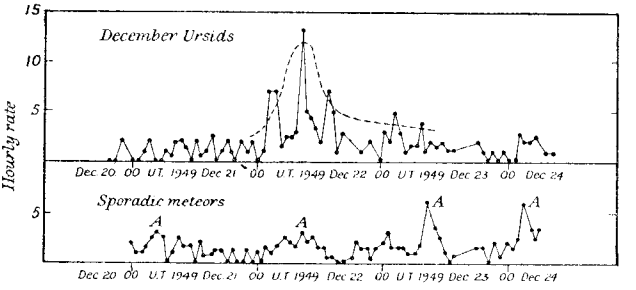
15
10
5
Hourly rate
December Ursids
Dec 20 00 U.T. 1949 Dec 21 00 U.T. 1949 Dec 22 00 U.T. 1949 Dec 23 00 Dec 24
5
Sporadic meteors
A
A
A
A
Dec 20 00 U.T. 1949 Dec 21 00 U.T. 1949 Dec 22 00 U.T. 1949 Dec 23 00 Dec 24

FIG. 158. The activity of the December Ursids as recorded by the radio-echo technique in 1949. The broken line is the smoothed hourly rate. The lower curve shows the hourly rate of sporadic meteors (those with range-time plots outside the theoretical envelope). *A* marks the influence of the apex component.

(*c*) *Radiant*

The radiant position quoted by Bečvář in his original announcement was α 233°, δ +82·6°. This position was markedly different from all subsequent visual and radio-echo determinations, and Ceplecha‡ has recently investigated the original data. During the progress of the shower, three meteors were recorded photographically and Ceplecha's reduction of these gives the following coordinates

α (1946)	δ (1946)
216° 53′	75° 48′
217° 12′	75° 55′
219° 27′	75° 16′

The weighted mean, corrected for diurnal aberration and zenithal attraction, is

$$\alpha\ (1950) = 217^\circ\ 05' \pm 4';\ \delta\ (1950) = +75^\circ\ 51' \pm 3'$$

on 1945 December 22·773 ± 0·051 U.T.

This differs widely from the position given by Bečvář which was obtained from sixteen meteors plotted by Dzubák. Fortunately, two of these plotted meteors were also photographed, and it became evident that the systematic errors in the visual data fully accounted for the difference

† Hawkins, G. S., and Almond, M. (1950), loc. cit.
‡ Ceplecha, Z. (1951), loc. cit.

TABLE 121

Hourly Rates of the Bečvář Meteor Stream, 1945 December 22

Time U.T.	*Hourly rate*	*Time U.T.*	*Hourly rate*
16h. 50m.	36	17h. 40m.	26
17 00	20	17 50	55
17 10	69	18 00	108
17 20	34	18 10	38
17 30	14	18 20	101

TABLE 122

Hourly Rate of the Ursid Stream subsequent to 1945

Source	*Technique*	*Time of maximum*	⊙ *at max.*	*Maximum hourly rate*
Bečvář† and Ceplecha‡	Visual	1946 Dec. 22	270° 52′	11
Prentice§ . .	Visual	1947 Dec.	270° 30′	20
Clegg, Hughes, and Lovell‖ . .	Radio-echo	1947 Dec. 22	270° 0′	15
Clegg, Lovell, and Prentice†† . .	Radio-echo	1948 Dec. 21d. 08h.	269° 23′	15
Hawkins and Almond‡‡ . .	Radio-echo	1949 Dec. 22d. 07h. 20m.	270° 12′	13
Hawkins and Almond§§ . .	Radio-echo	1950 Dec. 22	269° 48′	20
Jodrell Bank, unpublished	Radio-echo	1951 Dec. 23	270° 30′	13
	Radio-echo	1952 Dec. 22	270° 24′	9
	Radio-echo	1953 Dec. 23	271°	11

Bečvář|||| originally reported the stream to be of short duration, 4 hours only, but in the recent analysis Ceplecha‡ makes it clear that this short duration was determined by twilight on the one hand and moon and clouds after 18h. 20m. on 1945 December 22 on the other, and that the duration of the stream was probably much greater than 4 hours. The radio-echo observations in the years 1947 to 1953 have shown that the duration of the Ursid stream is, in fact, some 30 to 40 hours. A typical example of the trend of the activity of the stream is given in Fig. 158, this being the plot of the hourly rates of the stream and of the accompanying sporadic

† Bečvář, A. (1947), loc. cit.
‡ Ceplecha, Z., *Bull. Cent. Astr. Inst. Czech.* **11** (1951), 156.
§ Prentice, J. P. M. (1948), loc. cit.
‖ Clegg, J. A., Hughes, V. A., and Lovell, A. C. B. (1948), loc. cit.
†† Clegg, J. A., Lovell, A. C. B., and Prentice, J. P. M., *J. Brit. Astr. Assoc.* **60** (1949), 27.
‡‡ Hawkins, G. S., and Almond, M., ibid. **60** (1950), 251.
§§ Hawkins, G. S., and Almond, M., *Mon. Not. Roy. Astr. Soc.* **112** (1952), 219.
|||| Bečvář, A. (1946), loc. cit.

has a period of 3·3 years, or twice the mean period of these Geminid orbits. This topic will be discussed again in Chapter XXI, but there is no certain solution of the possible origin of such short-period meteor orbits.

4. The December Ursids (Bečvář's stream)

(*a*) *History*

At 16h. 30m. U.T. on the afternoon of 1945 December 22, one of the observers at the Skalnaté Pleso observatory in Czechoslovakia noticed a very high meteor frequency, and observation in the succeeding hours showed that an unexpected meteoric display was taking place. The event was reported by Bečvář,† who placed the radiant in Ursa Minor and gave the hourly rate as 169. Bečvář‡ again reported the return of the shower on 1946 December 22, but this time gave the hourly rate as 11. This shower was seen visually in England by Prentice§ in 1947 and was also located by the radio-echo technique.‖ Since that time the shower has been studied systematically by the radio-echo technique, but the hourly rate has never exceeded 15 to 20. In retrospect it appears possible that this is the same minor stream established by Denning†† from his observations between 1890 and 1910, and that the spectacular stream observed by Bečvář in 1945 may represent a condensation in the orbit or be related to it in some other manner.

(*b*) *Activity*

Bečvář† originally gave the hourly rate of the stream on the night of its discovery in 1945 as 169; but in a more recent analysis of the original data Ceplecha‡‡ states that this was the total frequency seen by four observers.§§ The true zenithal rates given by Ceplecha, as the mean of three observers, are listed in Table 121 for the period 16h. 50m., just after it was first observed, to 18h. 20m., when clouds and the moon stopped the observations. The mean rate over the 100 minutes of observation was 48 per hour.

As mentioned above, this high rate has not been encountered in subsequent years, the data for which are given in Table 122, the hourly rate being the maximum observed in all cases.

† Bečvář, A., *I.A.U. Circular*, no. 1026, Jan. 24, 1946.
‡ Bečvář, A., ibid., no. 1078, Feb. 4, 1947.
§ Prentice, J. P. M., *J. Brit. Astr. Assoc.* **58** (1948), 140.
‖ Clegg, J. A., Hughes, V. A., and Lovell, A. C. B., ibid., p. 134.
†† Denning, W. F., *Brit. Astr. Assoc. Observer's Handbook* (1922), p. 15.
‡‡ Ceplecha, Z., *Bull. Cent. Astr. Inst. Czech.* **11** (1951), 156.
§§ It should, perhaps, be mentioned that Bečvář, having been deposed from office, has had no opportunity of replying to these and other criticisms of his observations.

together with the mean radio-echo orbit computed by Hawkins and Miss Almond. It is evident from Table 120 and from Figs. 156, 157, that

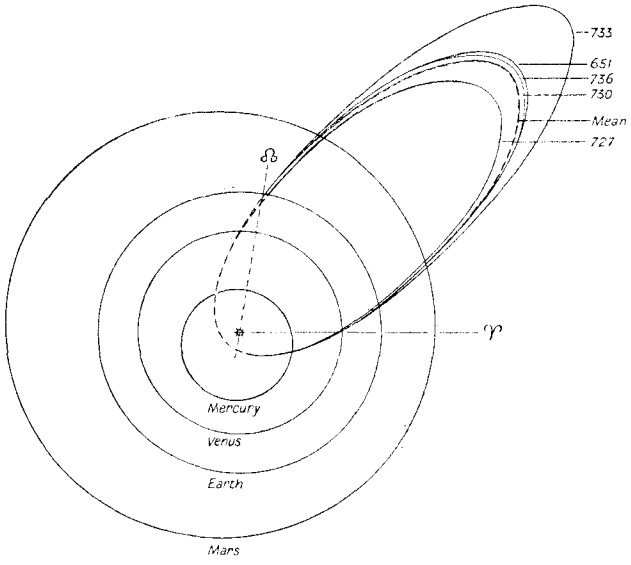

FIG. 156. Projection on the ecliptic of the Geminid orbits determined by the photographic technique. The notation corresponds to Table 120.

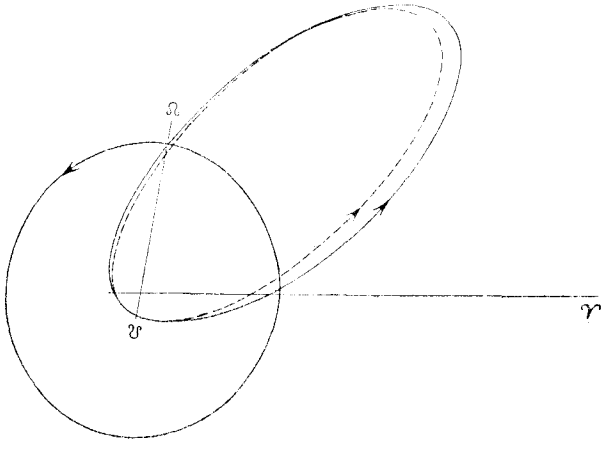

FIG. 157. The orbits of Geminid meteors projected on to the plane of the ecliptic. —— Mean orbit computed from the radio-echo observations. – – – Mean orbit given by Whipple from the photographic observations.

very close agreement exists between the photographic and radio-echo orbits. These orbits are unique compared with the orbits of known comets, planets, or asteroids. The shortest-period comet known (Encke's)

for diurnal motion, zenith attraction, and deceleration gave the corrected geocentric velocity $v_g = 34{\cdot}2$ km./sec., compared with the 34·72 km./sec. of Whipple's photographic measurements.

Taking into consideration the different mass groups covered by the various techniques, it is evident that the three determinations of the velocity of the Geminid meteors are in excellent agreement.

(*e*) *Orbit*

In 1931 Maltzev† speculated on the orbit of the Geminids. Although handicapped by lack of knowledge of the precise velocities, he brought forward arguments in support of the view that the orbit must be elliptical, an opinion which has been confirmed by recent work. The surprising nature of the ellipticity of the Geminid orbit was not revealed until the publication of Whipple's photographic measurements in 1947.‡ His results on the radiants and velocities of five doubly photographed meteors have been quoted above, and Table 120 gives the corresponding orbital data. Hawkins and Miss Almond§ have also computed a mean orbit from the radio-echo data, and these elements are included in Table 120 for comparison.

TABLE 120

Orbital Elements for the Geminid Meteors

Meteors	*Date*	Ω (1900·0)	ω	*Mean anomaly*	i	a	q	e	P
		° ′	° ′	° ′	° ′	*a.u.*	*a.u.*		*years*
Harvard No. 727	1937 Dec. 12·3774	259 25	325 01	−24 57	23 04	1·302	0·1398	0·893	1·49
Harvard No. 730	1937 Dec. 13·3256	260 22	324 44	−21 58	24 27	1·399	0·1360	0·903	1·66
Harvard No. 733	1937 Dec. 13·4254	260 29	324 25	−16 04	27 26	1·678	0·1270	0·924	2·17
Harvard No. 736	1937 Dec. 14·3796	261 27	323 28	−21 17	23 00	1·434	0·1434	0·900	1·72
Harvard No. 651	1936 Dec. 14·3077	261 37	324 04	−20 34	23 20	1·457	0·1380	0·905	1·76
Mean (omitting No. 733)	Dec. 13·6	260 43	324 19	−22 12	23 28	1·396	0·1393	0·900	1·65
Mean radio echo uncorrected	1948 Dec.	261·1 ± 0·5	325 ± 2	..	23 ± 3	1·31 ± ·04	0·14 ± ·02	0·89 ± ·01	1·50
Mean radio echo corrected for deceleration	1948 Dec.	261·1	325	..	23	1·4	0·14	0·89	1·66

The orbits of the photographic meteors are drawn in Fig. 156 projected on to the plane of the ecliptic. Fig. 157 shows Whipple's mean orbit,

† Maltzov, V. A., *Russ. Astr. J.* **8** (1931), 67.
‡ Whipple, F. L. (1947), loc. cit.
§ Hawkins, G. S., and Almond, M., loc. cit.

details for five have been given by Whipple† and values for the apparent relative velocity for three others by Jacchia,‡ as listed in Table 119.

Omitting no. 733 for which the determinations of all elements showed appreciable divergence, Whipple gives mean values for nos. 727, 730, 736, 651 as follows:

$$\text{Dec. } 13{\cdot}6 \begin{cases} v = 35{\cdot}95 \text{ km./sec.} \\ V = 36{\cdot}34 \quad ,, \\ v_g = 34{\cdot}72 \quad ,, \\ \bar{V} = 34{\cdot}14 \quad ,, \end{cases}$$

Measurements of the Geminid velocities by the radio-echo technique have been made in Great Britain and Canada. Preliminary British measurements, using the pulse diffraction technique§ in 1948 have been described by Ellyett and Davies.‖ More comprehensive measurements were made in 1949, when 122 velocities were obtained between December 9 and 15. These have been described in Chapter XII. Fig. 106 shows the histogram of the results, and the discussion on pp. 218, 219 showed that there must be a true spread in the Geminid velocities. A further 149 velocities measured in 1951 December gave similar results.††

An attempt to estimate the actual spread in heliocentric velocities was made by Hawkins and Miss Almond‡‡ using the same treatment as for the Quadrantids and Perseids. They combined the 1948 and 1949 measurements, and, with the same notation, found

$$\sigma_E = 1{\cdot}2 \text{ km./sec.}, \quad \sigma_S = 3{\cdot}5 \text{ km./sec.}, \quad \sigma_K = 1{\cdot}5 \text{ km./sec.},$$

$\sigma_A = 0{\cdot}3$ km./sec., $\sigma_0 = 4{\cdot}6$ km./sec., and hence $\sigma_H = 2{\cdot}3$ km./sec. This spread is considerably greater than the equivalent standard deviation of 0·23 km./sec. found in the photographic measurements. The reason for the difference is not known, but is presumably introduced because of the wide difference in range of mass groups covered by the photographic and radio techniques.

The Canadian measurements§§ were made by using the continuous-wave diffraction technique and non-directional aerial systems. The results, and McKinley's method of analysis, have been described in Chapter XII in connexion with the distribution of sporadic velocities. The mean apparent observed velocity was 35·25 km./sec. Corrections

† Whipple, F. L. (1947), loc. cit.

‡ Jacchia, L. G., *Tech. Rep. Harv. Coll. Obs.* (1948), no. 2 (Harvard Reprint Series, II–26).

§ See Chap. IV.

‖ Ellyett, C. D., and Davies, J. G., *Nature*, **161** (1948), 596.

†† Jodrell Bank, unpublished.

‡‡ Hawkins, G. S., and Almond, M., loc. cit.

§§ McKinley, D. W. R., *Astrophys. J.* **113** (1951), 225.

The significance of the much greater spread found in the radio-echo and visual work is not yet apparent. It may well be connected with the differing samples of mass groups observed in the various techniques.

(*d*) *Velocities*

Geminid velocities are not represented in the collection of British meteor data presented by Porter.† Maltzev‡ lists nine Geminids observed by Denning between 1892 and 1915 and three observed by Olivier in 1923; but in view of the subsequent precision photographic and radio-echo measurements no purpose would be served in discussing these visual observations.

TABLE 119

Photographic Determinations of the Velocities of Geminid Meteors

WHIPPLE§

Harvard meteor number	727	730	733	736	651
Date	1937 Dec. 12·3774	1937 Dec. 13·3256	1937 Dec. 13·4254	1937 Dec. 14·3796	1936 Dec. 14·3077
v Apparent relative velocity (km./sec.)	35·21	35·96	38·26	36·05	36·56
V No atmosphere velocity (km./sec.)	35·62	36·62	38·44	36·31	36·81
v_g Geocentric velocity (km./sec.)	34·01	34·97	37·04	34·74	35·14
$\bar{V}$ Heliocentric velocity (km./sec.)	33·46	34·16	35·67	34·39	34·53

§ Whipple, F. L. (1947), loc. cit.

JACCHIA‖

Harvard meteor number	1112	1265	1539
Date	1941 Dec. 11·27	1944 Dec. 14·22	1947 Dec. 14·20
v Apparent relative velocity (km./sec.)	36·64	35·95	35·66 / 35·53 ††

‖ Jacchia, L. G., *Tech. Rep. Harv. Coll. Obs.* (1948), no. 2 (Harvard Reprint Series II–26).

†† Corresponding to two heights of the trail, 67·3 and 65·4 km. respectively.

Eight values for the velocity of Geminid meteors determined by the double-camera photographic technique have been published. Complete

† Porter, J. G., *Mon. Not. Roy. Astr. Soc.* **103** (1943), 134; **104** (1944), 257.

‡ Maltzev, V. A., loc. cit.

magnetic effects are inadequate to produce finite deviations over intervals of less than hundreds of thousands of years on meteors with diameters of a centimetre.

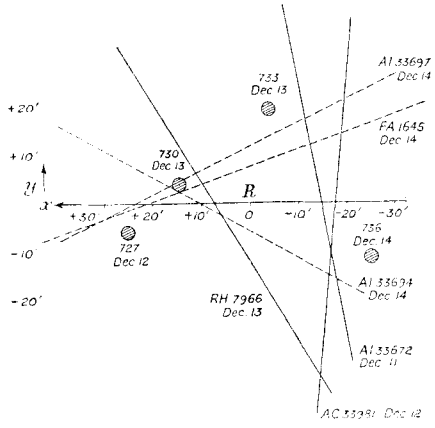

FIG. 154. Extended corrected trails and double-station radiants of photographic Geminids recorded in 1937.
(The notation is the Harvard plate numbering.)
R = mean calculated radiant.
⎓ = extended single trails. ⊘ = double-station meteor radiants.

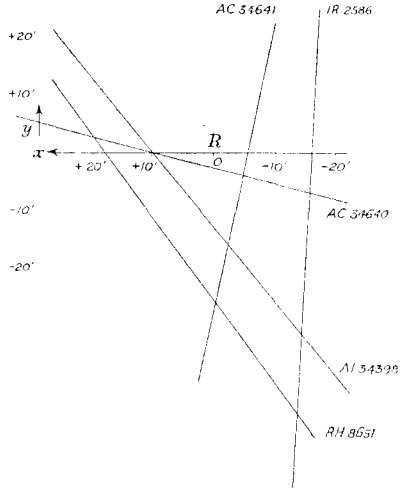

FIG. 155. The single-station trails of Geminids photographed on 1938 Dec. 14.
(The notation is the Harvard plate numbering.)

There are, however, surprising discrepancies in the measurements of the radiant diameter given by the three techniques. The radio observations indicate a radiant diameter not greater than 4°; the visual observations indicate a diameter of about 12° with a concentration in a region $4° \times 3°$ around the mean position.† From a detailed investigation of the photographic trails Whipple‡ found the random probable error of the radiant point of a Geminid to be $\pm 21'$. In view of the importance of ascertaining whether this represented a true cosmic spread in the spatial motions of the Geminid meteors as they approached the earth, Whipple investigated four other possible causes:

(i) Measuring error, which was found to contribute $\pm 2'$ at most to the spread.

(ii) Errors in zenith correction arising from uncertain radiant and time of apparition. These are unlikely to introduce errors of more than 3′ (corresponding to a degree error in the radiant position) or $\pm 8'$ due to uncertain time of apparition.

(iii) Deviations from linear motion in the atmosphere. A deviation of 20′ perpendicular to the trail would correspond to 60 microns per centimetre departure from linearity on the plate, whereas the average departure is only a few microns.

(iv) Spread in radiant arising from the combination of observations made in different years or nights. In this case the meteors observed in one night or in one year should show a smaller deviation from the mean radiant than $\pm 21'$. Fig. 154 shows the extended corrected trails of single-station Geminids and the radiants of double-station Geminids photographed in 1937, while Fig. 155 shows the single-station trails of 1938 December 14. It is evident from these figures that the Geminid meteors of a single year show random deviations of the same order as those observed in different years.

The conclusion from Whipple's investigation is that an actual cosmic spread of the order of $\pm 20'$ does exist in the Geminid meteors. As an explanation Whipple favours the idea that such a spread arises because of planetary perturbations. These introduce random effects because of the differing positions, and subsequently the differing orbital paths of the individual particles. Whipple makes the further interesting point that a full theory would provide some measure of the age of the Geminid stream. For example, effects due to light pressure§ and related electro-

† Prentice, J. P. M., private communication.

‡ Whipple, F. L. (1947), loc. cit.

§ See Chap. XX.

TABLE 116

Whipple's Determination of the Daily Motion of the Geminid Radiant from Thirty-six Single and Five Doubly Photographed Trails

	Apparent radiant		*Corrected radiant*	
Year and equinox .	1900·0	1945·0	1900·0	1945·0
Mean solar longitude .	260·34	260·97	260·34	260·97
Mean date U.T. (Dec.)	12·31 d.*	13·35 d.	12·31 d.*	13·35 d.
Mean α . . .	111° 54′	112° 38′	110° 27′	112° 11′
Mean δ . . .	+32° 56′	+32° 50′	+32° 30′	+32° 25′
Δα per day . .	+63′	+63′	+63′	+63′
Δδ per day . .	+3′	+3′	−4′	−4′
Total motion per day .	53′	53′	53′	53′

* G.M.T.

The radio-echo observations summarized by Hawkins and Miss Almond† are also in good agreement with the visual and photographic data. The data for the 1949†, 1950,† 1951,‡ and 1952‡ observations are given in Table 117.

TABLE 117

Radio-echo Observations of the Geminid Radiant Position

	1949			1950			1951			1952		
Date	*Solar longitude* ⊙	*Radiant* α	δ	*Solar longitude* ⊙	*Radiant* α	δ	*Solar longitude* ⊙	*Radiant* α	δ	*Solar longitude* ⊙	*Radiant* α	δ
	deg.	*deg.*	*deg.*	*deg.*	*deg.*	*deg.*	*deg.*	*deg.*	*deg.*	*deg.*	*deg.*	*deg.*
Dec. 7	..	..	..	254·4	107	+37	..	..	..	..	..	..
8	255·7	108	+33	255·4	101	31	..	..	..	..	..	..
9	256·7	108	36	256·4	108	30	256·2	110	36	256·9	110	32
10	257·7	110	36	257·4	108	32	257·2	112	36	257·9	111	33
11	258·8	110	30	258·5	111	32	..	..	..	259·0	112	31
12	259·8	111	32	259·5	112	32	259·2	111	31	260·0	113	31
13	260·8	112	30	260·5	113	30	260·2	113	31	261·0	114	32
14	261·8	115	33	261·5	115	31	261·3	116	36	262·0	116	32
15	262·8	114	34	..	..	..	262·3	114	29	..	..	..

The daily movement of the radiant point as determined by the visual, photographic, and radio studies is in close agreement, as indicated in Table 118.

TABLE 118

Daily Motion of the Geminid Radiant

	α	δ
Radio echo†	+1·3° ± 0·1°	−0·3° ± 0·1°
Photographic§	+1·05°	−0·66°
Visual (King)‖	+1·2°	−0·1°
(Maltzev)††	+1·0°	−0·1°

† Hawkins, G. S., and Almond, M., loc. cit.
‡ Jodrell Bank unpublished.
‖ King, A., loc. cit.
§ Whipple, F. L. (1947), loc. cit.
†† Maltzev, V. A., loc. cit.

TABLE 114

Ephemeris of the Geminid Radiant compiled by King in 1926 *and by Maltzev in* 1931 *from Visual Observations*

Date (*epoch* 1928)	*King*		*Maltzev*		*Date* (*epoch* 1928)	*King*		*Maltzev*	
	α	δ	α	δ		α	δ	α	δ
	deg.	*deg.*	*deg.*	*deg.*		*deg.*	*deg.*	*deg.*	*deg.*
Nov. 25	91·3	+33·8	94·1	+33·4	Dec. 7	106·4	+33·0	106·7	+32·6
26	92·5	33·7	95·2	33·4	8	107·7	32·9	107·8	32·6
27	93·8	33·7	96·2	33·3	9	108·9	32·8	108·8	32·5
28	95·1	33·6	97·3	33·2	10	110·1	32·7	109·9	32·4
29	96·4	33·6	98·3	33·1	11	111·3	32·6	110·9	32·4
30	97·7	33·5	99·4	33·0	12	112·5	32·5	111·9	32·3
Dec. 1	98·9	33·5	100·4	33·0	13	113·7	32·3	112·9	32·3
2	100·2	33·4	101·5	33·0	14	114·9	32·1	114·0	32·2
3	101·4	33·4	102·5	32·9	15	116·1	31·9	115·0	32·1
4	102·7	33·3	103·6	32·8	16	117·2	31·7	116·1	32·1
5	104·0	33·2	104·6	32·8	17	118·3	31·5	117·1	32·0
6	105·2	33·1	105·7	32·7					

Subsequent visual observations by Hoffmeister† and by British‡ and American§ observers have shown general agreement with the positions given in Table 114.

Whipple‖ has carried out a precise investigation of the Geminid radiant from the collected Harvard photographic data. Five double-station photographs obtained in 1936 and 1937 yielded the individual radiant data listed in Table 115. An additional thirty-six single trails photographed between 1903 and 1945 were used, after the application of special corrections, to give the mean radiant and daily motion listed in Table 116. These results are in close accord with the visual data referred to above.

TABLE 115

Whipple's Photographic Determinations of the Geminid Radiant from Five Doubly Photographed Trails

Meteor no.	*Date*	*Apparent radiant* α (1900)	δ (1900)	*Corrected radiant* α (1900)	δ (1900)
727	1937 Dec. 12·3774	112° 12′	+33° 00′	110° 56′	+32° 29′
730	1937 Dec. 13·3256	112° 41′	+32° 53′	111° 46′	+32° 33′
733	1937 Dec. 13·4254	112° 49′	+33° 28′	111° 29′	+32° 49′
736	1937 Dec. 14·3796	113° 16′	+32° 47′	112° 00′	+32° 15′
651	1936 Dec. 14·3077	113° 15′	+32° 20′	112° 26′	+32° 02′

† Hoffmeister, C., *Meteorströme* (Weimar, 1948).
‡ *Mem. Brit. Astr. Assoc.* **32** (1936).
§ Olivier, C. P., *Publ. McCormick Obs.* **5** (pt. i), 1929.
‖ Whipple, F. L., *Proc. Amer. Phil. Soc.* **91** (1947), 189.

TABLE 113

Activity of the Geminid Meteor Shower as observed by the Radio-echo Technique

Longitude of sun at maximum ⊙	*Date of maximum*	*Hourly rate at maximum*
deg.		
261·4	1946 Dec. 14	53
261·3	1947 Dec. 14	57
261·1	1948 Dec. 13	56
260·8–261·8	1949 Dec. 13–14	81
260·5	1950 Dec. 13	79
261·3	1951 Dec. 14	75
260·0	1952 Dec. 12	72
260·7	1053 Dec. 13	71

in sensitivity of the apparatus is plotted in Fig. 153 (*a*), while 153 (*b*) summarizes all the uncorrected information for the years 1946–50 inclusive. It seems evident from these data that the shower may be considered to have an almost constant activity from year to year. Also it appears that the stream density is asymmetrical about the maximum, the Earth encountering less debris after maximum than before. There is some indication that this asymmetry does not extend throughout all mass groups. For example, in Fig. 153 (*c*) the hourly rate curves for long-duration and short-duration echoes are compared. It is known that the long-duration echoes are associated with larger meteors than the short-duration echoes,† and hence it seems that the smaller meteors in the Geminid stream may be distributed fairly symmetrically around ⊙ = 259°.

(*c*) *Radiant*

The general catalogue of Denning‡ contains many determinations of the Geminid radiant. In 1923§ Denning stated that he first obtained convincing evidence of the motion of the radiant in 1885. The summary of the radiant ephemeris given by Denning in 1923 agrees closely with the mean ephemeris computed by King‖ in 1926 for the visual observations which were then available. However, Maltzev†† criticized the ephemeris given by King on the grounds that his treatment of the basic data was inadequate. The two ephemerides, both deduced from the same observational data, are given in Table 114.

† Greenhow, J. S., and Hawkins, G. S., *Nature*, **170** (1952), 355.
‡ Denning, W. F., *Mem. Roy. Astr. Soc.* (1899), loc. cit.
§ Denning, W. F., *Mon. Not. Roy. Astr. Soc.* **84** (1923), 46.
‖ King, A., ibid. **86** (1926), 638.
†† Maltzev, V. A., *Russ. Astr. J.* **8** (1931), 67.

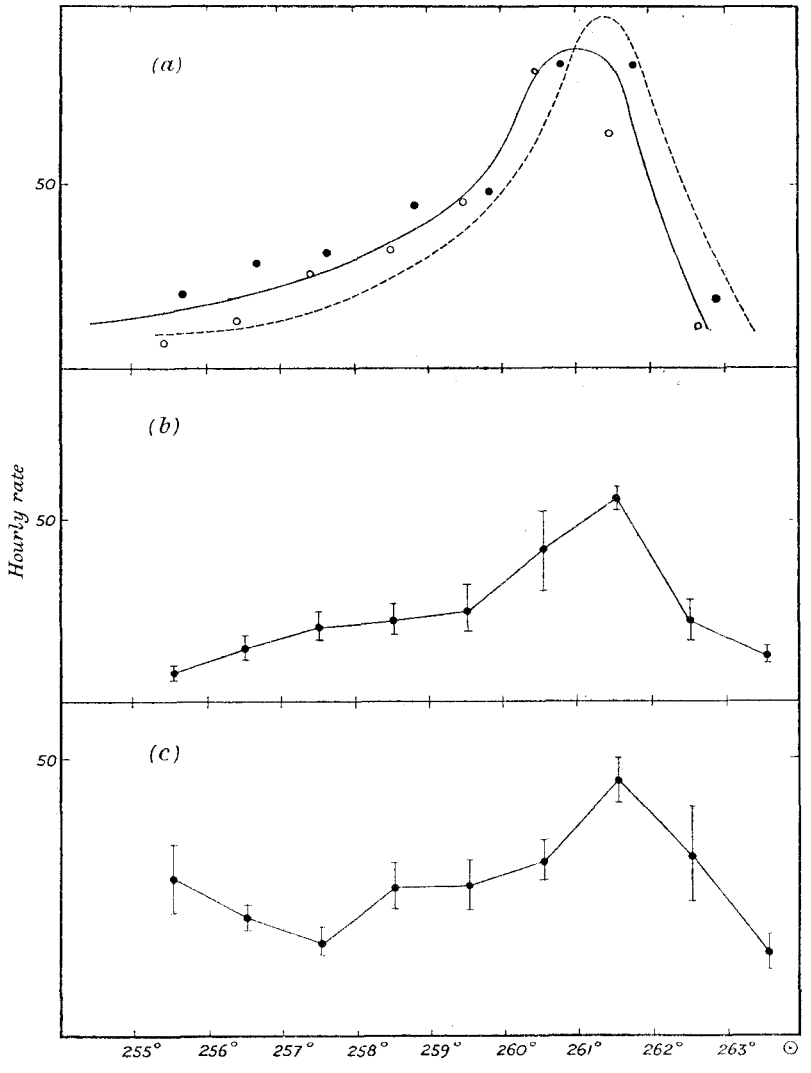

FIG. 153. (*a*) Hourly rate of the Geminid stream plotted against sun's longitude.

● 1949 } Radio-echo observations corrected for variations in sensitivity of
○ 1950 } equipment.
– – – – – Visual observations (Hoffmeister).

(*b*) Hourly rate of the Geminid stream plotted against sun's longitude, according to the radio-echo observations 1946–50 (uncorrected for sensitivity variations).

(*c*) *Percentage* of radio echoes from the Geminid meteors with durations exceeding 1 second plotted against sun's longitude.

connexion. There is, however, a major difficulty in that the plane of the meteor orbits and of the orbit of Encke's Comet differ by 10° or 15°. Whipple† has investigated this discrepancy in considerable detail. He has shown that the differing inclinations can be explained by the perturbing effect of Jupiter, and that a common origin for the meteors and the comet is highly probable. This topic will be considered more fully in Chapter XXI.

3. The Geminid shower

(*a*) *History*

The Geminid meteor shower, which reaches a maximum on December 13–14, provides one of the richest and most reliable meteor displays of the year. There do not appear to be any records of this shower in antiquity; in fact, according to King‡ the existence of the shower was first recognized in England by R. P. Greg in 1862 and in the United States by Marsh and Twining in the same year. Denning's§ general catalogue certainly includes many records of Geminid meteors going back to 1862, and he claims‖ to have established the movement of the radiant point in 1877. In more recent years Whipple's†† photographic meteor studies revealed the surprising fact that the orbit of the stream was one of unusually short period.

(*b*) *Activity*

Few systematic visual data of the activity of the Geminid stream are available—presumably due to the generally unfavourable sky conditions prevailing in December. The various records of the British visual observers‡‡ indicate that at least during the present century the shower has yielded a fairly constant hourly rate lying between 20 and 60 at maximum. A visual-rate curve deduced from information supplied by Hoffmeister§§ is shown in Fig. 153 (*a*). Since 1946 the shower has been observed systematically, using the radio-echo technique. The hourly rates at maximum for the various years are given in Table 113. The progress of the shower with date for the years 1949 and 1950 as observed on the radiant survey equipment‖‖ with the rates corrected for variation

† Whipple, F. L., loc. cit.
‡ King, A., *Mon. Not. Roy. Astr. Soc.* **86** (1926), 638.
§ Denning, W. F., *Mem. Roy. Astr. Soc.* **53** (1899), 203.
‖ Denning, W. F., *Mon. Not. Roy. Astr. Soc.* **84** (1923), 46.
†† Whipple, F. L., *Proc. Amer. Phil. Soc.* **91** (1947), 189.
‡‡ *Mem. Brit. Astr. Assoc.* **1** (1892), et seq.
§§ Private information quoted by Hawkins, G. S., and Almond, M., loc. cit.
‖‖ Aspinall, A., Clegg, J. A., and Hawkins, G. S., *Phil. Mag.* **42** (1951), 504 (see Chap. IV).

The orbits of the meteors of intermediate date, 705 and 710, lie between these two but are omitted for clarity. Fig. 152, taken from Miss Wright and Whipple,† illustrates similarly the progression in the northern Taurids. In both diagrams the projection is on to the plane of the ecliptic.

The planes of the orbits of these Taurid meteors lie very close to the planes of the orbits of the planets, and Whipple‡ pointed out that close approaches with Mercury, Venus, and Mars could occur. Table 112 gives Whipple's figures for the distance ΔZ perpendicular to the ecliptic between the meteor and planetary orbits at the times of equal radius vector and heliocentric longitude. (A positive sign for ΔZ indicates that the meteor passes north of the planetary orbit.)

TABLE 112

Minimum Distances of Taurid Meteors from Planetary Orbits

Meteor no.		697	705	712
Planet	*True anomaly*	ΔZ (*a.u.*)	ΔZ (*a.u.*)	ΔZ (*a.u.*)
Mercury .	−	−0·002	−0·010	0·022
	+	−0·016	−0·008	
Venus .	−	+0·038	+0·032	+0·026
	+	+0·052	−0·037	−0·026
Earth .	−	0·000	0·000	0·000
	+	−0·099	−0·072	−0·052
Mars .	−	−0·018	−0·020	−0·019
	+	−0·110	−0·082	−0·082

The Taurid stream spreads over at least 0·2 a.u. along the ecliptical plane, and hence, in view of the small values of ΔZ, it seems that the shower must be active for all four planets both before and after perihelion passage. This consideration led Whipple to make the remarkable prediction in 1940‡ that 'in the case of the earth, the radiant of the post-perihelion shower would be in the general direction of the sun, producing only day-time meteors unlikely to be observed except as fireballs in late June and early July'. We shall see later (Chap. XVIII) that the development of the radio-echo techniques led to the detection of this return shower as one of the prominent summer day-time meteor streams.

In addition to the orbital elements for the Taurid meteors, Table 111 gives the mean elements for Encke's Comet, the orbit of which is also shown in Fig. 152, projected on to the plane of the ecliptic together with the northern Taurid orbits. The similarity between the orbits of the comet and the meteors is very marked, and strongly suggests that the comet and the meteors must have a common origin or other close

† Wright, F. W., and Whipple, F .L., loc. cit.

‡ Whipple, F. L., loc. cit.

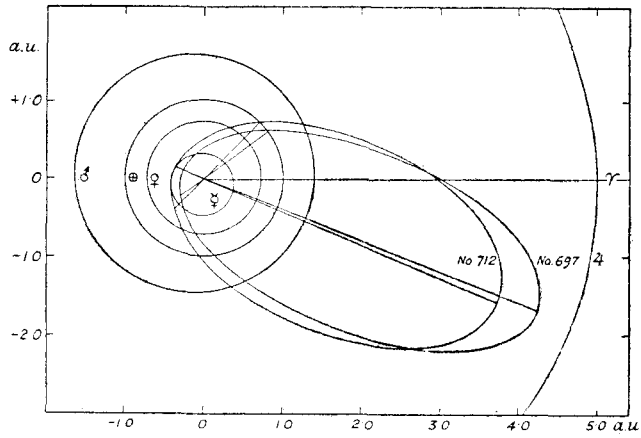

FIG. 151. Orbits of two southern Taurid meteors. Projection on the plane of the ecliptic.

No. 697, 1937 Oct. 31, e = 0·88, i = 6·3°.
No. 712, 1937 Nov. 10, e = 0·82, i = 4·6°.

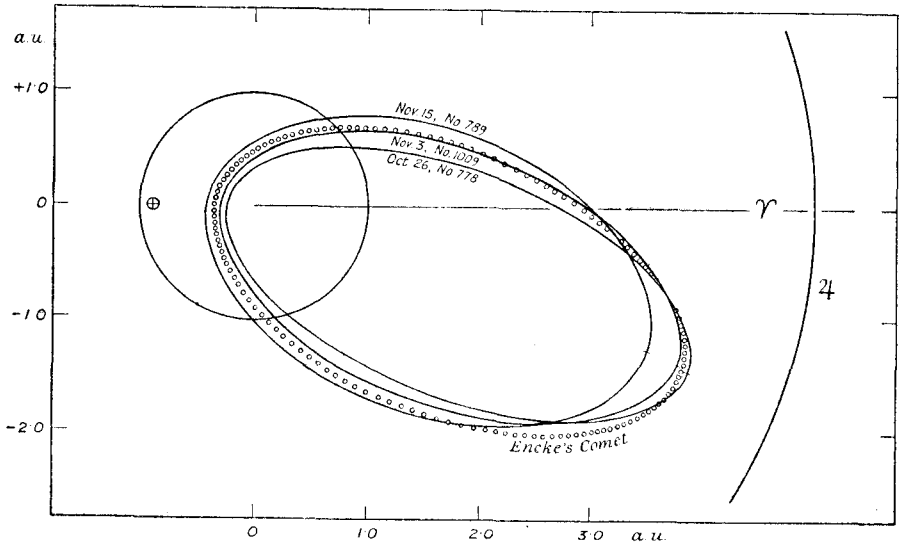

FIG. 152. Orbits of three northern Taurid meteors, compared with the orbit of Encke's Comet. Projection on the plane of the ecliptic.

in orbital characteristics with date are represented by the orbits drawn in Figs. 151 and 152. Fig. 151, taken from Whipple,† shows the orbits of two southern Taurids—697 of October 31 and 712 of November 10.

† Whipple, F. L., loc. cit.

invites comparison with the ideas of Knopf† and Hoffmeister‡ that the Taurid stream is of interstellar origin. A comparison of the mean latitude, longitude, and daily motion of the radiants used by Knopf shows very close agreement with the similar quantities for the Taurid-Arietid meteors listed in Table 111, and leaves little room for doubt that the same streams are under investigation. In the light of the photographic

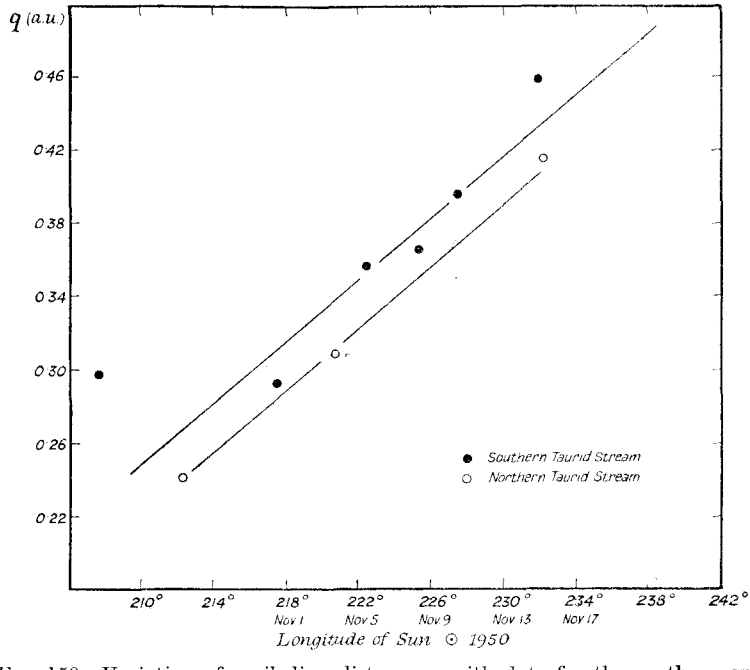

FIG. 150. Variation of perihelion distance q with date for the southern and northern Taurid streams.

measurements, the idea of the interstellar origin for these streams has therefore to be definitely abandoned, a conclusion later accepted by Hoffmeister.§

It was mentioned in (*d*) above that the heliocentric velocities do not show any marked change with date, but this is not the case for the other orbital elements. The most conspicuous correlation is that of perihelion distance q, which increases with date as shown in Fig. 150. a, e, ω, and i also show systematic variations with time. The aphelion distance q′ is not well correlated with date. The longitude of perihelion, π, shows no correlation, but its scatter is small within each stream. These changes

† Knopf, O., loc. cit.

‡ Hoffmeister, C., loc. cit.

§ Hoffmeister, C., *Meteorströme*, ch. 8.

TABLE 111

Orbital Elements for nine Taurid-Arietid Meteors computed by Miss Wright and Whipple

Meteor no.	*Stream*	*Date*	*Argument of perihelion* ω	*Longitude of ascending node* Ω	*Longitude of perihelion* $\pi = \omega + \Omega$	*Inclination to ecliptic* i	*Aphelion distance* q′ (*a.u.*)	*Semi-major axis* a (*a.u.*)	*Perihelion distance* q (*a.u.*)	*Eccentricity* e	*Orbital period* P *years*
			deg.	*deg.*	*deg.*	*deg.*					
697	Southern Taurids	1937 Oct. 31·3507	120·6	37·5	158·1	6·3	4·59	2·44	0·291	0·881	3·82
705		1937 Nov. 5·3594	113·5	42·6	156·1	5·5	4·59	2·47	0·354	0·858	3·88
710		1937 Nov. 8·2072	112·1	45·4	157·5	5·1	4·41	2·39	0·364	0·847	3·69
712		1937 Nov. 10·2343	109·5	47·6	156·9	4·6	4·07	2·23	0·394	0·824	3·33
1527		1947 Nov. 15·372	103·7	52·2	155·9	5·3	3·46	1·96	0·459	0·766	2·74
642	Southern Arietid	1936 Oct. 21·2972	122·2	27·2	149·5	6·0	3·52	1·91	0·296	0·845	2·64
778	Northern Taurids	1938 Oct. 26·3397	307·7	212·2	159·9	3·8	4·14	2·19	0·239	0·891	3·24
1009		1940 Nov. 3·3125	299·6	220·9	160·5	2·5	4·01	2·16	0·307	0·858	3·17
789		1938 Nov. 15·2697	287·8	232·4	160·2	3·2	3·71	2·06	0·414	0·799	2·97
Comet Encke		..	185·2	334·7	159	12·4	4·09	2·217	0·339	0·847	3·30

was pointed out by Whipple† and confirmed in the later analysis of Miss Wright and Whipple,‡ whose results are plotted in Fig. 149. Whipple also pointed out that although the observed velocities varied over a range of nearly 3·5 km./sec., the heliocentric velocities were almost constant, with an apparent decrease in time of apparition. Owing to

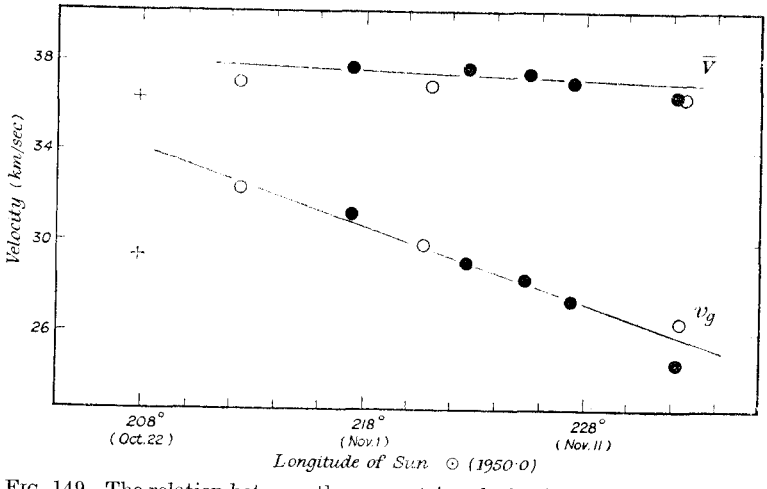

FIG. 149. The relation between the geocentric velocity (v_g) and the heliocentric velocity ($\bar{V}$) with dates for the Taurid-Arietid showers according to Miss Wright and Whipple.

● Southern Taurids. o Northern Taurids. + Southern Arietids.

the importance of any such variation of heliocentric velocity, Whipple† made a careful investigation of the errors of measurement, and concluded that it was not possible to make any certain deduction concerning the reality of this apparent variation of heliocentric velocity with time. The fuller data plotted in Fig. 149 also indicate a possible slight decrease in heliocentric velocity with time. The changes in the other orbital elements with date are, however, real, and these will be referred to below.

(*e*) *Orbits*

The orbital data for the nine meteors whose velocities are listed in Table 110 are tabulated in Table 111. These are taken from the data of Miss Wright and Whipple.‡ The results for five of the meteors (697, 705, 710, 712, 778) were also given earlier by Whipple.† One of the most striking features of these data is the short period of the orbits, and this immediately

† Whipple, F. L., loc. cit.
‡ Wright, F. W., and Whipple, F. L., loc. cit.

(d) Velocities

Porter† has analysed twenty-eight possible Taurids between the limits of November 2 and 19 from the British visual meteor data. The mean velocity is given as 25·7 km./sec. However, in view of the complexity of the radiants revealed by Miss Wright and Whipple,‡ and of their precise photographic determination of the velocities, no point would be served in discussing the details of the visual measurements.

TABLE 110

Velocities of the Taurids and Arietids according to Miss Wright and Whipple

	Southern Taurids					*Southern Arietid*	*Northern Taurids*		
Meteor number	697	705	710	712	1527	642	778	1009	789
Date	1937 Oct.	1937 Nov.	1937 Nov.	1937 Nov.	1947 Nov.	1936 Oct.	1938 Oct.	1940 Nov.	1938 Nov.
Corrected radiant* $\alpha°$	31·3507	5·3594	8·2072	10·2343	15·372	21·2972	26·3397	3·3125	15·2697
Corrected radiant* $\delta°$	51·27	53·17	55·27	56·15	58·65	42·29	47·4	52·20	58·36
v app. relative velocity km./sec.	+14·05	14·43	15·07	15·47	14·38	11·37	20·6	20·50	23·37
V no atmosphere velocity	32·1	30·9	30·0	29·2	24·6	30·6	33·3	31·2	27·6
v_g geocentric velocity	32·9	31·0	30·6	29·5	26·9	31·4	33·9	31·7	28·3
$\overline{V}$ heliocentric velocity	31·2	29·2	28·4	27·3	24·6	29·5	32·3	29·9	26·2
	37·7	37·8	37·6	37·3	36·6	36·3	37·1	37·1	36·9

* The slight discrepancies between these positions and those given in Table 107 are the result of a subsequent re-analysis of the data made by L. Jacchia.

Whipple§ presented the velocities of the seven Taurid meteors which were listed in Table 107. In the later publication of Miss Wright and Whipple,‡ five‖ of these which were suitable for orbital calculation were retained, and three more recent doubly photographed meteors added. In addition, one previously classed as sporadic†† (No. 642) has been included as a southern Arietid. The velocity data for these nine accurately measured meteors are given in Table 110.

The most striking characteristic of these velocities is the marked decrease in geocentric velocity with increasing solar longitude—a relation which appears to be independent of stream association. This feature

† Porter, J. G., *Mon. Not. Roy. Astr. Soc.* (1943), loc. cit.; (1944), loc. cit.

‡ Wright, F. W., and Whipple, F. L., loc. cit.

§ Whipple, F. L. (1940), loc. cit.

‖ These five (697, 705, 710, 712, 778) were the only ones of the original set completely photographed with double cameras and rotating shutters.

†† Whipple, F. L., *Proc. Amer. Phil. Soc.* **79** (1938), 499.

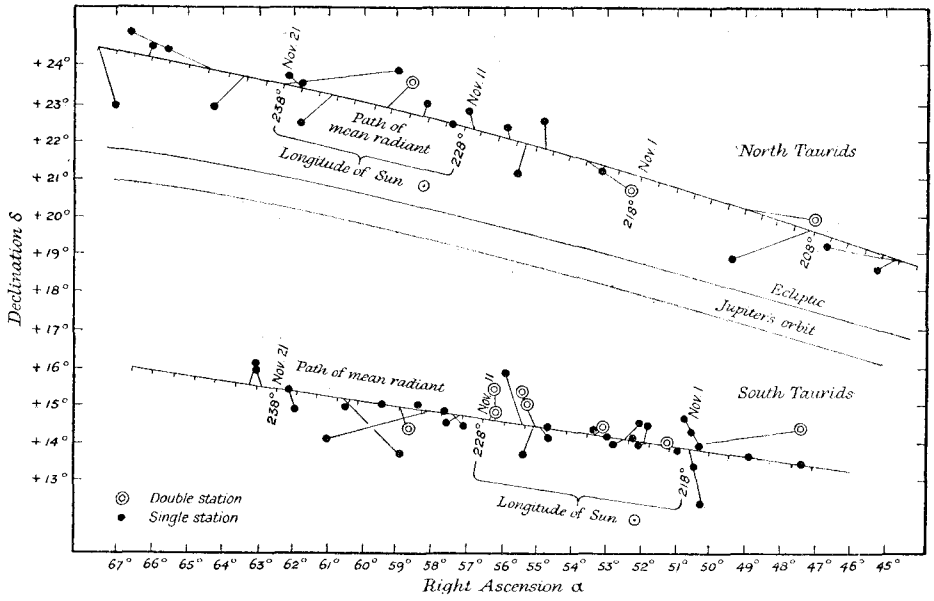

FIG. 147. Radiant paths for the northern and southern Taurid streams according to the photographic analysis of Miss Wright and Whipple. For each meteor trail in each shower a point represents the nearest position of the extended great circle to the calculated mean radiant of the instant. A line joins this nearest point to the radiant; hence the great circle for each trail is perpendicular to this joining line. The paths of the mean radiants are those given in Table 109.

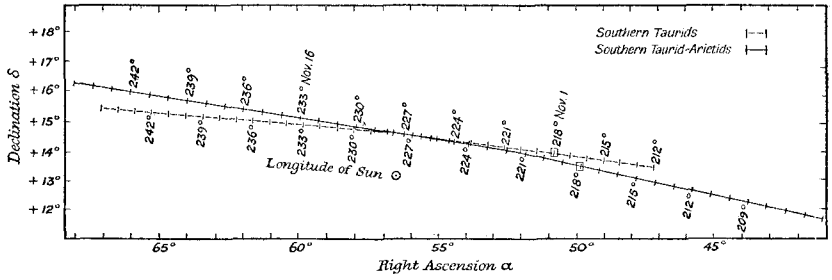

FIG. 148. Mean radiant paths for the combined southern Taurid-Arietid streams compared with those of the southern Taurid stream, according to the photographic analysis of Miss Wright and Whipple.

southern Taurid streams in which the individual meteor radiants are also plotted. Fig. 148 gives similar data for the combined southern Taurid-Arietid stream with the southern Taurids shown for comparison.

streams. There is some doubt as to whether the southern Arietids may not form a continuous stream with the southern Taurids. Therefore Miss Wright and Whipple also give a solution whereby both are combined into one moving radiant. The final solutions for the coordinates of these various streams are given in Table 108.

TABLE 108

The Radiants in Taurus and Aries according to the Photographic Analysis of Miss Wright and Whipple

	Southern Taurid-Arietid stream	*Southern Taurids*	*Northern Taurids*	*Southern Arietids*	*Northern Arietids*
Year and equinox	1950·0	1950·0	1950·0	1950·0	1950·0
Longitude of sun	223·26°	225·70°	227·74°	206·24°	227·26°
Mean date U.T. 1950	Nov. 6·26	Nov. 8·69	Nov. 10·72	Oct. 20·22	Nov. 10·24
Radiant at mean date α	53° 19′	55° 13′	56° 55′	41° 38′	41° 20′
Radiant at mean date δ	+14° 09′	+14° 29′	+22° 25′	+10° 19′	+19° 52′
$\Delta\alpha \cos\delta$ per day	+39′±1	+35′±1	+28′±1	..	..
$\Delta\delta$ per day	+8′±1	+5′±1	+8′±2	..	..
Total motion per day	40′	35′	29′	..	..

TABLE 109

Predicted Mean Radiant with Date for the Taurid-Arietid Streams according to Miss Wright and Whipple

(Epoch 1950·0)

		Right ascension						*Declination*					
	Longitude of sun	*Southern Taurid-Arietids*		*Southern Taurids*		*Northern Taurids*		*Southern Taurid-Arietids*		*Southern Taurids*		*Northern Taurids*	
	deg.	*deg.*	*min.*	*deg.*	*min.*	*deg.*	*min.*	*deg.*	*min.*	*deg.*	*min.*	*deg.*	*min.*
Oct. 17	203	39	53	..		44	35	+11	22	..		+19	01
20	206	41	51	..		46	04	11	49	..		19	29
23	209	43	50	..		47	33	12	16	..		19	55
26	212	45	49	46	56	49	01	12	41	+13	24	20	22
29	215	47	48	48	45	50	31	13	06	13	39	20	47
Nov. 1	218	49	48	50	33	52	02	13	29	13	54	21	11
4	221	51	49	52	22	53	33	13	52	14	08	21	35
7	224	53	49	54	11	55	04	14	14	14	21	21	57
10	227	55	50	56	01	56	36	14	34	14	34	22	19
13	230	57	52	57	50	58	08	14	54	14	45	22	40
16	233	59	54	59	40	59	41	15	13	14	56	23	00
19	236	61	56	61	30	61	14	15	30	15	06	23	20
22	239	63	58	63	20	62	48	15	47	15	15	23	38
25	242	66	01	65	10	64	22	16	02	15	23	23	55
28	245	68	04	67	00	65	57	16	16	15	30	24	12
Dec. 1	248	..		..		67	32	..		..		24	27

The variation of predicted mean radiant position with date is given in Table 109. This is shown graphically in Fig. 147 for the northern and

Denning's remarks on these streams indicate that the chief displays are generally given by the α-Arietids, ϵ-Arietids, and λ-Taurids. Little further information was gained about the situation until the photographic meteor studies of the region were undertaken by Whipple† and by Miss Wright and Whipple.‡ In the first publication Whipple† presented the accurate radiant coordinates of seven doubly photographed Taurids, as listed in Table 107.

TABLE 107

Whipple's First List of seven Photographic Taurid Radiants

Harvard number	*Date*	*Corrected radiant* α	δ
697	1937 Oct. 31·3507	51° 5′	14° 0′
705	1937 Nov. 5·3620	52 56	14 23
710	1937 Nov. 8·1968	55 12	15 4
	1937 Nov. 8·2176	54 59	15 1
712	1937 Nov. 10·2343	55 58	15 25
716	1937 Nov. 10·3842	56 10	14 49
719	1937 Nov. 22·046	64 1	15 56
778	1938 Oct. 26·3397	46 53	20 3

In comparing this list with Denning's radiants (Table 106) it is evident that one of Denning's chief radiants (λ-Taurids) is well represented in Table 107 (Nos. 697, 705, 710, 712, 716). Also No. 778 would appear to be associated with Denning's ϵ-Arietids. Whipple also suggested that a meteor previously analysed (No. 642) and classed as sporadic,§ with a radiant of α 41·9°, δ +13·7°, could more realistically be related to Denning's σ-Arietid radiant.

By far the most detailed analysis of the radiant structure is that carried out by Miss Wright and Whipple.‡ They analysed 102 meteors found on the Harvard photographic plates between 1896 and 1948 covering the period October 15–December 2. Ninety of these were single-station photographs and 12 double station. From this analysis they conclude that the major activity (49 meteors) is due to a subcentre which they call the southern Taurid stream, together with the northern Taurid stream (24 meteors), displaced 7° north of the southern Taurids but with a similar movement in right ascension. They also isolate two less active subcentres in Aries—the southern Arietids (or σ-Arietids) (8 meteors) and the northern Arietids (4 meteors) related to the respective Taurid

† Whipple, F. L., *Proc. Amer. Phil. Soc.* **83** (1940), 711.
‡ Wright, F. W., and Whipple, F. L. (1950), loc. cit.
§ See Chap. XI.

with a secondary maximum around November 11 ($\odot = 228°$). On the other hand, the northern Taurids show only a flat maximum in the middle of November. Miss Wright and Whipple suggest that the more concentrated southern Taurid stream may have developed more recently than the diffuse northern stream.

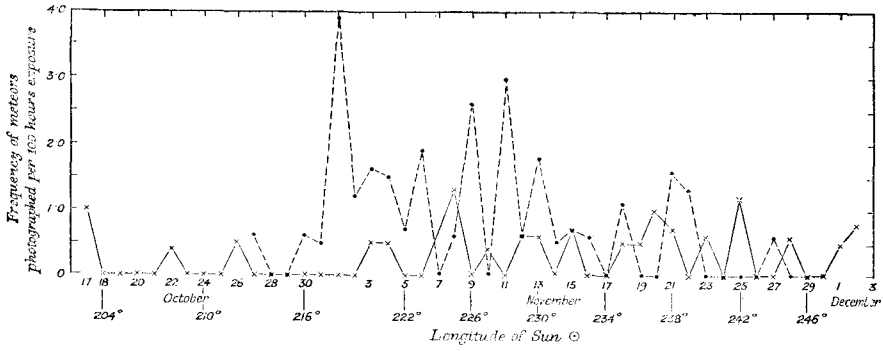

FIG. 146. Hourly rate of the southern and northern Taurid meteor streams according to Miss Wright and Whipple.

– – ● – – – ● – – Southern Taurid stream. — × — × Northern Taurid stream

(c) *Radiants*

The complex nature of the activity in Taurus was recognized by Denning,† who in 1928 published a list of thirteen active centres as given in Table 106.

TABLE 106

Denning's 1928 *List of the Radiants in Taurus and Aries*

Streams	*Extent of activity*	*Mean radiant* α *(deg.)*	δ *(deg.)*
1. β-Arietids .	Oct.–Nov.	21·6	+21·9
2. ξ-Arietids .	Sept.–Oct.	30·9	9·6
3. α-Arietids .	Sept.–Nov.	32·0	18·5
4. 39 Arietids .	Aug.–Oct.	40·5	30·9
5. σ-Arietids .	Oct.	41·9	13·7
6. ε-Arietids .	Oct.–Nov.	41·9	21·4
7. ζ-Arietids .	Oct.–Nov.	49·3	18·7
8. λ-Taurids .	Oct.–Nov.	55·7	14·2
9. ε-Taurids .	Oct.–Nov.	55·9	9·0
10. ζ-Taurids .	Nov. 1–17	60·1	28·9
11. γ-Taurids .	Oct.–Nov.	61·44	11·8
12. κ-Taurids .	Oct. 17–Dec. 1	63·5	22·3
13. ζ-Taurids .	Nov. 14–Dec. 15	80·5	23·3

† Denning, W. F., *J. Brit. Astr. Assoc.* **38** (1928), 302.

3 and 10, is broad, and the activity low—not more than 10 per hour for a visual observer. Nevertheless, the stream has recently emerged as one of great importance in meteor astronomy. The unusual persistence of the shower (nearly a month), coupled with the slow daily motion of the radiant, led Knopf† and Hoffmeister‡ to conclude that the shower orbits were hyperbolic, and hence that the Taurids were an interstellar meteor stream. But the investigations of Whipple§ in 1940 showed, on the contrary, that the orbits were of unusually short period and that the stream was probably associated with Encke's Comet. Still more recently, the radio-echo observations have shown that this night-time autumn Taurid shower is the return of the day-time β-Taurid shower (see Chap. XVIII). As remarked by Whipple,§ the dilution of the Taurid stream has disguised its character as one of the more important known showers, and the total population of the associated streams is probably comparable with that of any of the generally recognized streams.

(*b*) *Activity*

The group of meteor radiants in Taurus and Aries is complex and of relatively low activity. Consequently, the hourly rate from this region has not been investigated systematically and little is known about any annual variations in activity which may be present. The total interval of the shower is generally recognized as extending for nearly a month from October 26 to November 22, with the hourly rate reaching 10 to 20 over the broad maximum of November 3–10, although Denning‖ lists the activity of the group as extending from October to December 15. The radio-echo observations†† can only resolve the total activity, including the sporadic meteors, from this region of sky, but no significant variations have been detected since 1946—the maximum hourly rates being 18 (1946 November 9), 9 (1947 November 6), 14 (1950 November 9).

The photographic analysis of Miss Wright and Whipple‡‡ has enabled the activity of the various sub-showers to be isolated, and Fig. 146 shows the frequency of occurrence per 100 hours of exposure of meteors in the southern and northern Taurid streams (see below). The hourly rate of the southern Taurids rises abruptly to a maximum at the beginning of November ($\odot = 218°$) and is followed by a slow decline to late November,

† Knopf, O., *Astr. Nachr.* **242** (1931), 161.
‡ Hoffmeister, C., *Die Meteore* (Leipzig, 1937), p. 46.
§ Whipple, F. L., *Proc. Amer. Phil. Soc.* **83** (1940), 711.
‖ Denning, W. F., *J. Brit. Astr. Assoc.* **38** (1928), 302.
†† Hawkins, G. S., and Almond, M., *Mon. Not. Roy. Astr. Soc.* **112** (1952), 219.
‡‡ Wright, F. W., and Whipple, F. L., *Tech. Rep. Harv. Coll. Obs.* (1950), no. 6 (Harvard Reprint Series II–35).

On the other hand, Porter† considers that the great distance between the earth and the cometary orbit (0·15 a.u. at closest approach) makes any such connexion impossible, and points out that there are thirty-five comets which approach to within 0·05 a.u. of the earth and sixty to within 0·1 a.u., none of which show any accordance with meteor

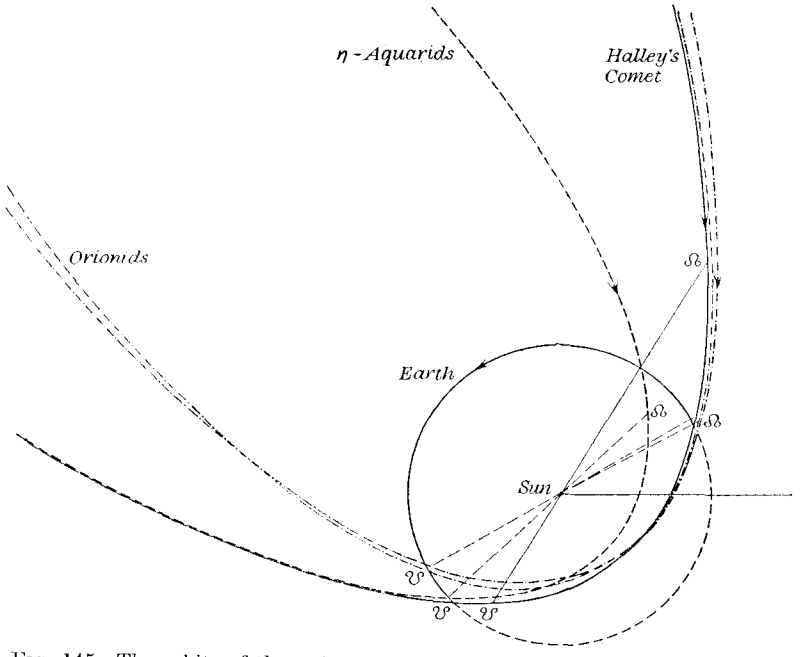

FIG. 145. The orbits of the η-Aquarid meteor stream and of Halley's Comet as given in Fig. 132, compared with two Orionid orbits as computed by Jacchia from photographic data.

showers. The orbit of the η-Aquarid stream has been compared in Fig. 132 with that of Halley's Comet. In Fig. 145 these are reproduced with the addition of the two Orionid orbits computed by Jacchia. It is evident that the association of the Orionids with the comet is plausible. As in the case of the η-Aquarid orbit, the period is less than that of the comet. More precise data on the orbit of the meteors are required before the situation can be clarified.

2. The Taurid shower and the radiants in Aries

(*a*) *History*

From about October 26 to November 22, meteors can be seen from a radiant in Taurus. The maximum, which occurs between November

† Porter, J. G., *Rep. Phys. Soc. Progr. Phys.* **11** (1948), 402.

Hoffleit† using the rotating-shutter technique described in Chapter XI. The velocities were 44 and 40 km./sec.; they regarded the low values as due to retardation in the earth's atmosphere.

Only two cases of accurate Orionid velocities determined from the double-camera work have so far been published‡ as follows:

Harvard serial no.	*Date*	*Velocity*
889	1939 Oct. 24·40	66·58 km./sec.
1382	1946 Oct. 23·29	65·28 km./sec.

So far there are no records of determinations of Orionid velocities by using radio techniques.

(*e*) *Orbit*

In 1911 Olivier§ first drew attention to the similarity between the orbits of the Orionids and of the η-Aquarid stream of May (see Chap. XIII). The possible connexion of the η-Aquarid stream with Halley's Comet has already been discussed. The idea has therefore emerged that the η-Aquarid and Orionid meteor streams are caused by the passage of the earth through the debris in the orbit of Halley's Comet before and after perihelion. The elements for the orbits of the η-Aquarids and Orionids and for Halley's Comet are compared in Table 105.

TABLE 105

Comparison of the Orbits of the η-Aquarids, Orionids, and Halley's Comet

	Source	Ω	ω	π	e	i	a	q
		deg.	*deg.*	*deg.*		*deg.*	*a.u.*	*a.u.*
Orionids . .	McIntosh‖	25·6	77·7	103·3	1	162·3	∞	0·604
	Jacchia 1939‡	30·22	85·7	..	0·944	163·4	9·84	0·548
	Jacchia 1946‡	29·31	87·8	..	0·915	162·9	6·32	0·537
η-Aquarids .	See Ch. XIII	43·1	83·0	126·1	0·91	160	5·0	0·47
Halley's Comet	See Ch. XIII	57·3	111·7	169·0	0·9673	162·2	17·946	0·587

The connexion of the two meteor streams with the cometary orbit has been strongly emphasized by Olivier,†† Svoboda,‡‡ and Hoffmeister.§§

† Millman, P. M., and Hoffleit, D., *Ann. Harv. Coll. Obs.* **105** (1937), 601.

‡ Jacchia, L. G., *Tech. Rep. Harv. Coll. Obs.* (1948), no. 2 (Harvard Reprint Series II–26).

§ Olivier, C. P., *Trans. Amer. Phil. Soc.* **22** (1911) (pt. i).

‖ McIntosh, R. A., *Mon. Not. Roy. Astr. Soc.* **90** (1929), 160.

†† Olivier, C. P., *Meteors*, ch. 8 (1925); *Comets* (1930).

‡‡ Svoboda, J., *Bull. internat. de l'Acad. d. Sci. de Bohème*, **23** (1914), 3; *Astr. Nachr.* **197** (1913), 203.

§§ Hoffmeister, C., *Meteorströme*, ch. 8; *Die Meteore* (Leipzig, 1937).

From these data Hoffmeister deduces a mean value of

$$\odot_{\max} = 206{\cdot}4^\circ,\ \alpha = 93{\cdot}7^\circ \pm 1{\cdot}0,\ \delta = +16{\cdot}1^\circ \pm 0{\cdot}3,$$

or, when corrected for zenithal attraction, α 93·5°, δ 15·9°, a position which is in good agreement with the mid-stream value given by Prentice (Table 102).

Contemporary radio-echo observations do not compete in resolution with the work of Prentice, but are in general agreement. The information given by Hawkins and Miss Almond† for the years 1949–50 is as follows:

	α	δ	$\odot_{\max}$
1949	95°	+13°	209·5°
1950	98°	+9°	207·2°

(*d*) *Velocities*

The analysis of the British visual meteor data by Porter‡ contains ten cases of possible Orionid velocities, the details of which are given in Table 104.

TABLE 104

Visual Velocity Measurements of possible Orionid Meteors

Date	*Radiant*		*Measured velocity*	*Theoretical parabolic velocity*
	α (*deg.*)	δ (*deg.*)	*km./sec.*	*km./sec.*
I. *From multiple observations*				
1930 Oct. 21	95	+5	69	66
Oct. 25	109	+22	46	71
II. *From duplicate observations*				
1928 Oct. 18	88	+13	65	66
Oct. 20	93	+15	34	67
Oct. 20	93	+18	33	68
Oct. 20	101	+16	32	70
Oct. 20	110	+13	21	72
Oct. 20	98	+19	41	69
Oct. 20	105	+25	17	71
Oct. 20	96	+14	68	68
			Mean velocity = 42·6 km./sec.	

In his later analysis Porter§ gives the mean velocity of thirty-five Orionids as 51·6 km./sec., but no details are given of the other twenty-five velocities omitted in the previous work.‡ The velocities of two Orionid meteors were measured in the photographic work of Millman and Miss

† Hawkins, G. S., and Almond, M., *loc. cit.*
‡ Porter, J. G., *Mon. Not. Roy. Astr. Soc.* **103** (1943), 134.
§ Porter, J. G., ibid. **104** (1944), 257.

from a region centred on α 92°, δ +15° for several days, but that this is due to the passage of successive subcentres through this position, and not, as Denning believed, to the existence of a stationary radiant in that position.

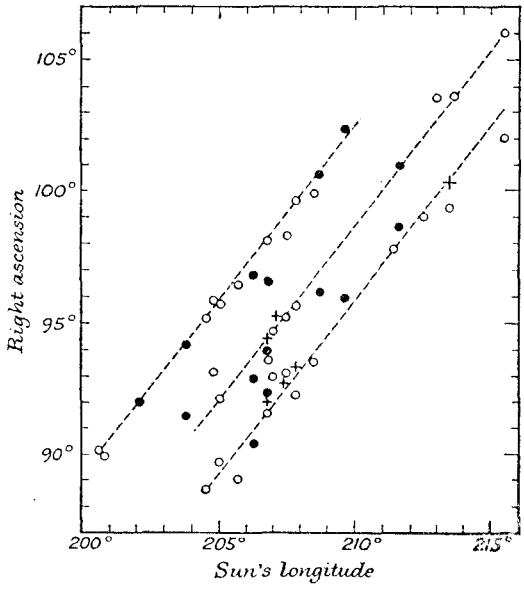

FIG. 144. The right ascension of the three main Orionid subcentres at declination +15°, plotted against sun's longitude, according to Prentice.
o – – – Observations of 1928–32. ● – – – Observations of 1933–5.
(The six positions marked + are from duplicate accordances. The others are determinations by a single observer (Prentice).)

Hoffmeister† gives details of the Orionid radiant from his own observations as listed in Table 103.

TABLE 103

Hoffmeister's Radiants for the Orionid Stream

Year	*Sun's longitude at maximum* ⊙	*Radiant* α	δ
	deg.	*deg.*	*deg.*
1931	203·7	95·5	+17·0
1933	205·6	91·0	+16·5
1931	205·7	92·7	+15·7
1933	206·1	91·0	+15·0
1931	207·7	97·3	+16·2
1933	209·9	94·5	+16·4

† Hoffmeister, C., *Meteorströme*, ch. 8.

The subcentres are clearly shown in the gnomonic maps of Fig. 143 which give the radiants observed on various nights in 1933 and 1935. Finally, in Fig. 144, the right ascension of the three main streams at

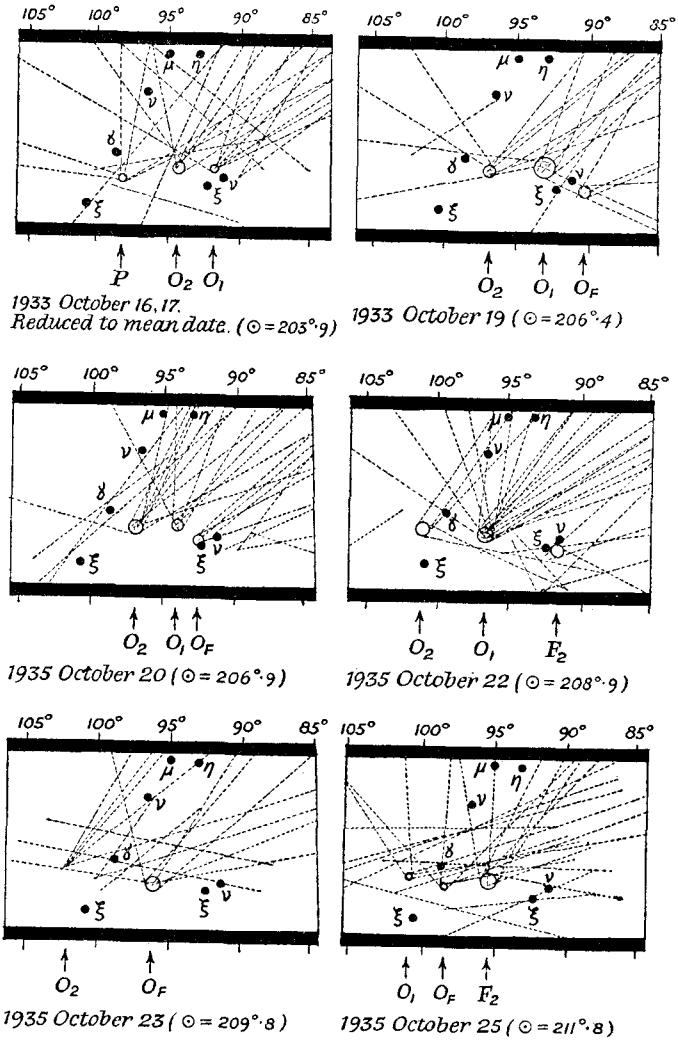

FIG. 143. Orionid radiants as observed by Prentice on successive days in 1933 and 1935. The notation corresponds to that of Table 102. (The P and F_2 streams are additional weak centres.)

δ +15° are plotted against the longitude of the sun. From these results it is clear how Denning may have been misled in his belief of stationary radiation. Fig. 144 shows that there is considerable activity

photographic records of three Orionids meteors indicating a motion of the expected amount from October 19, a date on which all observers agreed in placing the radiant at α 91°, δ +15°.

The shower was observed in 1928 by McIntosh† under good conditions in New Zealand. He found the radiants listed in Table 101, again clearly showing the movement of the radiant.

TABLE 101

Orionid Radiants 1928 *according to McIntosh*†

Date	*Radiant*		*No. of meteors*
	α *deg.*	δ *deg.*	
1928 Oct. 15·65	89·2	+14·2	15
16·64	90·0	15·0	9
18·65	91·6	14·6	4
20·62	92·5	14·2	12
23·64	93·5	14·9	3
24·64	99·4	13·7	9

The most detailed investigation of the radiant structure has been carried out by Prentice‡ between 1928 and 1939. His results not only show conclusively that the radiant is in daily motion, but also provide a plausible explanation of the reason why Denning was led to believe that the radiant was stationary. Prentice concluded that the Orionid meteors came principally from three sharply defined centres, situated at close intervals in declination +15°, and that these centres were in motion parallel to the ecliptic at a rate of approximately 1·3° per day. He also concluded that another stream was in similar motion at declination +18°. These results are summarized in Table 102, and Figs. 143 and 144.

TABLE 102

Prentice's Radiants for the Orionid Stream

	Mean position at long. of apex = 118°		*Daily motion in* α	*No. of radiants*	*No. of meteors*
	α *deg.*	δ *deg.*	*deg.*		
Leading stream (O_2) .	98·1	+14·9	1·30	10	46
Mid-stream (O_1) . .	94·4	15·5	1·34	9	41
Following stream (O_F) .	91·7	15·1	1·22	13	60
Northern stream . .	97·8	18·2	0·92	6	28

† McIntosh, R. A., *Mon. Not. Roy. Astr. Soc.* **90** (1929), 160.
‡ Prentice, J. P. M., loc. cit.

quoting observations made by Dole in America of a rich return in 1922, but one of low activity in 1925.

No subsequent observations of sufficient detail have yet been made to enable further judgement to be taken on Prentice's suggestion. Radio-echo observations† since 1946 give a fairly constant intensity for the stream as shown in Table 100, but the resolution is insufficient to yield any information about the activity of subcentres.

TABLE 100

Radio-echo Observations of the Orionid Activity

Year	⊙	*Date at maximum*	*Hourly rate*
1946	204·3	Oct. 18	18
1947	206·0	Oct. 20	14
1948	208·8	Oct. 22	20
1949	209·5	Oct. 23	20
1950	207·2	Oct. 21	17
1951	203·3	Oct. 18	12
1952	206·7	Oct. 20	10

(*c*) *Radiant*

Denning‡ held strongly to the opinion that the radiant of the Orionids was of a different character from that of the Perseids, in that it retained a fixed place amongst the stars during the three weeks of its activity. His observations, together with those of other British observers, showed that there were two active radiants at $\alpha = 91°$, $\delta = +15°$, and $\alpha = 97°$, $\delta = +16°$ which remained fixed. This view of the Orionid radiant remained almost unchallenged until 1911. Subsequent work, however, gradually led to the abandonment of the view of such stationary radiants. A very full discussion of the arguments surrounding these ideas has been given by Olivier,§ and since the subject of 'stationary radiation' is now closed no point would be served in discussing the matter here. In the particular case of the Orionids, evidence was steadily accumulated by Olivier‖ in America that the Orionid radiant was, in fact, moving in the direction of increasing right ascension, and, during the rich shower of 1922, Dole†† secured good radiants from October 17 to 29, showing the radiant to be in motion. Also, on 1922 October 20, King‡‡ secured

† Hawkins, G. S., and Almond, M., *Mon. Not. Roy. Astr. Soc.* **112** (1952), 219 (data for 1951, 1952 unpublished).

‡ Denning, W. F., *Mem. Roy. Astr. Soc.* **53** (1899), 203; *Mon. Not. Roy. Astr. Soc.* **73** (1913), 667.

§ Olivier, C. P., *Meteors*, chs. 10, 11.

‖ Olivier, C. P., *Trans. Amer. Phil. Soc.* **22** (pt. i) (1911); *Mon. Not. Roy. Astr. Soc.* **74** (1913), 37.

†† Dole, R. M., *Pop. Astron.* **31** (1923), 37; *Publ. Leander McCormick Obs.* **5** (1929), 38.

‡‡ *Bull. Harv. Coll. Obs.* (1922), no. 778; (1923), no. 783.

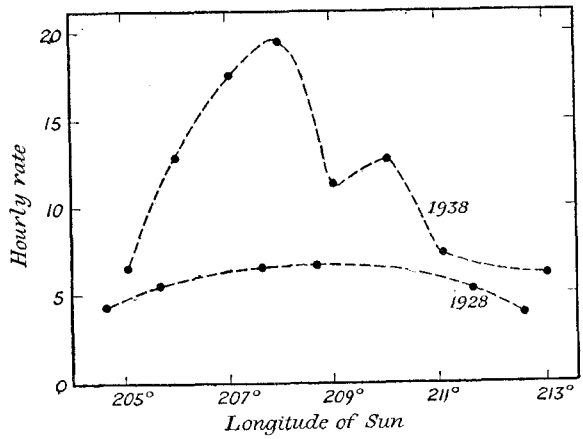

FIG. 141. Hourly rates of the Orionids according to Prentice for years of low (1928) and high (1938) activity.

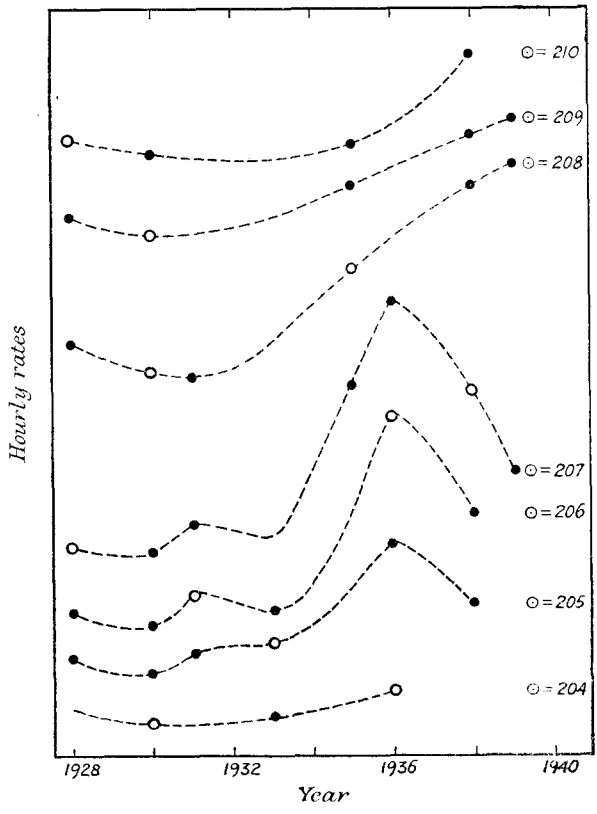

FIG. 142. The activity of the Orionid subcentres 1928–39. (The zeros of the ordinates are arbitrarily displaced.)

● – Observed rates, o – interpolated rates.

XV

THE MAJOR METEOR SHOWERS—III

THE PERMANENT STREAMS OF SEPTEMBER TO DECEMBER

THE period of September to December has long been recognized as a time of considerable meteoric activity. In the past it has contained some spectacular events, such as the great showers of Leonids, Bielids, and Giacobinids. These are discussed in Chapters XVI and XVII. The present chapter deals with the more permanent streams of the Orionids, Taurids, Geminids, and Ursids.

1. The Orionid shower

(*a*) *History*

The Orionid shower is active from about October 15–25, reaching a maximum on October 20–21. The hourly rate for a single visual observer is 10 to 20, but there are no records of any outstanding displays of this shower in the past. The shower has been the centre of great controversy, however, firstly because it was regarded by Denning as being a clear case of a 'stationary radiant', and secondly because of the probable connexion of the stream with the η-Aquarids and Halley's Comet.

(*b*) *Activity*

An extensive study of the shower between 1928 and 1939 has been made by Prentice.† The activity from 1928 to 1935 was very low, but it increased rapidly between 1933 and 1935. Representative curves given by Prentice‡ for a year of low activity (1928) and a year of high activity (1938) are shown in Fig. 141. Prentice also investigated the activity of the various subcentres into which the stream is divided, from which he concluded that the activity of the sub-groups is not synchronized. The effect is shown in Fig. 142, in which the hourly rates of the Orionids are plotted as ordinates against the years of observation for each integral value of sun's longitude, $\odot$, between 205° and 210°. For the early longitudes a decline in the hourly rate begins after 1936, but the activity at later longitudes is still increasing. Prentice further concludes that the Orionids may have a period of about seventeen years,

† Prentice, J. P. M., *J. Brit. Astr. Assoc.* **43** (1933), 376; **46** (1936), 329; **49** (1939), 148; **51** (1941), 167.

‡ Prentice, J. P. M. (1941), loc. cit.

TABLE 99

The Orbital Elements of the Perseid Stream and of Comet 1862 III

	☊	ω	i	e	q	a	*Period*
					a.u.	*a.u.*	*years*
Comet 1862 III .	137° 27′	152° 46′	113° 34′	..	0·9626	..	121·5
Schiaparelli . .	138° 16′	154° 28′	115° 57′	assumed parabolic	0·9643	..	..
Whipple . . .	141° 28′	155° 31′	119° 42′	0·9577	0·9680	22·89	109·5
Ceplecha . . .	140° 21′	150° 53′	112° 12′	0·9474	0·9506	18·11	..
Hawkins and Almond	139° 30′	153°	114°	0·93	0·97	14·4	..

The agreement of these various determinations is very satisfactory and the close connexion of the Perseid orbit with that of Comet 1862 III is also evident in Fig. 140, where the orbit determined by Hawkins and Miss Almond from the radio-echo data is projected on to the plane of the Comet's orbit.

in connexion with the Quadrantid velocities. Using the same notation, the corresponding values for the Perseids over the years 1948–51, inclusive, are $\sigma_E = 1{\cdot}7$ km./sec.; $\sigma_S = 2{\cdot}9$ km./sec.; $\sigma_R = 2{\cdot}1$ km./sec.; $\sigma_A = 0{\cdot}3$ km./sec., and, since $\sigma_0 = 4{\cdot}6$ km./sec., $\sigma_H = 2{\cdot}3$ km./sec. Thus the actual spread in heliocentric velocities may make a significant contribution to the dispersion of the velocities in Fig. 139.

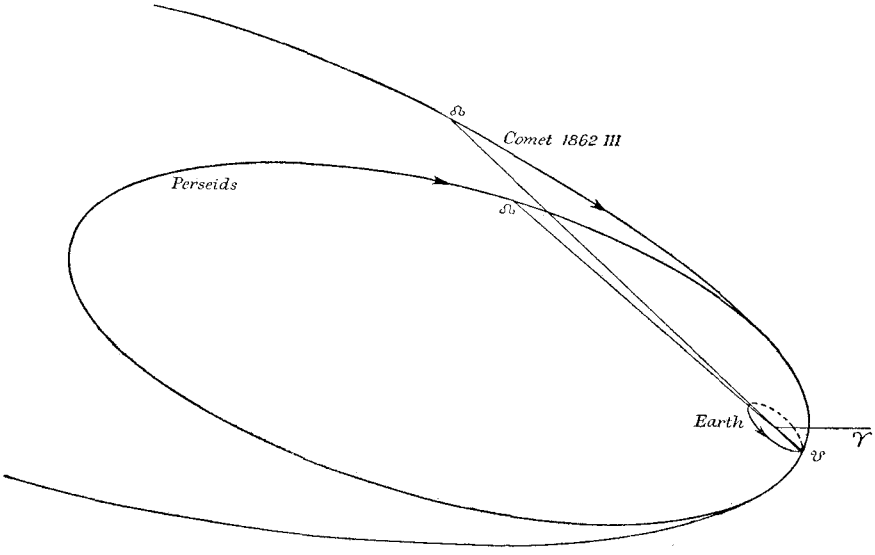

FIG. 140. The orbits of the Perseid meteor stream as determined by the radio-echo observations compared with the orbit of Comet 1862 III. (Projection is on the plane of the comet's orbit.)

(*e*) *Orbit*

As mentioned in (*a*) above, the work of Schiaparelli on the orbit of the Perseids provided the first clear illustration of the connexion between a meteor stream and a comet. The final calculation of the parabolic orbit for the Perseids was made by Schiaparelli,† based on A. S. Herschel's determination of the radiant in 1863 as $\alpha = 44°, \delta = +56°$. The elements are given in Table 99 compared with Comet 1862 III.

More recent computations of the orbit using the photographic and radio-echo measurements of the velocities have been given by Whipple,‡ Ceplecha,§ and Hawkins and Miss Almond.‖ These orbital elements are also given in Table 99.

† Schiaparelli, G. V., *Sternschnuppen*; see Olivier, loc. cit. p. 58.
‡ Whipple, F. L. (1938), loc. cit.
§ Ceplecha, Z., loc. cit.
‖ Hawkins, G. S., and Almond, M., loc. cit.

from which it was possible to isolate six Perseids, the average velocity of which was $62{\cdot}3 \pm 1{\cdot}6$ km./sec.

TABLE 98

Radio-echo Measurements of Perseid Velocities

Date	*No. of determinations*	*Mean velocity km./sec.*	*Remarks*
1949 Aug. 11	1	59·8	McKinley,† moving-head echo
		58·3	,, Doppler whistle
1948 Aug. 11–12	6	$62{\cdot}3 \pm 1{\cdot}6$	Manning, Villard, and Peterson‡
1948	27	$60{\cdot}7 \pm 4{\cdot}7$	Hawkins and Miss Almond§
1949	14	$60{\cdot}3 \pm 2{\cdot}9$	
1950	41	$61{\cdot}0 \pm 5{\cdot}0$	
1951	83	$59{\cdot}2 \pm 5{\cdot}3$	

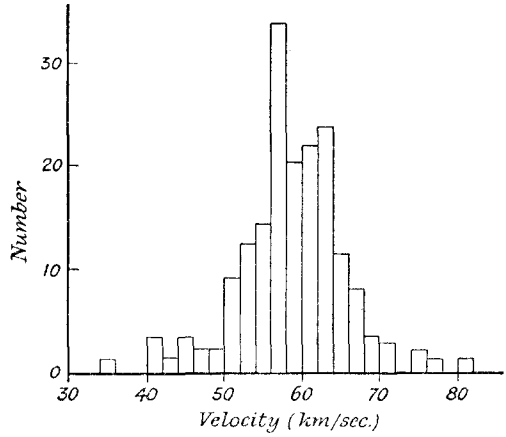

FIG. 139. Distribution of 165 Perseid velocities 1948–51 measured by the radio-echo diffraction technique.

The radio-echo measurements made at Jodrell Bank during the showers of 1948–51, inclusive, using the pulsed diffraction technique, have been summarized by Hawkins and Miss Almond.§ The details are included in Table 98, together with the other radio-echo measurements, and the distribution of velocities is shown in Fig. 139.

Hawkins and Miss Almond have investigated how much of the dispersion in the velocities might be caused by an actual spread of the velocities in the stream. The details of the analysis have been described on p. 255

† McKinley, D. W. R., *J. Appl. Phys.* **22** (1951), 202.
‡ Manning, L. A., Villard, O. G. and Peterson, A. M., ibid. **20** (1949), 475.
§ Hawkins, G. S., and Almond, M., *Mon. Not. Roy. Astr. Soc.* **112** (1952), 219.

Complete details for one (No. 689) have been given by Whipple† and the velocities, decelerations, and heights for nine others by Jacchia.‡ These are listed in Table 97.

TABLE 97

Perseid Velocities Photographically determined by the Double-camera Method

Harvard serial number	*Date*	*Velocity*
		km./sec.
689	1937 Aug. 15·2565	61·188
978	1940 ,, 8·19	59·95
1089	1941 ,, 11·30	59·88
1173	1942 ,, 5·18	59·76
1377	1943 ,, 7·27	60·88
1273	1945 ,, 11·34	59·23
1273	1945 ,, 11·34	58·83
1275	1945 ,, 12·32	60·04
1276	1945 ,, 12·35	58·54
1469	1947 ,, 13·24	60·21

The close agreement of these ten velocities, with a mean value of 59·85 km./sec., is in striking contrast to the wide scatter of those determined by visual observations (Table 96).

Ceplecha§ has given details of a Perseid photographed at three stations in Czechoslovakia, the velocity being 59·646 km./sec., in excellent agreement with the results of Table 97.

Radio-echo measurements of the velocities have recently been made in America, Canada, and Great Britain. One accurately determined velocity using a three-station 'moving-head' Doppler technique (see Chap. IV) has been discussed by McKinley.‖ This Perseid was recorded on 1949 August 11. The mean value from the moving-head records was 59·8 km./sec. and from the Doppler records 58·3 km./sec. The velocities at the beginning and end of the recorded path were 61·0 and 58·5 km./sec. respectively. These results are in excellent agreement with the photographic determinations listed in Table 97.

Manning, Villard, and Peterson†† used the Doppler technique at Stanford during the night of 1948 August 11–12 and measured sixty velocities,

† Whipple, F. L., *Proc. Amer. Phil. Soc.* **79** (1938), 499.

‡ Jacchia, L. G., *Tech. Rep. Harv. Coll. Obs.* (1948), no. 2 (Harvard Reprint Series II–26).

§ Ceplecha, Z., *Bull. Cent. Astr. Inst. Czech.* **2** (1951), no. 8, 114.

‖ McKinley, D. W. R., *J. Appl. Phys.* **22** (1951), 202.

†† Manning, L. A., Villard, O. G., and Peterson, A. M., *J. Appl. Phys.* **20** (1949), 475. (*Stanford Technical Rep.*, Sept. 30, 1948, no. 7).

TABLE 96

Visual Velocity Measurements of Possible Perseid Meteors

I. *From multiple observations*

Date	*Radiant* α *deg.*	δ *deg.*	*Measured velocity km./sec.*	*Theoretical parabolic velocity km./sec.*
1899 Aug. 9	41	+58	71	61
10	43	53	36	64
10	44	58	104	61
10	42	56	68	62
1924 Aug. 2	53	58	40	59
5	37	55	29	62
1932 Aug. 11	53	50	34	65
11	46	59	45	61
11	55	58	39	60
11	46	57	49	62
11	48	44	40	68
11	66	47	45	65
11	49	54	52	63
11	50	52	42	64
11	34	60	37	60
11	38	55	116	62
11	52	56	63	62
1939 Aug. 11	58	58	48	60
11	45	55	41	62
1940 Aug. 10	38	38	45	69
				Mean of multiples = 52 km./sec.

II. *From duplicate observations*

1877 Aug. 7	55	55	80	62
10	43	52	47	64
10	56	65	220	57
1895 Aug. 11	49	60	61	60
11	37	57	56	61
11	33	52	29	63
1897 Aug. 8	52	46	50	66
9	49	55	146	62
1898 Aug. 10	54	23	120	72
10	48	52	45	64
11	47	55	60	63
11	53	56	61	62
11	48	58	63	61
1899 Aug. 6	41	57	50	61
11	45	58	81	61
11	45	57	69	62
14	53	47	36	67
1901 Aug. 15	53	53	62	64
1902 Aug. 12	61	56	61	62
1922 July 28	36	43	45	66
30	38	45	60	66
Aug. 15	50	74	18	52
1923 Aug. 10	42	58	55	61
11	48	53	48	64
12	42	58	42	61
13	50	58	63	61
1924 July 31	38	49	28	64
				Mean of duplicates = 65 km./sec.

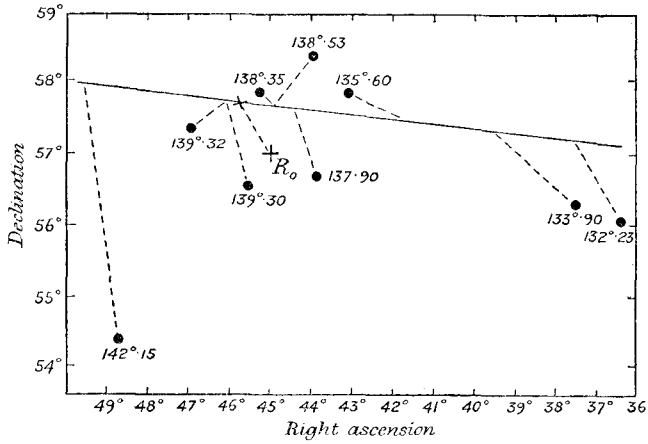

FIG. 138. The radiant positions of nine doubly photographed Perseid meteors, showing the daily motion of the mean radiant (full line). Each radiant is plotted in its actual position and joined by a broken line to the point on the mean path which corresponds to the time of observation of the meteor. The sun's longitude is given for each observation ($\odot = 139° \equiv$ Aug. 12). R_0 is the mean radiant position.

(d) Velocities

The analysis of the visual meteor data collected by Porter† gives 47 cases of possible Perseid velocities as listed in Table 96. There are 20 determinations from multiple observations and 27 from duplicate observations.

The mean velocity from the multiple observations is 52 km./sec. and from the duplicate observations 65 km./sec. In his analysis of the data Porter‡ later gives a mean value of 43·4 km./sec. for 152 Perseids occurring within the time limits of July 22 and August 19; but the individual details of the reductions additional to the forty-seven listed in Table 96 are not given. This figure of 43·4 km./sec. for the Perseid velocity is also quoted by Prentice§ as the result of the British visual measurements.

The velocities of two Perseid meteors were measured in the photographic work of Millman and Miss Hoffleit‖ using the rotating-shutter technique described in Chapter XI. The velocities were 50 and 41 km./sec.; they regarded the low values as due to retardation in the earth's atmosphere.

The velocities of several Perseid meteors have been accurately determined by Whipple and by Jacchia using the double-camera technique.

† Porter, J. G., *Mon. Not. Roy. Astr. Soc.* **103** (1943), 134.
‡ Porter, J. G., ibid. **104** (1943), 20.
§ Prentice, J. P. M., *Rep. Phys. Soc. Prog. Phys.* **11** (1948), 389.
‖ Millman, P. M., and Hoffleit, D., *Ann. Harv. Coll. Obs.* **105** (1937), 601.

indicated in Table 95. The radio-echo observations† of the radiant position, also given in Table 95 for 1950, 1951, and 1952, show a considerable scatter about these mean positions. This is to be expected in a diffuse radiant with active subcentres, since the radiant position is determined for only a short period during the passage of the radiant through the beam. The mean radiant assigned by Prentice‡ for the

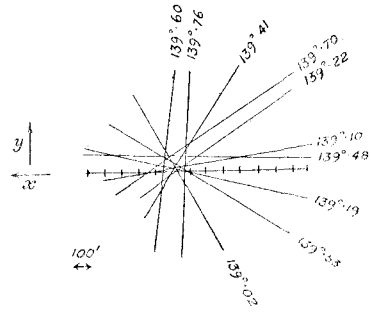

FIG. 137. The paths of ten Perseid trails photographically recorded near the time of maximum between ⊙ = 139°·02 and 139°·76.

period of the maximum is α 44°, δ +58° and it is classed as 'diffuse'. On the other hand, in a preliminary account of the photographic work on the Perseid meteors, Whipple§ states that at the time of maximum the radiation is from a relatively small area of the sky. This is well illustrated in Fig. 137, which shows the paths of ten trails photographically recorded between solar longitude 139°·02 and 139°·76.

The data for nine doubly photographed Perseid meteors have been given by Whipple,§ and the results are plotted in Fig. 138. The radiant motion is clearly in evidence. Whipple's values for the daily motion are $\Delta\alpha = +0°{\cdot}7$ per day, $\Delta\delta = +0°{\cdot}1$ per day. The inclusion of forty-nine singly photographed Perseid trails indicates the possibility of there being two moving Perseid radiants, the major one after August 7 and a minor one before August 9, but more observations are needed to verify this duplicity. The daily motion of the radiant from the smoothed radio-echo data is $\Delta\alpha = +0°{\cdot}6$, $\Delta\delta = +0°{\cdot}1$, in agreement with Whipple's value but differing from the values of $\Delta\alpha = +1°{\cdot}3$, $\Delta\delta = +0°{\cdot}3$ given by Denning.

† Hawkins, G. S., and Almond, M., *Mon. Not. Roy. Astr. Soc.* **112** (1952), 219 (except data for 1952 which are unpublished).

‡ B. A. A. Handbooks.

§ Whipple, F. L., *Sky and Telescope*, **6** (1947), no. 10, 10.

Olivier† assigns the credit for this discovery to Twining‡ although Denning's§ great series of observations showed that the motion existed over a considerable period of time, placing the matter beyond dispute. Discussions of the motion of the Perseid radiant have been given by Denning§ and by King.‖ Table 95 compares the average positions given

TABLE 95

Radiant Positions of the Perseid Shower

Date	*Visual*						*Radio-echo*					
	King		*Denning*		*Öpik*		1950		1951		1952	
	α	δ	α	δ	α	δ	α	δ	α	δ	α	δ
	deg.	*deg.*	*deg.*	*deg.*	*deg.*	*deg.*	*deg.*	*deg.*	*deg.*	*deg.*	*deg.*	*deg.*
July 27	25	+52	27·1	+53·2	..		..		..		..	
28	28	53	28·2	53·5	..		..		..		..	
29	..		29·3	53·8	..		28	+52	..		..	
30	..		30·5	54·1	..		31	56	..		..	
31	..		31·6	54·4	..		40	58	..		..	
Aug. 1	..		32·7	54·7	..		38	56	..		..	
2	..		33·9	55·0	..		42	55	..		..	
3	34·8	56	35·1	55·3	..		..		40	+60	41	+57
4	36	57	36·4	55·5	..		..		42	63	39	61
5	..		37·6	55·7	..		..		..		..	
6	38	56·5	38·9	56·0	..		33	52	39	50	39	56
7	..		40·2	56·2	38	+56	39	59	45	53	41	58
8	..		41·5	56·5	..		42	57	43	57	39	62
9	42	57	42·9	56·7	41	56	43	56	43	57	42	57
10	44	57·2	44·3	56·9	40	56	44	57	47	59	44	55
11	45·4	57·4	45·7	57·1	36–42	56–58	45	61	49	46	44	58
12	47·1	57·5	47·1	57·3	38	56	46	57	46	57	48	61
13	47·7	58·3	48·5	57·5	40	57	51	59	44	60	49	59
14	48·9	58·3	50·0	57·7	..		52	61	48	58	54	59
15	50·5	58·5	51·4	57·8	..		51	62	37	58	..	
16	..		52·9	58·0	..		49	56	55	59	..	
17	..		54·4	58·2	..		47	52	43	50	..	

by Denning and King, from which it will be seen that the general position and motion are well established. As a result of the observations in 1921, Öpik†† referred to the fact that the radiant covered a considerable area and gave the mean radiants as listed in Table 95. According to Prentice,‡‡ contemporary visual observations show that the Perseid radiant is very diffuse, with a diameter of 10–15°, the centre of which moves roughly as

† Olivier, C. P., *Meteors*, ch. 5.

‡ Twining, A. C., *Amer. J. Sci.* (*II*), **32** (1861), 444.

§ Denning, W. F., *Mem. Roy. Astr. Soc.* **53** (1899), 203; *Mon. Not. Roy. Astr. Soc.* **62** (1901), 161.

‖ King, A., *Mon. Not. Roy. Astr. Soc.* **76** (1916), 542; **88** (1927), 113.

†† Öpik, E. J., *Publ. Tartu. Obs.* **25** (1923), no. 4.

‡‡ Prentice, J. P. M., private communication.

TABLE 94

Hourly Rate of the Perseid Stream since 1900

Year	*Aug.* 10	*Aug.* 11	*Aug.* 12	*Aug.* 13
1901	55	49	..	..
1902	15	..	..	60
1903	..	..	30	..
1904	92	37	..	..
1906	10	..	..	..
1907	71	30	..	..
1908	15	..	..	..
1909	12	67	..	..
1910	46	..	..	..
1911	2	1	..	..
1912	2	12	..	..
1915	..	..	23	..
1920	(78)	(196)	(77)	(44) Öpik†
1921	(33)	(250) 250	(93)	(43) Öpik†
1924	weak	..	..	..
1925	weak	..	..	..
1926	average	..	..	..
1927	weak	..	..	..
1928	..	33	..	..
1929	weak	..	..	..
1930	weak	..	..	..
1931	..	73	64 (160)	Olivier gives 160
1932	24	48	..	Prentice‡
1933	weak	..	..	..
1934	18	29	..	Prentice‡
1935	19	..	..	,,
1936	..	..	12	,,
1939	13	35	25	,,
1940	18	29	..	,,
1946	..	..	23	Radio-echo data§
1947	(18)	(23)	(46) 26	(27) ,, ,,
1948	..	..	(21) 57	(10) ,, ,,
1949	..	..	57	,, ,,
1950	(14) 24	21	64	(16) 59 ,, ,,
1951	31	37	(44) 32	33 ,, ,,
1952	22	39	50	36 ,, ,,
1953	22	26	37	22 ,, ,,

† The values in parentheses for 1920 and 1921 are those given by Öpik, E. J. (*Publ. Tartu Obs.* **25** (1922–4), nos. 1 and 4), obtained by his statistical double count method. The rates are therefore not strictly comparable with those given elsewhere, which are the unreduced rates for a single observer. Even so, there is no doubt from the records of many other observers that the shower of 1921 was exceptionally strong.

‡ From observations of the British Astronomical Association privately communicated by J. P. M. Prentice.

§ The values in parentheses are from the visual records of the B.A.A. (see ‡).

1920, of the radio-echo observations† made in 1950, and of contemporary visual observations.‡ (The change of the epoch of maximum with date is apparent only. All maxima coincide when the scale is reduced to solar longitude.) The identity of the stream before July 28 and after August 17 is uncertain. Bredikhine§ first questioned the reality of these Perseid radiants derived from such low hourly rates at a time of the year when the activity is so complex. Since the visible sporadic rate in late July is about 20 per hour, it is evident that the observations of the Perseid stream when the hourly rate is less than about three or four cannot have great significance.

Even though the Perseid display is regarded as being constant in hourly rate, there have nevertheless been some significant changes. The 'normal rate' for a single observer under good sky conditions is generally given as about 50 per hour; but there have been several notable occurrences, the last of which, in 1921, gave an hourly rate of 250. On other occasions the returns have been very poor, particularly in 1911 and 1912, when, with only a few per hour, Denning‖ suggested that the shower might have disappeared.

Table 94 gives the hourly rate of the shower since 1900 as far as the data can be extracted from the very dispersed references. Where bad sky conditions or moonlight interfered with the observations, the observers estimate of the hourly rate has been quoted. Except where otherwise indicated, the results are those obtained by the observers of the British Astronomical Association.†† Various predictions have been made regarding a periodicity in the shower. For example, Denning‡‡ tabulated all the accounts of the ancient and modern displays of the Perseids going back to A.D. 714 July and decided that a period of 11·72 years was suggested by these observations. He predicted future maxima in 1932·88, 1944·60, 1956·32, 1968·04, but there is no evidence for any unusual return of the shower on the first two of these dates.

(c) *Radiant*

Early studies of the radiant position of the Perseids are unique in that they first demonstrated clearly the daily motion of a radiant point.

† Hawkins, G. S., and Almond, M., *Mon. Not. Roy. Astr. Soc.* **112** (1952), 219.
‡ Hawkins, G. S., measurements for 1944–7.
§ Bredikhine, T., *Bull. Imp. Nat. Moscow*, **1** (1888).
‖ Denning, W. F., *Observatory*, **35** (1912), 337.
†† Abstracted from the Memoirs and Journals of the British Astronomical Association.
‡‡ Denning, W. F., *Mon. Not. Roy. Astr. Soc.* **84** (1923), 45; **84** (1924), 178.

was first recognized in the period 1830–40 by Quételet, Herrick, and others, since when the shower has been observed systematically. The shower is particularly noteworthy because the computation of its orbit by Schiaparelli† between 1864 and 1866 led to the establishment of the connexion between it and Comet 1862 III, this being the first occasion on which any plausible relation was established between meteors and other celestial objects.

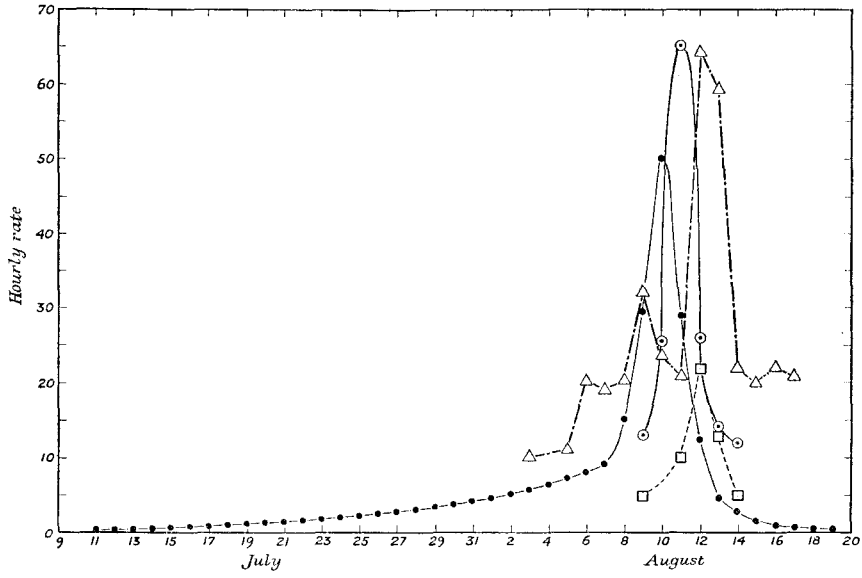

FIG. 136. Epoch of maximum of the Perseid meteor shower. –●–● Observations by Denning, 1869–98. –⊙–⊙ Observations by Öpik, 1921. (The ordinates of Öpik's hourly numbers have been reduced by 3 for ease of comparison, see footnote to Table 94.) △–△– Radio-echo observations, 1950. –□–□– Visual observations, 1944–7.

(*b*) *Activity*

One of the most complete investigations of the Perseid shower was made by Denning‡ during the years 1869–98. Between the dates of July 11 and August 19 he observed 6,479 meteors, 2,409 of which he identified as members of the Perseid stream, with hourly rates as shown in Fig. 136. The motion of the radiant point during this period will be referred to in (*c*). Subsequent observations have confirmed the general shape of the epoch of maximum as given by Denning. For example, Fig. 136 also gives the results of Öpik's§ observations made in Esthonia in

† Schiaparelli, G. V., *Sternschnuppen.*
‡ Denning, W. F., *Astr. Nachr.*, no. 3546.
§ Öpik, E. J., *Publ. Tartu Obs.* **25** (1922), no. 1.

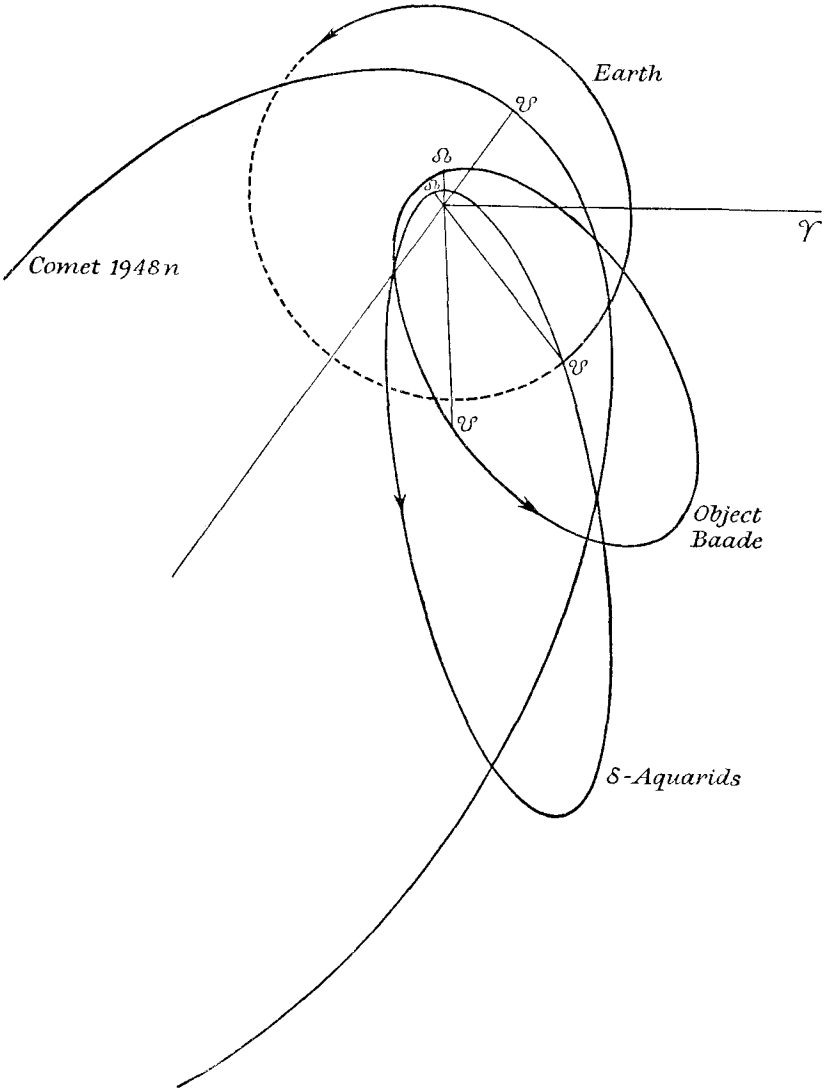

FIG. 135. The orbit of the δ-Aquarid stream, computed from the radio-echo observations by Miss Almond. The orbits of comet 1948 n and of Baade's object 1566 Icarus are shown for comparison. Projection is on the plane of the ecliptic.

from August 10–13 each year. It also extends for a considerable time on either side of the maximum with reduced hourly rates. The history of the shower, which can be traced back for over 1,200 years, has been described by Olivier.† The existence of the regular display in August

† Olivier, C. P., *Meteors*, ch. 5.

measurements and the McIntosh radiant. The various results are given in Table 93.

TABLE 93

Orbital Elements for the δ-Aquarid Meteor Stream

	Ω	π	ω	i	e	q	a	*Velocity heliocentric*
	deg.	*deg.*	*deg.*	*deg.*		*a.u.*	*a.u.*	*km./sec.*
McIntosh (1934 July 28) . .	304·7	104·3	..	55·8	1·0	0·0393	..	assumed parabolic
Watson .	305	..	..	56	1·0	0·039	..	assumed parabolic
Hoffmeister (Aug. 3) .	310·0	97·0	147·0	23·7	0·9264	0·118	1·5995	34·64
Lindblad (July 29) .	305·6	..	152·2	28·4	0·956	0·080	1·807	35·4
Almond (July 28) .	304·6±1	101±2	156±2	24±5	0·96±0·2	0·06± 0·015	1·5+0·6 −0·3	..
Comet 1948 n	233·0	..	183·8	13·25	0·809	0·558	2·922	..
1566 Icarus	87·777	..	30·875	23·02	0·82697	0·187	1·0784	..

The orbits given by Lindblad and Miss Almond are very similar, and since they are based on actual velocity measurements they must be regarded as significant. The errors given in Table 93 for Miss Almond's orbit indicate the effects of the spread in the measured velocity. The mean orbit, projected on to the plane of the ecliptic, is shown in Fig. 135. This orbit is very similar to that of a prominent day-time stream—the Arietids —and the relationship between the two will be discussed in Chapter XVIII. On account of the very elliptical nature of the orbit, there are few bodies in the solar system with which the stream is likely to be associated. Rigollet† suggested that the shower might be associated with Comet 1948 n which has a markedly elliptical orbit, but the closest approach is 0·22 a.u. and the association does not seem plausible. Rigollet‡ has also suggested that the stream may be associated with the minor planet 1566 Icarus discovered on 1949 June 26 by Baade. The orbital elements for the comet and for Baade's object are tabulated in Table 93 and also shown in Fig. 135 for comparison with the δ-Aquarid orbit.

2. The Perseid shower

(*a*) *History*

The Perseid meteor shower is one of the most regular visible meteoric events, yielding hourly rates of about 50 over the period of maximum

† Rigollet, R., *Ann. d'Astrophys.* **14** (1951), no. 2.

‡ Rigollet, R., *Documentation des Obs. Inst. d'Astrophys.* **6** (Paris, 1952).

the δ-Aquarid velocities using the Jodrell Bank technique. There were 155 velocities measured using a dipole aerial in the period 1952 July 26–29, but the stream was not sufficiently prominent over the sporadic background to yield a measurable velocity group. On the other hand, with the more directive aerials of equipment IV (Chap. XII), used during transit of the δ-Aquarid radiant between 02h. and 03h. on 1952 July 28, 29, thirty-seven velocities were measured with a prominent group

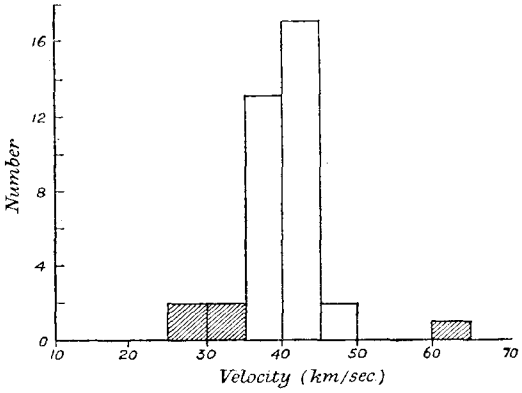

FIG. 134. The velocity distribution of δ-Aquarid meteors as measured by the radio-echo technique.

as shown in Fig. 134. Thirty-five of the velocities were between 35 and 49 km./sec. with a mean of 40·5±2·7 km./sec. The remaining five, which are shown shaded in Fig. 134, had large deviations from the root mean square value and were probably sporadic. In order to show that the grouping was characteristic of the δ-Aquarid shower, a check experiment was made under similar conditions on 1952 August 8. No grouping of velocities was found.

(e) Orbit

Orbital elements for the δ-Aquarid stream have been given by McIntosh† and Watson,‡ assuming a parabolic velocity, and by Hoffmeister,§ assuming his indirectly derived value for the heliocentric velocity of 34·6 km./sec. Orbits based on the actual velocity measurements have been calculated by Lindblad,‖ using McKinley's velocity and the McIntosh radiant, and by Miss Almond,†† using her own velocity

† McIntosh, R. A., loc cit. (1934).
‡ Watson, F., *Between the Planets* (Blakiston).
§ Hoffmeister, C., *Meteorströme* (Weimar, 1948).
‖ Lindblad, B. A., loc. cit.
†† Almond, M., loc. cit.

McIntosh, the spread of the radiant is very small.† The daily movement of the radiant point by about one degree in right ascension is well marked.

(*d*) *Velocities*

There are few published velocity measurements for the δ-Aquarid shower. For example, all the visual data collected by Porter‡ yield only six measurements of possible δ-Aquarid velocities and these are spread over a very wide range, as shown in Table 92.

TABLE 92

Visual Velocity Measurements of possible δ-Aquarid Meteors

Date	*α*	*δ*	*Measured velocity*	*Theoretical parabolic velocity*
	deg.	*deg.*	*km./sec.*	*km./sec.*
1898 July 30	340	−21	55	46
1898 Aug. 11	343	−12	19	43
1899 Aug. 1	336	−16	32	44
1923 Aug. 2	346	−16	74	49
1924 July 24	317	−27	14	37
1924 July 29	333	−16	30	44

Prentice§ quotes a mean observed velocity of 29 km./sec., but the sources of the individual data are not given. The theoretical parabolic geocentric velocity for the six possible δ-Aquarids is given in column 5 of Table 92.

The value given by Prentice§ of 29 km./sec. for the geocentric velocity corresponds to a heliocentric velocity of 32 km./sec. Hoffmeister‖ quotes a heliocentric velocity of 34·6 km./sec. McIntosh†† calculated a value of 54·1 km./sec. (that is a hyperbolic orbit) from the zenith attraction of the radiant. However, Davidson‡‡ later showed that the method used by McIntosh for calculating the velocity was incorrect.

Recently it has been possible to measure the velocity of the shower by the radio-echo technique. Thus in the work on the sporadic distribution McKinley§§ gives a velocity distribution for the period 1949 July 26–29 with a sharp peak centred at 40·41 km./sec. (Fig. 114, Chap. XII). Miss Almond‖‖ has also given the results of a specific experiment to measure

† Whipple, F. L., *Sky and Telescope*, **6** (1947), no. 70, 10, states that unpublished photographic results indicate that the radiant is diffuse.
‡ Porter, J. G., *Mon. Not. Roy. Astr. Soc.* **103** (1943), 134.
§ Prentice, J. P. M., *Phys. Soc. Rep. Prog. Phys.* **11** (1948), 389.
‖ Hoffmeister, C., *Meteorströme* (Weimar, 1948).
†† McIntosh, R. A., *Mon. Not. Astr. Soc.* **96** (1936), 704.
‡‡ Davidson, M., ibid. **97** (1937), 75.
§§ McKinley, D. W. R., *Astrophys. J.* **113** (1951), 258.
‖‖ Almond, M., *Jodrell Bank Annals*, **1** (1952), 22.

(c) *Radiant*

The most complete radiant data are those given by McIntosh† from the observations made in New Zealand between 1926 and 1933 and shown in Table 91. Also tabulated for comparison are the radiant coordinates given by Hoffmeister.‡ Hoffmeister states that the radiant is very diffuse and that the concentration does not greatly differ over 20°. The radiant is unfavourably placed for radio-echo determinations in the northern hemisphere, but the following information given by Hawkins and Miss Almond§ may be compared with Table 91.

$\odot$ (1950) 124°·5 $\alpha = 339°$, $\delta = -14°$, diam. 3°.

$\odot$ (1951) 123°·4 $\alpha = 336°$, $\delta = 0°$, diam. 6°.

TABLE 91

Radiant Coordinates of the δ-Aquarid Stream

Date	$\odot$ 1951	*McIntosh*		*Hoffmeister*	
		α	δ	α	δ
		deg.	*deg.*	*deg.*	*deg.*
July 22	118° 22′	334·9	−19·2	..	..
23	119 19	335·8	18·8	..	..
24	120 17	336·8	18·4	..	..
25	121 14	337·7	18·1	..	..
26	122 11	338·6	17·7	333·0	−13·0
27	123 09	339·6	17·4	..	..
28	124 06	340·5	17·0	..	..
29	125 03	341·4	16·6	..	..
30	126 01	342·4	16·3	..	..
31	126 58	343·3	15·9	..	..
Aug. 1	127 55	344·3	15·9	342·4	−17·7
2	128 53	345·1	15·1	..	..
3	129 50	346·0	14·8	..	..
4	130 48	346·9	14·4	..	..
5	131 45	347·8	14·0	..	..
6	132 43	348·7	13·6	341·5	−17·2
7	133 40	349·7	13·1	..	..
8	134 38	350·6	12·7	..	..
9	135 35	351·5	12·2	346·5	−16·5
10	136 33	352·4	11·8	..	..

The various observations are in reasonable agreement, but undoubtedly the greatest weight must be attached to the New Zealand observations where the radiant appears near the zenith, and where, according to

† McIntosh, R. A., loc. cit.

‡ Hoffmeister, C., *Meteorströme* (Weimar, 1948), ch. 9.

§ Hawkins, G. S., and Almond, M., loc. cit.

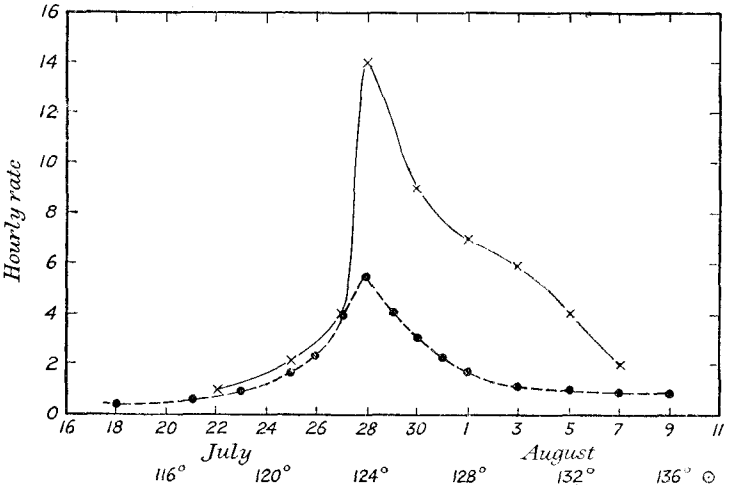

FIG. 133. The epoch of maximum of the δ-Aquarid shower.
–●– –●– – Denning 1869–98. –×–×– McIntosh 1926–33.

maximum is shown at ⊙ = 122° (July 26); hence it is not possible to attach any significance to this discrepancy. Moreover, the recent radio-echo observations† give data in agreement with the Denning–McIntosh results as follows:

Maximum	⊙	*Hourly rate* (*see note in text*)
1949 July 29	125°·8	24
1950 July 28	124°·5	38
1951 July 27	123°·4	41

As regards the hourly rate given by the radio-echo observations, owing to the low declination of the radiant it was not possible to separate the δ-Aquarid stream from the appreciable sporadic background rate. Hence these figures include both the sporadic and δ-Aquarid rates, and are to be compared with the total rates given by McIntosh,‡ at the maximum, of 34 per hour. Lindblad§ has published details of some radio-echo observations of the δ-Aquarid shower made in 1950. He interprets the results as indicating a maximum on July 28–29 in agreement with the visual results, but he also finds evidence that a large number of very faint δ-Aquarids crossed the earth's orbit 3·5 days before the main stream. Lindblad attributes this separation to the Poynting–Robertson effect (see Chap. XX).

† Hawkins, G. S., and Almond, M., *Mon. Not. Roy. Astr. Soc.* **112** (1952), 219.
‡ McIntosh, R. A., loc. cit.
§ Lindblad, B. A., *Meddl. fr. Lunds Astronom. Obs.* (1950), Ser. I, no. 179 (1952).

XIV

THE MAJOR METEOR SHOWERS—II

THE PERMANENT STREAMS OF JULY AND AUGUST

AFTER the η-Aquarid shower in early May, the night-time activity remains very low until late July, the major events being concentrated in the day-time sky (Chapter XVIII). The period of late July and August is, however, one of the richest of the whole year, and contains two major showers (the δ-Aquarids and the Perseids) and a large number of streams of a minor character, some of which—such as the α-Capricornids, Cygnids, and Lacertids—are the best known and the most active of the minor streams.

1. The δ-Aquarid shower

(a) History

The δ-Aquarids attain a maximum about July 28. The shower has a low declination and is most readily observed in the southern hemisphere—it is, in fact, perhaps the most prominent of the showers visible in the southern hemisphere. In his records of ancient showers, Newton† lists two (A.D. 784 July 14 and A.D. 714 July 19) which correspond to the epoch of the δ-Aquarids (1850 July 29 and 1850 August 2 respectively) and which Olivier‡ considers to be notable past occurrences of this shower. Apart from this, there are no records of unusual occurrences of the shower during the period of its observation by trained observers since the second half of the nineteenth century.

(b) Activity

Plots of the hourly rate of the shower according to observations made by Denning§ in the northern hemisphere between 1869 and 1898, and by McIntosh‖ in New Zealand between 1926 and 1933 are shown in Fig. 133. Both sets of observations agree in showing a rather rapid rise to maximum on July 28 followed by a slow decrease. Information on the shower has also been given by Hoffmeister,†† who, whilst agreeing with the general trend of the activity as shown in Fig. 133, places the maximum at $\odot = 130°$ (August 3). In the accompanying diagram,‡‡ however, the

† Newton, H. A., *Amer. J. Sci.* (*II*), **36** (1863), 145; **37** (1864), 378.
‡ Olivier, C. P., *Meteors*, ch. 5 (1925).
§ Denning, W. F., *Mem. Roy. Astr. Soc.* **53** (1899), 203.
‖ McIntosh, R. A., *Mon. Not. Roy. Astr. Soc.* **94** (1934), 583.
†† Hoffmeister, C., *Meteorströme* (Wiemar, 1948), ch. 9.
‡‡ Hoffmeister, C., ibid., ch. 9, fig. 29.

same major axis as Halley's Comet. Also given in Table 90 are the orbital elements calculated by Hoffmeister† for the meteor stream, and those calculated by McIntosh‡ from the New Zealand observations.

Olivier, Hoffmeister, and McIntosh considered that the elements of the orbit as given in Table 90 were in good enough agreement to justify the belief that the meteor stream is associated with Halley's Comet, and it was believed that the Orionids (see Chapter XV) were also associated with this comet. Recently, however, Miss Almond§ has computed the orbit of the stream on the basis of the velocity indicated by the radio-echo measurements referred to above, 64 km./sec. Taking the radiant as α 338°, δ $\pm$0° on May 4, the orbital elements are given in Table 90, and the orbits are plotted in Fig. 132. The period of the shower appears to be 11 years, that is only about one-seventh of that of Halley's Comet. The orbit is, however, closely aligned with that of the comet after perihelion. At the ascending node the calculated orbit again passes close to the orbit of the earth on November 21, that is a month later than the date of the Orionid shower. Further velocity determinations of greater accuracy are evidently necessary before this interesting situation can be fully clarified.

† Hoffmeister, C., *Astr. Nachr.* **196** (1913), 309.
‡ McIntosh, R. A., loc. cit.
§ Almond, M., Jodrell Bank, unpublished.

Recently a certain amount of information on the η-Aquarid velocities has been obtained from the radio-echo measurements. In 1951 Hawkins and Miss Almond† measured three η-Aquarid velocities as 63·7, 63·0, and 58·8 km./sec. Also, in the velocity measurements made by McKinley‡ and discussed in Chapter XII, a peak in the distribution between 1949 May 3 and 5 (Fig. 114) can be identified with the η-Aquarid shower, and indicates a mean velocity of 64 km./sec.

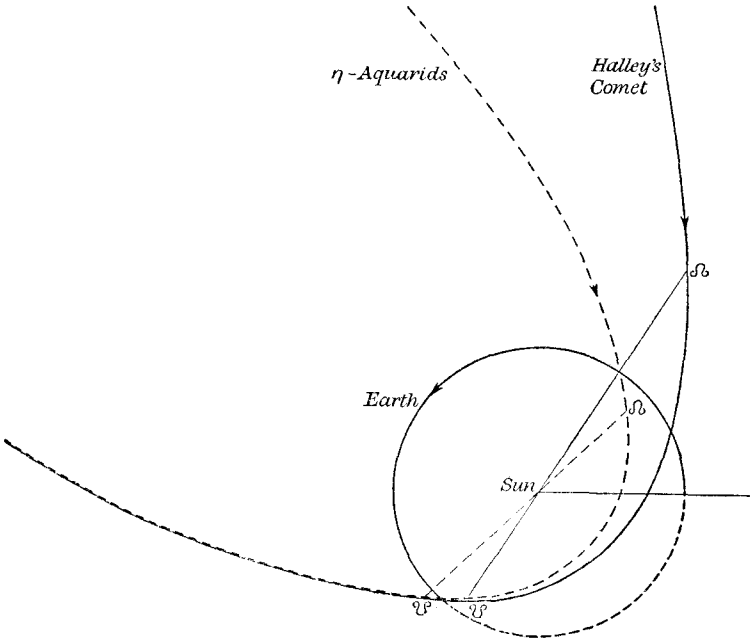

FIG. 132. The orbit of the η-Aquarid meteor stream, as calculated by Miss Almond from the radio-echo data, compared with the orbit of Halley's Comet.

(e) Orbit

Full details of the discussions which centred around the orbit of the η-Aquarid stream and its relation to Halley's Comet have been given by Olivier.§ Table 90 gives Olivier's results for the orbital elements of the stream, these being a weighted mean of the elements computed for eight radiants derived from observations of about ninety meteors. The elements are calculated in two ways: firstly by assuming a parabolic velocity for the meteors, and secondly by assuming that they have the

† Hawkins, G. S., and Almond, M., *Jodrell Bank Annals*, **1** (1952), 22.
‡ McKinley, D. W. R., *Astrophys. J.* **113** (1951), 225.
§ Olivier, C. P., *Meteors*, ch. 8.

TABLE 90

Orbital Elements of the η-Aquarid Shower compared with Halley's Comet

	Assuming parabolic orbit					*Assuming same major axis as the Comet*						
	☊	ω	π	i	q	☊	ω	π	i	q	e	a
	deg.	*deg.*	*deg.*	*deg.*	*a.u.*	*deg.*	*deg.*	*deg.*	*deg.*	*a.u.*		*a.u.*
Halley's Comet . . .	..	..	..	..	..	57·3	111·7	169·0	162·2	0·5871	0·9673	17·946
Olivier (1900–13) . . .	45·0	108·4	153·4	161·8	0·664	45·0	108·1	152·0	162·0	0·658	0·9638	17·947
Hoffmeister (1913) . . .	..	..	..	..	..	45·2	99·7	144·9	162·6	0·595	0·967	17·946
McIntosh (1929) . . .	..	..	..	..	..	46·1	95·1	141·3	161·7	0·553	0·969	17·947
McIntosh (1935) . . .	..	..	..	..	..	43·6	97·3	140·9	162·2	0·5616	0·9687	17·946
Almond (1951), assuming v = 64 km./sec. and α 338°, δ ±0° .	..	..	..	..	..	43·1	83·0	126·1	160·0	0·47	0·91	5·0

the radiant is a very clear case of one in daily motion. From weighted means of the New Zealand observations referred to previously, McIntosh† has given the ephemeris in Table 89 for the movement of the radiant. The observations of Hoffmeister, and the radio-echo measurements referred to in (*b*) all give similar results for the coordinates.

TABLE 89

Ephemeris of the η-Aquarid Radiant

Date	α	δ	*Date*	α	δ
1935	*deg.*	*deg.*	1935	*deg.*	*deg.*
April 28	330·4	−3·1	May 8	339·3	+0·2
29	331·3	−2·8	9	340·2	+0·6
30	332·2	−2·5	10	341·0	+1·0
May 1	333·1	−2·2	11	341·9	+1·3
2	334·0	−1·9	12	342·8	+1·7
3	334·8	−1·6	13	343·7	+2·1
4	335·7	−1·3	14	344·6	+2·5
5	336·6	−0·9	15	345·5	+2·9
6	337·5	−0·5	16	346·4	+3·3
7	338·4	−0·1			

(*d*) *Velocities*

There is scarcely any published information on the velocity of meteors of the η-Aquarid stream. The paucity of data is well illustrated by the fact that in the entire published data of the British Astronomical Association since 1890 only two doubly observed η-Aquarid meteors are listed.‡ The first was a very bright meteor observed on 1900 May 3. The data were reduced both by Denning and by Herschel with the following results:

Denning α 337°, δ ±0° v = 45 km./sec.

Herschel α 335°, δ −2° v = 37 to 43 km./sec.

More recently, Porter§ has corrected the data and gives

α 327°, δ +6° v = 38 km./sec.

For the second, observed on 1921 May 4, Porter gives

α 308°, δ +10° v = 68 km./sec.

The theoretical parabolic velocities, calculated from the elongations, are 68 and 67 km./sec. respectively.

† McIntosh R. A., loc. cit.

‡ *Mem. Brit. Astr. Ass.* **10** (pt. i) (1901); Porter, J. G., *Mon. Not. Roy. Astr. Soc.* **103** (1943), 134.

§ Porter, J. G., loc. cit.

Africa. Owing to the lack of knowledge about sky conditions and corrections for radiant altitude, no significance can be attached to the difference in hourly rates. Both series of results, which are plotted in Fig. 131, indicate that the maximum is attained between May 4 and May 6, that is between $\odot = 43°$ and $\odot = 45°$. The data are summarized in Table 88 together with the results of radio-echo observations in the northern hemisphere since 1947, which confirm this epoch of maximum.

TABLE 88

Epoch of Maximum of the η-Aquarid Shower

Date of maximum	*Sun's longitude* ⊙ *(deg.)*	*Hourly rate at maximum*	*Authority*
(1928–33) May 4–6	..	10	McIntosh†
1933 May 5	44	36	Hoffmeister‡
1947 May 4	43	7	Clegg, Hughes, and Lovell§
1949 May 8	47	10	Aspinall, Clegg, and Lovell‖
1950 May 6	45	12	Aspinall and Hawkins††
1951 May 1‡‡	40	16	Hawkins and Almond§§
1952 May 4	43·6	15	Almond, Bullough, and Hawkins‖‖

The shower evidently possesses a broad maximum, and the activity extends over a considerable time. For example, in 1929 McIntosh† identified meteors from this radiant from April 21 to May 12, which gives the breadth of the stream as about 35×10^6 miles. There is no information in any of the available results which indicates any marked annual changes in the activity of the shower.

(*c*) *Radiant*

An account of the early discussions on the radiant coordinates of the η-Aquarid shower has been given by Olivier.††† Some of the earlier determinations were vitiated because the observers took the mean for several successive nights, whereas Olivier‡‡‡ and Dole§§§ showed that

† McIntosh, R. A., loc. cit.

‡ Hoffmeister, C., loc. cit.

§ Clegg, J. A., Hughes, V. A., and Lovell, A. C. B., *Mon. Not. Roy. Astr. Soc.* **107** (1947), 369.

‖ Aspinall, A., Clegg, J. A., and Lovell, A. C. B., ibid. **109** (1949), 352.

†† Aspinall, A., and Hawkins, G. S., ibid. **111** (1951), 18.

‡‡ It seems likely that the early maximum in 1951 may be spurious, due to the masking of the radio-echo results by a transient stream, or by a grouping of sporadic radiants.

§§ Hawkins, G. S., and Almond, M., *Jodrell Bank Annals*, **1** (1952), 2.

‖‖ Almond, M., Bullough, K., and Hawkins, G. S., ibid. **1** (1952), 22.

††† Olivier, C. P., *Meteors*, ch. 8.

‡‡‡ Olivier, C. P., *Publ. Astr. Soc. Pac.* **22** (1910), 141.

§§§ Dole, R. M., *Observatory*, **44** (1921), 242.

sphere. There are no well-attested cases of any spectacular past occurrences of this shower, although Olivier† mentions that if the node were stationary the showers of A.D. 401 April 9 (≡ A.D. 1850 April 29), A.D. 839 April 17 (≡ A.D. 1850 April 30), A.D. 927 April 17 (≡ A.D. 1850 April 29), and A.D. 934 April 18 (≡ A.D. 1850 April 30) in Newton's lists‡ might possibly be past displays of η-Aquarids. Nevertheless, consider-

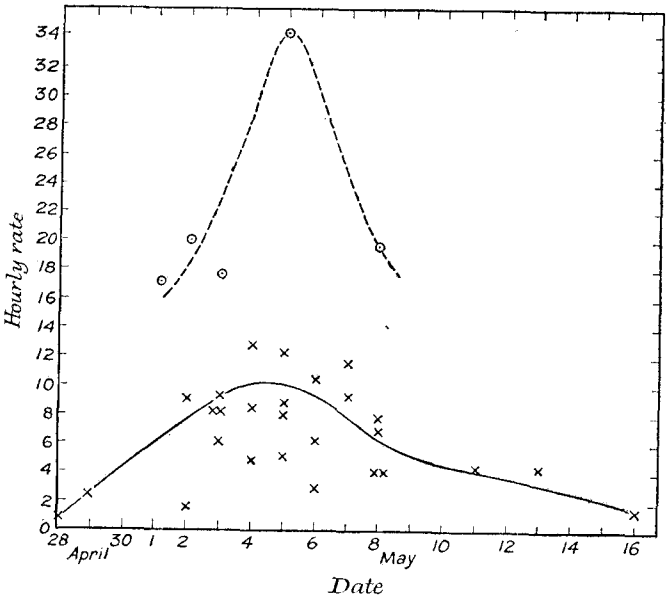

FIG. 131. Epoch of maximum of the η-Aquarid shower.
–×–× Observations from 1928 to 1933 by McIntosh in New Zealand.
–⊙–⊙ Observations in 1933 by Hoffmeister in South Africa.

able interest is attached to the shower because of its possible connexion with Halley's Comet. Various suggestions to this effect have appeared since 1868,§ but it will be seen in § 4 (c) that the contemporary view on this matter is somewhat undecided. On account of the low declination of the radiant, the shower cannot be readily observed in the northern hemisphere and most of the information about it comes from observations made in South Africa and New Zealand.

(*b*) *Activity*

The activity of the η-Aquarid stream has been established by the visual observations of McIntosh‖ in New Zealand, and of Hoffmeister†† in South

† Olivier, C. P., *Meteors*, ch. 8.
‡ Newton, H. A., loc. cit.
§ See Olivier, loc. cit., for a full account.
‖ McIntosh, R. A., *Mon. Not. Roy. Astr. Soc.* **90** (1929), 157; **95** (1935), 601.
†† Hoffmeister, C., *Meteorströme* (Weimar, 1948), ch. 8.

TABLE 86

Radio-echo Determinations of the Velocity of Lyrid Meteors

Date	*Velocity km./sec.*	*Reference*
1948 April 21	48	Millman and McKinley†
,, ,,	48	
,, ,,	50±3	
1948 April 22	47·0±2·0	Ellyett†
	46·5±3·0	
	46·1±0·4	
1949 April 21	49·0 (beginning)	McKinley†
	43·4 (end)	

(*e*) *Orbit*

As mentioned in (*a*) above, the close relationship between the Lyrid shower and Comet 1861 I was established through the work of Weiss, Pape, and Galle in 1867. The elements of the comet's orbit are given in Table 87, with the elements of the Lyrid orbit as originally computed by Galle,‡ together with the mean Lyrid orbit as derived from the contemporary radiant and velocity data presented in (*c*) and (*d*).

TABLE 87

Orbital Elements for Comet 1861 I and the Lyrid Meteor Shower

	Epoch	*Radiant*	☊	ω	i	e	q	*Velocity (geocentric)*	*Period (years)*
			deg.	*deg.*	*deg.*		*a.u.*	*km./sec.*	
Comet 1861 I	..	..	30·3	213·4	79·8	0·9835	0·9270	48	415
Galle's Lyrid orbit	1864 April 20	α 277·5° δ 34·6°	30	206	89	0·9829	0·955	..	?
Contemporary Lyrid orbit	1950 April 21	α 271° δ 31°	30·5	210	81	0·88	0·90	46·6	19·8

At the descending node, the comet approaches to within 0·002 a.u. of the earth's orbit, and the connexion of the Lyrid shower with the comet is highly probable. The great age for which the shower has been active is no doubt due to the high inclination (80°) of the orbit which makes planetary perturbations improbable.

4. The η-Aquarid shower

(*a*) *History*

The η-Aquarid shower occurs early in May with an hourly rate of about 10 in the northern hemisphere and 20–30 in the southern hemi-

† Loc. cit. on p. 262.

‡ Galle, J. G., loc. cit.

he obtained convincing evidence for the motion of the Lyrid radiant in 1885, and in 1923 gave an ephemeris showing a movement from α 269°, δ +33° on April 18 to α 278°, δ +33° on April 26. Subsequently, a large number of radiant positions were determined by visual observers, but no precise agreement as to the coordinates has been reached. For example, Prentice† compares group Lyrid radiants determined by reliable observers in U.S.A. and G.B. as in Table 85.

Prentice concludes that such discrepancies cannot be due solely to errors of observation and that the Lyrid shower must have double or multiple centres. The most recent visual data on the radiant are those given by Prentice‡ for the 1930 and 1931 returns as follows:

1930 April 21, $\alpha = 273{\cdot}0°$, $\delta = +31{\cdot}5°$, diameter 1·8° (10 meteors).

1931 April 22, $\alpha = 272°$, $\delta = +32{\cdot}5°$, diameter 2·5° (4 meteors).

There is no published record of subsequent radiant determinations, but, in the most recent summaries, Prentice§ lists the Lyrids as centred on $\alpha = 271°$, $\delta = +31°$ with multiple centres.

The radiant coordinates given by the radio-echo technique‖ are listed as $\alpha = 273°$, $\delta = +30°$, with a mean radiant diameter of 8°, but owing to the low hourly rate more weight must be attached to the visual observations.

(*d*) *Velocities*

The data on the velocity of Lyrid meteors are meagre. For example, since 1895 only six velocity determinations, visually determined, are given in the published records of the British observers as follows: 30, 48, 53, 61, 62, 64 km./sec. The scatter is so great that the values are worthless. Three radio-echo determinations have been given by Millman and McKinley,†† one by McKinley,‡‡ and three by Ellyett§§ as listed in Table 86.

The velocity of one Lyrid meteor, photographically determined by the double-camera technique, has been listed by Jacchia.‖‖ It is Harvard no. 1065, photographed on 1941 April 23·32 with velocities of 48·47 km./sec. at 87·5 km. altitude and 48·00 km./sec. at 80·0 km. altitude.

† Prentice, J. P. M., *J. Brit. Astr. Ass.* **40** (1930), 136.
‡ Prentice, J. P. M., *Mem. Brit. Astr. Ass.* **32** (pt. i) (1936).
§ Prentice, J. P. M., *Brit. Astr. Ass. Handbook*, 1947–50.
‖ Hawkins, G. S., and Almond, M., loc. cit.
†† Millman, P. M., and McKinley, D. W. R., *J. Roy. Astr. Soc. Can.* **42** (1948), 121.
‡‡ McKinley, D. W. R., *J. Appl. Phys.* **22** (1951), 202.
§§ Ellyett, C. D., unpublished (Ph.D. thesis, Manchester, 1948).
‖‖ Jacchia, L. G., *Tech. Rep. Harv. Coll. Obs.* (1948), no. 2 (Harvard Reprint Series II–26).

over several succeeding nights. The data plotted in Fig. 130 show a sharp maximum on April 21 on both occasions.

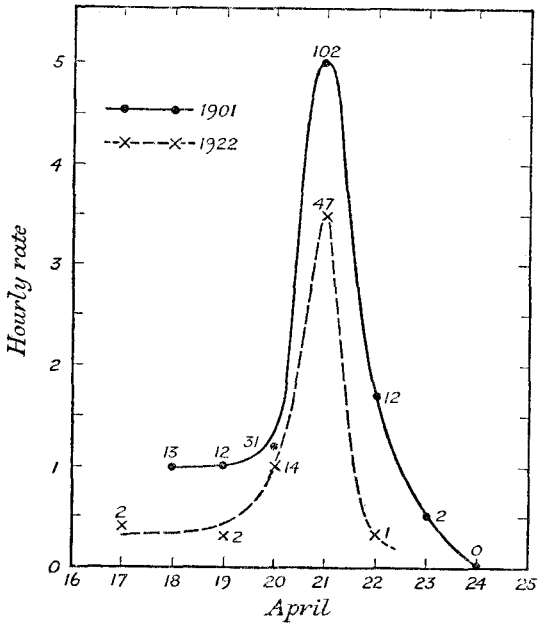

FIG. 130. Epoch of Lyrid maximum as given by the visual observations of 1901 and 1922. (The number by each plotted point gives the number of meteors observed.)

TABLE 85

Lyrid Radiants

Date	*Radiant*		*No. of meteors*	*Observers*
	α *deg.*	δ *deg.*		
1922 April 21·76	270·0	+32·6	17	U.S.A.
1922 April 21	271	+34	7+	G.B.
,, 21	271	+33	4+	,,
1928 ,, 21	272	+33	4	,,
,, 21	272	+33·25	11	,,
1923 ,, 20·85	280	+37·1	28	U.S.A.
1922 ,, 21·82	280·2	+37·4	5–13	,,
1923 ,, 23·8	281·6	+35·6	19	,,

(*c*) *Radiant*

The first radiant coordinates for the Lyrid shower appear to have been given by Herrick as α 273°, δ +45°, 1839 April 18. Denning† states that

† Denning, W. F., *Mon. Not. Roy. Astr. Soc.* **84** (1923), 46.

evidence of intense activity during this period except for the 1922 return. Then on 1922 April 21 a rate of more than 1 per minute appears to have been recorded by observers in eastern Europe.† The British observers, although working under good conditions, did not record this high rate, but the account‡ speaks of 'very fine Lyrids' being observed with a maximum at April 21d. 10h. 45m.

TABLE 83

Maximum Hourly Rates of the Lyrid Meteor Shower

Year	*Hourly rate*	*Year*	*Hourly rate*
1884	22	1922	3 to 100**
1893	5	1930	7
1895	6	1947	7
1896	Very low	1948	20
1898	6	1949	10
1899	Very low	1950	6
1901	8	1951	11
1903	4	1952	Very low
1912*	1	1953	7

* Davidson, loc. cit.
** See remarks in text.

In reviewing the work of the American Meteor Society for 1919–25 Prentice§ refers to this discrepancy and gives the comparison in Table 84 between the observations of H. N. Russell in Greece and his own observations in Great Britain.

TABLE 84

The Lyrid Shower of 1922

Date	*Hourly rate in Great Britain*	*Hourly rate in Greece*
1922 April 20	0·5	..
1922 April 21	3	96

He concludes that the rich portion of the shower must be extremely narrow. Nothing is yet known about the question of periodicity in the Lyrid shower. Comet 1861 I, with which the shower is associated, has a period of 415 years, but the historical data are insufficient to check if there is any related periodicity in the shower. Although the hourly rates are low, the epoch of maximum is shown to be sharp from the visual observations of 1901‖ and 1922†† for which published data are available

† *Pop. Astron.* **31** (1923), 172.
‡ *Mem. Brit. Astr. Ass.* **24** (pt. iii) (1923).
§ Prentice, J. P. M., *J. Brit. Astr. Ass.* **40** (1930), 136.
‖ *Mem. Brit. Astr. Ass.* **11** (pt. i) (1902).
†† Ibid. **24** (pt. iii) (1923).

that a close similarity existed between the orbit of Comet 1861 I and that of the Lyrid meteors. In his work on the past history of the major meteor showers, Newton† was able to trace the history of the Lyrids for some 2,500 years. Some of these displays must have been very remarkable. Thus Olivier‡ quotes from Biot's *Chinese Catalogue*: 'March 27 15 B.C.§ after the middle of the night, stars fell like a rain; they were 10° to 20° long: this phenomenon was repeated continually. Before arriving at the earth they were extinguished.' The last great shower appears to have been in 1803, when, according to contemporary newspaper accounts collected by Herrick in 1839, an observer is stated to have counted 167 meteors in 15 minutes 'and could not number them all'. It was about this time that the work of Arago (1835), Benzenberg (1838, 1839), and Herrick (1838, 1839) first confirmed the regular appearance of a shower with its radiant in Lyra, around April 21, although the numbers observed were small. Owing to the weak displays which have been given by this shower during the past century, comparatively little accurate information is available about it.

(*b*) *Activity*

Although it is inferred from some of the historical accounts mentioned above that the Lyrid shower must have given great displays in the past, its activity during the era of trained observers has been very low. For example, the records of maximum activity as deduced from the observations of the British Astronomical Association‖ in 1884 and from 1893 to 1930, and of the radio-echo observations†† since 1947 are given in Table 83. Denning‡‡ observed the stream carefully in 1884 since he believed that Herrick's idea of a 27-year period had some foundation. The rate observed of 22 per hour is considerably higher than that found subsequently, but later returns do not support the idea of the 27-year period. Davidson§§ has given an account of the careful observations under good conditions in 1912, but the rate was only 1 per hour.

It is, of course, likely that some of the visual observations represent a lower limit owing to poor sky conditions or to the fact that the observations may not have covered the period of maximum, but there is no other

† Newton, H. A., *Amer. J. Sci.* (*II*), **36** (1863), 145; **37** (1864), 378.
‡ Olivier, C. P., *Meteors*, ch. 6.
§ Corresponds to A.D. 1850 April 21.
‖ *Mem. Brit. Astr. Ass.* **1** (1892); **3** (1894); **4** (1895); **5** (1896); **6** (1897); **7** (1898); **8** (1899); **9** (1900); **10** (1901); **11** (1902); **12** (1903); **13** (1904); **14** (1905); **24** (1923); **32** (1936).
†† Hawkins, G. S., and Almond, M., loc. cit.
‡‡ Denning, W. F., *Observatory*, **7** (1884), 217.
§§ Davidson, M., *J. Brit. Astr. Ass.* **22** (1912), 364.

An ejection velocity of 20 km./sec. would be required and the idea does not seem plausible. It must be concluded, therefore, that at present no relation of the meteor stream with other bodies in the solar system can be established.

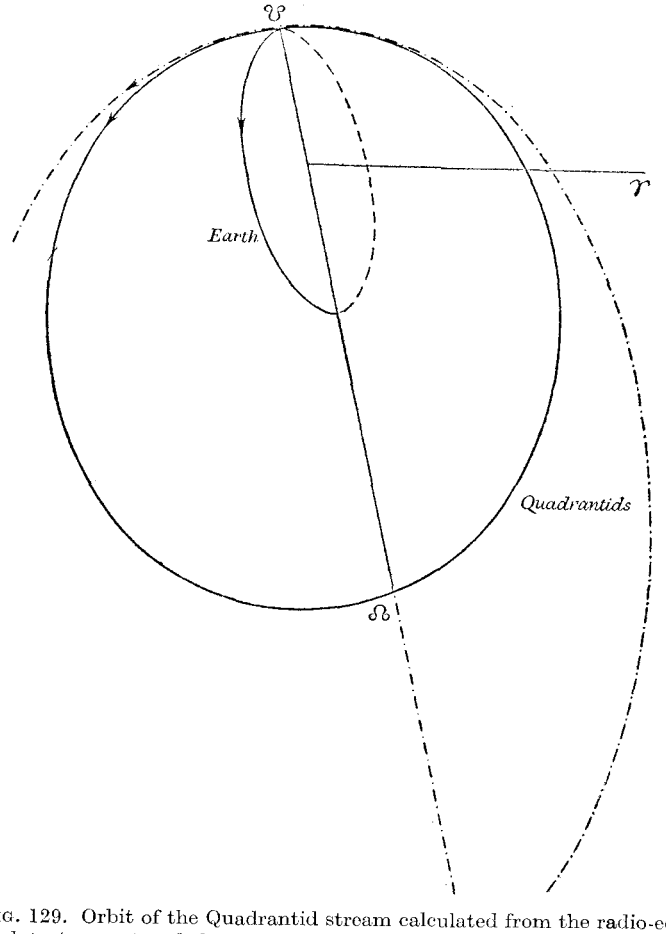

FIG. 129. Orbit of the Quadrantid stream calculated from the radio-echo data (———) and the photographic data on one meteor (– · – · –).

3. The Lyrid shower

(*a*) *History*

Although at the present time the Lyrid meteor shower gives only poor displays, it is nevertheless renowned as a shower of considerable antiquity which in the past has yielded displays of great intensity. Also, between 1860 and 1870 the calculations of Weiss,† Pape,‡ and Galle§ established

† Weiss, E., *Astr. Nachr.* **68** (1867), 382.
‡ Pape, C. F., ibid. **55** (1861), 206.
§ Galle, J. G., ibid. **69** (1867), 33.

computes the width of the stream to be $1{\cdot}5 \times 10^6$ miles and states that there is no corresponding comet. In 1919 Pokrovsky and Shaine noticed that the coordinates of the Quadrantids were nearly those of Comet 1860 I, which, like Biela's comet, was remarkable because of its division into two parts. Actually the epochs differ by a month and the association does not seem very plausible. The comparison is given in Table 81.

Hoffmeister† observed the Quadrantids in 1933 and considered that there was evidence for a long-period orbit. The parabolic elements which he computed are also given in Table 81. He was unable to find any plausible cometary association.

The orbital elements computed by Hawkins and Miss Almond‡ from the radio-echo data are given in Table 82.

TABLE 82

Orbital Elements for the Quadrantids computed from the Radio-echo and Photographic Data

	☊ (*deg.*)	ω (*deg.*)	i (*deg.*)	e	q (*a.u.*)	a (*a.u.*)
Radio-echo: Quadrantids	282·5±0·5	166±3	67±2	0·44±0·03	0·97±0·04	1·7±0·1
Radio-echo: Quadrantids with deceleration correction	282·5	166	67	0·46	0·97	1·8
Jacchia (photographic)	282·1	168	74	0·72	0·93	3·4

The limits of error were obtained from the estimated error of the radiant determination and the probable error in the velocity distribution. The coordinates were corrected for zenithal attraction and diurnal aberration. The influence of the correction for deceleration (computed according to the method and data given by Whipple§ and Jacchia‖) is shown separately in Table 82.

The orbit is of short period and high inclination and is therefore unlike any known cometary orbits. The exceptional nature of the Quadrantid orbit has since been confirmed by Jacchia†† who has calculated the orbital elements from one doubly photographed meteor in 1951. This information is also given in Table 82, and the two orbits are shown in Fig. 129. The orbit intersects that of a near-parabolic comet (Comet 1939*a*, Kozik–Peltier) in two places at distances of 1·3 and 1·7 a.u. from the sun, and the possibility of ejection of material (see Chap. XXI) at either of these points to form the meteor stream has been considered.

† Hoffmeister, C., loc. cit. ‡ Hawkins, G. S., and Almond, M., loc. cit.
§ Whipple, F. L., loc. cit.
‖ Jacchia, L. G., *Tech. Rep. Harv. Coll. Obs.* (1948–9), nos. 2, 3, 4.
†† Jacchia, L. G., private communication.

σ_E may be obtained from the errors in the measurement of individual velocities as described in § 1 (*c*), Chapter XII, σ_R from the observed radiant positions and diameters, and σ_S from the measured background rate of sporadic meteors. σ_A can be estimated from the equations for deceleration given by Whipple,† and hence σ_H can be estimated. For the 1951 Quadrantid measurements Hawkins and Miss Almond obtain $\sigma_E = 1{\cdot}0$ km./sec., $\sigma_S = 1{\cdot}1$ km./sec., $\sigma_R = 1{\cdot}7$ km./sec., $\sigma_A = 0{\cdot}3$ km./sec., and since $\sigma_0 = 3{\cdot}4$ km./sec., $\sigma_H = 2{\cdot}5$ km./sec.

This result indicates that an actual spread in heliocentric velocities may make a significant contribution to the dispersion of the velocities in Fig. 128.

(*e*) *Orbit*

A preliminary attempt to define an orbit for the Quadrantid stream was made in 1873 by Kirkwood,‡ who, from qualitative observations, derived a period of thirteen years. Fisher§ computed a heliocentric velocity of 39·1 km./sec. for the Quadrantid meteors at the node, using the mean radiant and velocity data compiled by him for the observations up to 1927. He concludes that this result is not incompatible with the heliocentric velocity of 41·8 km./sec. derived on the assumption of a 14·6 year period. Parabolic elements for the stream were computed in 1908 by Wenz‖ and in 1913 by Davidson†† as given in Table 81.

TABLE 81

Parabolic Elements for the Quadrantids as computed by Wenz, Davidson, and Hoffmeister, compared with Comet 1860 I

	Epoch	Radiant		☊	i	π	q
		α (deg.)	δ (deg.)	deg.	deg.	deg.	a.u.
Wenz . .	1908 Jan. 3d. 20h.	239	+48	282·6	70·0	83·1	0·972
Davidson .	1913 Jan. 2d.–3d.	232	+51	282	72·8	96·2	0·981
Hoffmeister .	1925·0	227·1	+46·4	282·2	81·5	92·7	0·977
Comet 1860 I	..	..	..	324·0	79·3	173·8	1·197

In commenting on this orbit Davidson points out that the motion is direct, and that 11·25 days after perihelion the particles are at a distance of 1 a.u., moving with a velocity of 41·6 km./sec. This leads to a geocentric velocity in the earth's atmosphere of 45·3 km./sec. Davidson

† Whipple, F. L., *Rev. Mod. Phys.* **15** (1943), 246.
‡ Kirkwood, D., *Proc. Amer. Phil. Soc.* **13** (1873), 501.
§ Fisher, W. J., loc. cit.
‖ Wenz, W., *Bull. de la Soc. Astronom. de France*, **22** (1908), 365.
†† Davidson, M., *J. Brit. Astr. Ass.* **23** (1913), 233.

system was in use at the beginning of the shower and is unlikely to be associated with the Quadrantid radiant. The remaining 25 velocities give a mean of $37{\cdot}1 \pm 3{\cdot}5$ km./sec. A further 37 velocities were measured during the Quadrantid epoch of 1951 January and 25 velocities during the epoch of 1952 January. The distribution for the 1951 measurements, which is shown in Fig. 128 (*b*), has a mean of $39{\cdot}3 \pm 3{\cdot}4$ km./sec. The

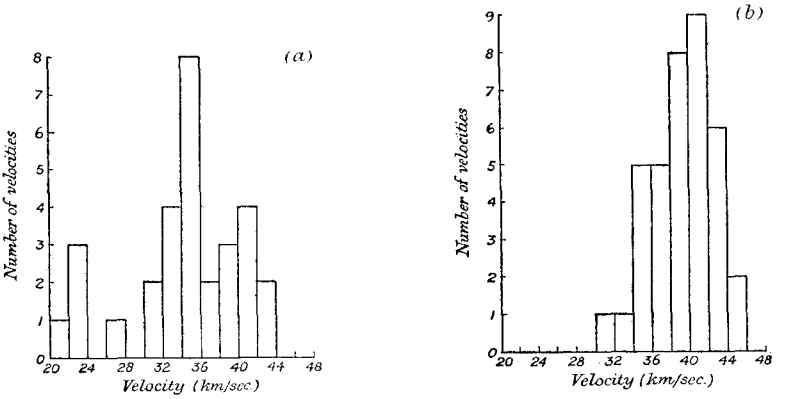

FIG. 128. The velocity distribution of the Quadrantid meteors measured by the radio-echo diffraction technique. (*a*) January 1948. Mean $37{\cdot}1 \pm 3{\cdot}5$ km./sec. (neglecting the low-velocity group). (*b*) January 1951. Mean $39{\cdot}3 \pm 3{\cdot}4$ km./sec.

mean value for the complete 87 velocities (1948, 1951, 1952) is 39·6 km./sec.

Hawkins and Miss Almond† have investigated how much of this velocity spread can be attributed to an actual spread in the heliocentric velocity of the individual meteors in the stream. The standard deviation of the observed geocentric distribution (σ_0) can be written as

$$\sigma_0^2 = \sigma_E^2 + \sigma_R^2 + \sigma_S^2 + \sigma_A^2 + \sigma_H^2,$$

where σ_E = standard deviation caused by random errors in the measuring technique;

σ_R = standard deviation resulting from the variation of apparent elongation of radiant points;

σ_S = standard deviation introduced by sporadic meteors;

σ_A = standard deviation caused by differential atmospheric deceleration;

σ_H = standard deviation introduced by a real spread in the heliocentric velocities.

† Hawkins, G. S., and Almond, M., loc. cit.

the radio-echo observations as seen from Table 80 which gives the coordinates for the showers of 1950, 1951† and 1952, 1953.‡

TABLE 80

Radiant Coordinates for the Quadrantid Shower determined by the Radio-echo Technique

Date	Solar longitude ⊙	Radiant coordinates		Radiant diameter deg.
		α (deg.)	δ (deg.)	
1950 Jan. 1	280·6	233	+52	10
Jan. 3	282·6	231	+47	12
Dec. 28	275·9	224	+52	5
Dec. 30	278·0	228	+46	5
1951 Jan. 1	280·0	231	+46	5
Jan. 2	281·0	228	+51	8
Jan. 3	282·1	232	+49	< 3
Jan. 5	284·1	236	+51	4
Jan. 6	285·1	236	+50	10
Jan. 7	286·2	227	+49	6
1952 Jan. 2	280·8	227	+56	6
Jan. 3	281·8	233	+47	4
Jan. 4	282·8	233	+48	3
Jan. 5	283·9	224	+52	4
Jan. 6	284·9	232	+50	6
1953 Jan. 1	280·5	221	+50	8
Jan. 2	281·6	214	+47	10
Jan. 3	282·6	231	+50	5
Jan. 4	283·6	231	+46	7

(*d*) *Velocities*

Fisher§ lists fourteen velocities determined from doubly observed meteors between 1903 and 1918. The values range from 25·8 to 77·3 km./sec. with a mean of 41·8 km./sec. Omitting the four most widely dispersed values, the mean reduces to 38·5 km./sec. There do not appear to be any other published velocity determinations of Quadrantid meteors until the advent of the radio-echo diffraction technique in 1948. Then, on 1948 January 3 and 4, Ellyett and Davies‖ measured 30 velocities, the distribution of which is shown in Fig. 128 (*a*). The low-velocity group (mean 22·4 km./sec.) was obtained when a non-directional aerial

† Hawkins, G. S., and Almond, M., loc. cit.
‡ Jodrell Bank observations, unpublished.
§ Fisher, W. J., loc. cit.
‖ Ellyett, C. D., and Davies, J. G., *Nature*, **161** (1948), 596; Davies, J. G., and Ellyett, C. D., *Phil. Mag.* **40** (1949), 614.

During the night of 1929 January 2–3, Fisher and Miss Olmsted† recorded three Quadrantid meteors photographically. Their final value for the mean radiant was α 231·8°, δ +48·3°. All subsequent observations have

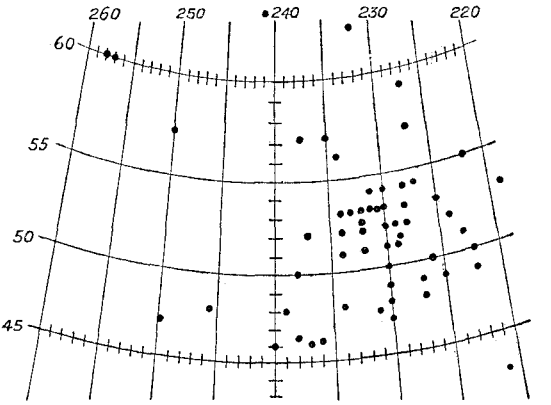

FIG. 126. Radiant positions of the Quadrantid shower (plotted on great circle chart) as given by Fisher for singly observed meteors between 1860 and 1927.

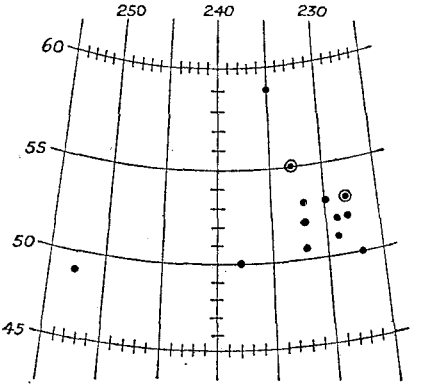

FIG. 127. Radiant positions of the Quadrantid shower (plotted on great circle chart) as given by Fisher for doubly observed meteors between 1860 and 1927.

confirmed that the Quadrantid radiant is spread over a wide area. Prentice‡ remarks that the radiant is exceedingly complex and apparently covers a wide area at least 20° in diameter with centre about α 230°, δ +50°. The spread in radiant position has been confirmed by

† Fisher, W. J., and Olmsted, M., *Circ. Harv. Coll. Obs.* (1930), no. 347.
‡ Prentice, J. P. M., loc. cit.

by Hawkins and Miss Almond.† The curve of activity against solar longitude is given in Fig. 125 for the years 1951, 1952, 1953. This shows good agreement with the curve given by Prentice (Fig. 124) for the epoch of maximum and for the duration of the shower. The maximum rates‡ determined by the radio-echo apparatus are given in Table 79.

TABLE 79

Maximum Rates of the Quadrantid Shower determined by the Radio-echo Apparatus

Date	*Solar longitude* $\odot$	*Maximum hourly rate*
1947 Jan. 3	282·6	34
1948 Jan. 4	283·0	76
1949 Jan. 3	282·5	41
1950 Jan. 3	282·6	70
1951 Jan. 3	282·1	90
1952 Jan. 4	282·8	104
1953 Jan. 3	282·6	170

There is no evidence from these various data of any marked periodicity in activity. This is contrary to earlier views since Denning and Mrs. Wilson§ considered that the Quadrantids might have a period of $13\frac{1}{4}$ years. Also, from the maxima between 1860 and 1927 Fisher|| considered that a mean cycle of 14·6 years was indicated. On this basis another maximum would be expected in 1936; but Prentice†† gives a rate of only 35 for that year, whereas he considers the return of 1932 (80 per hour) to have been very rich. The more reliable radio-echo data (Table 79) as yet gives no support to the idea of any periodicity. The activity in 1953 appears to have been the greatest recorded for over forty years.

(*c*) *Radiants*

According to Fisher,|| Stillman Masterman first determined the Quadrantid radiant in 1863 as α 238°, δ +46° 26′. In 1864 Herschel obtained a value of α 234·0°, δ +50·9°. Many subsequent determinations showed similar discrepancies. The various determinations up to 1927 have been collected by Fisher and are plotted in Fig. 126 for singly observed meteors and in Fig. 127 for doubly observed meteors. The radiant points cluster around α 232°, δ +52° but are widely scattered.

† Hawkins, G. S., and Almond, M., *Mon. Not. Roy. Astr. Soc.* **112** (1952), 219. Except the information for 1952–3 which is unpublished.

‡ The parameters of the radio apparatus were adjusted so that the hourly rates recorded corresponded to those seen by a visual observer under good sky conditions. This applies to all the radio-echo rates quoted in Chapters XIII–XVIII.

§ Denning, W. F., and Wilson, F., *Mon. Not. Roy. Astr. Soc.* **78** (1918), 198.

|| Fisher, W. J., loc. cit.

†† Prentice, J. P. M., loc. cit.

period according to Prentice is given in Fig. 124. These determine the epoch of maximum at approximately $\odot = 282° 57'$ and show that the

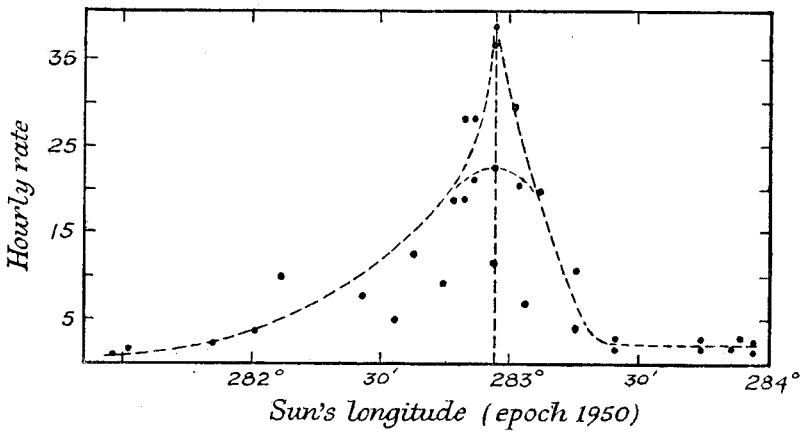

FIG. 124. The hourly rate of the Quadrantid meteor shower plotted against longitude of the sun according to Prentice from visual observations between 1921 and 1940.

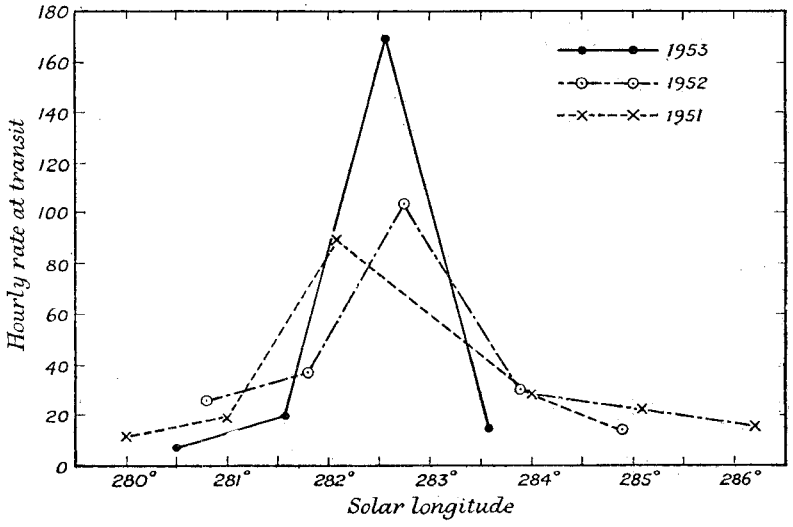

FIG. 125. The hourly rate of the Quadrantid shower at transit as given by the radio-echo observations, plotted against solar longitude for 1951, 1952, and 1953.

major part of the activity of the shower is over in about 20 hours. Telescopic observations during 1947–9 have been reported by Rigollet.† The radio-echo information on the stream since 1946 has been presented

† Rigollet, R., *Ann. d'Astrophys.* **14** (1951), 181.

published the same suggestion at about this time. Since 1860 there are records of fairly regular observations of the shower, mainly by observers in the British Isles. These have been hindered greatly by the poor weather conditions of early January and the short life of the shower. Since 1946, however, systematic observations have been made by the radio-echo technique.

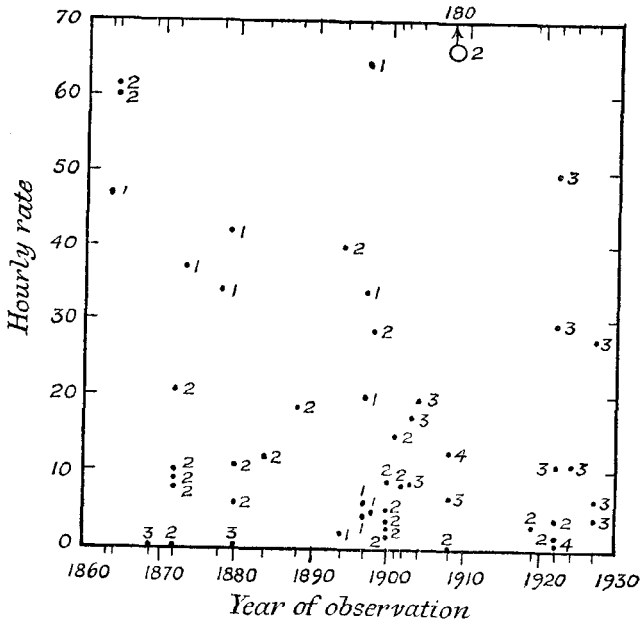

FIG. 123. The hourly rate of the Quadrantid meteor shower from observations between 1860 and 1930 according to data collected by Fisher. The small numbers by the plotted points are the dates in January to which the observation refers.

(*b*) *Activity*

According to Fisher,† useful counts of the Quadrantid rate were made only in 24 Januaries out of a possible 68 between 1860 and 1927. His summary of the available information is given in Fig. 123. The greatest maxima apparently occurred in 1864 (60 per hour); 1879 (> 42 per hour); 1897 (64 per hour); 1909 (180 per hour); 1922 (50 per hour). Information on the activity of the shower is also given by Prentice‡ from 1921 to 1940. The maximum rate during this period appears to have occurred in 1932 (80 per hour) although the results are influenced by unfavourable weather. The hourly rate plotted against longitude of the sun over this

† Fisher, W. J., loc. cit.

‡ Prentice, J. P. M., *J. Brit. Astr. Ass.* **51** (1940), 19.

TABLE 78

The Major Meteor Streams

Shower	*Date of maximum*	*Classification and chapter*
Quadrantids . . .	Jan. 3	Permanent Chap. XIII
Lyrids	April 21	,, ,, ,,
η-Aquarids	May 4–6	,, ,, ,,
Pons–Winnecke . . .	June 28	Lost Chap. XVII
δ-Aquarids	July 28	Permanent Chap. XIV
Summer day-time streams .	May, June, July	Permanent and Periodic Chap. XVIII
Perseids	Aug. 10–14	Permanent Chap. XIV
Giacobinids	Oct. 10	Periodic Chap. XVI
Orionids	Oct. 20–23	Permanent Chap. XV
Taurids . . .	Nov. 3–10	,, Chap. XV
Leonids	Nov. 16–17	Periodic Chap. XVI
Bielids	Nov.–Dec.	Lost Chap. XVII
Geminids	Dec. 12–13	Permanent Chap. XV
Ursids	Dec. 22	,, Chap. XV

Denning† published in 1899 lists 4,367 radiants, and the modern compilations of Hoffmeister‡ and Öpik§ give attention to many more streams than those listed in Table 78. However, the showers described in the present book are those which are widely recognized as being of a major character, and for which information is available from a variety of sources.

2. The Quadrantid shower

(*a*) *History*

The Quadrantid shower is one of the most intense showers at present active. It is short-lived and the sharp maximum occurs over a period of a few hours between January 2–4. Fisher‖ has given the complete history of this shower and collected the known data up to 1927. It is named after an obsolete constellation *Quadrans Muralis* found in early nineteenth-century star atlases—located at the junction of the areas of Draco, Hercules, and Bootes. The occurrence of the shower has not been traced back for any considerable time. In 1861 Wartmann†† recognized the period January 2–3 to be a noteworthy one from his observations since 1853. Quetelet‡‡ claims first publication in 1839. Herrick§§ also

† Denning, W. F., *Mem. Roy. Astr. Soc.* **53** (1899), 203.
‡ Hoffmeister, C., *Meteorströme* (Weimar, 1948).
§ Öpik, E. J., *Circ. Harv. Coll. Obs.* (1934), no. 388.
‖ Fisher, W. J., ibid. (1930), no. 346.
†† Wartmann, *Bull. Ac. R. Brux.* **8** (2) (1841), 226.
‡‡ Quetelet, A., *Catalogue des principales apparitions d'étoiles filantes*, 1839.
§§ Herrick, E. C., *Amer. J. Sci. (II)*, **39** (1840), 334.

XIII

THE MAJOR METEOR SHOWERS—I

THE PERMANENT STREAMS OF JANUARY TO JUNE

1. Introduction

THE major meteor showers are the dominant observational events in meteor astronomy. They occur when the earth sweeps through concentrations of debris in space. About a dozen major showers have been recorded visually and several recur annually, indicating that the debris is itself moving in an orbit around the sun. After a few days the earth generally moves out of the debris; hence, although the showers can be a spectacular occurrence, their contribution to the total number of meteors entering the atmosphere is somewhat less than the sporadic meteor contribution.

The meteors in a given stream travel in roughly parallel paths in the earth's atmosphere. Their apparent point or area of divergence is the radiant position. By convention, the shower takes its name from the constellation, or star, near which this position lies. If the radiant position and the velocity of the meteors in the earth's atmosphere are known, the orbit of the stream can be computed as described in Chapter V. The available information about the major showers varies a great deal. For some, the orbits are known with precision, and the association of the debris with other constituent bodies in the solar system has been established.

In many cases the showers are observed every year with about the same intensity, indicating that the debris is fairly uniformly dispersed around the orbit. For purposes of classification we shall refer to these as permanent streams. In others the debris is localized in the orbit and the streams exhibit a marked periodicity (Chap. XVI). In one or two cases major meteor streams have completely vanished (Chap. XVII). Finally, the radio-echo techniques have revealed the existence of intense meteor streams active in the summer day-time. These are discussed in Chapter XVIII.

Table 78 summarizes the major showers which are dealt with here. These all give displays (or have done in the past) with visual hourly rates exceeding 20 to 50. In addition to the showers listed there are a number of minor streams occurring at various times during the year with rates of only a few per hour. For example, the great catalogue of

of the sporadic meteors moved in very short period orbits. The analysis of the British visual meteor data also failed to show the existence of these very high velocities. Criticism and counter-criticism effectively led to an impasse, but since 1948 the new radio-echo techniques have been applied to this problem and have yielded results which are opposed to the hyperbolic theory. Neither in the British nor in the Canadian work is there any indication of the high velocities demanded in the conclusions of Hoffmeister and Öpik. Hoffmeister† has concluded that his own observations can be interpreted in the light of the new results, but Öpik,‡ even in the face of the new results, does not move from his belief in the hyperbolic theory.

The complication of Öpik's results and his analysis are evident from Chapter IX, and now that the non-hyperbolic theory is widely accepted the task of explaining his conclusions remains. If the validity of the basic observational data is accepted, there remains only the question of the validity of the statistical analysis which has already been queried by Olivier.§ At any moment there is a wide spread in the velocity distribution of sporadic meteors and the distribution itself is asymmetrical. It does not seem impossible that the application of conventional stellar statistics to such a problem may lead to erroneous results, but no one has yet attempted the task of such a quantitative investigation of Öpik's results.

Hence, although Öpik's results remain an enigma, the contemporary conclusions to be drawn from the surveys of the previous chapters is that only a small percentage, if any, of the sporadic meteors are moving with hyperbolic velocities; and that the few cases of small hyperbolic velocities which probably exist more likely arise from planetary perturbations than from the interstellar origin of the meteors.

† Hoffmeister, C., private communication.
‡ Öpik, E. J., *Irish Astr. J.*, loc. cit.
§ Olivier, C. P., *Pop. Astron.* **46** (1938), 325.

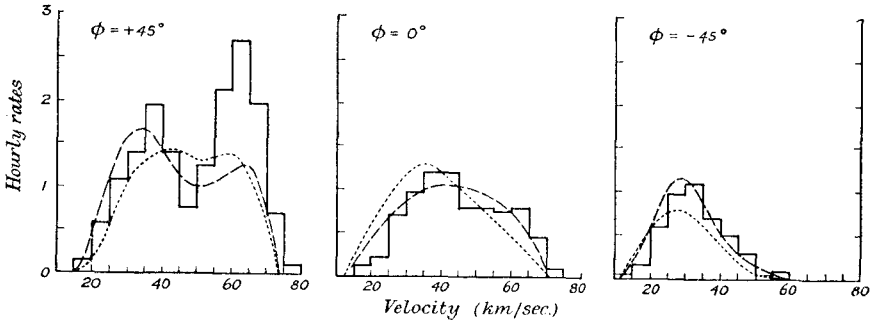

FIG. 122. Observed and theoretical velocity distributions in McKinley's experiment for elevation of apex $\phi = +45°$, 0°, −45°.

——— Observed distribution. – – – Theoretical, assuming equal numbers $\bar{V} = 36$ and 42 km./sec., no 30 km./sec., and the non-uniform distribution of Fig. 121. ..... Theoretical visual curves on the same assumption.

All curves normalized to the observed distribution for $\phi = 0°$.

to have originated in interstellar space. In fact there are thirty-two meteors (0·3 per cent.) in the interval 75–79 km./sec.; but if these were interstellar it is difficult to see why an appreciable number was not found with velocities greater than 80 km./sec. It seems preferable to regard this small hyperbolic component as due to interplanetary meteors which have suffered perturbations. In any case there is no indication whatsoever of the preponderance of hyperbolic velocities found by Öpik and Hoffmeister (Chaps. IX and VI).

As regards the equivalent visual magnitudes of the meteors, McKinley does not enter into a detailed analysis. From a comparison of the visual and radio-echo rates he considers that the average meteor studied probably had a magnitude of +4 or +5, with a limiting magnitude of +7 or +8. This range of magnitudes is comparable with that covered in the work of Almond, Davies, and Lovell (see § 1).

3. General conclusions on the velocity of sporadic meteors

During the last twenty-five years a large fraction of the work in meteor astronomy has been concerned with the problem of the origin of the sporadic meteor component. In the period between the two world wars the investigations of Hoffmeister and Öpik led to the belief that most of the sporadic meteors had an origin in interstellar space and travelled with markedly hyperbolic velocities in the solar system. Then the precise photographic measurements failed to show such high velocities; on the contrary, the surprising result was obtained that some

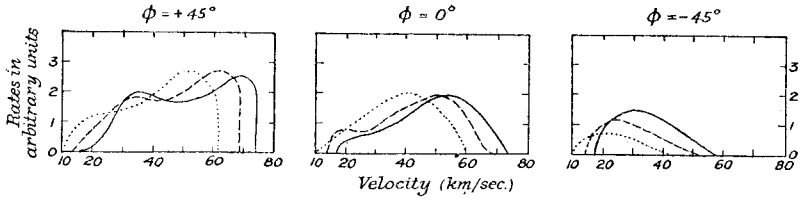

FIG. 120. Theoretical velocity distributions for elevation of apex $\phi = +45°, 0°, -45°$.
——— $\bar{V} = 42$ km./sec. – – – $\bar{V} = 36$ km./sec. ..... $\bar{V} = 30$ km./sec.

ellipticity) and by eliminating $\bar{V} = 30$ km./sec., which removes the very elliptical orbits. The adopted density distribution for this case, compared with the previously assumed uniform case, is shown in Fig. 121. The densities on the $\bar{V}$ circles in (*c*) are then modified according to this

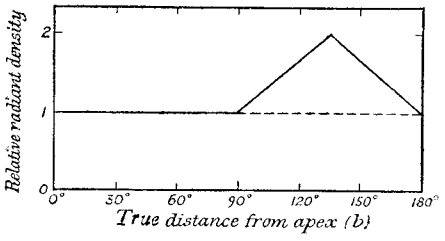

FIG. 121. Assumed theoretical distribution of radiants as a function of distance from the apex (*b*).
– – – Uniform distribution. ——— Adopted non-uniform distribution.

distribution and the numerical integration repeated as in (*c*). The final theoretical curves are shown in Fig. 122, assuming equal numbers of $\bar{V} = 36$ and 42 km./sec. meteors but none of $\bar{V} = 30$ km./sec.

(*e*) *Discussion*

Examination of Fig. 122 shows a reasonably good agreement between the theoretical and observed distributions; except that in the case of $\phi = +45$ the number of high velocities exceeds those predicted. It is possible to change the density distribution of Fig. 121 to obtain a better fit by increasing the radiants in the region b = 0°–30°. Other reasons for the discrepancy may be that faster meteors produce relatively more ionization and hence more are detectable in the high-velocity range.

McKinley points out that so many variable parameters are involved in deriving the theoretical curves in (*c*) that it is possible to fit the data from very dissimilar theoretical postulates. It is clear, however, that none of the 10,000 meteors studied by McKinley can be definitely asserted

equal angular elements so that the transformation of points on the $\overline{V}$ circles to the v_g circles can be effected by drawing great circles through the apex at equal intervals of the angle Z. The number of radiants selected on the $\overline{V}$ circle then has to be multiplied by sin b.

(ii) The distance z is computed for each point on the v_g circles selected by 10° increments of the angle Z, by means of the spherical triangle defined by the apex, zenith, and the selected point.

(iii) Each point on the v_g circle is now multiplied by the P(z) function corresponding to the zenith distance of the point according to Fig. 118.

(iv) The sum of the modified densities on the v_g circle is then the rate of meteors of velocity v_g which will be detected by the radio system for the particular values of a and $\overline{V}$ selected in (i). As an example, the curves in Fig. 120 are the theoretical distributions for elevation of apex $\phi = +45°$, 0°, $-45°$, and for $\overline{V} = 42$, 36, 30 km./sec. in each case.

(d) Comparison of the Observational Data with the Theoretical Distributions

The appropriate observational data for comparison with the theoretical curves such as those of Fig. 120 were selected by first determining the local times corresponding to the particular values of ϕ for each of the operating periods. Only a limited amount of the total information can be used in these comparisons—for example, ϕ reaches $+45°$ only from June to December, and $-45°$ only from December to June. Moreover, the observing hours in which the strong major showers occurred were necessarily rejected. The histograms in Fig. 122 show the observational data for the selected values of $\phi = +45°$, 0°, and $-45°$. An attempt was then made to fit these curves by a synthesis of the various theoretical distributions. None of the possible combinations yielded a satisfactory fit, the closest approach being obtained by synthesizing equal numbers of 36 and 42 km./sec. meteors but with few 30 km./sec. meteors.

McKinley therefore investigated the alternative assumption of a non-uniform radiant distribution, assuming first that there were more direct than retrograde orbits (that is the inclinations of the orbits favoured the interval $0° \pm 90°$), and that the ellipticities were large—more nearly parabolic than circular.

In the analytical method, described in (c) above, these conditions were implied by postulating more radiants with $b > 90°$ than with $b < 90°$ (the parameter b is a measure of the combined effect of inclination and

v_g and $\bar{V}$ are the geocentric and heliocentric velocities respectively, the appropriate transformations are

$$v_g^2 = \bar{V}^2 + 900 + 60\bar{V}\cos b,$$

$$v_g \sin c = \bar{V} \sin b.$$

Owing to the earth's attraction, the meteor will appear with an apparent velocity v, and a correction Δz to the zenith angle z of the radiant will be required, given by

$$v^2 = v_g^2 + 125,$$

$$\tan\frac{\Delta z}{2} = \frac{v - v_g}{v + v_g}\tan\frac{z}{2}.$$

$\bar{V}$ may be regarded as a parameter, and selected values assigned to all the radiants over the celestial sphere. Table 77 then shows typical values of v, c, and Δz for uniform values of b and for three values of the parameter $\bar{V}$.

TABLE 77

Typical Transformations for McKinley's Velocity Distribution

	$\bar{V} = 30$			$\bar{V} = 36$			$\bar{V} = 42$		
b	v	c	Δz	v	c	Δz	v	c	Δz
0°	61·03	0°	0° 58′	66·94	0°	0° 48′	72·86	0°	0° 41′
15	60·51	7·5	1 0	66·39	8·2	0 50	72·27	8·8	0 42
30	59·02	15·0	1 2	64·75	16·4	0 52	70·50	17·1	0 44
45	56·55	22·5	1 8	62·04	24·6	0 57	67·61	26·5	0 48
60	53·15	30·0	1 18	58·32	33·0	1 4	63·63	35·5	0 54
75	48·90	37·5	1 32	53·66	41·5	1 16	58·67	44·8	1 4
90	43·88	45·0	1 56	48·18	50·2	1 35	52·81	54·5	1 19
105	38·20	52·5	2 34	41·98	59·2	2 6	46·22	64·8	1 44
120	32·02	60·0	3 44	35·23	68·9	3 2	39·11	76·1	2 27
135	25·53	67·5	6 4	28·18	79·8	4 55	31·73	89·3	3 48
150	19·14	75·0	11 54	21·22	93·8	9 16	24·63	106·9	6 35
165	13·65	82·5	30 20	15·32	117·4	21 18	18·84	134·2	12 22
180	11·18	90·0	90 0	12·69	180·0	39 24	16·40	180·0	17 36

The correction Δz only becomes serious for meteors with low heliocentric velocities with radiants near the antapex. It has therefore been neglected by McKinley in deriving the theoretical velocity distribution. The conversion of the $\bar{V}$ radiants to the v radiants could be achieved by means of a surface integral over the sphere, including the probability function P(z); but a simplified method of numerical integration was preferred according to the following procedure:

(i) For a selected value of a, uniform density of radiants may be represented by uniform and equal line density along each of the $\bar{V}$ circles at equal increments of b. The $\bar{V}$ circles are divided into

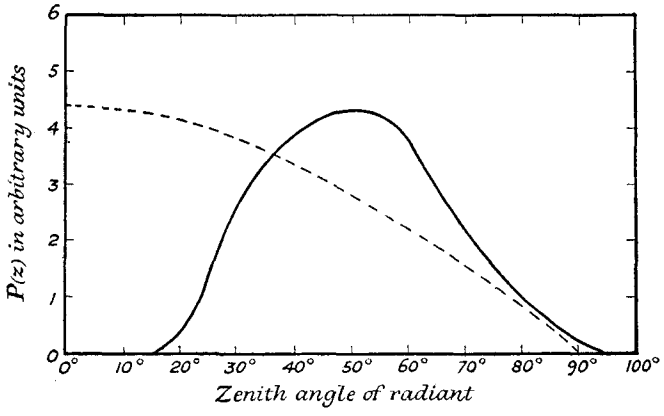

FIG. 118. The probability function P(z) for McKinley's observations.
——— Empirical radio probability.
– – – – Theoretical visual probability.

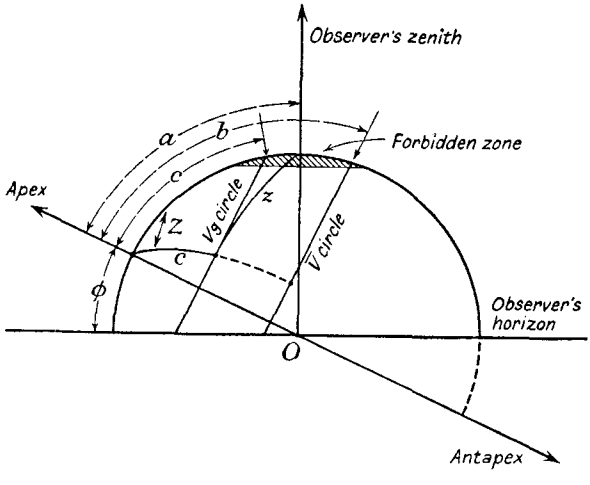

FIG. 119. Diagram for calculation of theoretical velocity distribution in McKinley's experiment.

(c) *The Theoretical Velocity Distribution*

The theoretical velocity distribution applicable to the measurements made by McKinley can be derived in the following way, assuming that the meteor radiants are uniformly distributed. In Fig. 119 the observer is at O, and the apex is at elevation ϕ relative to the observer's horizon, or at a distance a from the observer's zenith. Small circles on the celestial sphere labelled $\overline{V}$ and v_g are drawn such that a true radiant on the $\overline{V}$ circle will appear, owing to the earth's motion, to lie on the v_g circle. If

the mean deceleration to be $-2{\cdot}5$ km./sec.^{2} and V = 36·0 km./sec. The finally corrected value v_g for the geocentric velocity is then obtained from equation (6) (p. 221). This gives v_g = 34·2 km./sec., which is in reasonable agreement with Whipple's† value of 34·7 km./sec., derived from photographic measurements.

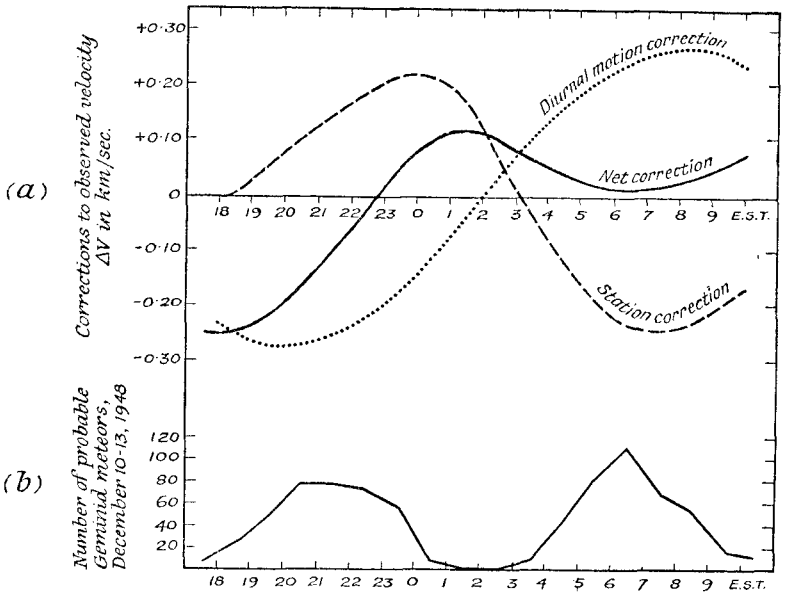

FIG. 117. (*a*) ..... Diurnal motion correction for Geminid meteors. – – – Statistical correction for average position of Geminid meteors due to spacing of transmitter and receiver. ——— Net correction to be applied to observed velocities. (*b*) Observed hourly rates of probable Geminid meteors (1948 data).

McKinley next deduces a relation between the radio meteor rates and zenith angle of the radiant from the information given in Fig. 117 (*b*). The transit time of the radiant was 02h. 10m. E.S.T. The meteor numbers for corresponding times on either side of transit were summed and plotted against zenith angle of the radiant yielding the full-line curve of Fig. 118. The ordinate P(z) represents the probability that the radio system will detect a meteor when the radiant is at a given zenith distance. This function is then used in the analysis of the sporadic distribution. Also given in Fig. 118 is P(z) = cos z which represents to a first order the probability function for a visual observer.

† See Chap. XV.

periods it can be shown that the proportion of non-Geminids is unlikely to exceed 15 or 20 per cent. of the total. The mean velocities from Fig. 116 are

1948	851 meteors	35·2 km./sec.
1949	234 ,,	35·5 ,,
	Mean	35·25 ,,

These velocities are mean apparent observed velocities and require the following corrections to obtain the geocentric velocity.

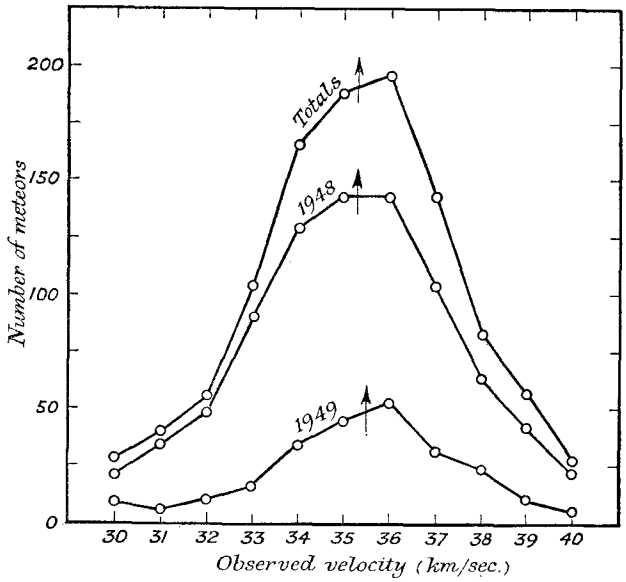

FIG. 116. The velocity distribution of probable Geminid meteors as measured by McKinley: (*a*) in 1948 Dec. 851 observations, mean velocity 35·2 km./sec. (*b*) in 1949 Dec. 234 observations, mean velocity 35·5 km./sec.

(i) *Correction for diurnal motion.* Fig. 117 shows the diurnal-motion correction for Ottawa, and also the average correction which should be applied to the observed velocities each hour to allow for the separation of the receiver and transmitter. The resulting net correction, which is also shown in Fig. 117, when averaged over the observational period, amounts to −0·036 km./sec. McKinley therefore adopts 35·2 km./sec. as the observed velocity corrected for diurnal motion.

(ii) *Correction for deceleration and zenithal attraction.* In order to correct for deceleration, McKinley assumes that the average mass of the meteors is about 1 milligram, and that the average zenith distance of origin is 50°. Using equations deduced by Whipple,† he then derives

† Whipple, F. L., *Rev. Mod. Phys.* **15** (1943), 243.

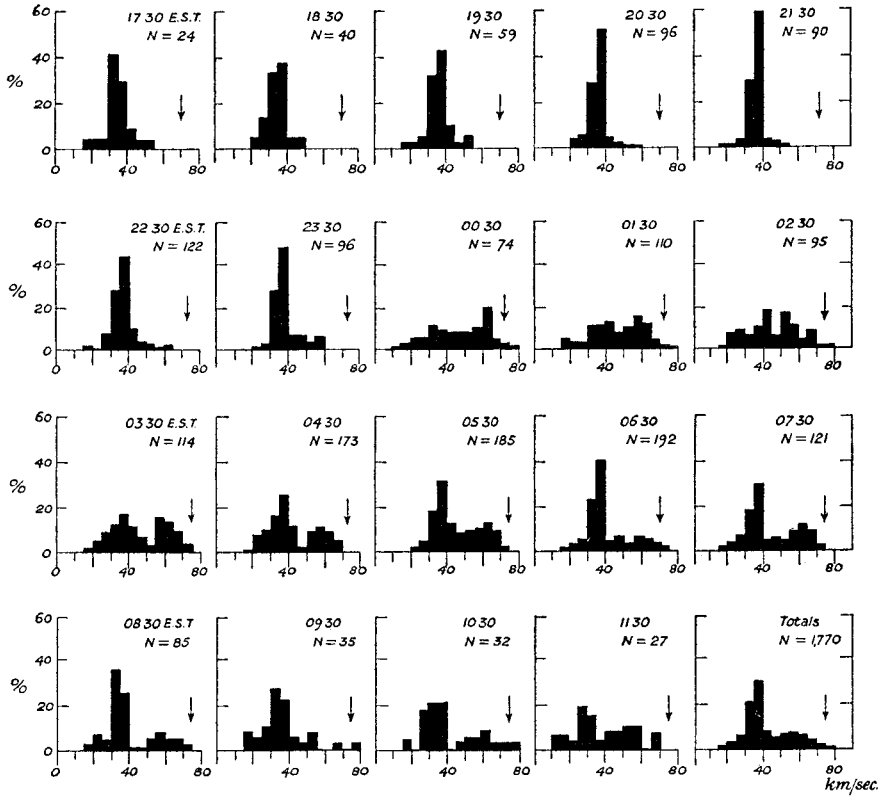

FIG. 115. The hourly distribution of velocities measured by McKinley between 17h. and 12h. E.S.T. on 1948 Dec. 10–13.

Ordinates: per cent. of total measured in hourly intervals (all histograms are normalized).
Abscissae: velocity in km./sec.

Geminid shower is shown in Fig. 115. In these graphs the data for the corresponding hour of each of the three nights have been added. Near transit of the radiant (around 02h. E.S.T.), when the radiant was high in the sky, the ranges were beyond those recorded by the apparatus.† The velocity group between 30 and 40 km./sec. has been analysed further into unit steps and is shown in Fig. 116 for both the 1948 and 1949 Geminid showers. These distributions must contain meteors which do not arise from the Geminid radiant; but by comparison with other

† The variation in range of the recorded echoes with radiant altitude arises because of the specular reflection property of the trails and has been discussed in Chap. IV.

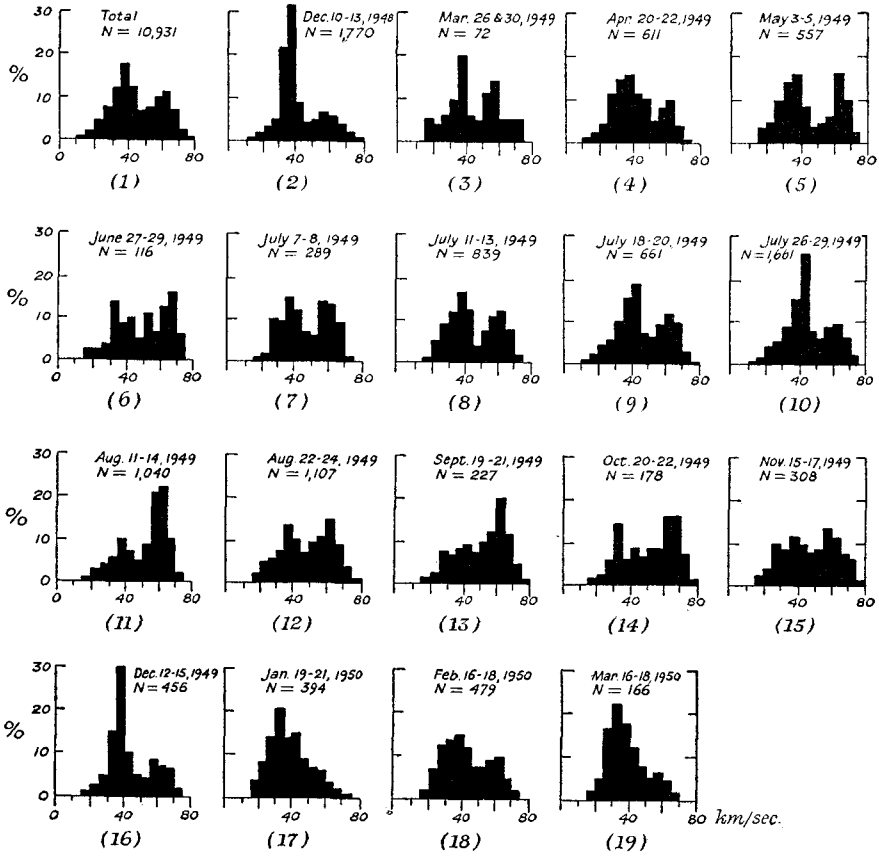

FIG. 114. The velocity distributions measured by McKinley from 1948 Dec. to 1950 March. The histograms represent the total distributions for the periods indicated, usually covering from 48 to 72 hours continuously.

Ordinates: per cent. of total in period (all histograms are normalized).
Abscissae: velocity in km./sec.

the summer day-time streams† Fig. 114 (6)–(10)—is also evident. Preparatory to the statistical analysis of these observations, McKinley made a detailed examination of the Geminid shower in order to investigate the errors in the analysis and to deduce a probability function of general application.

(*b*) *Analysis of the Geminid Shower Velocities*

The hourly distribution of velocities from 17h. to 12h. E.S.T. for the three nights 1948 December 10–13 covering the maximum of the

† See Chap. XVIII.

of the meteors observed in the apex experiments may have had velocities in excess of the parabolic limit. It is possible, of course, that a result of this nature may be due to planetary perturbations.

(v) *Effect of meteor magnitude on the velocity distribution.* The sample of 860 meteors measured in the main lobe of the aerial systems during the apex experiments has been tested for any change in velocity distribution with magnitude. The results are given in Fig. 113 (*a*)–(*f*), from which it is clear that no significant change occurs in the velocity distribution over a range of five magnitudes.

2. McKinley's measurements of meteor velocities

Simultaneously with the work described in § 1 above, McKinley† carried out a series of measurements in Ottawa using the continuous-wave technique for measuring velocities (see Chap. IV). The transmitter generated 1·5 kw. on a wave-length of 10·0 m. The aerial consisted of a half-wave dipole, mounted a quarter wave-length above ground, giving a broad beam. The receiving system was located 7·5 km. distant from the transmitter and used a similar aerial. A separate pulsed transmitter and receiver were used for measuring the meteor ranges. The method of recording the meteor velocities, giving a continuous envelope of the Fresnel diffraction pattern, instead of the discontinuous envelope of the pulse system, has been described in Chapter IV. McKinley's arrangement is sharply distinguished from the arrangement used by Almond, Davies, and Lovell in the aerial system. Whereas the aerial system described in § 1 was highly selective, McKinley's system is effectively non-selective, and records meteors independently of their direction of approach, apart from a small region in the neighbourhood of the zenith.

(*a*) *Details of Observations*

The velocity data were collected over 15 months from 1948 December to 1950 March. The equipment was operated for at least one 48-hour period per month in order to accumulate observational data over an entire calendar year. By this means McKinley collected 10,933 echoes of good quality suitable for velocity analysis. Velocity distributions of the total number observed in each operating period are given in Fig. 114, with the numbers normalized for comparison. Fig. 114 (1) shows the distribution for all measured velocities. The trend to higher velocities in the autumn months is well marked, and the influence of the pronounced showers—Geminids‡ Figs. 114 (2) and (16); Perseids§ Fig. 114 (11); and

† McKinley, D. W. R., *Astrophys. J.* **113** (1951), 225.

‡ See Chap. XV.

§ See Chap. XIV.

TABLE 76

Mean Errors of Velocity Measurement at 70 km./sec.

Experiment (apex)	1948	1949	1950	1951	*Total*
No. of meteors . .	11	43	36	62	152
R.m.s. error km./sec. .	3·5	5·5	4·3	4·3	4·6

The r.m.s. error of the seven velocities in Table 75 is 8·6 km./sec., and when compared with the r.m.s. error of the 70-km. group in Table 76 it is evident that the seven meteors have unusually large errors, and that

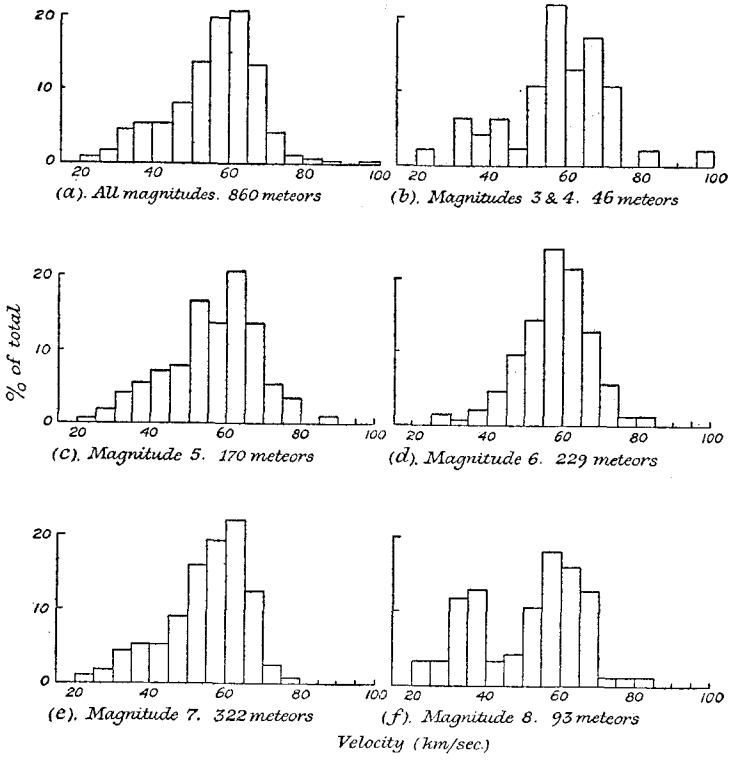
% of total
(a). All magnitudes. 860 meteors
(b). Magnitudes 3 & 4. 46 meteors
(c). Magnitude 5. 170 meteors
(d). Magnitude 6. 229 meteors
(e). Magnitude 7. 322 meteors
(f). Magnitude 8. 93 meteors
Velocity (km/sec.)

FIG. 113. The velocity distribution (*a*) for all magnitudes of meteors in the apex experiments, (*b*) for magnitude groups 3 and 4, (*c*) for magnitude group 5, (*d*) for magnitude group 6, (*e*) for magnitude group 7, (*f*) for magnitude group 8.

their true velocities may lie within the parabolic limit. Even so, it can be shown on statistical grounds that the number is more than would be expected, and, although the number is too small for any definite conclusion to be reached, the fact cannot be excluded that about 1 per cent.

(iii) *The effect of side lobes.* Each of the aerial systems had a subsidiary lobe at high elevation in an easterly direction. Although the power radiated in this lobe was small, meteors recorded in it were at short range, and hence the sensitivity was relatively high. The meteors thus recorded were distinguished by their short range, and their contributions in the histograms of Figs. 101, 102, 103, 104, and 105 are unshaded. The most probable radiant point for these meteors is low in the west, that is, near the antihelion point in the apex experiment, and near the helion point in the antapex experiment. The exact elongation is not known, but estimates based on the most probable elongation indicate that the velocities of these meteors are also non-hyperbolic. The theoretical curves have been normalized to distributions which omit these short-range meteors, since they do not arise from the parts of the sky considered in deriving the theoretical distribution.

(iv) *The high velocity tail.* In the apex experiments 860 meteors were measured in the main lobes of the aerials. Seven of these yielded velocities exceeding 80 km./sec. Although this is less than 1 per cent. of the total, it is interesting to examine whether this actually represents a hyperbolic component, or whether the high velocities can be attributed to errors of measurement. The details of the seven measurements are listed in Table 75.

TABLE 75

Details of Seven Velocities in excess of 80 *km./sec.*

Date	*Time d. h. m.*	*Velocity km./sec.*	*Range km.*	*Amplitude × receiver noise level*	*Electron density $\times 10^{10}$/cm. path*
1948 Nov. .	2 09 33	80·5± 2·9	275	7	29
1949 Nov. .	2 06 12	83·3± 6·9	380	5	30
1949 Nov. .	12 06 50	82·4± 5·0	700	6	136
1949 Nov. .	19 05 40	96·9±12·6	615	9	119
1949 Dec. .	10 06 26	87·0± 9·6	460	7	42
1950 Nov. .	18 05 21	80·4± 8·1	700	6	26·8
1951 Nov. .	26 07 10	83·5±11·1	180	9	4·9

The errors quoted are calculated from the number of pulses in each zone, and although this yields a high value for the error (see § 1 (*c*)), the figures can be compared directly with those obtained in other velocity ranges. The corresponding errors for meteors in the velocity group 65–75 km./sec. measured in the same experiments are given in Table 76.

(equipments II, III, IV) as well as 4 m. (equipment I), and also by the observed antapex distribution. Deceleration can also be eliminated, since the radio-echo velocity measurements on the shower meteors (Chap. XIII et. seq.) show that this effect is small. The low value of the peak velocity therefore appears to be a real effect.

The two possible sources of the discrepancy lie in the basic assumptions from which the theoretical curves were derived. Firstly, it was assumed that the parabolic orbits were distributed at random. The apparatus was sensitive to radiants contained in a strip of sky cutting the ecliptic at the apex and continuing along a line of constant ecliptic longitude from this point. But the area which would produce velocities of 60 km./sec. from meteors moving at parabolic heliocentric velocity lies near the zenith, 45° from the apex and in ecliptic latitude 45°. Hence, if the results are to be explained in this way, a very large concentration of radiants would be required in this area. Such a concentration is completely at variance with the visual and radio-echo results on the distribution described in Chapter VI. Secondly, it was assumed that the meteors were moving in parabolic orbits. On this basis and the assumption of random directions, over half the meteors come from the zone of sky close enough to the apex to yield velocities between 67 and 73 km./sec. Any reduction in the heliocentric velocity will increase the concentration in this area. Thus the observed distributions give a measure of the heliocentric velocity distribution, which may be estimated by subtracting the earth's orbital velocity from the observed velocity peak. Hence the results are compatible with sporadic meteors moving with a heliocentric velocity of about 34 km./sec., that is, in elliptical orbits with periods of about two years. The complete observational disagreement between these conclusions and those of Öpik is extremely pronounced.

(ii) *The antapex experiments.* The early results, especially those obtained with equipment I, were criticized by Öpik† on the grounds that the apparatus possessed an instrumental cut-off which precluded the measurement of high velocities. The antapex experiments were primarily designed to answer this criticism, and the distributions in Figs. 102, 104 show that the lack of high velocities is a real effect. The discrepancy between the observational and theoretical curves is similar to that observed in the apex experiments. On account of the broad shape of the distribution it is difficult to analyse the cause of the discrepancy in any detail, although general support is given to the conclusions reached in (i) above.

† Öpik, E. J., *Irish Astr. J.* **1** (1950), 80.

TABLE 73

Comparison of Magnitudes obtained from Visual Rates and Electron Densities

	From visual rate (magnitude at peak frequency)	*From electron density (magnitude at peak frequency)*
	+	+
1949 apex .	6·0	5·5
1950 apex .	7·5	7·0
1951 apex .	8·5	8·0

TABLE 74

Number of Meteors observed in Different Magnitude Groups during the Radio-echo Apex Experiments

Magnitude† m	*Electron line density* $\alpha_0 \times 10^{10}$	1948 *apex*	1949 *apex*	1950 *apex*	1951 *apex*	*Total*
3 and 4	> 100	9	29	8	..	46
5	39·8 —100	37	118	14	..	169
6	15·9 — 39·8	20	36	169	7	232
7	6·31— 15·9	..	..	128	187	315
8	2·51— 6·31	..	..	1	93	94

(*g*) *Discussion of Results*

A comparison of the experimental and theoretical distributions in Figs. 100–5 shows immediately that the results are in serious conflict with the measurements of Öpik, and that if any meteors move with hyperbolic velocities they must represent only a small fraction of the total number. Nevertheless, the experimental distributions show considerable disagreement when compared with the theoretical distributions calculated on the basis of a random distribution of parabolic orbits. The significance of these departures is discussed in this section.

(i) *The apex experiments.* The theoretical distributions calculated on the basis of parabolic orbits show that the most probable velocity should be nearly 72 km./sec., whereas in each case the observed distribution peaks at about 60 km./sec. The possibility of instrumental causes for this cut-off has been excluded by measurements on a wave-length of 8 m.

† Group 5 denotes magnitudes 5·0–5·9 inclusive, and similarly for the other groups.

that described in § 1 (*d*) (iii) above. Assuming a mean position of 45° for the apex during the course of the experiments, the relative numbers of meteors passing through a square kilometre of the 95 km. surface from a square degree in different parts of the sky is first calculated. The total of these numbers is then normalized to the appropriate number in column 5 of Table 4 (p. 10), and hence the true number of meteors falling on a square kilometre of horizontal surface from a given area of sky is obtained. The number of meteors of given magnitude observed by the radio apparatus is obtained by summing the product of the number from a given area of sky and the collecting area of the aerial for that magnitude and radiant direction, the sum being taken over all parts of the sky to which the aerial is sensitive. The subsequent procedure of comparison between the visual and radio data may be illustrated by reference to the 1950 apex experiment.

On the above basis the magnitude distribution peaked at +5·7 and the hourly rate was 2·1 for an assumed visual rate of one per hour (according to the normalization carried out against Table 4). At 06h. in the autumn mornings the true visual rate is 10 per hour. Thus the above radio rate has to be increased to 21 for the assumed magnitude distribution. The true magnitude range is then obtained from a comparison of this figure with the actual radio-echo rate. The observed rate was 292 per hour, and hence the assumed magnitude scale must be shifted by 2·5 log(292/21) or 2·9 magnitudes, giving a magnitude distribution with maximum at (5·7+2·9) = 8·6. Actually in this experiment only 40 per cent. of the echoes could be classed as 'velocity type'; the majority of the remainder were long-duration echoes having been recorded by the apparatus after trail distortion. On this basis the above scaling is modified to magnitude 7·6 at the peak of the distribution.

Similar analysis was applied to the 1949 and 1951 apex experiments; the results are given in Table 73 compared with the magnitude estimates for the electron density calculations. The method could not be applied satisfactorily to the antapex experiments owing to lack of data on the correct visual rate to be assumed.

In view of the uncertainties regarding the ionizing and luminous efficiencies of meteors on the one hand, and the uncertainty regarding the collecting area of a visual observer for meteors of a given magnitude on the other, the agreement between the two estimates must be regarded as very reasonable.

The final assessment of the numbers of meteors in the various magnitude groups observed during the apex experiments is given in Table 74.

TABLE 72

Distribution of Electron Densities observed in the Experiments on the Velocity Distribution

Line density, α_0, *electrons/cm.* $\times 10^{10}$	*Zenithal magnitude* m, *calculated from* α_0 *using eq.* (14)	*Number of meteors in the various experiments*					
		Equipment I 1948 *Apex*	*Equipment II* 1949 *Apex*	*Equipment II* 1950 *Antapex*	*Equipment III* 1950 *Apex*	*Equipment III* 1951 *Antapex*	*Equipment IV* 1951 *Apex*
398–631	3·5–3·0	..	1	4	..	..	..
251–398	4·0–3·5	..	..	3	1	..	..
159–251	4·5–4·0	2	2	5	4	..	..
100–159	5·0–4·5	7	26	17	3	..	..
63·1–100	5·5–5·0	12	37	26	4	..	..
39·8–63·1	6·0–5·5	25	81	25	10	2	..
25·1–39·8	6·5–6·0	16	24	4	55	4	1
15·9–25·1	7·0–6·5	4	12	..	114	7	15
10·0–15·9	7·5–7·0	..	..	..	117	13	31
6·31–10·0	8·0–7·5	..	..	..	11	5	156
3·98–6·31	8·5–8·0	..	..	..	1	2	68
2·51–3·98	9·0–8·5	..	..	..	..	2	24
1·59–2·51	9·5–9·0	..	..	..	..	..	1

factor. The work of Greenhow and Hawkins† on this subject has been referred to in Chapter III, from which it appears that the most reasonable value to assume for the ionizing efficiency is 0·2, at least for values of $\alpha_0 < 10^{13}$ electrons/cm. path. On the basis of the results for the Perseid meteor shower, the relation between zenithal magnitude m and α_0 is given as

$$\mathrm{m} = 35 - 2{\cdot}5 \log \alpha_0. \qquad (14)$$

Since the major number of velocities in the experiments described above were of the same order as the Perseid velocities (60 km./sec.), this relation has been used to obtain the visual magnitudes for the line densities listed in Table 72.

(ii) *Magnitude estimates from comparison of the visual and radio-echo rates.* An alternative method of estimating the range of magnitudes covered in these experiments consists in a comparison of the rates observed visually and by the radio-echo apparatus. This comparison can be made if the relative collecting areas for meteors of different magnitudes are known both for the visual observer and for the radio-echo equipment. The case of the visual observations has been discussed in Chapter II, and the relevant data for the number of meteors of different magnitudes seen by a visual observer is contained in Table 4 (p. 10).

The calculation of the collecting area for the radio apparatus follows

† Greenhow, J. S., and Hawkins, G. S., *Nature*, **170** (1952), 355.

are shown as the full lines together with the histograms of the experimental distributions in Figs. 100–5. A discussion of these curves is given in § 1 (*g*).

(*f*) *The Range in Magnitudes of the Measured Meteors*

Two methods were used to investigate the range of equivalent visual magnitudes covered in this work on the sporadic distribution. The first method involved the calculation of the electron densities in the trails and a subsequent conversion to visual magnitude, while the second method involved a comparison of the radio echo and visual meteor rates.

(i) *The electron densities and conversion to visual magnitudes.* The relation between the electron densities in the meteor trails, the parameters of the apparatus, and the signal strength of the radio echo has been discussed in Chapter III. It was found that the meteors investigated with the equipments described in § 1 (*a*) produced electron line densities, α_0, such that equation (6) of Chapter III could be used without significant error. For each equipment the wave-length λ and transmitter power P are known. For each meteor the range R is measured, and the received power $\bar{\omega}$ can be calculated from the measured signal noise ratio of the radio echo. In the case of the remaining parameter—the power gain of the aerial G—the value to be used is not that quoted in § 1 (*a*) for the main axis of the aerial, but the value which is effective in the direction of the observed echo. This depends on the range R, and azimuth from the axis of the aerial. The azimuth for the individual echo is not known, but a method of calculating the most probable value of the sensitivity ($G/R^{\frac{3}{2}}$) for each case has been described by Almond, Davies, and Lovell.† Hence the individual electron densities can be calculated from equation (6) of Chapter III. The data are summarized in Table 72 for the various apex and antapex experiments.

The conversion of these line densities to equivalent visual magnitudes requires a knowledge of the ionizing efficiency of meteors. In reviewing the subject in 1948, Herlofson‡ concluded that the ionizing efficiency was 0·01 (the probability that an evaporated meteor atom will produce an electron by collision), and on this basis a meteor of visual magnitude +1 should produce 10^{12} electrons/cm. path. Although the early radio-echo results appeared to support this estimate, a better understanding of the radio-wave scattering processes (Chap. III) soon made it apparent that this estimate of the ionizing efficiency must be too low by a large

† Almond, M., Davies, J. G., and Lovell, A. C. B., *Mon. Not. Roy. Astr. Soc.* **111** (1951), 585.

‡ Herlofson, N., *Rep. Phys. Soc. Progr. Phys.* **11** (1948), 444.

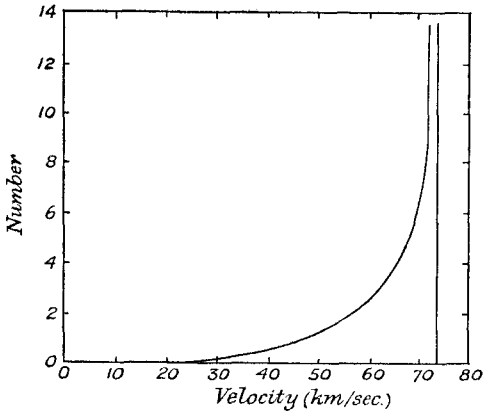

(*a*)

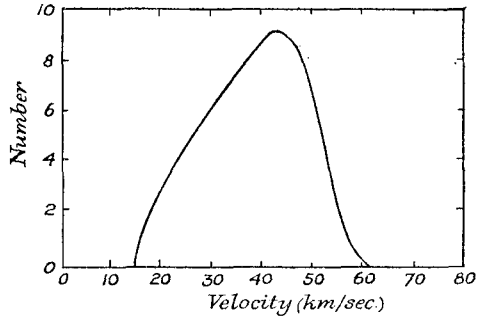

(*b*)

FIG. 112. The theoretical velocity distributions calculated for equipment II (§ 1 (*a*)).

(*a*) The distribution for the 1949 apex experiment.
(*b*) The distribution for the 1950 antapex experiment.

(*e*) *Comparison of the Theoretical and Experimental Distributions*

The theoretical distributions for the various equipments and experiments described in §§ 1 (*a*) and (*b*) were calculated as described above. In order to obtain convenient curves with which the various experimental distributions could be compared, the errors of measurement, assessed as described in § 1 (*c*), were superimposed on the theoretical distributions. For each 1 km./sec. interval the proportion of meteors which would remain in the interval or be shifted 1, 2, 3, etc., km./sec. either side was calculated. Summation of the numbers in each interval then gave the final distribution for comparison with the experimentally observed distribution. These error-corrected theoretical curves

had their reflecting points on the contour $\mathbf{q}_0 = 0{\cdot}23$, and the largest area in each case has been taken as the one extending outwards to this contour. Of the total of forty-five segments, all except the one nearest to the zenith were situated symmetrically in pairs, on either side of the axis of the beam, so that only twenty-three radiant positions were required.

(iv) *Calculation of the velocity distribution.* The collecting areas of Table 71 can be used to find the numbers of meteors from each segment detected by the apparatus, provided the functions $F(\alpha_0')$ and $f(v)\sin\beta$ of (8) and (12) are known. $F(\alpha_0')$ depends on the mass distribution of the meteors, and, on the basis of the evidence given in Chapter VII, $F(\alpha_0')$ has been taken as $1/\alpha_0'$. Equation (10) then gives the number of meteors N_l from the l-th segment as

$$N_l = \tfrac{1}{2}\eta_l \log\gamma \sum_{p=1}^{n} (\boldsymbol{a}_{p-1}+\boldsymbol{a}_p). \qquad (13)$$

As regards the function f(v), Clegg showed that the internal evidence from the experiments suggested that $f(v) = v^\sigma$ with $\sigma = 1$.†

It may be assumed, therefore, that the meteors detected out to the farthest contour $\mathbf{q}_0 = 0{\cdot}23$ were those of such a velocity and radiant altitude that $v\sin\beta$ had its maximum value $(v\sin\beta)_m$. In the apex experiments this condition was fulfilled for particles emanating from the segment at an altitude of 70°, while for the antapex experiment the corresponding altitude was 35°. In the case of a segment for which $v\sin\beta$ is lower than the maximum value by a factor γ^{-p}, where p is a positive integer, the outermost collecting area must be taken as the one extending outwards to the contour $\mathbf{q}_p = 0{\cdot}23\,\gamma^p$. For segments for which $v\sin\beta$ does not differ from $(v\sin\beta)_m$ by an integral power of γ the areas can be estimated by interpolation. After correcting the figures of Table 71 in this way for each radiant position in turn, the appropriate values of $\sum_{p=1}^{n} (\boldsymbol{a}_{p-1}+\boldsymbol{a}_p)$ can be found for the various segments. Since η is known from (9), the relative values of N_l can be determined from (13) and, using (4), can be plotted as a function of velocity.

Examples of the theoretical velocity distributions obtained in this manner are shown in Fig. 112 (*a*) and (*b*).

† This value, derived from the experimental results, is not in agreement with the value calculated by Öpik (*Tartu Obs. Publ.* **30** (1940), no. 5) of $\sigma = 2{\cdot}5$. The assumption of a higher value for σ shifts the peaks of the theoretical distributions in Fig. 112 to higher velocities. It will be seen in § 1 (*g*) that such an assumption would serve to strengthen further the deductions made from the experiments. A value of $\sigma < 1$ would shift the maximum of the curves in Fig. 112 to lower velocities. However, it is not possible to justify on theoretical grounds values of $\sigma < 1$.

the position of the line mm′, corresponding to the height of maximum ionization, is estimated. The area extends laterally to the points x, y, where this line cuts the contour q_0, and its boundary cuts the inner contours at points where the electron density has fallen by successive multiples of the chosen factor γ. The vertical distances of these points above and below mm′ can be read off from Fig. 111. To find the corresponding distances along the echo plane, which is inclined at an angle β to the vertical, we must multiply by $\sec\beta$. Corresponding areas for meteors of other mass groups can be drawn in a similar manner.

As an example, the collecting areas for the aerial system used in equipment II (§ 1 (*a*)), corresponding to the various segments of Fig. 109, are given in Table 71.

TABLE 71

Collecting Areas of Aerial System

χ *deg.*	β *deg.*	*Collecting areas in km².*						
		$q_6 = 2{\cdot}07$	$q_5 = 1{\cdot}44$	$q_4 = 1{\cdot}00$	$q_3 = 0{\cdot}69$	$q_2 = 0{\cdot}48$	$q_1 = 0{\cdot}34$	$q_0 = 0{\cdot}23$
83·5	10	..	386	1 350	2 580	3 800	5 150	6 450
92	10	645	1 820	2 900	4 030	5 150	6 540	8 050
100	10	65	965	1 830	2 990	4 350	5 860	7 080
85	20	..	370	1 450	2 580	3 540	5 060	7 250
93·5	20	645	1 770	3 310	4 760	6 120	7 020	9 170
102·5	20	166	677	1 925	3 060	4 180	5 320	6 830
86·5	30	..	96·5	1 350	2 580	4 030	5 320	6 920
96	30	680	2 160	3 640	4 990	5 630	7 730	9 170
105·5	30	322	1 060	2 060	3 280	4 180	5 320	6 550
88	40	..	..	370	1 930	3 600	5 310	7 570
98·5	40	805	2 250	3 600	5 220	6 920	8 370	9 660
109·5	40	129	1 130	2 090	3 150	4 180	5 410	6 700
90	50	..	..	..	1 290	3 220	5 480	7 570
102	50	900	2 250	3 700	5 960	7 510	9 350	11 920
116	50	..	935	1 770	2 740	3 860	5 320	6 510
91·5	60	..	..	..	..	645	2 570	5 800
108	60	645	2 540	4 570	6 770	9 180	10 950	13 350
126	60	481	1 450	2 800	3 770	5 080	6 450	7 950
94	70	..	..	..	..	..	..	..
119	70	805	3 000	5 800	8 220	10 700	13 700	16 730
154	70	..	741	2 090	3 280	4 770	5 800	7 410
100·5	80	..	..	..	..	..	..	..
180	80	805	3 220	8 050	11 300	14 500	19 300	23 400

The two left-hand columns indicate the azimuth χ and the altitude β of the centre points of the segments relative to the axis of the aerial beam. Other columns show the measured areas for values of the limiting sensitivity contour differing by factors of $q = 1{\cdot}44$. It was found experimentally that the most distant meteors detected by the apparatus

meteors from the l-th segment will therefore be

$$N_l = \tfrac{1}{2}\eta_l \sum_{p=0}^{n} (a_{p-1}+a_p) \int_{\alpha_0^m/\gamma^{p}}^{\alpha_0^m/\gamma^{p-1}} F(\alpha_0')\, d\alpha_0'. \qquad (10)$$

Hence, if $F(\alpha_0')$ is known, and if the collecting areas can be constructed, a relationship can be found between η_l and the observed hourly rate.

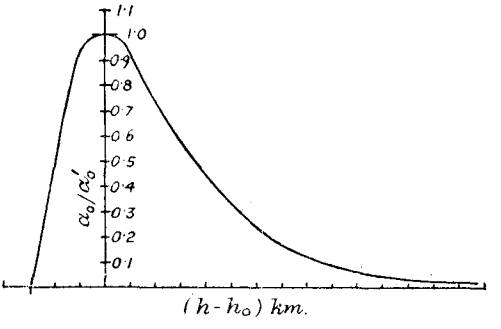

FIG. 111. Theoretical curve for the variation of ionization α_0 of a meteor with height h. The maximum ionization α_0' occurs at height h_0.

The shapes and sizes of the collecting areas depend on the variation of electron density along the trail. Clegg used the relationship derived by Herlofson† for the relation between the electron density α_0 and the height h in the atmosphere:

$$\alpha_0 = \frac{9}{4}\alpha_0'\left\{1-\frac{1}{3}\exp\left(\frac{h_0-h}{H}\right)\right\}^2 \exp\left(\frac{h_0-h}{H}\right), \qquad (11)$$

where α_0' is the maximum ionization used above, h_0 is the height of maximum ionization, and H is the scale height. In this α_0' is given by

$$\alpha_0' \propto \boldsymbol{m} f(v)\sin\beta, \qquad (12)$$

where $\boldsymbol{m}$ is the meteor mass, v the initial velocity, and β the altitude of the radiant. In the present case the dependence of h_0 on $\boldsymbol{m}$, v, and β has not been taken into account, since the errors introduced thereby in computing the field of view of the apparatus are small. The value of α_0/α_0' as a function of $(h-h_0)$ for $H = 10$ km. is plotted in Fig. 111.

This curve can be used directly to find the overall collecting area of the apparatus for any given radiant position. Consider, for example, the delineation of the area xwyz of Fig. 110. A plan of the echo plane, showing the configuration of the sensitivity contours is first constructed, and

† Herlofson, N., *Rep. Phys. Soc. Prog. Phys.* **11** (1947), 444.

radiant position is described by Clegg† in an appendix to the original paper.

Consider meteors of a certain mass group which produce their maximum electron density corresponding to α_0' at height mm′, and assume that they are just detectable out to points xy, on the contour $\mathbf{q}_0$ (Fig. 110). Meteors of the same mass which cross the echo plane closer to the axis of the beam cut contours of higher value and will be detectable above and below mm′. A curve xwyz can be defined inside of which meteors of this class can be observed. Similar areas can be defined for meteors in other mass groups with values of α_0 differing from α_0' by factors $\gamma^{\pm p}$, where p is an integer. The conditions determining the shapes of these areas are discussed below. Experimentally it is found that there is a fairly well-defined range limit beyond which no echoes appear, and the largest area which need be considered corresponds to this limit. The value of $\alpha_0 = \alpha_0^{\mathrm{m}}$ corresponding to this area can be found from the parameters of the apparatus.

The number of meteors falling on the earth from the l-th segment with electron density values between α_0' and $\overline{\alpha_0'+\mathrm{d}\alpha_0'}$ can be written as

$$\mathrm{dN}_{\alpha_0' l} = \eta_l \, \mathrm{F}(\alpha_0') \, \mathrm{d}\alpha_0', \tag{8}$$

where $\mathrm{F}(\alpha_0')$ is a predetermined function, and

$$\eta_l \propto \left(\frac{\mathrm{N}_\epsilon}{\mathrm{N}}\right) \Delta \mathrm{S}, \tag{9}$$

ΔS being the area of the segment.

A series of curves similar to xwyz, corresponding to $\alpha_0^{\mathrm{m}}, \frac{\alpha_0^{\mathrm{m}}}{\gamma}, \ldots, \frac{\alpha_0^{\mathrm{m}}}{\gamma^{\mathrm{p}}}$ can be constructed for any radiant position, and their areas $\boldsymbol{a}_0, \boldsymbol{a}_1, \ldots \boldsymbol{a}_{\mathrm{p}}$ measured. The number n of such curves will be finite, the smallest having an area $\boldsymbol{a}_{\mathrm{n}-1}$, the area $\boldsymbol{a}_{\mathrm{n}}$ corresponding to $\alpha_0^{\mathrm{m}}/\gamma^{\mathrm{n}}$ being zero. Consider the trails between α_0^{m} and $\alpha_0^{\mathrm{m}}/\gamma$; the largest will be detected in the area $\boldsymbol{a}_0$, but the smallest only in $\boldsymbol{a}_1$. The effective collecting area for this group is therefore approximately equal to $\frac{1}{2}(\boldsymbol{a}_0+\boldsymbol{a}_1)$ and the total hourly number detected will be

$$\tfrac{1}{2}(\boldsymbol{a}_0+\boldsymbol{a}_1)\eta_l \int_{\alpha_0^{\mathrm{m}}/\gamma}^{\alpha_0^{\mathrm{m}}} \mathrm{F}(\alpha_0') \, \mathrm{d}\alpha_0'.$$

Similar expressions follow for other groups and the total echo rate N_l for

† Clegg, J. A., *Mon. Not. Roy. Astr. Soc.* **112** (1952), 399.

The echoes from the meteors emanating from a single segment are all returned from the neighbourhood of a plane surface perpendicular to the direction of the radiant and passing through O. In Fig. 110 the radiant is in the direction OR, at altitude β. OABC is the earth's surface and the echo plane OXYA is inclined at $(90°-\beta)$ to the horizontal. The

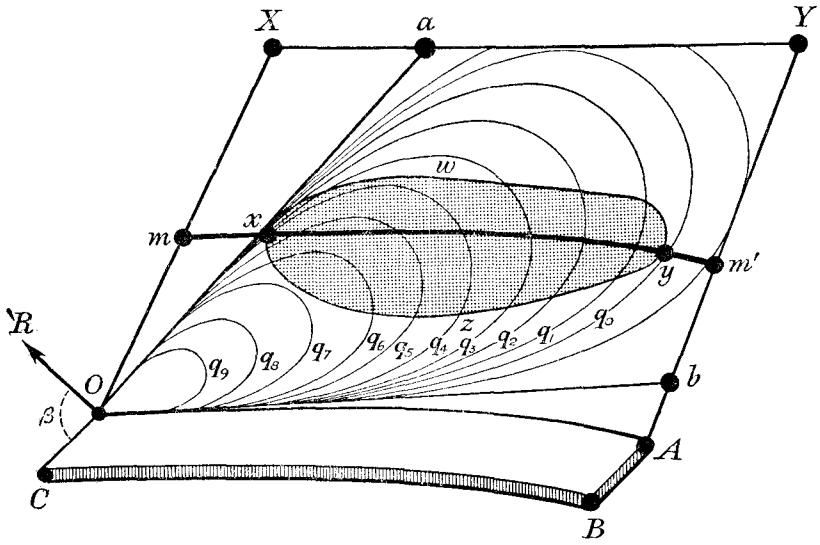

FIG. 110. Sensitivity contours on the echo plane. Oa, Ob represent the limits of the aerial coverage. The shaded area xwyz represents the collecting area of the apparatus for meteors of a given mass group.

aerial polar diagram is represented, as in Chapter IV, by contours on this plane corresponding to different values $\mathbf{q}_0, \mathbf{q}_1, \ldots$ of the overall sensitivity of the apparatus. Then for a trail whose reflecting point lies on the contour $\mathbf{q}_p$ the amplitude Z of the echo is given by equation (3) of Chapter IV,

$$Z = k\mathbf{q}_p \alpha_0, \tag{7}$$

where k is a constant depending on the parameters of the apparatus, and α_0 is the electron line density in the trail.† It is convenient to choose the $\mathbf{q}$ values such that $\mathbf{q}_{p+1} = \gamma \mathbf{q}_p$, where γ is a numerical factor greater than unity, determined by the required contour spacing. A geometrical method for constructing the contours for a given aerial system and any

† It is assumed that the electrons behave as individual scatterers: that is, equation (6) of Chap. III applies. In the magnitude range covered by the series of experiments this assumption is justifiable. For more densely ionizing meteors the quantity α_0 in (7) could not be assumed to be the line density (see Chap. III) and the collecting areas derived here would need modification.

same velocity and direction of flight, and they can be treated as members of a single shower with a point radiant situated in the centre of the segment. The elongations of the centre points of the segments from A can be measured, and the values of v_g and N_ϵ/N found from the curves in Fig. 108.

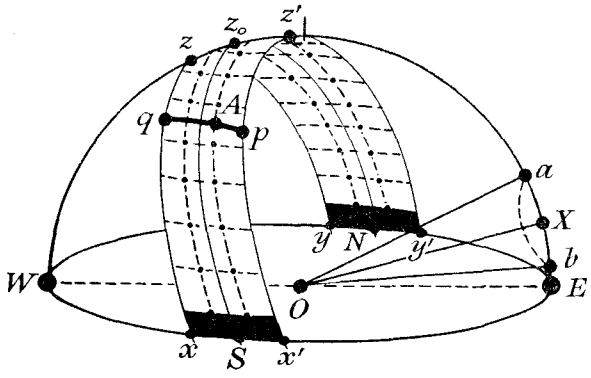

FIG. 109. Segments of celestial sphere representing radiants within the aerial coverage. The shaded areas close to xx', yy', which are 5° in vertical width, contribute a negligible number of meteors, and have been ignored.

Each of the apex and antapex experiments referred to above extended over several months, and in computing N_ϵ/N and v_g mean values were taken for the declination of A. Observations were made over periods of approximately 2 hours, during which A moved some distance across the strip via the path pq, and a mean position was assumed. It was found sufficient to divide the strip xzy, x'z'y', into forty-five segments of equal area, in the way shown in the figure. The elongation ϵ of the centre point of each segment from the apex, and the altitude and azimuth relative to the direction OE was measured by constructing a model of Fig. 109 on a sphere.

(iii) *The effective collecting area of the apparatus.* The probabilities of detection of meteors by the apparatus will differ for the various segments in Fig. 109, and in order to determine the relationship between the true hourly numbers of meteors from the various segments, and the corresponding radio-echo rates, the effective collecting area of the apparatus must be found for the individual radiant positions. This effective area has already been discussed in Chapter IV for meteors of a single shower. For the individual segments in Fig. 109 the treatment given by Clegg† is as follows.

† Clegg, J. A., *Mon. Not. Roy. Astr. Soc.* **112** (1952), 399.

and at that time thought that a more active shower which he had observed on 1914 September 23, 24, at α 270°, δ +50° might be the related display.

In 1920 Davidson† published corrections to his former calculations which arose because the value of ω for the comet had been taken to be 191° 28′ instead of 171° 28′. The new calculated position of the radiant was α 251·5°, δ +55·9°, the comet's distance from the earth's orbit being $5\frac{1}{2}$ million miles. Later, however, Crommelin‡ pointed out that according to the elements of the comet given for the 1926 return, the orbit of the earth and the comet actually intersected, and that the radiant should be at about October 10, α 265°, δ +54°. A further investigation by Davidson‡ agreed with this view and placed the radiant at α 261°, δ +53·5°. Very great interest therefore attached to the 1926 return, and the observations left no doubt that an appreciable meteor shower occurred as predicted. The earth crossed the orbit even closer to the comet in 1933 and 1946 and the showers then witnessed are classed amongst the few great meteoric storms which have occurred during the past century. Fisher§ has since investigated the ancient records of meteor showers and from an analysis of the relative position of the earth and the comet at the various dates concludes that returns of the Giacobinid shower may also have been witnessed in A.D. 585, 859, 1385, 1841, and 1847.

(*b*) *Activity*

The Giacobinid shower has now been observed on four returns, 1926, 1933, 1946, and 1952. In 1926, the earth crossed the cometary orbit 70 days before the comet; in 1933, 80 days after the comet, and, in 1946, 15 days after the comet. In 1939 the orbit was crossed 136 days before the comet and no shower was observed, but in 1952, when the orbit was crossed 195 days ahead of the comet, an intense shower was recorded in daylight by the radio-echo apparatus.

The 1926 observations have been described by Prentice‖ and by Denning.†† Prentice observed in a clear sky for 3 hours between 20h. 20m. and 23h. 20m. on October 9 and estimated the hourly rate from the radiant in Draco to be about seventeen. By far the most spectacular event of this return was, however, the occurrence of a great fireball on 1926 October 9d. 22h. 16m. U.T. from the Draco radiant. Thirty-five

† Davidson, M., *Mon. Not. Roy. Astr. Soc.* **80** (1920), 739.
‡ This information is given by Denning, W. F., ibid. **87** (1926), 104.
§ Fisher, W. J., *Bull. Harv. Coll. Obs.* (1934), no. 894, 15.
‖ Prentice, J. P. M., *J. Brit. Astr. Assoc.* **44** (1934), 108.
†† Denning, W. F., *Mon. Not. Roy. Astr. Soc.* **87** (1926), 104.

observations were found to be suitable for analysis. The original data were computed by King† and a full description of the observations was published later by Porter and Prentice.‡ This fireball was of zenithal magnitude −7 and left a long-enduring train which persisted for between 32 and 40 minutes.

Records of the watches in the intervening years 1927–32 inclusive have been given by Prentice§ and show no activity from the shower. On 1933 October 9, however, when the earth crossed the orbit 80 days behind the comet, a great meteoric storm was witnessed in many parts of the world. Most of the observers in England§ were handicapped by cloud, but King‖ has collected and summarized many reports from other parts of the British Isles and from observers widely scattered in Europe. It is evident from these reports that the total duration of the shower was only some 4 to 4·5 hours and that the maximum occurred at 20h. on 1933 October 9. The numbers were so great that few observers were able to count the rate, but it seems clear that the rate at maximum must have been 4,000 to 6,000 per hour. The most detailed information is that obtained by de Roy†† in Belgium and by Sandig and Richter‡‡ in Leipzig, who undertook telescopic observations. A comparison of these visual and telescopic data has been made by Watson.§§ The hourly-rate curve obtained by de Roy (Fig. 161), shows a sharp maximum of about 5,400 per hour at 20h. 15m. U.T. He also made magnitude estimates of 534 meteors over two periods shown as I and II in Fig. 161. These observations confirm the statement of nearly all observers that the majority of the meteors were faint. The analysis of this magnitude distribution and of the telescopic magnitude distribution will be discussed in Chapter XIX. Emanuelli‖‖ made a critical analysis of a great number of observations which were published on the 1933 shower, from which he concluded that the maximum was at 20h. 4m., when the hourly rate was 19,000.

Attempts to observe the shower in England at the 1939 and 1940 return have been described by Prentice.††† No Giacobinid meteors were found but in view of the short period characteristics of the shower in

† See Denning, W. F. (1926), loc. cit., and Prentice (1934), loc. cit.
‡ Porter, J. G., and Prentice, J. P. M., *J. Brit. Astr. Assoc.* **49** (1939), 337.
§ Prentice, J. P. M., *J. Brit. Astr. Assoc.* **44** (1934), 110.
‖ King, A., ibid., p. 111.
†† de Roy, F., *Gazette Astronomique*, **20** (1933), 170.
‡‡ Sandig, H., and Richter, N., *Astr. Nachr.* **250** (1933), 170.
§§ Watson, F., *Bull. Harv. Coll. Obs.* (1934), no. 895, 9.
‖‖ Emanuelli, P., *Coelum*, **9** (1939), 161.
††† Prentice, J. P. M., *J. Brit. Astr. Assoc.* **50** (1939), 27; **51** (1940), 18.

1933 and 1946 it appears that daylight may have interfered with the observations, since the predicted time of maximum fell after dawn in 1939 and during the afternoon in 1940.† However, there are no reports of any appreciable shower from other parts of the world.

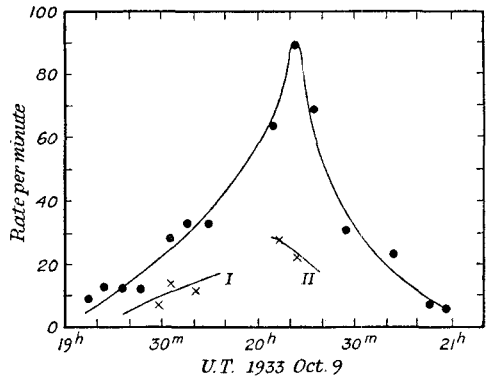

FIG. 161. The activity of the Giacobinid shower on 1933 Oct. 9 according to the visual observations of de Roy. I and II represent the times when magnitude estimates were made of 534 meteors.

The return of the shower in 1946 was well observed visually, photographically, and by the new radio-echo technique in many parts of the world. The shower was again a spectacular occurrence, of short duration —not more than 5 to 6 hours—and with a sharp peak at 1946 October 10d. 3h. 40m. to 3h. 50m.

The activity as found by the various techniques is illustrated in the composite diagram of Fig. 162. The visual records are those compiled by Wylie‡ from six observing groups in America, the photographic records are those given by Jacchia, Kopal, and Millman§ from the Canadian observations and the radio-echo records are from the results obtained in England by Lovell, Banwell, and Clegg‖ at Jodrell Bank. Very similar radio-echo results were also obtained by Appleton and Naismith†† at Slough and by Hey, Parsons, and Stewart‡‡ at Byfleet.

It is evident from these observations that the characteristics of the

† The experience of 1952 when a shower was observed by the radio-echo technique in day-time, with the comet even farther from perihelion, supports the suggestion that the shower may have been missed in 1939 and 1940 because of daylight.

‡ Wylie, C. C., *Sky and Telescope*, **6** (1947), no. 66, 11.

§ Jacchia, L. G., Kopal, Z., and Millman, P. M., *Astrophys. J.* **111** (1950), 104.

‖ Lovell, A. C. B., Banwell, C. J., and Clegg, J. A., *Mon. Not. Roy. Astr. Soc.* **107** (1947), 164. †† Appleton, E. V., and Naismith, R., *Proc. Phys. Soc.* **59** (1947), 461.

‡‡ Hey, J. S., Parsons, S. J., and Stewart, G. S., *Mon. Not. Roy. Astr. Soc.* **107** (1947), 176.

shower were very similar to those of the 1933 return. The hourly rate at maximum according to the visual plots of Wylie was 4,200. According

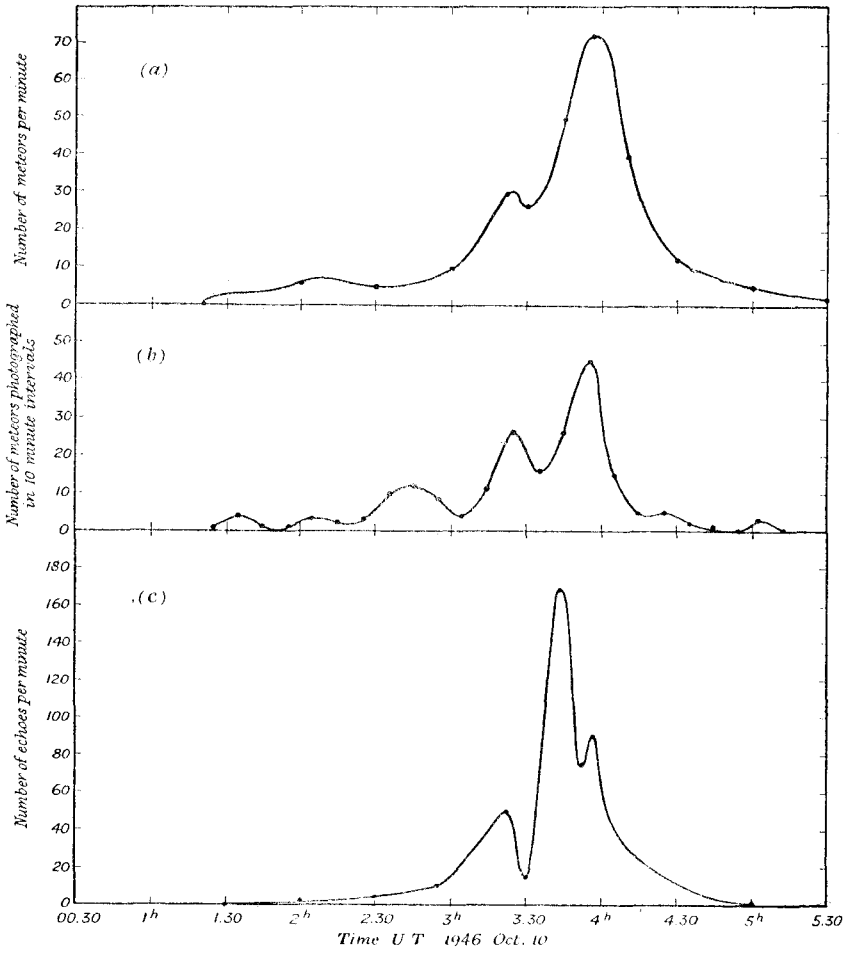

FIG. 162. The activity of the Giacobinid meteor shower on 1946 Oct. 10.

(*a*) Visual, (*b*) photographic, (*c*) radio-echo.

to the ciné-film analysis of the radio-echo results of Lovell, Banwell, and Clegg, 67 echoes were recorded in 24 seconds at the peak, giving an equivalent hourly rate of 10,000; but within ± 5 minutes of this peak the hourly rate had decreased to 3,000 and within ± 30 minutes to 60. The sensitivity of this apparatus was such as to give a close relation to the hourly rates seen by a single visual observer.

Prentice† has summarized the results of the British visual observations. Averaging over 7- or 8-minute intervals yielded a maximum observed rate of 965 which, when allowance was made for the low altitude of the radiant, gave an equivalent zenithal rate of 2,250. Also, using de Roy's magnitude distribution for the 1933 shower, Prentice makes an allowance for the strong moonlight and concludes that the 1946 return was only half as rich as that of 1933. This conclusion is not borne out by the visual results of Wylie or by the radio-echo observations, both of which indicate that the shower was at least as intense as the 1933 return.

An interesting feature of the activity shown in Fig. 162 is the sudden temporary decrease at about 3h. 30m., evident in the visual, photographic, and Jodrell Bank radio records. Jacchia, Kopal, and Millman‡ remark that a similar drop is also evident in the final frequency curve compiled from all the Canadian visual observations.

It is also seen that the radio-echo rates appear to have reached a maximum a few minutes before the visual and photographic maxima, but a subsidiary maximum occurred at the time of the visual and photographic maxima. Experience on other showers, and with the sporadic background, showed that the hourly rates given by the radio apparatus and a visual observer were very similar. Although the radio apparatus samples fainter meteors, its restricted collecting area balances the difference. It may be, therefore, that this high peak at 3h. 40m. consisted of meteors too faint to be visible, and that a separation of meteor masses has already taken place in the Giacobinid stream. It will be noticed that the subsidiary maximum at 3h. 48m. agrees well in time and hourly rate with the visible maximum.

Subsequent radio-echo surveys in 1947–51 showed no unusual activity at the time of the passage of the earth through the orbit of the comet. On 1952 October 9, however, the radio-echo apparatus recorded an intense shower during daylight hours in the afternoon.§ The shower commenced at 14h. 30m. U.T. and rose rapidly after 15h. to a maximum at 15h. 30m. After this time the shower declined quickly, and by 16h. 30m. the activity had fallen to a small fraction of the maximum. The equivalent visual hourly rate during the period of maximum was estimated at 200. One or two meteors at the end of the shower in the early evening were observed visually.§ The summarized data on the activity of the shower are given in Table 125.

† Prentice, J. P. M., *Observatory*, **67** (1947), 3; *J. Brit. Astr. Assoc.* **57** (1947), 86.
‡ Jacchia, L. G., Kopal, Z., and Millman, P. M. (1950), loc. cit.
§ *Brit. Astr. Assoc. Circ.* (1952), no. 337.

TABLE 125

Activity of the Giacobinid Shower

Date	*Earth at node*	*Hourly rate at maximum*
1926	70 days before comet	17
1933	80 days after comet	4,000–6,000
1939	136 days before comet	..
1946	15 days after comet	4,000–6,000
1952	195 days before comet	200

(*c*) *Radiant*

From the observation of fourteen meteors during the first appreciable shower in 1926, Prentice† gave the mean corrected radiant as α 260°, δ +51·5°, with a radiant diameter of 7°. The computation of the radiant of the great fireball was made by King‡ from thirty-five observations and is given as α 262°, δ +55°. The very close agreement of these positions with the predicted radiant position (see (*a*)) left little doubt of the association of the shower with the comet.

During the great shower of 1933 many radiant positions were computed, a large number of which have been collected by King.§ Representative determinations are listed in Table 126.

TABLE 126

Visual Determinations of the Giacobinid Radiant during the 1933 *Return*

Observer	*Number of meteors used in determining the radiant*	*Radiant position* α	δ	*Diameter*
		deg.	*deg.*	*deg.*
Ellison, Armagh	..	267	+55	3
Milligan, Omagh	..	264·5	54·5	..
Dods, Eskdalemuir	..	265·25	52·3	..
Walmesley, Perth	..	265	55	..
Mourant, Jersey	..	256·5	54	..
de Roy, Antwerp	16	262	55	7
Ryves, Spain	..	266	53·5	..
Forbes-Bentley, Malta	..	262·5	55	..
Sytinskaja, Leningrad	110	267·2	55·9	(Corrected α 262·1 δ +55·8)
Astapowitsch, Stalinabad	80	258·0	57·5	..
Malzman, Odessa	18	267	57	..
Schwarzman, Odessa	15	265	15	..
Results of 25 observers on the Continent	Limits	263 to 282	47 to 60	..

† Prentice, J. P. M. (1934), loc. cit.

‡ Quoted by Denning, W. F. (1926), loc. cit., and by Porter, J. G., and Prentice, J. P. M. (1939), loc. cit.

§ King, A. (1934), loc. cit.

Accurate photographic determinations of the radiant position were made by Jacchia, Kopal, and Millman† during the 1946 shower. They used three cameras, behind one rotating shutter, mounted so as to cover 4,000 square degrees of the sky. Over the period of the Giacobinid shower sixteen exposures were made on each camera, the average exposure time being 15 minutes. By this means they obtained photographic information of 204 Giacobinid meteors, each plate containing the photographed trails of a number of meteors. The cameras were stationary; hence the individual radiant points of all the meteor trails on one exposure defined a curve on the film, resulting from the composition of the proper motion of the radiant and the diurnal motion of the sky. The proper motion was computed on the assumption that the meteor particles followed the orbit of the Giacobinid comet exactly and this was combined with the diurnal motion to give the apparent path of the radiant on the films. A visual watch was carried out simultaneously with the photographic recording and 27 meteors visually observed were identified with 27 of the photographed meteors. The time of apparition of these 27 meteors was therefore known accurately. In Table 127, which gives the results of the computation of the radiants, these 27 visually identified meteors are included separately in 6 groups.

TABLE 127

Photographic Determination of the Giacobinid Radiant during the 1946 Return

Exposure set or visual meteor group	*Mean time* 1946 *Oct.* 10	*Number of meteors in group*	*Apparent radiant* (1947·0)		*True radiant corrected for diurnal aberration and zenithal attraction* (1947·0)	
			α	δ	α	δ
			deg.	*deg.*	*deg.*	*deg.*
731–732	1·501	7	266·500	55·048	261·765	54·039
735	2·583	19	267·235	55·822	261·988	54·143
1	2·667	7	266·959	55·782	261·692	54·027
736	2·833	9	267·257	56·057	261·923	54·205
2	2·943	3	267·432	56·125	262·078	54·210
737	3·117	10	267·422	56·177	262·033	54·124
3	3·202	5	267·495	56·223	262·092	54·110
738	3·307	29	267·732	56·261	262·317	54·081
4	3·460	4	267·580	56·405	262·141	54·121
739	3·600	28	267·519	56·463	262·075	54·051
5	3·763	4	267·312	56·618	261·859	54·071
740	3·800	42	267·511	56·692	262·055	54·130
741	4·050	9	267·324	56·773	261·898	54·004
6	4·750	4	267·403	57·357	262·136	54·048

† Jacchia, L. G., Kopal, Z., and Millman, P. M. (1950), loc. cit.

A least squares solution for the true radiant gave

$$1946 \text{ Oct. } 10{\cdot}16 \quad \begin{cases} \alpha = 262{\cdot}07^\circ \pm 0{\cdot}13 & (1947{\cdot}0) \\ \delta = +54{\cdot}09^\circ \pm 0{\cdot}04 \end{cases}$$

with a daily motion of $\begin{cases} \Delta\alpha = +2{\cdot}1^\circ \pm 0{\cdot}9 \\ \Delta\delta = -0{\cdot}1^\circ \pm 0{\cdot}4. \end{cases}$

The motion of the true radiant is direct at a rate of $1{\cdot}3^\circ \pm 0{\cdot}6$ per day, but the authors point out that the reality of this is in doubt because of the relatively large probable error.

For the twenty-seven trails which were also visually observed it was possible to determine the distance of the projected trails from the mean computed radiant. The average value was 7·2′, giving a probable error of spread of 6·2′. The authors conclude that most of this spread can be accounted for by observational errors and that the true cosmic spread was probably less than 2 or 3 minutes of arc. This is very much smaller than the cosmic spread of many other of the major showers (for example, Taurids 17′ Geminids 13·5′; see Chap. XV). This small spread is in marked contrast to the large radiant diameter found in the visual observations.

(*d*) *Velocities*

Until the 1946 return there were no well-attested measurements of the velocities of the Giacobinid meteors. Most of the visual observers had remarked that the meteors were slow in accordance with the original predictions made by Davidson,† and the velocity of the 1933 fireball was computed by King‡ from thirty-five observations to be 32 km./sec. The meteors were so clearly moving in the orbit of the comet, however, that little doubt existed as to their velocity. Computation of the relative velocity of the earth and the meteors was made by Jacchia, Kopal, and Millman§ using Cunningham's‖ orbit for the comet. They obtained the value of 20·433 km./sec. before correction for zenith attraction. The computed geocentric velocity corrected for diurnal aberration and zenith attraction is given in Table 128 for the duration of the shower. The authors expressed confidence that these velocities were correct to 1 in 1,000, since the observed position of the radiant on October 10·16 differed by only 4·5′ from its computed position, this divergence being less than the probable error.

† Davidson, M. (1915), loc. cit.
‡ See Porter, J. G., and Prentice, J. P. M. (1939), loc. cit.
§ Jacchia, L. G., Kopal, Z., and Millman, P. M. (1950), loc. cit.
‖ Cunningham, L. E., *Harvard Announcement Card*, no. 775.

TABLE 128

Computed Velocities of the Giacobinid Meteors 1946

1946 *Oct.* 10 *U.T.*	v_g (*km./sec.*)	1946 *Oct.* 10 *U.T.*	v_g (*km./sec.*)
1·5	23·105	3·5	23·079
2·0	23·095	4·0	23·080
2·5	23·086	4·5	23·084
3·0	23·081	5·0	23·090

The only velocity measurements actually made during the 1946 shower appear to be the radio-echo measurements of Hey, Parsons, and Stewart.† These were remarkable as being the first velocity measurements ever made by radio-echo methods. The technique, in which the reflection from the head of the approaching meteor is observed, has been described in Chapter IV. Twenty-two measurements were made, giving the data listed in Table 129.

TABLE 129

Radio-echo Measurements of the Giacobinid Velocities 1946

1946 *Oct.* 10 *U.T.*	*Velocity* (*km./sec.*)	1946 *Oct.* 10 *U.T.*	*Velocity* (*km./sec.*)
h. m.		h. m.	
00 56	23·4	04 32	23·1
01 19	23·2	04 36	18·6
01 21	23·3	04 43	19·3
01 21	20·5	04 58	25·2
01 43	22·5	04 59	29·8
01 56	24·0	05 02	21·1
03 52	24·3	05 04	19·9
03 59	24·9	05 06	22·7
04 14	25·1	05 07	22·9
04 17	23·5	05 15	25·5
04 31	22·9	06 29	21·9

The weighted mean of the velocities, 22·9$\pm$1·3 km./sec., uncorrected for zenith attraction or diurnal aberration, has to be compared with the computed value, quoted above, of 20·433 km./sec.

(*e*) *Orbit*

The observations described above confirm Davidson's original prediction that the debris associated with the Giacobini–Zinner Comet is responsible for the meteor showers observed in 1926, 1933, 1946, and 1952. As far as the meteor showers are concerned, chief interest, therefore,

† Hey, J. S., Parsons, S. J., and Stewart, G. S. (1947), loc. cit.

TABLE 130

Changes in the Orbit of Comet Giacobini–Zinner since 1900

Year	*Eccentricity* e	*Perihelion distance* q	*Distance between earth's and comet's orbits at node*	*Earth at node*
1900	0·733	0·9319	−0·0619	..
1913	0·720	0·9759	−0·0181	..
1926	0·717	0·9947	+0·0005	70 days before comet
1933	0·716	0·9994	+0·0054	80 days after comet
1939	0·717	0·9955	+0·00125	136 days before comet
1946	0·717	0·9957	+0·00142	15 days after comet
1952	0·718	0·9887	−0·0057	195 days before comet

The information in this table relating to the changes in the eccentricity and perihelion distance since the discovery of the comet in 1900 has been given by Porter.†

TABLE 131

Elements of the Giacobini–Zinner Comet 1946 *and Predicted Elements for* 1953

Authority	*Perihelion passage* T (*U.T.*)	ω	Ω	i	e	a	q	*Mean daily motion n*	*Period* P
		deg.	*deg.*	*deg.*		*a.u.*	*a.u.*	*deg.*	*years*
Cripps‡ . . .	1946 Sept. 18·4991	171·83098	196·28334	30·73015	0·7166767	3·514279	0·9957	0·1496064	6·5880
Dinwoodie§ . . .	1953 April 17·01691	171·90847	196·23070	30·82765	0·7179204	3·504931	0·98867	0·1502052	6·56174

† Porter, J. G., *Rep. Phys. Soc. Progr. Phys.* **11** (1948), 402. I am indebted to Dr. Porter for kindly supplying the data for 1952.
‡ Cripps, F. R., *Brit. Astr. Assoc. Handbook* (1946), p. 38.
§ Dinwoodie, C., ibid. (1952), p. 44.

centres on the effect of perturbations, especially in regard to possible future close encounters of the earth and the comet. The relation between these approaches and the intensity of the meteor shower has been given in Table 125. Future returns of the comet will be awaited with great interest. The 1946 elements of the comet and the predicted elements for the subsequent return in 1953, after allowing for the perturbations by Earth, Jupiter, and Saturn, are given in Table 131.

2. The Leonid shower

(*a*) *History*

The history of the remarkable Leonid shower has been related by Olivier.† The spectacular events during the night of 1833 November 12, when meteors were described as 'falling from the sky like snowflakes', represents, perhaps more than any other event, the beginning of scientific interest in meteor astronomy. Likewise, the failure of the shower to return as predicted in 1899 represents in the opinion of Olivier 'the worst blow ever suffered by astronomy in the eyes of the public'. The display of 1833 drew attention to the accounts of a similar spectacle observed during the night of 1799 November 11. The well-known account by Humboldt, who observed this event in South America, referred to 'thousands of meteors and fireballs moving regularly from north to south with no part of the sky so large as twice the moon's diameter not filled each instant by meteors'. It was during the 1833 display, however, that serious scientific observations were first made, particularly by D. Olmsted, A. C. Twining, and many others who noticed that the meteors appeared to be radiating from a point. In 1863 and 1864 Newton‡ predicted the dates on which previous occurrences of the Leonid shower should have been witnessed and succeeded in tracing its occurrence back to A.D. 585, and also predicted that the shower would return again in November 1866. In 1866 Schiaparelli's orbit for the Leonids was published in his *Sternschnuppen* and the close connexion of this orbit with that of the newly discovered Comet 1866 I was immediately realized. A period of 33·25 years was assigned to the shower, and the expected appearance of another great display on 1866 November 13 was confirmed, although the rate does not appear to have been as great as that in 1833. In the years following this shower J. C. Adams and Stoney investigated the Leonid orbit and the possibility of perturbations in detail. In spite of the caution advanced by such calculations—in

† Olivier, C. P., *Meteors*, ch. 4.

‡ Newton, H. A., *Silliman's Journal* (II), **36** (1863), 146; **37** (1863), 377; **38** (1864), 53.

particular that on the critical date in November 1899 the earth would be 1,300,000 miles from the Leonid orbit—another great shower was confidently expected in November 1899.†

The failure of the shower to manifest itself undoubtedly led to a serious diminution of interest in meteor astronomy. At the next perihelion passage in 1932, although a major shower occurred, there was no great meteoric storm such as had been witnessed a hundred years earlier. It now seems certain that the main part of the Leonid orbit has been removed from the earth's orbit by successive perturbations, and the recurrence of the tremendous meteoric storms of the Leonids in the future seems unlikely.

(*b*) *Activity*

The period of the Leonid stream is 33·25 years and the debris still seems to be closely grouped around the comet. Even during the epoch of the great meteoric storms, appreciable activity only seems to have been recorded for a few years either side of the maximum, the shower otherwise appearing with low intensity. Some of the available data on the activity around the appropriate times of perihelion passage are given in Table 132. The hourly rates quoted are the maximum observed in any part of the world. As will be mentioned later, the shower is of short duration and in several cases observers in England, for example, have recorded only comparatively low rates because the maximum has occurred in daylight, whereas in some parts of America the full maximum has been visible.

† The following account, given by the Director of the Meteor Section of the British Astronomical Association (W. F. Denning), reveals the high state of expectancy which prevailed—*Mem. Brit. Astr. Assoc.* **9** (pt. i) (1900), 6: 'Another failure! Yet it was thought that the display of 1899 would more than compensate for the weak showers of 1897 and 1898. The failure is much deplored in view of the universal effort to witness the phenomenon and secure useful observations. No meteoric event ever before aroused such an intense and widespread interest, or so grievously disappointed anticipation. The scientific journals and newspapers all contained references to the subject, and the occurrence was predicted in such confident terms to take place that the public became enthusiastic, and looked forward to its appearance as a certainty. Many people regard the prescience of the astronomer as something marvellous, he can foretell the moment of an eclipse that will occur generations hence, and no thought of questioning either his accuracy or veracity ever enters their heads. Thus everyone expected that when they looked up to the sky on the night of November 14-15 they would see it full of meteors. But the fiery storm did not appear. The firmament, with its glittering stars and silver moon, was just as still as on an ordinary mid-November night. Only now and then, indeed, a shooting star rapidly streaked along the sky to prove that the Leonids were present in a weak and scattered shower in place of the dense and brilliant display that had been awaited. The finest celestial sight of a generation had failed to come at its appointed time, and the disappointment was all the keener in some quarters from the impression which prevailed that another chance of witnessing it would not occur until 1933.'

TABLE 132

Activity of the Leonid Shower

Date	*Hourly rate*	*Source*
1799 Nov. 11	Great storm	Humboldt
1831 Nov. 13	? Considerable shower	see Olivier†
1832 Nov. 12–13	? ,, ,,	
1833 Nov. 12	Great storm (10,000 ?)	
1866 Nov. 13	5,000	see Olivier†
1867 Nov. 13	1,000 + (moon)	
1868 Nov. 13	1,000	
1897 Nov.	Very low	British Astronomical Association‡
1898 Nov. 14	50–100	
1899 Nov. 14	40	
1900 Nov.	Very low	
1901 Nov. 14	200+	
1902 Nov.	Very low	
1903 Nov. 15–16	250§	
1904 Nov. 14	20–50	
1906 Nov. 16	20–30‖	
1930 Nov. 16	30–80	British Astronomical Association‡
1931 Nov. 16	30–90	
1932 Nov. 16–17	240 (see Crommelin††)	
1946 Nov. 17	24	Radio-echo rates‡‡
1947 Nov. 16	3	
1948 Nov. 14	11	
1949 Nov. 16	7	
1950 Nov. 16	11	
1951 Nov. 17	< 8	
1952 Nov.	No record	
1953 Nov. 17	< 7	

During the period for which systematic observations have been possible using the radio-echo techniques, no major return of the shower has taken place. The radio-echo rates for the years 1946–53 are included in Table 132.

The association of close grouping of the debris near the comet with a small cross-section is again in evidence in the case of the Leonids. All reports of the great meteoric storms refer to the short duration of the shower. For example, in England during the 1866 return the maximum occurred at about 01h. on November 13 and the shower was over by 04h. Denning§ has given the hourly-rate curve for the unexpectedly rich return of 1903 as shown in Fig. 163. The extreme sharpness of the maximum bears a strong resemblance to the sharp curve of activity

† Olivier, C. P., *Meteors* (1925), ch. 4.

‡ *Mem. Brit. Astr. Assoc.* **6** (1897) et seq.

§ Denning, W. F., *Mon. Not. Roy. Astr. Soc.* **64** (1903), 125.

‖ See ibid. **67** (1907), 275. †† *J. Brit. Astr. Assoc.* **43** (1933), 99.

‡‡ Hawkins, G. S., and Almond, M., *Mon. Not. Roy. Astr. Soc.* **112** (1952), 219, and unpublished Jodrell Bank data.

found for the other periodic shower—the Giacobinids—discussed earlier in this chapter. The small cross-section of the stream is again indicated by the analysis of the thirty-six Leonid meteors photographed at

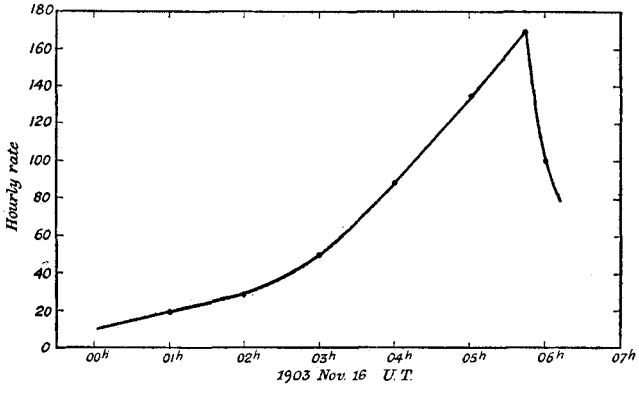

FIG. 163. Hourly rate of the Leonid shower on 1903 Nov. 16 as given by Denning.

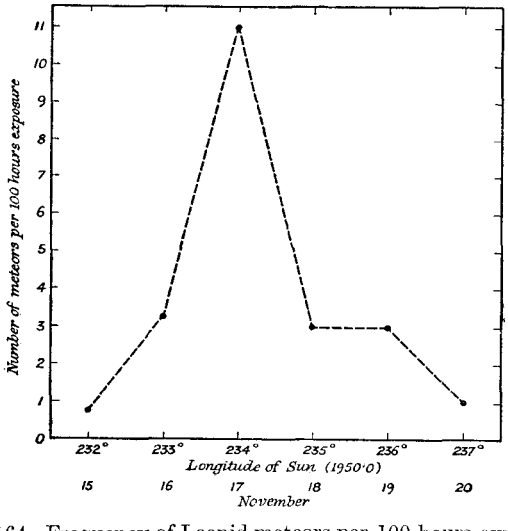

FIG. 164. Frequency of Leonid meteors per 100 hours exposure on the Harvard photographic plates 1898–1951.

Harvard from 1898 to 1951.† The frequency per 100 hours exposure is shown in Fig. 164. One-half of the photographic meteors appeared within a 24-hour interval around the maximum.

(c) *Radiant*

The great shower in November 1833 was the first occasion on which it became evident that the meteors were apparently radiating from a point.

† Wright, F. W., *Tech. Rep. Harv. Coll. Obs.* (1951), no. 7 (Harvard Reprint Series, II–38).

The credit for this observation is generally given to D. Olmsted and A. C. Twining, but according to Olivier† the facts were also clearly stated by several other observers. The scientific preparations for the expected return in 1899 were so extensive that although the storm did not then materialize a large number of radiant positions were determined in the subsequent years, both by photography and by visual observation. Denning‡ gave the radiant as α 150·65°, δ +23·1° for the mean of seventeen doubly observed Leonids in the years 1896–1903. This showed good agreement with the more extensive determinations§ made in 1903, a sample of which is as follows:

Blum (Paris)	α 151·5°	δ +22·5°	(48 meteors)
Denning (Bristol)	α 151°	δ +22°	(33 meteors)
Olivier (Virginia)	α 151°	δ +22°	(78 meteors)

In 1932 King‖ presented an analysis of his own observations of the Leonids in the years 1899–1904 and 1920–31 with particular reference to the motion of the radiant. These observations are quoted in Table 133.

TABLE 133

Visual Observations of the Leonid Radiant according to King‖

Date G.M.A.T.	*Sun's longitude*	α	δ	*No. of meteors*	*Radiant diameter*
	⊙ *deg.*	*deg.*	*deg.*		*deg.*
1899 Nov. 15·62	144·3	151·5	+22	7	4
1900 Nov. 15·61	144·0	151·5	22	3	3
1903 Nov. 15·86	143·5	150	22·5	10	..
1904 Nov. 15·61	144·0	150·5	21	8	..
1920 Nov. 13·97	142·5	150	22·5	7	..
1920 Nov. 15·56	144·1	152	23	7	4·3
1925 Nov. 15·54	143·9	150·5	23	3	..
1927 Nov. 17·56	145·4	152	22·5	4	0·5
1928 Nov. 15·59	144·2	150·25	22	10	1·75
1928 Nov. 16·60	145·2	151·75	22	6	2
1930 Nov. 15·58	143·7	151	22	6	3
1930 Nov. 16·57	144·7	152	21·5	8	1·75
1931 Nov. 16·60	144·5	152	22·2	22	1·66
1931 Nov. 17·58	145·5	153	22	8	4

After adjusting the dates for epoch and correcting for precession to 1932, King gave the weighted means listed in Table 134.

† Olivier, C. P., *Meteors* (1925), ch. 4.
‡ Denning, W. F., *Mon. Not. Roy. Astr. Soc.* **64** (1903), 125.
§ Denning, W. F., ibid. **64** (1904), 354.
‖ King, A., ibid. **93** (1932), 109.

TABLE 134

Change of Mean Radiant Position of Leonids with Date according to King

Date 1932 *G.M.A.T.*	⊙ *deg.*	*Mean position*		*No. of radiants*
		α (*deg.*)	δ (*deg.*)	
Nov. 13·97	142·5	150·2	+22·4	1
Nov. 15·42	144·0	151·0	22·2	7
Nov. 16·09	144·7	152·0	21·9	4
Nov. 16·82	145·4	152·5	22·2	2

This appears to be the first collected observational evidence of the shift of the radiant. King's predicted ephemeris for the radiant based on this shift is given in Table 135.

TABLE 135

King's predicted Ephemeris of the Leonid Radiant

Date 1932 *G.M.A.T.*	*Radiant*		*Date* 1932 *G.M.A.T.*	*Radiant*	
	α (*deg.*)	δ (*deg.*)		α (*deg.*)	δ (*deg.*)
Nov. 12·5	148·3	+23·2	Nov. 16·5	152·3	+21·8
Nov. 13·5	149·3	22·8	Nov. 17·5	153·3	21·4
Nov. 14·5	150·3	22·5	Nov. 18·5	154·3	21·0
Nov. 15·5	151·3	22·1	..	..	

King's ephemeris is in close agreement with the mean radiants given by Huruhata† from an analysis of the visual Japanese observations made in 1934, listed in Table 136.

TABLE 136

The Visual Leonid Radiant 1934 *according to Huruhata*†

Date 1934 *G.M.A.T.*	*Radiant*	
	α *deg.*	δ *deg.*
Nov. 3·8	141	+27
Nov. 7·8	145	25·5
Nov. 9·8	146	25
Nov. 10·8	147	24·5
Nov. 14·8	151	22·5
Nov. 15·8	151·8	22·2
Nov. 16·8	152·7	21·8
Nov. 17·8	153·3	21·5

† Huruhata, M., *Mem. Jap. Astr. Assoc.* **3** (1935), 327.

Photographic determinations of the Leonid radiant were first made in 1898 at Yale and Harvard. The Yale results have been discussed by Elkin.† The mean radiant determined from seven trails was at α 151·3°, δ +22·5°, with a spread of about half a degree in each coordinate. At the same time a considerable number of trails were also photographed at Harvard. A discussion of three trails which appeared on one plate on 1898 November 14 has been given by Hogg.‡ The mean position was at R.A. 10h. 03m. 1s., δ +22·36° (1900), but the trails did not intersect in a point, the spread lying between 12′·5 and 33′·6, from which Hogg concluded that the luminous air paths could not be exactly parallel. The analysis of the further fifteen trails obtained with the guided cameras on 1898 November 14 has been given by Fisher and Miss Olmsted.§ The weighted mean position of the radiant was found to be α 151° 00·5′, δ +22° 38·1′. Fisher and Miss Olmsted‖ also give the results of the analysis of three Leonid trails on a single plate exposed on 1901 November 14. The weighted mean radiant was at α 150° 49·7′, δ +23° 27·3′, the triangle of intersection of the three trails extending for 8′.

The latest analysis of the Harvard photographic Leonid data has been given by Miss Wright.†† The analysis included thirty trails photographed at one station and six doubly photographed trails in the period 1898 to 1951. The trails previously analysed by Fisher and Miss Olmsted are included in the series. The results of this analysis are given in Table 137, which gives the data for the corrected Leonid radiant at maximum, in Table 138, which gives the predicted position of the corrected radiant from November 15 to November 20, and in Fig. 165, which gives the path of the mean radiant and the positions of the individual determinations.

TABLE 137

Corrected Leonid Radiant at Maximum from the Harvard Photographic Data

Mean long. of sun at max.	233°·94	Equinox 1950·0
Right ascension α at max.	152° 17′	
Declination δ at max.	+22° 17′	
$\Delta\alpha \cos\delta$ (per day)	+39′±3′	
$\Delta\delta$ (per day)	−25′±3′	
Total daily motion	46′	

† Elkin, W. L., *Astrophys. J.* **10** (1899), 25.
‡ Hogg, F. S., *Bull. Harv. Coll. Obs.* (1928), no. 857, 6.
§ Fisher, W. J., and Olmsted, M., ibid. (1929), no. 870, 7.
‖ Fisher, W. J., and Olmsted, M., ibid., p. 12.
†† Wright, F. W., *Tech. Rep. Harv. Coll. Obs.* (1951), no. 7 (Harvard Reprint Series, II–38).

TABLE 138

Predicted Mean Radiant Position (1950·0) from the Harvard Photographic Data

Date U.T. Nov.	⊙ *(deg.)*	α *(deg.)*	δ *(deg.)*
15	232·5	151°·17′	+22° 53′
16	233·5	151 59	22 28
17	234·5	152 41	22 03
18	235·5	153 23	21 38
19	236·5	154 06	21 14
20	237·5	154 48	20 49

The agreement between the visual and photographic radiant determinations is extremely good.

(d) Velocities

As soon as the well-marked period of 33·25 years for the recurrence of the Leonid stream had been established, the velocity of the meteors could be computed accurately. The geocentric velocity outside the atmosphere should be 72 km./sec. The discrepancy between this value and the earlier measurements of the velocity of the Leonid meteors was put forward as strong evidence for considerable deceleration in the atmosphere. Thus, in the early photographic work described in Chapter XI, Millman and Miss Hoffleit† measured the velocity of three Leonids as 61·3, 78, and 61·1 km./sec. and derived a mean heliocentric velocity of 31 km./sec. instead of the expected value of 41·5 km./sec. In his analysis of the British visual meteor data, Porter‡ found the mean of twenty-seven Leonid determinations to be 57·8 km./sec. It now seems evident, however, that these low values must be due to errors of measurement, since the contemporary measurements using the double-station photographic technique give results in close agreement with the expected velocity and show only small decelerations. Six double-station measurements have been published by Miss Wright,§ according to the analysis made by Jacchia.‖ The results are given in Table 139.

The random errors in measuring the velocities of the Leonid meteors are considerably larger than for most doubly photographed meteors, owing to the fact that the trails are short and faint. The average number of breaks in the trail was only six, resulting in a weak velocity determina-

† Millman, P. M., and Hoffleit, D., *Ann. Harv. Coll. Obs.* **105** (1937), 601.
‡ Porter, J. G., *Mon. Not. Roy. Astr. Soc.* **104** (1944), 257.
§ Wright, F. W. (1951), loc. cit.
‖ One of these (No. 792) was published previously by Jacchia, L. G., *Tech. Rep. Harv. Coll. Obs.* (1948), no. 2.

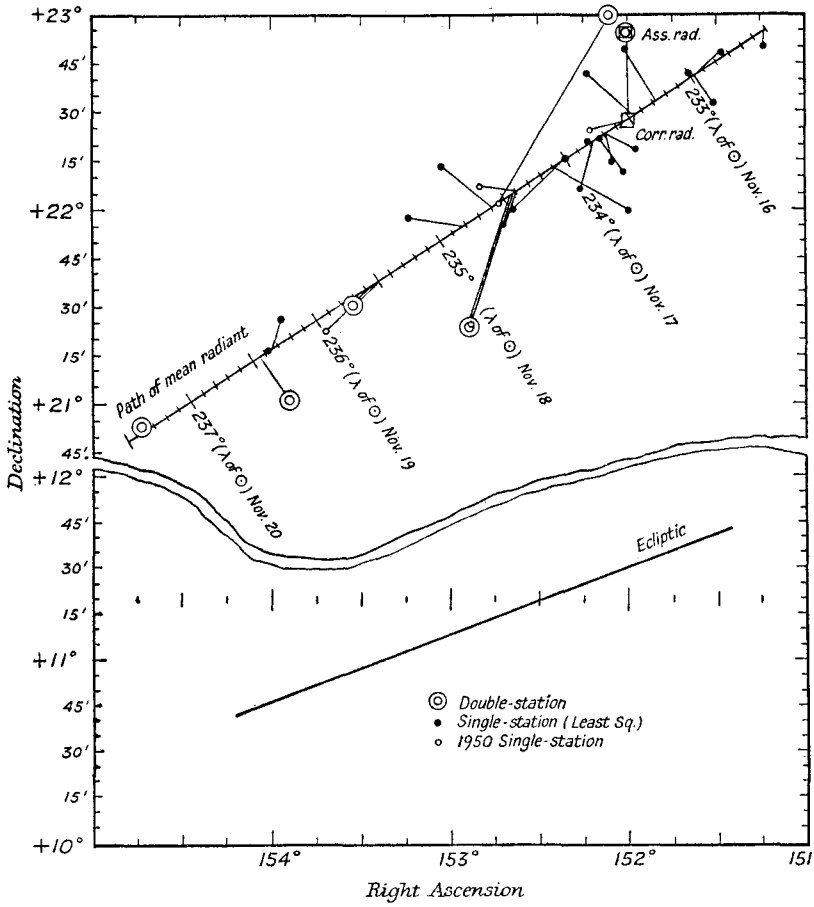

FIG. 165. The path of the mean Leonid radiant as given by the Harvard photographic results. For each meteor trail of the single-station meteors a black dot represents the nearest point of the extended great circle to the calculated mean radiant of the instant. The line from each point to the radiant is perpendicular to the great circle for each trail. The double circles refer similarly to the meteor trails photographed simultaneously at two stations.

tion and a very poor measure of deceleration. The mean apparent relative velocity of 71·8 km./sec. must therefore be considered to be in excellent agreement with the anticipated value from the orbital characteristics of the parent comet.

(*e*) *Orbit*

The first significant speculations on the orbit of the Leonids were made in 1863 and 1864 by Newton, who listed five possible periods for the shower. In 1866 Schiaparelli published an orbit on the assumption that

TABLE 139

The Velocities of Six Leonid Meteors determined by the Double-station Technique

	Meteor No. (Harvard notation)					
	792	2176	2179	2181	1360	1447
Date U.T. . . .	1938 Nov. 16·374	1950 Nov. 17·3917	1950 Nov. 17·4732	1950 Nov. 18·4796	1946 Nov. 19·340	1946 Nov. 20·287
Sun's longitude ⊙ .	233°·50	234°·46	234°·54	235°·55	236°·45	237°·41
Apparent radiant α	152° 05′	152° 43′	152° 11′	153° 40′	153° 53′	154° 32′
Apparent radiant δ	+23° 04′	+21° 26′	+22° 59′	+21° 32′	+21° 07′	+21° 02′
Corrected radiant α	152° 00′	152° 59′	152° 09′	153° 32′	..	154° 43′
Corrected radiant δ	+22° 55′	+21° 21′	+22° 58′	+21° 30′	..	+20° 54′
Apparent relative velocity v km./sec. .	71·8	70·5	72·9	71·9	71·7	71·8
No atmosphere velocity V km./sec. .	72·2	70·5	72·9	71·9	..	72·3
Geocentric velocity v_g km./sec. . .	71·1	69·3	71·8	70·9	..	70·8
Heliocentric velocity $\bar{V}$ km./sec. . .	42·0	40·0	42·6	41·5	..	41·4

33·25 years was the correct period, and, as mentioned earlier, the identification of this orbit with that of the Comet Temple 1866 I followed immediately. After this identification Schiaparelli† gave the orbits for the stream compared with that of the comet as listed in Table 140.

Simultaneously, Adams‡ suggested that the motion of the node should enable a decision to be reached between the five possible periods suggested by Newton. The observed motion was 102·6″ annually with respect to the equinox, or 52·6″ with respect to the stars, which is 29′ in 33·25 years. Adams's calculation of the perturbations by Jupiter, Saturn, and Uranus, assuming a period of 33·25 years, gave a motion of 28′. The excellent agreement finally settled the argument in favour of the largest of Newton's five periods. Adams's elements for the orbit are given in Table 140. The orbits of five of the Leonids doubly photographed at Harvard and referred to earlier are also given in Table 140. Miss Wright§ points out that an error of only 0·2 km./sec. in the velocity could account for the difference of 12 years in the mean period given for the five meteors and that of the comet.

The task of investigating the perturbations of the orbit in the years following the 1866 return was carried through by Stoney and Downing.‖ They found that the stream made close approaches to Saturn in 1870 and to Jupiter in 1898, whereby the perihelion distance was decreased from

† Schiaparelli, J. V., *Sternschnuppen* (1871), p. 57.
‡ Adams, J. C., *Mon. Not. Roy. Astr. Soc.* **27** (1866–7), 247.
§ Wright, F. W. (1951), loc. cit.
‖ Stoney, G. H., and Downing, A. M. W., *Proc. Roy. Soc.* A, **64** (1898–9), 403.

TABLE 140

The Orbits of the Leonids and of Temple's Comet 1866 I

Authority		*Perihelion passage*	π (= $\omega + \Omega$) *Longitude of perihelion*	Ω *Ascending node*	i *Inclination*	q *Perihelion distance (a.u.)*	e *Eccentricity*	a *Semi-major axis (a.u.)*	*Period (years)*
Schiaparelli 1871	Leonids	Nov. 10·092	56° 25·9′	231° 28·2′	162° 15·5′	0·9873	0·9046	10·34	33·25
	Comet 1866 I	Jan. 11·160	60 28·0	231 26·1	162 41·9	0·9765	0·9054	10·344	33·176
Adams 1867 .	Leonids		58 19	..	163 14	0·9855	0·9047	10·3402	33·25
Harvard photographic (1938–1950)	Leonid No. 792		46·2	233·1	161·6	0·986	..	30·3	..
	Leonid No. 2176		44·7	234·5	163·3	0·982	..	4·6	..
	Leonid No. 2179		50·9	234·5	161·6	0·987	..	27	..
	Leonid No. 2181		49·0	235·5	163·0	0·985	..	13·2	..
	Leonid No. 1447		52·8	237·4	163·2	0·986	..	10·7	..
	Mean		..	..	..	0·985	0·923	12·8	45·6

0·9855 to 0·9729 and the period changed by one-third of a year. Finally, just before the expected 1899 return, Stoney showed that on the critical date Adams's orbit was 1,300,000 miles inside the earth's orbit. Unfortunately, as we have seen, insufficient notice was taken of these cautions about the improbability of a great return of the Leonids in 1899.

As far as is known, the laborious calculations necessary to establish the effect of future perturbations on the orbit of the stream have not been made. From the comparatively weak returns of 1899 and 1932, it is evident that at the critical date the earth is now far removed from the dense part of the stream. Whether successive perturbations will increase or decrease the distance between the earth and the main swarm is not yet known.

XVII

THE MAJOR METEOR SHOWERS—V

THE LOST STREAMS

In the eighteenth and nineteenth centuries great meteoric streams of the type already described in connexion with the Giacobinids and Leonids were found to be associated with Biela's Comet. After 1899, however, the shower almost completely disappeared. This disappearance, together with the strange disruption of Biela's Comet, gives to the Bielid shower a unique position in meteor astronomy. In more recent times a strong shower associated with the Pons–Winnecke Comet has also disappeared. No doubt many similar disappearances have occurred in the past, but the two showers discussed in this chapter are the only prominent ones of this type for which there is reliable information.

1. The Bielid (or Andromedid) shower

(*a*) *History*

In 1826 Biela discovered a faint comet, but when its orbit was computed it was realized that the same comet had been previously observed by Montagne in 1772 and by Pons in 1805. The period of the comet was 6·6 years, and it was observed again in 1832 when it passed within 20,000 miles of the earth's orbit. In 1839 the comet was unfavourably placed and was not seen, but on 1845 December 29 Herrick and Bradley of Yale saw a small companion comet beside the main one. The companion comet grew in brightness and developed a tail. It seemed that violent forces were disrupting the comet. At the next return in 1852 both comets were faint and separated by over a million miles. They were last seen in September 1852, and in spite of most careful searches were never seen again on any subsequent return. In 1872 and 1885, however, when the earth crossed the orbit of the vanished comet, there were tremendous displays of meteors. Strong showers were also witnessed at the appropriate times in 1892 and 1899, but since then no appreciable shower of these Bielid meteors has been observed.

(*b*) *Activity*

The occurrences of prominent meteor showers connected with Biela's Comet have certainly been traced back to 1741,† while Klinkerfues‡

† Olivier, C. P., *Meteors* (1925), ch. 7.

‡ Klinkerfues, W., *Göttinger Nachrichten* (April 30, 1873), p. 275, translated by W. J. Fisher in *Popular Astronomy*, **39** (1931), 573.

brings forward arguments to show that the great shower and comet of A.D. 524, together with other subsequent notable historic showers, might have been associated with Biela's Comet. Owing to the rapid regression of the node, the dates of apparition of the shower show considerable changes. Fisher† has investigated these changes in detail from 1741 to 1926 in order to predict the possible dates of future occurrences of the showers. The available information on the activity and dates of apparition from 1741 is listed in Table 141.

TABLE 141

The Activity of the Bielid Stream

Source	*Date*	*Hourly rate*
Krafft (St. Petersburg)	1741 Dec. 5	'Large number'
Brandes (Bremen)	1798 Dec. 7	~ 400/hour
Raillard (France)	1830 Dec. 7	'Many'
Flaugergues (Toulon), Webb (England), Herrick and Newton (U.S.A.), Quetelet (Brussels)	1838 Dec. 6	~ 100/hour
Heis (Aachen)	1847 Dec. 6	~ 150/hour
Zeziolo (Bergamo)	1867 Nov. 30	?
Many observers	1872 Nov. 27	Meteoric storm, 2,000–6,000/hour
Many observers (see Newton‡)	1885 Nov. 27	Meteoric storm, 75,000/hour ?
Many observers (see Newton§)	1892 Nov. 23	~ 300/hour
Denning‖	1899 Nov. 24	~ 100/hour
Denning††	1904 Nov. 21	~ 20/hour
Prentice‡‡	1940 Nov. 27–Dec. 4	~ 5/hour
R. M. Dole (U.S.A.)§§	1940 Nov. 15	~ 30/hour

The information about any appreciable return of the stream after 1899 is very uncertain. Olivier‖‖ states that from the 1899 return until 1924 the number of Bielid meteors was insufficient to enable a radiant to be determined, but Denning†† gives an account of an apparent Bielid shower observed in November 1904 both in Ireland and in Sweden. Prentice‡‡ has described the attempts to observe Bielid meteors from 1921 to 1940. Nothing of interest was observed until 1940, when from November 27 to December 4 definite Bielid activity was observed,

† Fisher, W. J., *Proc. Nat. Acad. Sci. Wash.* **12** (1926), 728, corrected in **13** (1927), 578.
‡ Newton, H. A., *Amer. J. Sci.* (3), **31** (1886), 409.
§ Newton, H. A., ibid. **45** (1892), 61.
‖ Denning, W. F., *Mon. Not. Roy. Astr. Soc.* **60** (1900), 374.
†† Denning, W. F., ibid. **65** (1905), 851.
‡‡ Prentice, J. P. M., *J. Brit. Astr. Assoc.* **51** (1941), 92.
§§ See note by Prentice, J. P. M., *Brit. Astr. Assoc. Handbook* (1947), p. 42.
‖‖ Olivier, C. P., loc. cit.

although the rate was only a few per hour. In the same year, on November 15, R. M. Dole in the U.S.A. reported the occurrence of a fairly strong shower of Bielid meteors. Radio-echo observations in 1946, 1947,† and 1948‡ failed to record any significant activity from the Bielid radiant; neither has there been any in the succeeding years up to 1953.§

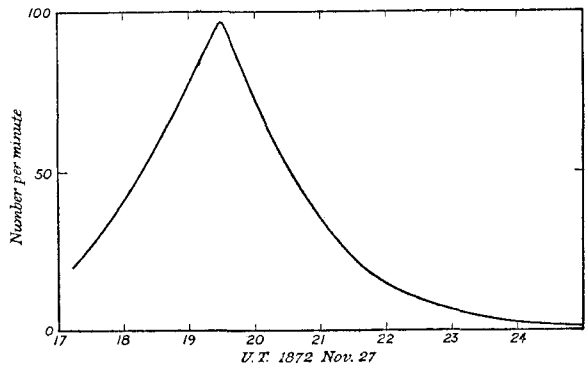

FIG. 166. The curves of activity of the great Bielid meteoric storm of 1872 Nov. 27.

As is the case with all the great meteoric storms which have been observed, the duration of the Bielid displays of 1872 and 1885 was very short, the earth passing through the dense part of the swarm in a few hours. A curve of activity for the 1872 Bielid shower has been given by Watson‖ and is reproduced in Fig. 166. The behaviour of the shower in 1885 was similar; according to Newton†† the principal shower was over in 6 hours. The much lower activity of the later returns seems to have been more diffuse. Thus, according to Denning,‡‡ the shower of 1899 was seen on November 23 and 24, and the Bielid meteors of 1904 from November 16 to November 22. Since this shower occurred only 5 years after the 1899 return, and since the period of the comet is 6·6 years, the comet was 15 months from perihelion and Denning inferred that the meteors must be spread out over a considerable arc of the orbit. The only subsequent observations, in 1940, confirm this dispersion of the debris.

† Lovell, A. C. B., and Prentice, J. P. M., *J. Brit. Astr. Assoc.* **58** (1948), 140.
‡ Clegg, J. A., Lovell, A. C. B., and Prentice, J. P. M., ibid. **60** (1949), 25.
§ Jodrell Bank unpublished radio-echo observations.
‖ Watson, F., *Between the Planets* (Blakiston, 1947), p. 127.
†† Newton, H. A., *Amer. J. Sci.* (3), **31** (1886), 409.
‡‡ Denning, W. F. (1900), loc. cit.

(*c*) *Radiant*

A radiant position for the Bielid stream appears to have been first given by Heis on 1847 December 6. This, and subsequent details of radiant determinations, are listed in Table 142.

TABLE 142

Radiant Position of the Bielid Stream

Authority	*Date*	*Radiant* α	*Radiant* δ	*Radiant area*	*Remarks*
		deg.	*deg.*	*deg.*	
Heis. .	1847 Dec. 6	25	+40	..	..
		21	54	..	..
Zezioli .	1867 Nov. 30	17	48	..	..
Newton† .	1885 Nov. 27	24·54	44·74	several degrees	Mean of 90 radiants
Denning‡ .	1899 Nov. 24	23	42·25	2–3	
Elkin§ .	1899 Nov. 24	23·8	39·7	..	One photographed meteor
Elkin‖ .	1905 Nov. 18	25·01	46·08	..	One photographed meteor
Denning††	1904 Nov. 21	21	50	..	..
		26·03	44·16	..	..
Prentice‡‡	1940 Nov. 30	23	44·5	2·5	4 meteors
	1940 Dec. 2	29	45·5	7·5	6 meteors
	1940 Dec. 4	23	41·5	0	4 meteors

The two photographic records in Table 142 were obtained by Elkin§‖ during the initial photographic work at Yale. There are no published records of any subsequent photographic determinations of the radiant.

(*d*) *Velocities*

As in the case of the other streams with well-marked periodicities, the velocity of the Bielid meteors can be determined from the periodicity, the expected geocentric velocity being 16 km./sec. The only photographic velocity determination for comparison with this is the original one obtained by Elkin§ in the work referred to above. His measured velocity was 20·2 km./sec., which reduced to a geocentric velocity of 16·8 km./sec. in reasonable agreement with the expected value. There are no records of visual measurements of the velocity of Bielid meteors in Porter's analysis§§ of the British meteor data. During the radio-echo watch for Bielid meteors in 1948‖‖ one velocity of 19·6±2·0 km./sec. was determined. Although this is consistent with the uncorrected velocity of the

† Newton, H. A. (1886), loc. cit.
‡ Denning, W. F. (1900), loc. cit.
§ Elkin, W. L., *Astrophys. J.* **12** (1900), 4.
‖ See Olivier, C. P., *Astr. J.* **46** (1937), 41.
†† Denning, W. F. (1905), loc. cit.
‡‡ Prentice, J. P. M. (1941), loc. cit.
§§ Porter, J. G., *Mon. Not. Roy. Astr. Soc.* **103** (1943) 134; **104** (1944), 257.
‖‖ Clegg, J. A., Lovell, A. C. B., and Prentice, J. P. M. (1949), loc. cit.

Bielid meteors, little weight can be attached to it since the radiant is unknown.

(*e*) *Orbit*

According to Olivier,† both Weiss and d'Arrest announced almost simultaneously in 1867 that the Andromeda meteors moved in the orbit of Biela's Comet, the history of which has been referred to above. Weiss, in 1868, clearly pointed out the effect of the rapid decrease in the longitude of the node and predicted that the shower of 1872 should occur about November 28, not in December as the previous returns had done. The great meteoric storm of 1872 November 27 confirmed this prediction. Table 143, compiled from data given by Olivier,† lists Newton's positions for the node and inclination of the comet's orbit, and Hind's values for the minimum distance between the orbits of the earth and the comet at the various returns. (Since the comet disappeared in 1852, the figures for 1859 and 1866 are predictions only.)

TABLE 143

The Changes in the Orbit of Biela's Comet

Date	☊	i	*Distance (comet orbit–earth orbit)*	*Sun's longitude ⊙ on dates of occurrence of Bielid showers*	
	deg.	*deg.*	*a.u.*	*Date*	*deg.*
1772	258·7	17	−0·06545	..	..
..	..	..	..	1798	256·2
1806	252·4	13·6	+0·01321	..	..
1826	251·2	13·6	+0·00892	..	..
1832	..	..	+0·00087	..	..
1833	249·0	13·2	..	..	..
..	..	..	..	1838	256·1
1839	..	..	−0·00009	..	..
1846	246·5	12·6	−0·01680	..	..
..	..	..	..	1847	257·7
1852	246·3	12·6	−0·01130	..	..
1859	246·1	12·4	+0·00567	..	..
1866	246·0	12·0	+0·01295	..	..
..	..	..	..	1867	248·4
..	..	..	..	1872	246·1
..	..	..	..	1885	245·8

The consistency between the changes in the orbit of the comet and the times of apparition of the shower is apparent from Table 143.

The close connexion between the orbital elements of the meteor stream observed in 1885 and those of the comet was shown by Corrigan‡ in 1886. His data are given in Table 144.

† Olivier, C. P., *Meteors*, ch. 7.

‡ Corrigan, S. J., *Sidereal Messenger*, **5** (1886), 144 (see Olivier, loc. cit.).

TABLE 144

Orbital Elements of Biela's Comet and the Associated Meteor Streams

Authority		*Long. of Perihelion* π	*Long. of node* Ω	i	*Perihelion distance*	e	a (*a.u*)
Corrigan†	Biela's Comet .	109° 40′	246° 29′	12° 33′	0·8606	0·7559	3·526
„	Meteor stream 1885 Nov. 27 .	108° 16′	245° 57′	13° 08′	0·8578	..	..
Elkin‡	Single meteor 1899 Nov. 24 .	108° 48′	242° 22′	12° 04′	..	0·7923	4·110
Prentice§	Nov. 1940. .	109°·3	250°·7	13°·2	0·875	0·757	3·6

The only determination for an individual meteor is that given by Elkin,‡ which agrees well with the cometary elements. Also given in Table 144 are the elements for the stream observed by Prentice§ in 1940, which is in good agreement with the elements of the comet. This agreement is in many ways somewhat surprising, since the observations made by Prentice were from November 27 to December 2, whereas, according to the rapid regression of the node observed in the nineteenth century, the shower would have been expected to occur in early November. Prentice believes that there may now be several meteoric currents associated with Biela's Comet, as indeed was suggested by Klinkerfues‖ in 1873. The remarkable history of the comet and of the associated meteor streams lends particular interest to future observations of any return of the Bielid meteors.

2. The Pons–Winnecke meteors

(*a*) *History*

On 1819 June 12 Pons discovered a new comet, and although its period was computed as 5·62 years it was not until 1858 March 8 that it was rediscovered by Winnecke. Since then it has been regularly observed. The aphelion of the comet's orbit lies very close to Jupiter, and since the period of the comet is almost exactly half that of Jupiter it suffers considerable perturbations at each alternate revolution. These perturbations brought the orbit of the comet very close to that of the earth. On 1916 June 28 the orbit was, in fact, only 3 million miles from the earth and a strong shower of meteors was observed. Subsequently the perturbations increased the separation of the orbits, and although there are records of meteors from the shower during the 1921 and 1927 returns the shower is now regarded as completely lost.

† Corrigan, S. J., loc. cit. (see Olivier, loc. cit.).
‡ Elkin, W. L. (1900), loc. cit.
§ Prentice, J. P. M. (1941), loc. cit.
‖ Klinkerfues, W. (1873), loc. cit.

(*b*) *Activity*

The only appreciable display of the Pons–Winnecke meteors occurred during May and June 1916. A very sharp maximum seems to have occurred on 1916 June 28, which was seen by observers in England† but not in America. Denning‡ gave the rate as 32 per hour, but other observers gave 100 per hour, whereas in America the rate did not exceed 6 per hour. Olivier§ gives details of the low hourly rate of meteors belonging to this shower from 1916 May 20 to July 10. The disparity in the rates observed in England and America on June 28 indicates that the dense part of the swarm must have been extremely localized since only 6 hours elapsed between the English and American observations.

The expectations of a great display when the comet returned to perihelion in 1921 were not fulfilled. Very few Pons–Winnecke meteors were observed either in England or in America, although the Japanese observers‖ reported a strong shower of very faint meteors. At the next return in 1927 the only reports of significant numbers of Pons–Winnecke meteors came from Russia†† and from Dole‡‡ in America. There are no further accounts of observations of this meteor stream.

(*c*) *Radiant*

The observed radiant positions as collected by Olivier§ for the 1916 shower are given in Table 145.

TABLE 145

Radiant Positions of the Pons–Winnecke Shower 1916

Source	*Date*	*Radiant* α	δ	*No. of meteors*
	1916	*deg.*	*deg.*	
A.M.S.§§ . .	May 21·6	224·5	+25·3	8
,,	May 26·68	230·3	27·4	7
,,	May 27·25	231·0	27·5	7
,,	May 27·67	232·1	26·8	4
,,	May 30·14	232·7	28	15
,,	June 3·7	234·4	27·5	16
,,	June 4·68	235·8	25·6	9
British observers .	June 28·5	203	53	100
Denning . .	June 28·5	231	54	69
,,	June 28·5	223	41	
A.M.S. . . .	July 3·67	206·7	61·2	5

† *Nature*, **97** (1916), 388.
‡ Denning, W. F., *Observatory*, **36** (1916), 356.
§ Olivier, C. P., *Mon. Not. Roy. Astr. Soc.* **77** (1916), 71.
‖ *Kyoto Publications*, **5**, no. 5; *Observatory*, **45** (1922), 81.
†† *Observatory*, Nov. 1927. ‡‡ Dole, R. M., *Observatory*, **51** (1928), 25.
§§ American Meteor Society.

It appears from these observations that a number of distinct radiants were active simultaneously, especially on the night of maximum, June 28. The connexion between these various groups was investigated by Smith,† who computed an ephemeris for the A.M.S. radiants determined in late May and early June for comparison with the theoretical Pons–Winnecke radiant and with the British radiants of June 28. His ephemerides are given in Table 146.

TABLE 146

Ephemeris of the Pons–Winnecke Radiant

1916	☊	*Ephemeris of the A.M.S. radiant (parabolic elements)*		*Ephemeris of the A.M.S. radiant (elliptical elements)*		*Ephemeris of Pons–Winnecke radiant*	
		☊+ω = 283° 24′		☊+ω = 287° 36′		☊+ω = 271° 36′	
		α	δ	α	δ	α	δ
May 21	60° 05′	229° 04′	25° 50′	227° 55′	22° 48′	222° 39′	33° 52′
31	69 41	231 35	29 38	228 56	29 43	222 49	40 19
June 10	79 15	232 30	35 03	228 45	35 57	221 00	45 58
20	88 48	231 11	40 34	226 55	41 18	216 41	50 37
30	98 20	227 07	45 36	222 43	45 37	209 22	53 24
July 10	107 52	220 08	49 13	216 53	48 11	200 31	54 24

Smith concludes that the A.M.S. radiants of late May and early June would have drifted with time towards the British radiants of June 28 and to the theoretical position of the Pons–Winnecke radiant. Even so, the agreement is not good, and since the node differs by 30° it seems that the meteors must have been separated from the orbit of the comet.

(d) Velocities and Orbit

There are no records of any velocity determinations of the Pons–Winnecke meteors, and the orbital data have therefore been computed by assuming either parabolic or elliptical elements. As regards the orbit of the comet, it has been subject to unusually severe perturbations as mentioned above, owing to its close approach to Jupiter at aphelion. The changes in the elements from 1858 to 1945 have been listed by Porter‡ as in Table 147.

In 1916 the perihelion point was inside the earth's orbit, but successive perturbations then caused the perihelion point to move outside the orbit, and the distance has now increased so much that further occurrences of the Pons–Winnecke meteor shower seem extremely unlikely. The connexion

† Smith, F. W., *Mon. Not. Roy. Astr. Soc.* **93** (1932), 156.
‡ Porter, J. G., *Rep. Phys. Soc. Progr. Phys.* **11** (1948), 402.

TABLE 147

Changes in the Orbital Elements of the Pons–Winnecke Comet

Date	☊	i	e	q	*Distance (comet–earth)*	*Computed radiant* α	δ
				(*a.u.*)	(*a.u.*)	*deg.*	*deg.*
1858	113·5°	10·8°	0·755	0·769	−0·231	..	..
1886	104·1	14·5	0·726	0·885	−0·128	204	+45
1915	99·4	18·3	0·701	0·972	−0·041	208	54
1921	98·1	18·9	0·678	1·041	+0·030	205	57
1939	96·8	20·1	0·670	1·102	+0·092	205	59
1945	94·4	21·7	0·654	1·160	+0·150	207	60

of the meteor stream observed in 1916 May–June with the Pons–Winnecke comet was pointed out by Denning† and by Olivier.‡ The possibility of reconciling the various radiants observed with the single cometary orbit has been discussed above.

† Denning, W. F., *Observatory*, **40** (1917), 95; *Nature*, **97** (1916), 388, 457.

‡ Olivier, C. P., *Circ. Harv. Coll. Obs.* (1916), p. 614; *Mon. Not. Roy. Astr. Soc.* **77** (1916), **71.**

XVIII

THE MAJOR METEOR SHOWERS—VI

THE DAY-TIME STREAMS

(*a*) *History*

THE evolution of the radio-echo technique for the study of meteors enabled a systematic survey to be made of meteoric activity, unhampered by cloud or daylight. The day-time results were of particular interest since they yielded the first information about the meteor streams falling on the sunlit side of the earth. During the summer of 1945 Hey and Stewart† delineated two day-time radiants between June 6 and 13, and during the daylight hours of 1946 May, June, and July, Prentice, Lovell, and Banwell‡ found a high general level of meteoric activity. At that time the real significance of the results was not apparent, since little evidence existed of the relation between the number of radio echoes and the number of visible meteors. During the autumn and winter of 1946–7 the workers at Jodrell Bank made a careful survey of the known meteor showers, from which it was apparent that, with the particular apparatus in use, a close relation existed between the number of radio echoes and the number of meteors seen by a visual observer. The results obtained with this apparatus in daylight were not exceptional until May. Then, during the investigation of the η-Aquarid shower on 1947 May 1, it was found that the well-known shower with its radiant near η-Aquarii was not an isolated event, but merely the beginning of a great belt of meteoric activity extending towards the sun, observable only in daylight. Initially the main radiant was in Pisces, but the phenomena developed with great rapidity, and by the end of June at least seven centres of considerable activity had been delineated, extending in the ecliptic up to right ascension 90°. The day-time activity continued throughout July and August, and comparison with the known major showers indicated that it was without precedent in extent and duration. Preliminary announcements of the discovery of this remarkable activity were made on 1947 June 26§ and September 18,§ and a full acount of the observations was given by Clegg, Hughes, and Lovell.‖ In subsequent years much

† Hey, J. S., and Stewart, G. S., *Proc. Phys. Soc.* **59** (1947), 858.

‡ Prentice, J. P. M., Lovell, A. C. B., and Banwell, C. J., *Mon. Not. Roy. Astr. Soc.* **107** (1947), 155.

§ Lovell, A. C. B., *Brit. Astr. Assoc. Circ.* (June 26, 1947), no. 282; (Sept. 18, 1947), no. 285.

‖ Clegg, J. A., Hughes, V. A., and Lovell, A. C. B., *Mon. Not. Roy. Astr. Soc.* **107** (1947), 369.

more detail was obtained about this day-time activity. The 1948 observations† showed that the main phenomena were recurrent, and preliminary velocity measurements were made.‡ In 1949 and 1950 the orbits of the main streams were first clearly delineated,§ and these results were confirmed in 1951‖ and 1952.†† It is now clear that the dominant streams of the summer sequence are the Arietids and ζ-Perseids in early June, and the β-Taurids in late June. These have returned in great strength in each year of observation and their orbital characteristics are now well established. A number of other less active streams—apparently not all recurrent—have comprised the activity in May and July. Unless otherwise stated, the account in this chapter is a survey of the original papers from Jodrell Bank referred to above.

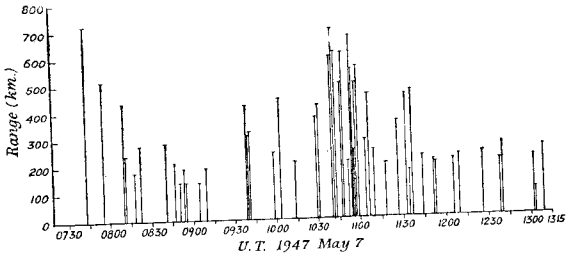

FIG. 167. Range-time plots of echoes with aerial directed at azimuth 90° on 1947 May 7 showing the well-known η-Aquarid shower in transit at 07h. 40m. and the day-time shower in Pisces at 10h. 40m.

(*b*) *Activity*

The original investigation in 1947 was made with a single directional aerial, and one of the early range-time plots (see Chap. IV), which indicated beyond doubt the existence of a new series of showers, is shown in Fig. 167. This figure contains the results with the aerial directed at azimuth 90° on May 7 between 07h. 20m. and 13h. 20m. The η-Aquarids transited at 07h. 40m., and after some scattered activity another clearly defined radiant passed through the beam at 10h. 40m. The activity of this new radiant (which was found to lie in Pisces) at that stage was 13 per hour, or twice the activity of the η-Aquarids. After early May, in each year, a very rapid increase in activity has occurred. The extent of this is well indicated by the range-time plots shown in Fig. 168 covering

† Aspinall, A., Clegg, J. A., and Lovell, A. C. B., ibid. **109** (1949), 352.
‡ Ellyett, C. D., ibid., p. 359.
§ Aspinall, A., and Hawkins, G. S., *Mon. Not. Roy. Astr. Soc.* **111** (1951), 18; Davies, J. G., and Greenhow, J. S., ibid., p. 26; Almond, M, ibid., p. 37.
‖ Hawkins, G. S., and Almond, M., *Jodrell Bank Annals*, **1** (1952), 2.
†† Almond, M., Bullough, K., and Hawkins, G. S., ibid., p. 13.

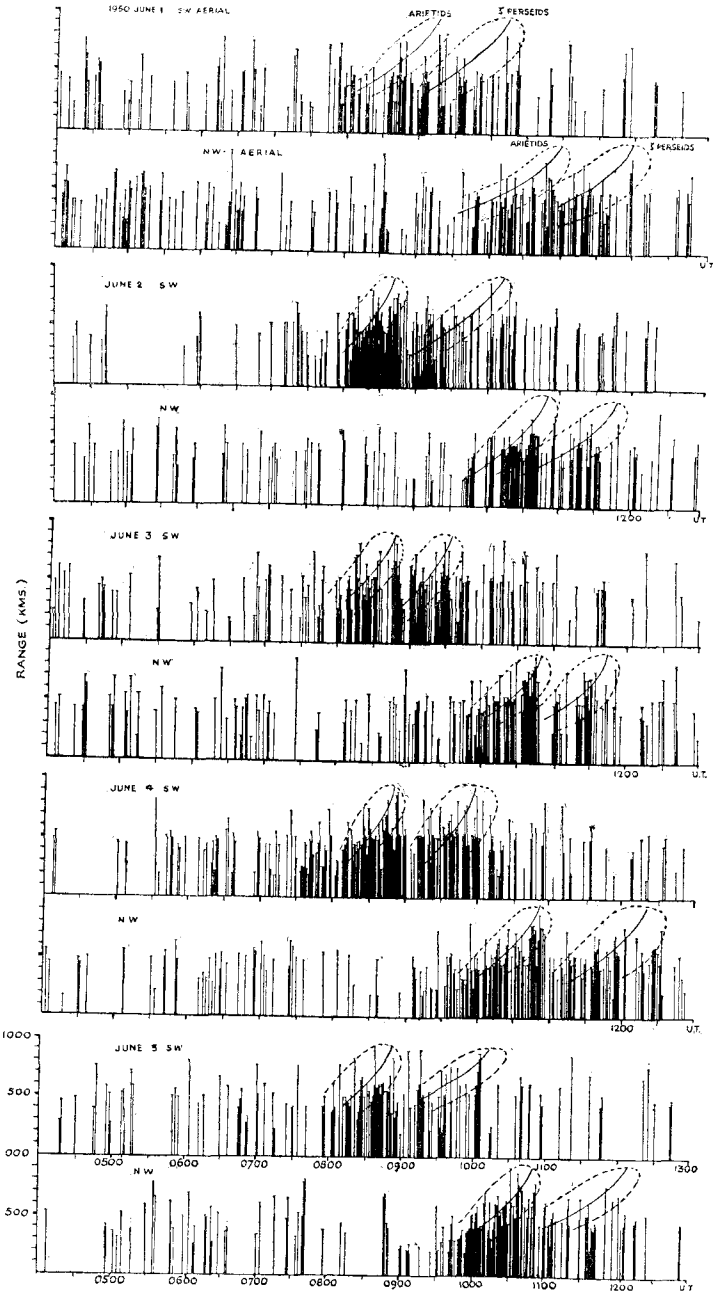
1950 JUNE 1 SW AERIAL
ARIETIDS
ζ PERSEIDS
NW-1 AERIAL
ARIETIDS
ζ PERSEIDS
U.T.
JUNE 2 SW
NW
1200
U.T.
JUNE 3 SW
NW
1200
U.T.
JUNE 4 SW
NW
1200
U.T.
RANGE (KMS.)
1000
500
000
JUNE 5 SW
0500
0600
0700
0800
0900
1000
1100
1300
NW
500
0500
0600
0700
0800
0900
1000
1100
1200
U.T.

FIG. 168 (*a*)

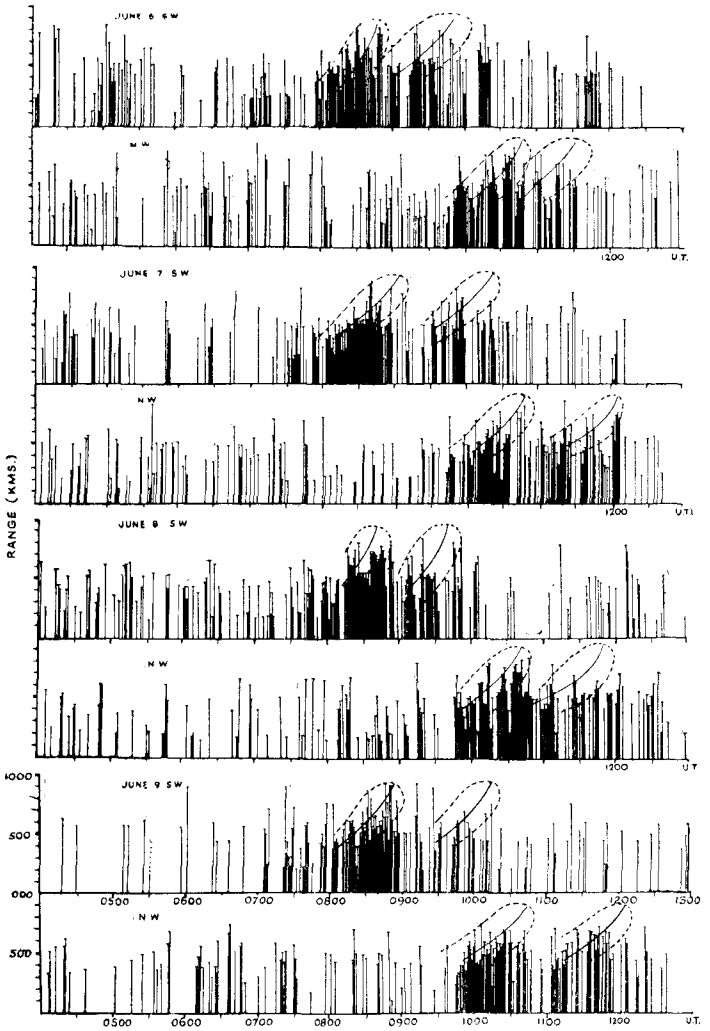
JUNE 6 SW
NW
1200
U.T.
JUNE 7 SW
NW
1200
UT
JUNE 8 SW
NW
1200
U.T
RANGE (KMS.)
1000
500
000
JUNE 9 SW
0500
0600
0700
0800
0900
1000
1100
1200
1300
NW
500
0500
0600
0700
0800
0900
1000
1100
1200
U.T.

FIG. 168 (*b*)

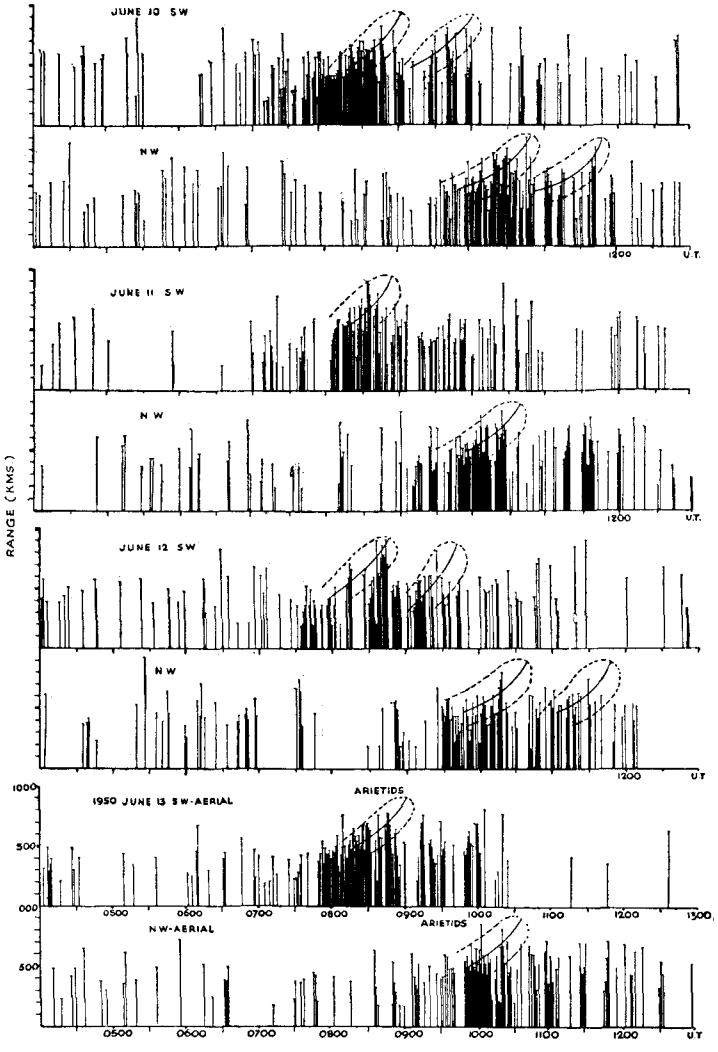

FIG. 168 (*c*)

FIG. 168. Portions of the range-time plots covering the period of the Arietid and ζ-Perseid streams in 1950 June. The apparatus used was the radiant-survey apparatus described in Chapter IV: and the plots are those for the twin aerials for each day.

the period of activity of the Arietids and ζ-Perseids in June 1950 as measured on the radiant-survey apparatus (Chap. IV). In interpreting these records it must be remembered that the rate is equivalent to that which would be visible to a single observer under good dark-sky conditions. In each year the richest stream of the sequence has been the Arietids, and the outstanding activity and duration of the shower may

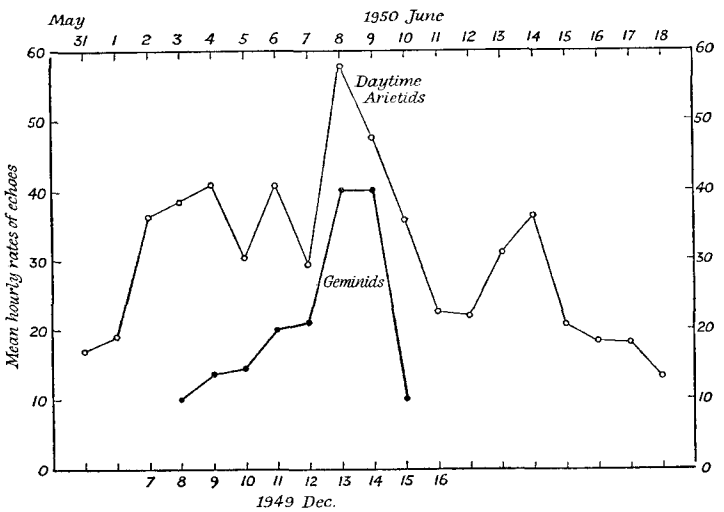

FIG. 169. Comparison of the mean hourly rates of the night-time Geminid shower in 1949 December, and the day-time Arietid shower in 1950 June.

be seen from Fig. 169, where the mean hourly rates are compared with those for the well-known night-time Geminid shower (Chap. XV). The general levels of activity for the summer months of 1947, 1948, and 1950 are shown in Figs. 170 (*a*), (*b*), (*c*), respectively, while Fig. 170 (*d*) shows the corresponding night activity for comparison.

With the methods of recording used with the single-aerial equipment in 1947–9 it was not possible to determine the daily activity of the individual radiants, but maximum hourly rates could be assigned and are given in Table 148,† which also contains the detailed rates of the individual radiants for 1950–2.

† The results for 1949 were somewhat meagre owing to the fact that the equipment was in process of change from the single-aerial working to the twin aerials of the meteor-survey equipment. The broad features of the activity, dominated by the Arietids, were still apparent.

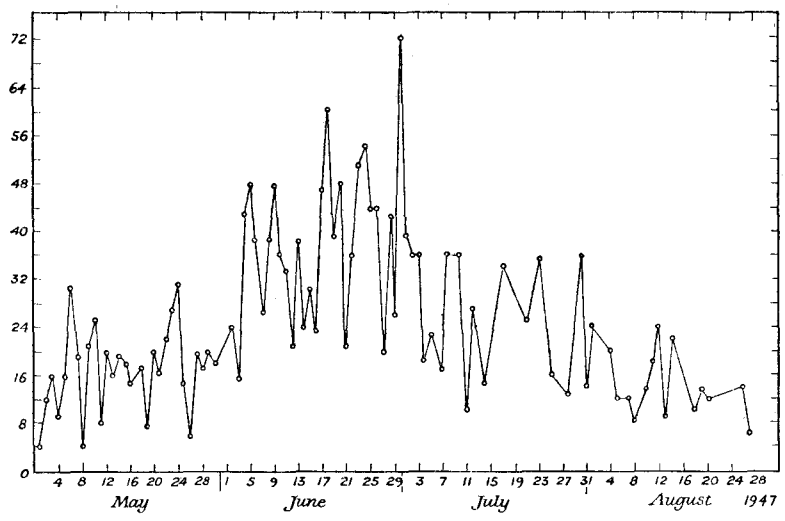

FIG. 170 (*a*). Mean hourly rate per radiant 1947 May–August.
Ordinates: number of echoes per hour.

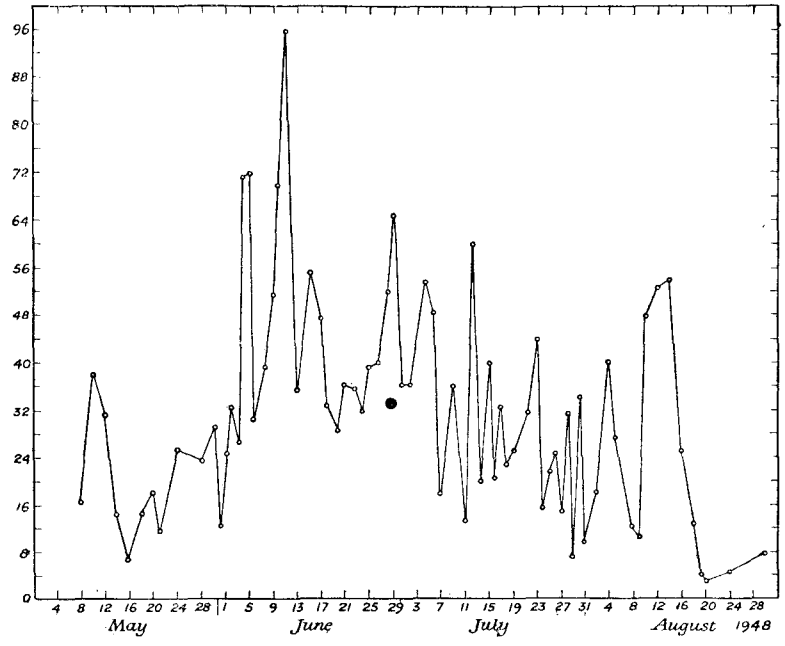

FIG. 170 (*b*). Mean hourly rate per radiant 1948 May–August.
Ordinates: number of echoes per hour.

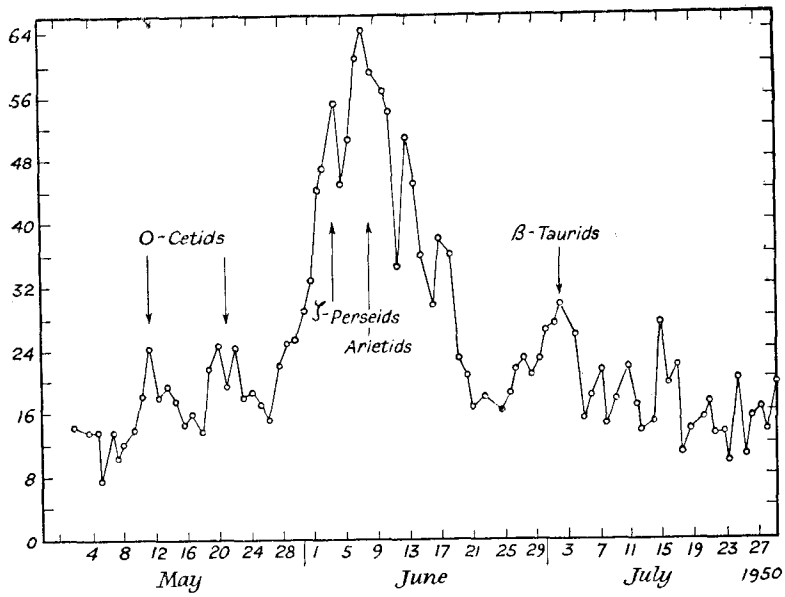

FIG. 170 (*c*).

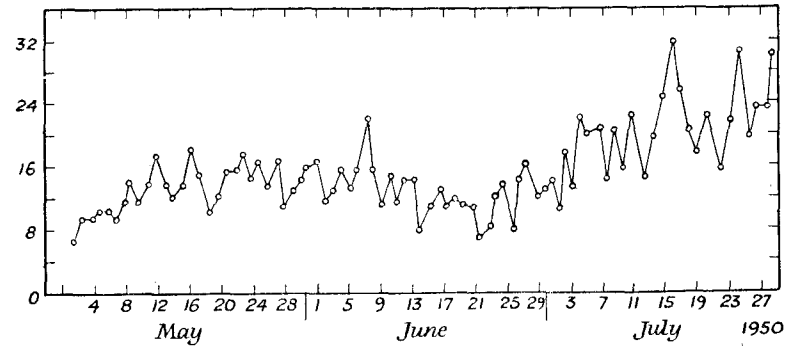

FIG. 170 (*d*).

FIG. 170 (*c*) and (*d*). The day- and night-time meteor activity during the summer of 1950.

Ordinates: 170 (*c*). Maximum hourly rate of echoes during day-time 06h. 00m.–18h. 00m. U.T.

Ordinates: 170 (*d*). Maximum hourly rate of echoes during night-time 18h. 00m.–06h. 00m. U.T.

TABLE 148

Activity of the Day-time Meteor Radiants

Stream	*Date*	1947	1948	1950	1951	1952
η-Aquarids	May 1	..	..	..	9	..
	May 4	13	..	..	..	15
	May 6	..	..	12	..	..
Piscids	May 7	28	..	The original Piscid stream was not delineated in 1950–2		
	14	..	14			
ν-Piscids	May 12	The ν-Piscids and the o-Cetid streams were not delineated in 1947–8 but may have been associated with the minor streams which were then found to be connected with the 1947 Piscids.		..	12	Not delineated
	13			..	16	
o-Cetids	14			18	23	
	15			..	25	Not delineated
	16			18	..	
	17			..	18	
	21			22	..	
	23			18	..	
Arietids†	May 29	..	..	..	25	13
	30	..	..	..	18	..
	31	..	..	18	16	21
	June 1	..	..	20	16	32
	2	..	..	36	22	23
	3	..	..	39	37	39
	4	..	60	41	27	35
	5	..	40	31	24	40
	6	44	..	41	12	72
	7	..	..	30	34	76
	8	..	..	57	34	54
	9	..	..	31	43	49
	10	..	..	37	..	..
	11	..	..	23	30	48
	12	..	..	23	44	48
	13	..	..	32	22	46
	14	..	..	38	19	18
	15	..	..	22	20	30
	16	..	..	19	..	26
	17	..	..	16	12	..
	18	..	..	14	..	35
ζ-Perseids	June 1	..	34	20	23	13
	2	..	..	20	23	15
	3	..	..	39	..	15
	4	..	..	29	17	29
	5	..	..	18	..	20
	6	..	..	20	32	28
	7	..	..	22	33	37
	8	..	..	23	39	32
	9	40	..	16	29	48
	10	..	..	17	..	..
	11	..	..	..	33	25

† In the publication of the 1947 results the Arietid stream was labelled Stream D. In the publication of the 1948 results this Arietid stream was wrongly interpreted as consisting of two radiants labelled D (ξ-Perseids) and H (Arietids). The close proximity of two such active streams as the Arietids and ζ-Perseids made the interpretation difficult until the meteor-survey apparatus became operative in 1950.

TABLE 148 (*cont.*)

Activity of the Day-time Meteor Radiants

Stream	*Date*	1947	1948	1950	1951	1952
ζ-Perseids (*cont.*)	June 12	In the publication of the		19	38	28
	13	1947 results the ζ-Perseids		..	24	..
	14	were labelled stream E		12	14	..
	15	and in the 1948 results		7	22	16
	16	stream D′.		9	..	..
54-Perseids .	June 21–9	60 (June 25)	36 (June 26)		Not delineated	
β-Taurids. .	June 24	..	..	..	16	..
	25	..	..	..	11	..
	26	..	..	14	24	26
	27	65	..	23	16	29
	28	..	..	15	21	23
	29	..	..	14	..	..
	30	..	..	12	23	21
	July 1	..	..	19	17	25
	2	..	..	29	14	25
	3	..	35	21	19	..
	4	..	..	20	24	..
	5	..	..	..	19	..
α-Orionids .	July 12–17	Not delineated	50 (July 12)		Not delineated	
ν-Geminids .	July 12–17	Not delineated	60 (July 12)		Not delineated	
λ-Geminids .	July 12–17	Not delineated	32 (July 12)		Not delineated	
θ-Aurigids .	July 23-Aug. 4	Not delineated	20 (July 25)		Not delineated	

Since 1950 the activity of these streams has been obtained from the range-time plots by a standardized method which makes direct comparison possible between the activities in the various years. The meteor rates are standardized by comparison with the sporadic activity over the period of the individual shower. The only assumption in this standardization is that the density of sporadic meteors is constant at any particular position of the earth's orbit. The 1950 conditions, which gave a radio-echo rate comparable with the visual rate for a single observer during the major night-time showers, has been taken as standard. In that year the mean hourly rate of sporadic meteors was 6·3 for the Arietid and Perseid epochs and 9·6 for the Taurid epoch, and these now form the standard of comparison.

It will be evident from Table 148 that the major sequence of the Arietids, ζ-Perseids, and β-Taurids has recurred over the five years of the investigation. The activity in mid-May and during July is very confused, however, and although the general level of the activity has remained consistently high during these epochs there has been no similar

consistency in the coordinates of the radiants delineated. The original Piscid stream of 1947 and 1948 May was not in evidence on the 1950, 1951 records, which, however, showed radiants near ν-Piscium and o-Ceti. On the 1952 records none of these radiants could be delineated. The major 54-Perseid stream was found only in 1947 and 1948 and the four streams, α-Orionids, ν-Geminids, λ-Geminids, θ-Aurigids, of July only in 1948. Further investigations in subsequent years will be required before it can be ascertained whether these streams are moving in long-period orbits or whether they represent isolated occurrences.

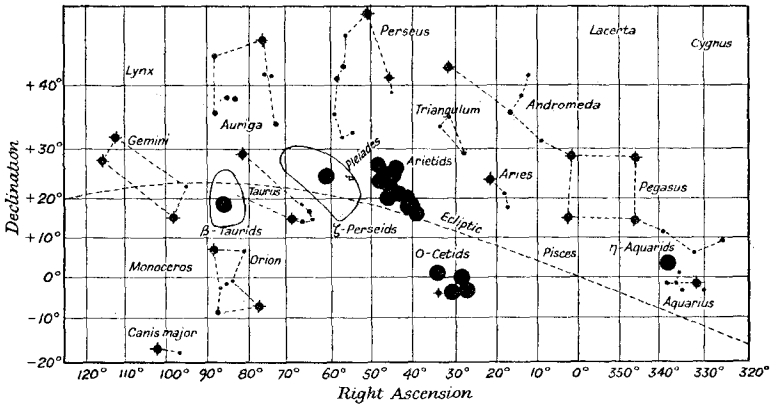

FIG. 171 (*a*). The radiant positions of the 1950 day-time meteor streams shown on a Mercator projection. Individual radiant positions are plotted for the Arietids, η-Aquarids, and o-Cetids. The diameter of a radiant represents the probable error in its position. For the ζ-Perseids and β-Taurids the weighted mean position is given, and the area shows the scatter of the radiants in each group.

(*c*) *Radiants*

The radiants of the streams in 1947 and 1948 were delineated by using the single movable aerial. With this technique it was rarely possible to measure both right ascension and declination on the same day. Since 1950 the radiant-survey apparatus has been in operation, and this must be regarded as giving the more precise information. The full information on the mean radiant positions is given in Table 149, while Table 150 contains the day-to-day radiant determinations of the streams delineated since 1950.

The radiant positions of the streams measured in 1950–2 are shown on the Mercator projections in Figs. 171 (*a*), (*b*), (*c*). Similar diagrams for the radiants of the 1947 and 1948 results have been given in the appropriate publications. The sequence of radiant positions for the Arietid stream

given in Table 150 shows a definite eastward trend in right ascension with an abnormal motion away from the ecliptic. The daily change in coordinates has been deduced by using a weighted least mean-square

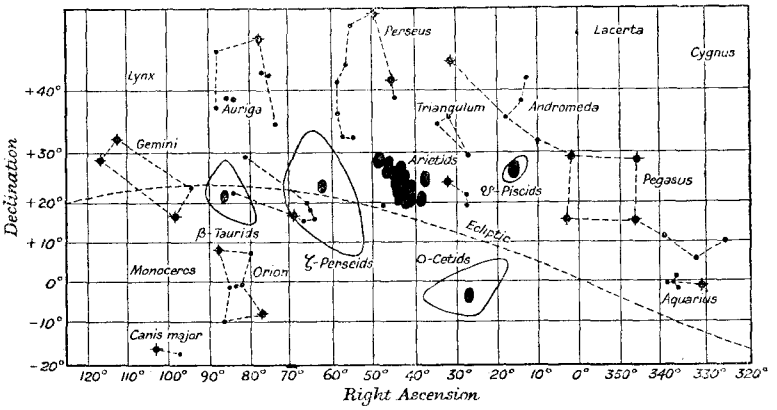

FIG. 171 (*b*). The radiant positions of the 1951 day-time meteor streams shown on a Mercator projection. Individual radiant positions are plotted for the Arietids, the area of a radiant representing the probable error in its position. For other streams the weighted mean position is given and the area shows the scatter of the radiants in each group.

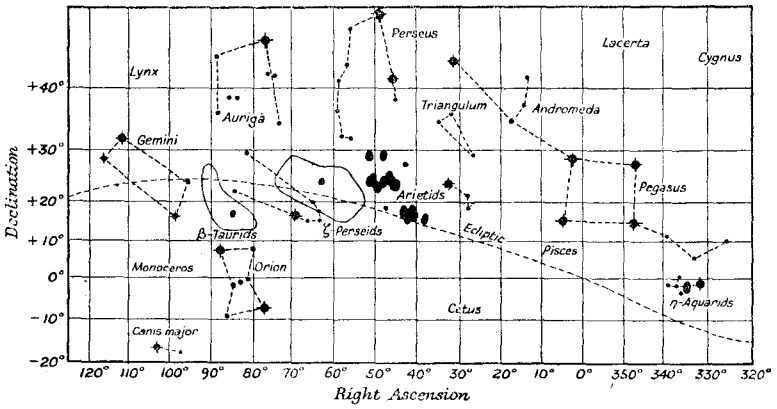

FIG. 171 (*c*). The radiant positions of the 1952 day-time meteor streams shown on a Mercator projection. Individual radiant positions are plotted for the Arietids; otherwise the weighted mean position is given and the area shows the scatter of the radiants in each group.

method and the ephemeris of the radiant obtained from the combined 1950–2 results is given in Table 151. The radiant of the ζ-Perseid stream also shows a pronounced eastward trend with abnormal motion away from the ecliptic. In the case of the β-Taurid stream the eastward trend

TABLE 149. *Mean Radiant Positions of the Day-time Meteor Streams*

Stream	1947				1948				1950				1951				1952			
	Time of maximum ⊙	*Duration* △⊙	*Mean radiant* α	δ	*Time of maximum* ⊙	*Duration* △⊙	*Mean radiant* α	δ	*Time of maximum* ⊙	*Duration* △⊙	*Mean radiant* α	δ	*Time of maximum* ⊙	*Duration* △⊙	*Mean radiant* α	δ	*Time of maximum* ⊙	*Duration* △⊙	*Mean radiant* α	δ
	deg.	*deg.*	*deg.*	*deg.*	*deg.*	*deg.*	*deg.*	*deg.*	*deg.*	*deg.*	*deg.*	*deg.*	*deg.*	*deg.*	*deg.*	*deg.*	*deg.*	*deg.*	*deg.*	*deg.*
η-Aquarids	43	−3 +6	338·4	00·0	44	−0 +4	336·0	00·0	45	..	338·5	+03·0	40	..	313	−04	43·6	±0	336	−2
Piscids	46	−2 +6	26·3	+24·6	49	−8 +11	26·4	+26·2	Not identified								Not identified			
Stream B (1947)	47	−2 +2	355·5	+05·0	Possible identification but not certain owing to lack of declination measurement				Not identified								Not identified			
Stream C′ (1948)	Listed as minor radiants				52	−10 +3	034·4	+20·3	Not identified								Not identified			
ν-Piscids	Not identified				Not identified				Not identified				51	−1 +1	16	27	Not identified			
o-Cetids	Not identified				Not identified				59	−6 +2	29·4	−02·7	54	−1 +2	26	−08				
Arietids†	75	−6 +7	049·0	+29·1	74	−10 +9	048·9	+27·9	77	−8 +9	044·3	+22·6	80	−13 +6	43·7	+24·5	76	−8 +12	46·0	+22·4
ζ-Perseids‡	77	−6 +4	056·6	+15·0	70	−6 +15	066·2	+31·8	72	−1 +12	058·4	+22·8	77	−7 +6	062·2	+22·4	78	−8 +8	62·4	+21·4
54-Perseids	93	−2 +2	067·6	+34·0	94	−5 +2	070·0	+32·1	Not identified								Not identified			
β-Taurids	95	−7 +0	082·0	+25·0	101	−7 +1	092·5	+26·3	99	−5 +2	086·2	+18·7	98	−6 +5	087·0	+20·0	96	−2 +4	85·4	+17·3
α-Orionids	Not identified				110	−0 +4	086·8	+11·8	Not identified								Not identified			
ν-Geminids	Not identified				110	−0 +4	098·0	+21·0	Not identified								Not identified			
λ-Geminids	Not identified				110	−0 +4	110·3	+15·0	Not identified								Not identified			
θ-Aurigids	Not identified				122	−2 +10	085·6	+38·3	Not identified								Not identified			

† In the publication of the 1947 results the Arietid stream was labelled D; and in the 1948 results it was wrongly interpreted as consisting of two

TABLE 150

Daily Radiant Positions of the Day-time Streams 1950–2

Stream	*Date*	1950 *Radiant* α	1950 *Radiant* δ	1950 *Radiant diameter*	1951 *Radiant* α	1951 *Radiant* δ	1951 *Radiant diameter*	1952 *Radiant* α	1952 *Radiant* δ	1952 *Radiant diameter*
		deg.	*deg.*	*deg.*	*deg.*	*deg.*	*deg.*	*deg.*	*deg.*	*deg.*
η-Aquarids	May 1	..	..	..	313	−4	< 3	..	..	..
	4	..	..	..	..	..	..	336	−2	< 3
	6	338·5	+3·0	< 3	..	..	..	..	..	..
ν-Piscids	May 12	..	..	..	15	+28	5	..	..	..
	13	..	..	..	17	+26	8	..	..	..
o-Cetids	14	27·5	−3·5	< 3	20	+4	7	..	..	..
	15	..	..	..	26	−8	< 3	..	..	..
	16	..	..	..	..	..	..	..	..	..
	17	..	..	..	38	−3	11	..	..	..
	18	28·5	0·0	< 3	..	..	..	..	..	..
	19	..	..	..	..	..	..	..	..	..
	20	..	..	..	..	..	..	..	..	..
	21	29·5	−5·0	10	..	..	..	..	..	..
	22	..	..	..	..	..	..	..	..	..
	23	34·0	+1·0	< 3	..	..	..	..	..	..
			+			+			+	
Arietids	May 29	..	..	..	42	20	4	36	17	3
	30	..	..	..	43	23	4	..	..	..
	31	43·0	26·0	< 3	43	20	< 3	38	14	< 3
	June 1	43·0	27·0	< 3	39	28	< 3	40	15	< 3
	2	39·0	16·0	< 3	38	26	3	41	17	< 3
	3	39·5	18·5	< 3	42	22	4	42	14	3
	4	42·5	17·5	< 3	41	22	3	42	16	< 3
	5	41·5	20·0	< 3	41	20	< 3	43	17	< 3
	6	42·0	21·0	< 3	44	25	< 3	46	23	3
	7	44·5	23·5	< 3	44	27	< 3	46	23	< 3
	8	45·5	21·0	< 3	42	25	< 3	48	24	< 3
	9	46·0	25·0	< 3	45	26	3	45	23	< 3
	10	48·5	23·5	< 3	No record			No record		
	11	46·0	26·5	< 3	45	26	3	47	24	< 3
	12	46·5	25·0	< 3	45	21	3	49	23	< 3
	13	48·0	27·0	< 3	46	27	3	51	29	3
	14				45	23	4	51	24	3
	15	Position not determined owing to solar radio noise interference			47	27	3	48	29	< 3
	16				..	..	..	51	24	< 3
	17				49	29	8	..	..	..
	18				..	..	..	51	24	4
	19				..	..	..	47	25	3
			+			+				
ζ-Perseids	June 1	58·0	28·0	< 3	55	8	7	58	26	6
	2	57·5	27·0	< 3	55	17	5	63	25	4
	3	53·5	19·5	< 3	..	..	..	69	28	8
	4	58·5	14·0	< 3	56	14	3	56	18	< 3
	5	60·5	24·0	< 3	..	..	..	59	23	4
	6	54·5	23·5	4	59	28	8	63	23	7
	7	62·0	25·0	3	61	20	4	60	19	3
	8	63·5	20·0	< 3	62	22	9	62	27	9
	9	66·0	25·0	< 3	66	33	8	60	15	5

TABLE 150 (*cont.*)

Stream	Date	1950 Radiant α	1950 Radiant δ	1950 Radiant diameter	1951 Radiant α	1951 Radiant δ	1951 Radiant diameter	1952 Radiant α	1952 Radiant δ	1952 Radiant diameter
		deg.	*deg.*	*deg.*	*deg.*	*deg.*	*deg.*	*deg.*	*deg.*	*deg.*
ζ-Perseids (*cont.*)	10	63·5	23·0	< 3	No record			No record		
	11	..	..	..	66	29	11	63	+23	5
	12	62·5	22·0	< 3	65	28	8	67	+24	7
	13	..	..	..	65	33	9	Radiant ill-defined		
	14	69·5	24·0	< 3	61	18	4	..	..	..
	15	72·0	28·0	3	70	18	8	69	+21	3
	16	71·5	29·5	< 3	..	..	..	..	..	..
	17	..	..	..	..	..	..	73	+23	3
β-Taurids	June 24	..	..	..	80	15	< 3	..	..	..
	25	..	..	..	80	15	< 3	..	..	..
	26	80·5	15·0	< 3	80	15	< 3	81	+13	3
	27	87·5	17·0	< 3	89	18	3	86	+13	5
	28	86·0	19·0	< 3	85	21	5	88	+17	6
	29	88·5	24·0	< 3	..	..	..	..	..	..
	30	86·0	26·5	< 3	87	20	..	90	+25	3
	July 1	85·5	21·0	< 3	87	19	< 3	90	+22	< 3
	2	86·5	17·5	7	88	29	4	83	+15	4
	3	86·5	17·5	5	89	26	5	..	..	..
	4	88·5	13·0	< 3	91	21	8	..	..	..
	5	..	..	..	88	20	4	..	..	..

is again evident, but the motion is toward the ecliptic. The ephemerides for these streams, obtained as above, are also included in Table 151. The mean daily motion of the Arietid radiant is $\Delta\alpha = +0°{\cdot}7$, $\Delta\delta = +0°{\cdot}6$; for the ζ-Perseids $\Delta\alpha = +1°{\cdot}1$, $\Delta\delta = +0°{\cdot}4$, and for the β-Taurids $\Delta\alpha = +0°{\cdot}8$, $\Delta\delta = +0°{\cdot}4$.

(*d*) *Velocities*

The first velocity measurements of the day-time streams were made in 1948, when between June 25 and August 6 the velocities of sixty-one meteors were obtained using the radio-echo diffraction technique. Unfortunately, this covers a period of confused activity, and with the single aerial then in use the identification of the measured meteors with specific streams presented some difficulty. The homogeneous groups which were identified appeared to relate to the 54-Perseid and θ-Aurigid streams for which apparent geocentric velocities of $37{\cdot}5 \pm 3{\cdot}7$ km./sec. and $32{\cdot}9 \pm 2{\cdot}7$ km./sec. were obtained respectively. These values gave approximate heliocentric velocities of $39{\cdot}1 \pm 2{\cdot}6$ km./sec. for the 54-Perseids and $27{\cdot}5 \pm 1{\cdot}4$ km./sec. for the θ-Aurigids, indicating that the orbits of the streams were elliptical. As these two streams have not been identified in subsequent years, it has not been possible to confirm the results.

With the introduction of the twin-aerial survey equipment for

TABLE 151

Ephemerides of the Motion of the Radiants of the Day-time Arietids, ζ-Perseids, and β-Taurids

Longitude of sun ⊙	70°	72°	74°	76°	78°	80°	82°	84°	*Mean daily motion*
Arietid radiant position α	39·5°	40·9°	42·3°	43·6°	45·0°	46·4°	47·7°	49·1°	+0·7°±0·03°
Arietid radiant position δ	+18·9°	+21·1°	+21·3°	+22·6°	+23·8°	+25·0°	+26·3°	+27·5°	+0·6°±0·05°
ζ Perseid radiant position α	54·6°	56·8°	59·0°	61·3°	63·5°	65·7°	67·9°	70·1°	+1·1°±0·05°
ζ Perseid radiant position δ	+20·1°	+20·9°	+21·7°	+22·5°	+23·3°	+24·1°	+24·9°	+25·7°	+0·4°±0·10°
Date: June 1950	1·0	3·1	5·2	7·3	9·4	11·5	13·6	15·7	..

Longitude of sun ⊙	92°	94°	96°	98°	100°	102°	..	..	*Mean daily motion*
β-Taurid radiant position α	81·6°	83·3°	84·9°	86·6°	88·2°	89·9°	..	..	+0·8°±0·08°
β-Taurid radiant position δ	+16·7°	+17·6°	+18·4°	+19·3°	+20·1°	+20·9°	..	..	+0·4°±0·14°
Date: June–July 1950	June 24·1	26·2	28·3	30·4	July 2·5	4·6	..	..	..

radiant measurement, the single-aerial system was directed exclusively to the measurement of velocities during the summer day-time period. In 1949 the measurements could only be made between May 30 and June 18, during which time twenty-two velocities of Arietid meteors were obtained, giving a mean velocity of $38{\cdot}5 \pm 4{\cdot}0$ km./sec. In 1950 a full programme of measurements was carried out which resulted in velocity determinations for the o-Cetids, Arietids, ζ-Perseids, and β-Taurids. In 1951 the velocities of the Arietids and ζ-Perseids were determined again, while the 1952 measurements yielded results for the Arietids and β-Taurids. The details for the various streams are given below, and the results summarized in Table 152.

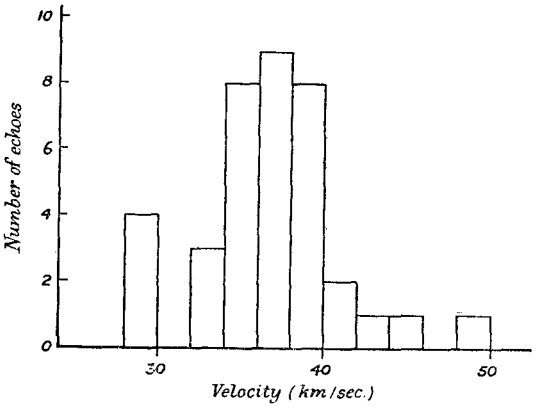

FIG. 172. Distribution of o-Cetid velocities, 1950.

(i) o-*Cetids.* The velocity of thirty-seven o-Cetid meteors was measured between 1950 May 13 and May 23. The distribution is shown in Fig. 172, the mean velocity being $36{\cdot}7 \pm 4{\cdot}2$ km./sec.

(ii) *Arietids.* The measurement of the Arietid velocities presents some difficulty because of the proximity of the radiant to that of the ζ-Perseid radiant, the separation in right ascension being only 20 degrees. During the period of early June, when both streams are highly active and when it is necessary to measure the velocities of both streams, a special technique has been employed. Whereas normally the radiant can be followed by a single movable aerial, in this case the aerial is maintained on a fixed azimuth during the transit of both radiants. Range-time plots are then made of the echoes yielding velocity measurements as shown in Fig. 173. The selection of velocities for each radiant is made by taking those which fall within the appropriate range-time envelopes. Fig. 173 shows the

results of this technique over the period 1950 May 31–June 12. The Arietid envelope contained forty-four velocity measurements and the

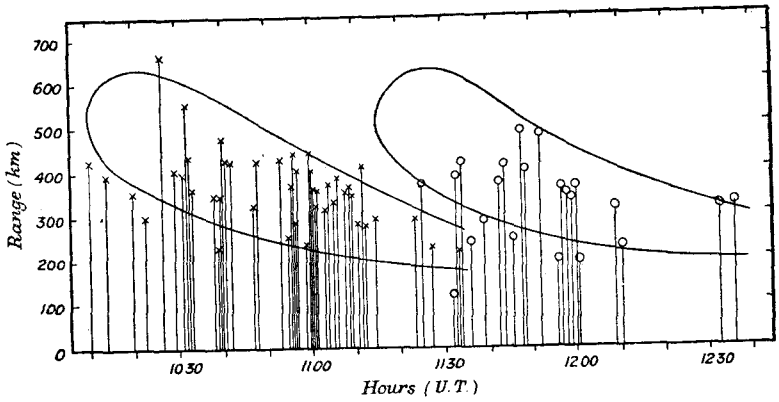

FIG. 173. Range-time distribution of echoes giving velocity determinations (1950 May 31–June 12).

× Arietid echoes. ○ ζ-Perseid echoes. —— theoretical range-time distributions.

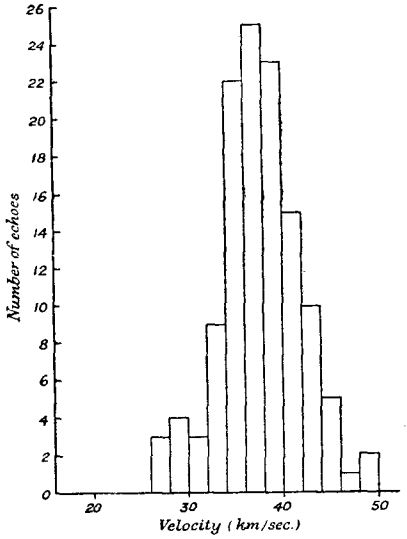

FIG. 174. Distribution of 122 Arietid velocities, 1950.

ζ-Perseid envelope twenty-one. In this year after June 12 the aerial was moved to follow the Arietid radiant between June 12 and 16, giving a further seventy-eight velocities. The distribution of the 122 velocities is shown in Fig. 174, the mean being $37{\cdot}7 \pm 4{\cdot}3$ km./sec. The same technique was employed in 1951 and 1952 with similar results.

(iii) *ζ-Perseids.* The measurement of the ζ-Perseid velocities has been referred to above, and the results for 1950 are included in Fig. 173. The appropriate histogram of the twenty-one ζ-Perseid velocities is shown in Fig. 175 (*a*), and that of the twelve measured in 1951 in Fig. 175 (*b*). The velocity of the stream was not determined in 1952.

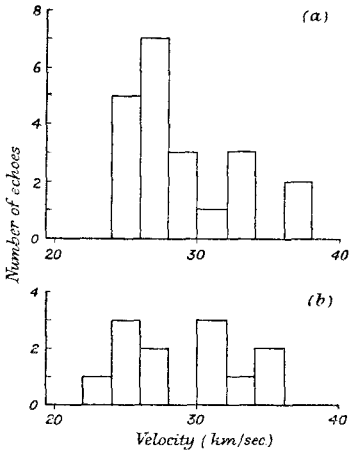

Fig. 175. (*a*) Distribution of ζ-Perseid velocities, 1950. (*b*) Distribution of ζ-Perseid velocities, 1951.

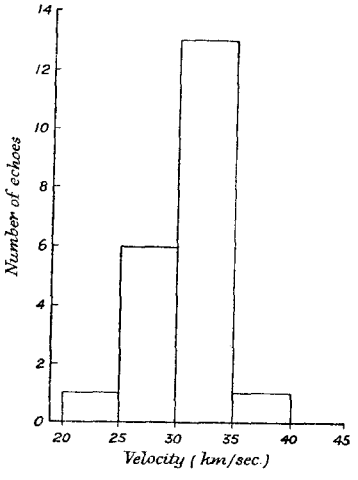

FIG. 176. Distribution of β-Taurid velocities, 1950, 1952.

(iv) *β-Taurids.* The velocities of ten β-Taurid meteors were determined in 1950. No measurements were obtained in 1951, but in 1952 a further eleven velocities were obtained. The combined results are shown in Fig. 176.

The velocity distribution for each of these showers shows an appreciable spread about the mean. This is partly due to the unavoidable inclusion of sporadic meteors in the group, but, even for the Arietid radiant where the shower rate is greatly in excess of the sporadic rate, the spread remains large. In the 1950 observations the r.m.s. error for the individual determinations in the Arietid group was 2·4 km./sec., while the standard deviation of the group was 4·3 km./sec. Hence there must exist a considerable true spread in the velocities of individual meteors in these groups. The significance of this is discussed below.

(*e*) *Orbits*

After the discovery of the day-time streams, the delineation of their orbits became a matter of great interest. Both Hoffmeister† and

† Hoffmeister, C., *Forschungen und Fortschritte* (Oct. 1947), nr. 19/20/21; *Die Meteorströme.*

TABLE 152

The Velocity Measurements of the Summer Day-time Streams

Stream / Year	o-Cetids		Arietids		Perseids	
	Number	v±dv km./sec.	Number	v±dv km./sec.	Number	v±dv km./sec.
1948	..	..	..	..	..	..
1949	..	..	22	38·5±4·0	..	..
1950	37	36·7±4·2	122	37·7±4·3	21	28·8±3·2
1951	..	..	39	38·7±4·4	12	29·0±3·9
1952	..	..	28	38·5±3·2	..	..

Stream / Year	54-Perseids		β-Taurids		θ-Aurigids	
	Number	v±dv km./sec.	Number	v±dv km./sec.	Number	v±dv km./sec.
1948	15	37·5±3·7	..	..	5	32·9±2·7
1949	..	..	..	..	..	..
1950	..	..	10	31·4±4·1	..	..
1951	..	..	..	..	..	..
1952	..	..	11	31·5±2·7	..	..

Whipple† had independently suggested that meteor streams moving in short-period orbits might give rise to showers incident on the sunlit hemisphere of the earth. In fact, we have already mentioned in Chapter XV that from the detailed study of the orbit of the November Taurids, Whipple predicted that the Taurid orbit should intersect the earth's orbit after perihelion passage 'producing only day-time meteors unlikely to be observed except as fireballs in late June and early July'. It was realized in 1947 that the radiant of the β-Taurid shower of late June was most probably the day-time return of the autumn Taurids, and this was confirmed when it became possible to calculate the orbit in 1950. The preliminary velocity measurements made in 1948 for the 54-Perseid and θ-Aurigid streams indicated that the orbits were of short period, but little precise information was obtained until the more comprehensive measurements of 1950 gave data for the o-Cetid, Arietid, ζ-Perseid, and β-Taurid streams. The information obtained in the years 1950–2 is summarized below.

(i) *o-Cetids.* It has only been possible to calculate the orbit of this shower from the 1950 observations and the details are given in Table 153.

The observed radiant has been corrected for zenith attraction and diurnal aberration. The shift in $\Delta\Omega$ was not sufficient to produce a

† Whipple, F. L., *Proc. Amer. Phil. Soc.* **83** (1940), 711.

detectable change in velocity and the orbit is computed from the mean radiant and velocity. The mean date has been used to determine the node. The spread in the elements was estimated from the radiant movement and velocity spread. The velocity spread primarily determines Δa, Δe, and Δq; Δi is influenced both by Δv and by $\Delta\alpha$, and $\Delta\omega$ primarily by $\Delta\alpha$. The orbit of this stream projected on to the plane of the ecliptic

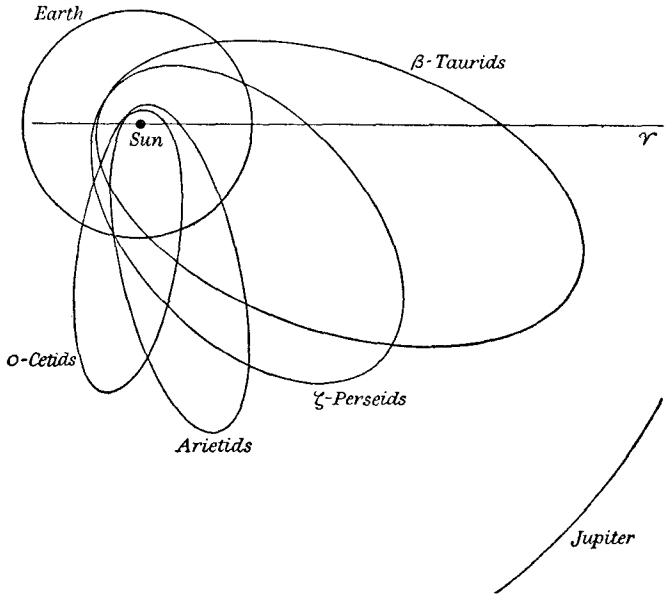

FIG. 177. Orbits of summer day-time meteor streams projected on to the plane of the ecliptic.

is shown in Fig. 177. Since ω is 211° and i 34°, the orbit does not approach the earth except in May.

(ii) *Arietids.* It has been possible to compute the elements of the Arietid orbit in each of the years 1950–2, and the results are given in Table 154. The details of the corrections and the estimates of the spread are as described for the o-Cetids. The radiant shows a steady change in right ascension and declination, and orbits for the first and last dates, with the same semi-major axis as the mean orbit, have been computed from the smoothed radiant positions. Although the shape remains almost unchanged, both i and π vary with position in the shower, and the line of apsides swings gradually forward.

The mean orbits for the various years agree satisfactorily within the limits of experimental error. The projection on the plane of the ecliptic

TABLE 153

Observational Data and Orbital Elements for the o-Cetid Shower

Mean date 1950	Radiant α deg.	Radiant δ deg.	Corrected radiant α deg.	Corrected radiant δ deg.	Corrected radiant λ deg.	Corrected radiant β deg.	Observed velocity v km./sec.	Helio-centric velocity $\bar{V}$ km./sec.	a a.u.	e	q a.u.	i deg.	ω deg.	π deg.	Ω deg.	ΔΩ deg.
May 19	29·4±2	−2·7±2	29·0±2	−3·7±2	26·0±2	−13·6±2	36·7±4·2	32·5±2·7	1·3±0·4	0·91±0·04	0·11±0·03	34±7	211±3	89±3	238·0	9

TABLE 154

Observational Data and Orbital Elements for the Arietid Stream

Date	Corrected radiant α deg.	Corrected radiant δ deg.	Corrected radiant λ deg.	Corrected radiant β deg.	Velocity Observed v±dv km./sec.	Velocity Heliocentric $\bar{V}$ km./sec.	a a.u.	e	q a.u.	i deg.	ω deg.	π deg.	Ω deg.	ΔΩ deg.
1950 June 1 .	38·4	+15·5	41·6	+1·0	..	..	1·5	0·94	0·09	3	28	98	70·3	..
June 8 (mean orbit) .	43·8±1	21·9±1·5	48·0±1	5·7±1·5	37·7±4·3	34·0±2·9	1·5±0·7	0·94±0·04	0·10±0·03	18±5	29±2	106±2	77·0	18
June 18	51·1	31·1	57·2	12·7	..	..	1·5	0·92	0·12	34	33	120	86·6	..
1951 May 30 .	39·3	20·7	43·4	5·1	..	..	1·6	0·91	0·15	11	38	..	67·3	..
June 8 (mean orbit) .	43·4	23·9	48·0	7·0	38·7±4·4	34·8±3·0	$1·6^{+3·5}_{-0·5}$	0·94±0·04	0·09±0·03	21±8	29±3	106	76·8 ±0·5	20
June 18 .	47·1	26·7	52·0	8·8	..	..	1·6	0·97	0·06	40	22	..	85·4	..
1952 June 9 .	45·5	21·7	49·2	4·4	38·5±3·2	34·8±2·5	$1·6^{+0·8}_{-0·3}$	0·95±0·03	0·09±0·02	13±4	29±2	106	77·5 ±0·5	21

is shown in Fig. 177. Although the inclination is high at the end of the shower, it is low enough at the beginning to consider the possibility that the stream might intersect the earth's orbit again after perihelion passage. The predicted radiant of this return shower is at α 336°, δ −11° on July 28—a time and position coinciding with the δ-Aquarid shower (Chap. XIV). The orbit of the δ-Aquarid stream has been

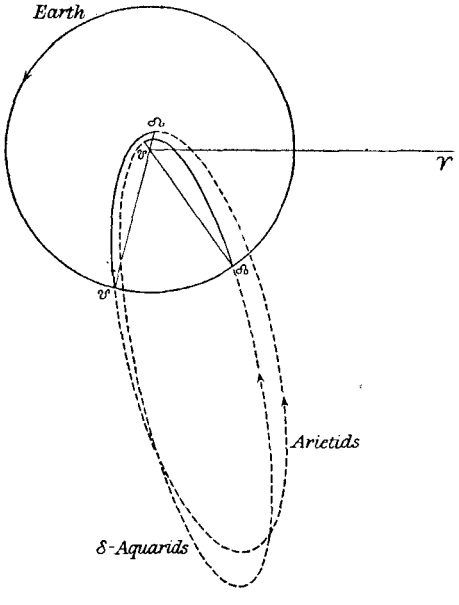

FIG. 178. Mean orbits of the δ-Aquarids and the day-time Arietids projected on to the plane of the ecliptic.

discussed in Chapter IV. A comparison of the elements given in Table 93 (Chap. XIV) with those of the Arietids in Table 154 and of the projection on the plane of the ecliptic in Fig. 178 shows the similarity of the orbits. There is close agreement between the values of π. The inclination of the δ-Aquarid orbit is 24° and the stream is 0·31 a.u. away from the earth at its second approach on June 9. From the duration of 16 days of the day-time Arietids the width of the stream must be at least 0·27 a.u. There is also evidence that the δ-Aquarid stream lasts 18 days in the southern hemisphere.† Hence, as the system of orbits is so broad, it seems probable that the two showers are connected and are produced by one extended meteor stream.

† McIntosh, R. A., *Mon. Not. Roy. Astr. Soc.* **94** (1934), 583.

TABLE 155

Observational Data and Orbital Elements for the ζ-Perseid Stream

Date	Corrected radiant α deg.	δ deg.	λ deg.	β deg.	Velocity: Observed v±Δv km./sec.	Velocity: Helio-centric $\bar{V}\pm\Delta\bar{V}$ km./sec.	a a.u.	e	q a.u.	i deg.	ω deg.	π deg.	Ω deg.	ΔΩ deg.
1950 June 8	61·0±2	+22·8±2	63·6±2	+3·0±2	28·8±3·2	34·8±2·0	1·7±0·5	0·79±0·08	0·35±0·04	4±2	61±4	138±4	77·0	16
1951 June 2	51·1	+12·4	52·3	−4·7	..	..	1·6	0·84	0·27	7	232	..	250·1	..
June 9	61·6	21·2	63·7	+0·4	29·0±3·9	34·7±3·0	$1\cdot6^{+8\cdot0}_{-0\cdot3}$	0·79±0·1	0·34±0·05	0·4±2	59±2	..	77·8±0·5	..
June 17	68·8	27·5	71·2	+5·5	..	..	1·6	0·78	0·36	6	62	..	84·5	..

TABLE 156

Observational Data and Orbital Elements for the Day-time β-Taurid Stream and the Night-time Taurids

Date	Corrected radiant α deg.	δ deg.	λ deg.	β deg.	Velocity: Observed v±Δv km./sec.	Velocity: Helio-centric $\bar{V}\pm\Delta\bar{V}$ km./sec.	a a.u.	e	q a.u.	i deg.	ω deg.	π deg.	Ω deg.	ΔΩ deg.
β-Taurids 1950 June 30	85·7±2	+17·9±2	85·9±2	−4·6±2	31·4±4·1	36·7±2·8	$2\cdot2^{+3\cdot1}_{-0\cdot8}$	0·85±0·10	0·34±0·04	6±3	224±4	162±4	278·1 ±0·5	8
β-Taurids 1952 June .	84·9	+16·1	85·0	−7·2	31·5±2·7	37·3±2·0	$2\cdot5^{+2\cdot6}_{-0\cdot3}$	0·86±0·10	0·36±0·03	9±4	246±4	162±4	276·4 ±0·5	6
November night-time northern Taurids:														
No. 778 .	..	..	..	..	..	37·1	2·19	0·891	0·239	3·9	307·7	160·1	212·41	..
789 .	..	..	..	..	..	36·9	2·06	0·799	0·414	3·2	287·8	160·2	232·40	..
1009 .	..	..	..	..	..	37·1	2·16	0·858	0·307	2·5	299·6	160·5	220·92	..

(iii) *ζ-Perseids.* The ζ-Perseid orbit has been computed from the 1950 and 1951 measurements. The eastward trend of the radiant and its motion away from the ecliptic were more pronounced in 1951, and for that year orbits for the first and last dates have also been computed, showing a system similar to the Arietids. The elements are given in Table 155, and the mean orbit projected on to the plane of the ecliptic is shown in Fig. 177.

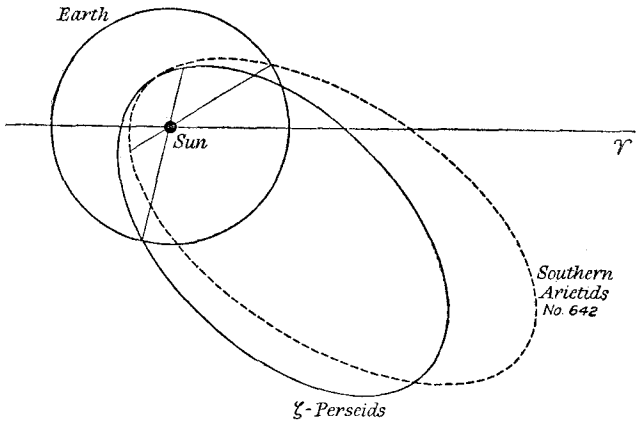

FIG. 179. Orbits of the ζ-Perseid meteor stream and an individual southern Arietid meteor.

The inclination changes sign during the progress of the shower and hence a portion of the ζ-Perseid stream must lie in the plane of the ecliptic, giving another intersection during the winter months. The predicted shower arising from this encounter should occur on October 11 at right ascension 28°, declination +12°. This is in the position of the southern Arietid stream, delineated by Whipple using the Harvard photographic technique, discussed in Chapter XV. The mean orbit of the ζ-Perseid stream is drawn for comparison with Whipple's orbit for the southern Arietid No. 642 in Fig. 179, and there seems little doubt that the summer day-time ζ-Perseid system and the autumn night-time S-Arietid systems must be closely related.

(iv) *β-Taurids.* The β-Taurid orbit has been computed from the 1950 and 1952 observations. The elements are given in Table 156, and the orbit projected on to the plane of the ecliptic is shown in Fig. 177.

Whipple's prediction of a return of the November Taurid stream in the summer day-time has been mentioned previously. The delineation of the orbit of the β-Taurid stream leaves little doubt that this stream is,

in fact, arising from the intersection of the November Taurid orbit after perihelion. The elements of the orbits for three of Whipple's photographically determined northern Taurids are given in Table 156 and

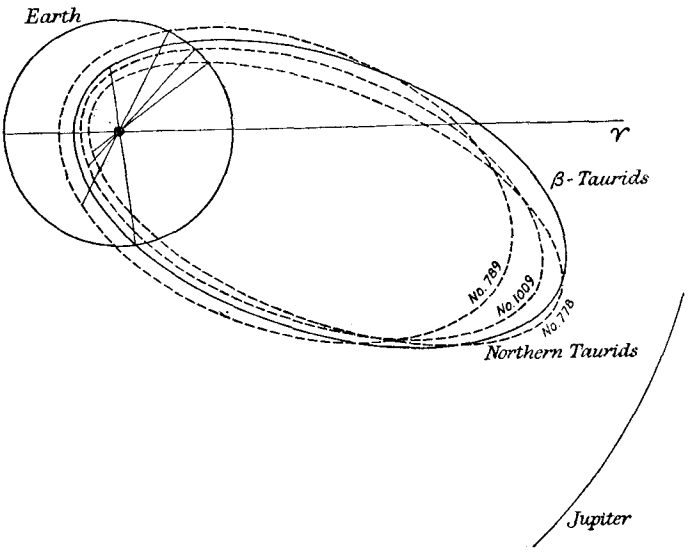

FIG. 180. Orbits of the day-time β-Taurid stream compared with three of the orbits of the night-time November northern Taurid stream.

these three orbits are drawn in Fig. 180 together with the β-Taurid orbit. The relation of these orbits to that of Encke's Comet has been referred to in Chapter XV and will be discussed again in Chapter XXI.

XIX

THE NUMBER AND MASS DISTRIBUTION OF THE SHOWER METEORS

THE number and mass distribution of sporadic meteors and the resultant space density was discussed in Chapter VII. From the available observational evidence it was concluded that the relation between change of numbers dN with magnitude m could be expressed in the form

$$dN = \varkappa^m \, dm. \tag{1}$$

Independent determinations of $\varkappa$ give values lying between 2·0 and 2·7. In terms of the mass distribution m

$$dN = \frac{dm}{m^p}, \tag{2}$$

where $p = 2$, corresponds to the base $\varkappa = 2{\cdot}5$ in (1). The relations have been established by measurements on the sporadic meteor distribution in the magnitude range from about −4 to +9. These figures give a space density per magnitude group of about $5{\cdot}0 \times 10^{-26}$ gm./c.c. and by extrapolation a space density of about 10^{-24} gm./c.c. for all sporadic meteors. Unfortunately little work has yet been done on the corresponding distributions for meteors in the major showers, the data being limited mainly to a few visual and photographic measurements. Radio-echo measurements described in § 2 give hope of much more detailed information in the near future.

1. Visual and photographic determinations of the frequency distribution

The distribution of luminosities in the meteors of the Perseid shower has been studied by Öpik† using the double-count method described in Chapter II. His results are summarized in Table 157. The mean value for the base $\varkappa$ in equation (1) is 2·5 or the same as Watson's value for the sporadic distribution.

The observations of the great Giacobinid shower of 1933 October 9 made by de Roy‡ and by Sandig and Richter§ have been referred to in Chapter XVI. Fig. 161 (Chap. XVI) shows the two periods during the shower when de Roy made his naked-eye estimates of the magnitudes

† Öpik, E. J., *Publ. Tartu Obs.* **25** (1922), no. 4.
‡ de Roy, F., *Gazette Astronomique*, **20** (1933), 170.
§ Sandig, H., and Richter, N., *Astr. Nachr.* **250** (1933), 170.

TABLE 157

Distribution of Luminosities in the Perseid Shower according to Öpik

Zenithal magnitude	4 to 4·5	3·5 4	3·0 3·5	2·5 3·0	2·0 2·5	1·5 2·0	1·0 1·5	0·5 1·0	0·0 0·5	−0·5 0·0	−1·0 −0·5	−1·5 −1·0	−2·0 −1·5	−2·5 −2·0	−3·0 −2·5	−3·5 −3·0	−4·0 −3·5
1921																	
Number	19	51	93	85	83	73	34	22	5	3	4	2	1	0	0	0	0
% .	18	21	25	14	10	8	3	0·1	0·25	0·2	0·25	0·04	0·02	0	0	0	0
1920																	
Number	30	60	85	85	75	50	35	14	8	3	2	2	1	0	0	1	..
% .	25	21	18	13	11	5	4	1	0·6	0·17	0·08	0·09	0·05	0	0	0·04	..

of 534 meteors. Sandig and Richter made magnitude estimates of 101 meteors through a 70 mm. telescope. Their data have been discussed by Watson.† The distribution of numbers observed against magnitude is shown in Fig. 181 (*a*) and (*b*). The period II observations of de Roy (see

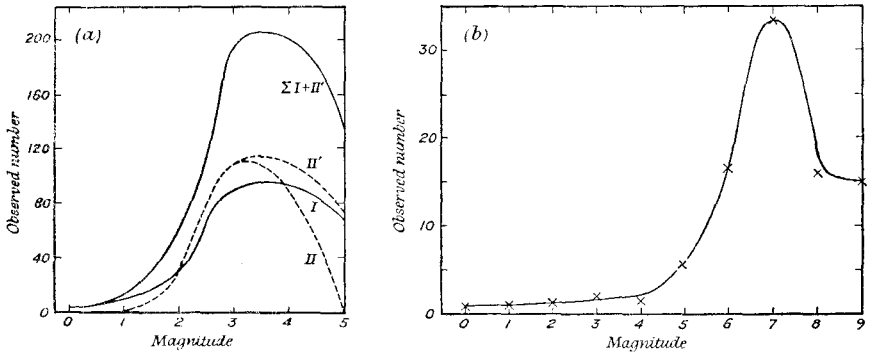

FIG. 181. (*a*) Naked-eye magnitude distribution made during the 1933 Giacobinid shower by de Roy. For observing periods I and II, see Fig. 161 (Chap. XVI). II′ is II corrected for effects of moonlight. (*b*) Telescopic magnitude distribution made during the 1933 Giacobinid shower by Sandig and Richter.

Fig. 161, Chap. XVI) were carried out in moonlight; and these have been corrected by Watson as shown at II′ in Fig. 181 (*a*). Watson then applies corrections as discussed in Chapter II for the numbers missed by the observer, and also deduces that a factor of 220 would bring the telescopic observations to the same conditions as the naked-eye observations. The final results are given in Table 158, and the distribution of this corrected N against magnitude is shown in Fig. 182. The slope of this curve gives $\varkappa$ as 2·5, in agreement with Öpik's value for the Perseid meteors.

† Watson, F., *Bull. Harv. Coll. Obs.* (1934), no. 895.

TABLE 158

The Frequency Distribution Observed by de Roy and by Sandig and Richter during the 1933 *Giacobinid Shower, as corrected by Watson*

Magnitude	*True naked eye*	*Number telescopic*	$220 \times$ *Telescopic*	$\log_{10} N$
0	1	..	..	0
1	8	..	..	0·90
2	60	..	..	1·78
3	223	2	(440 ?)	2·35
4	433	2	440	2·64
5	1415	6	1320	3·14
6	..	22	4840	3·68
7	..	51	11220	4·05
8	..	91	20020	4·30

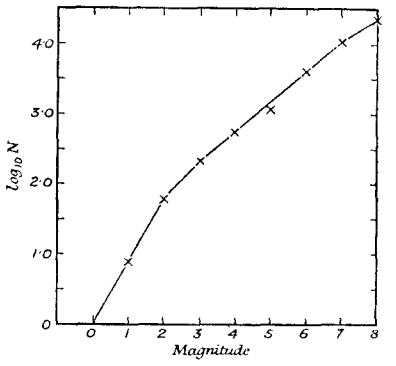

FIG. 182. The corrected frequency distribution of the 1933 Giacobinid shower.

Watson compares this Giacobinid distribution with the Perseid distribution found by Öpik, and with observations of Leonid meteors made in 1933 at Oak Ridge, Blue Hills, Hopkinton, and Wellesley. The three distributions are compared in Fig. 183. The shape of the Leonid curve is also substantiated by Leonid observations made by Millman.† The Leonid and Perseid distributions show sharp kinks at about +1 mag. and +3 mag. respectively. The most rational conclusion to be drawn from this is that these showers are lacking in faint meteors compared with the Giacobinid shower. It will be seen that this result is in agreement with the predictions of dispersion of small particles from showers of great age (see Chap. XX).

Photographic measurements of the frequency distribution during the 1946 return of the Giacobinid shower were made by Jacchia, Kopal,

† Millman, P. M., *J. Roy. Astr. Soc. Can.* **28** (1934), no. 3.

and Millman.† The distribution of the apparent panchromatic magnitudes m_p at maximum brightness for 177 meteors is given in Table 159.

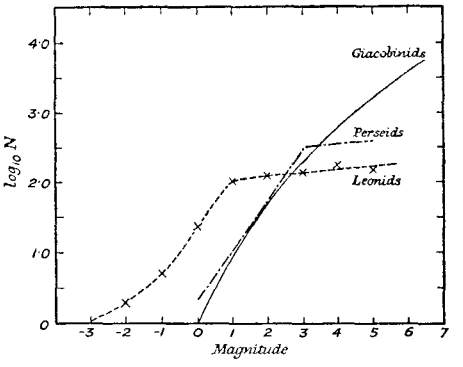

FIG. 183. The Giacobinid frequency distribution of Fig. 182 compared with the frequency distribution for the Leonids and Perseids.

TABLE 159

Distribution of Apparent Photographic Magnitudes for the 1946 *Giacobinid Shower*

Panchromatic magnitude m_p	*Number of meteors* N
−8	1
−7	0
−6	4
−5	5
−4	16
−3	33
−2	52
−1	(46)
0	(20)

The count at magnitudes −1 and 0 must be incomplete since these magnitudes are near the threshold of the camera used. From magnitudes −2 to −6, the increase is expressed by

$$\log_{10} N = 2{\cdot}50 + 0{\cdot}34 m_p,$$

leading to a value for the base $\varkappa$ of 2·2. This is in reasonable agreement with the value of $\varkappa = 2{\cdot}5$ found above from the analysis of the 1933 Giacobinid shower. Jacchia, Kopal, and Millman† also state that a value of $\varkappa = 2{\cdot}5$ was found in the Canadian visual observations of the

† Jacchia, L. A., Kopal, Z., and Millman, P. M., *Astrophys. J.* **111** (1950), 104.

1946 Giacobinid shower. The authors point out that the values of m_p used above are affected by distance and by short-lived explosions on the trail, and that a better index of the frequency distribution is given by the integrated absolute magnitude

$$\mathbf{M}_p = -2{\cdot}5 \log \int I \, dt,$$

where the integral $\int I \, dt$ is taken as unity when m_p reduced to 100 km. distance is zero. The distribution of these integrated magnitudes is listed in Table 160.

TABLE 160

Distribution of Integrated Absolute Photographic Magnitudes for the 1946 *Giacobinid Shower*

$\mathbf{M}_p$	N
−6	3
−5	5
−4	13
−3	21
−2	51
−1	42
0	(33)
+1	(3)

In this case the increase is best expressed by

$$\log_{10} N = 2{\cdot}20 + 0{\cdot}29\mathbf{M}_p,$$

giving a value of $\varkappa = 1{\cdot}95$. This is in marked contrast to the higher values of $\varkappa$ found in the photographic work on the sporadic meteors. It seems possible that the assumption of constant $\varkappa$ over this range of negative magnitudes is not justified. Evidently such a value could not extend indefinitely into the brighter magnitude region.

2. Radio-echo methods for determining the frequency distribution

It will be clear from Chapter III that the radio-echo techniques provide a method for determining the electron line densities α_0 for individual meteors, either by measurement of the amplitude of the Fresnel zone patterns in cases where $\alpha_0 < 10^{12}$ electrons/cm. path or by measurement of the durations of the radio-echo in cases where $\alpha_0 > 10^{12}$ electrons/cm. path. In the case of homogeneous velocity groups, as provided by the major showers, the establishment of the distribution of α_0's would then give the frequency distribution of magnitudes or mass directly. Preliminary application of this idea was made by Lovell,

Banwell, and Clegg† in the radio-echo measurements of the Giacobinid shower in 1946, and Lovell‡ has referred to further measurements on the 1946 Geminid shower and on the 1947 Quadrantid shower. In the light of recent developments these results cannot be regarded as reliable since at that time it was thought that formula (6) of Chapter III could in all cases be used to obtain the line density α_0. The revised method based on the correct formulae of Chapter III can now be employed with confidence to determine the frequency distribution, but results are not yet available.

An alternative radio-echo method for determining the mass distribution has recently been devised by Kaiser and Evans.§ It can be shown‖ from the theory of the evaporation of meteors that the rate of evaporation as the meteor penetrates the atmosphere is given by

$$\mathbf{n} \simeq \tfrac{9}{4}\,\mathbf{n}_{\max}\left(\frac{p}{p_{\max}}\right)\left(1-\frac{1}{3}\left(\frac{p}{p_{\max}}\right)\right)^2, \tag{3}$$

where p is the atmospheric pressure at the point in question and $p_{\max}$ the pressure at the point of maximum evaporation given by

$$p_{\max} \simeq \tfrac{8}{3}\,\mathrm{lg}\,\rho_{\mathrm{m}}\left(\frac{\boldsymbol{r}_\infty}{\mathrm{V}^2}\right)\cos\chi, \tag{4}$$

l and ρ_{m} being the latent heat of evaporation and density of the meteor, g the acceleration due to gravity, $\boldsymbol{r}_\infty$ the radius and V the velocity of the meteor before it enters the atmosphere, and χ the zenith angle. The rate of evaporation, $\mathbf{n}_{\max}$, at the maximum point is given by

$$\mathbf{n}_{\max} \simeq \frac{4}{9}\left(\frac{G}{HA}\right)(\tfrac{4}{3}\pi\,\boldsymbol{r}_\infty^3\,\rho_{\mathrm{m}}\,\mathrm{V}\cos\chi), \tag{5}$$

where H is the scale height, A the atomic weight, and G Avogadro's number.

Equation (3) can be used to plot the shape of the evaporation curve as the meteor penetrates the atmosphere. For constant V it will also be evident from equations (3), (4), and (5) that the extension of this curve in height depends on $\boldsymbol{r}_\infty$ and hence the mass of the meteor. If the height distribution of the meteors in a homogeneous velocity group is determined, the width of the distribution to half amplitude will therefore depend on the range of meteoric masses included in the sample. It has

† Lovell, A. C. B., Banwell, C. J., and Clegg, J. A., *Mon. Not. Roy. Astr. Soc.* **107** (1947), 164.

‡ Lovell, A. C. B., *Rep. Phys. Soc. Progr. Phys.* **11** (1948), **415.**

§ Kaiser, T., and Evans, S., *Mon. Not. Roy. Astr. Soc.* **114.**

‖ Herlofson, N., *Rep. Phys. Soc. Progr. Phys.* **11** (1948), **444.**

been shown by Kaiser and Evans that the relation between the half amplitude width of the height distribution Δh, and the exponent p in equation (2) is given by

$$\frac{\Delta h}{H} = 3{\cdot}39(3p-\tfrac{7}{2})^{-\frac{1}{2}}. \tag{6}$$

So far only preliminary applications of the idea have been made to the determination of p, using the technique of height determination described by Clegg and Davidson.† The results indicate that the value of p is 1·7 for the Geminid shower, but is considerably greater for the daytime Arietid shower. The method has also been applied to the sporadic distribution by selecting groups with homogeneous velocity. The various groups all yield a value of $p = 2$; corresponding to the base $\varkappa$ in equation (1) of 2·5.

It has been a common observation in many of the radio-echo studies that the relative increase in numbers of echoes during a major nighttime shower show a ratio of increase over the sporadic background which is less than the corresponding ratio found in visual observations. The discrepancy becomes increasingly marked in radio equipment of high sensitivity which detects meteors near the limit of naked-eye visibility, and the effect has always been particularly prominent in the Perseid shower.‡ The peculiarity has been discussed by McKinley§ and by McKinley and Millman,‖ and undoubtedly arises because of the lack of small meteors in the showers of considerable antiquity. Reference to Fig. 183 and § 1 also indicates that this result is well known from visual observations in the case of the Perseid and Leonid showers. The cosmological reasons for this disappearance of small particles in old showers will be discussed in Chapter XX.

3. The total meteoric mass entering the earth's atmosphere from the shower meteors

The total daily mass and energy brought into the earth's atmosphere every day by the sporadic meteors has been estimated in Tables 23 and 24 of Chapter VII. By making the same assumption about the mass-luminosity relationship it is possible to modify these tables to include the effect of the meteors in the major showers. Although this can be

† Clegg, J. A., and Davidson, I. A., *Phil. Mag.* **41** (1950), 77.

‡ See, for example, the comments made by Prentice, J. P. M., Lovell, A. C. B., and Banwell, C. J., *Mon. Not. Roy, Astr. Soc.* **107** (1947), 155, concerning the radio-echo studies of the 1946 Perseids.

§ McKinley, D. W. R., *Canad. J. Phys.* **29** (1951), 403.

‖ McKinley, D. W. R., and Millman, P. M., *Proc. Inst. Radio Engrs.* **37** (1949), 364.

done in detail by reference to the figures of the activity of the major showers given in Chapters XIII to XVIII it is sufficient for the present purpose to scale the activity from the radio-echo survey of the overall activity shown in Fig. 184. This shows the variation of activity of the

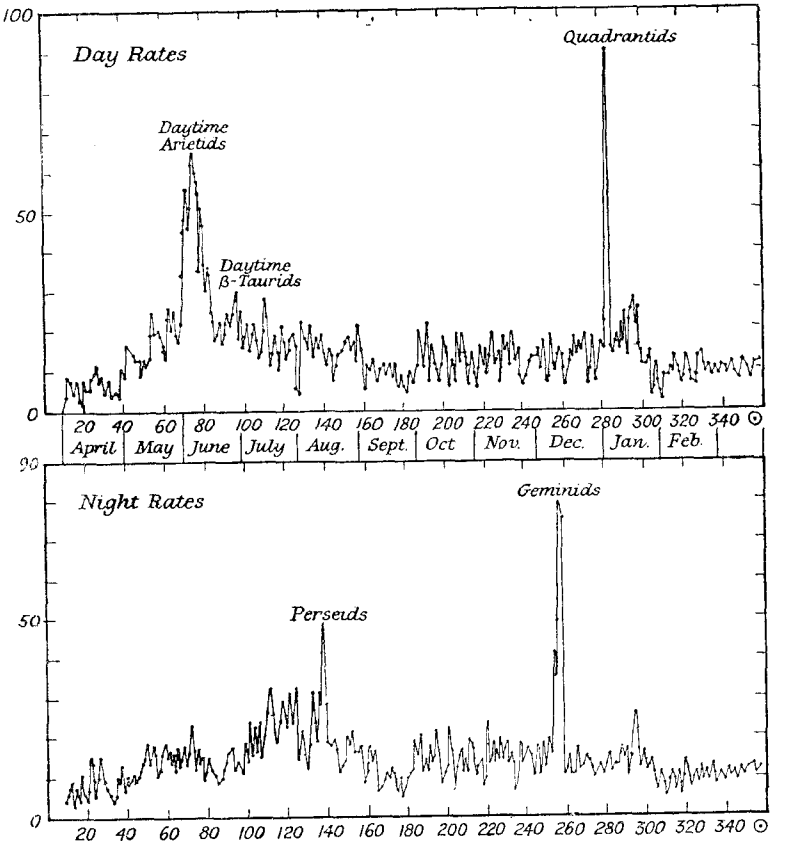
100
Day Rates
Quadrantids
Daytime Arietids
50
Daytime β-Taurids
0
20 40 60 80 100 120 140 160 180 200 220 240 260 280 300 320 340 ⊙
April May June July Aug. Sept. Oct Nov. Dec. Jan. Feb.
90
Night Rates
Geminids
50
Perseids
0
20 40 60 80 100 120 140 160 180 200 220 240 260 280 300 320 340 ⊙

FIG. 184. The variation of meteor activity throughout the year for day and night periods as determined by the radio-echo technique.

sporadic background throughout the year for day and night periods, and the peaks due to the major showers. From these curves the data of Tables 23 or 24 (Chap. VII) can be scaled directly to give the contribution of the showers. The data in Fig. 184 have been selected to show the maximum sporadic activity during the day or night, whereas an average is required for comparison with Tables 23 and 24. The ratios of shower to sporadic activity in Fig. 184 have therefore been doubled to allow for this. The scaling is accomplished from the ratios of the areas under the

shower peaks to the average area under the sporadic background. This gives the increase per hour of the shower meteors over the sporadic meteors averaged during the time for which the shower is active. The daily increase in mass may be obtained by assuming that the shower radiant is above the horizon for an average of 12 hours per day, and the total mass brought in by the shower is then given by multiplication of this column by the number of days for which the shower is active. The various scaling factors derived from Fig. 184 are given in Table 161. In Table 162 the result of applying these scaling factors to the sporadic meteor estimates in Table 23 (Chap. VII) are given for five of the most prominent major showers. The other recurrent showers of lesser activity such as the Orionids, Lyrids, etc., are classed together under 'other showers'.

TABLE 161

Scaling Factors for the Major Showers over the Sporadic Background derived from Fig. 184

(The units are arbitrary)

		Arietids+ ζ-Perseids	*β-Taurids*	*Quadrantids*	*Perseids*	*Geminids*	*Other showers*
Area of sporadic peak (day and night) . .	4,491	..	..	..	..	..	..
Area of sporadic (average) .	2,245	..	..	..	..	..	..
Average sporadic per day .	3·1	..	..	..	..	..	..
Number of days of activity .	..	16	11	2	9	6	23
Area above sporadic background . .	..	194	25	63	57	142	140
Average per day	..	12·1	2·2	31	6·3	23	6·1
Ratio $\frac{\text{shower}}{\text{sporadic}}$.	..	3·9	0·7	10	2	7·2	2

The more detailed information in Table 24 (Chap. VII) can, of course, be converted in the same manner. The information in the column headed 'Sporadic meteors' in Table 162 is taken directly from Table 24 (Chap. VII). The reservations made in that chapter regarding the sporadic mass estimates still apply to the estimates made here for the shower meteors. There is, of course, the additional doubt as to the range of magnitudes for which the inverse square law of mass distribution applies in the case of the showers. The evidence presented earlier in this chapter makes it extremely unlikely that the fainter magnitude groups still

TABLE 162

Meteoric Mass entering the Earth's Atmosphere in Various Magnitude Groups due to the Major Showers

Meteor magnitudes	*Sporadic meteors mass*			*Arietids and ζ-Perseids mass*			*β-Taurids mass*			*Quadrantids mass*			*Perseids mass*			*Geminids mass*			*Other showers mass*			*Mass total all showers*
	hour	*day*	*year*	*hour*	*day*	*total*	*hour*	*day*	*total*	*hour*	*day*	*total*	*hour*	*day*	*total*	*hour*	*day*	*total*	*hour*	*day*	*total*	
	kg.	*kg.*	*kg.* $\times 10^3$	*kg.*	*kg.*	*kg.* $\times 10^3$	*kg.*	*kg.*	*kg.* $\times 10^3$	*kg.*	*kg.*	*kg.* $\times 10^3$	*kg.*	*kg.*	*kg.* $\times 10^3$	*kg.*	*kg.*	*kg.* $\times 10^3$	*kg.*	*kg.*	*kg.* $\times 10^3$	*kg.* $\times 10^3$
> -10	22·9	550	200	89·3	1072	17	16·0	192	2·1	229	2748	5·59	43·8	525	4·7	164·9	1978	11·9	43·8	525	12·1	53·7
−4 to −9	5	120	43·8	19·5	234	3·7	3·5	42	0·4	50	600	1·20	10	120	1·1	36·0	432	2·6	10	120	2·7	11·7
−3 to +9	10·8	260	94·9	42·1	505	8·1	7·56	90·7	1·0	108	1296	2·59	21·6	259	2·3	77·8	933	5·6	21·6	259	5·9	25·5
+10 to +30	16·7	400	146	65·1	781	12·5	11·7	140·4	1·5	167	2004	4·00	33·4	400	3·6	120·2	1442	8·6	33·4	400	9·2	39·4
Total	55·4	1330	485	216·1	2592	41·5	38·7	464·4	5·1	554	6648	13·29	110·8	1329	11·9	398·9	4786	28·7	110·8	1329	29·9	130·4

exist in showers such as the Perseids. Even so, within the fairly wide range of uncertainty of these estimates, Table 162 yields information of considerable interest. It will be seen that during the course of a year the recurrent showers bring a meteoric mass into the earth's atmosphere which is only about one-third to one-quarter of that brought in by sporadic meteors. Amongst the showers, the great Arietid and ζ-Perseid day-time showers in June contribute nearly a third of the total shower mass.

The occasional spectacular occurrences of some of the periodic showers such as the Giacobinids are not included in Table 162; but the mass brought into the atmosphere on these occasions must be very great. If we consider the most recent occurrence—that of the Giacobinid shower in October 1946—the appropriate scaling factor in Table 161 would be about 700, and even although the shower only lasted for a few hours the total mass would be of the order of 70×10^3 kg., a figure comparable with the total mass of all recurrent showers for a whole year.

4. The total mass and density of meteoric particles in the orbits of the major showers

From the mass estimates of the previous section it is possible to speculate on the total mass and density of the meteoric material in the orbits of the major showers, on the assumption that the density is uniform around the orbit. This latter assumption is fully justified for the recurrent showers listed in Table 162. From the data about the various shower orbits given in the previous chapters it is possible to calculate the linear length of the various orbits. Also from i and ω and the number of days for which the shower is active, the cross-section of the stream can be found. Hence the total volume containing the meteoric particles in the entire orbit can be calculated. The number of meteors swept up by the earth in time t are those contained in a cylinder of volume

$$\pi r_e^2 \, \mathrm{tv},$$

where r_e is the radius of the earth's atmosphere (6,400 km.) and v the relative velocity of the earth and the meteors. Hence by putting t = 1 hour or 1 day and using the appropriate mass swept up for the individual showers in Table 162, the density in the orbit can be calculated. For v, the geocentric velocity of the particular shower meteors has been used. The data calculated for the showers discussed earlier in this chapter are given in Table 163.

As expected, the densities in the orbit are somewhat higher than for the sporadic meteors, being of the order of 10^{-23} to 10^{-24} gm./c.c. compared

with 10^{-24} to 10^{-25} gm./c.c. for the sporadic distribution. The total mass in each orbit is about 10^{12} kg. (10^9 tons).

TABLE 163

The Density and Total Mass in the Orbits of the Major Showers

	Arietids	*ζ-Perseids*	*β-Taurids*	*Quadrantids*	*Perseids*	*Geminids*
(1) Circumference of orbit (km.)	$9{\cdot}4\times10^8$	$12{\cdot}6\times10^8$	$15{\cdot}9\times10^8$	$17{\cdot}2\times10^8$	$67{\cdot}3\times10^8$	$9{\cdot}7\times10^8$
(2) Width of active region (km.)	$3{\cdot}9\times10^7$	$3{\cdot}5\times10^7$	$1{\cdot}5\times10^7$	$0{\cdot}5\times10^7$	$2{\cdot}1\times10^7$	$1{\cdot}5\times10^7$
(3) Total volume around orbit (km.)^3	$11{\cdot}8\times10^{23}$	$12{\cdot}4\times10^{23}$	$2{\cdot}9\times10^{23}$	$0{\cdot}3\times10^{23}$	$23{\cdot}7\times10^{23}$	$1{\cdot}7\times10^{23}$
(4) Volume containing meteors swept up in one day (km.)^3	$4{\cdot}3\times10^{14}$	$3{\cdot}2\times10^{14}$	$3{\cdot}4\times10^{14}$	$4{\cdot}4\times10^{14}$	$6{\cdot}6\times10^{14}$	$4{\cdot}0\times10^{14}$
(5) Density in orbit (kg./km.^{3})	$6{\cdot}0\times10^{-12}$		$1{\cdot}4\times10^{-12}$	$15{\cdot}1\times10^{-12}$	$2{\cdot}4\times10^{-12}$	$12{\cdot}0\times10^{-12}$
(6) Total mass (kg.)	$7{\cdot}2\times10^{12}$		$0{\cdot}4\times10^{12}$	$0{\cdot}5\times10^{12}$	$5{\cdot}7\times10^{12}$	$2{\cdot}0\times10^{12}$

Notes. (1) Calculated from major and minor axes of orbits.
(2) Calculated from number of days of duration of shower and i and ω of the orbit.
(3) From (1) and (2).
(4) From $\pi r_e^2 tv$ with r_e = radius of atmosphere (6,400 km.), t = one day and v = geocentric velocity of shower meteors.
(5) From (4) and mass per day in Table 162.
(6) From (4) and (5).

For comparison with these figures it is possible to speculate on the mass of meteor debris associated with a new periodic shower such as the Giacobinids. In the previous section it was estimated that during the few hours of activity of the shower about 7×10^4 kg. of debris entered the atmosphere. From line 4 of Table 163 it can be estimated that this debris must be contained within a volume of about 2×10^{13} km.^{3} Thus the density of matter in the active region is about 3×10^{-9} kg./km.^{3}, or a thousand times higher than the density calculated for the recurrent showers. The meteors are very localized in the orbit and from Chapter XVI it can be estimated that they are unlikely to extend for more than about 100 days around the orbit or, say, 10^8 km. Since the earth sweeps through the active part of the stream in about 2 hours the cross-section is around 10^{10} km.^{2} Thus the total volume containing the debris is only about 10^{18}/km.^{3}, and the total meteor mass about 10^9 or 10^{10} kg. Even allowing for large factors of uncertainty this mass is 100 to 1,000 times less than the total mass in the recurrent streams of Table 163. Of course, in this estimate the mass of material in the comet itself which is still an entity in the case of the Giacobinid shower has not been included. The significance of these mass and density estimates will be discussed in Chapter XXI.

It is also interesting to notice that the individual particles are widely scattered in space even in the most concentrated showers. Reference to Table 24 of Chapter VII shows that in the sporadic background a body of mass 1 mgm. occurs on the average in 10^{23} c.c. ($\sim 10^{7}$ cu. miles) of space, and one of mass 1 gm. in about 10^{26} c.c. ($\sim 10^{10}$ cu. miles) of space. Even in a most concentrated display like the Giacobinid shower the corresponding estimates only rise to 10^{19} c.c. ($\sim 10^{3}$ cu. miles) for a body a mass 1 mgm. and 10^{22} c.c. ($\sim 10^{6}$ cu. miles) for a body of mass 1 gm.

XX

THE DISPERSIVE EFFECTS IN METEOR STREAMS

THE discussions in previous chapters of this book have indicated that most of the meteoric matter in the solar system is widely dispersed. Perhaps one-quarter or one-fifth of the total is, however, associated with the major showers—debris moving in specific orbits, or closely related orbits, in many cases dispersed uniformly around the orbit. There are various effects capable of dispersing meteoric debris. As regards the shower meteors it seems natural to assume that the debris originally existed in one conglomerate—such as a comet—and that these dispersive forces have scattered the debris in the course of time around and about the orbit. On this view the periodic streams, such as the Giacobinids, where the debris is still localized, are comparatively young and are still in the initial processes of dispersion, whereas the recurrent streams such as the Perseids where the debris is uniformly scattered around the orbit, are of great age. There is a good deal of circumstantial evidence in support of this general view, and the main idea of dispersion is not now seriously questioned.

A further extrapolation of this idea leads to the view that the sporadic meteor content of the solar system is the result of the ultimate dispersive effects on matter which was originally closely conglomerated. On this question, however, there is not yet good evidence or agreement, since this sporadic matter might equally well be primeval. A solution of this particular problem would evidently be of great importance as regards the origin of the solar system, and the more detailed investigation of the individual orbits of sporadic meteors which may be expected during the next few years may provide the basic data for the investigation.

The present chapter is mainly concerned with the forces which disperse the debris in the orbits of the major showers, and with the possibilities of estimating the age of the showers from the extent of the dispersion.

1. The effect of planetary perturbations

It is easy to show that the main disturbances are caused by Jupiter and Saturn. If the attractive force of Jupiter on a body at unit distance is represented by 1,000, then the appropriate values for other members of the solar system at unit distance are Sun ($\sim 10^6$), Saturn (300),

Neptune (54), Uranus (46), Earth (3·2), Venus (2·6), Mars (0·34), Mercury (0·15). Thus, except in the case of a very close approach to the smaller planets, the main perturbations are always due to Jupiter or Saturn. The main effect is to accelerate the motion of the body along the line, body-planet. The composition of this acceleration with that along the line, body-sun, may give rise to various changes in the orbit. The exact calculation of the perturbations, which is described in the standard texts, is a complex procedure. The following simplified treatment which illustrates the particular problem under discussion here is due to Porter.†

The standard equations of motion including the effect of an attracting body of mass $m_1(x_1, y_1, z_1)$ at distance ρ from the body are of the form

$$\frac{d^2x}{dt^2} = -k^2 \sum m_1 \frac{x_1 - x}{\rho^3}, \tag{1}$$

where k^2 is written as the gravitational constant (see Chap. V). This is with reference to the centre of mass of the whole system. Alternatively in heliocentric coordinates with r and r_1 the radii vectores of the body and planet

$$\frac{d^2x}{dt^2} + k^2(1+m)\frac{x}{r^3} = k^2 m_1\left(\frac{x_1 - x}{\rho^3} - \frac{x_1}{r_1^3}\right). \tag{2}$$

Equation (2) with the corresponding ones in y and z can be used to compute the perturbations of the body as described in the standard texts. Alternatively (2) can be written in the form

$$\frac{d^2x}{dt^2} + k^2(1+m)\frac{x}{r^3} = m_1 \frac{dR}{dx}, \tag{3}$$

where $m_1 R$ is the perturbative function. Except where great accuracy is required it is convenient to determine the variations in the elements as distinct from the coordinates. In this case a simplification results by taking a new set of axes in the plane of the orbit and moving with the body. The X axis is along the line body-sun; the Y axis in the plane of the orbit, 90° in front of the body, and the Z axis perpendicular to the orbit plane. The coordinates of the body are then r, 0, 0. From equation (2), $\bar{S}$, $\bar{T}$, and $\bar{W}$ are computed, and are regarded as the attractive forces along the axes defined above. Then from the equations in Chapter V the following relations for variations of the elements are obtained, where t is the interval in days. In these equations φ is the angle of eccentricity

† Porter, J. G., *Comets and Meteor Streams*, Chapman & Hall, 1952.

($e = \sin\varphi$), and E the eccentric anomaly, otherwise the notation is the same as in Chapter V.

$$
\left.
\begin{aligned}
t\frac{d\Omega}{dt} &= r\sin(\omega+\nu)\operatorname{cosec} i\,\bar{W} \\
t\frac{di}{dt} &= r\cos(\omega+\nu)\bar{W} \\
t\frac{d\varphi}{dt} &= a\cos\varphi\sin\nu\,\bar{S}+a\cos\varphi(\cos E+\cos\nu)\bar{T} \\
t\frac{d\pi}{dt} &= -\frac{p}{e}\cos\nu\,\bar{S}+\frac{p+r}{e}\sin\nu\,\bar{T}+2\sin^2\tfrac{1}{2}i\frac{d\Omega}{dt} \\
t^2\frac{dn}{dt} &= -\frac{3k\omega}{\sqrt{a}}\left(e\sin\nu\,\bar{S}+\frac{p}{r}\bar{T}\right) \\
t\frac{dM}{dt} &= (p\cos\nu\cot\varphi-2r\cos\varphi)\bar{S}-\cot\varphi\sin\nu\,(p+r)\bar{T}
\end{aligned}
\right\}. \qquad (4)
$$

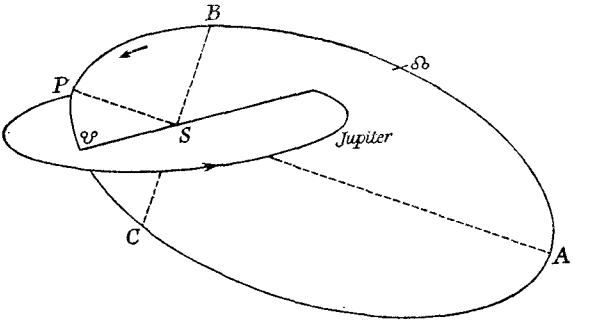

FIG. 185. Effect of perturbations.

The qualitative effects of the perturbations may readily be seen from equations (4). The orthogonal component $\bar{W}$, always due, in practice, to the major planets, will be negative as the body moves forward from the ascending node (as $\omega+\nu$ increases from 0 to 180°), and will be positive in the remaining part of the orbit. Thus the change in node given by $d\Omega/dt$ in (4) will always be negative. Hence the effect of a planetary perturbation on a body is always to cause the node of the orbit to retrogress if the motion is direct, and to advance if the motion is retrograde. This is a common effect and its importance for the case of meteor streams is evident from previous chapters of the book. The main effects of the perturbations given by equations (4) may be summarized by reference to Fig. 185.

(*a*) Node: affected by $\bar{W}$ only, which changes sign at ☊. Thus the node retrogresses for direct motion.

(*b*) Inclination: affected only by $\bar{W}$. Maximum positive value at ☊ and maximum negative value at ☋.

(*c*) Major axis: attraction $+\bar{T}$ always increases major axis. $+\bar{S}$ has no effect at perihelion and aphelion, but increases the major axis in the region PCA and decreases it in the second half ABP.

(*d*) Line of apsides: $+\bar{S}$ causes PA to move forward when the body is in the region CAB and backwards in the region BPC. $+\bar{T}$ causes forward movement of PA when the body is in the region PCA, and backward in the region ABP.

(*e*) Eccentricity: $+\bar{S}$ increases e during path PCA and decreases e during path ABP. $+\bar{T}$ has maximum positive effect at P and maximum negative effect at A. The effect is zero at the two points where r = b.

Equations (4) give the rate of change of the elements with time and the total effect has to be obtained by integration. There are various methods of performing these calculations which are described in the standard texts. The final effect depends not only on the closeness of approach to the planet but also on the duration of the attraction, and is therefore greatly dependent on the nature of the orbit. In particular, particles moving in orbits of high inclinations can only suffer severe perturbations when a close approach to a planet occurs at the node. Undoubtedly this fact accounts for the stability of such meteor streams as the Perseids and Lyrids which are of great antiquity. On the contrary the striking effect of perturbations by Jupiter on an orbit of short period and low inclination is well evidenced by the case of the Pons–Winnecke meteor stream. The changes in the elements of this orbit between 1858 and 1945 have been listed in Table 147 of Chapter XVII. During this time the perihelion point moved from inside, to outside the earth's orbit, and the orbit itself has become larger and more circular, with greater inclination. The distance of nearest approach to the earth's orbit has now increased so much that a further occurrence of the Pons–Winnecke meteor shower appears very unlikely.

Even when the conditions are not such as to give rise to these extreme effects, the changing position of the node caused by the orthogonal component $\bar{W}$ must always be present—a point which formed the basis of the identification of the Leonid orbit with comet 1866 I as described in Chapter XVI. Further, the collective perturbations which arise from

many revolutions of the particles around the sun will eventually cause a conglomerate to disperse around the orbit—each individual particle following its own orbit within the main stream and suffering perturbations different from its neighbour. Hence, although the perturbative effects may not be violent enough to swing the entire orbit away from the earth as in the case of Pons–Winnecke, even in the most favourably placed orbits such as the Perseids there will be a constantly changing position of the node and an eventual dispersion of the particles around and about the orbit.

2. The ejection of meteoric material from comets

Although there is general acceptance of the fact that many of the major meteor showers are moving in cometary orbits, the idea that they arise from the partial or complete disintegration of the comet is by no means universally accepted. Nevertheless, there are now powerful reasons for the belief, and in this case the mode of ejection of the meteoric material would be a prominent factor in the dispersal of the material. The idea that meteor streams are formed by the ejection of material from comets appears first in 1877 in the work of Bredikhine. The most recent developments of the idea due to Whipple† will be referred to in Chapter XXI. Whipple shows on the basis of the cometary model that the meteoric particles will be ejected from the comet at an appreciable rate when it is within about 2 a.u. of the sun, and that the velocity of ejection Δu will be given by

$$\Delta u = \left(\frac{r_c}{Lr}\right)^{\frac{1}{2}} \frac{3{\cdot}28}{q^{3/8}} \text{ m./sec.}, \tag{5}$$

where r_c is the radius of the comet in km., $1/L$ is the heat absorption coefficient, r is the radius of the meteoric particle in cm., and q the perihelion distance of the comet in a.u. Evidently the variation in ejection velocity with r and q will be a prominent effect in the dispersion of the meteoric particles. The particular case of the Perseid stream has been studied by Hamid.‡ For $r_c = 5$ km., $r = 0{\cdot}1$ cm., $L = 2$, $q = 1$ a.u. the velocity of ejection given by (5) is 16·5 m./sec. The ejection will be in all directions with a preference in the direction of the sun. The change in the angular orbital elements due to the ejection velocity $< 0°{\cdot}1$, but the change in the period is shown to be appreciable. Hence after only a few dozen revolutions in the orbit the ejected meteoric material will be distributed along the entire orbit.

† Whipple, F. L., *Astrophys. J.* **111** (1950), 375; **113** (1951), 464.
‡ Hamid, S., Harvard (doctoral dissertation), 1950.

This mechanism of ejection can therefore give rise to a distribution of the meteors around the orbit, but since the effect on the angular elements is small, the cross-section of the stream will not be greatly increased. The widening of the stream will occur through the effects of the succeeding planetary perturbations discussed in § 1. Hamid shows that the observed dispersion of the photographic radiants of the Perseid meteors can be adequately explained on this basis if the shower has endured for about 200 revolutions of the parent comet.

3. The Poynting–Robertson effect

In 1903 Poynting† considered the effects on the motion of a small body in the solar system when it absorbed and subsequently re-emitted solar radiation. He concluded that there would be a tangential drag, which would decrease the angular momentum of the body and eventually cause it to fall into the sun. It is now generally recognized that this effect exists and that it is of great importance in meteor astronomy, but the correct explanation of the drag was not given until 1937. Poynting attributed the drag to a back pressure of radiation tending to retard the motion of the emitting body; he conceived this as due to a crowding-up of radiation in front of the particle and to a corresponding thinning-out behind. His value for the magnitude of this force was $\frac{1}{3}\Theta\bar{V}/\mathbf{c}^2$, where Θ is the rate at which the particle is radiating energy, $\bar{V}$ its velocity through space, and $\mathbf{c}$ the velocity of light. The gravitational force varies as the cube of the linear dimensions of the body whereas Θ depends on the square of the linear dimensions. Thus the drag should become increasingly marked as the size of the body decreases. Poynting estimated that a body of radius 1 cm. and density 5·5 at the earth's distance from the sun and with the earth's velocity could make 10^8 revolutions before falling into the sun, whereas a body of radius 10^{-3} cm. would only make 10^5 revolutions.

The next contribution to the subject was made by Larmor‡ in 1913, who gave an alternative treatment on classical electromagnetic theory of the retarding force on a body moving with velocity $\bar{V}$ arising from its own radiation. Larmor's value for the force was $\Theta\bar{V}/\mathbf{c}^2$—three times that obtained by Poynting. It was pointed out,§ however, that the braking effect of such a force was in contradiction with relativity theory,

† Poynting, J. H., *Phil. Trans. Roy. Soc.* A **202** (1903), 525; *Collected Scientific Papers*, Art. **20** (Cambridge, 1920), 304.

‡ Larmor, J., *Proc. 5th Internat. Congress Mathematics*, **1** (Cambridge, 1913), 197.

§ *Observatory*, **40** (1917), 278.

and in a detailed investigation Page† showed that a moving body does not suffer retardation as a consequence of its own radiation alone. Subsequently Larmor‡ admitted the correctness of this result and agreed that an isolated body cooling in space would not be retarded, since the back thrust of the radiation would be compensated by the increase of velocity resulting from the conservation of momentum as the mass decreased. But he then pointed out the true cause of the Poynting drag and resolved the paradox '. . . for Poynting's particle describing a planetary orbit the radiation from the sun comes in, which restores the energy lost by radiation from the particle, and so establishes again the retarding force $-\Theta\bar{V}/c^2$ . . .'.

The original misconception about the existence of this force arose because of the use of a stationary frame referred to the particle, in which case the process of absorption and re-emission does not introduce any net force. On the other hand when the particle is considered in the solar reference frame there is a force proportional to the velocity of the particle.§ The force is clearly of very great interest in meteor astronomy since it leads to a separation of the meteoric particles according to their size, an effect which, as will be shown, is very marked in periods of time which are astronomically small.

The full relativistic treatment of the effect was given by Robertson‖ in 1937, and his results are now generally accepted. The simplified Newtonian approximations, involving only first order terms in $\bar{V}/c$, are sufficiently exact for use in the general meteor problems considered here. In this case the equations of motion for the particle are expressed in terms of the two vectors

$$\bar{\boldsymbol{V}} = \frac{\mathrm{d}\boldsymbol{x}}{\mathrm{d}t}, \qquad \boldsymbol{n} = \frac{\boldsymbol{l}}{c}, \tag{6}$$

where $\boldsymbol{n}$ is the unit vector in the direction of the incident beam. Robertson's equations of motion for the particle then become

$$m\frac{\mathrm{d}\bar{\boldsymbol{V}}}{\mathrm{d}t} = \mathrm{f}\left(1-\frac{\bar{\boldsymbol{V}}_{\mathrm{n}}}{c}\right)\boldsymbol{n} - \mathrm{f}\frac{\bar{\boldsymbol{V}}}{c}, \tag{7}$$

† Page, L., *Phys. Rev.* **11** (1918), 376; **12** (1918), 371.

‡ Larmor, J., *Poynting's Collected Scientific Papers* (Cambridge, 1920), p. 757.

§ In terms of quantum theory, the quanta emitted by the sun carry a purely radial momentum and hence, when absorbed by a particle moving in the solar system, will produce a tangential dragging force in addition to normal radiation pressure. Since the re-radiated quanta are isotropic with respect to the particle there is no recoil effect due to its own radiation.

‖ Robertson, H. P., *Mon. Not. Roy. Astr. Soc.* **97** (1937), 423.

where $\overline{V}_n$ is the component of the velocity $\overline{V}$ in the direction $\boldsymbol{n}$. The first term is due directly to the radiation pressure in the direction of the beam, weakened by the Doppler factor $(1-(\overline{V}_n/\mathbf{c}))$. The tangential drag is given by the second term.†

For a particle moving in the solar system $\boldsymbol{n}$ is the unit vector along the radius vector from the sun, and the energy density, d, will fall off inversely as the square of the distance from the sun. If b is the earth–sun distance, and Ξ the solar constant ($\Xi = 1{\cdot}35\times10^6$ ergs/sec./cm.^{2}) then at distance r from the sun

$$\left.\begin{aligned} d &= \frac{\Xi b^2}{\mathbf{c}\mathrm{r}^2}, \qquad \mathrm{f} = \frac{\boldsymbol{m}\kappa\mathbf{c}}{\mathrm{r}^2} \\ \text{where} \qquad \kappa &= \frac{\mathrm{A}\Xi b^2}{\boldsymbol{m}\mathbf{c}^2} = \frac{3\Xi b^2}{4\boldsymbol{r}\rho\mathbf{c}^2} = \frac{2{\cdot}51\times10^{11}}{\rho\boldsymbol{r}} \end{aligned}\right\}. \tag{8}$$

In the second expression for κ the cross-section A and mass $\boldsymbol{m}$ of the particle are given in terms of a sphere of density ρ and radius $\boldsymbol{r}$, large compared with the wave-length of the incident radiation.

Adding to equation (7) the gravitational force $\gamma(\boldsymbol{M}\boldsymbol{m}/\mathrm{r}^2)$ in the direction $-\boldsymbol{n}$, the equations of motion in polar coordinates (r, θ) in the plane of the orbit with the sun as pole are given by

$$\frac{\mathrm{d}^2\mathrm{r}}{\mathrm{dt}^2} - \mathrm{r}\left(\frac{\mathrm{d}\theta}{\mathrm{dt}}\right)^2 = -\frac{\bar{\mu}}{\mathrm{r}^2} - \frac{2\kappa}{\mathrm{r}^2}\frac{\mathrm{dr}}{\mathrm{dt}}, \tag{9}$$

$$\frac{1}{\mathrm{r}}\frac{\mathrm{d}}{\mathrm{dt}}\left(\mathrm{r}^2\frac{\mathrm{d}\theta}{\mathrm{dt}}\right) = -\frac{\kappa}{\mathrm{r}}\frac{\mathrm{d}\theta}{\mathrm{dt}}, \tag{10}$$

where $\bar{\mu} = \mu_0 - \kappa\mathbf{c}$ is the solar gravitational constant, $\mu_0\,(=\gamma\boldsymbol{M})$, reduced by $\kappa\mathbf{c}$ as representing the repulsive effect of the direct radiation pressure. Equation (10) integrates to give

$$\mathbf{H} = \mathrm{r}^2\frac{\mathrm{d}\theta}{\mathrm{dt}} = \mathbf{h} - \kappa\theta, \tag{11}$$

where $\mathbf{H}$ is the instantaneous value of the angular momentum and $\mathbf{h}$ the initial value.

From these equations Robertson calculated the secular perturbations

† The interpretation of the effect in terms of classical notions is clear from equation (7). The particle absorbs energy at the rate $\mathbf{c}\mathrm{f} = \mathbf{c}.\mathrm{A}d$. This is re-radiated isotropically about the particle which is moving with velocity $\overline{V}$ and therefore carries away electromagnetic momentum at the rate $(\mathbf{c}\mathrm{f}/\mathbf{c}^2)\overline{V}$. Since mechanical and electromagnetic momentum is conserved this process must cause the particle to lose momentum at the rate $\mathrm{f}\overline{V}/\mathbf{c}$ which therefore appears as the retarding force given by the last term in equation (7).

for an osculating ellipse of semi-major axis a and eccentricity e as follows:

$$\frac{da}{dt} = -\frac{\kappa(2+3e^2)}{a(1-e^2)^{\frac{1}{2}}}, \tag{12}$$

$$\frac{de}{dt} = -\frac{5\kappa e}{2a^2(1-e^2)^{\frac{1}{2}}}. \tag{13}$$

For the advance of perihelion Roberston obtained

$$\frac{d\pi}{dt} = \frac{3\gamma^{\frac{1}{2}}M^{\frac{1}{2}}\bar{\mu}}{c^2a^{\frac{5}{2}}(1-e^2)}. \tag{14}$$

The most striking consequence of this retardation is that any particle moving in the solar system will eventually be swept into the sun;† in fact it follows from (11) that a particle cannot survive for $h/2\pi\kappa$ revolutions about the sun. (The case mentioned earlier, considered by Poynting, of a particle of radius 1 cm., $\rho = 5{\cdot}5$ in a circular orbit at the earth's distance would survive $1{\cdot}55 \times 10^8$ revolutions—in close agreement with Poynting's value of 10^8 revolutions.)

The time scale, and other consequences of this retardation for particles of meteoric size have been considered in detail by Wyatt and Whipple.‡ As far as π is concerned, $d\pi/dt$ in (14) is only significant for large and dense bodies where $\bar{\mu} \simeq \gamma M$; and the change is insignificant for meteoric particles (in the case of Mercury, for example, the change amounts to only 43″ per century). For small particles the changes in e and a are of most interest. For an initially circular orbit (12) integrates to give the total time of fall into the sun as

$$t = \frac{a^2}{4\kappa} = 7{\cdot}0 \times 10^6 r\rho a^2 \text{ years}, \tag{15}$$

where the radius r is in cm., density ρ in gm./c.c., and the initial distance a in astronomical units. For an eccentric orbit (12) and (13) give the relation between a and e, which on integration gives

$$a = \frac{Ce^{4/5}}{1-e^2}. \tag{16}$$

The constant C in (16) can be computed, given a_0 and e_0 at any arbitrary time

$$C = a_0 e_0^{-4/5}(1-e_0^2). \tag{17}$$

From (16) and (13) a relation may be obtained involving only e and t

$$\frac{de}{dt} = -\frac{5\kappa(1-e^2)^{3/2}}{2C^2e^{3/5}}. \tag{18}$$

† Unless, of course, the radiation pressure balances the gravitational attraction—this critical limit being given by $r\rho > 5{\cdot}72 \times 10^{-5}$ gm./cm.²

‡ Wyatt, S. P., and Whipple, F. L., *Astrophys. J.* **111** (1950), 134.

Hence (for $e_0 > e$)

$$(t-t_0) \text{ years} = -\frac{2C^2}{5\kappa}\int_{e_0}^{e}\frac{e^{3/5}\,de}{(1-e^2)^{3/2}} = 1{\cdot}13\times10^7 r\rho C^2\int_{e}^{e_0}\frac{e^{3/5}\,de}{(1-e^2)^{3/2}}, \tag{19}$$

where r and ρ are in c.g.s. units. C^2 with dimensions $(\text{a.u.})^2$ is obtained from (17) by using the constants of the orbit. The integral cannot be found directly, but the integrand is independent of the particle, and numerical integrations suffice for all cases. Wyatt and Whipple calculated values of the function

$$G(e_0) = \int_{e}^{e_0}\frac{e^{3/5}\,de}{(1-e^2)^{3/2}} \tag{20}$$

for various values of e as given in Table 164. Substitution of r, ρ, and C^2 then gives the total time for the particle to spiral into the sun.

TABLE 164

Data for Calculation of Time of Fall of a Particle into the Sun as a Result of the Poynting–Robertson Effect

e	$G(e_0)$	$\frac{(t-t_0)}{10^7 r\rho q^2}$ *years*	e	$G(e_0)$	$\frac{(t-t_0)}{10^7 r\rho q^2}$ *years*
0·00	..	0·704	0·78	0·771	4·10
0·05	0·0052	0·778	0·80	0·846	4·42
0·10	0·0158	0·858	0·81	0·889	4·60
0·15	0·0305	0·946	0·82	0·934	4·79
0·20	0·0489	1·04	0·83	0·983	5·00
0·25	0·0710	1·15	0·84	1·04	5·23
0·30	0·0969	1·27	0·85	1·10	5·49
0·35	0·127	1·40	0·86	1·16	5·77
0·40	0·162	1·55	0·87	1·23	6·08
0·45	0·202	1·72	0·88	1·32	6·43
0·50	0·249	1·92	0·89	1·41	6·83
0·55	0·305	2·15	0·90	1·51	7·29
0·60	0·370	2·42	0·91	1·63	7·82
0·62	0·400	2·54	0·92	1·78	8·45
0·64	0·432	2·68	0·93	1·96	9·22
0·66	0·468	2·82	0·94	2·17	10·17
0·68	0·506	2·98	0·95	2·45	11·39
0·70	0·548	3·16	0·96	2·82	13·06
0·72	0·595	3·36	0·97	3·37	15·50
0·74	0·647	3·57	0·98	4·30	19·60
0·76	0·705	3·82	0·99	6·37	28·89

Wyatt and Whipple simplified the calculations further for the total time of fall by writing (16) as

$$C^2 = q^2(1+e)^2e^{-8/5} \tag{21}$$

[where $q = a(1-e)$].

Then (19) becomes

$$(t-t_0) \text{ years} = 10^7 r\rho q^2 \left[\frac{1{\cdot}13(1+e_0)^2}{e_0^{8/5}} \int_e^{e_0} \frac{e^{3/5}\, de}{(1-e^2)^{3/2}} \right]. \qquad (22)$$

The quantity $\left[\frac{1{\cdot}13(1+e_0)^2}{e_0^{8/5}} \int_e^{e_0} \frac{e^{3/5}\, de}{(1-e^2)^{3/2}} \right]$ is also tabulated in Table 164, and from this the total time of fall into the sun of a particle of radius r and density ρ can be readily obtained by substitution of the perihelion

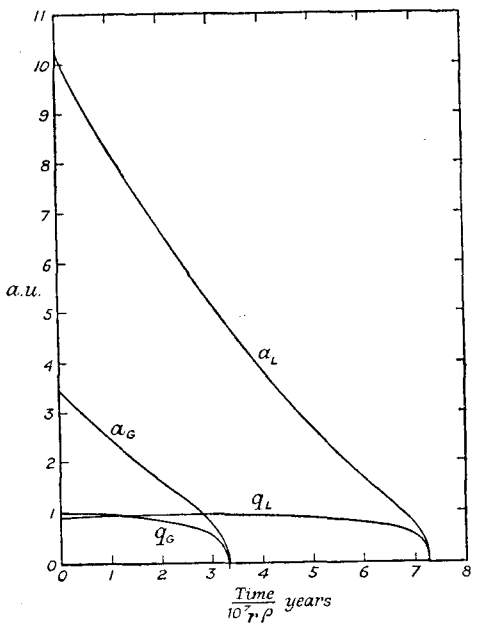

FIG. 186. The changes in semi-major axis a, and perihelion distance q as a function of time due to the Poynting–Robertson effect. Subscript L refers to the Leonid orbit and G to the Giacobinid orbit.

distance q in a.u. For the calculation of the time required for the particle to change between two arbitrary eccentricities, it is, of course, necessary to compute by using $G(e_0)$.

The change of the semi-major axis a and the perihelion distance q with time for particles in the present Giacobinid and Leonid orbits have been calculated by Wyatt and Whipple and are shown in Fig. 186. The decrease in a is fairly linear; that in q very slow until the final

stages. The calculations for the total time of fall into the sun of the particles in some of the major showers are given in Table 165. Whipple's photographic elements (Chap. XV) have been taken for the orbit of the Geminid meteors, and Yamamoto's† elements for the orbits of the presumed parent comets for the remaining showers. These associations agree with the conclusions of Chapters XIII to XVII with the exception of the doubtful Orionid–Halley Comet relationship. The total time of fall computed from the data of Table 164 is given in column 6. For comparison, column 7 gives the corresponding times for a circular orbit calculated from (15).

TABLE 165

Times of Fall into the Sun of Meteoric Particles in the Major Shower Orbits

Shower	*Parent comet*	a	e	C	$\frac{(t-t_0)}{10^7 r\rho}$ *years*	$\frac{(t-t_0)_{circ}}{10^7 r\rho}$ *years*
Geminids .	?	1·396	0·900	0·289	0·143	1·4
Taurids . .	Encke	2·210	0·8498	0·6995	0·605	3·4
Bielids . .	1852 III	3·5259	0·75592	1·8902	2·79	8·7
Giacobinids .	1933 III	3·520	0·7160	2·241	3·32	8·7
Orionids ? .	Halley ?	17·96	0·9673	1·186	5·10	230
Leonids . .	1866 I	10·325	0·90542	2·0145	7·24	75
Perseids .	1862 III	24·277	0·96035	1·9491	12·2	410
Lyrids . .	1861 I	55·665	0·98346	1·8508	18·6	2200

It is evident from these results that the lifetime of small meteoric bodies in the solar system is short, astronomically. For example, a particle of radius 0·05 cm. and density 4 gm./cm.^{3}, corresponding to about a fifth magnitude meteor moving in the orbit of Halley's Comet would be drawn into the sun in about 10,000,000 years.

A further factor of extreme interest in meteor astronomy is the possibility of observing the Poynting–Robertson effect in the major showers by virtue of the selective effect arising from differing particle size and density—the smaller ones being drawn towards the sun much faster than the larger ones. Wyatt and Whipple estimated the order of times required to separate meteors of magnitude +5 and −2 so that the earth would pass from one limit to the other in 5 days. In order to do this the showers in Table 165 with inclinations less than 40° were considered, and their inclinations assumed to be zero. The perihelion advance was neglected and the earth's orbit taken as circular. The density of the meteors in each shower was taken as 4 gm./cm.^{3} and the

† Yamamoto, A. S., *Pub. Kwasan Obs.* **1** (1936), no. 4.

radii calculated from the luminosity-mass relationships discussed in Chapters VII and XIX. The estimates are given in Table 166.

TABLE 166

Times of Separation of Meteors of Magnitude −2 and +5 due to Poynting–Robertson Effect

Shower	*Time (years)*
Geminids	7×10^4
Taurids	5×10^5
Giacobinids	1×10^6
Bielids	2×10^6
Leonids	3×10^6
Orionids ?	5×10^6

Wyatt and Whipple state that such a separation effect has not been observed. However, in the case of the Geminid shower the radio-echo data listed in Chapter XV show that there is, in fact, a very marked separation of particle sizes. The most active region of the shower is near the end and consists of a marked concentration of heavier particles compared with the earlier activity of the shower. In other words the dispersion is exactly of the type to be expected from the operation of the Poynting–Robertson effect over a period of some 10^4 years. It is well known that the Perseid shower contains mainly large particles, and in this case it seems likely that the smaller content has been sifted away from the original orbit by the Poynting–Robertson effect. The high inclination of the orbit provides a ready explanation why these smaller particles moving in an orbit of reduced major axis are no longer intercepted by the earth. As regards the other showers listed in Table 166, sufficient radio-echo data are available only for the Giacobinid shower. No separation is found, a result to be expected in view of the showers' recent origin. In the case of the day-time showers, which are intercepted on the sunlit side of the earth, it is clear that the Poynting–Robertson effect will act to produce the heavy particles at the beginning of the shower. An inspection of the radio-echo data has not revealed any separation in particle sizes with time, which may indicate that the day-time streams have an origin more recent than the time scale of Table 166. The perturbative effects discussed earlier in this chapter are non-selective as regards particle sizes; moreover, the showers of low inclination considered in Table 166 are those most susceptible to planetary perturbations. Hence the showers may have been dispersed in a non-selective manner within the time scale of Table 166; thus, in cases where the Poynting–Robertson effect is not observed, the times in Table 166 can only be regarded as an upper limit to the age of the shower.

4. The Yarkovsky effect

According to Öpik,† Yarkovsky published a pamphlet in St. Petersburg about 1900 dealing with the effect of radiation pressure on a rotating particle. The effect arises on account of the excess of radiation emitted by the 'evening' hemisphere over the 'morning' hemisphere. It appears that a very slight excess of the evening over the morning temperature might produce a drag of the same order as the Poynting–Robertson effect. If the rotation and orbital motion are in the same direction the Yarkovsky effect is opposite to the Poynting–Robertson effect; if the rotation is opposite to the orbital motion the two effects work in the same direction.

Öpik gives the ratio of the Yarkovsky effect (y) to the Poynting–Robertson effect (P_g) as

$$\frac{y}{P_g} = -\frac{c}{U}\frac{2}{3}\frac{\Delta T}{T}\cos\Theta, \tag{23}$$

where c is the velocity of light, U the orbital velocity, T the absolute temperature, ΔT the difference of surface radiative temperatures between the evening and morning points at equinox, and Θ the inclination of the equator of rotation to the plane of the orbit.

For a stony sphere in the solar system with period of axial rotation W (in seconds), moving in an orbit with semi-major axis a (a.u.) Öpik gives

$$\Delta T = \frac{1}{6a^2}\sqrt{W} \text{ deg. absolute} \tag{24}$$

taking into account appropriate values for the conductivity, specific heat, and solar constant. Equation (24) remains valid provided the daily temperature oscillations die out well outside the centre of the particle, that is provided

$$r > \tfrac{1}{5}\sqrt{W}, \tag{25}$$

where r is the radius of the particle.

Otherwise if

$$r < \tfrac{1}{5}\sqrt{W} \tag{26}$$

then (approximately)

$$\Delta T = \frac{5}{6}\frac{r}{a^2}. \tag{27}$$

Substitution in (23) gives

$$y/P_g = -3{\cdot}97\cos\Theta\frac{\sqrt{W}}{a} \tag{28}$$

† Öpik, E. J., *Proc. Roy. Irish Acad.* **54** (1951), 165. (Öpik states that his reference to this pamphlet is from memory only.)

and $$y/P_g = -19{\cdot}8 \cos \Theta \frac{r}{a^2} \tag{29}$$

corresponding respectively to (24) and (27).

For retrograde motion ($180° > \Theta > 90°$) y works in the same direction as P_g, leading to an accelerated rate of decrease of the major axis. For direct motion ($0° < \Theta < 90°$) the effects are opposite and da/dt is decreased or even inverted so that the particle spirals away from the sun. For given W or r the ratio depends on a—and for a certain value a_0 the ratio is -1, and the two effects will cancel.

In applying the idea to meteor particles Öpik draws attention to his estimates† that for an age of 3×10^9 years these particles will possess an average period of rotation as a result of collisions with smaller dust particles of

$$\overline{W} = \frac{r^{3/2}}{1800} \text{ sec.} \tag{30}$$

for $0{\cdot}01 < r < 5$ cm., and of

$$\overline{W} = \frac{r}{18000} \text{ sec.}$$

for $r < 0{\cdot}01$ cm.

Even if these periods are underestimated by a factor of 10 (which would be the case if the age or frequency of collisions were overestimated), it is clear that the cases represented by (24), (25), and (28) will be predominant. Thus from (28)

$$y/P_g = -0{\cdot}3 \cos \Theta \, r^{3/4}/a \quad \text{for } r > 0{\cdot}01$$

and $$y/P_g = -0{\cdot}09 \cos \Theta \, r^{1/2}/a \quad \text{for } r < 0{\cdot}01.$$

Putting $\cos \Theta = \frac{1}{3}$ the 'equilibrium' conditions ($y/P_g = -1$) will be attained in the following cases

r (cm.)	10^{-3}	10^{-2}	10^{-1}	1	3	10
a_0 (a.u.)	(0·002)	(0·006)	(0·04)	0·2	0·5	1·1

A solid particle is unlikely to exist at a distance closer than 0·01 a.u. to the sun, thus the equilibrium distances a_0 are only likely to have significance for large particles $r = 1$ to 10 cm. The Yarkovsky effect is thus probably negligible for meteoric particles, except for those of large size in the fireball class.

5. Conclusion

The summary of possible dispersive effects in this chapter leads to the impression that planetary perturbations, coupled with the possibility

† Öpik, E. J., *Pub. Tartu Obs.* **28** (1936), no. 6.

of differential ejection velocities from the original conglomerate, are the main influences dispersing meteoric debris around the orbit. The Poynting–Robertson effect introduces a selective drag which in the course of time will separate out the particles in a shower according to their size, eventually causing all to fall into the sun—the small ones faster than the large ones. The Yarkovsky effect would not seem to be an important dispersive influence except possibly for the larger meteoric bodies in which case it might either aid or hinder the Poynting–Robertson drift, depending on whether the motion in the orbit is retrograde or direct.

The possibility of other dispersive influences has been mentioned by Whipple.† Meteors must carry a positive charge, as a result of photo-electric effects due to the sun's radiation, and if the sun has a magnetic field a motion of the line apsides must result—greater for smaller meteors than for large ones. Simple electrostatic effects might also tend to disrupt an originally compact stream. No detailed calculations have yet been made on these topics but their magnitude hardly seems likely to be a greater selective influence than the Poynting–Robertson effect within the time scale of the major showers.

† Whipple, F. L., *Proc. Amer. Phil. Soc.* **83** (1940), 711; **91** (1947), 189.

XXI

COSMOLOGICAL RELATIONSHIPS OF METEORS

1. The association of the major showers with comets

THE extent of the relation of major showers with comets has been discussed in earlier chapters of the book. Mainly as a result of the work of Schiaparelli, it was realized in 1866 that the orbit of the Perseid shower was closely related to that of Comet 1862 III, and the orbit of the Leonid shower with that of Comet 1866 I. Subsequently, other close associations were recognized, and Table 167 summarizes the possible cometary-meteor stream associations known at the present time.

TABLE 167

Cometary-Meteor Stream Associations

Meteor shower	*Comet*	*Date*	*Radiant*	*Closest approach of cometary orbit (Comet–Earth)*	*Remarks*
			α δ	a.u.	
Quadrantids	(?)Kozik-Peltier 1939a	Jan. 3	230 +50	..	Doubtful
Lyrids	1861 I	April 21	271 +34	−0·002	..
η-Aquarids	(?)Halley	May 6	336 −1	−0·064	Doubtful
Orionids		Oct. 20	95 +15		
β-Taurids (day-time)	Encke	June 30	90 +20	..	Common orbits originally. Now separated due to perturbations (see text)
Taurids		Nov. 10	55 +20	..	
ζ-Perseids (day-time)		June 10	60 +22	..	
S-Arietids		Oct. 20	41 +10	..	
Pons–Winnecke	Pons–Winnecke	June 30	208 +54	−0·042	..
Perseids	1862 III	Aug. 11	45 +58	+0·010	..
Giacobinids	Giacobini–Zinner	Oct. 10	262 +54	+0·004	..
Leonids	1866 I	Nov. 15	151 +23	−0·052	..
Bielids	Biela	Nov. 30	23 +44	−0·018	..
Ursids	Tuttle 1939 k	Dec. 22	200 +80	+0·100	..

There are four main criteria by which the identity of the orbits of the comet and the meteor stream must be judged. (i) Similarity of orbits, provided the comet makes a sufficiently close approach to the earth.

(ii) Recurrence of the shower in a period compatible with that of the comet. (iii) Regression or advance of the date of the shower, corresponding to the movement of the node of the comet. (iv) Daily movement of the radiant in the case of a long enduring stream. Of the possible associations listed in Table 167 only six would receive universal recognition on this basis as undisputed cases of the relation of a meteor stream and a comet (Lyrids, Pons–Winnecke, Perseids, Giacobinids, Leonids, and Bielids), and two of these are now lost streams (Pons–Winnecke and Bielids). In dealing with the relations between comets and meteors two other major factors have to be considered. Firstly there are a number of major showers for which there seems to be no possibility of a cometary relationship—these are considered in § 3 below. Secondly there are a large number of comets which, on the basis of Table 167, might be expected to give rise to meteor showers. Lists of such comets approaching the earth's orbit within 0·25 a.u. were drawn up in 1875 by Herschel† and in 1920 by Davidson.‡ Porter has considered the matter again recently.§ There are some sixty-eight cases of long period or parabolic comets which should approach the earth sufficiently closely to produce a meteor stream but there are no major showers which can be associated with these. For comets moving in elliptical orbits of date later than 1700, approaching the earth to within 0·1 a.u., Porter gives the data listed in Table 168. Of the nineteen cases in this Table there are only six close relationships of the classic type, together with a highly probable association (the Ursids) and a doubtful relationship (the η-Aquarids). Occasionally, claims are made for the association of a minor shower with a cometary orbit, and at one time Denning published a list of twenty-eight such accordances. These have never received independent confirmation and, moreover, it seems very likely that many of Denning's minor streams represent fictitious groupings of sporadic meteors.

The failure to find meteor streams associated with the majority of the elliptical comets in Table 168, and for sixty-eight parabolic comets with equally close approaches, and the existence of several major showers without parent comets (see § 3) has led authors such as Porter‖ to urge caution over the widespread view that meteors are the debris of comets. The possible mode of formation of meteor streams from comets in the few cases where the connexion is clearly established will be discussed in § 4.

† Herschel, A., *Rep. on Meteors to Brit. Assoc.*, 1875.

‡ Davidson, M., *Mon. Not. Roy. Astr. Soc.* **80** (1920), 739.

§ Porter, J. G., *Comets and Meteor Streams* (Chapman & Hall, 1952); *J. Brit. Astr. Assoc.* **62** (1952), 101.

‖ Porter, J. G., ibid.; *Rep. Phys. Soc. Progr. Phys.* **11** (1948), 402.

TABLE 168

Comets with Elliptical Orbits approaching the Earth to within 0·100 *a.u.*

Comet	*Period (years)*	*Possible meteor radiant* α	δ	*Date*	*Closest at longitude*	*Distance of closest approach (Comet–Earth)*	*Remarks*
						a.u.	
1819 IV Blanpain	5·1	332	−40	Jan. 9	☊+29°	+0·077	..
1743 I	5·4	350	−10	Feb. 11	☊+52°	+0·026	..
1907 II Grigg-Mellish	164	308	−61	Mar. 30	☊	−0·002	..
1861 I	417	271	+34	Apr. 21	☊	−0·002	Lyrids (see Table 167)
Grigg–Skjellerup	5·0	109	−37	Apr. 26	☊	−0·098	..
Halley	76·3	336	−1	May 6	☋−11°	−0·064	η-Aquarids(?) (see Table 167)
1930 VI Schwassmann–Wachmann	5·4	218	+45	June 8	☋	+0·006	..
Pons–Winnecke	6·1	204	+56	June 30	☋	+0·028	Pons-Winnecke (see Table 167)
1770 I Lexell	5·6	273	−21	July 5	☋−32°	+0·015	..
1862 III	120	45	+58	Aug. 11	☋	+0·010	Perseids (see Table 167)
Finlay	6·7	278	−37	Sept. 29	peri	+0·055	..
Giacobini–Zinner	6·6	262	+54	Oct. 10	☋	+0·004	Giacobinids (see Table 167)
1866 I Tempel	33·2	147	+24	Nov. 11	☋−4°	−0·024	Leonids (see Table 167)
1743 I	5·4	22	+4	Nov. 14	☊−39°	−0·021	..
1852 III Biela	6·6	23	+42	Nov. 28	☋−2°	+0·008	Bielids (see Table 167)
1770 I Lexell	5·6	256	−25	Dec. 5	☊−62°	−0·025	..
1917 I Mellish	145	103	+9	Dec. 15	☊−5°	−0·061	..
1881 V Denning	8·5	277	−35	Dec. 17	☊+18°	+0·037	..
1926 IV Tuttle	13·5	219	+74	Dec. 22	☋	+0·100	Ursids (see Table 167)

2. The case of Encke's Comet and the November Taurid and day-time β-Taurid meteor streams

Encke's Comet, although of short period, does not appear in Table 168, since the distance of approach $> 0{\cdot}1$ a.u. Whipple's work on the orbits of the Taurid meteors, described in Chapter XV showed that the orbits of these meteors were remarkably similar to that of the comet with respect to a, e, and π, but that the planes of the comet and the meteor orbits differed by 10° to 15°. Later, as described in Chapter XVIII it also became clear that the day-time β-Taurid meteors of June–July moved in similar orbits to the November Taurids. The discrepancy in the inclinations apparently removed all possibility of a common origin or connexion between these meteors and Encke's Comet, the first criterion given in § 1 not being satisfied. However, the stream makes close approaches to the terrestrial planets, and by studying the effects

of successive perturbations, particularly by Jupiter, Whipple† has been able to show that a common origin of Encke's Comet and the Taurid stream is probable.

The ratio of the periods of Encke's Comet (3·3 years) with the period of Jupiter (11·86 years) is nearly 2 to 7; hence at aphelion a near approach to Jupiter occurs every seven revolutions (about 1 a.u. minimum). In his approximate theory of the secular perturbations, Whipple assumes that the observed perturbations arise from this cause only, and that the elements a and e are statistically constant with time.‡ The systematic changes with time in the angular elements ω, Ω, and i are given in Table 169.

TABLE 169

Observed Perturbations for Encke's Comet

Difference in mean date	$\Delta\omega$	$\Delta\Omega$	Δi
	deg.	*deg.*	*deg.*
1812(2) to 1832(7)	+0·38	−0·19	−0·24
1832(7) to 1855(7)	+0·65	−0·43	−0·25
1855(7) to 1873(4)	+0·20	−0·10	+0·01
1873(4) to 1891(7)	+0·30	−0·16	−0·22
1891(7) to 1914(7)	+0·71	−0·49	−0·35
1914(7) to 1931(3)	+0·26	−0·00	−0·00
Mean perturbation. .	+0·42	−0·25	−0·18
Standard deviation .	±0·21	±0·16	±0·14

With the notation of Chapter XX, § 1, the perturbing forces $\bar{S}$, $\bar{T}$, $\bar{W}$ per unit mass due to Jupiter will be given by

$$\bar{S} = \mathbf{k}^2 m\left(\frac{\xi - \mathrm{r}}{\rho^3} - \frac{\xi}{\mathrm{r}_1^3}\right), \tag{1}$$

$$\bar{T} = \mathbf{k}^2 m\left(\frac{\eta}{\rho^3} - \frac{\eta}{\mathrm{r}_1^3}\right), \tag{2}$$

$$\bar{W} = \mathbf{k}^2 m\left(\frac{\zeta}{\rho^3} - \frac{\zeta}{\mathrm{r}_1^3}\right), \tag{3}$$

where m is the mass of Jupiter, $\mathbf{k}^2$ the Gaussian constant, ξ, η, and ζ the coordinates of Jupiter with origin at the sun (oriented with respect to the comet's orbit in the sense $\bar{S}$, $\bar{T}$, $\bar{W}$), r and r_1 the radii vectores of the comet and planet respectively, and ρ the distance between the comet and Jupiter. Within the limits of accuracy desired the mean

† Whipple, F. L., *Proc. Amer. Phil. Soc.* **83** (1940), 711.

‡ In fact, the orbit shows an abnormal decrease in a which has been the cause of much speculation. Whipple (*Astrophys. J.* **111** (1950), 375) has recently given a new theory of this abnormality.

value of the tangential force $\bar{T}$ can be taken as zero, also the solar attractions ξ/r_1^3 and ζ/r_1^3 can be absorbed in a constant k_0 together with $\mathbf{k}^2m$. A mean value of $1/\rho^3$ can then be found such that the value of ζ exactly at aphelion of the comet and opposition of Jupiter may be used. The longitude of Jupiter then becomes $(\pi+180^\circ)$ and

$$\zeta = r_1 \sin\omega' \sin i' \tag{4}$$

(ω', i', Ω', etc., are the elements of the comet reduced to the plane of Jupiter's orbit).

With these approximations (1), (2), and (3) become

$$\left.\begin{aligned} \bar{S} &= k_0\left(\frac{\xi-r}{\rho^3}\right) \\ \bar{T} &= 0 \\ \bar{W} &= k_0\frac{r_1}{\rho^3}\sin\omega' \sin i' \end{aligned}\right\}. \tag{5}$$

From standard theory† the perturbations in π, Ω', and i' are given by

$$na^{3/2}\sqrt{p}\frac{\Delta\pi}{\Delta t} = -\frac{p}{e}\cos\nu\bar{S} + \frac{p+r}{e}\sin\nu\bar{T} + r\sin u\frac{\tan i'}{2\bar{W}}, \tag{6}$$

$$na^{3/2}\sqrt{p}\frac{\Delta\Omega'}{\Delta t} = r\frac{\sin u}{\sin i'}\bar{W}, \tag{7}$$

$$na^{3/2}\sqrt{p}\frac{\Delta i'}{\Delta t} = r\cos u\,\bar{W}, \tag{8}$$

where ν is the true anomaly of the comet, u its longitude from the ascending node, n the mean motion, and Δt the effective time for which the forces act. p is the *semi-latus rectum* $= a(1-e^2)$.

On the assumption that the perturbations occur at aphelion, $\nu = 180^\circ$ and $u = \omega'+180^\circ$. Substitution in equations (6), (7), and (8) combined with equations (5) give

$$\frac{\Delta\pi}{\Delta t} = -k_0\frac{p}{e}\left(\frac{\xi-r}{\rho^3}\right) - k_0\frac{rr_1}{\rho^3}\sin^2\omega' \sin i' \tan\frac{i'}{2}, \tag{9}$$

$$\frac{\Delta\Omega'}{\Delta t} = -k_0\frac{rr_1}{\rho^3}\sin^2\omega', \tag{10}$$

$$\frac{\Delta i'}{\Delta t} = -k_0\frac{rr_1}{\rho^3}\sin\omega' \cos\omega' \sin i'. \tag{11}$$

† For example, Moulton, F. R., *An Introduction to Celestial Mechanics* (Macmillan, 1923), p. 404.

The second term in (9) is numerically small and may be neglected. This equation and (11) may be used without further modification to obtain average values of the perturbations per close approach; but in (10) the $\sin^2\omega'$ term will be inaccurate when $\sin\omega'$ is near zero. Whipple averages $\sin^2\omega'$ over a range l in longitude on each side of aphelion and replaces $\sin^2\omega'$ by $\frac{1}{2}(1-k_3\cos 2\omega')$ where $k_3 = \sin 2l/2l$ is determined from the observed mean ratio of $\Delta\Omega'/\Delta i'$ per close approach.

Finally for the fundamental equations Whipple obtains

$$\left.\begin{aligned} \frac{d\pi}{dt} &= k_1 \\ \frac{d\Omega'}{dt} &= -k_2(1-k_3\cos 2\omega') \\ \frac{d\omega'}{dt} &= k_4-k_5\cos 2\omega' \\ \frac{di'}{dt} &= -k_6\sin\omega'\cos\omega'\sin i' \end{aligned}\right\} \qquad (12)$$

where $k_4 = k_1+k_2$ and $k_5 = k_2k_3$.

In these equations the unit of time is the average interval between close approaches, and all quantities which are not angular elements are combined as constants (k_1, etc.). Integration of equations (12) then gives

$$\left.\begin{aligned} \pi &= \pi_0+k_1t \\ \cos 2\omega' &= \frac{k_5-k_4\sin k_7(t-t_0)}{k_4-k_5\sin k_7(t-t_0)} \\ \Omega' &= \pi-\omega' \\ \log\tan\frac{i'}{2} &= k_8-k_9\log(k_4-k_5\cos 2\omega') \end{aligned}\right\} \qquad (13)$$

where π_0, ω_0' and i_0' are the values at $t = 0$ (1855) and where

$$k_7 = 2\sqrt{(k_4^2-k_5^2)},$$

$$\sin k_7t_0 = -\frac{k_5+k_4\cos 2\omega_0'}{k_4-k_5\cos 2\omega_0'},$$

$$k_8 = \log\tan\frac{i_0'}{2}+k_9\log(k_4-k_5\cos 2\omega_0'),$$

$$k_9 = k_6/4k_5.$$

From the mean values of the observed perturbations (Table 169) and the initial values of the elements of the comet referred to Jupiter's plane

(Table 170), the values of the constants as given in Table 170 are obtained. The unit of time is the average interval between close approaches (about 21 years) and the zero of time is 1855.

TABLE 170

Elements of Comet Encke and three Taurid Meteors referred to Jupiter's Orbit (1920) *and the Values of the Perturbation constants*

	Comet Encke	*Meteor* 642	*Meteor* 710	*Meteor* 778	*Perturbation constants*
ω'	188°·0	134·8	125·9	337·9	k_1 0·00290
Ω'	331·0	15·0	31·5	227·5	k_2 0·0463
π	158·8	149·8	157·3	159·7	k_3 0·942
i′	13·9	5·7	4·5	4·5	k_4 0·0492
Dihedral angle between orbit planes of meteor and comet ϵ'	0·0	10·6	12·3	15·6	k_5 0·0436
					k_6 0·0924
a(a.u.)	2·217	1·910	2·349	2·191	k_7 0·0456
e	0·847	0·845	0·844	0·891	k_7 t_0 30°·6
Aphelion distance (a.u.)	4·09	3·52	4·33	4·14	t_0 11·7
					k_8 −2·047
					k_9 0·530

The period of revolution of $\omega'(4\pi/k_7)$ is 276 intervals or about 5,800 years, and the period of variation of i′ is half that of ω', or about 2,900 years, and lies within the range i′ = 16°·0 to i′ = 3°·6. The perturbed elements calculated as above are shown in Fig. 187 as functions of the number of close approaches with Jupiter.

In associating the Taurid meteors with the comet, Whipple presumes that at some stage in the past a remote comet disintegrated into smaller ones and that the Taurid meteors are the disintegration products of one or more components of the original. In this case the relation between ω' and i′ obtained above for the comet should also apply to the Taurid meteors. The appropriate calculations carried out as above for meteors Nos. 642, 710, and 778 give values for the inclination i′ of 5°·1, 3°·9,† and 4°·5† respectively, in very good agreement with the observed values (Table 170) of 5·7°, 4·5°, and 4·5°. It appears, therefore, that the only serious discrepancy in the orbits of the Taurid meteors and Encke's Comet—that of the inclination—can be explained satisfactorily in terms of perturbations due to close approaches with Jupiter at aphelion.

† According to Brouwer (*Astr. J.* **52** (1947), 190), the correct calculated values for meteors 710 and 778 should be i′ = 4°·5 and 8°·7 respectively, the original values of i′ = 3°·9 and 4°·5 being in error due to a numerical slip. This correction worsens somewhat the agreement in the calculated inclination of 778 with the observed value.

Subsequently Brouwer† carried out a more rigorous treatment of the perturbation theory as applied to Encke's Comet, and confirmed the results obtained by Whipple in the approximate empirical theory outlined above.

The perturbations depend on the aphelion distance of the orbit and Whipple points out that it should be possible to estimate the times elapsed since the separation of the meteor streams from the comet by

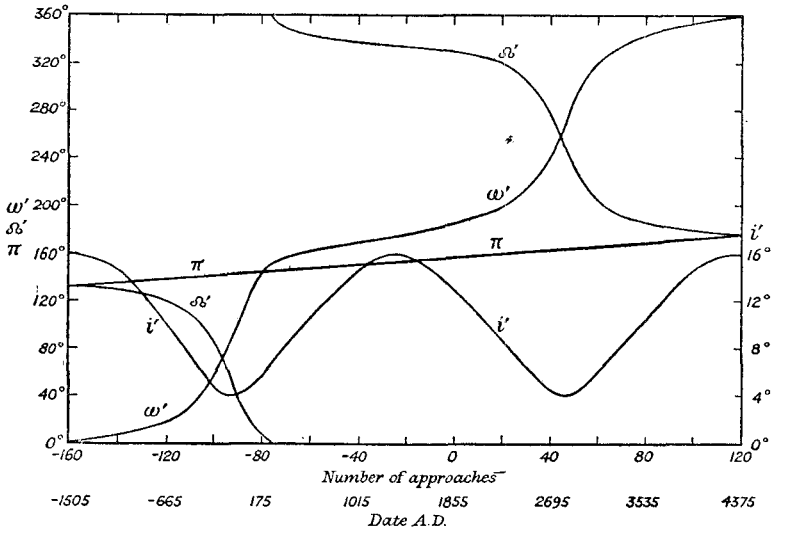

FIG. 187. Perturbed orbital elements for Encke's Comet as calculated by Whipple.

comparing ω' and Ω' for the various orbits. Taking a mean aphelion distance for the four best determined Taurids in the earlier work, Whipple estimates a minimum value of 5,000 years from considerations of the value of ω'. Unfortunately this leads to a discrepancy in π which should have changed by $+15°$, but for which the observed difference is negligible. A partial reconciliation can be achieved by adjusting the value of ω' but this leads to ages of from 5,000 to 20,000 years for the four meteors in question. From other considerations related to deviations between the correlations of the elements, Whipple obtains an age of 14,000 years. More recently the topic has been reconsidered by Whipple and Hamid,‡ who have recalculated the secular perturbations on the basis of Brouwer's more rigorous treatment of the perturbation theory†

† Brouwer, D., *Astr. J.* **52** (1947), 190.

‡ Whipple, F. L., and Hamid, S. E. D., *Harv. Abstract* (see also *Sky and Telescope* **9** (1950), 248).

including the later Taurid data obtained by Wright and Whipple† making a total of nine meteors. For five of the orbits the values of π tend to converge to the value of Encke's Comet 6,000 years ago; and for three orbits π diverges appreciably. They also find that the orbit planes of four meteors coincided well with that of Encke's Comet 4,700 years ago, and that three other orbit planes coincide with each other but not with that of the comet, about 1,500 years ago. They also find that the 4,700-year orbit set tends to cross near the solar distance 3.0 a.u. before aphelion, and those of the 1,500-year set near aphelion.

From these facts Whipple and Hamid conclude that the meteor streams were formed by a violent ejection of material from the comet some 4,700 years ago and by a subsequent ejection 1,500 years ago from a body moving in an orbit of similar shape and π, but with greater aphelion distance—probably a component of the comet which split away at an unknown time in the past. It is also concluded that the velocity of ejection was about 3 km./sec.; and that the ejection occurred at a distance $r \gg q$. These conclusions are not consistent with Whipple's theory of the mode of formation of meteor streams by cometary ejection (see § 4), and the authors propose that the ejections from Comet Encke were the result of encounters with asteroidal bodies. The calculated points of ejection lie near the asteroidal plane, and one of the points is in the region of the greatest concentration of asteroids.

The main conclusions arising from this theory of Whipple and his associates is, therefore, that the complex system of Taurid–Arietid streams active in October–November probably had a common origin with Encke's Comet several thousand years ago. Further, in view of the similarity of the orbit of the day-time β-Taurid stream with the autumn Taurids, and of the day-time ζ-Perseid stream with the autumn Southern Arietids it must also be presumed that two of the most prominent summer day-time streams have a similar origin.

The above theory has been given considerable attention in this chapter since it represents almost the only contemporary effort to investigate in detail the complex problems surrounding the possible association of meteor streams and comets. Moreover it presents a probable solution of the origin of a series of prominent major showers.

3. The major meteor showers without cometary associations

The list of showers given in Table 167 as possibly associated with certain comets omits several of the important major showers. These all

† Wright, F. W., and Whipple, F. L., *Tech. Rep. Harv. Coll. Obs.*, no. 6 (1950).

have orbits of short period and association with cometary objects seems extremely unlikely. A list of the main showers in question, for which orbits have been determined, is given in Table 171.

TABLE 171

Major Meteor Showers without Cometary Association

Meteor shower	*Date*	*Radiant* α	*Radiant* δ	*Semi-major axis* a (*a.u.*)
(?) Quadrantids .	Jan. 3	230°	+50°	2·0
δ-Aquarids . .	July 28	340°	−17°	1·6
Geminids . .	Dec. 13	111°	+32°	1·5
Arietids (day-time)	June 8	44	+24	1·6
o-Cetids (day-time)	May 19	29·4	−2·7	1·3

All the summer day-time streams appear to move in short period orbits. The ζ-Perseid and β-Taurids have been associated with Encke's Comet above, but the Arietids and o-Cetids have no cometary association and are included in Table 171. The only two other streams in the summer sequence for which velocities have been determined are the 54-Perseids and θ-Aurigids, both with similar short period orbits, but these streams have not been included since the data rest on measurements in one year only. Of the night-time streams the Geminids and δ-Aquarids have no obvious cometary connexion. The Quadrantids were also included in Table 171 as possessing a doubtful association with Comet Kozik–Peltier. This could only be so if the comet ejected the Quadrantid material at a particular point of its orbit, and at present the classification of this stream must remain doubtful. Some similar doubt must exist on the question of the Orionids, and η-Aquarids; but the nature of their orbits and their connexion with Halley's Comet is reasonable enough to justify their inclusion in the cometary class. Although the number of showers listed in Table 171 is less than those listed as possessing cometary association in Table 167, nevertheless they include some of the showers which are most prominent at the present time. The existence of such great amounts of debris moving in orbits of short period presents one of the most interesting aspects of meteor astronomy, for which at present there is no satisfactory solution.

Whipple's photographic studies† first showed beyond doubt that the Geminid meteors were moving in orbits which were unique compared with the orbits of known comets, planets, and asteroids. The comet of shortest known period, Encke's, has a period of 3·3 years, or twice that

† Whipple, F. L., *Proc. Amer. Phil. Soc.* **91** (1947), 189.

of the mean period of the Geminids. Even the period of the unusual asteroids Eros and Apollo is longer than the average Geminid. The eccentricity of the orbit is also greater than that of any asteroid. As regards the possibility of the Geminids having a cometary association it is clear that a comet in the present Geminid orbit would disintegrate rapidly owing to the frequent perihelion passages at such a small distance from the sun. The small aphelion distance also makes it difficult to account for the short period as resulting from the perturbing effect of Jupiter. If it is assumed that the parent of the Geminid stream was originally a member of the Jupiter comet family then some unknown forces must have reduced its aphelion distance from about 5 a.u. to 2·65 a.u. It is possible that although the orbit now only approaches the earth's orbit closely, in the past it may have been oriented to permit of large perturbations by Venus or Mars. The action of Jupiter on such an orbit over periods of thousands of years might produce large changes in the inclination in the same manner as discussed for the Taurid meteors and Encke's Comet.

Maltzev† considered the possibility that the Geminids were separated from a parabolic comet by the close approach of the comet to the sun, with specific reference to the great comet of 1680. The orbits are near, a little after perihelion, in close proximity to the sun. Plavec‡ has also referred to certain perturbations of the Geminid orbit. He calculated the secular perturbations in Whipple's elements for the Geminid orbit due to Jupiter and the earth over a hundred years with the results given in Table 172.

TABLE 172

Perturbations of the Geminid Orbit by Jupiter and the Earth in 100 *years and changes in the least distance of the Orbit from the Earth*

Elements epoch 1937	*Secular perturbations by*		*Year*	☊	*Date of maximum*	*Radius vector*	*Distance from earth*
	Jupiter	*Earth*					
			A.D.			(*a.u.*)	
π 225° 02′	−0·1′	−1·1′	1700	264° 33′	Dec. 17. 7	0·8503	0·1337
☊ 260° 43′	−95·0′	−2·2′	1900	261° 18′	Dec. 14. 5	0·9665	0·0178
i 23° 28′	+47·8′	+0·7′	2100	258° 03′	Dec. 11. 4	1·0912	−0·1066
e 0·900	−0·001	0·000					
a 1·396	..	..					

The rapid retrogression of the node is of particular interest, since it would cause the date of maximum of the shower to change by one day

† Maltzev, V. A., *Astr. J. U.S.S.R.* **8** (1931), 67.
‡ Plavec, M., *Nature*, **165** (1950), 362.

in sixty years. Also the point of intersection of the orbit with the plane of the ecliptic does not move parallel with the earth's orbit but cuts it at a steep angle. This gives rise to a rapid change in the least distance of the shower from the earth as listed in Table 172. Taking the width of the debris as about 0·1 a.u., these calculations indicate that the Geminids can only be visible for about 400 years, and that they probably appeared about 1700 and will disappear about 2100. Plavec claims to have established the retrogression of the node, and draws attention to the fact that although at present the Geminids are one of the strongest showers there is little reference to their occurrence even 100 years ago.

It will be evident from the above discussion that the origin of the Geminid meteor stream remains an enigma, as does that of the remaining streams listed in Table 171. As yet there has been no serious speculation on the origin of the day-time o-Cetids, δ-Aquarids, and day-time Arietids. The remarkable similarity in the shape of the orbits of the two latter streams has been referred to in Chapter XVIII, but their different inclinations may present an obstacle to the idea of a common origin.

The topics discussed so far in this chapter have been investigated at great length from a phenomenological aspect by Hoffmeister.† This work is a major attempt towards a separation and classification of the chief statistical components of meteor phenomena, which Hoffmeister considers under the headings of ecliptical, cometary, and interstellar. Although it is no longer possible to attach any significance to the idea of an interstellar component, Hoffmeister's classification under the other headings agrees well with the contents of this chapter. He includes many other streams which are not generally regarded as of a major character in support of the classification. As regards the ecliptical component, under which heading could be included the short-period streams discussed in this section, Hoffmeister concludes that the system is not related to comets but that it forms part of the system of minor planets. The similarity of the orbits to some of the minor planets is indeed striking, and the idea of a planetary origin for these short-period meteor streams is both plausible and attractive. The question of these short period orbits will be referred to again in § 5.

4. The mode of formation of meteor streams from comets

Although the cosmological associations for some of the major meteor streams is obscure it would be hard to deny in view of the evidence

† Hoffmeister, C., *Meteorströme*, Weimar, 1948—a short summary is given by Hoffmeister in the *Observatory*, **70** (1950), 70.

presented in § 1 that at least some of the important meteor streams appear to have a close association with comets. Evidently there are two broad possibilities, either the meteoric debris is the primeval material from which the comet is forming, or conversely, the debris is the result of some disintegration process in the comet. In Chapter XIX it was estimated that the total mass of meteoric material in the orbits of the major meteor streams was about 10^{12} kg. This is somewhat less than the cometary masses—a recent estimate† of the mass of Halley's Comet is about 10^{16} kg.—and this fact would appear to favour the ejection or disintegration hypothesis. The methods by which comets could give rise to meteor streams appear to have been first discussed seriously by Schiaparelli who formed the view that meteor streams arise from comets because of the dispersive forces which occur when the comet makes close approaches to the sun or a planet. Later, Bredikhine developed the ejection theory, as mentioned in Chapter XX. A summary of these earlier ideas has been given by Olivier.‡ The most recent and detailed theory of the formation of meteor streams from comets is due to Whipple§ whose views will be summarized here.

(*a*) *Whipple's Comet Model*

Whipple proposes a new comet model whose nucleus is visualized as consisting of a conglomerate of ices such as H_2O, NH_3, CH_4, CO_2 or CO, C_2N_2, and other materials volatile at low temperature ($< 50°$ K.), but on approaching the sun, vaporization of the ices occurs through externally applied solar radiation. This leaves an outer matrix of non volatile insulating meteoric material. Meteoric material below some limiting size will blow away because of the low gravitational attraction of the nucleus, and will begin the formation of a meteor stream. Some of the larger or denser particles may also be removed by shocks, but the largest particles will remain on the surface to produce an insulating layer. After a short time the loss of gas will be materially reduced by the insulation provided by this matrix. Whipple shows that the heat transfer through such thin meteoric layers in a vacuum is limited chiefly by the radiative rate, and that it is inversely proportional to the effective number of layers. It is shown that an appreciable time lag in heat transfer can occur for a rotating cometary nucleus. The low central temperature is maintained by vaporization of the ices. This cometary model is capable of explaining the peculiarities in the orbital behaviour of certain comets.

† Vorontsov-Velyaminov, B., *Astrophys. J.* **104** (1946), 226.
‡ Olivier, C. P., *Meteors*, ch. 17.
§ Whipple, F. L., *Astrophys. J.* **111** (1950), 375; **113** (1951), 464.

For example, if the nucleus is rotating in the forward sense with respect to its revolution, the time lag in heat transfer will result in the vaporized ices being emitted with a component towards the antapex of motion. The momentum transfer will propel the nucleus forwards, reduce the mean motion and increase the orbital eccentricity, as observed for comets such as C. Wolf and C. d'Arrest. Retrograde motion will produce an acceleration in mean motion and a decrease in eccentricity as observed for Comet Encke. Whipple shows that the present orbital changes could be produced by a mass loss of from 0·002 to 0·005 units per orbital revolution, provided the force is proportional to the solar energy flux, and cuts off at a distance of about 2 a.u.

As regards the ejection of the meteoric material, Whipple considers the material which has already been carried some distance from the nucleus, in order to avoid the complicated forces which are likely to arise near the surface. He assumes that the escape is sufficiently rapid so that it is only necessary to consider the gases escaping from the sunlit hemisphere. If the ices utilize a fraction 1/n of the solar radiation for sublimation; if the nucleus is spherical of radius R_c and density ρ_c; and if the mean heat of sublimation of the ices is Π calories per gramme, then the mass of ices Δm sublimated per second at a distance r(a.u.) from the sun is given by

$$\Delta m = \frac{\pi R_c^2 \Xi}{n \Pi r^2}, \tag{14}$$

where Ξ is the solar constant (= 0·032 cal. cm.$^{-2}$ sec.$^{-1}$ at 1 a.u.).

At a distance R ($\gg R_c$) from the nucleus it is assumed that the gas escapes over the hemisphere $2\pi R^2$ with an outward velocity given by

$$u = \left(\frac{8kT_g}{\pi A}\right)^{\frac{1}{2}}, \tag{15}$$

where **k** is Boltzmann's constant, T_g the temperature and A the molecular weight of the gas. The momentum transferred per second per square centimetre at a distance R is then

$$\frac{(u \Xi R_c^2)}{(2nr^2 \Pi R^2)}. \tag{16}$$

It is believed that meteoric particles are irregular and rough and hence will have a large accommodation coefficient for gaseous encounters. For simplicity Whipple assumes the coefficient to be unity, and that the particles are spherical of radius ***r*** and density ρ_s. If the cometary gas is stopped by these particles and re-emitted immediately with thermal

velocities, the drag coefficient is approximately that for free molecular flow.

Thus the outward force on a slowly moving particle is given by

$$\frac{13\pi u \boldsymbol{r}^2 \Xi R_c^2}{18 n r^2 \Pi R^2}. \tag{17}$$

The total force will be reduced by gravity so that the net outward acceleration becomes

$$\frac{d^2R}{dt^2} = \frac{(C_1 - C_2 R_c)R_c^2}{R^2} \tag{18}$$

where

$$C_1 = \frac{39 u \Xi}{72 n r^2 \boldsymbol{r} \rho_s \Pi} \tag{19}$$

and

$$C_2 = 4\pi\rho_c \frac{\Upsilon}{3}. \tag{20}$$

The relative velocity V_∞ of the particle at infinity with respect to the cometary nucleus is then given by

$$V_\infty^2 = 2C_1 R_c - 2C_2 R_c^2. \tag{21}$$

Whipple shows that a reasonable value for the gas temperature T_g in (15) is $T_g = 300/\sqrt{r}$ °K. giving

$$u = \left(\frac{8 \times 300° \text{ K.}}{\pi A}\right)^{\frac{1}{2}} \frac{1}{(r_{a.u.})^{\frac{1}{4}}}. \tag{22}$$

Taking $\rho_c = 1$ gm. cm.$^{-3}$, $\rho_s = 4$ gm. cm.$^{-3}$, $A = 20 \times 1{\cdot}661 \times 10^{-24}$ gm., and expressing $\boldsymbol{r}$ in cm., R_c in km., and r in a.u. equation (21) reduces to

$$V_\infty = \left(\frac{1}{n \boldsymbol{r} r^{9/4}} - 0{\cdot}052 R_c\right)^{\frac{1}{2}} R_c^{\frac{1}{2}} 328 \text{ cm. sec.}^{-1} \tag{23}$$

As an example of orders of magnitude of V_∞ Whipple considers the case of a new comet for which the sublimation efficiency n is unity, of radius 1 km. at distance 1 a.u. from the sun. Meteoric particles of radius 1 cm. and density 4 gm. cm.$^{-3}$ would be ejected with a velocity of about 3 metres per second.

Equation (23) indicates that the ejection of meteoric debris should be more violent and frequent near perihelion. Also, for the same (1/n), large comets should eject particles with greater velocities than small comets. Whipple uses this prediction to assess the theory in terms of the frequency of bright meteors as represented in the Harvard photographic collection and gives the data of Table 173.

TABLE 173

Relation of Comet Brightness and Meteor Characteristics

Meteor shower	*Associated comet*	*Comet brightness*	q (*a.u.*)	*Shower length (days)*	*Nature of photographed meteors*
Perseids . .	1862 III	Bright	0·97	30	Strong
Leonids . .	1866 I	Lost	0·98	5	Medium
Lyrids . . .	1861 I	Bright	0·92	4	Weak
Bielids . . .	Biela	Lost	0·86	5	Weak
Geminids . .	?	..	0·14	4	Strong
η-Aquarids . .	Halley (?)	Bright	0·59	6	Weak
Orionids . .	Halley (?)	Bright	0·59	10	Medium
Giacobinids . .	1933 III	Faint	1·00	1	Weak (?)
Taurids . .	Encke	Medium	0·39	40	Strong
δ-Aquarids . .	?	..	0·04	10	Strong
Quadrantids . .	?	..	0·99	2	Weak

In general the predictions of the theory are confirmed—the most widely dispersed showers like the Perseids and Taurids, and possibly the η-Aquarids and Orionids, arising from massive comets; while the faint comets—Giacobini–Zinner, Biela, and 1866 I produce concentrated showers. The evidence is not conclusive since large comets have produced concentrated showers, on the other hand all the faint comets in Table 173 have produced concentrated showers.

The maximum radius r_{max} of ejected meteoric material can be obtained from equations (18–23) as

$$r_{max} = \frac{19}{nr^{9/4}R_c} \text{ cm.}, \qquad (24)$$

where R_c is in km. and r in a.u.

The maximum radius is sensitive to the perihelion distance, and for close approaches corresponds to extremely bright fireballs. In Table 173 there are three perihelion distances less than 0·5 a.u. and in each case the showers are strong photographically. From a perusal of the von Niessl–Hoffmeister fireball catalogue (Chapter VIII) Whipple also concludes that the showers with small perihelion distances definitely tend to show unusually bright meteors.

It is clear that Whipple's new theory offers a most promising approach to the problem of the physical relationships of meteors and comets. More precise testing of the theory should rapidly become possible as the new photographic and radio-echo data on meteors accumulates.

(*b*) *The Ejection and Evolution of the Perseid Stream from Comet* 1862 III

The prominence, age, and clear association of the Perseid meteor stream with Comet 1862 III has always attracted much interest in regard

to the mode of formation of such an extensive region of debris from the comet. The first serious speculations appear to have been made in the nineteenth century by Bredikhine, who, as mentioned previously, favoured the theory of ejection of the meteoric matter from the cometary nucleus. Schulhof considered that such ejections could not possibly form such an extensive stream as the Perseids without planetary perturbations. The most recent treatment along these lines is by Hamid,† whose work on this subject has been mentioned in Chapter XX. On the basis of Whipple's comet model, Hamid calculates the velocity of ejection of the Perseid meteors from the comet to be 16·5 metres per second. A few dozen revolutions would suffice for the ejected material to be scattered around the orbit but without perturbations the shower would be very short ($\ll 1$ day). On the basis of Whipple's model the ejection will occur at an appreciable rate only when its distance from the sun is 2 a.u. or less. It is therefore necessary to calculate how long it has been since the comet's perihelion distance was within 2 a.u. of the sun. Hamid shows that the comet must have been captured by Jupiter and that the ejection of the meteors occurred after capture. By a detailed treatment of the effects of the perturbations due to Jupiter and Saturn he concludes that the present configuration of the stream could arise from an ejection which took place about 40,000 years ago.

5. The origin of sporadic meteors

A good deal of attention has been given earlier in this book to the problem of the velocity of sporadic meteors, and the conclusion now seems inescapable that they must be contained in the solar system as distinct from the interstellar view which has prevailed for so long. Perhaps of equal significance is the increasing amount of evidence from the radio-echo and photographic data that their orbits, far from being hyperbolic, are in fact of short period, and bear more resemblance to the orbits of the 'planetary' shower meteors discussed in § 3 than to the longer period orbits of the cometary shower meteors. Whipple‡ drew attention to this peculiarity in the first publication of the accurate photographic results, which included the orbits of four sporadic meteors. Three of these had orbits only slightly inclined to the ecliptic and of short period. The fourth had retrograde motion in an orbit of long period. Whipple pointed out that the first type of orbit was similar to the orbits of the asteroids with perihelion distances less than unity, and emphasized

† Hamid, S. E., Doctoral dissertation (Harvard, 1950).
‡ Whipple, F. L., *Proc. Amer. Phil. Soc.* **79** (1938), 499.

this peculiarity by compiling the data given in Table 174. This table gives the orbital elements for the three sporadic meteors in question, the three asteroids with perihelion distances less than unity and the five comets of periods less than seven years and perihelion distances less than unity. The orbital similarities between the asteroids and the meteors are most marked. Subsequently, similar types of orbits were found for several major showers as discussed in § 3, and recently, as mentioned above, there are now very strong grounds for believing that the orbits of many of the sporadic meteors are of this asteroidal type.

TABLE 174

Comparison of the Orbits of Short-period Sporadic Meteors, Asteroids, and Comets

	q	a	e	i
				deg.
Sporadic meteors				
Whipple No. 642†	0·296	1·91	0·84	6·0
Whipple No. 660.	0·968	2·22	0·56	4·3
Whipple No. 670.	0·618	3·21	0·81	1·9
Mean	0·627	2·45	0·74	4·1
Asteroids (q < 1)				
Apollo‡	0·647	1·48	0·56	6·4
Anteros§	0·441	1·86	0·76	1·4
1937 UB‖	0·618	1·64	0·63	6·2
Mean	0·569	1·66	0·65	4·7
Comets†† (P < 7 *years:* q < 1)				
Encke	0·332	2·21	0·85	12·6
Grigg–Skjellerup	0·908	2·93	0·69	17·4
Brorsen I	0·590	3·11	0·81	29·4
Giacobini–Zinner	1·000	3·52	0·72	30·7
Biela	0·856	3·52	0·76	12·6
Mean	0·737	3·06	0·77	20·5

The questions raised by these remarks and the contents of § 3 may be of deep significance in studies of the origin of the solar system. It may be anticipated that during the next decade a large amount of accurate information will be obtained by photographic and radio-echo studies, on the orbits of individual sporadic meteors. In this case the basic

† Meteor No. 642 was subsequently classified as a Southern Arietid (see Chap. XV).
‡ Whipple, F. L., and Cunningham, L. E., *Ann. Harv. Coll. Obs.* **105** (1937), 537.
§ Herget and Miss Davis, *Harv. Announcement Card* (1936), no. 366.
‖ Cunningham, L. E., ibid. (Jan. 1938), no. 440.
†† Yamamoto, A. S., *Pub. Kwasan Obs.* **1** (1936), no. 4.

material will be available for a detailed theoretical study of the origin of these short-period meteors. The major problem to be settled is whether these meteors are the debris of the primeval matter from which the solar system was formed, or whether they are the result of some subsequent planetary or cometary break-up. In this connexion it is interesting to notice that the Poynting–Robertson effect sets a rather short time-scale at which any such break-up could have occurred. The mean semi-major axis for the asteroids is about 3 a.u. and if the sporadic meteors were formed by a planetary disintegration at about this distance from the sun their orbits would mostly be within that of Jupiter with an apse near the planet's orbit. Wyatt and Whipple† have calculated the times of fall into the sun of particles with radius r moving in orbits of this type assuming their density to be 4 gm./c.c., according to the method given in Chapter XIX. Their results for various possible types of short-period orbits are given in Table 175.

TABLE 175

Times of Fall into the Sun for Meteors with an Asteroidal Type of Origin

Perihelion distance q (*a.u.*)	*Aphelion distance* q′ (*a.u.*)	*Semi-major axis* a (*a.u.*)	*Eccentricity* e	*Constant* C *equation* 19 *Chap. XX*	*Time of fall* t (*years*)
5	5	5	0·00	..	$70\times10^7\times r$
3	3	3	0·00	..	$25\times10^7\times r$
3	5	4	0·25	11·4	$11\times10^7\times r$
1	3	2	0·50	2·60	$1{\cdot}9\times10^7\times r$
1	5	3	0·67	2·31	$2{\cdot}9\times10^7\times r$

It can be seen from this table that for a time-scale of 3×10^9 years all bodies with radius of less than 4 cm. must have been swept into the sun. For a planetary break-up occurring 6×10^7 years ago, as suggested by Bauer‡ particles originating in the asteroidal belt of radius less than 0·08 a.u. must have been swept into the sun. Similar calculations have been made by Öpik§ who also introduces another important factor—that of the filtration of the particles through collisions with the planets. According to Öpik's calculations Jupiter presents a major obstacle, and within the cosmic time-scale will have cut off practically all particles over 2 mm. in diameter, although letting through fairly well those of 0·2 mm. diameter. If this view is correct then no meteor within the visual

† Wyatt, S. P., and Whipple, F. L., *Astrophys. J.* **111** (1950), 134.
‡ Bauer, C. A., *Phys. Rev.* **74** (1948) 501.
§ Öpik, E. J., *Proc. Roy. Irish Acad.* **54** (1951), 165.

and normal telescopic range of observation can belong to the primordial dust, but must have a more recent origin.

Such considerations imply a lack of faint meteors and militate against the idea of an origin in the asteroidal belt within a reasonable time-scale. If the primeval, or planetary, type of origin has to be abandoned for these, or other reasons, then the possibility of dispersion from the orbits of the cometary shower meteors presents an alternative. Although at first sight a highly plausible source for sporadic meteors, we have already seen earlier in this chapter the difficulty of explaining the evolution of large amounts of meteoric debris moving in short period orbits, from a cometary type of parentage.

6. Meteors and the zodiacal light

Although various theories have been advanced to account for the zodiacal light there can be little doubt that it is due basically to an extensive cloud of particles lying in the plane of the ecliptic and illuminated by the sun.† The evidence that this cloud of particles lies in the solar system is also conclusive. Recent treatments of the problem by Allen‡ and van de Hulst§ in which the importance of diffraction of sunlight by the zodiacal particles is emphasized, as well as scattering, has led to speculations of considerable interest. Both authors show that one part of the light of the solar corona (the Fraunhofer component) can be explained as due to diffractional scattering by small zodiacal particles. Allen's solution requires a particle density of 2×10^{-23} gm. c.c. at 1 a.u. from the sun on the assumption that the particles are of radius 10^{-3} cm. Van de Hulst assumes a distribution of particle sizes similar to that found in the meteoric matter and his solution requires a particle density of 5×10^{-21} gm. c.c.; throughout the interplanetary medium with a thickness perpendicular to the plane of the ecliptic of about 0·1 a.u. Evidently van de Hulst's solution, involving a plausible distribution of particle sizes appears preferable. Here we are particularly concerned with the relation of this interplanetary matter, responsible for the zodiacal light and the Fraunhofer component of the corona, to the meteoric matter in the solar system.

Van de Hulst's solution requires a density some 10^4 times greater than that of meteoric matter in the solar system inferred in Chapters VII and XIX. The preferred radii for the van de Hulst particles is between 1 mm.

† A convenient summary of the various views on the zodiacal light is given by Mitra, S. K., in *The Upper Atmosphere*, ch. 10, Royal Asiatic Society, Bengal, 1948.

‡ Allen, C. W., *Mon. Not. Roy. Astr. Soc.* **106** (1946), 137.

§ van de Hulst, H. C., *Astrophys. J.* **105** (1947), 471.

and 0·1 mm. and hence on the basis of his analysis faint meteors should be 10,000 times more plentiful than actually observed. Van de Hulst considers that his figure for the number of particles required to explain the zodiacal light and the Fraunhofer component is unlikely to be in error by a factor of 2, and even if one allows a factor of uncertainty of 10 or more in the meteor densities there is still a very large discrepancy to be explained. He considers a possible explanation to be that only a very small fraction of the interplanetary particles have velocities high enough to cause visible meteors, and suggests that the majority of the particles might move in nearly circular orbits similar to the planets and asteroids.

In an interesting comment on this idea Öpik† points out that van de Hulst's explanation of the discrepancy cannot be correct for the following reasons. Considering a two-body problem where the particles are subject only to the attraction of a planet of mass m and radius r_p; the number of particles intercepted by a planet in unit time is

$$\pi\sigma^2\rho\mathbf{u},$$

where σ is the effective target radius for capture, $\mathbf{u}$ the relative velocity, and ρ the space density. σ is the distance of the asymptote of the hyperbolic orbit from the centre of the planet when the periastron distance is r_p. Then the velocity in periastron is

$$U = \sqrt{(\mathbf{u}^2+S^2)},$$

where S, the velocity of escape from the surface of m, is given by

$$S = \sqrt{\left(\frac{2\gamma m}{r_p}\right)}.$$

Conservation of angular momentum gives

$$\sigma\mathbf{u} = Ur_p$$

hence

$$\sigma^2 = r_p^2\left(1+\frac{S^2}{\mathbf{u}^2}\right)$$

and the intensity Ψ of a meteor shower produced by the cloud and intercepted by m becomes

$$\Psi = \frac{(\pi\sigma^2\rho\mathbf{u})}{(\pi r_p^2)} = \rho u\left(1+\frac{S^2}{\mathbf{u}^2}\right).$$

Ψ is a minimum for $\mathbf{u} = S$ and approaches infinity as $\mathbf{u} \to \infty$ and as $\mathbf{u} \to 0$. Thus the condensing action of the planets gravitational field would, in fact, give rise to a meteor shower of infinite intensity from the

† Öpik, E. J. (1951), loc. cit.

'quiescent cloud' proposed by van de Hulst. In the case of the earth the problem is complicated by the presence of the sun, but Öpik shows that the broad considerations are not changed. Öpik's own explanation is that meteors of radius $6 > r > 10^{-2}$ cm. must be practically absent near the four inner planets, owing to the sweeping action of Jupiter combined with the Poynting–Robertson drift. On the other hand, for particles of radius $\sim 10^{-3}$ cm. Öpik calculates that the drift is too fast for the sweeping action of Jupiter to be significant. The time-scale in these calculations is 3×10^9 years. If this view is correct, particle sizes of 10^{-3} cm. and less might well predominate in the zodiacal light particles, whereas those in the range 0·03 to 6 cm. would be scarce. Much larger particles, at present in the vicinity of the earth, probably originated in the asteroidal ring, and hence might be expected to be relatively plentiful. Öpik's suggestions therefore give an explanation of the discrepancy between the space density of interplanetary matter calculated from the observed meteor frequency and that actually believed to exist according to van de Hulst's zodiacal light theory. A crucial test of van de Hulst's theory and of Öpik's views would be the observation of very faint meteors of magnitude 16 to 20. These would correspond to the particles of radius $< 10^{-3}$ cm. which escape the sweeping action of Jupiter and would therefore be expected to be some 10,000 times more numerous than predicted from the extrapolation of the number distribution of visual meteors.

APPENDIX I

NOTE ON SYMBOLS

The notation for the most frequently recurring quantities have been standardized as listed below.

VELOCITY

$\overline{\mathrm{V}}$ always refers to *heliocentric* velocity of meteors.
V apparent velocity of meteor outside earth's atmosphere.
$\mathrm{V_E}$ orbital velocity of earth.
V_E rotational velocity of earth.
V heliocentric velocity of interstellar particle.
$\overline{V}$ mean heliocentric velocity corresponding to centre of radiation (Chap. IX).
v geocentric velocity of meteor.
$\mathrm{v_p}$ geocentric parabolic velocity of meteor.
$\mathrm{v_g}$ geocentric velocity corrected for zenithal attraction.
$\mathrm{v_0}$ velocity at mid-point of trail.
v′ mean group velocity (Chap. XII).
v percentage speed (Chap. X).
v discrete values of space velocity (Chap. IX).
$\boldsymbol{v}$ velocity of interstellar particle.
w (with suffix) angular velocity (Chap. IX)
w theoretical angular velocity (Chap. IX).
U orbital velocity of particle (Chap. XX).
U velocity of particle in periastron (Chap. XXI).
u velocity of cometary ejection (Chap. XX).
$\mu = \mathrm{V_E}/\overline{\mathrm{V}}$.
$\Lambda = \mathrm{v}/\mathrm{V_E}$.
$\Lambda_0 = \overline{\mathrm{V}}/\mathrm{V_E} (= 1/\mu)$.

ORBITAL ELEMENTS

☊ ascending node.
☋ descending node.
i inclination.
a semi-major axis.
b semi-minor axis.
e eccentricity.
q $= \mathrm{a}(1-\mathrm{e})$ perihelion distance.
q′ $= \mathrm{a}(1+\mathrm{e})$ aphelion distance.
p $= \mathrm{a}(1-\mathrm{e}^2)$ *semi-latus rectum*
ω angle of perihelion.
π $= (☊+\omega)$ longitude of perihelion.
T time of perihelion passage.
ν true anomaly.
M mean anomaly.
n mean daily motion in degrees.
t date.

φ angle of eccentricity ($e = \sin\varphi$).
E eccentric anomaly.
H hour angle.
P period of orbit.

MISCELLANEOUS ASTRONOMICAL NOTATION

α (occasionally R.A.) right ascension
δ (occasionally decl.) declination

In the case of a meteor radiant the coordinates are printed in the text as $\alpha 90°$, $\delta +15°$; indicating right ascension 90°, declination +15°.

β latitude of radiant (used as altitude of radiant in Chap. XII).
λ longitude of radiant.
λ_a longitude of apex.
ϵ elongation of radiant ($\Delta\epsilon$ elongation correction).
ϵ obliquity of ecliptic.
α elevation of point on ecliptic.
η distance from radiant.
χ zenith angle.
Υ vernal equinox.
ϕ elevation of apex.
ψ latitude.
W period of axial rotation.
z measured zenith distance.
z corrected zenith distance.
Ξ solar constant.
b earth–sun distance.
m magnitude.
m meteor mass.
r meteor radius.
m used for mass (unspecified).
r_e radius of earth.
r_e radius of earth's atmosphere.
L length of meteor path.
M mass of sun.
$\odot$ longitude of sun.

RADIO NOTATION

α_r phase.
θ, ϕ polar diagram angles.
λ wave-length.
σ mean power density.
τ pulse width (τ_0 time in c.w from f_1 to f_2).
$\bar{\omega}$ received power.
$\bar{\omega}_0$ basic receiver noise level.
ω wave frequency.
ψ phase difference.
$f_1 f_2$ transmitter frequency.

f_0 pulse recurrence frequency.
G aerial power gain.
$E_1, E(x)$ field strength.
I_r intensity reflected wave.
N noise factor.
P transmitter power.
P_e external noise.
W_0 power density.
$\overline{W}$ mean transmitter power.
Z echo amplitude (signal noise ratio).

MISCELLANEOUS NOTATION

c velocity of light.
e electron charge.
g acceleration due to gravity.
h height.
k Boltzmann's constant, also $\mathbf{k}^2 = \gamma$ (gravitational constant).
l latent heat of evaporation.
m electron mass.
n rate of evaporation.
p atmospheric pressure.
t time.
t time relative to point.
t interval in days.
A atomic (molecular) weight.
D diffusion coefficient.
G Avogadro's number.
H scale height.
I luminosity.
$1/L$ heat absorption coefficient.
α_0 no. of electrons per cm. path in meteor trail.
N no. of electrons.
T temperature.
$\overline{S}$ $\overline{T}$ $\overline{W}$ attractive forces.
γ gravitational constant.
$\mu_0 = \gamma M$.
$\mu = \gamma(M+m)$ acceleration at unit distance.
μ_e acceleration at unit distance from earth.
II heat of sublimation.
ρ density.

APPENDIX II

SUMMARY OF RECENT WORK

THE main part of the text was written towards the end of 1951 and early 1952. In this Appendix a summary is given of subsequent results which became available up to the end of 1953.

CHAPTER IV

1. *A new radio-echo technique for the measurement of the orbits of single meteors*

The radio-echo techniques for the measurement of meteor radiants described in Chapter IV are applicable only to shower meteors or to rare single meteors of exceptional brightness. At Jodrell Bank, Davies and Gill† have recently extended the velocity measuring technique of Davies and Ellyett‡ to the delineation of both radiants and velocities of individual meteors. In addition to the transmitter and receiver used for the velocity measurements, two further receivers are employed, spaced about 4 km. east and south of the home station. The echoes received at these stations are transmitted by radio link to the home station where they are photographed alongside the direct echo on a single film. Thus in addition to the diffraction pattern yielding the meteor velocity, the time displacements between the occurrence of the pattern at the three receivers can be measured, and these time displacements lead to a knowledge of the meteor radiant. Since the separation of the receivers is of the order of a length of a Fresnel zone, meteors yielding velocity measurements on one receiver do so on all three. The accuracy in velocity measurement is about 2 per cent. and in radiant position about 2°.

A preliminary experiment on the Geminid meteors in 1953 December yielded orbits in good agreement with those obtained by Whipple.§ The method is now being used to study the orbits of sporadic meteors. Between one and two hundred orbits can be obtained in the course of 24 hours.

2. *The radio echo from the head of a meteor trail*

On pp. 73, 74 it was mentioned that no satisfactory explanation existed for the occasional echoes observed from the head of the meteor trails, used for velocity measurements by the range-time method. An explanation in terms of the diffraction theory given in Chapter IV has now been offered by Browne and Kaiser.‖ No assumptions are invoked beyond those commonly accepted as necessary to explain the specularly reflected echo. The theory predicts intensities of the head echo in agreement with observation. It also predicts that the intensity of the head echo relative to that of the specularly reflected echo should be proportional to the radio wave-length and inversely proportional to the difference in range between the two echoes.

CHAPTER VI

Visual work on the distribution of sporadic meteor orbits

On pp. 108 et seq. reference was made to the visual work of Prentice and the B.A.A. observers on the distribution of sporadic meteors. The analysis has now

† Davies, J. G., and Gill, J. C. Not yet published.

‡ See Chap. IV, p. 78.

§ See Chap. XV.

‖ Browne, I. C., and Kaiser, T. R., *J. Atmos. Terr. Phys.* **4**, (1953), 1.

been completed but not yet published. The final analysis for 1,000 meteors confirms the longitude and latitude distribution of apparent radiants shown in Figs. 61 (*a*) and (*b*), and of the true radiants shown in Fig. 69.

CHAPTER XI

The double camera investigation of the velocity distribution of sporadic meteors

In a footnote on p. 211 reference was made to the fact that the Super Schmidt cameras were working satisfactorily in September 1952. Unfortunately no results of the investigation are yet available for publication, but according to private information from Dr. F. L. Whipple and Dr. L. G. Jacchia the results are consistent with the distribution derived from the radio echo work (Chapter XII).

CHAPTER XIII

1. *The Quadrantid shower*

The text refers to the visual data collected by Prentice for the years 1921 to 1940. In a recent paper Prentice† has now published his observations for the years 1941 to 1953. A new determination of the epoch of maximum gives $\odot = 282° 53'$ in close agreement with the previous value. The paper also contains a discussion of a possible 13-year period in the activity.

In 1952 Alcock and Prentice‡ succeeded in determining 13 Quadrantid radiants from duplicate observations. The results show a spread in α from 231° to 243° and in δ from $+40°$ to $+60°$.

A recent discussion of the orbit of the Quadrantid stream has been given by Bouška.§ His calculations are based on the observational data given in the text, and further consideration is given to the possible relationship of the stream either with Comet Tuttle I or with Comet Kozik–Peltier.

Recently Millman and McKinley‖ have published the results of a radio-echo investigation of the 1951 Quadrantid shower, using the technique described in Chapter IV. They obtain a mean geocentric velocity of $40{\cdot}9 \pm 0{\cdot}5$ km./sec. Using data on the radiant position obtained from other sources they calculate the mean orbit with eccentricity 0·74, inclination 70°, and period 7·2 years, in general agreement with the photographic and Jodrell Bank orbit described in Chapter XIII.

2. *The Lyrid shower*

In view of the discrepancies in the position of the Lyrid radiant discussed on pp. 261–2, some recent measurements in Czechoslovakia published by Ceplecha†† are of interest. Correction for zenith attraction has been made and the list should be compared with Table 85, p. 261.

The spread in the radiant position is evident and the measurements support the conclusion of Prentice that the discrepancies cannot be due solely to errors of observation.

† Prentice, J. P. M., *J. Brit. Astr. Ass.* **63** (1953), 175.
‡ Alcock, G. E. D., and Prentice, J. P. M., ibid. 186.
§ Bouška, J., *Bull. Cent. Astr. Inst. Czech.* **4** (1953), 165.
‖ Millman, P. M., and McKinley, D. W. R., *J. Roy. Astr. Ass. Can.* **47** (1953), 237.
†† Ceplecha, Z., *Bull. Cent. Astr. Inst. Czech.* **3** (1952), 95.

APPENDIX II

Date	Radiant		No. of meteors
	α deg.	δ deg.	
1947 April 20·66	273·3±0·7	+33·0±0·7	6
1947 April 21·75	273·2±1·1	36·6±0·7	9
1947 April 21·79	272·4±0·6	34·1±1·3	8
1947 April 21·79	279·5±0·4	37·3±0·6	6
1947 April 21·79	272·5±0·9	38·3±0·7	5
1947 April 22·23	270·8±0·0	35·0±0·0	3
1949 April 22·29	277·8±0·9	32·6±0·6	14
1949 April 22·29	273·3±0·8	34·7±0·5	14

CHAPTER XIV

1. *The δ-Aquarid shower*

Rigollet† has published the results of telescopic observations of eight δ-Aquarids made in July 1951. The magnitudes range from +6 to +9, and the computed radiant positions are in good agreement with those in Table 91 (p. 272).

Lindblad‡ has discussed some implications of the short period orbit of the δ-Aquarids, particularly the temperature effects due to the closeness of approach of the debris to the sun. He also refers to the possible occurrence of gaps in the velocity distribution which he suggests might be associated with resonance effects.

Ceplecha§ has given the results of visual measurements of the radiant in Czechoslovakia as follows:

1948 July 30·34 α 337·7°±0·8°, δ −9·4°±1·0° (6 meteors).
1948 July 30·52 α 348·3°±0·8°, δ −10·5°±0·4° (6 meteors).

These results, obtained on the same night, are not in very good agreement with the coordinates quoted in Table 91 (p. 272).

2. *The Perseid shower*

Since the completion of Chapter XIV a number of important papers on the Perseid stream have been published. In particular, Miss Wright and Whipple‖ have given a comprehensive account of the Harvard photographic work on this shower which considerably extends the preliminary account of this work given in Chapter XIV. The analysis is based on 115 photographs in the Harvard series over the years 1893 to 1952 in the interval July 28 to August 24. Twenty-three meteors were photographed simultaneously at two stations and ninety-two at one station only.

The mean radiant is found to be at α 45° 56′, δ +57° 45′ (corrected) on August 12, at $\odot_{1950} = 139{\cdot}0°$. The daily motion is Δα 43′±2′, Δδ 7′±2′, in close agreement with the values given previously in Chapter XIV. Table III in this publication may be compared directly with Table 95 (p. 280) for the daily radiant position.

In the twenty-three doubly photographed meteors, eleven are used for orbital

† Rigollet, M. R., *J. des Observateurs*, **35** (1952), 170.
‡ Lindblad, B. A., *Observatory*, **73** (1953), 157.
§ Ceplecha, Z., *Bull. Cent. Astr. Inst. Czech.* **3** (1952), 95.
‖ Wright, F. W., and Whipple, F. L., *Tech. Rep. Harv. Coll. Obs.* (1953), No. 11 (Harvard Reprint Series II—47).

calculation. These include numbers 978, 1089, 1173, 1275, 1276, 1469, already listed on p. 284, together with five other later reductions (2049, 2034, 2801, 2033, 2046). Numbers 689, 1377, and 1273 in the previous list are rejected for the orbital calculations but are used with nine others for radiants, heights, and miscellaneous data. The mean apparent relative velocity v for the eleven meteors is $60{\cdot}01 \pm 0{\cdot}23$ km./sec. compared with 59·85 km./sec. from the preliminary data in Table 97 (p. 284). The 'no atmosphere' velocity $V = 60{\cdot}44 \pm 0{\cdot}21$ km./sec., the geocentric velocity $v_g = 59{\cdot}30 \pm 0{\cdot}21$ km./sec., and the heliocentric velocity $\overline{V} = 41{\cdot}29 \pm 0{\cdot}17$ km./sec.

The mean orbital elements are as follows:

Ω	ω	i	q	l/a
$138{\cdot}1° \pm 0{\cdot}5$	$151{\cdot}2° \pm 0{\cdot}7$	$113{\cdot}7° \pm 0{\cdot}3$	$0{\cdot}951 \pm 0{\cdot}003$ a.u.	$0{\cdot}048 \pm 0{\cdot}016$(a.u.)$^{-1}$

The correspondence of these elements with those of Comet 1862 III is even closer than the preliminary data quoted in Table 99 (p. 287).

Measurements of the radiant position made in Czechoslovakia in 1947 and 1948 have been given by Ceplecha.† The results of combined photographic and visual measurements in 1952 have been published by Paroubek, Šášky, and Vozárová.‡

Extensive discussions of the Perseid stream have been given by Guigay§ and by Ahnert-Rohlfs.‖ From observations in the U.S.S.R. Astapovich†† concluded that an easterly branch of the Perseid stream existed, about 7° south in declination and 10° west in right ascension from the main radiant. This branch was found to be active from 1926 August 6 to August 15 and its association with Comet 1870 I was suggested. Miss Wright and Whipple were unable to find any indication of this stream in the Harvard analysis referred to above.

CHAPTER XV

1. *The Orionid shower*

The 1953 radio-echo data for addition to Table 100 is as follows:

1953 Oct. 23 $\odot$ 209·4 deg. Hourly rate $\gtrsim 6$.

2. *The Taurid shower*

For comparison with § 2 (*b*), p. 297, the maximum rates during the Taurid epoch observed with the radio-echo equipment in the years 1951–3 are as follows:

	$\odot$ *deg.*	*Hourly rate*
1951 Nov. 7	223·7	25
1952 Nov. 7	224·5	16
1953 Nov. 8	226·2	8

3. *The Geminid shower*

The following radio-echo observations made at Jodrell Bank during the 1953 Geminid shower are given for comparison with Tables 113, 117, and Fig. 153 (*a*).

† Ceplecha, Z., *Bull. Cent. Astr. Inst. Czech.* **3** (1952), 95.
‡ Paroubek, A., Šášky, R., and Vozárová, M., ibid. **6** (1953),144.
§ Guigay, G., *J. des Observateurs*, **31** (1948), No. 1.
‖ Ahnert-Rohlfs, E., *Veroff. der Sternwarte in Sonneberg*, **2** (1952), No. 1.
†† Astapovich, I., *Bull. Obs. Corp. Astr.-Godet. Soc. U.S.S.R.* No. 19 (1933).

Date		Solar longitude ⊙	Radiant α	Radiant δ	Hourly rate
		deg.	deg.	deg.	
1953	Dec. 8	255·6	110	+30	12
1953	Dec. 9	256·7	110	33	22
1953	Dec. 10	257·7	112	33	26
1953	Dec. 11	258·7	111	33	20
1953	Dec. 12	259·7	113	34	57
1953	Dec. 13	260·7	113	33	71
1953	Dec. 14	261·7	115	30	61

CHAPTER XVI

The Giacobinid shower

As described on p. 331, an intense Giacobinid shower was observed during the afternoon of 1952 October 9 when the earth crossed the orbit 195 days ahead of the comet. From the history of the activity given in Table 125 it seemed possible that when the earth crossed the orbit 170 days behind the comet on 1953 October 9 a meteoric storm might occur. Extensive preparations were made for this event but the results were entirely negative, the rate of Giacobinid meteors being zero. The reasons for this are not yet clear, but since a great shower was observed in 1933 when the earth crossed the orbit 80 days after the comet, it seems likely that perturbations may have removed the debris further from the earth's orbit.

CHAPTER XVIII

The day-time meteor streams

The radio-echo observations, on p. 443, made at Jodrell Bank during the summer of 1953 are given for comparison with Tables 148 and 150.

CHAPTER XIX

1. *Visual determinations of the frequency distribution of the shower meteors*

The results of an investigation made in Czechoslovakia of the frequency distribution in the 1952 Perseid shower have been given by Kresák and Vozárová.† For meteors down to third apparent magnitude (zenithal magnitude +4) they find the base $\varkappa$ in equation (1), p. 384, to be 2·85. This is to be compared with the value of 2·5 for the same magnitude range obtained by Öpik (p. 384). Between zenithal magnitudes +4 to +6 Kresák and Vozárová find that the number remains approximately constant.

2. *Radio-echo determinations of the frequency distribution*

On p. 389 reference was made to a new radio-echo method for determining the mass distribution. The method involved the measurement of the height distribution and the full theory has been considered in two papers by Kaiser‡ and the practical application has been described by Evans.§ A summary of the results on the mass distribution of five major showers is given below. In all cases the range of magnitudes was from +4 to +7 (zenithal).

† Kresák, L., and Vozárová, M., *Bull. Cent. Astr. Inst. Czech.* **4** (1953), 139.
‡ Kaiser, T., *Mon. Not. Roy. Astr. Soc.* **114**, No. 1.
§ Evans, S., ibid.

Shower	*Date* 1953	*Solar longitude* ⊙	*Radiant position* α	δ	*Radiant diam.*	*Hourly rate*
		deg.	*deg.*	*deg.*	*deg.*	
o-Cetids	May 17	56·1	11	−2	3	8
Arietids	May 28	66·8	48	+24	3	11
	29	67·7	39	18	3	16
	30	68·7	48	23	3	13
	31	69·6	48	34	6	21
	June 2	71·5	43	29	3	24
	3	72·5	38	28	3	31
	4	73·4	43	25	3	40
	5	74·4	41	16	4	53
	6	75·3	46	27	3	40
	7	76·3	44	16	4	64
	8	77·3	44	25	3	54
	9	78·2	47	24	3	43
	10	79·2	47	17	3	67
	11	80·1	45	25	4	50
	12	81·1	48	24	3	37
	13	82·0	45	30	3	33
	14	83·0	46	24	4	17
	15	83·9	46	24	3	20
	16	84·9	52	25	3	23
ζ-Perseids	June 2	71·6	60	+26	3	16
	3	72·5	57	29	5	24
	4	73·5	63	25	6	34
	5	74·5	60	25	4	30
	6	75·4	62	24	3	34
	7	76·4	60	17	3	33
	8	77·3	62	23	7	29
	9	78·3	69	24	3	20
	10	79·2	66	17	7	31
	11	80·2	65	17	11	26
	12	81·1	68	28	7	26
	13	82·1	68	25	10	30
	14	83·1	72	24	12	19
	15	84·0	63	20	5	23
	16	85·0	67	17	8	13
β-Taurids	June 28	96·4	82	+14	3	24
	29	97·4	84	14	4	24
	30	98·3	96	24	3	18
	July 2	100·2	80	24	8	26
	3	101·2	87	12	4	24

Quadrantids. Observed in 1953 and 1954, the Quadrantids show a normal distribution of heights corresponding to an inverse power law of mass distribution with an exponent p in equation (2), p. 384, of 1·68.

Day-time Arietids. Observed in 1952 and 1953 the Arietids are exceptional in that the value of p in the mass law is considerably higher than the value for sporadic meteors and is of the order of 2·5.

Day-time β-Taurids. Apparently a normal shower in that the mass distribution roughly obeys a power law with an exponent $p = 1{\cdot}75$. Observed in 1953 only.

Perseids. Notable visually for the large number of brilliant meteors, the Perseids are found to have the lowest value of p observed which is 1·56. The distribution of heights is such that a moderate deviation from a power law may not produce any considerable effect. Some cut off in the mass distribution must undoubtedly occur for the brightest meteors. Results obtained in 1952 and 1953 agree closely and no marked variation has been observed during the period of the shower.

Geminids. Observed in 1951 and 1952 the Geminids have normal distribution of masses with $p = 1{\cdot}66$ during the period December 9–12. The remainder of the period, December 13–15, is characterized by a remarkable departure from a power law distribution which takes the form of a strong concentration of meteors in a range of magnitudes centred on +5. Fainter meteors appear to be considerably reduced in number.

CHAPTER XX

The Poynting–Robertson effect

Plavec† has discussed the influence of the Poynting–Robertson effect on close pairs of meteors. He considers that meteor pairs may be originally binary systems, and shows that the Poynting–Robertson effect is the most important force governing such systems. The dispersion of such pairs is shown to be very rapid and hence the occurrence of true double meteors in the earth's atmosphere is likely to be very rare. Plavec also applies these ideas to the disintegration of a meteor stream as a whole.

CHAPTER XXI

(*a*) *The structure of the Perseid meteor shower*

The evolution of the Perseid shower was discussed on pp. 428–9. Further reference to Hamid's theory has been made by Miss Wright and Whipple,‡ who compare the implications of the recent Harvard analysis with the predictions of the theory.

A discussion of the structure of the Perseid shower has also been given in two papers from Czechoslovakia.§ It is concluded that no local accumulations exist in the orbit up to a diameter of 100,000 km., except those due to random distribution. Also, excluding the general decrease of density from the centre to the borders of the stream, it is found that the distribution of meteors in the shower is random. Application of the Poynting–Robertson effect indicates that the age of the Perseid shower is about 10^7 years. This has to be compared with the age of 4×10^4 years given by Hamid (p. 429) from considerations of perturbation effects.

(*b*) *The relation between minor planets and meteor streams*

A brief discussion of the similarity between certain meteor showers and minor planets has been given by Plavec.‖ He concludes that there is no evidence that the short-period showers and minor planets have a common origin, and suggests that a general generical connexion between the two is more probable.

† Plavec, M., *Bull. Cent. Astr. Inst. Czech.* **4** (1953), 60.

‡ Wright, F. W., and Whipple, F. L., *Tech. Rep. Harv. Coll. Obs.* No. 11 (1953) (Harvard Reprint Series II—47).

§ Kresák, L., and Vozárová, M., *Bull. Cent. Astr. Inst. Czech.* **4** (1953), 128, 139.

‖ Plavec, M., ibid. **4** (1953), 195.

INDEX OF AUTHORS

Adams, J. C., 150, 337, 346, 347, 348.
Alcock, G. E. D., 4.
Allen, C. W., 432.
Almond, M., 9, 48, 212, 230, 237, 246, 252, 255, 256, 257, 265, 267, 268, 269, 272, 273, 274, 275, 276, 285, 286, 287, 294, 312, 316, 317, 318, 320, 322, 324, 325.
Appleton, E. V., 23, 27, 329.
Arago, 259.
Army Operational Research Group, 28.
d'Arrest, 353.
Aspinall, A., 65, 112, 265.
Astapowitsch, 332.

Baade, W., 275.
Backhouse, T. W., 7, 8, 9.
Baker, J. G., 17, 18, 19.
Banwell, C. J., 28, 29, 50, 329, 330, 358, 389.
Barnett, M. A. F., 23.
Bauer, C. A., 431.
Bauschinger, J., 94.
Bečvář, A., 319, 320, 321, 322.
Benzenberg, 3, 142, 259.
Beverage, H. H., 28.
Bhar, J. N., 26.
Blum, 341.
Bochníček, Z., 322.
Boothroyd, S. L., 12, 14, 130, 131, 159, 163.
Bowen, E. G., 27.
Bradley, 349.
Brandes, 3, 142, 350.
Bredikhine, T., 278, 401, 425, 429.
Breit, G., 23.
Brorsen, 430.
Brouwer, D., 420.
Bullough, K., 265.
Burland, M. S., 16.

Carroll, P., 19.
Ceplecha, Z., 9, 16, 284, 286, 287, 319, 320, 321, 322, 323, 324, 325.
Clegg, J. A., 43, 50, 55, 56, 61, 65, 76, 77, 220, 223, 225, 226, 228, 265, 320, 322, 329, 330, 358, 389, 390.
Closs, R. L., 45.
Cook, E. M., 4.
Corrigan, S. J., 353, 354.
Coulvier-Gravier, F. A., 97, **143, 144.**
Cripps, F. R., 336.
Crommelin, 327, 339.
Cunningham, L. F., 334.

Davidson, I. A., 390.
Davidson, M., 5, 92, 94, 97, 103, 191, 256, 259, 273, 326, 327, 334, 335, 414.
Davies, J. G., 9, 48, 67, 76, 78, 79, 212, 219, 230, 237, 246, 254, 316.
Denning, W. F., 3, 96, 97, 101, 102, 145, 154, 190, 249, 252, 259, 261, 266, 270, 271, 277, 278, 280, 281, 288, 290, 291, 292, 293, 297, 298, 299, 308, 310, 319, 326, 327, 340, 341, 350, 351, 352, 355, 357, 414, 415.
Dinwoodie, C., 336.
Dobson, G. M. B., 16, 198.
Dods, 332.
Dole, R. M., 265, 290, 350, 351, 355.
Downing, A. M. W., 346.
Dzubák, 321.

Eastman, 143.
Eastwood, E., 28.
Eckersley, T. L., 23, 27.
Eddington, A. S., 166.
Elkin, W. J., 14, 15, 198, 352, 354.
Ellison, 332.
Ellyett, C. D., 67, 76, 78, 79, 254, 262, 263, 316.
Emanuelli, P., 328.
Evans, S., 389, 390.

Fedinsky, V. V., 16, 198.
Fisher, R. A., 134.
Fisher, W. J., 16, 142, 143, 145, 146, 147, 148, 149, 150, 198, 249, 250, 252, 253, 254, 256, 327, 343, 350.
Flaugergues, 350.
Forbes-Bentley, 332.

Galle, J. G., 147, 154, 258, 263.
Ghose, B. N., 26.
Giacobini, 326, 335, 336, 413, 415, 428, 430.
Goodall, W. M., 23, 24, 27.
Greenhow, J. S., 46, 231.
Greg, R. P., 308.

Hamid, S., 401, 402, 420, 421, 429.
Hansell, C. W., 28.
Harang, L., 27.
Hardcastle, J. A., 92.
Hargrave, D., 163, 164.
Hawkins, G. S., 65, 112, 231, 252, 255, 256, 257, 265, 268, 272, 285, 286, 287, 294, 312, 316, 317, 318, 320, 322, 324, 325.
Heis, 350, 352.
Heising, R. A., 23, 24.
Herlofson, N., 76, 226, 230.
Herrick, E. C., 249, 259, 261, 277, 349, 350.
Herschel, A. S., 122, 154, 190, 252, 266, 286, 414.
Hey, J. S., 28, 29, 43, 50, 51, 52, 74, 75, 76, 329, 335, 358.
Hind, 353.
Hoffleit, D., 16, 21, 198, 200, 201, 203, 207, 282, 294, 344.
Hoffmeister, C., 1, 8, 9, 97, 103, 104, 105, 106, 107, 108, 118, 119, 122, 131, 132, 141, 142, 143, 144, 145, 146, 147, 149, 150, 152, 153, 246, 247, 249, 257, 264, 265, 266, 267, 269, 270, 272, 273, 274, 293, 294, 295, 297, 305, 308, 309, 311, 376, 424, 428.
Hogg, F. S., 343.
Hughes, V. A., 265, 320, 322, 358.

Hulst, H. C. van de, 432, 433, 434.
Humboldt, 337, 339.
Huruhata, M., 342.
Huygens, 40.

Ingram, L. J., 27.
Ito, Y., 26.

Jacchia, L. G., 16, 21, 22, 205, 208, 209, 210, 257, 262, 282, 284, 295, 296, 315, 316, 329, 331, 333, 344, 386, 387.
Jones, L. F., 28.

Kaiser, T., 45, 389, 390.
King, A., 190, 280, 290, 308, 310, 311, 312, 328, 332, 334, 341, 342.
Kirkwood, D., 150, 256.
Kleiber, J. A., 146.
Klinkerfues, W., 349, 354.
Kopal, Z., 16, 329, 331, 333, 334, 386, 387.
Knabe, 133.
Knopf, 150, 151, 297, 503.
Krafft, 350.

Lane, J. H., 15.
Laplace, 94.
Larmor, J., 402, 403.
Lindblad, B. A., 271, 274, 275.
Lindemann, F. A., 16, 198.
Lovell, A. C. B., 9, 28, 29, 43, 48, 50, 76, 77, 97, 212, 230, 237, 246, 265, 320, 322, 329, 330, 358, 388, 389.

McCrosky, R. E., 19.
McIntosh, R. A., 264, 265, 266, 267, 269, 270, 271, 272, 273, 274, 275, 291, 295.
McKinley, D. W. R., 52, 53, 54, 73, 74, 75, 76, 82, 85, 132, 237, 238, 239, 240, 241, 242, 243, 244, 245, 246, 262, 263, 268, 273, 274, 284, 285, 316, 390.
Malzman, 332.
Maltzev, V. A., 145, 146, 147, 150, 310, 311, 312, 315, 317, 423.
Manning, L. A., 74, 76, 82, 284, 285.
Maris, H. B., 24.
Marsh, 308.
Masterman, S., 252.
Mercer, K. A., 28.
Milligan, 332.
Millman, P. M., 16, 21, 52, 53, 54, 73, 74, 75, 76, 132, 133, 135, 198, 200, 201, 203, 207, 262, 263, 282, 294, 329, 331, 333, 334, 344, 386, 387, 390.
Mindhara, T., 26.
Mitra, S. K., 26.
Montagne, 349.
Mourant, 332.

Nagaoko, H., 24.
Naismith, R., 23, 27, 329.
Newton, H. A., 3, 86, 150, 259, 264, 270, 337, 345, 346, 350, 351, 352, 353.
Niessl, G. von, 103, 141, 142, 143, 144, 145, 146, 147, 149, 150, 151, 153, 428.
Nielsen, A. V., 92, 154.

Olivier, C. P., 1, 4, 12, 16, 86, 94, 96, 97, 188, 189, 198, 203, 247, 259, 264, 265, 267, 268, 269, 270, 276, 280, 290, 295, 315, 337, 339, 341, 350, 353, 355, 357, 425.
Olmsted, D., 3, 86, 337, 341.
Olmsted, M., 202, 253, 343.
Öpik, E. J., 1, 2, 6, 7, 9, 10, 11, 12, 13, 106, 124, 128, 130, 131, 132, 136, 154, 155, 156, 157, 158, 159, 160, 161, 163, 164, 165, 166, 167, 169, 170, 171, 173, 175, 177, 178, 179, 181, 183, 184, 185, 186, 187, 188, 189, 193, 195, 196, 197, 201, 207, 210, 233, 234, 246, 247, 249, 277, 279, 280, 384, 385, 386, 410, 411, 431, 433, 434.

Pape, C. F., 258, 263.
Parsons, S. J., 74, 75, 76, 329, 335.
Peterson, A. M., 76, 82, 284, 285.
Peterson, H. O., 28.
Pickard, G. W., 26.
Piddington, J. H., 27.
Pierce, J. A., 27, 28, 50.
Plavec, M., 423, 424.
Pokrovsky, 257.
Pons, 349, 354.
Porter, J. G., 4, 5, 6, 12, 86, 94, 95, 154, 188, 189, 190, 191, 192, 193, 195, 196, 266, 273, 282, 294, 296, 302, 315, 328, 337, 344, 352, 356, 398, 414.
Poynting, J. H., 271, 402, 403, 405, 406, 407, 408, 409, 410, 412, 431, 434.
Prentice, J. P. M., 1, 4, 12, 28, 29, 96, 103, 110, 111, 188, 189, 190, 250, 251, 252, 253, 260, 262, 273, 280, 281, 282, 288, 289, 290, 291, 292, 293, 294, 319, 320, 322, 327, 328, 331, 332, 350, 352, 354, 358.
Prior, 143.

Quäck, E., 26.
Quételet, A., 249, 277, 350.

Raillard, 350.
Richter, N., 328, 384, 385, 386.
Rigollet, R., 251, 275.
Robertson, H. P., 271, 402, 403, 404, 405, 406, 407, 408, 409, 410, 412, 431, 434.
Roy, de F., 328, 329, 331, 332, 384, 385, 386.
Russell, H. N., 260.
Ryves, 332.

Sandig, H., 328, 384, 385, 386.
Schaeberle, 203.
Schafer, J. P., 23, 24, 27.
Schiaparelli, G. V., 3, 86, 94, 96, 99, 101, 102, 103, 110, 118, 120, 122, 277, 286, 287, 337, 345, 346, 347, 413, 425.
Schmidt, 96, 97.
Schulhof, 429.
Schwarzman, 332.
Shaine, 257.
Shapley, H., 12.
Skellett, A. M., 24, 27.
Smith, F. W., 356.

Stanjukowitsch, K. P., 16, 198.
Stewart, G. S., 28, 29, 43, 50, 51, 52, 74, 75, 76, 329, 335, 358.
Stoney, G. H., 337, 346, 348.
Svoboda, J., 295.
Syam, P., 26.
Sytinskaja, H. N., 21, 332.

Taylor, A. H., 27.
Thomson, M. M., 16.
Torwald Køhl, 143, 144.
Turner, 202.
Tuve, M. A., 23.
Twining, A. C., 3, 86, 280, 308, 337, 341.

Vanýsek, V., 322.
Villard, O. G., 76, 82, 284, 285.

Walmesley, 332.
Wartmann, 249.
Waters, H. H., 16.
Watson, F., 4, 14, 123, 124, 125, 129, 130, 131, 132, 135, 136, 137, 138, 139, 151, 152, 153, 274, 328, 351, 384, 385, 386.
Watson-Watt, R. A., 27.
Webb, 350.
Weiss, E., 258, 263, 353.
Wells, R. C., 19.
Wenz, W., 256.
Whipple, F. L., 1, 2, 16, 17, 19, 20, 104, 202, 203, 204, 205, 206, 207, 209, 210, 211, 240, 241, 256, 257, 281, 282, 284, 286, 287, 297, 298, 299, 300, 301, 302, 303, 304, 306, 307, 308, 311, 312, 313, 315, 316, 317, 318, 377, 382, 383, 401, 405, 406, 407, 408, 409, 412, 415, 416, 418, 419, 420, 421, 422, 423, 425, 426, 427, 428, 429, 430, 431.
Whitney, W. T., 16.
Wilkins, A. F., 27.
Williams, J. D., 133, 134, 135.
Wilson, F., 252.
Wilson, R., 163, 164, 183.
Winnecke, 354.
Wolf, C., 96, 97.
Wright, F. W., 297, 298, 299, 300, 301, 302, 303, 304, 307, 343, 344, 346, 421.
Wyatt, S. P., 405, 406, 407, 408, 409, 431.
Wylie, C. C., 150, 329, 330, 331.

Yagi, 38, 39, 41, 67.
Yamamoto, A. S., 408.
Yarkovsky, 410, 411, 412.
Young, L. C., 27.

Zenker, 15.
Zeziolo, 350, 352.

INDEX OF SUBJECTS

References in italics are to pages on which figures are given, while those with an asterisk are to pages on which the information is contained in tables

aberration, diurnal, 92–93.
accordance, defined, 190.
accordances: duplicate, reduction of, 191–3; multiple, reduction of, 191–2.
aerial arrays, 37–39.
— coverage, 222.
— power gain, *see* power gain.
— system: collecting area, defined, 56, effective, *56*, of Jodrell Bank equipment, 227*, and radiation pattern of aerial, 56; elevation of, for measuring velocity, 212; electronic switching of, 41; of Jodrell Bank, 67, Pl. ii, 212–13, 227*; used in observation, 35–41, 67; for measuring velocity, 212–13.
aerials: directional characteristics, 222; lobes, side, 38–39, effect of, 235; radiation pattern of, and collecting area of aerial system, 56; reciprocity theorem and, 36; sensitivity contours of, 58.
— types: broadside arrays, 38–39.
— — dipole, half-wave, 39, 237, centre-fed, 36–37.
— — narrow-beam: for measuring velocity of sporadic meteors, 212–37; collecting area of, 223–8.
— — single directional: summer day-time streams investigated by, 359–63, their radiants determined by, 368, their velocities measured by, 372, 374.
— — wide-beam: for measuring velocity of sporadic meteors, 237–46.
age of showers, 397.
AI patrol camera, 17, 202, 209, 210.
amplitude variation-time methods for measuring meteor velocity, 73, 76–85.
— variations of scattered echoes, 78–79.
Andromeda meteors, movement in orbit of Biela's comet, 363–4.
angular velocity: calculation of, 155, 156; correction to rocking mirror method, 156*; correlation between height and, 164; distribution of, 105–6; measurement of, 12, by use of rotating shutters, 14; observed waves and, 182; reduction to zenithal angular velocity, 182; of shower meteors, *184*.
— — zenithal: angular velocity reduced to, 182; relation between height and, 157*.
'anomalies', 87, *88*.
antapex: defined, 213; experiments, 213, 223, 228, 230, 232, 234.
Anteros, 430*.
apex: defined, 213; experiments, 213, 223, 228, 230, 232, 233–4, 235, 237.
Apollo, 423, 430*.
apparent density of radiants, working formula for, 171.
— velocity of meteor, defined, 90.
δ-Aquarid shower, 270–5; activity, 270–1; classification, 249*; cometary association, 275, 422; geocentric velocity, 273; heliocentric velocity, 273; hourly rates, 270–1; shower length, 428*; orbit, 274–5, 276*, 380, elements of, 275*; origin, 424; radiants, 52, 272–3; radiant coordinates, 272*, 440; radiant positions, 440; time of occurrence, 249*, 270; velocities, 273–4.
— — (1952), 274.
η-Aquarid shower, 175, 263–9, 288, 295–6, 358; activity, 264–5, 359, 366*; breadth of stream, 265; classification, 249*; comet associated with, 264, 269, 413*, 414, 415*, 422; hourly rates, 263–4, 265*; shower length, 428*; orbit, 268–9, elements, 267*, 269; periodicity, 269; radiants, 265–6; radiant coordinates, 266*, 370*, 371*; radiant position, 370*, 371*; time of occurrence, 249*, 263, 265; velocities, 266–8.
area of visibility, effective, for meteors of different magnitudes, 129*.
argument of perihelion, defined, 87.
Aries, radiants in, *see* Arietid (night-time) shower.
Arietid (night-time) shower, 275, 296–308; activity, 297–8; geocentric velocity, 303; heliocentric velocity, 303; hourly rates, 297, 367; orbit, 303–8, elements, 304*; origin, 421; radiants, 298–301; radiant position, 300–1; velocities, 302–3.
α-Arietid shower, 299; radiants, 298*.
δ-Arietid shower, 413*.
ε-Arietid shower, 299; radiants, 298*.
ζ-Arietid shower, radiants, 298*.
σ-Arietid shower, radiants, 298*, 299.
northern Arietid shower, 299.
southern Arietid shower, 299, 300, 302*; origin, 421.
Arietid summer day-time stream, 359, 443; activity, 363, 366*, 443*; classification, 359; cometary association, 422*; mass brought into earth's atmosphere by, 394; orbit, 378, 379*, 380, density and mass of

particles in, 395*, elements, 379*; origin, 424; radiant coordinates, 370*, 371*; radiant positions, 370*, 371*; velocities, 373*, 374–5, 377*.
Arizona expedition, 1, 7, 130, 152, 155; meteor streaming observed by, 171; velocity measurements by, 163–81, of Öpik and of Boothroyd, 159–63, Öpik's analysis compared with Porter's British analysis, 195–7; visual techniques of, 10–14.
arrays, *aerial*, 37–39, 67.
'artificial meteors', 9, 104.
asteroids: orbits, 430*; Anteros, 430*; Apollo, 423, 430*; Eros, 423; 1937 UB, 430*.
astronomical notation, 436.
astronomy, meteor, beginnings of scientific interest in, 337.
— radio, techniques, 1.
atmosphere, earth's: mass, meteoric, entering, 135–8, 390–4; mass and energy brought into, by sporadic meteors, 138*; paths of meteor showers in, 248; velocity of Perseids affected by, 282.
— upper, meteor heights and, 2.
atmospheric absorption, effect on magnitude of, 6.
attention, coefficient of, 8.
attraction, earth's, and meteors, 90, 142, 175.
θ-Aurigid stream: activity, 367*; geocentric velocity, 372; heliocentric velocity, 372; orbit, 377; radiant coordinates, 370*; radiant position, 370*; velocity, 377*.

beam, aerial: direction of, for measuring velocity, 213; shape, range-time relationship of radio echoes and, 56; width, and radiant position, 52.
beat frequency for continuous wave method, 32; and range accuracy, 35.
Bečvář's stream, 319–25.
Bielid (Andromedid) shower, 288, 326, 349–54; activity, 349–51; classification, 249*; comet associated with, 349, 353–4, 413*, 414, 415*; hourly rate, 350*, 351; shower length, 351, 428*; orbit, 353–4, elements, 354*; periodicity, 351; radiants, 351; radiant coordinates, 351*; time of occurrence, 249*, 351; velocities, 351–3.
Boltzmann's constant, 47.
Boothroyd, Arizona results of, 159–63.
British meteor data on velocity of sporadic meteors, Porter's analysis, 190–7.

Cambridge, Mass., 17, 202, 209.
cameras: AI patrol, 17, 202, 209, 210; copying, 19; double camera technique, 14, 202–11, 439; FA patrol, 17, 202, 209, 210; used in Harvard techniques, 16–20; KA, 209; KB, 209; Ross Xpres, 17, 20*; rotating shutter, 14, 16, 17, 19–20, measurement of velocity by, 198; Schmidt, 14, 20*; super Schmidt, 17, 18–20, *18*, 20*, 210–11.
α-Capricornid stream, 270.
cathode-ray tube in radio-echo observation, 30, 31, 41–43.
Cauchy's approximations for Fresnel integrals, 80.
o-Cetid stream: activity, 366*, 443*; cometary association, 422*; orbit, 377–8, elements, 379*; origin, 424; radiant coordinates, 370*, 371*; radiant positions, 370*, 371*; velocity, 374, 377*.
Clegg method of measuring meteor radiants, 55–73.
coefficients: attention, 8; perception, 8.
collecting area of aerial system, *56*, 227*; defined, 56; effect of electron density on, 226; limits of, 59; and mass of meteor, relationship between, 57–58; power gain, 44, 49.
— — of narrow-beam aerials, 223–8.
— — of an observer, estimation of, 9, 10*.
— — for telescopic observations, *124*.
colour correction for photometric magnitudes, 22.
cometary index, variation of, *121*, 122.
comets: meteor showers associated with, 413–24, *see also separate showers and streams*; meteor showers having no association with, 414, 415*; meteor streams formed from, 424–9; meteoric material ejected from, 401–2; orbits, 430*, identification with orbits of meteor streams, 413–14; Whipple's model, 425–8, 429.

COMETS:

Biela (1852 III), 257, 349, 350, 353*, 354, 413*, 415*, 428*, 430*.
Blanpain (1819 iv), 415*.
Brorsen I, 430*.
d'Arrest, 426.
Denning (1881 v), 415*.
Encke, 297, *306*, 307, 308, 318–19, 383, 413*, 415–21, 426, 428*, 430*; perturbations for, 416*.
Finlay, 415*.
Giacobini–Zinner, 335, 336*, 413*, 415*, 428, 430*.
Grigg–Mellish (1907 II), 415*.
Grigg–Skjellerup, 415*, 430*.

COMETS (*cont.*):
Halley, 264, 268, 269, 288, 295, *296*, 408, 413*, 415*, 422, 428*; estimated mass of, 425.
Kozik–Peltier (1939*a*), 257, 413*, 422,
Lexell (1770 I), 415*. [439.
Mellish (1917 I), 415*.
Pons–Winnecke, 349, 354, 413*, 415*.
Schwassmann–Wachmann, 415*.
Temple, *see* 1866 I.
Tuttle: I, 439; (1926 iv), 415*; (1939k), 324, 413*.
Wolf, 426.
1680, 423.
1743 I, 415*.
1860 I, 257.
1861 I, 259, 260, 263, 413*, 415*, 428*; orbital elements, 263*.
1862 III, 277, 286, 287, 413, 413*, 415*, 428*, 428–9.
1866 I (Temple), 337, 346, 347*, 400, 413, 413*, 415*, 428*; orbit, 347*.
1870 I, 441.
1900 III, 326, 327, 331.
1933 III, 428*.
1948 n, 275.
components, meteor: directly moving, 119; ecliptical, 104, 106; hyperbolic, 103, 119, 210, 213, 246; interstellar, 104, 424; meteor, sporadic, origin of, 246; solar, 210; velocity, transverse heliocentric, 183*.
computation of orbit: of a meteor, 54, 94–95; of meteor streams, 248.
constants: Boltzmann's, 47; gravitational, 89, 91, 141, 398.
continuous-wave technique for observing diffraction pattern, 79–85; for measuring velocity, 32, 35, 82–85, 237–46.
— — — with frequency modulated for radio observation, 31–32.
— — diffraction technique, velocity of Geminids determined by, 316–17.
corrections for: deceleration, 240–1; diurnal motion, 240; lens distortion, 202; photometric measurements of magnitude, 21–22; velocity, angular, in rocking mirror method, 156*; zenithal attraction, 240–1.
cosmological relationships of meteors, 413–34.
counting of meteors, 7–10.
critical aspect effect of meteor trails, 50.
cross-bearings for observing paths, 191.
cross-section for scattering, formula for, 43.
curve-fitting method of measuring meteor velocity, 75.
Cygnid stream, 270.
daily frequency of sporadic meteors, 131, *132*.
data, reduction of, for photographic plates, 20–22.
debris, dispersion of, 397–412.
deceleration: correction for, 240–1; effect of, 234; measurement of, 73, 75, 76.
December Ursids, *see under* Ursids.
declination, effect of, 171.
— of radiant, determination of, 63, 65, 67–68.
density: electron, 225; conversion to visual magnitudes, 230–2; effect on collecting area, 226.
— distribution of meteors, von Niessl's expression for, 103; relation between height and, 203, 204.
— of particles in orbits of shower meteors, 394–6.
— of radiants: apparent, working formula, 171; surface, 169.
— space, per magnitude group, 384.
detector, type of, and signal obtained, 80.
determination: of declination of radiants, 63, 65, 67–68; of radiant coordinates, 63–65; of right ascension of radiants, 63.
differential refraction, 202.
diffraction from a line source, radio-echo production in terms of, 73.
— pattern: continuous wave technique for observing, 79–85; Fresnel, 237; of radiants, 438; of reflected waves, 78–79; of trail, Pl. iii.
— photographs, use of, to estimate errors in velocity measurements, 214.
— theory, and radio echoes, 74, 76.
diffusion, equation for, 166.
dipoles: centre-fed half wave, 36–37; half wave, aerial, 39, 237; power gain expressed in terms of, 44; Hertzian, 36, 37.
directivity, 36, 38, 39.
directly moving component, 119.
— — meteors, 118.
dispersion, theory of, 397; observational error and velocity, 184; maximum-error, 185.
dispersive effects in meteor streams, 397–412.
display system of radio-echo observation, 41–43.
distribution: frequency, *see under* frequency; mass, *see under* mass; of projection ratios, 173, 174*; space, *see under* space; true, equation for, 166; of velocities, angular, 105–6, geocentric tangential, 168*, heliocentric, 175–9, 180*, 181*, 234; space, 173–5, 175*–6*, Öpik's calculations, 167–81.

diurnal aberration, 92–93.
— distribution of sporadic meteors, 96–122, *97*; Hoffmeister's investigations, 103–8, *107*, *119*; compared with Schiaparelli's theory, 101–2, 103.
— motion, corrections for, 240.
— rotation of the earth, effect of, 112.
— variation in meteor rates, 8–9, 28.
— — of mean hourly rates of radio echoes, 51.
Doña Ana, 17, 209.
Doppler method: 'fast Doppler', 85; 'slow Doppler', 82–85; velocity of Perseids measured by, 284–5.
Doppler whistle, 74; defined, 80 n.
double-camera technique, 14, 202–11, 439; Jacchia's analysis of data, 208–9; velocity distribution determined by, of Geminids, 315*, of Lyrids, 262, of Orionids, 295, of Perseids, 282, 284.
double-count method, 7–8.
double station technique, velocities of Leonids determined by, 346*.
Draconid meteor showers, *see* Giacobinid shower.
drag, tangential, 402.
duplicate observation, 3.
duration: formula for, 183; of shower meteors, *184*.

E region: effect of meteors on, 23, 24–28; electron density of, 23, 26.
earth: atmosphere of, velocity of meteor in, 90–91, energy and mass brought into, by sporadic meteors, 138*; attraction of, and meteors, 90, 142, 175; attractive force of, 398; diurnal rotation, effect of, 112; mean distribution of sporadic meteors round, *118*; modulation of sporadic orbit round orbit of, *121*, 122; number of meteors falling to, 225; orbital velocity of, 175; perturbations due to, 423*.
ecliptic latitude, distribution of sporadic meteors in, 110.
ecliptical component, 104, 106, 424.
— meteors, 108.
ejection of meteoric material, 401–2; radius, 428; velocity, 401, 429.
electron density of E region, 23, 26.
— — of meteors, 225; conversion to visual magnitudes, 230–2.
— — in meteor trail, 44–46, 57; effect on collecting area, 226.
— line density, 388.
electronic switching of aerial systems, 41.
elongation of the radiant: height and, 193; height, velocity, and, 193–5; velocity and, 195, *196*; velocity, geocentric, and, 213.
— of true radiant, 93–94.
energy brought into earth's atmosphere by sporadic meteors, 138*.
equations of meteoric motion, 86–95.
Eros, 423.
evaporation of meteors, 2, 136; rate, 389.

FA patrol camera, 17, 202, 209, 210.
'fast Doppler' method, 85.
fatigue, effect of, 105.
field correction for magnitude obtained by photometric measurement, 22.
fireballs: day-time meteors observed as, 307; defined, 142; duration, 147; heights of appearance and disappearance, 146, *147*; heliocentric velocity, 146*; hyperbolic velocity, 142, 143, 148; path lengths, 148, *148*, *149*; periodicity of, 143, *144*; radiants, 143, *145*; apparent radiants, 150, 151, *152*; concentration of radiants, 153; true radiant, 151. From Draco radiant (1926), 327–8, 332; of 1933, 334.
— catalogue, von Niessl–Hoffmeister, 142–54.
Fraunhofer component, 432, 433.
frequency: of different magnitudes, 129–30; of meteors, Williams's analysis, 133–5; of projection ratios, 167–73.
— daily, of sporadic meteors, 131, *132*.
— distribution of meteors, 130–5, 384–90, 442–3; radio-echo techniques and, 135, 388–90. Of Geminid (1946), 389; Giacobinid (1933), 386*, (1946), 386–8, 389; Leonid (1933), 386; Perseid, 386; Quadrantids (1947), 389; of shower meteors by visual observation, 384–8.
Fresnel diffraction pattern, 237.
— integral, 45, 77; Cauchy's approximations for, 80.
— zones, 49, 79, 214, 438; oscillations, 35; pattern, 48, 388.

galactic noise, 47, 48.
Geminid shower, 147, 148, 189, 202, 237, 308–19, 444; activity, 308–10, 441–2; classification, 249*; cometary association, 422*, 422–3; heliocentric velocity, 316; hourly rate, 308–10, *363*, 441–2; shower length, 428*; life of, 424; orbit, 308, 317–19, 422–4, density and mass of particles in, 395*, elements, 317*; origin, 423, 424; particle sizes, separation of, 409; radiant, 310–14; radiant coordinates, 311*, 312*, 313; radiant position, 310–14; time of occurrence

249*, 308; velocity, 238–43, 315–17, distribution, *240*.
Geminid shower (1946): frequency distribution, 389; magnitude, 387*, 388*.
— — (1947), 53.
— — (1949), 69, 214, 220; velocity distribution, *218*.
— — (1950), 69.
— — (1953), orbit determined by radio-echo technique, 438.
λ-Geminids: activity, 367*; radiant co-ordinates, 370*; radiant position, 370*.
ν-Geminids: activity, 367*; radiant co-ordinates, 370*; radiant position, 370*.
geocentric velocity of meteor, 142, 145, 241; calculation of, 220–2; defined, 90; standard deviation, 255; relation between elongation of meteor radiant and, 213; formula, 221; relationship with solar longitude, 302–3; relation between zenithal magnitude and, 180*. δ-Aquarids, 273; Arietid, 303; θ-Aurigid, 372; Bielids, 352; Leonids, 344; 54-Perseids, 372; Quadrantids, 256, 439; Taurids, 303; *see also separate showers and streams*.
— — parabolic, 273.
— tangential velocities, distribution of, 168*.
Giacobinid (Draconid) shower, 288, 326–37; activity, 327–32; age, 397; classification, 249*; comet associated with, 326, 332, 335–7, 413*, 414, 415*; hourly rate, 327, 328, 330, 331; shower length, 328, 428*; magnitude, 328; orbit, 335–7, density and mass of particles in, 395; particle sizes, separation of, 409; radiants, 332–4; radiant coordinates, 326, 332, 334; radiant position, 327, 332; recorded in day-time by radio-echo technique, 326, 327, 331; time of occurrence, 249*; velocity, 326, 334–5.
— — (1933): frequency distribution, 386; magnitude, 384–5.
— — (1946), 16, 29, 74, 76; frequency distribution, 386–8, 389; shower length, 329; magnitude, 387*, 388*; mass brought into earth's atmosphere by, 394.
— — (1952), 331, 442.
gnomic projection, effect on Great Circle by, 19.
gravitational constants, 141, 398; for velocity of meteor in its orbit, 89, 91.
Great Circle, effect of gnomic projection on, 19.

Harvard collection of photographic plates, 14, 143, 299, 311.
Harvard techniques for meteor photography, 16–22, 198–211, 440–1.
height of fireballs, 146, *147*.
— meteor, 3; correlation between angular velocity and, 164; in upper atmosphere measurements, 2; data, source of, 3; relation between density and, 203, 204; determination of, 202–3; ionization varying with, *226*; of hyperbolic meteors, 197; meteor, shower, average, 193, 194*; meteor, sporadic, average, 193, 194*; observation of, 10–12; radiant, elongation, and, 193; and radio-echo range, 61; relation between velocity and, 2, 194*; relation between velocity, elongation, and, 193–5; relation between zenithal angular velocity and, 157*.
— mean, shower meteors, 195; sporadic meteors, 195; use of, 155, 156.
heliocentric velocity of fireballs, 146*.
heliocentric velocity, 104, 106, 141, 142, 316; relation between concentration of meteors and, 234; defined, 90; distribution of, 175–9, 180*, 181*, 234. Arietid, 303; θ-Aurigid, 372; Leonid, 344; 54-Perseid, 372; Taurid, 303; *see also separate showers and streams*.
— — parabolic, 234.
— — projected, distribution of, 159–62.
— space velocities for sporadic meteors, *187*.
— tangential velocity, relation between zenithal magnitude and, 188*.
Herschel's determination of radiant co-ordinates of Perseid shower, 286.
Hertzian dipole, 36, 37.
Hey and Stewart method of measuring meteor radiants, 50–52.
Hoffleit's and Millman's photographic measurements of velocity, 198–201.
Hoffmeister's investigation of diurnal variation, 103–8, *107*, *119*, 247.
— von Niessl–, fireball catalogue, 142–54.
hyperbolic meteor component, 103, 119, 210, 213, 246.
— shape of radio echo, 54, 73, 75, 76.
— stream in Taurus, 146, 150.
— velocity of fireballs, 142, 143, 148.
— — of meteors, 103, 108, 118, 130, 196, 201, 207, 209, 210, 233, 246, 247.

Icarus, minor planet 1566, 275.
infra visual meteors, 11, 13.
intensity of reflected wave, formula for, 78.
intensity-modulated range-time display, *42*, 73, 82, 85; radio echo photographed on, Pl. i; trace, 82.

interplanetary particles, velocity of, and formation of meteors, 433.
interstellar clouds, velocity of, 141.
— component, 104, 424.
— origin of sporadic meteors, 141.
— particles of matter: masses of, 139; radii of, 139; velocity of, in solar system, 141.
— space, density of matter in, 139.
— streams, 143, 146, 150.
ionization: by meteors, 23, 24–28, *25*, 230, 245; at head of a meteor, 74, 438; according to height of meteor, *226*; and return of radio echo, 73.

Jacchia's analysis of double-camera data, 208–9.
Jodrell Bank Experimental Station: radiant survey apparatus at, 65–73, *66*, Pl. ii; radio-echo techniques for measuring velocity of sporadic meteors, 212–37. Giacobinids, observation of, 329; δ-Aquarid velocities measured by, 273–4; Perseid velocities measured by, 285–6. Investigation of summer day-time streams at, 358–83.
Jupiter: attractive force, 397; orbit of, perturbations due to, 308; perturbations due to, 346, 354, 356, 397, 398, 400, 416, 423, 429; sweeping action of, 434.

Lacertid stream, 270.
lens distortion, correction for, 202.
Leonid shower, 147, 148, 175, 288, 337–48; activity, 338–40; classification, 249*; comet associated with, 337, 346, 400, 413, 413*, 414, 415*, 428*; frequency distribution of, 386; geocentric velocity, 344; heliocentric velocity, 344; hourly rates, 338, 339*, *340*; orbit, 345–8, Schiaparelli's determination of, 337, 345–6; periodicity, 337, 338; radiants, 340–4, path of, *345*; radiant coordinates, 341, 342*, 343; radiant position, 341, 342*; time of occurrence, 249*; velocities, 344–5, 346*.
— — (1833), 3, 4, 86.
— — (1931), 24.
— — (1932), 16, 24, 26.
— — (1933), 16; frequency distribution of, 386.
— — (1940), 27.
longitude of perihelion, 87.
— solar, relationship with geocentric velocity, 302–3.
— distribution of sporadic meteors, 110, 120.
luminosity: distribution in Perseid shower, 384, 385*; magnitude error and, 193; relation between mass, velocity, and, 136; relation between meteors seen and, 7; relation between velocity and, 108, 179–81, 187, 210; and zenithal magnitude, 6.
Lyrid shower, 147, 175, 258–63; activity, 259–61; age, 400; classification, 249*; comet associated with, 259, 260, 263, 413*, 414, 415*; hourly rate, 259–60; shower length, 428*; orbit, 263, elements, 263; periodicity, 259; radiants, 261–2; radiant coordinates, 261, 440*; radiant position, 259, 262, 439; time of occurrence, 249*, 259; velocities, 262–3.
— — (1922), 260–1.
— — (1946), 29.

McKinley's measurement of meteor velocities, 237–46.
— and Millman's method for measuring meteor radiants, 52–55.
magnitude: atmospheric absorption and, 6; estimate of, from comparing visual and radio-echo rates, 231–3; observer's field and, 7; field of vision as a function of, 8; frequency of different, 129–30; proportional to logarithm of intensity, 135; relation between line density and, 46; mass to be attributed to a given, 136, and, *137*; measurement of, use of photometry for, 21–22; number of meteors of given, calculation of, 232; relation between change of number and, 384; and number of meteors observed, 123; observed, correction to zenithal, *131*; range of, 230–3, relationship between power gain and, 49; effect on velocity distribution of, 237; visual, conversion of electron density to, 230–2; zenithal, defined, 6, relation between geocentric velocity and, 180*, relation between heliocentric tangential velocity and, 188*, and luminosity, 6. Giacobinid, 328, (1933), 384–5, (1946), 387*, 388*.
— correction, 6–7, 6*, scale, 128.
— error, and luminosity, 193.
magnitude function, 8.
— group, space density per, 384.
— scales, correlation of naked eye and telescopic observations, 128*.
magnitudes, stellar, 6.
map plotting of observed paths, 3, 4, 190.
Mars: attractive force, 398; orbit of, Taurids and, 307; perturbations, 423.
mass, meteoric: in earth's atmosphere, 135–8, 390–4; magnitude and, 136, 137*;

in meteor streams, 425; relationship between velocity, luminosity, and, 136.
mass of Perseid meteors of second magnitude, 136.
— of particles in orbits of shower meteors, 394–6.
mass distribution of meteors, 135–8; determined by Kaiser and Evans, 389–90; relationship between echoes recorded and, 49.
— — of shower meteors, number and, 384–96.
matter, density of, in interstellar space, 139.
— meteoric, density of, in solar system, 139.
mean heights, use of, 155, 156.
Mercury: attractive force, 398; orbit of, Taurids and, 307.
meteoric mass entering earth's atmosphere, 135–8, 390–4.
— material: ejection from comets of, 401–2; total mass of, in orbits, 425.
— — ejected, 401–2; radius, 428; velocity, 401, 429.
— motion, fundamental equations, 86–95.
meteorites, 2, 138, 154; micro-, 2; Pultusk, 154.
meteor(s): activity, variation in, *391*; 'artificial', 9, 104; close-pairs of, 444; components, *see under* components; cosmological relationships of, 413–34; counting of, 7–10; density distribution of, von Niessl's expression for, 103; directly moving, 118; ecliptical, 108; effect on E region by, 23, 24–28, *25*; earth's attraction and, 90, 142, 175; evaporation, *see* evaporation; formation of, velocity of interplanetary particles and, 433; heights, *see* heights; hyperbolic, frequency, 180*, height of, 197; and ionization, 23, 24–28, *25*, 74, 230, 245; densely ionizing, 73, 74, 82, 224 n.; infra visual, 11, 13; of given magnitude, observed, calculation of, 232, *see also* magnitude; mass, relationship between collecting area and, 57–58, *see also* mass; number of, falling to earth, 225, relationship between radio echo and visual totals, 358; hourly number of, relation between radio echo rates and, 223; true number of, falling on a square kilometre, 232; observation of, by radio techniques, 1, 30–49; observation, probability of, of different classes of, 125–6; orbit, *see* orbit; path length, *see* path length; photography of, *see* photography; physics, 2; radiants, *see* radiants; correspondence between radio echoes and, 28–30; radio waves propagated by, 24–28; rates, *see* rates; streaming observed in Arizona expedition, 171; structure of, 444; zodiacal light and, 432–4; velocity, *see* velocity.
— showers of: age of, 397; classed as summer day-time streams, 359, 366*–7*; comets associated with, 413–24; having no associations with comets, 421–4, 422*; frequency distribution determined by radio echo, 388–90; major, 248–383; naming of, 248, 249*; occurrence of, 248; orbits of, computation, 248, mass and density of particles in, 394–5; origin of, 401; particles in, disappearance of, 390; paths of, 248; radiant position of, defined, 248; *see also the various named showers.*
— streams of: daylight, 1, *see also* summer day-time streams; dispersive effects in, 397–412; formation of, 401, 424–9, Schiaparelli on, 425; intensity, 172*; lost, 349–57; total mass of meteoric material in, 425; orbit, computation of, 86–95, identification with orbits of comets, 413–14; periodic, 326–48; permanent, defined, 248, (January to July) 248–69, (July to August) 270–87, (September to December) 288–325; perspective and, 56; planetary origin of some, 424; and minor planets, 444; width of, 402; *see also the various named streams.*

METEORS, SHOWERS AND STREAMS

δ-Aquarid shower, 270–5; activity, 270–1; classification, 249*; cometary association, 275, 422; geocentric velocity, 273; heliocentric velocity, 273; hourly rates, 270–1; shower length, 428*; orbit, 274–5, 276*, 380, elements of, 275*; origin, 424; radiants, 52, 272–3; radiant coordinates, 272*, 440; radiant positions, 440; time of occurrence, 249*, 270; velocities, 273–4. (1952), 274.
η-Aquarid shower, 175, 263–9, 288, 295–6, 358, 359, 366*; activity, 264–5, 359, 366*; breadth of stream, 265; classification, 249*; comet associated with, 264, 269, 413*, 414, 415*, 422; hourly rates, 263–4, 265*; shower length, 428*; orbit, 268–9, elements, 267*, 269; periodicity, 269; radiants, 265–6; radiant coordinates, 266*, 370*, 371*; radiant position, 370*, 371*; time of occurrence, 249*, 263, 265; velocities, 266–8.

Arietid (night-time) shower, 275, 296–308; activity, 297–8; geocentric velocity, 303; heliocentric velocity, 303; hourly rates, 297, 367; orbit, 303–8, elements, 304*; origin, 421; radiant positions, 300–1; velocities, 302–3.
α-Arietid shower, 299; radiants, 298*.
δ-Arietid shower, 413*.
ϵ-Arietid shower, 299; radiants, 298*.
ζ-Arietid shower, radiants, 298*.
σ-Arietid shower, radiants, 298*, 299.
northern Arietid shower, 299.
southern Arietid shower, 299, 300, 302*; origin, 421.
Arietid summer day-time stream, 359, 443; activity, 363, 366*, 443*; classification, 359; cometary association, 422*; mass brought into earth's atmosphere by, 394; orbit, 378, 379*, 380, density and mass of particles in, 395*, elements, 379*; origin, 424; radiant coordinates, 370*, 371*; radiant positions, 370*, 371*; velocities, 373*, 374–5, 377*.
θ-Aurigid stream: activity, 367*; geocentric velocity, 372; heliocentric velocity, 372; orbit, 377; radiant coordinates, 370*; radiant positions, 370*; velocity, 377*.
Bečvář's stream, *see* Ursids, December.
Bielid (Andromedid) shower, 288, 326, 349–54; activity, 349–51; classification, 249*; comet associated with, 349, 353–4, 413*, 414, 415*; hourly rate, 350*, 351; shower length, 351, 428*; orbit, 353–4, elements of, 354*; periodicity, 351; radiants, 351; radiant coordinates, 351*; time of occurrence, 249*, 351; velocities, 351–3.
α-Capricornid stream, 270.
o-Cetid stream: activity, 366*, 443*; cometary association, 422*; orbit, 377–8, elements, 379*; origin, 424; radiant coordinates, 370*, 371*; radiant positions, 370*, 371*; velocity, 374, 377*.
Cygnid stream, 270.
Geminid shower, 147, 148, 189, 202, 237, 308–19, 444; activity, 308–10, 441–2; classification, 249*; cometary association, 422*, 422–3; heliocentric velocity, 316; hourly rate, 308–10, *363*, 441–2; shower length, 428*; life, 424; orbit, 308, 317–19, 422–4, density and mass of particles in, 395*, elements, 317*; origin, 423, 424; particle sizes, separation of, 409; radiant, 310–14; radiant coordinates, 311*, 312*; 313; radiant position, 310–14; time of occurrence, 249*, 308; velocity, 238–43, 315–17, distribution, *240*. (1946): frequency distribution, 389; magnitude, 387*, 388*. (1947), 53. (1949), 69, 214, 220; velocity distribution, *218*. (1950), 69. (1953), orbit determined by radio-echo technique, 438.
λ-Geminid stream: activity, 367*; radiant coordinates, 370*; radiant position, 370*.
ν-Geminid stream: activity, 367*; radiant coordinates, 370*; radiant position, 370*.
Giacobinid (Draconid) shower, 288, 326–37; activity, 327–32; age, 397; classification, 249*; comet associated with, 326, 332, 335–7, 413*, 414, 415*; hourly rate, 327, 328, 330, 331; shower length, 328, 428*; magnitude, 328; orbit, 335–7, density and mass of particles in, 395; particle size, separation of, 409; radiants, 332–4; radiant coordinates, 326, 332, 334; radiant position, 327, 332; recorded in daytime by radio-echo, 326, 327, 331; time of occurrence, 249*; velocity, 326, 334–5. (1933): frequency distribution, 386; magnitude, 384–5. (1946), 16, 29, 74, 76; frequency distribution, 386–8, 389; shower length, 329; magnitude, 387*, 388*; mass brought into earth's atmosphere by, 394. (1952), 331, 442.
Lacertid stream, 270.
Leonid shower, 147, 148, 175, 288, 337–48; activity, 338–40; classification, 249*; comet associated with, 337, 346, 400, 413, 413*, 414, 415*, 428*; frequency distribution, 386; geocentric velocity, 344; heliocentric velocity, 344; hourly rates, 338, 339*, *340*; orbit, 345–8, Schiaparelli's determination of, 337, 345–6; periodicity, 337, 338; radiants, 340–4, path of, *345*; radiant coordinates, 341, 342*, 343; radiant position, 341, 342*; time of occurrence, 249*; velocities, 344–5, 346*. (1833), 3, 4, 86. (1931), 24. (1932), 16, 24, 26. (1933), 16; frequency of, 386. (1940), 27.
Lyrid shower, 147, 175, 258–63; activity, 259–61; age, 400; classification, 249*; comet associated with, 259, 260, 263, 413*, 414, 415*; hourly rate, 259–60; shower length, 428*; orbit, 263,

METEORS, SHOWERS AND STREAMS (*cont.*):
elements, 263; periodicity, 259; radiants, 261–2; radiant coordinates, 261, 440*; radiant position, 259, 262, 439; time of occurrence, 249*, 259; velocities, 262–3. (1922), 260–1. (1946), 29.
Orionid shower, 147, 148, 189, 288–96; activity, 288–90, 441; classification, 249*; comet associated with, 269, 288, 295–6, 408, 422; hourly rate, 288, *289*, 290*; shower length, 428*; orbit, 295–6; position, 291; radiants, 290–4; radiant coordinates, 290, 291, 293, 294; radiant position, 291; time of occurrence, 249*, 288; velocities, 294–5.
α-Orionid stream: activity, 367*; radiant coordinates, 370*; radiant position, 370*.
Perseid shower, 147, 148, 175, 231, 237, 275–87, 444; activity, 277–8; age, 397, 400; classification, 249*; comet associated with, 277, 286, 413, 413*, 414, 415*, 428*, 428–9, 441; frequency distribution, 386; heliocentric velocity, 286; hourly rates, 275, *277*, 278, 279*, 367; life, 276, 278; luminosity distribution, 384, 385*; orbit, 286–7, 401, density and mass of particles in, 395*, Schiaparelli's computation of, 277, 286, elements, 287*, 441; origin of, 428–9, 444; periodicity, 278; radiants, 4, 278, 280–2, 286, dispersion of, 402; radiant coordinates, 280*, 281, Herschel's determination of, 286; radiant position, 278, 280–2, 440, 441; structure of, 444; time of occurrence, 249*, 276, 277, 278; velocities, 281, 282–6. (1920), 8. (1921), 8. (1946), 29. (1947), 96.
— — of second magnitude, mass of, 136.
54-Perseid stream: activity, 367*; geocentric velocity, 372; heliocentric velocity, 372; orbit, 377; radiant coordinates, 370*; radiant position, 370*; velocity, 377*.
ζ-Perseid stream: activity, 363, 366*–7*, 443*; classification, 359; comet associated with, 413*; mass brought into earth's atmosphere by, 394; orbit, 382, density and mass of particles in, 395*, elements, 381*; origin, 421; radiant coordinates, 370*, 371*–2*; radiant positions, 370*, 371*–2*; velocity, 373*, 374, 376, 377*.
Piscid stream: activity, 366*; radiant coordinates, 370*, 371*; radiant positions, 370*, 371*.
ν-Piscid stream: activity, 366*; radiant coordinates, 370*; radiant positions, 370*.
Pons–Winnecke, 354–7; activity, 355; classification, 249*; comet associated with, 413*, 414, 415*; hourly rate, 355; orbit, 356–7, elements, 357*; perturbations due to Jupiter, 357*, 400, 401; radiants, 355–6; radiant coordinates, 355*; radiant position, 355*; time of occurrence, 249*, 355; velocities, 356–7.
Quadrantid shower, 147, 249–58, 443; activity, 249–52; classification, 249*; cometary association, 257, 413*, 422, 439; geocentric velocity, 256, 439; heliocentric velocity, 255, 256, 257; hourly rate, 250–2; shower length, 428*; orbit, 256–8, density and mass of particles in, 395*, elements, 257*; parabolic elements, 256; periodicity, 252; position, 249; radiants, 252–4; radiant coordinates, 254*, 439; radiant position, 253; time of occurrence, 249; velocities, 254–6. (1946), 29. (1947), frequency distribution, 389.
shower: angular velocity, *184*; classification, 248; durations of, *184*; frequency distribution, 384–90, 442–3; height, 193, 194*, mean, 195; number and mass distribution of, 384–96; times of fall into sun, 408*.
solar: frequency, 180*.
sporadic: activity, seasonal variation of, 120–2, average, 193, 194*; component, origin of, 246; distribution of, 49, in ecliptic latitude, 110, 120, major showers and, 96, Prentice's investigations, 108–11, radio-echo investigations of, 112–17; distribution, diurnal, 96–122, *97*, compared with Schiaparelli's theory, 101–2, 103, Hoffmeister's investigations of, 103–8, *107*, *119*; distribution, mean, round the earth, *118*; distribution, seasonal, 96–122, *97*, compared with Schiaparelli's theory, 102–3, 120; distribution, true, 117–19, 185; diurnal variation, 113–14; daily mass of, *137*; daily frequency, 131, *132*; heights, mean, 195; mass distribution, 9, 123–40; mass and energy brought into earth's atmosphere by, 138; number of, 9, 123–40; orbit of, 247, 429, 430*, distribution of, 438–9, modulation of,

around earth's orbit, *121*, 122; origin, 1, 141, 163, 207, 210, 246–7, 429–32; space distribution of, 138–40; velocity of, 141–247, British data on, 190–7, Öpik's measurements of, 155–89, photographic measurements of, 198–211, radio-echo techniques for measuring, 212–46; velocity distribution, 2, 49, 119, double-camera investigation of, 439; velocity, heliocentric space, *187*.
space, distribution of, 186*.
summer day-time streams, 118, 122, 238, 297, 326, 358–83; activity, 359–68, 443*; classification, 249*; observed as fireballs, 307; hourly rates, *363*, *364–5*; orbits, 378–83; radiants, 368–72; radiant coordinates, 370*–2*; radiant positions, 368, *369*, 370*–2*; revealed by radio echoes, 248, 307, 358–9; showers classed as, 359, 366*–7*; times of occurrence, 249*; velocities, 372–6. (1947), 65, 71.
— — Stream B: radiant coordinates, 370*; radiant positions, 370*.
— — Stream C′: radiant coordinates, 370*; radiant position, 370*.
Taurid shower, 202, 205, 296–308; activity, 297–8; age, 420, 421; classification, 249*; comet associated with, 297, 307–8, 413*, 415–21; geocentric velocity, 303; heliocentric velocity, 303; hourly rate, 297, 367, 441; shower length, 428*; orbit, 303–8, 377, and orbits of Mercury, Venus, and Mars, 307, elements, 304*; origin, 305, 421; radiants, 298–301; radiant coordinates, 298*, 299*; radiant position, 300–1; time of occurrence, 249*, 296–7; velocities, 302–3.
β-Taurid stream, 297, 444; activity, 367*, 443*; classification, 359; comet associated with, 413*, 415–21; orbit, 382–3, density and mass of particles in, 395*, elements, 381*; origin, 421; radiants, 298*, 377; radiant coordinates, 370*–1*; radiant positions, 370*, 372*; velocities, 373*, 374, 376, 377*.
γ-Taurid stream, radiant, 298*.
ϵ-Taurid stream, radiant, 298*.
ζ-Taurid stream, radiant, 298*.
κ-Taurid stream, radiant, 298*.
λ-Taurid, 299; radiant, 298*.
northern Taurid stream, 299, 302*, 307.
s-(southern) Taurid stream, 299, 300, *301*, 302*.
ξ-Taurid stream, radiant, 298*.
Ursid stream, December (Bečvář's stream), 319–25; activity, 319–21; classification, 249*; comet associated with, 324–5, 413*, 414, 415*; hourly rate, 319–21, 323; orbit, 323–5, elements, 324*; radiant, 321–2; radiant coordinates, 321*, 322*; radiant position, 321, 322*; time of occurrence, 249*, 320; velocities, 323.
micro-meteorites, 2.
Milky Way, The, galactic noise from, 48.
Millman and Hoffleit's photographic measurements of velocity, 198–201.
— and McKinley's method for measuring meteor radiants, 52–55.
modulation frequency caused by Fresnel zone oscillations, 35.

Neptune, attractive force of, 398.
von Niessl's expression for density distribution of meteors, 103.
von Niessl–Hoffmeister fireball catalogue, 142–54.
nodes of orbit: defined, 86–87; effect of perturbations on, 399.
noise, relation of, to detection of meteor echo, 47.
— galactic, 47, 48.
— receiver, 46–48.
notation: astronomical, miscellaneous, 436; miscellaneous, 437; radio, 436–7.
number: change of, relation between magnitude and, 384; and mass distribution of shower meteors, 384–96; of meteors observed, magnitude and, 123.
Nyquist's theorem, 46–47.

Oak Ridge, 17, 202, 209.
observation: duplicate, 3–4; photographic techniques, 14–22, 198–211, 212; radar techniques for, 32; radio-echo techniques for, 23–49, 67, 212–46; reticule method for, 10–12, 188; rocking mirror method for, 106; telescopic, 123–40, applied to Giacobinids, 328, Boothroyd's method, 159–63; visual techniques, 3–14, 141–97, 212; of Arizona expedition, 10–14.
observational error dispersion: Öpik's corrections for, 166–7; and velocity, 184.
occulted trail, first photograph of, 15.
Öpik, work of, 155–89; analysis of Arizona data of, compared with Porter's British analysis by, 195–7; calculation of distribution of space velocities by, 167–81; correction for observational error dispersion by, 166–7.
optical diffraction theory and electron density in meteor trail, 44–46.

orbits, comets: identification with orbits of meteors, 413–14.
— meteor: 'anomalies', 87, *88*; computation of, 54, 94–95; determination by triangulation, 73, 76; elements of, 86–87, *see also separate showers and streams*, symbols, 435–6; retrograde motion defined, 86; nodes defined, 86–87; plane of, *87*; radio-echo measurement of, 258, 269, 317, 318, 438; velocity of meteor in its, 88–90.
— sporadic meteors, 247; comparison with those of asteroids and comets, 430*; distribution of, 438–9.
— meteor streams: computation of, 248; identification with orbits of comets, 413–14.
— spatial, computation of, 86–95.
Orionid shower, 147, 148, 189, 288–96; activity, 288–90, 441; classification, 249*; comet associated with, 269, 288, 295–6, 408, 422; hourly rate, 288, *289*, 290*; shower length, 428*; orbit, 295–6; position, 291; radiants, 290–4; radiant coordinates, 290, 291, 293, 294; radiant position, 291; time of occurrence, 249*, 288; velocities, 294–5.
α-Orionid stream: activity, 367*; radiant coordinates, 370*; radiant position, 370*.

Palomar, Mount, 14.
parabolic regression method of measuring meteor velocity, 75.
— velocity, 108, 141, 268, 323; Schiaparelli's equation, 99.
— constants for velocity of meteor in its orbit, 89.
— limiting velocity of meteor in its orbit, 90.
— limit, 119; and telescopic observation, 130.
— geocentric velocity, 273.
— heliocentric velocity, 234.
paraboloidal aerial, 39–40.
parallactic displacement, 3.
particles, meteoric: in meteor showers, disappearance of, 390; mass and density of, in orbits of meteor showers, 394–6; equations of motion of, 403; effect of radiation pressure on, 410–11; separation of, according to size, 403, 409; rate of fall into sun, 402, 405, 456*; time of fall into sun, 431; in space, velocity of, 141; velocity, 427.
path, meteor: data on, accuracy of, 4; determination by wand or extended string, 4, 190, from segmented trails, 20; map-plotting of, 3, 4, 190; and number of meteors observed, 123; observation of, 10–12; perturbations and, 96.
— of meteor showers, 248.
path length, meteor: source of data on, 3; for different magnitudes, 129*.
— — of fireballs, 148, *148*, *149*.
perception, coefficient of, 8.
perihelion: argument of, defined, 87; longitude of, 87.
periodic phenomenon, idea of, 86.
— streams of meteors, 326–48.
periodicity: comet, Pons–Winnecke, 354; fireballs, 143, *144*; of meteors, *see separate showers and streams*.
Perseid shower, 147, 148, 175, 231, 237, 275–87, 444; activity, 277–8; age, 397, 400; classification, 249*; comet associated with, 277, 286, 413, 413*, 414, 415*, 428*, 428–9, 441; frequency distribution, 386; heliocentric velocity, 286; hourly rates, 275, *277*, 278, 279*, 367; life, 276, 278; luminosity distribution, 384, 385*; orbit, 286–7, 401, density and mass of particles in, 395*, Schiaparelli's computation of, 277, 286, elements, 287*, 441; origin, 428–9, 444; periodicity, 278; radiants, 4, 278, 280–2, 286, dispersion of, 402; radiant coordinates, 280*, 281, Herschel's determination, 286; radiant position, 278, 280–2, 440, 441; structure of, 444; time of occurrence, 249*, 276, 277, 278; velocities, 281, 282–6.
— — of second magnitude, mass of, 136.
54-Perseid stream: activity, 367*; geocentric velocity, 372; heliocentric velocity, 372; orbit, 377; radiant coordinates, 370*; radiant position, 370*; velocity, 377*.
ζ-Perseid stream: activity, 363, 366*–7*, 443*; classification, 359; comet associated with, 413*; mass brought into earth's atmosphere by, 394; orbit, 382, density and mass of particles in, 395*, elements, 381*; origin, 421; radiant coordinates, 370*, 371*–2*; radiant positions, 370*, 371*–2*; velocity, 373*, 374, 376, 377*.
— — (1920), 8.
— — (1921), 8.
— — (1946), 29.
— — (1947), 96.
perspective, and meteor streams, 56.
perturbations: calculation of, 398–401; constants, 419*; effect of, *399*; fundamental equations, 417–19; and paths of meteors, 96. Due to Jupiter, 346, 354,

356, 397, 398, 400, 416, 423, 429; to Mars, 423; to Saturn, 346, 397, 398, 429; to sun, 401; to Venus, 423.
photographic techniques of observation, 14–22, plates, data from, reduction of, 20–22; double camera, 202–11; frequency distribution of shower meteors determined by, 384–8; Harvard, 1, 16–22, 143; velocity of sporadic meteors measured by, 198–211, Millman and Hoffleit's results, 198–201, Whipple's results, 202–8.
photometry: magnitude measured by, 21–22; and meteor trails, 21.
Piscid stream: activity, 366*; radiant coordinates, 370*, 371*; radiant positions, 370*, 371*.
ν-Piscid stream: activity, 366*; radiant coordinates, 370*; radiant positions, 370*.
planets: meteors associated with, 307, 346; origin of short-period meteor streams from, 424; perturbations due to, effect of, 397–401.
— minor, relation of meteor streams and, 444.
plasma resonances, 45.
Poisson's equation, 152.
polar diagrams of aerial systems, 36, 38, 40, 41, 61, 224.
Polar Year Expedition of 1932, 27.
Pons–Winnecke meteors, 354–7; activity, 355; classification, 249*; comet associated with, 413*, 414, 415*; hourly rate, 355; orbit, 356–7, elements, 357*; perturbations due to Jupiter, 357*, 400, 401; radiants, 355–6; radiant coordinates, 355*; radiant position, 355*; time of occurrence, 249*, 355; velocities, 356–7.
Porter's analysis of British meteor data, 190–7; compared with Öpik's, 195–7.
power density, 36; flux of power formula, 36, 37; of scattered radiation, formula for, 44.
— gain (G) of an aerial system, 36, 37, 40, 41, 48–49, 67, 212, 230; and collecting area, 44, 49; expressed in terms of a half-wave dipole, 44; and magnitude range, 49.
Poynting–Robertson effect, 271, 402–9, 431, 444.
Prentice's investigation on distribution of sporadic meteors, 108–11.
projection ratios: distribution, 173, 174*; frequency of, 167–73; spread in, limits, 185, and velocity, 184.
pulse rate for radio observation, 30, 35.
pulse shape, relationship of band width to, 34.
— spectrum, 33.
— techniques: for observing diffraction pattern, 78–79; for observation, 30–31, *31*, 32, 33, 35; for reflection of radio waves, 24, 27; for measuring velocity of sporadic meteors, 212–37.
— width, 32–33, 35, 41; and range accuracy, 48.
Pultusk meteorite, 154.

Quadrantid shower, 147, 249–58, 443; activity, 249–52; classification, 249*; cometary association, 257, 413*, 422, 439; geocentric velocity, 256, 439; heliocentric velocity, 255, 256, 257; hourly rate, 250–2; shower length, 428*; orbit, 256–8, density and mass of particles in, 395*, elements, 257*; parabolic elements, 256; periodicity, 252; position, 249; radiants, 252–4; radiant coordinates, 254*, 439; radiant position, 253; time of occurrence, 249; velocities, 254–6.
— — (1946), 29.
— — (1947), frequency distribution, 389.

radar, and meteor observation, 32.
radiant: calculation of, 220–2; corrections to observed, 91–94; data on, source of, 3; declination of, determination of, 63, 65, 67–68; defined, 86; density, apparent, working formula, 171; surface, 169; determination of, 49, accuracy of, 4, error of, from reticule observations, 12; diffuseness of, 70; elevation, defined, 52, and range distribution of echo, 52; elongation of, relation between geocentric velocity and, 213, relation between height, velocity, and, 193–5; errors, 191; measurement of, 1, 50–73, Clegg method, 55–73, Hey and Stewart method, 50–52, McKinley and Millman's method, 52–55; variation in number visible, Schiaparelli's theory, 96–101; right ascension, determination of, 63; survey apparatus at Jodrell Bank, 65–73; zenith angle, relation between radio meteor rates and, 241; *see also separate showers*.
— apparent, *90*; determination of, 110, 202; distribution, *117*.
— space, 151, *152*, *153*.
— 'stationary', 288, 290, 291, 292, 293.
— true, 93; elongation of, 93–94.
— coordinates: defined, 51 n.; determination of, 63–65; visual observation of, 190; *see also separate showers*.

radiant position: aerial beam width and, 52; defined, 51, 248; determination of, 68; variation and range of echo rate and, 56; *see also separate showers.*
— of fireball, 143, *145*; apparent, 150, 151, *152*; concentration, 153; true, 151.
radiation, relation between retardation and, 402–3.
— pattern of aerial and collecting area of system, 56.
— pressure: effect on a rotating particle of, 410–11; from the sun, 138.
radiators: centre-fed half-wave dipole; 36–37; Hertzian dipole, 36, 37.
radio apparatus for the study of meteors, 30.
— astronomy, techniques, 1.
— echo: amplitude, formula, 224; meteor activity, variation in, determined by, *391*, activity of Giacobinids observed by, 329, 330, 331; correspondence between meteor and, 28–30; critical aspect of trail, 50; duration of, 42, 46, short-duration, 26, of short duration similar to random noise impulses, 66; diffraction theory and, 74, 76; diffraction technique, velocities measured by, 254, 285, 372; frequency distribution determined by, 135, 388–90, 442–3, fundamental equations of, 43–49; hourly rates of, mean, diurnal variation, 51; hourly rates of meteors estimated by, 252*, 265*, 271, *277*, 290*, 297, 308, 310*, 339*; relationship between mass distribution and, 49, Kaiser and Evans method to determine, 389–90; relationship between number recorded and wave-length, 49; relation to noise, 47; observation by means of, 23–49; orbits calculated from, 258, 269, 317, 318, 438; photographs of, on an intensity-modulated range-time display, Pl. i; production in terms of diffraction from a line source, 73; meteor radiants measured by, 50–73, Clegg method, 55–73, Hey and Stewart method, 50–52, McKinley and Millman's method, 52–55; relation between zenith angle of radiant and meteor rates, 241; radiant coordinates determined by, 254*, 262, 294, 312*, 313, 322; radiant positions observed by, 280*, 281; range of, 58–63, limit, 225; range distribution of, and elevation of radiant, 52; range-time curves, 61–63; range-time display and shape of, 54; range-time relationship of, and beam shape, 56; rate, 58–63, formula, 225–6, relation between hourly number of meteors and, 223, variation and range of, and radiant position, 56, comparison with visual rate to estimate magnitude, 231–3; relation between receiver noise level and number of echoes obtained, 46–48; shape of, 54, 73, 75, 76, defined, 54, hyperbolic, 54, 73, 75, 76; signal obtained dependent on type of detector, 80; of sporadic distribution, 112–17; measure of strength, 47; summer day-time streams revealed by, 248, 307, 358–9; from head of trail, 438; transient, 27, 28, 43, 49; velocity of meteors measured by, 73–85, 212–46, 254, 263*, 268, 273, 274*, 284, 285*, 286, 316, 323, 335*, 352.
— — notation, 436–7.
— — techniques for study of meteors, 30–49; for measuring meteor velocities, 73–85.
— waves: formula for intensity of reflected wave, 78; frequencies, critical, 23, 25–26; length, for radio-echo observation, 43–49, for measuring velocity, 212, and echoes recorded, 49; propagation of, meteors and, 24–28; reflection of, pulse technique for, 23, 24, 27; scattering of, 230–1, into skip zone, 27.
range accuracy: and beat frequency, 35; and rounding of pulse, 33; and pulse width, 48; and receiver band width, 34, 35.
— measurement by pulse or frequency modulated method, 32.
range-time curves of radio echoes, 61–63.
— display and shape of radio echo, 54.
— — methods for measuring meteor velocity, 73–76.
— — plots: and determination of radiant position, 68; showing velocity measurements, *375*. Of Geminid showers (1949, 1950), 69, *70*; of summer day-time streams, *71*.
— — relationships of radio echoes and aerial beam shape, 56.
— — trace of echoes, 82, 83, 84, Pl. i.
rates, meteor: diurnal variation in, 8–9, 28; diurnal variation of sporadic, *115*; determined by radio echo, 231–3, relation between zenith angle of radiant and, 241; visual, 9, 10*, 231–3.
receiver band width, and meteor observation, 32–35, 47.
— noise, 46–48.
reciprocity theorem: and aerials, 36; and magnitude, 205.
recording system of radio-echo observation, 41–43.

recurrence frequencies, velocity determination and, 48.
refraction, differential, 202.
retardation, relation between radiation and, 402–3.
reticule method of observation, 10–12, 188; for recording trails, 181.
retrograde motion of orbit, defined, 86.
right ascension of radiants, determination of, 83.
rocking mirror method of measuring angular velocities, 12–14, 156; apparatus, 155; corrections to, 156*; frequency measured by, 182; used in Tartu, 181–9.
rotating-shutter technique for measuring velocity, 14, 16, 17, 19–20, 198, 207, 282, 295, 333.

Saturn: attractive force, 397; perturbations due to, 346, 397, 398, 429.
scattering, 43–45; amplitude variation of, 78; cross-section formula, 43; diffraction theory and, 74, 76; diffractional, by zodiacal particles, 432; effects, abnormal, 27–28; fundamental, formula, 57; by ionized meteor trail, 30; power density formula, 44; of radio wave, 230–1, into skip zone, 27.
Schiaparelli: computation of orbit of the Leonids, 337, of Perseids, 277, 286; on formation of meteor streams, 425; equation of, for parabolic velocity, 99, 101, 102; theory of, for variation in number of meteor radiants visible, 96–101, compared with observed diurnal variation, 101–2, 103, compared with observed seasonal variation, 102–3, 120.
Schmidt camera, 14, 20*; super, 17, 18–20, *18*, 20*, 210–11.
Scorpius, streams in, 150, 151.
seasonal variation: of sporadic meteor activity, 96–122, compared with Schiaparelli's theory, 102–3, 120.
segmented trails, measurement of, 202.
showers of meteors, *see under* meteors.
skip zone, scattering of radio waves into, 27.
'slow Doppler' method, 82–85.
solar component of meteors, 210.
— longitude, relationship with geocentric velocity, 302–3.
— system: density of meteoric matter in, 139; origin of, 397; origin of sporadic meteors in, 207, 210; velocity of interstellar particles in, 141.
Soledad, 17, 20, 209, 211.
space density per magnitude group, 384.
— distribution of sporadic meteors, 138–40.
space radiants, 151, *152*, *153*.
— velocities, 159, 173–5, 175*–6*, Öpik's calculations, 167–81; for sporadic meteors, 186*; heliocentric, for sporadic meteors, 187.
spatial orbit, *see under* orbit.
sporadic meteors, *see under* meteors.
'stationary radiant', 288, 290, 291, 292, 293.
Stewart and Hey method of measuring meteor radiants, 50–52.
stream intensity, 172*.
streams of meteors, *see under* meteors.
string, extended, use of, for observing path, 4, 190.
summer day-time streams, 118, 122, 238, 297, 326, 358–83; activity, 359–68, 443*; classification, 249*; observed as fireballs, 307; hourly rates, *363*, *364–5*; orbits, 378–83; radiants, 368–72; radiant coordinates, 370*–2*; radiant positions, 368, *369*, 370*–2*; revealed by radio echoes, 248, 307, 358–9; showers classed as, 359, 366*–7*; times of occurrence, 249*; velocities, 372–6.
— — Stream B: radiant coordinates, 370*; radiant positions, 370*.
— — Stream C′: radiant coordinates, 370*; radiant positions, 370*.
— — — (1947), 65, 71.
sun: attractive force, 397; perturbations due to, 401; radiation pressure of, 138; rate of fall of a particle into, 402, 405, 406*; times of fall of meteoric particles into, 408*, 431.
surface density of radiants, 169.
symbols: orbital elements, 435–6; velocity, 435.

tangential drag, 402.
Tartu observations, 181–9.
Taurid shower, 202, 205, 296–308; activity, 297–8; age, 420, 421; classification, 249*; comet associated with, 297, 307–8, 413*, 415–21; geocentric velocity, 303; heliocentric velocity, 303; hourly rate, 297, 367, 441; shower length, 428*; orbit, 303–8, 377, and orbits of Mercury, Venus, and Mars, 307, elements, 304*; origin, 305, 421; radiants, 298, 301; radiant coordinates, 298*, 299*; radiant position, 300–1; time of occurrence, 249*, 296–7; velocities, 302–3.
β-Taurid stream, 297, 443; activity, 367*, 443*; classification, 359; comet associated with, 413*, 415–21; orbit, 382–3, density and mass of particles in, 395*, elements, 381*; origin, 421; radiants,

298*, 377; radiant coordinates, 370*, 371*; radiant positions, 370*, 372*; velocities, 373*, 374, 376, 377*.
γ-Taurid stream, radiant, 298*.
ϵ-Taurid stream, radiant, 298*.
ζ-Taurid stream, radiant, 298*.
κ-Taurid stream, radiant, 298*.
λ-Taurid stream, 299; radiant, 298*.
northern Taurid stream, 299, 302*, 307.
s-(southern) Taurid stream, 299, 300, *301*, 302*.
ξ-Taurid stream, radiant, 298*.
Taurus, hyperbolic stream in, 146, 150.
telescopic observation, 123–40.
three-point method of measuring meteor velocity, 75; of measuring velocity of Perseids, 284.
timing errors in visual techniques, 4–5.
trails, meteor: critical aspect effect of, 50; density of, and duration of echo, 46; diffraction pattern of, Pl. iii; electron density in, 44–46, effective, 57; fixed reticule for recording, 181; formation of, modulation frequency caused by Fresnel zone oscillations during, 35; head of, radio echo from, 438; height of meteor determined from, 202–3; occulted, first photograph of, 15; photometry of, 21; power scattered from, and peak transmitter power, 48; scattering by ionized, 30; segmented, 20, 198, 202; specularly reflecting properties of, 55, 213. Of Giacobinid stream, 334; of Leonids, 343, 344; of Perseids, *281*.
transient echoes, 27, 28, 43, 49.
transmitter: for radio observation, 30, for continuous wave techniques, 237; power of, and radio observation, 35, and power scattered from meteor trail, 48.
— band width, formula for, 33.
— pulse: rate, 212; width, 32–35, 41.
triangulation, determination of orbit of meteor by, 73, 76.

Uranus, 346; attractive force of, 398.
Ursids, December (Bečvář's stream), 319–25; activity, 319–21; classification, 249*; comet associated with, 324–5, 413*, 414, 415*; hourly rate, 319–21, 323; orbit, 323–5, elements, 324*; radiant, 321–2; radiant coordinates, 321*, 322*; radiant position, 321, 322*; time of occurrence, 249*, 320; velocities, 323.

van de Hulst's theory of zodiacal light, 432–4.
velocity, meteor: according to apex experiments, 233; apparent, defined, 90; Arizona measurements, 183–81; data on, source of, 3; defined, 86; determination of, meteor height and, 2, and recurrence frequencies, 48, from segmented trails, 20; deviation, mean standard, 218; distribution, 2, 220, 242–5, calculation of, 228, effect of magnitude on, 237, theoretical and experimental compared, 229–30; relation between elongation and, 195, *196*; relation between elongation, height, and, 193–5; relation between height and, 194*; –luminosity relation, 108, 179–81, 187, 210; relationship between luminosity, mass, and, 136; correction for magnitudes obtained by photometric measurement, 22; measurement of, 1, by continuous wave method, 32, 35, 82–85, by curve-fitting method, 75, from diffraction photographs, errors in, 214, by radio techniques, 73–85, by range × dR/dt method, 75, by rotating-shutter camera, 14, 16, 17, 19–20, 198, 207, 282, 295, 333, by visual observation, 12–14; observational error dispersion and, 184; probable, 233; spread in projection ratios and, 184; symbols, 435.
— — angular: calculation of, 155, 156; distribution of, 105–6; correlation between height and, 164; measurement of, by means of rotating shutters, 12–14, correction to, 156*; observed waves and, 182; reduction to zenithal angular velocity, 182.
— — — zenithal: angular velocity reduced to, 182; relation between height and, 157.
— — geocentric, 142, 145, 241; calculation of, 220–2; defined, 90; forumla, 221; relation between elongation of meteor radiant and, 213; relationship with solar longitude, 302–3; relation between zenithal magnitude and, 180*; *see also separate showers*.
— — — parabolic, 273.
— — — tangential, distribution of, 168*.
— — heliocentric, 104, 106, 141, 142, 210, 255, 256, 257, 316; relation between concentration and, 234; defined, 90; distribution of, 175–9, 180*, 181*, 234; *see also separate showers*.
— — — parabolic, 234.
— — — projected, distribution of, 159–62.
— — — tangential, relation between zenithal magnitude and, 188*.
— — — transverse, components of, 183*

velocity, meteor, hyperbolic, 103, 108, 118, 130, 195, 196, 201, 207, 209, 210, 233, 246, 247.
— — — parabolic, 141, 268, 323; Schiaparelli's equation for, 99, 101, 102.
— of densely ionizing meteors, measurement of, 73, 74, 82.
— orbital, of earth, 175.
— of fireballs: compared with velocity of meteors, 150*.
— — — heliocentric, 146*.
— — — hyperbolic, 142, 143.
— of interplanetary particles and formation of meteors, 433.
— of interstellar clouds, 141.
— of interstellar particles in solar system, 141.
— of meteor: in earth's atmosphere, 90–91; in free fall, 142; in its orbit, 88–90; compared with velocity of fireballs, 150*.
— of meteoric particles, 427; in space, 141.
— of meteors, sporadic, 141–247; British data, 190–7; distribution, 49, 119, double camera investigation of, 439; measurement of, by photographic methods, 198–211, by radio-echo techniques, 212–46; space distribution, 186*, Öpik's calculations, 167–81, heliocentric, 159–61, 187.
— of shower meteors, angular, *184*.
Venus: attractive force of, 398; orbit of, and Taurids, 307; perturbations due to, 423.
visibility, area of, effective, for meteors of different magnitudes, 129*.
vision, field of, difference in magnitude and, 7; a function of magnitude, 8.
visual observation, *see under* observation.
— rates, compared with radio-echo rates to estimate magnitude, 231–3.

wand, use of, for determining path, 4, 190.
Whipple's comet model, 425–8, 429.
— photographic measurements of velocity, 202–8.

Yagi arrays, 38–39, 41, 67.
Yarkovsky effect, 410–11.

zenith attraction, 91–92, 104; correction for, 240–1.
— angular velocity: angular velocity reduced to, 182; height and, 157*.
— distance, 106.
— magnitude: defined, 6; geocentric velocity and, 180*; heliocentric tangential velocity and, 185*; and luminosity, 6.
zodiacal light: meteors and, 432–4; origin of, 432.
— particles, 432–4.

PRINTED IN
GREAT BRITAIN
AT THE
UNIVERSITY PRESS
OXFORD
BY
CHARLES BATEY
PRINTER
TO THE
UNIVERSITY

METEOR ASTRONOMY

LOVELL

5235
523.5
LOV

OXFORD